CROSS SECTIONAL COMPACTNESS AND BRACING REQUIREMENTS FOR
HPS70W GIRDERS

By

Steven J. Thomas

BS, The Pennsylvania State University, 2000

Submitted to the Graduate Faculty

of the School of Engineering

in partial fulfillment

of the requirement for the degree of

Master of Science

University of Pittsburgh

2002

UNIVERSITY OF PITTSBURGH

CIVIL AND ENVIRONMENTAL ENGINEERING

This thesis was presented

by

Steven J. Thomas

It was defended on

April 18, 2002

and approved by

Dr. Jeen-Shang Lin, Associate Professor, Civil and Environmental Engineering

Dr. John F. Oyler, Associate Professor, Civil and Environmental Engineering

Dr. Morteza A.M. Torkamani, Associate Professor, Civil and Environmental Engineering

Thesis Advisor: Dr. Christopher J. Earls, Associate Professor, Civil and Environmental Engineering

CROSS SECIONTAL COMPACTNESS AND BRACING REQUIREMENTS
FOR HPS70W GIRDERS

Steven J. Thomas, M. S.

University of Pittsburgh, 2002

The present study employs experimentally verified nonlinear finite element modeling techniques for the study of high performance steel (HPS) I-shaped bridge girders. Evaluations as to the appropriateness of using the current AISC LRFD Structural Steel Building Design Specification (1999) and AASHTO LRFD Bridge Design Specification (1998) provisions for maintaining cross-sectional compactness, an appropriate lateral bracing placement, and a sufficient lateral bracing stiffness for the purpose of plastic analysis and design are carried out within the context of applications involving A709 HPS483W high performance steel.

It appears that the current AISC and AASHTO provisions are not applicable to bridge girders made from A709 HPS483W steel. That is, all criteria relating to flange and web compactness, unbraced length, and bracing stiffness, when considering A709 HPS483W steel, are unconservative. New lateral bracing requirements are proposed, altering both the position of the bracing as well as the required bracing stiffness. In addition, new flange and web compactness criteria are developed for use with A709 HPS483W steel.

DESCRIPTORS

High Performance Steel (HPS)   Compactness

HPS Bridge Girder Design   Lateral Bracing

Plastic Analysis and Design   Nonlinear Finite Element Analysis

Rotation Capacity   Ductility

ACKNOWLEDGEMENTS

"Success is the journey, not the destination." A lot of people in this world tend to get caught up in believing that "success" is measured by how much money they make, how big their house is, what kind of car they drive, etc. However, I feel that success is not quite that simple. It is true that I succeeded in completing this report, and earning my masters degree, however, those accomplishments are merely the end result of the most successful two years of my life. If it is argued that success is measured by money, then I will claim my family and friends as my "money." Without the people in my life and the support and encouragement they have provided, there is no doubt in my mind that I would not have *succeeded* in completing this report and earning my degree. I may have finished, but I would not have done so successfully if it were not for all the amazing people that helped me along the way.

I must begin by thanking my grandmother, Helen Kimball. Through the course of the past two years my grandmother has not only been the most loving, encouraging, and supporting grandmother, but she has also become a true friend. In addition, I believe it has been her prayers that have allowed me to reach where I am today. Words simply cannot express how much I appreciate who she is and everything she has done for me.

I would also like to thank my whole family: my Mom, Patricia Thomas, my Dad, Herbert Thomas, Jr., my brother Dan Thomas, my sister, Maureen Nikitas, and my sister and brother in law, Karen Thomas and Mike Nikitas. These six people are not only

family, they are my best friends, and without their support and encouragement, this report would not exist. I have been blessed by God to be given such a wonderful family.

My time in Pittsburgh has seen its ups and downs. By far, it has involved the most challenging times in my life, thus far. I am forever indebted to all of my wonderful friends for all of their help, understanding, patience, and true friendship. All of their efforts and sacrifices will always be remembered and greatly appreciated.

I would like to thank Laura Volle for helping me chose to stay at the University of Pittsburgh and finish what I had started. She was forced to deal with me during a tough time when I desperately needed a friend – she not only filled the role, but she excelled and I will be forever grateful.

In addition, John Martinoli, Dave Dinan, and Nick Greco have played significant roles in contributing to my finishing this report and graduating. Their support has been paramount to my success, both in the "journey" and in the "destination." John has been the friend I never knew I had. Dave has been Dave – that is the best way to describe it. Nick – well, it is true that one is influenced by the attitudes of those around them. Nick's motivation, discipline, and determination has served as a foundation upon which I have been able to accomplish my goals and finish this report. Additionally, his patience and friendship while dealing with me as an "office-mate" is greatly appreciated. I would also like to thank Ed Telega and Megan Forsythe for their patience as friends, their continued willingness to help make my life a little easier, and most importantly, their constant reassurance that I could accomplish my goals.

I must also thank Dr. Christopher J. Earls. His roles as an advisor, a professor, and a friend have been crucial. On numerous occasions in the past two years I have presented Dr. Earls with some very challenging situations, both academically and personally. His sincere concern, advice, and trust in me will be forever appreciated. At times when most would have made a different decision, he stood by me and had faith in my abilities. In addition to teaching me a great deal about structural engineering, Dr. Earls taught me about life and about myself. For that, I am extremely thankful.

In addition, I must thank all of my students, particularly those I have had this last semester. They have been exceptionally patient and understanding, and therefore, very helpful towards my completing this report. I would also like to thank the Federal Highway Administration for their financial support. Finally, I would like to express my gratitude to our President, George W. Bush, for providing excellent leadership to our nation during this very sensitive time in history – united we stand.

I believe in surrounding myself with only those who lift me higher. In doing so, the journey leading up to the completion of this report has been far more a success than simply the destination of completing it.

TABLE OF CONTENTS

LIST OF TABLES

LIST OF FIGURES

xiv

xvi

NOMENCLATURE

b_f	Flange width
b	Flange width
C_d	Relative bracing factor based on single/double curvature
d	Depth of cross-section
E	Modulus of elasticity of steel
F_y	Steel yield stress
F_{yc}	Compression flange steel yield stress
F_b	Intermediate stress value
F_u	Steel ultimate stress
h	Depth of entire web
h_o	Distance between flange centroids
I	Moment of Inertia
K	Spring stiffness
L	Span length of simply supported beam
L_b	Laterally unbraced length
L_{pd}	Limiting laterally unbraced length for plastic analysis
M_y	Moment causing the extreme cross-sectional fiber to yield
M_p	Full plastic capacity of cross-section
M_u	Required flexural strength
M_1	Smaller moment at end of unbraced length of beam
M_2	Larger moment at end of unbraced length of beam
P_{br}	Required brace strength
P_p	Concentrated load resulting in the attainment of M_p
R	Rotation capacity of cross-section
r_y	Radius of gyration about the out-of-plane axis
t_f	Flange thickness

t_w	Web thickness
ß	Bracing stiffness
$ß_{br}$	Required bracing stiffness
ε_y	Yield strain
ε_b	Intermediate strain vlaue
ε_{st}	Strain hardening strain
ε_u	Ultimate strain
$?_f$	Flange slenderness ratio
$?_{flange}$	Flange slenderness ratio
$?_p$	Limiting slenderness parameter for plastic analysis
$?_w$	Web slenderness ratio
$?_{web}$	Web slenderness ratio
θ_p	Cross-sectional rotation resulting in the attainment of the theoretical plastic moment
θ_u	Cross-sectional rotation attained when the moment-rotation curve drops below M_p on the unloading branch

Acronyms

AASHTO	American Association of State Highway and Transportation Officials
AISC	American Institute of Steel Construction
ASCE	American Society of Civil Engineers
ASTM	American Society for Testing and Materials
FHWA	Federal Highway Administration
HPS	High Performance Steel
LRFD	Load and Resistance Factor Design

1.0 INTRODUCTION

The manner in which a structure is designed weighs heavily upon the material from which it is constructed. In today's society buildings are growing taller, bridges are spanning longer distances, and, as a result, the materials of construction are being relied upon more heavily to keep up with these constantly increasing demands. One construction material that is keeping pace with these demands is steel. New high performance steel grades have been introduced for use in civil structural applications. These new grades of steel hold out the promise of new and exciting advances in structural engineering while at the same time present formidable challenges that must be addressed.

Common practice in the design of steel members is to design the member such that plastic moment redistribution is not required to resist external actions. Even though this is currently the most common method of design, it is not the most practical method in terms of economical member proportioning as well as ease of analysis. When dealing with indeterminate structures, an alternate method based upon plastic design techniques enables smaller sections to be selected to resist the same load level. This alternate method fully exploits the mechanical behavioral characteristics of the steel by notionally allowing the entire cross section to yield and form a plastic hinge. This method is predicated upon the plastic hinge forming at a point along the member in such a way that inelastic rotation can be sustained so that the moment redistribution required for mechanism formation can take place.

In order for a plastic hinge to form and behave ductily, the cross sectional proportioning and bracing of the steel member are of great importance. The AISC LRFD Design Specification for Structural Steel Buildings (1999) and the AASHTO LRFD Bridge Design Specification (1998) prescribe web and flange limits of cross sectional plate slenderness known as "web compactness" and "flange compactness" requirements, respectively. If a member is "non-compact," it is considered likely that a cross sectional plate component in a member will buckle prior to developing sufficient structural ductility to allow for moment redistribution in the structural system. Similarly, these specifications also promulgate standards for the lateral bracing of flexural members. Without adequate lateral bracing (considering unbraced length, bracing strength and bracing stiffness), the member will globally buckle and unload before a plastic collapse mechanism can form. This must also be accounted for when designing the structure.

As a result of advancements in steel-making technology, the steel that is being used today can be significantly different than that of ten or twenty years ago; while A36 had formerly enjoyed a position of dominance in steel construction, it has been all but completely phased out by a newer, stronger, 50 ksi yield steel grade (A992). However, just as A36 is being phased out and replaced by A992, a similar transition is beginning to replace existing grades by what is referred to as high performance steel (HPS).

High performance steel is a designation given to several new steel compositions that have relatively high yield strength (generally greater than or equal to 70 ksi), exhibit good notch toughness, and have little or no preheat requirements for welding. Many of these HPS grades may exhibit mechanical properties significantly different from

traditional mild carbon steels. They may have yield stress levels very close to their ultimate stress levels resulting in virtually no strain hardening behavior. In addition, they may possess less overall material ductility as quantified by plastic strain. This is in contrast to the traditionally used mild carbon steels that have yield stresses between 36 and 50 ksi, a distinct yield plateau, and a significant strain hardening slope in both tension and compression.

Currently there is much interest in employing HPS as widely as possible. As a result, existing design specifications are being called upon to predict the response of the HPS component and systems with the same level of accuracy and safety that had been achieved with earlier constructional steel grades (i.e. A36, A992, etc.). Given that many specification provisions and capacity equations are semi-empirical in nature, it seems unlikely that design approaches and provisions tailored to experimental tests carried out on A36 members can be extended to the new HPS grades without some careful investigation.

Based on the research outlined in this study it is clear that the current specifications' provisions for compactness and bracing are inadequate when applied to doubly symmetric I-shaped A709 HPS483W steel girders. Verified nonlinear finite element modeling techniques are used to conduct parametric studies in which the flange and web slenderness ratios are varied as well as the unbraced length and bracing stiffness. The results are used to provide recommendations for new criteria that apply to plastic analysis and design of doubly symmetric I-shaped A709 HPS483W steel girders.

1.1 Background

This section of the report provides context from which to explain the basis for, and meaning of, the research findings and recommendations reported in subsequent chapters herein.

1.1.1 General Beam Behavior

The general behavior of a singly or doubly symmetric beam bent about the strong axis is shown in Figure 1. This behavior may be classified into three categories.

1. Plastic: The plastic range is characterized by the ability of the cross section to reach the plastic moment, M_p, and maintain this strength through a sufficient *rotation capacity* (to be explained later in this section) in order that moment redistribution may take place in indeterminate structures.

2. Inelastic: The inelastic range is characterized by the ability of some or all of the cross section to have yielded but only a small amount of inelastic deformation takes place before unloading below M_p occurs. This unloading is due to instabilities occurring in the form of local flange or web buckling or global lateral-torsional buckling.

3. Elastic: The elastic range is characterized by buckling taking place while the cross section is still fully elastic.

Regardless of the behavior category, failure of the beam will result from one or more of the following; local plate buckling of the compression flange, local plate

buckling of the web in flexural compression, or lateral-torsional buckling (Yura, Galambos, and Ravindra, 1978). The following graph (Figure 1) provides a visual representation of the three behavioral categories described above.
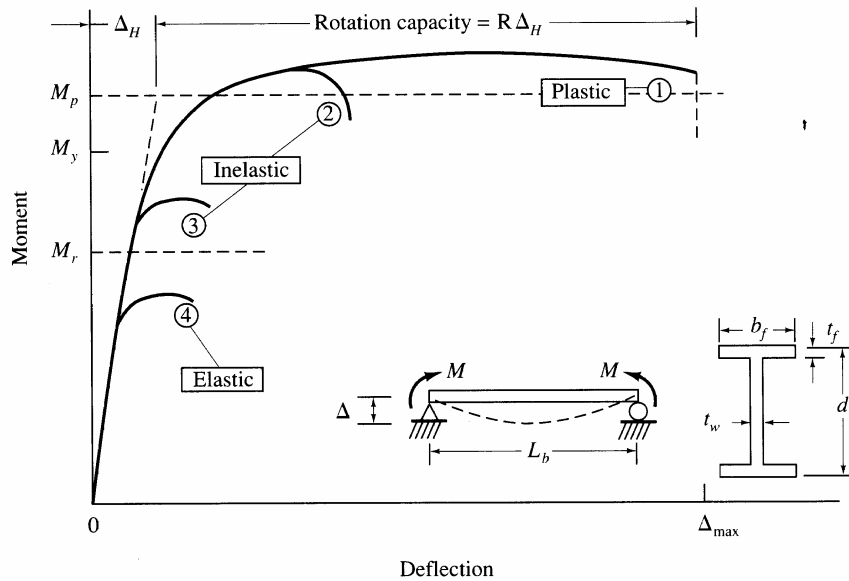
Figure 1 Beam Behavior (Yura, Galambos, Ravindra 1978)

The research included herein deals with these three failure modes and their occurrence within the plastic range of beam response. In order to apply the philosophy of plastic design and analysis for the purpose of exploiting moment redistribution in an indeterminate structure, the moment-rotation behavior of the steel beam must be completely understood.

1.1.2 Plastic Analysis and Design

Plastic analysis and design enables the full cross sectional capacity of a beam to be used by notionally allowing a *plastic hinge* to form. This hinging occurs when the plastic moment strength, M_p, is reached at a discrete point along the beam (i.e. the entire cross section has yielded). At such a location, the cross section can no longer resist increasing moment and hence large rotations occur, with constant resistance, M_p, being maintained. In the case of an indeterminate structure, such a scenario allows for moment re-distribution to occur. However, it is critical that in addition to the cross section reaching its plastic moment capacity, the beam must also be ductile enough to maintain M_p while continuing to deform (rotate) through a sufficient angle so that moment redistribution can take place. A common ductility measure is termed *rotation capacity* and is defined by ASCE (ASCE 1971) as $R = \{(\theta_u / \theta_p) - 1\}$. θ_u is the rotation when the moment capacity drops below M_p on the unloading branch of the M-θ plot and θ_p is the theoretical rotation at which the full plastic capacity is achieved based on elastic beam stiffness. This definition is described graphically in Figure 2. In this figure, θ_1 corresponds to θ_p, and θ_2 corresponds to θ_u in the ASCE definition.

$$R = \left(\frac{\Theta_2}{\Theta_1}\right) - 1$$
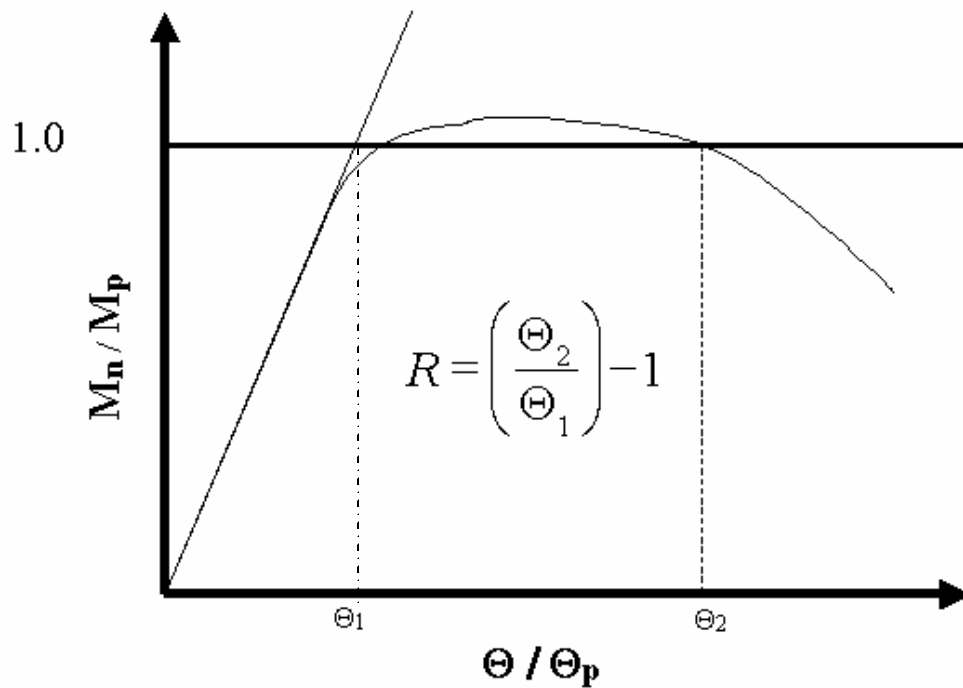
Figure 2 Definition of Rotation Capacity

For the purposes of employing plastic design and analysis, the AISC LRFD specification and the AASHTO LRFD specification require a minimum rotation capacity value of 3.

1.1.3 Local and Global Buckling Criteria

Once the concept of plastic design and analysis is understood, the next step is to design the beam so that it will be capable of forming a plastic hinge of sufficient rotation capacity without failing in any of the three instability modes previously mentioned. In order to facilitate this the AISC LRFD Specification for Structural Steel Buildings (1999) and the AASHSTO LRFD Bridge Design Specification (1998) have prescribed limits for

the width/thickness ratio of the compression flange, the depth/thickness ratio of the web, and the distance between points of lateral support.

Even with adequate lateral support a beam may fail to provide sufficient deformation because of local failures. Therefore, the application of plastic design and analysis mandates that the beam cross-section be *compact*. A compact cross section is considered as such when λ (the width/thickness ratio) for the flange and the web are both less than a limiting value, λ_p.

For the flange;

$$\lambda_f = \frac{b_f}{2t_f} \leq \lambda_p = 0.382\sqrt{\frac{E}{F_{yc}}} \tag{1-1}$$

Once 29000 ksi is substituted in for the elastic strain modulus, E, the above equation is reduced to the following;

$$\lambda_f = \frac{b_f}{2t_f} \leq \lambda_p = \frac{65}{\sqrt{F_{yc}}} \tag{1-2}$$

where F_{yc} is in ksi.

For the web (assuming a doubly symmetric cross section);

$$\lambda_w = \frac{h_w}{t_w} \leq \lambda_p = 3.76\sqrt{\frac{E}{F_{yc}}} \tag{1-3}$$

Again, once 29000 ksi is entered in for E, the above can be reduced to;

$$\lambda_w = \frac{h_w}{t_w} \leq \lambda_p = \frac{640}{\sqrt{F_{yc}}} \tag{1-4}$$

where F_{yc} is in ksi.

As long as the width/thickness ratios of the cross-sectional plate components are below these limits, then the cross section is considered compact, and thus theoretically able to undergo sufficient deformations required for collapse mechanism formation. Figure 3 shows graphically the relationship between these ratios and the expected moment capacity of a beam.
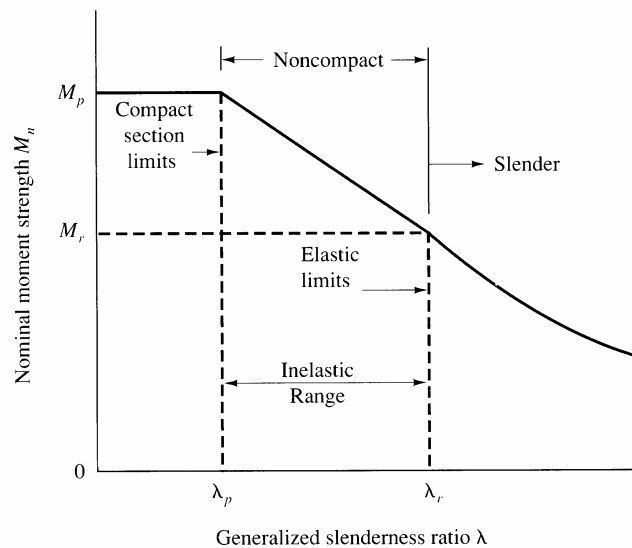
Figure 3 Nominal Strength M_n vs Generalized Slenderness Ratio λ for Limit States of Flange and Web Local Buckling (Salmon and Johnson 1996)

Once the beam's cross section has been selected such that it satisfies the compactness limits, it is capable of attaining the plastic moment as well as achieving sufficient rotation capacity for moment redistribution. This capability, however, depends heavily on the lateral bracing provided so as to prevent lateral-torsional buckling. Therefore, AISC and AASHTO permit the application of plastic design and analysis to a

compact section provided that the laterally unbraced length (L_b) does not exceed the prescribed maximum (L_{pd}).

$$L_b \le L_{pd} = \left[0.124 - 0.0759 \left(\frac{M_1}{M_2} \right) \right] \left(\frac{E}{F_y} \right) r_y \qquad (1\text{-}5)$$

Upon substituting in E = 29000 ksi this equation becomes;

$$L_b \le L_{pd} = \left[3600 - 2200 \left(\frac{M_1}{M_2} \right) \right] \left(\frac{r_y}{F_y} \right) \qquad (1\text{-}6)$$

When designing by plastic analysis, M_2 is equal to M_p since M_2 is defined as the larger moment at the end of the beam's unbraced length. M_1 is defined as the smaller moment at the end of the beam's unbraced length. Additionally, the ratio (M_1/M_2) is taken positive when the moments cause reverse curvature and negative for moments causing single curvature.

According to the specifications, as long as the beam cross section is compact and laterally braced in accordance with this limitation, it can be depended upon to develop a plastic hinge and redistribute its moments appropriately for applications involving plastic design and analysis. Figure 4 shows the effect of laterally unbraced length on the beam's expected moment capacity.
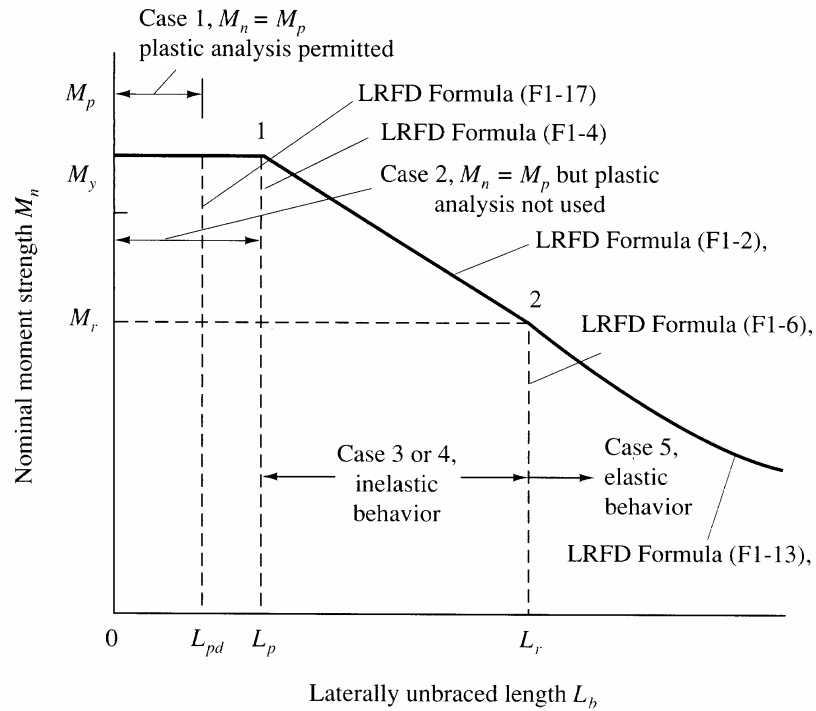
Figure 4 Nominal Strength M_n of "Compact" Sections as Affected by Lateral-Torsional Buckling (Salmon and Johnson 1996)

Once the appropriate bracing location is established, strength and stiffness requirements for the bracing member must be specified. In the case of nodal or discrete bracing, AISC LRFD (1999) requires the bracing strength (P_{br}) to be;

$$P_{br} = \frac{0.02 M_u C_d}{h_o} \tag{1-7}$$

For this equation, M_u is the required flexural strength. Therefore, when applying plastic design and analysis M_u will equal M_p. C_d is 1.0 for single curvature or 2.0 for double curvature. The distance between flange centroids is equal to h_o. In addition to the

bracing force, a minimum bracing stiffness (β_{br}) must be satisfied. This required bracing stiffness is as follows;

$$\boldsymbol{b}_{br} = \frac{10 M_u C_d}{L_b h_o \boldsymbol{f}} \tag{1-8}$$

All variables are the same for this equation as for the required bracing force with the addition of L_b, the unbraced length, and $\phi = 0.75$.

It is common practice in the design process to consider global buckling effects (due to lateral-torsional instabilities) as being separate and independent from those of local buckling (due to flange and web plate instabilities); this is a simplification of reality. In its guide and commentary on plastic design in steel, the American Society of Civil Engineers (ASCE) (ASCE 1971) states: "Even though local and lateral torsional buckling in the inelastic range are manifestations of the same phenomena, namely, the development of large cross sectional distortions at large strains, they have been treated as independent problems in the literature dealing with these subjects. This is mainly due to the complexity of the problem." Despite the fact that local and lateral-torsional buckling phenomena interact with one another, a great deal of success has been achieved in keeping them separate for purposes of design, and experience supports this approach.

1.1.4 High Performance Steel

While such an approach, based on de-coupling local and global buckling modes, has worked for common constructional steel grades, a question has come to pass with the addition of high performance steel (HPS) into the design field. Do all these limitations, assumptions, and behavior theories apply to steels with different material compositions and mechanical responses?

High performance steel is a designation given to several new steel compositions that have relatively high yield strength (generally greater than or equal to 70 ksi), exhibit good notch toughness, and have little or no preheat requirements for welding. Many of these HPS grades may exhibit mechanical properties significantly different from traditional mild carbon steels. They may have yield stress levels very close to their ultimate stress levels resulting in virtually no strain hardening behavior. In addition, they may possess less overall material ductility as quantified by plastic strain. This is in contrast to the traditionally used mild carbon steels that have yield stresses between 36 and 50 ksi, a distinct yield plateau, and a significant strain hardening slope in both tension and compression.

Despite such significant differences in material characteristics and behavior, the current design specifications, perhaps, over-simplify the difference in material characteristics between grades by simply scaling the critical values with factors related only to the value of the material's yield strength (i.e. $1/\sqrt{F_y}$). It seems unlikely that such a single scaling factor, based on yield stress alone, could be able to account for all of the

behavioral changes that accompany the differences that are characteristic of various HPS uniaxial material responses. In fact, new research is providing evidence that these differences may play a significant role in affecting member level behavior in terms of the evolution of local and global inelastic buckling phenomena and their impact on structural ductility (Earls 1999, 2000a, 2000b, Earls and Shah 2001). From the results of these studies it has been observed that geometric factors such as flange slenderness, web slenderness, beam unbraced length, bracing stiffness, etc., when taken alone, or in combinations, did not seem to accurately predict structural ductility as measured by plastic hinge rotation capacity. These observations raise concern about the applicability of current flexural design provisions in American steel building and bridge specifications (AISC LRFD 1999, AASHTO LRFD 1998) for use in designs involving high performance steels. As a result, various HPS grades are being studied in an attempt to identify trends in flexural ductility and moment rotation capacity as impacted on by flange slenderness, web slenderness, unbraced beam length, and bracing stiffness.

1.2 Literature Review

The validity of adapting current flexural design provisions to HPS applications has motivated several investigations. The present section provides a brief literature review conducted to identify the recent findings related to this issue. In particular, research involving the finite element method applied to similar situations as those studied herein, are surveyed.

In the steel building and bridge design specifications (AISC LRFD 1999, AASHTO LRFD 1998) local buckling and lateral torsional buckling are considered as being separated and unrelated phenomena. The strategy of independent consideration of local buckling and lateral-torsional buckling in steel I-shaped beam and girder design has been supported by much laboratory testing carried out on specimens made mostly from common structural grades of steel. While there appears to be little doubt of the utility in applying such notional de-coupling to applications with current low to medium strength steel grades, there is evidence that the practice of separate consideration of cross-sectional slenderness and beam slenderness is not prudent for applications involving new high performance steels (Earls 1999, Earls 2000a,b). This evidence comes from the results of experimentally verified nonlinear finite element studies of compact I-shaped beams of building type proportions made from HSLA80 and other high performance steel grades (HSLA80 is a type of high performance steel, having a yield strength of approximately 586MPa, used by the US Navy in double-hull ship construction).

From the numerical tests reported in these earlier studies it was observed that geometric factors such as flange slenderness, web slenderness, beam unbraced length, etc., when taken alone or in combinations, did not seem to accurately predict structural ductility as quantified by plastic hinge rotation capacity of high performance steel bridge girders. Such observations raise concern about the applicability of current flexural design provisions in the American steel building and bridge specifications (AISC LRFD 1999, AASHTO LRFD 1998) for use in designs involving high performance steels.

A parametric study of A709 Gr. HPS483W was conducted by Earls and Shah (2001) in which an unsymmetric cross section was subjected to three-point bending in an effort to investigate the influence of flange and web compactness on bridge girder rotation capacity.   Numerous finite element tests were carried out using the experimentally verified techniques involving the commercially available multipurpose finite element program ABAQUS (ABAQUS 1998). The parametric study involved changing the flange and web slenderness values as well as the lateral bracing distance, with the resulting rotation capacities being recorded and analyzed. Some preliminary recommendations were made based on the results of the tests that indicated the current AASHTO and AISC local and global buckling criteria tended to be unconservative when being applied to A709 Gr. HPS483W.

A great deal of research work has been reported in the literature related to the application of the finite element method to the modeling of entire bridges or small sub-assemblies of bridges. A number of researchers (White et al. 1997, Moen et al. 1999, Huang 1994, Earls 1999, 2000 a, b) have successfully modeled bare steel girders by

discretizing the entire bare steel members into a dense mesh of high order nonlinear shell elements. A survey of past literature has yielded examples of such bare steel flexural studies considering a moment gradient loading.

White and his co-researchers (White et al. 1998, White et al. 1997, White 1987) performed finite element studies using nonlinear, shear deformable, quadratic shell elements. This research focused on bridge girder size I-sections made from grade 50 steel (F_y=345 MPa) subjected to a moment gradient loading. White's research was aimed at the development of simplified moment-rotation relationships for inelastic design of continuous span beam and girder bridges (White et al. 1997). White exploited the symmetry of the loading and structural geometry about the negative moment region at the pier and hence modeled only one half of the subject bridge girders. He verified his modeling techniques with experimental tests found in the literature. White's models incorporate a shell finite element that is similar to the formulation used by ABAQUS in its S9R5.

Moen et al. (1999) considered the finite element modeling of I-shaped beams made from aluminium so as to develop a validated model as a basis for future parametric studies aimed at obtaining more accurate cross-sectional classifications for such members. Moen et al. verified their models against experimental tests and they also exploited the same mid-span symmetry that White used.

Huang (Huang 1994) also used nonlinear shell finite elements to model bridge beams under moment gradient (made from steel with up to a 430 MPa yield stress). Huang did not exploit symmetry about the mid-span stiffener when

modeling the entire negative moment region over the pier. Huang's models were composed of a graded mesh of ABAQUS S9R5 shell elements. The strategy of using a graded mesh is frequently employed when computational resources are limited. Mesh gradation is most appropriate in situations where it is certain that important structural response will occur in regions of the mesh well away from the coarser regions of the graded mesh where solution accuracy may be less reliable.

Additional research efforts in modeling high performance steel beams under moment gradient loading using nonlinear finite element techniques have been reported by several researchers (Axhag 1998, Azizinamini 1998, Earls 1999, 2000a, b, Earls and Shah 2001, Green et al. 1994, Ricles 1998).

1.3 Scope

In light of the recent research mentioned in the previous section, the validity of current provisions in the AISC LRFD Structural Steel Building Design Specification (1999) and AASHTO LRFD Bridge Design Specification (1998) for maintaining compactness, an appropriate lateral bracing placement, and a sufficient lateral bracing stiffness are called into question as they apply to the plastic analysis and design of continuous span I-shaped girders made from high performance steel. The difference in chemical composition of the new HPS steels (as compared with conventional mild carbon steel grades) translates into differences in certain mechanical properties such as strain hardening modulus, yield ratio, and the presence of a yield plateau. All of these

18

parameters have a profound impact on the inelastic response of HPS girders (Earls 1999, White et al. 1994, Huang 1994) and so too on subsequent compactness and bracing requirements as applied to the negative moment region of continuous span highway bridges (Earls 1999, Earls and Shah 2001).

As a result, a research program has been conducted at the University of Pittsburgh in cooperation with the New York Thruway Authority and the Federal Highway Administration that is focused on assessing the validity of employing the current compactness and bracing criteria as they relate to the plastic analysis and design of highway bridge girders utilizing A709 HPS483W steel. Recommendations regarding new criteria for compactness and lateral bracing, as they relate to the application of plastic analysis and design for the proportioning of continuous span HPS highway bridge girders, will be made in subsequent sections of this report.

The current work uses finite element modeling to conduct parametric studies for the purpose of investigating the influences of flange and web compactness, unbraced length and bracing stiffness on bridge girder rotation capacity. The finite element models are constructed using the commercial multipurpose finite element program, ABAQUS. These techniques are experimentally validated through two verification studies, both carried out at the University of Pittsburgh (Earls and Shah 2001, Greco and Earls, 2002). In these verification studies, ABAQUS models are tested and the results are compared to experimental data from the laboratory testing of the corresponding full-size bridge girders. The experimental tests used for comparison were carried out at the University of Pittsburgh (Morcos 1988) and at Lehigh University (Green et al. 2002). The models

utilize dense meshes of shell elements that are formulated for use in the large strain regime of structural response. Both geometric and material nonlinearities are modeled in the studies. Similarly, both local and global instabilities are captured with these modeling techniques.

A description of the nonlinear finite element modeling techniques used for the parametric study reported herein is contained within Chapter 2. These methods are shown to agree very well with the experimental tests carried out by Morcos (Morcos 1998) and Green (Green et al. 2002). The corresponding verification studies are outlined and discussed in Chapter 2. Chapter 3 provides a detailed explanation of the modeling procedure applied for the parametric study and Chapter 4 discusses the results obtained. Conclusions from this study and recommendations for modifying the current provisions are contained in Chapter 5.

2.0 FINITE ELEMENT METHOD

The Finite Element Method (FEM) may be viewed as a general structural analysis procedure that permits the calculation of stresses and deflections in two- and three-dimensions. The basic concept behind the Finite Element Method is that the structure being considered may be conceptualized and analyzed as an assemblage of individual structural components or elements. The name, finite element analysis, arises because there exists only a finite number of elements in any given model to represent an actual continuum with an infinite number of degrees of freedom.

2.1 A General Description of the Finite Element Method

Although the paper was written over 35 years ago, Clough's "The Finite Element Method in Structural Mechanics" (Clough 1965) provides a very simple, clear, and accurate explanation of the basics of the FEM. Therefore, it will be used in this report as a reference for explaining the basics behind the FEM. The concept of the FEM originated when an effort was made to improve on the Hrennikoff-McHenry "lattice analogy" for representing plane stress systems. The method actually began to develop when efforts were made to formulate a numerical analysis procedure for evaluating the two-dimensional state of stress in the surface elements of airplane wings. Its generalized background is based on the matrix transformation theory of structures, however there exists no theoretical necessity of using matrix methods in FEM analysis.

21

There are three basic phases that make up the finite element analysis procedure: First is *structural idealization* in which the original system is subdivided into its assemblage of discrete elements. This phase is conducted by the engineer and is a critical aspect in conducting an accurate analysis. This is because in order for the idealization to provide a reasonable and accurate representation of the actual continuum, each element must be established so that it deforms similarly to the deformations that occur in the corresponding region of the continuum. Otherwise, as load is applied, the elements would distort independently of one another, except at the nodes, and gaps or overlappings would develop along their edges. The idealization would therefore be much more flexible than the continuum. In addition, sharp stress concentrations would develop at each nodal point and the result would be an idealization that poorly resembled the actual structure. Thus, considering the deformation pattern of an element, and ensuring compatibility to adjacent elements' patterns, is the most important criterion in conducting this first phase.

The second phase is the *evaluation of the element properties.* This is the "critical phase" of the analysis procedure as it involves the setting up of the force-deflection relationship by use of a flexibility or stiffness matrix. The essential elastic characteristics of an element are represented by this force-displacement relationship which is a means of relating the forces applied at the nodes to the resulting nodal deflections. The standard procedure for developing the stiffness matrix, used to create this relationship, of one-, two-, or three- dimensional elements is as follows:

1. Express internal displacements, v, in terms of displacement functions, M:

$$\{v(x,y)\} = [M(x,y)]\{\alpha\} \qquad (2\text{-}1)$$

where $\{\alpha\}$ represents the amplitudes of the displacement functions.

2. Evaluate nodal displacement components in terms of the generalized coordinates:

$$\{v\} = [A]\{\alpha\} \qquad (2\text{-}2)$$

where [A] is obtained by substituting the nodal point coordinates into [M].

3. Express the generalized coordinates in terms of nodal displacements, i.e. invert the above equation.

$$\{\alpha\} = [A]^{-1}\{v\} \qquad (2\text{-}3)$$

4. Evaluate the element strains, obtaining the matrix [B] by appropriate differentiation of the displacement functions in [M].

5. Evaluate the element stresses, obtaining the stress-strain matrix, [D], which represents the specific elastic characteristics of the finite element material.

6. Compute the generalized coordinate stiffness,[k], of the element.

$$[k] = ?_{vol} [B]^{T}[D][B] \text{ dvol} \qquad (2\text{-}4)$$

7. Transform coordinates from the generalized to the desired nodal point stiffnesses.

$$[k] = [A]^{-1}[k] [A]^{T} \qquad (2\text{-}5)$$

The third phase of the finite element analysis procedure is the *structural analysis of the element assemblage*. As in any analysis, the main problem is to simultaneously satisfy equilibrium, compatibility, and force-deflection relationships. The basic

23

operations for approaching this problem include the use of the Displacement Method which is easiest for dealing with highly complex structures. They are:

1. Evaluate the stiffness properties of the individual structural elements, and express them in a convenient local coordinate system.

2. Transformation from the local coordinate system to the global structure coordinate system.

3. Superposition of the individual element stiffnesses contributing to each nodal point in order to obtain the total assemblage nodal stiffness matrix [K].

4. Formulation and solution of the equilibrium equations which express the relationship between applied nodal forces {F} and the resulting nodal displacements {d},

$$\{F\} = [K]\{d\} \qquad\qquad (2\text{-}6)$$

5. Evaluation of the element deformations from the nodal displacements and determination of the element forces from the element deformations.

The matrix techniques used in the finite element analysis are essentially linear procedures that the validity for depends on superposition. However, it is also possible to analyze non-linear systems. Generally, non-linearities may apply to finite element analysis in either of two ways:

1. The element properties (element stiffness) may vary with the deformation of the elements.

2. The geometry of the assemblage may change sufficiently under the load influencing the equilibrium relationships of the structure.

Non-linearities may also occur within the individual element in either of two ways:

1. As a result of a non-linear stress-strain relationship

2. As a consequence of significant changes in geometry during deformation of the element

In order to address these non-linear problems with the FEM, either of two methods may be used. First is *incremental load analysis.* This method proceeds by applying the loading in very small increments and changing only the necessary characteristics after each increment. The second method is the *iterative procedure*. This method begins with a linear analysis and then proceeds by altering the necessary properties after each iteration until the appropriate relationships are satisfied.

The FEM is an extremely powerful tool that provides a "unified approach" by which any type of structural configuration may be analyzed. As long as complete compatibility of the deformations is provided, both internally and along the element boundaries, the strain energy of the finite element idealization represents a lower bound to that of the true solution. In addition, the idealization will converge towards the true solution as the mesh size is reduced.

2.2 ABAQUS

The research reported herein employs the commercially available multipurpose finite element program ABAQUS. ABAQUS is widely recognized as a very appropriate tool for use in structural analysis problems involving a high degree of geometric and material nonlinearity. It provides the user with an extensive library of elements that can model virtually any geometry. It has a wide variety of material models that can simulate the behavior of most typical engineering materials such as metals, rubber, polymers, composites, reinforced concrete, crushable and resilient foams, and geotechnical materials such as soils and rock. In addition to structural applications, the program can also be used to simulate scenarios in areas of heat transfer, mass diffusion, thermal management of electrical components, acoustics, soil mechanics, and piezoelectric analysis. For the purpose of conducting nonlinear analyses ABAQUS is capable of automatically choosing appropriate load increments and convergence tolerances as well as continually adjusting them during the analysis to ensure that an accurate solution is obtained efficiently (ABAQUS 1998). Use of the program is split up into three distinct stages: *preprocessing* in which all aspects of the model are defined through the creation of an input file, *simulation* in which the program actually solves the numerical problem defined in the model, and *postprocessing* through which the results can be evaluated and analyzed in a variety of ways to assist the user. Assuming all three stages are conducted appropriately, ABAQUS is capable of providing extremely reliable results for a wide variety of situations.

2.3 Morcos Verification Study

In order to produce reliable data when performing parametric finite element tests it must be shown that the modeling strategies being employed are accurate and able to predict the behavior of the modeled components in a variety of scenarios. A reliable numerical model should be able to predict both global behavior (such as load vs. deflection) and local behavior (such as local strains and stresses) in a manner consistent with observed experimental responses of the subject structure. In general, numerical models produce results that are very much affected by the assumptions inherent in the formulation of the analytical technique. For instance, assumptions related to the type of stress-strain curve, lateral bracing stiffness, initial imperfection, etc., could potentially alter the numerical results in a finite element beam analysis. Such assumptions are extremely important when non-linear finite element analysis techniques are employed. Therefore, it is always a good practice to verify the results of numerical modeling techniques against some experimental results to ensure the reliability and accuracy of the numerical model.

With this in mind, a verification study of experimental data obtained from the laboratory testing of Morcos and Schilling (Morcos 1988) is referenced and used to validate this research. The previously mentioned verification study was conducted by Earls and Shah (2001) who used various modeling techniques to investigate the effects of different parameters on the flexural behavior of plate girders.

2.3.1 Overview of Experimental Specimen

Morcos (Morcos 1988) presented results from the experimental testing of three different full-scale steel plate bridge girder specimens that were tested in the Watkins-Haggart structures lab at the University of Pittsburgh. The proportions of the three girders varied in such a way that insight into the influence of web compactness on rotation capacity could be studied within the context of grade 345 steel. The specimens were simply supported and subjected to a concentrated load acting at mid-span in order to simulate the moment gradient loading condition present in the girder section adjacent to the pier of a two span continuous girder bridge. Morcos' specimen "S" was specifically chosen for the verification study due to the large inelastic deformations that were shown to be possible during the experimental testing. Specimen "S" was fabricated from plates of ASTM 572 grade 345 steel. Table 1 displays the material properties of this steel while Figure 5 shows the girder's geometric properties and Figure 6 shows the beam's profile.

Table 1 Mechanical properties of ASTM 572 grade 345 (Earls and Shah 2001)

	Actual plate thickness (mm)	Static yield stress (MPa)	Tensile strength (MPa)	% Elongation (2in.gauge length)
Flange	13	405.41	581.23	43
Web	5	387.48	492.30	39.7
Min. Requirements		345	448	21
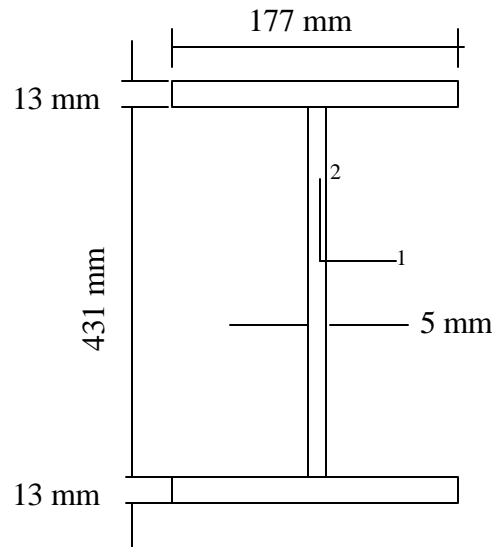
Length, L= 3.654 m

L/r_{min} = 86.64

Moment of Inertia, I(11)= 0.26023x10^{-3} m^4

Moment of Inertia, I(22)= 0.12019x10^{-6} m^4

Polar moment of Inertia, I(11)+ I(22) = 0.27225x10^{-3} m^4

Radius of gyration, r_{min} (r_{22}) = 0.196246 m

Radius of gyration, r_{max} (r_{11}) = 0.042175 m

Plastic Moment Capacity, M_p= 504.1 kN-m

P_p = 551.9 kN

Figure 5 Geometric Properties of Verification Specimen (Earls and Shah 2001)
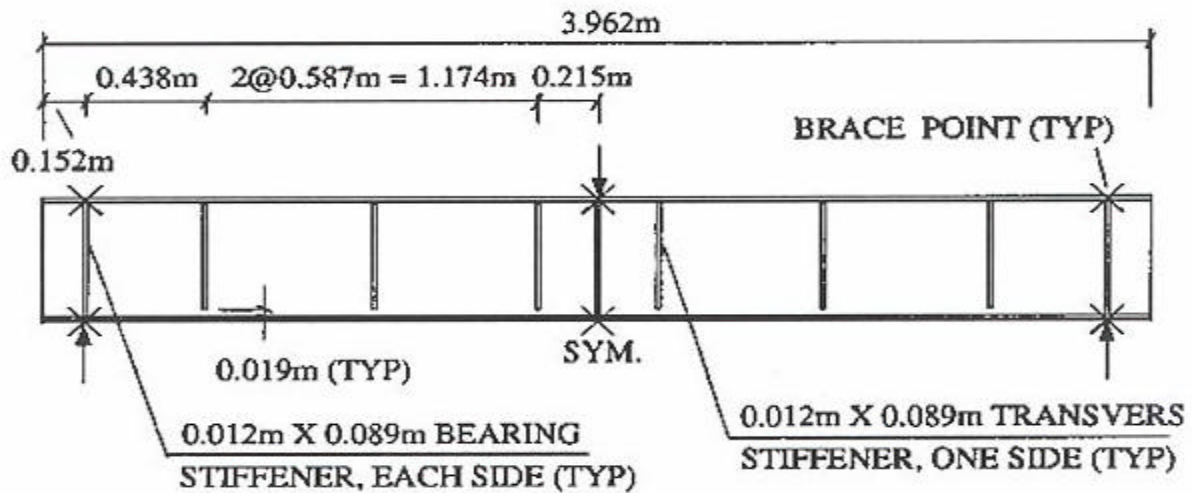
Figure 6 Profile of Verification Specimen (Earls and Shah 2001)

2.3.2 Finite Element Modeling Considerations

The finite element analysis program ABAQUS v. 5.8-14 was used for this verification study in which a number of finite element modeling techniques were applied and evaluated. This was done for the purpose of determining the most accurate modeling approach for predicting actual bridge girder response. The different modeling parameters considered were:

1) Different types of 3-d shell elements

2) Mesh density

3) Geometric imperfections

4) Lateral bracing stiffness

An input file was generated to duplicate the testing scenario as it occurred in the Watkins-Haggart structural engineering laboratory at the University of Pittsburgh.

In order to assess the influences of the above parameters on modeling accuracy, the parameters were varied and the corresponding model responses were compared against the experimental data. Two different element types were considered: the S4R (4 noded, reduced integration shell elements) and the S9R5 (9 noded, reduced integration shell elements with four membrane points). Through varying the remaining parameters, models were compared to the experimental data for both element types. The comparison work was accomplished by observing the moment-rotation and the load-deflection responses from the model and actual physical test. In addition, subsequent buckling modes in the plastic hinge region were studied carefully using the graphical post-processing facilities of ABAQUS.

2.3.3 Verification Results

Figures 7 and 8 demonstrate a relatively favorable agreement between the finite element model and the experimental results. The finite element models used to generate the results depicted in Figures 7 and 8 possess an element aspect ratio of one (dimensions: 12 mm x 12 mm) and a seed imperfection based on the first buckling mode and scaled to a maximum value of L/1000 ("L" being the overall span length of the simply supported beam). In each of the figures a given element type is evaluated as bracing stiffness varies. It is clear that both element types are sufficient for such analyses. Additionally, Figure 9 demonstrates the agreement

between the modal manifestations exhibited by the finite element models and those observed by Morcos to be present in the experimental test beam.

For more information regarding this verification study, refer to Earls and Shah (2001).
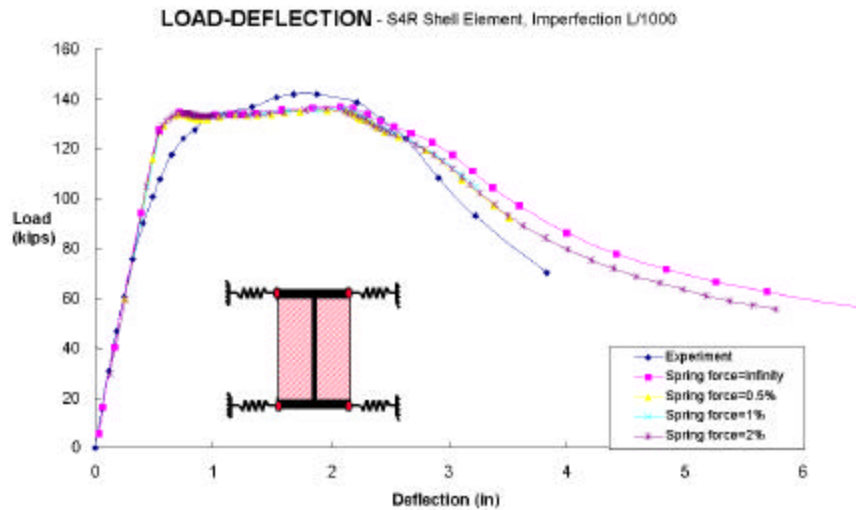
Figure 7 Verification Agreement Between ABAQUS Modeling and Experimental Testing (S4R) (Earls and Shah 2001)
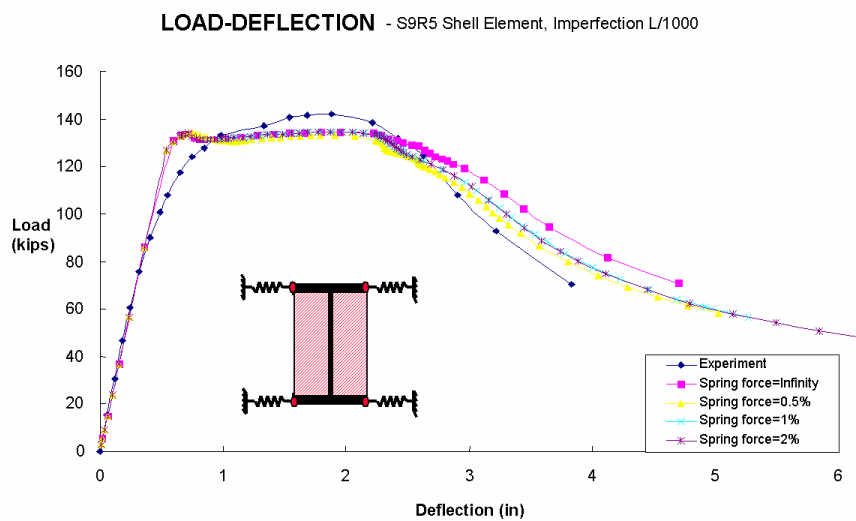
Figure 8 Verification Agreement Between ABAQUS Modeling and Experimental Testing (S9R5) (Earls and Shah 2001)
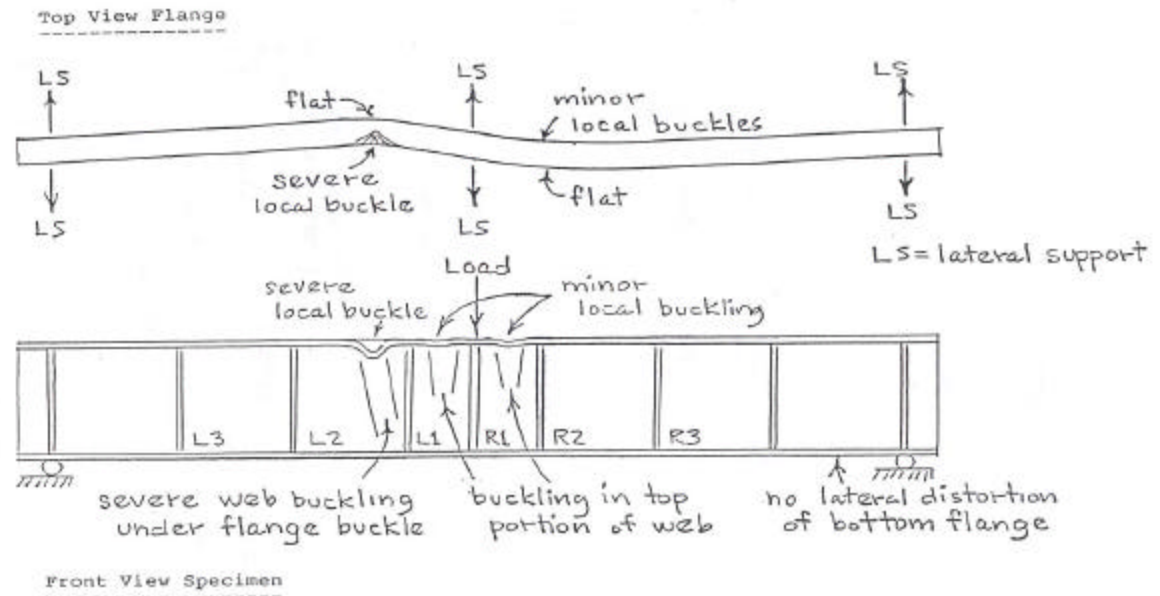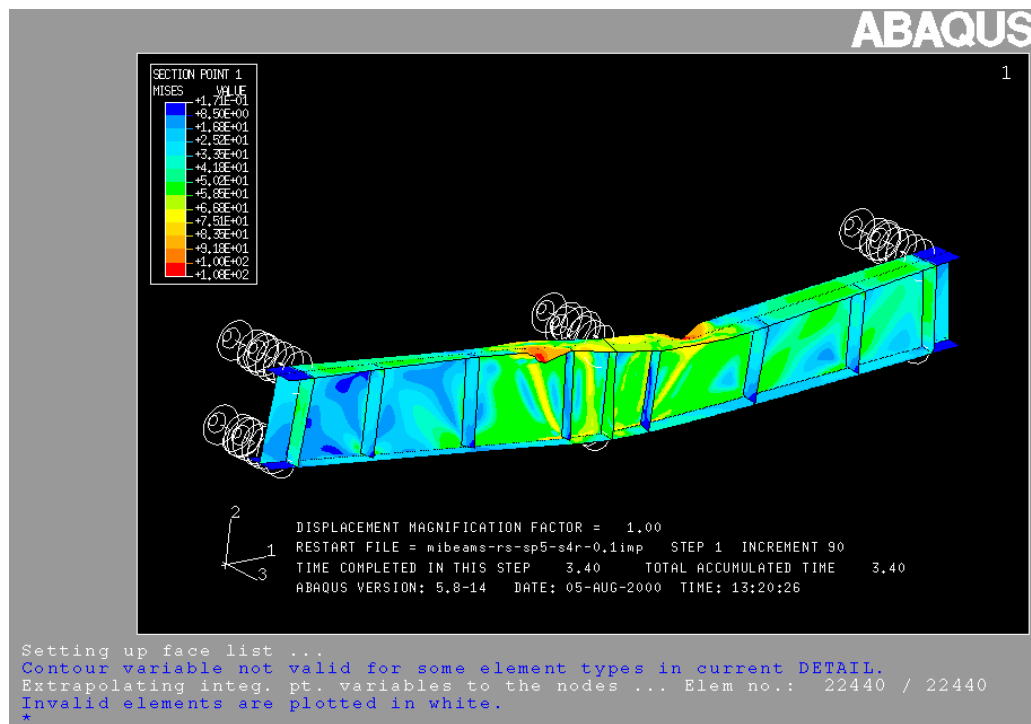
Figure 9 Comparison of Experimental and Finite Element Buckling Modes
(Earls and Shah 2001)

2.4 Green Verification Study

Greco and Earls (2002) conducted an additional verification study to compliment the work performed by Earls and Shah (2001), discussed in the previous section. The experimental testing used to compare and verify the ABAQUS modeling techniques was carried out by Green et al. (2002) in the Fritz Laboratory at Lehigh University.

2.4.1 Overview of Experimental Specimen

Green et al. (2002) presented results from the experimental testing of a series of beam specimens that were tested in Fritz Laboratory at Lehigh University. Green's Test Specimen 5 was chosen for this verification study. The specimen is a simply supported doubly symmetric A36 beam subjected to a concentrated load acting at mid-span. The beam has a flange slenderness of 5.86, a web slenderness of 51.61, and a b/d ratio of 0.306. The beam's profile and cross-section are shown in Figure 10. Flexible lateral bracing is located on the beam as indicated in this figure by an "x."
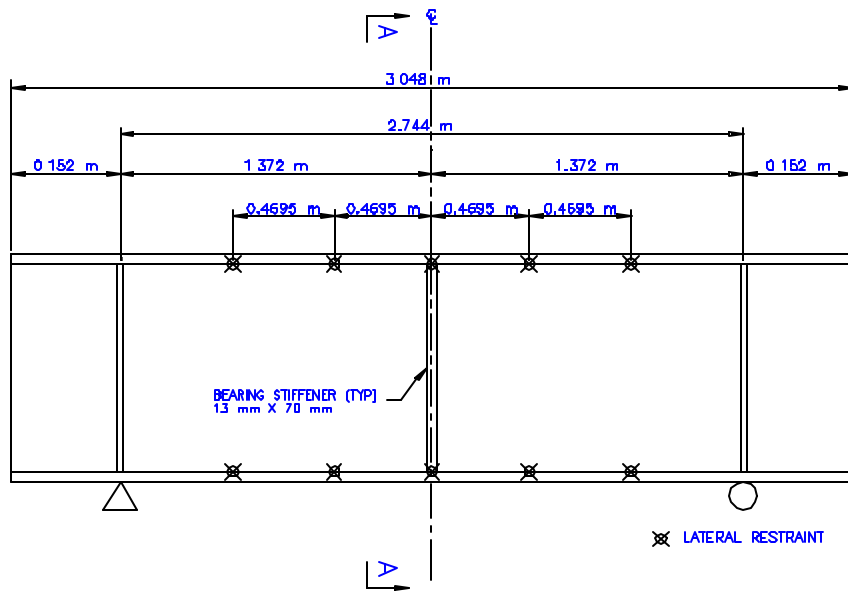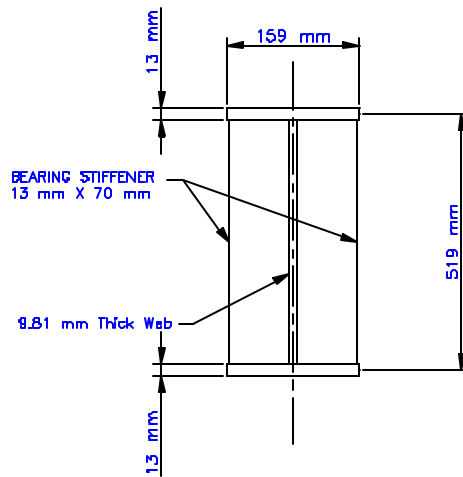
Figure 10 Profile of Green's Test Specimen 5 (Greco and Earls, 2002)

2.4.2 Finite Element Modeling Considerations

The verification analytical model developed for this study was built using the same ABAQUS S4R shell elements as those used for the parametric study reported herein. The finite element mesh used to formulate this model possessed an aspect ratio of approximately one and a seed imperfection was applied based on the first buckling mode scaled to a maximum value of L/1000 ("L" being the distance between the roller and pinned supports). The flexible bracing was modeled through the application of the ABAQUS SPRING1 element to the top and bottom flange at the four locations that correspond to the bracing locations in the experimental tests. The combined spring stiffness at each location on the beam was taken as six times the required AISC lateral bracing stiffness, discussed in Chapter 1 of this report.

2.4.3 Verification Results

Figures 11 and 12 demonstrate the close agreement that exists between the rotation capacities achieved for the analytical finite element model and that reported for the experimental results. Green et al. (2002) achieved a rotation capacity of 9.69 for Test Specimen 5, while Greco and Earls (2002) reported 9.6 for their analytical verification study. Further agreement between the two studies is shown through Figures 13 and 14 in the comparison of their failure modes. The figures compare pictures taken of Test

Specimen 5 (after it was tested) to screen captures of ABAQUS' predicted failure shape.

For more information regarding this verification study, refer to Greco and Earls (2002).
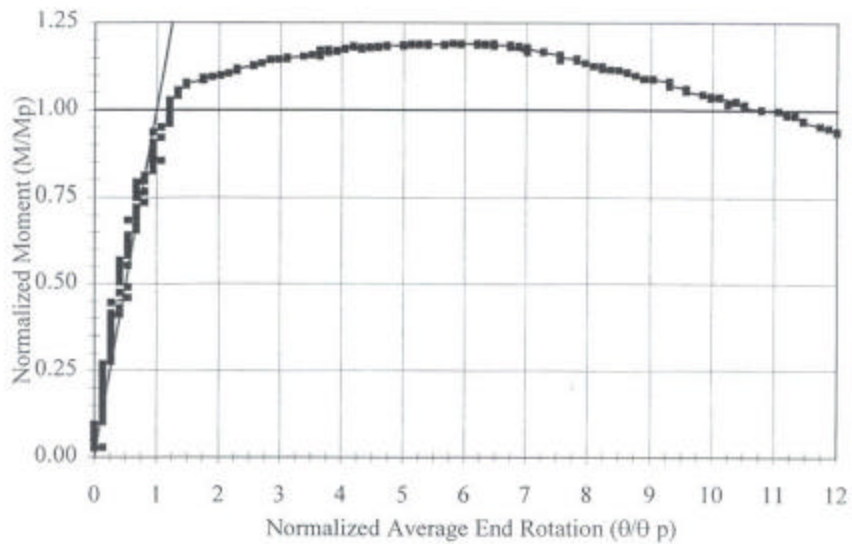
Figure 11 Test Specimen 5 Experimental Moment Gradient Response
(Green et al. 2002, Greco and Earls 2002))
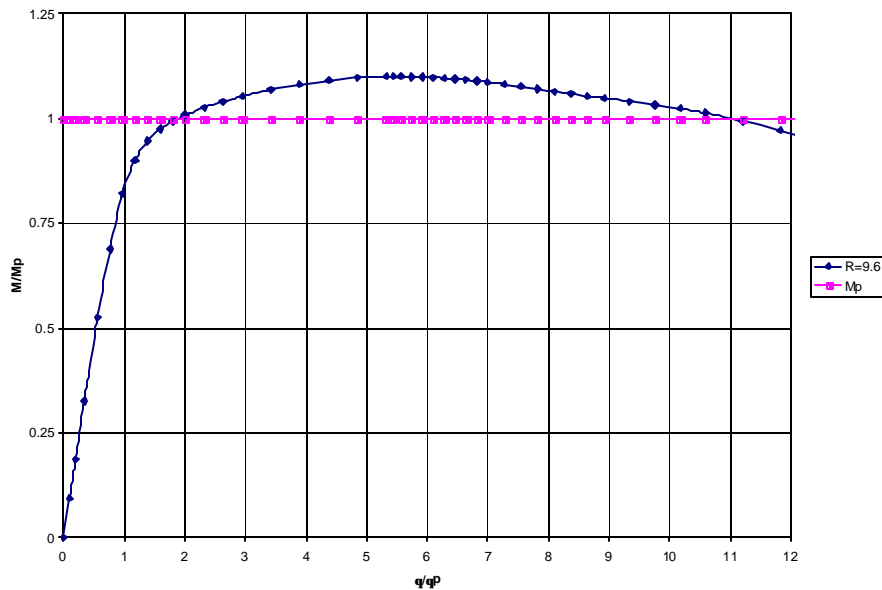
Figure 12 Test Specimen 5 Analytical Verification Model Moment Gradient Response
(Greco and Earls 2002)
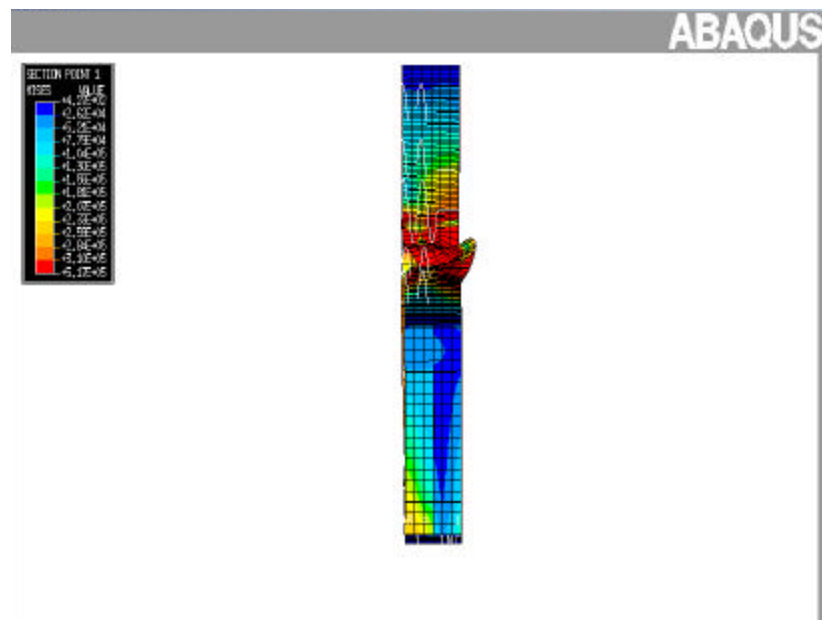
Figure 13 Longitudinal View Showing Lateral Compression Flange Movement in Midspan Region (Greco and Earls 2002)
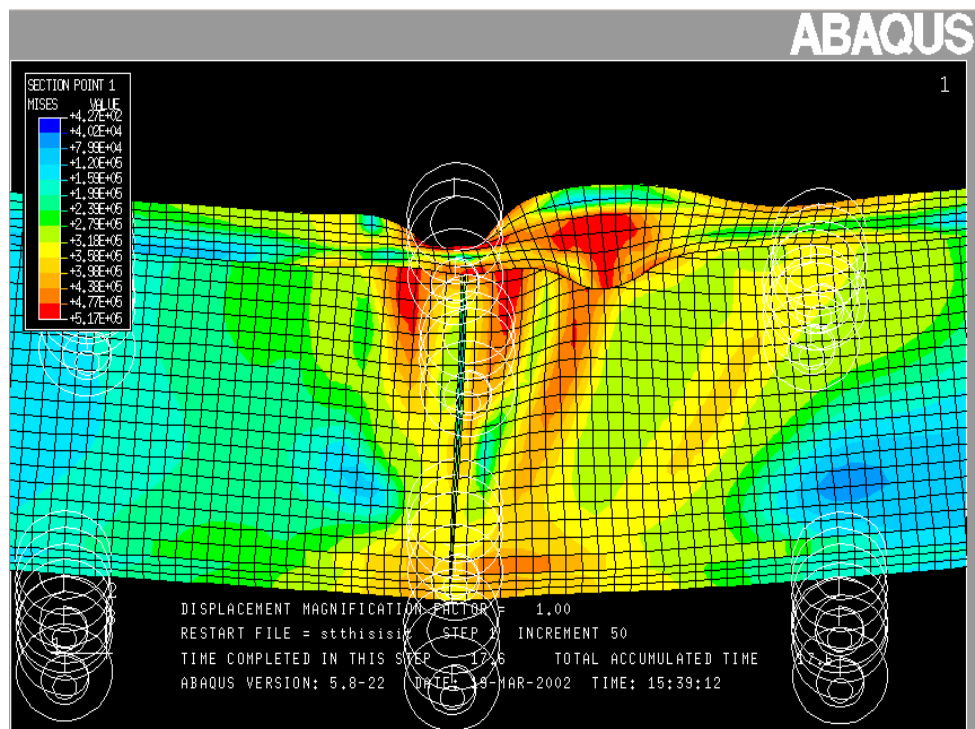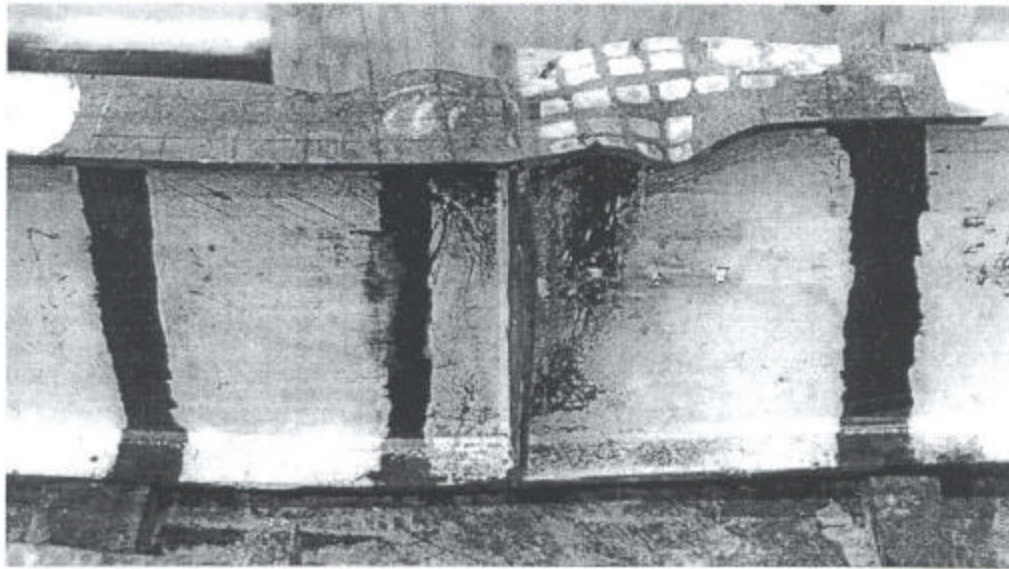
Figure 14 View of Midspan Region Showing Compression Flange Local Buckling (Greco and Earls 2002)

3.0 MODELING PROCEDURE

This Chapter details the procedure by which the current parametric study is conducted. The set up and geometry of the model are described, followed by the techniques used in the finite element idealization. Finally, the specifics and motivation behind the parametric study are addressed.

3.1 Geometric Case Considered

The behavior investigated in this research involves the formation of a plastic hinge in a high performance steel two-span continuous girder. In a continuous two-span girder, the first hinge will occur at the center support. If sufficient rotational ductility is available in the beam section located over the support, a collapse mechanism will form in each of the spans at a load higher than that needed to form the first hinge. Figure 15 depicts the loading scenario just described as well as the corresponding moment diagram. This figure defines what is termed the "hogging moment" region of the beam. Since the present study investigates plastic hinge rotation capacity, it is the hogging moment region that is of interest because it is the critical region associated with moment redistribution in this beam configuration.
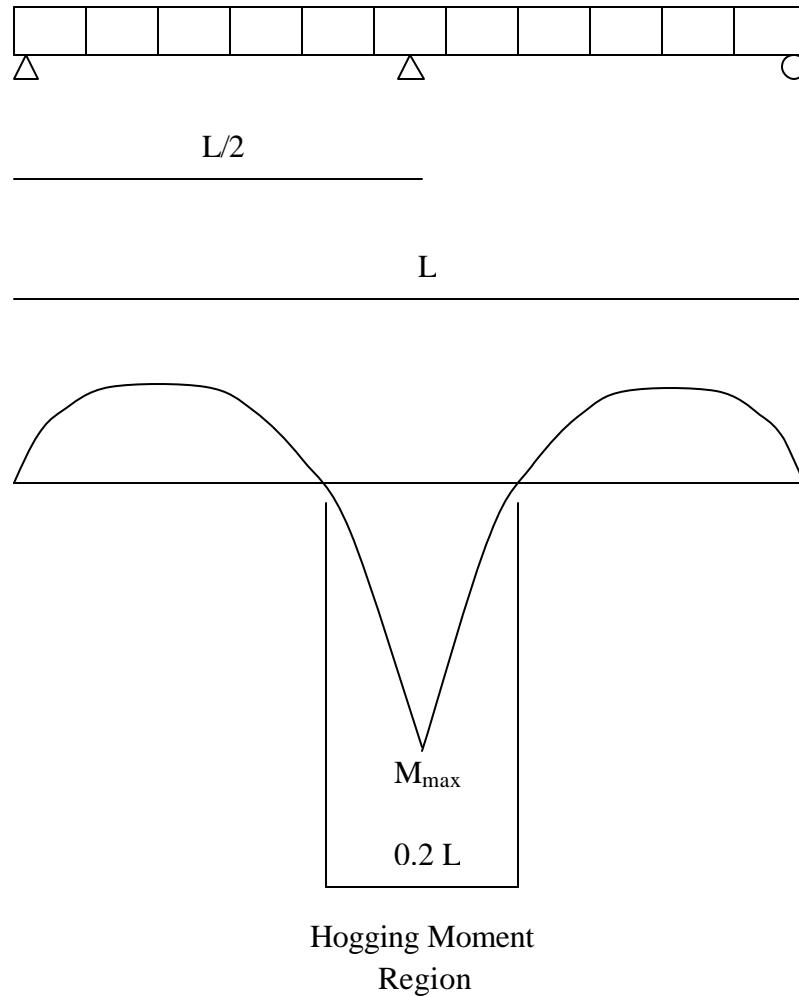
Figure 15 Hogging Moment Region of Continuous Span Girder

To model the hogging moment region, a single concentrated load (which represents the middle support reaction) is applied at the mid span of a simply supported beam. The supports of the simply supported model are placed at the inflection points of the actual continuous span (where the moment equals zero as it switches from negative to positive under a uniformly distributed loading) at a distance of 0.2 times the length of the double span (0.2 of L, as shown in Figure 15) (Barth et al. 2000). Compare the moment

diagram in Figure 16 for a simply supported beam to that of the hogging moment region from Figure 15. It can be seen how the moment diagram in Figure 16 can be used to model the area of interest in the continuous span girder since the curvature of the parabolic moment diagram region adjacent to the middle support is quite small and thus closely approximated by straight lines.

$$M_{max}$$
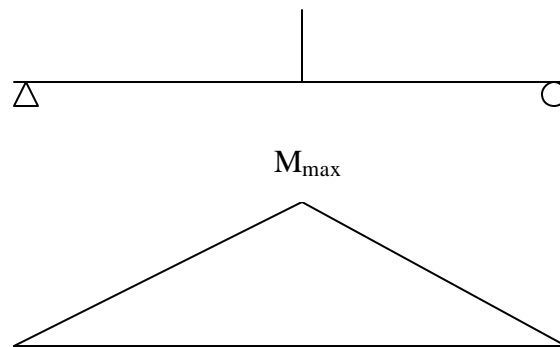
Figure 16 Simply Supported Model of Hogging Moment Region

3.2 Finite Element Idealization

The finite element model used for analysis carried out as part of this research is proportioned using a high performance steel highway bridge girder from the New York State Thruway Authority HPS bridge inventory as a guide. The HPS grade under consideration is A709 HPS483W (70 ksi). The actual yield strength used in the present work is 540.5 MPa (78.4 ksi) as per Aziznamini (1998). A simply supported span of 15.25 meters is used to model the hogging moment region of this bridge girder. An

additional unloaded girder length is present as a 7.625 meter overhang (L/2) at both

supports. These additional lengths of girder exist to help simulate the warping torsional

restraint that would be provided by adjacent beam segments in the actual continuous

bridge girder. The cross sectional geometry of the New York State Thruway Authority

bridge girder is compact according to current AASHTO LRFD (1998) and AISC LRFD

(1999) specifications. The girder's flange-width to beam-depth ratio (b/d) remains

approximately 0.52 (b_f = 0.406 m, h_w = 0.781 m) throughout all parametric studies

reported herein (shown in Figure 18).

A simulated knife-edge concentrated load is applied at mid span of the finite

element model to produce a moment gradient similar to that produced by the middle

support reaction in the hogging moment region of the continuous girder. This load is

applied incrementally so as to accurately trace the nonlinear moment-rotation response of

each case.

Full-depth stiffeners are located at the supports, load point, and all bracing

locations. At each of these locations lateral bracing is applied at all four flange tips of the

cross-section. Flexible bracing is provided at intermediate points located between the

load and the supports, the positions of which are uniformly varied as a parameter of the

present study. The stiffness of these intermediate braces is also uniformly varied as a

parameter of the present study. Ideal lateral bracing (i.e. ideal meaning infinite stiffness

and strength) is provided at all other bracing locations. These additional bracing

locations are present at both supports, the load point, and at the free ends of the

overhanging sections. Since the additional beam extensions are providing warping

restraint, and correspond to an additional unbraced beam length, their free ends are also braced.

Figure 17 shows the model geometry and the associated boundary conditions used for the parametric study while Figure 18 shows the cross-sectional geometry.
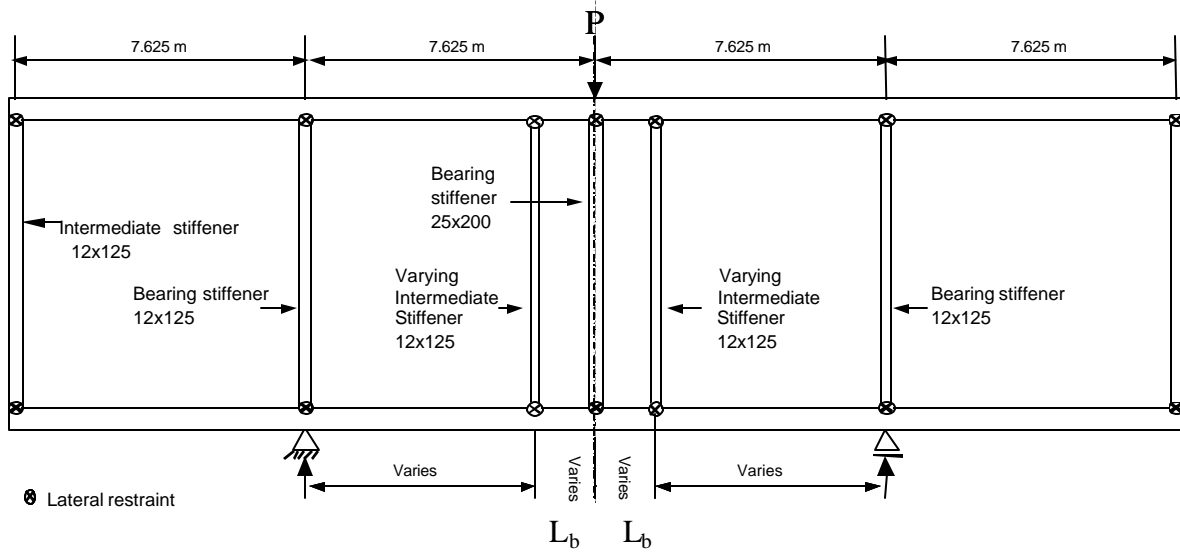
Figure 17 Model Geometry and Boundary Conditions Used in Parametric Study

t_f (varies)

t_w (varies)

t_f (varies)

0.781 m

0.406 m
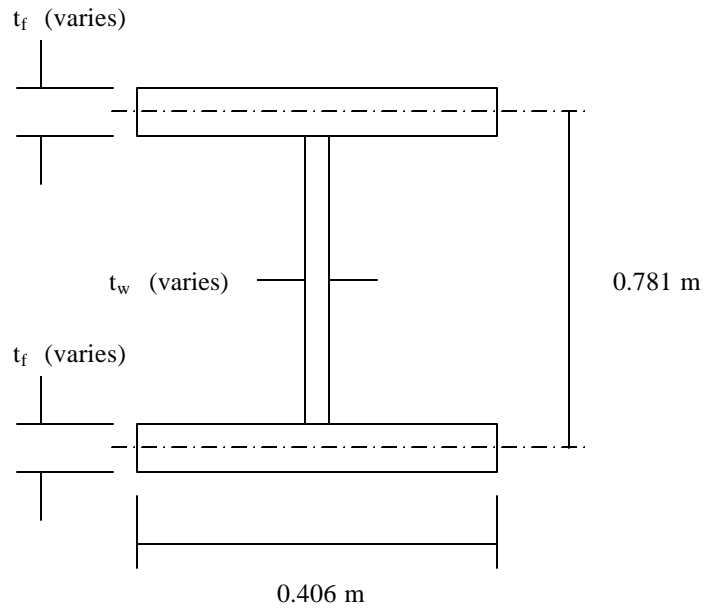
Figure 18 Cross Sectional Geometry

3.3 Finite Element Modeling Details

3.3.1 Finite Element Mesh

The commercially available multipurpose finite element program ABAQUS has been employed in all of the numerical studies reported herein. ABAQUS' success in modeling nonlinear structural problems has been well documented as previously noted in this report based on the research of one of the writers (Earls 2000 a, b, Earls and Shah 2002) and verification studies described in the previous chapter. These earlier studies employ modeling strategies that are very similar (and in some cases identical to) the

current work where inelastic local and global buckling phenomena are investigated through the use of nonlinear shell elements. Due to the complexity of the nonlinear response being studied, a very dense mesh of nonlinear shell elements is used in the modeling to capture inelastic local and global buckling behaviors.

The girder, which has overall dimensions of 30.5 meters in length, 0.406 meters in width, and 0.781 meters in depth, is created with approximately 50,000 elements, 29 mm by 29 mm in size. The S4R nonlinear, finite strain, shell element from the ABAQUS element library is selected for use in this parametric study based on the ability of this shell to accurately model local buckling deformations and the spread of plasticity effects (as proven by its superior performance in the verification study described in Chapter 2 of the current report). These elements are oriented along the planes of the middle surfaces corresponding to the constituent plate components of the members. When changing the component plate slenderness ratios in the current parametric study, only the thickness of these elements is altered.

The simple support conditions are provided by restraining all the nodes across the bottom flange (at the support locations) in all three global directions for the pin support and in the vertical and out of plane horizontal direction for the roller. Additional restraints in the out-of-plane direction are enforced at all stiffener locations. While rigid out-of-plane restraint is provided at the load point, supports, and free ends, flexible lateral bracing is applied to the remaining intermediate stiffeners (located between the load and the supports) through the use of ABAQUS' SPRING1 elements. These elements act as linear springs possessing a stiffness that is specified in the input file. The stiffness values

are varied uniformly as part of the parametric study. These out-of-plane bracing restraints are applied to the four flange tips of the braced cross-section. Figure 19 shows a schematic of how this bracing was idealized in the finite element model.
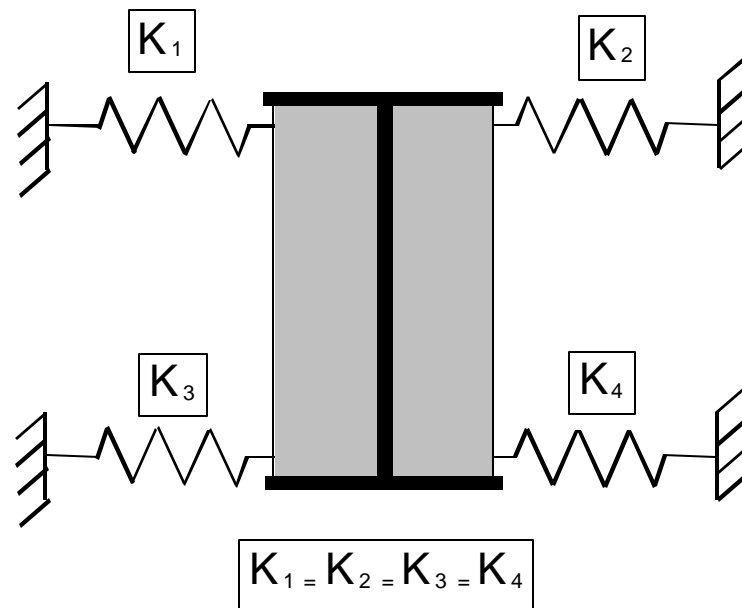
Figure 19 Schematic of Idealized Lateral Bracing Using ABAQUS SPRING1 Elements

3.3.2 Constitutive Law

In modeling the mechanical properties of A709 HPS483W steel, a uniaxial representation of the constitutive law is incorporated into the ABAQUS input deck in terms of true stress and logarithmic strain. ABAQUS then uses the von Mises yield criterion to extrapolate a yield surface in three-dimensional principal stress space from

this information.   The corresponding metal plasticity model is characterized as an associated flow plasticity model with isotropic hardening being used as the default hardening rule (Earls 2000a). Figure 20 graphically depicts the constitutive law used in this research for A709 HPS483W steel.
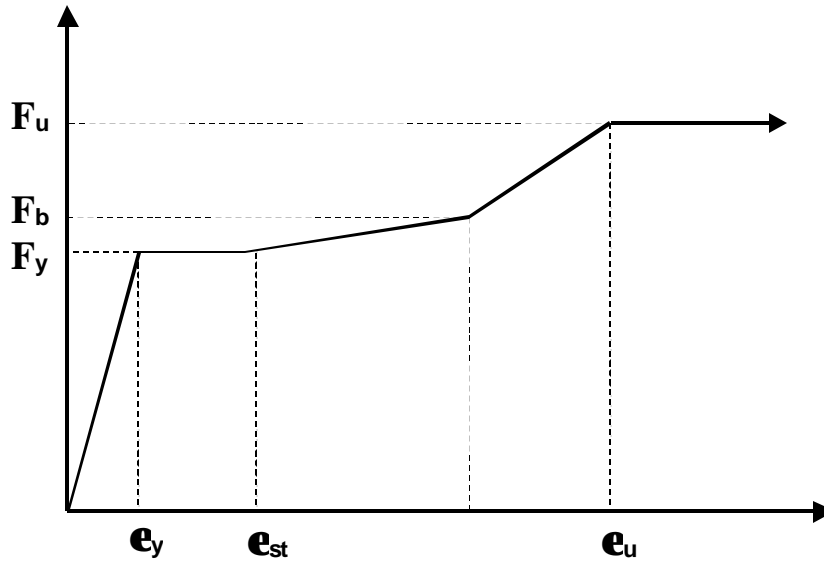
Material	F_y	F_u/F_y	F_{st}/F_y	e_{st1}/e_y	e_{st2}/e_y	e_u/e_y
HPS483W	539MPa	1.19	1.15	4.64	19.9	46.4

	s_{true}(MPa)	$e_{\ln}^{pl}$
Yielding	540.627	0.
Strain Hardening (on-set)	550.799	0.009667822
Strain Hardening	653.885	0.049084972
Intermediate Strain Hardening	704.579	0.091786387
Ultimate	720.592	0.114179156

Figure 20 A 709 HPS483W Constitutive Law

3.3.3 Seed Imperfection

In instances of modeling inelastic buckling with a finite element program, it is important that the modeling solution be carefully monitored so that any potential bifurcation in the equilibrium path is carefully evaluated in order to ensure that the equilibrium path being followed corresponds to the lowest energy state of the system. While there exist numerous strategies for accomplishing this (Teh and Clarke 1999), the method of seeding the finite element mesh with an initial displacement field is employed in these studies (ABAQUS 1998). In this strategy, an approximation to the first buckling mode of the girder is developed by subjecting the mesh to a linearized-eigenvalue buckling analysis. A seed imperfection is then superimposed on the finite element model via the lowest buckling mode's displacement field.

The primary role of applying such geometric imperfections is to provide a perturbation to the perfect model geometry. It is meant to initiate a response in the girder that is asymptotic to the ideal equilibrium path of the structure. As long as the imperfections are small enough so that they do not affect the girder's gross cross-sectional properties, this asymptotic response will be close to the girder's ideal response. Based on previous research (Yura and Helwig 2001), as well as the verification study described in Chapter 2 of this report, a maximum scaling factor of L/1000 is applied to the first buckling mode for the seed imperfections in all modeling reported herein. This means that the displacement field obtained from the buckling analysis is scaled so that the maximum displacement anywhere in the mesh is equal to one-one-thousandth of the

entire span length of the girder (L = 15.25 meters in the case of this research) (Earls and Shah 2001).

3.4 Preliminary Bracing Study

The purpose of the research reported herein is to investigate the validity of employing the current compactness and bracing criteria as they relate to the development of rotation capacity for the purpose of utilizing plastic analysis and design techniques with A709 HPS483W bridge girders. As a result, a parametric study in which the slenderness ratios for the web and flange, the unbraced length, and the lateral bracing stiffness are varied is carried out.

Due to the complexity of the parametric study, it is executed iteratively in two primary phases: (1) preliminary work; and (2) exhaustive parametric study. The first phase of this research is designed to develop a basis by which the second phase could be efficiently executed. In the preliminary phase, a typical girder cross sectional geometry is chosen to provide the basis of future parametric studies to be carried out. Based on the equations for flange and web compactness given in Chapter 1 (using Fy = 78.4 ksi = 540.5 MPa), λ_p for the flange equal to 7.34 and λ_p for the web equal to 72 are computed from the current specifications (AASHTO LRFD 1998, AISC LRFD 1999). With these limits in mind, a cross section with $\lambda_{flange} = 4.5$ (60% of its compactness limit) and $\lambda_{web} = 54$ (75% of its compactness limit) is initially considered. As mentioned previously, the

width and depth of the cross section do not change, only the thicknesses of the flange and web are altered when adjusting cross-section plate slendernesses.

Throughout the preliminary phase of the research the slenderness ratios remains constant at the λ_{flange} and λ_{web} just defined. The parameters that are varied in this phase are the unbraced length and the corresponding bracing stiffness. Based on recent research that has indicated good results when using unbraced lengths related to the depth of the girder (Earls 1999, Earls and Shah 2001), the following unbraced lengths are considered: d/2, d, 1.5d, and 2d. Because the depth of the cross section remains constant (0.781 m), these lengths become 0.3905 m, 0.781 m, 1.1715 m, and 1.562 m, respectively. Through the remainder of this report these lengths will be referred to in terms of their relation to d.

In addition, the lateral bracing stiffness is also varied to be between one times the value recommended by AISC (refer to Chapter 1) and 10 times this recommended value. As shown in Chapter 1, these bracing stiffness values are dependent upon the ultimate moment capacity (M_p) which changes with a change in cross sectional geometry, as well as upon the unbraced length, which changes as part of the parametric study. Therefore, the AISC recommended bracing stiffnesses are different for each study and had to be calculated accordingly on a case-by-case basis. Some of the most common applicable bracing stiffness values are tabulated in Appendix E. Ideal bracing (i.e. infinite stiffness) at all bracing locations is also considered.

Figures 21 through 26 present moment rotation results for some of the modeling conducted as part of the preliminary work. These plots are used to help identify any

trends that may exist between the changes in unbraced length and rotation capacity. That is, for every plot in Figures 21 through 26, unbraced length is the only parameter that varies, thus allowing for the evaluation of this parameter's influence on rotation capacity. The plots show a clear trend in the optimal unbraced length; in every case, using an unbraced length of "d," the depth of the girder, emerges as the superior bracing configuration.

Moment Gradient Chart: $b_f/2t_f = 4.5$, $h/t_w = 54$, 6.5 AISC β_{br}
Unbraced Length varies
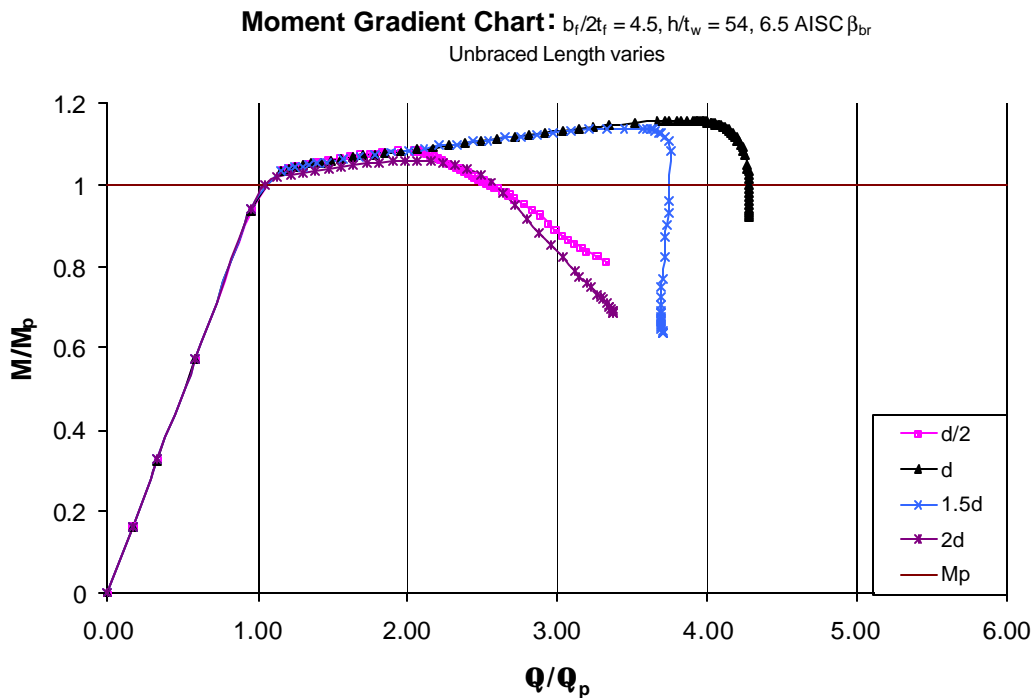
Figure 21 Moment Rotation Plot ($b_f/2t_f = 4.5$, $h/t_w = 54$, 6.5 AISC β_{br}, Unbraced Length Varies)

Moment Gradient Chart: $b_f/2t_f = 4.5$, $h/t_w = 54$, 7 AISC β_{br}
Unbraced Length varies
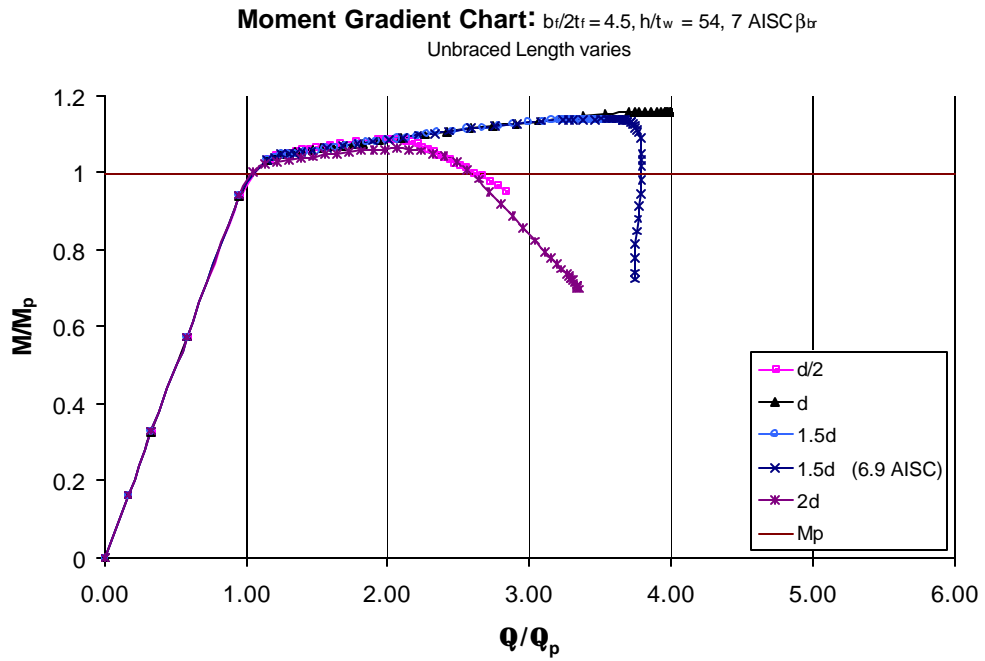
Figure 22 Moment Rotation Plot ($b_f/2t_f = 4.5$, $h/t_w = 54$, 7 AISC β_{br}, Unbraced Length Varies)

Moment Gradient Chart: $b_f/2t_f = 4.5$, $h/t_w = 54$, 7.3 AISC β_{br}
Unbraced Length varies
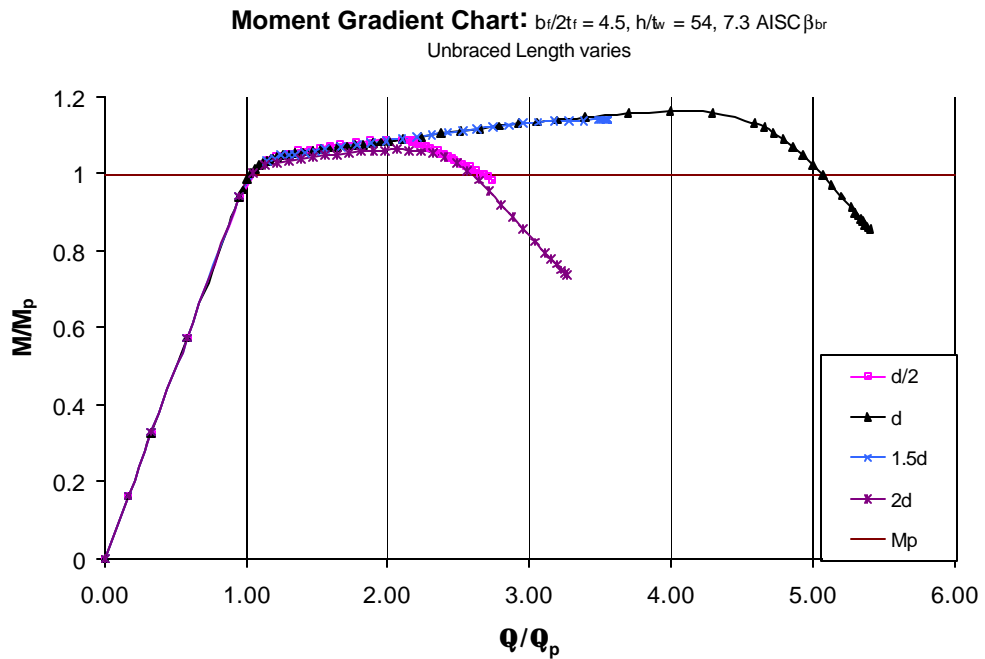
Figure 23 Moment Rotation Plot ($b_f/2t_f = 4.5$, $h/t_w = 54$, 7.3 AISC β_{br}, Unbraced Length Varies)
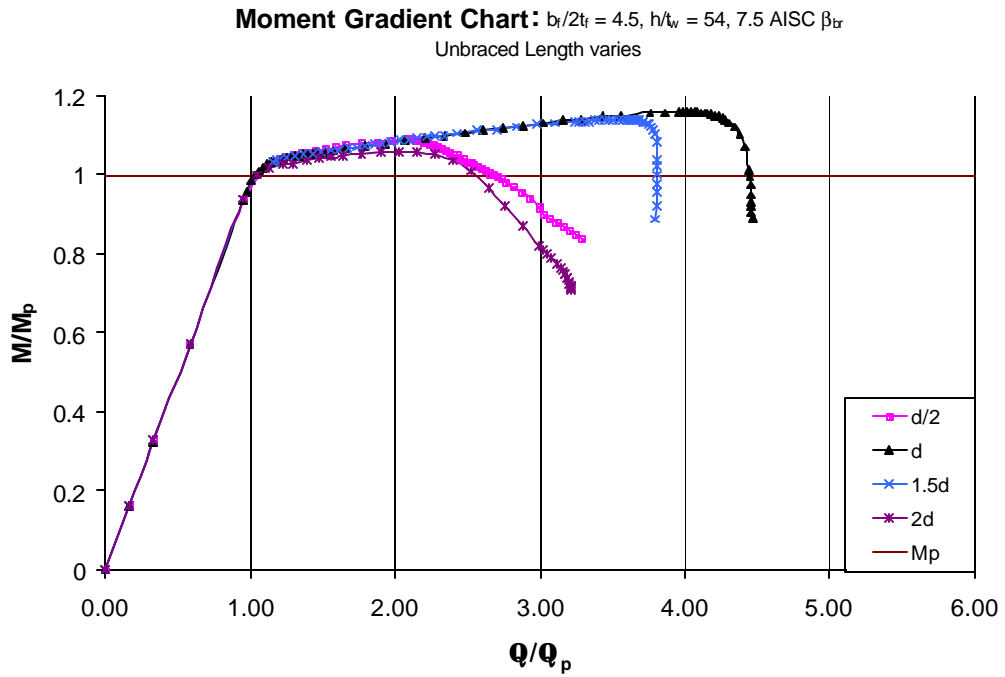
Figure 24 Moment Rotation Plot ($b_f/2t_f$ = 4.5, h/t_w = 54, 7.5 AISC β_{br}, Unbraced Length Varies)
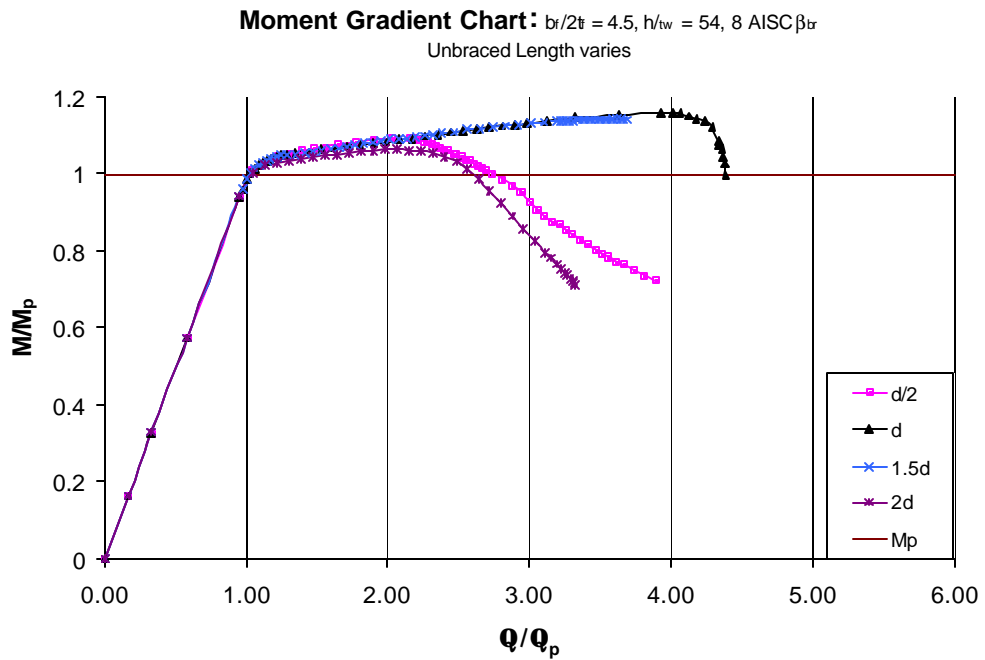
Figure 25 Moment Rotation Plot ($b_f/2t_f$ = 4.5, h/t_w = 54, 8 AISC β_{br}, Unbraced Length Varies)
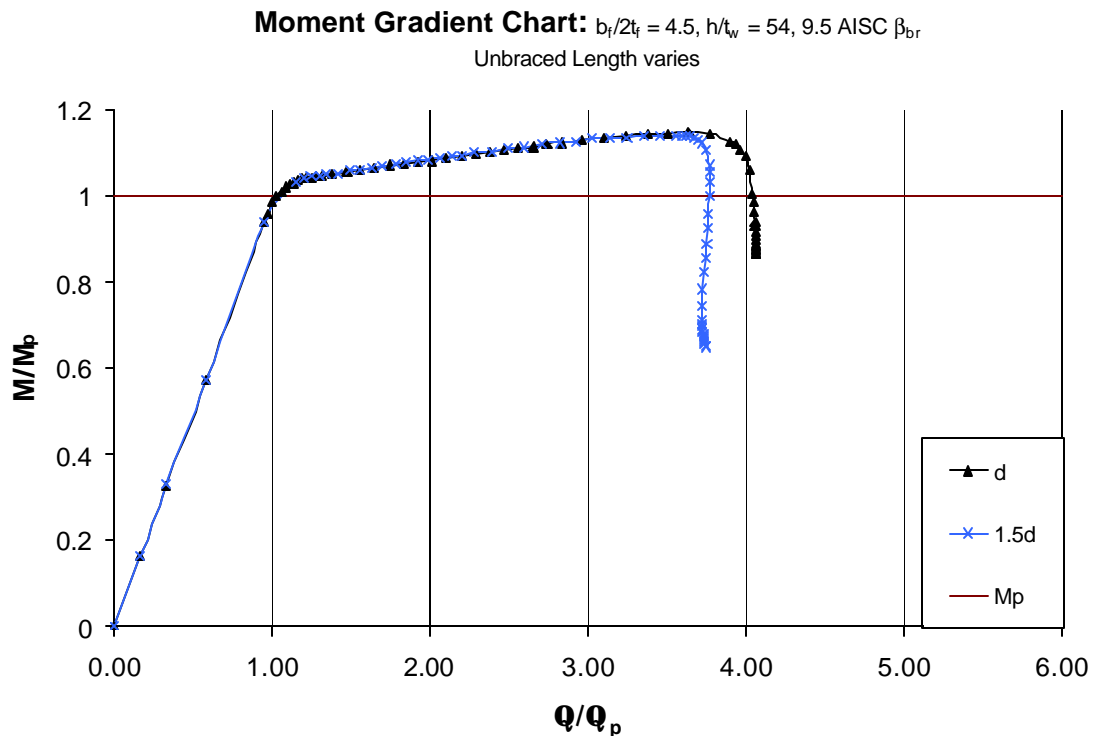
Figure 26 Moment Rotation Plot ($b_f/2t_f = 4.5$, $h/t_w = 54$, 9.5 AISC β_{br}, Unbraced Length Varies)

Noting that "d" appears to be optimal, Figure 27 shows a plot that compares the various bracing stiffnesses for this one unbraced length. This plot shows a gradual increase in rotation capacity as the bracing stiffness approaches 7.3 times the AISC recommended value (i.e. a maximum at 7.3), and then a gradual decrease in moment rotation response as the bracing stiffness continues to increase beyond 7.3 times the recommended value.

In addition to producing these optimal values for the two varied parameters, the results from the preliminary work provide a good basis for the parametric study executed as part of the exhaustive parametric study. Figures 21 through 26 also show that 1.5d is the second best bracing configuration, while 2d and 0.5d are the worst, with 0.5d tending

to be slightly better than 2d. Additionally, figure 27 shows that as long as the bracing stiffness is within the range of 5 times and 9.5 times the AISC recommended value, the girder is capable of reaching a rotation capacity of 3.0 or better. Hence the ductility is sufficient for use with plastic design and analysis methodologies.

Moment Gradient Chart: $b_f/2t_f = 4.5$, $h/t_w = 54$, $L_b = 1d$
Bracing Stiffness varies

Legend:
- 1 AISC
- 5 AISC
- 6.5 AISC
- 6.75 AISC
- 7 AISC
- 7.3 AISC
- 7.5 AISC
- 8 AISC
- 9.5 AISC
- Infinite Stiffness
- Mp

Y-axis: M/M_p
X-axis: Q/Q_p
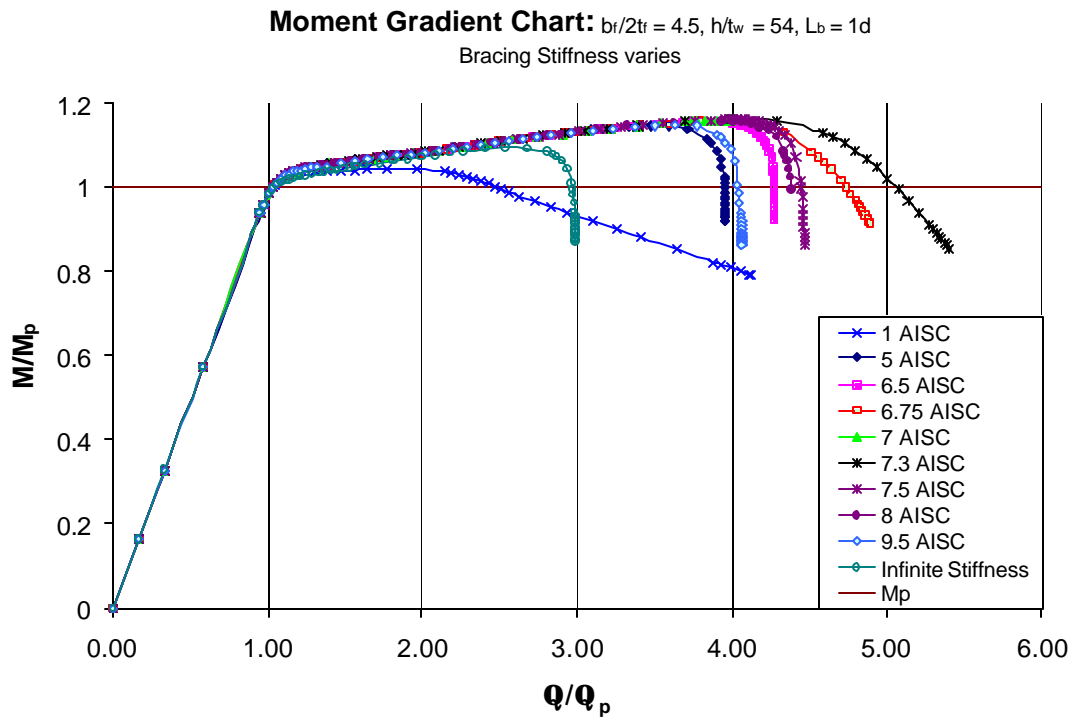
Figure 27 Moment Rotation Plot ($b_f/2t_f = 4.5$, $h/t_w = 54$, $L_b = 1d$, Bracing Stiffness Varies)

3.5 Primary Exhaustive Parametic Study

The goal of this portion of the research is to vary all four parameters (flange and web slenderness ratios, unbraced length, and bracing stiffness) in an appropriate manner so as to accurately, efficiently, and logically investigate the effects that all parameters have on the rotational ductility of HPS girders. The information derived from the preliminary parametric study is used to inform the direction of the parametric study carried out in this portion of the research.

The flange and web slenderness ratios (λ_{flange} and λ_{web}) are both varied as percentages of their specified limits per the current specifications (AASHTO LRFD 1998, AISC LRFD 1999). In both cases, 100%, 75%, and 50% are chosen as percentages considered. This gives λ_{flange} = 7.34, 5.5, or 3.5 and λ_{web} = 72, 54, or 36 for the parameters considered in reference to cross-sectional plate slenderness. To choose the parameters for the unbraced length and bracing stiffness, the results from the preliminary parametric study are used as a guide. The unbraced lengths considered are 0.5d, d, and 1.5d; the parameter, 2d, was eliminated based on its inferior performance in the preliminary work. The bracing stiffness is varied between 5 and 9.5 times the AISC recommended values, with the main focus on the multiples 6.5, 7.3 and 8.0. In addition to these values, several other values are considered for each parameter when deemed appropriate for a particular case. Flange slenderness ratios as low as 2.0 and web slenderness ratios as low as 18 are occasionally considered in this portion of the research.

Additionally, a wide array of bracing stiffness values arose on rare occasions in certain particular cases.

A total of approximately 200 detailed analyses are carried out as part of this second phase of the research. The results obtained from the model data are reduced in a variety of organization styles. All reduced data is available in the appendices wherein sample calculation sheets for applicable values, as well as tables of such values, are also available.

4.0 DISCUSSION OF RESULTS

Upon completion of each finite element test, ABAQUS post processing facilities are used to extract the support reactions and rotations that are present after each load increment. Microsoft Excel is then used to manipulate this data to calculate the internal moment and the girder rotation at each load increment. These results are normalized and plotted in a manner consistent with that described in Figure 2, located in Section 1.1.2 of this report. From this plot, the rotation capacity, as defined by ASCE (ASCE 1971), is calculated. All rotation capacities thus obtained as part of the current research have been tabulated in Appendix A. This table is presented in a variety of ways such that the results can be compared based on different combinations of tested parameters.

4.1 Reduction of Data

There exists a great deal of parametric data produced as part of the research reported herein. Therefore, it has been presented in a variety of ways so as to facilitate a clear understanding of all the information. The matrix of parameters tested consisted of approximately 200 different combinations of 4 different parameters ($b_f/2t_f$, h/t_w, L_b, β), and investigated the influence of each of these (alone and together) on the girder ductility. As a result, the data has been reduced and presented in two general ways: moment-rotation plots and interaction plots.

4.1.1 Moment-Rotation Plots

Each finite element test produces a moment-rotation response plot. These plots can be compared by combining them on the same graph and observing the effects that a change in the parameters has on girder ductility. The moment-rotation plots produced from this research are presented using four different methods.

The first presentation method combines the plots such that only the flange slenderness ratio varies. This presentation format highlights the influence that a change in flange slenderness has on rotational ductility using a given combination of web slenderness, unbraced length, and bracing stiffness parameters. A graph for every such combination is presented in Appendix B.1.

The remaining methods are very similar to the first, except that in each method a different parameter varies (while the other three parameters are held constant). Appendix B.2 contains the graphs in which only web slenderness varies. The graphs in Appendix B.3 show the effects of changing just the unbraced length, while Appendix B.4 has the graphs in which only bracing stiffness varies. Finally, Appendix B.5 presents moment-rotation plots for any remaining combinations that are not applicable in any of the previous graphs (i.e. graphs where multiple parameters change simultaneously).

4.1.2 Interaction Plots

Although the moment-rotation plots provide a good means of comparing all the data, the interaction plots included in Appendix C are designed to provide: (1) a means for observing the effectiveness of the current AISC and AASHTO compactness and bracing criteria for use with A709 HPS483W girders, (2) a means to highlight interaction between these investigated parameters, and (3) an organized presentation style that underscores any trends in the results.

There exist six different types of these interaction plots in which one of the parameters is graphed against another parameter. With four parameters, there are six possible combinations of two, leading to the six types of plots. On each plot, points are marked that indicate combinations of the four parameters that have been tested. Each point is annotated with the rotation capacity that is achieved for that combination of parameters. For ease in reading the graphs, each rotation capacity equal to or greater than 3.0 is highlighted in gray. In addition, the current AISC and/or AASHTO specified criteria are shown on each graph as they apply to A709 HPS483W steel for that combination of parameters to as to indicate where the current "safe zone" is (i.e. where, according to the current specifications, the girder should be capable of achieving a rotation capacity of at least 3.0).

It should be noted that specified values surrounded by parentheses and preceded by a ">" symbol (e.g. "(>3.2)") indicate slow convergence during the finite element test where ABAQUS was not permitted to continue with the test. In these instances, it is not

possible to report the precise rotation capacity for the given parametric combination, however it is possible to report a conservative value based on the progress of the ABAQUS solution prior to termination of the job; this conservative value is what is reported. The occurrence of this type of modeling outcome only affected about 10% of the tests.

The first type of interaction plot now discussed graphs web slenderness against flange slenderness. Examples of this type of plotting can be seen in Figures 28, 29, and 30. For each combination of unbraced length and bracing stiffness, one of these plots has been produced. For each of these plots there exist numerous combinations of flange and web slenderness ratios for which finite element tests are run. The corresponding rotation capacity for each of these individual tests is shown at its respective point on the graph.

The remaining five types of interaction plots are set up in a very similar manner; the only difference being that each type of plot considers a different combination of two parameters to plot against one another. Figures 31, 32, and 33 are examples of plotting web slenderness vs. unbraced length. Figures 34, 35, and 36 plot flange slenderness vs. unbraced length while examples of plotting web slenderness against bracing stiffness are given by Figures 37 through 40. The final two plot types are flange slenderness vs. bracing stiffness, shown in Figures 41 through 44, and unbraced length vs. bracing stiffness shown in Figures 45, 46, and 47. All the interaction plots are located in Appendix C. The observations from these interaction plots will be described in the following section.

4.2 Observations

That data produced from this research can be considered in three ways:

(1) How do the current AISC and AASHTO limiting criteria hold up when applied to A709 HPS483W steel?

(2) To what degree do any of the four parameters interact with each other as they influence the girder's ductility?

(3) What trends exist regarding the influence of each individual parameter on A709 HPS483W girder ductility?

4.2.1 Validity of Current AISC and AASHTO Compactness and Bracing Criteria

The principle focus of this research is to investigate the validity of employing the current compactness and bracing criteria as they relate to the plastic analysis and design of girders fabricated from A709 HPS483W steel. According to the current AISC LRFD and AASHTO LRFD design specifications, all tests conducted as part of this research satisfy the current compactness and bracing criteria, and therefore should all achieve a rotation capacity of 3.0 or greater. By highlighting only the combinations that reached 3.0, it becomes very easy to evaluate the adequacy of the current criteria.

In order to achieve sufficient rotation capacity, the flange must be compact according to current specification provisions. This means that for A709 HPS483W steel $\lambda_f = b_f/2t_f \leq \lambda_p = 7.34$. That is, the current specifications state that as long as $\lambda_f \leq 7.34$,

and assuming all other parameters (i.e. h/t_w, L_b) are within their limits, then the girder will be able to display sufficient ductility to achieve mechanism formation. Since all tests conducted herein involved the parameters being within the specifications' critical limits, the data clearly shows that the current flange compactness criterion is not adequate. Figures 28, 29, 30, 34, 35, 36, 41, 42, and 44 all clearly show that a flange slenderness ratio equal to 7.34 is too high to achieve a rotation capacity of 3.0. In fact, it can be seen from Table A-1 that with the exception of one combination, none of the models that had a flange slenderness of 7.34 achieved a rotation capacity greater than 1.8.

Similar to the flange, the web must also be compact to be considered useful for applications requiring moment redistribution. For this, the specifications require that for A709 HPS483W steel $\lambda_w = h/t_w \leq \lambda_p = 72$. That is, as long as $\lambda_w \leq 72$, and assuming all other parameters (i.e. $b_f/2t_f$, L_b) are within their limits, then the girder will be able to achieve sufficient rotation capacity to be considered for mechanism formation. The data presented in Figures 28 through 33 and 37 through 40 clearly show that the current web compactness criterion is also inadequate. A web slenderness of 72 is too high to achieve a rotation capacity of 3.0. It can be seen from Table A-4 that no combination of parameters having this web slenderness ratio exhibited a rotation capacity greater than 2.0.

The AASHTO LRFD Bridge Design Specification accounts for possible interaction between the web and compression flange slenderness ratios. It does this by allowing only one of the ratios to exceed 75% of λ_p at one time (AASHTO LRFD 1998). This interaction consideration is shown on the web slenderness vs. flange slenderness

interaction plots. Through Figures 28, 29, 30, 40, and 44 it can be seen that even this interaction consideration is insufficient in predicting the girder's ductility. Combinations were considered that accounted for 75% of both of the cross-sectional slenderness ratios separately as well as together, but under none of these situations did the rotation capacity exceed 2.2.

The AISC LRFD Specification for Structural Steel Buildings permits plastic analysis for compact sections when "the laterally unbraced length, L_b, of the compression flange adjacent to plastic hinge locations associated with the failure mechanism does not exceed L_{pd}" (AISC LRFD 1999). That is to say that as long as $L_b \leq L_{pd}$, and the cross section is compact, then the girder should be ductile enough to be considered for plastic design and analysis. Considering that the four unbraced lengths used in this parametric study are all less than L_{pd} (L_{pd} is generally between 5.5 and 6.5 times the depth of the beam for all tests run as part of this research) then the girders should respond with adequate ductility. However, as Figures 31 through 36 and 45, 46, and 47 all demonstrate, there exist many circumstances where this is not the case. Combinations exist for each unbraced length (0.5d, 1d, 1.5d, and 2d) where the cross section is compact but the rotation capacity is less than the required 3.0.

In addition to a required unbraced length, AISC also specifies a required bracing stiffness. Unlike the other three parameters' criteria, this required stiffness is not dependant upon the method of design. AISC simply provides a minimum bracing stiffness value, as described in Chapter 1 of this report, that must be satisfied for the bracing to be considered adequate. Figures 37, 44, and 46 show that AISC's required

bracing stiffness is far too small to be adequate for plastic analysis. A test run with one times the AISC recommended value achieved a rotation capacity of 1.5, whereas other tests run with all the same parameters, except for larger bracing stiffness values, achieved rotation capacities above 3.0. In addition, Figures 38 and 42 show examples of how a change in the bracing stiffness alone can affect whether or not the girder is considered sufficiently ductile. In these cases, all bracing stiffness values are above the current AISC required value.

The results of this research clearly show the inapplicability of the current compactness and bracing criteria for use in the design of A709 HPS483W girders. The compactness criteria scaling factor, based on yield strength alone, is not useful in applications involving A709 HPS483W steel. Additionally, the lateral bracing requirements in the current specifications are unsuitable for applications with HPS and must also be re-evaluated.

4.2.2 Interaction Between Chosen Parameters

Although it is known that local and global buckling phenomena are coupled in their effects on the flexural response of I-shaped beams and girders, a great deal of success has been achieved by treating them separately for the purposes of design. This success, however, has primarily been related to applications with mild carbon steel grades, rather than HPS grades such as are under investigation in this research. The results reported and presented herein allow for some preliminary observations to be made

regarding the significance of such interaction effects when considering A709 HPS483W steel. These observations are easiest made using the six interaction plots, and relate to the effects that each of the four parameters has on the other parameters.

Referring to the web slenderness vs. flange slenderness interaction plots presented in this chapter as well as those in Appendix C.1, it is clear that the two parameters interact with one another. The plots show that as the web slenderness increases, the flange slenderness must decrease in order to maintain sufficient ductility for mechanism formation. It appears that the ASSHTO interaction consideration is appropriate; it just needs to be modified for application with HPS grades. This interaction appears to end once the web slenderness reaches 54, a value above which sufficient ductility appears impossible, regardless of the flange slenderness value. This phenomenon will be discussed further in the following sub-section.

By comparing all of the web slenderness vs. flange slenderness plots it can be seen that the interaction between the two parameters also depends upon the unbraced length. This relation between local and global buckling becomes more clear when considering the web and flange slenderness vs. unbraced length plots. In virtually every case, as web slenderness decreases from 54, or flange slenderness decreases from 5.5, the allowable range of unbraced length seems to increase. In order for the beam to remain sufficiently ductile; (1) if either of the slenderness ratios are altered, then the unbraced length may also need to be changed, or (2) if the unbraced length changes then one or both of the slenderness ratios may have to be adjusted.

All of the interaction plots that consider bracing stiffness clearly show that as long as the other parameters are collectively sufficient to produce mechanism formation (i.e. in accordance with the results reported herein), then, assuming the bracing stiffness is also adequate (i.e. in accordance with the acceptable range reported herein), the beam rotation capacity will reach 3.0 with A709 HPS483W steel. Therefore, bracing stiffness appears to exhibit no interaction effects with any of the other parameters.

4.2.3 Trends in the Parameters' Effects on Ductility

Thus far, the results of this research have proven the inadequacy of employing current criteria for compactness and bracing to A709 HPS483W beam design. In addition, the philosophical approach of de-coupling local and global phenomena from one another when assessing beam ductility seems to be inappropriate. It is also evident that specific trends are present for each of the parameters as they affect the ductility of A709 HPS483W steel. By referring to the interaction plots presented in this chapter as well as those located in Appendix C, numerous observations can be made regarding these trends for each individual parameter.

Table 2 summarizes some of the results discussed in the following paragraphs. This table assumes adequate lateral bracing stiffness (according to the acceptable range reported herein) and shows the combinations for which mechanism formation can and cannot be relied upon in design. Although this table only shows data for a fraction of the

total combinations considered, it provides a good means of observing the trends evident

throughout the results.

Table 2 Summary of Trends Evident Throughout Parametric Study

Adequate Bracing Stiffness			Flange Slenderness (λ_f)			
			3.5	4.5	5.5	7.34
w e b	36	0.5d		-	-	-
		1d		✔	✔	-
		1.5d		✔	-	-
s l		2d	✔	✔		
e n d e r	54 (λ_w)	0.5d	-	-	-	-
		1d	✔	✔	-	-
		1.5d	-	-	-	-
		2d		-		
n e s s	72	0.5d	-	-	-	
		1d	-	-	-	
		1.5d	-	-	-	
		2d		-		

"✔" indicates sufficient rotation capacity was achieved
"-"   indicates sufficient rotation capacity was <u>not</u> achieved

Considering practical web slenderness ratios (λ_w) for highway bridge girders (i.e.

greater than or equal to 36), the maximum flange slenderness (λ_f) for which a rotation

capacity of 3.0 or greater is achieved is $\lambda_f = 5.5$ (75% the current AISC λ_p for the flange).

This, however, only occurs when $\lambda_w \leq 36$ (50% of the current λ_p for the web) and the

unbraced length (L_b) is 1d. No other bracing distance is sufficient under this situation.

The same situation occurs when $\lambda_f = 4.5$ and $\lambda_w = 54$; L_b must be 1d. However, having λ_f

= 4.5 proves to be more versatile in achieving sufficient ductility than if it equals 5.5. This is because the rotation capacity will reach 3.0 when $\lambda_w = 36$ and a corresponding L_b that may be between 1d and 2d, unlike the case for which $\lambda_f = 5.5$ wherein it can only be 1d. The interaction plots tend to show that $\lambda_f = 3.5$ is inferior to $\lambda_f = 4.5$. This is to say that evidence exists showing that as λ_f decreases from 4.5 to 3.5, the rotation capacities also decrease (this is due to the occurrence of vertical flange buckling). Considering these observations, it appears as though $\lambda_f = 4.5$ is the optimal value for flange slenderness. The best and most reliable results are achieved at this value. Flange slenderness values above 4.5 require strict limitations on web slenderness and unbraced length, whereas flange slendernesses below 4.5 results in less ductility due to the occurrence of vertical flange buckling.

The maximum λ_w for which the girder may be considered for plastic analysis and design is $\lambda_w = 54$ (75% the current AISC λ_p for the web). There exist no cases when $\lambda_w >$ 54 that the rotation capacity exceeds 2.4 and very few where it even reaches 2.0. Meanwhile, the only combinations with $\lambda_w = 54$ for which the section is considered sufficiently ductile are when $\lambda_f \leq 4.5$ and $L_b = 1d$. No other bracing distance is adequate under this situation. Similarly, L_b must equal 1d when $\lambda_w = 36$ and $\lambda_f = 5.5$. However, if $\lambda_f \leq 4.5$, with $\lambda_w = 36$, then L_b may be between 1d and 2d. All data shows that as λ_w decreases, the rotation capacity increases, assuming all other parameters remain the same.

The results clearly show that using the appropriate unbraced length is critical in allowing the girder to be considered for mechanism formation. No cases are observed

where $L_b = 0.5d$ produces a rotation capacity exceeding 1.9. However, the data clearly shows that $L_b = 1d$ is the optimal situation for virtually all of the parametric combinations considered. At the same time, $L_b = 1d$ should also be the minimum unbraced length allowed for plastic design. However, a range of allowable unbraced lengths exists between 1d and 2d when $\lambda_f \leq 4.5$ and $\lambda_w \leq 36$.

Although AISC specifies a required minimum bracing stiffness (β), it has been previously noted that this recommended value is too low. The data shows that as long as β is between 5.5 and 9.5 times AISC's recommended value, and all other parameters are adequate (based on the recommendations herein), then the girder will achieve a sufficient ductility so as to be considered for mechanism formation. Furthermore, the optimal β appears to be approximately 7.3 times the AISC recommended value. Some cases deviate slightly from this value, but remain between 6.5 and 8.0 times AISC. The case of infinite bracing stiffness has been shown to be far from ideal in its effect on beam ductility. In combinations where only the bracing stiffness varies, an infinite stiffness produces a rotation capacity far less than 3.0 while stiffness values that fall within the range of 5.5 to 9.5 times AISC's recommendation result in rotation capacities greater than 3.0.

The data produced from this research is reduced and presented in a variety of ways to facilitate interpretation. This chapter has summarized the interpretation process by discussing the main observations that can be made from the results. From the results it has been noted that: (1) the current AISC and AASHTO compactness and bracing criteria are inapplicable for use with A709 HPS483W steel, (2) there exist obvious

71

interaction effects between some of the parameters considered in this research: this calls into question the future viability of the current philosophical approach wherein cross-sectional compactness and bracing requirements are considered separately, and (3) practical trends in the data lend themselves to useful design recommendations which are presented in Chapter 5.

4.3 Examples of Interaction Plots Used for Discussion

The following figures provide examples of each style of interaction plot. In addition, they are chosen to supplement the discussion of results included within this chapter. When analyzing the results, all of the data in all of the interaction plots (located in Appendix C) are considered. The ones placed in this chapter merely provide a basic overview of all the results.
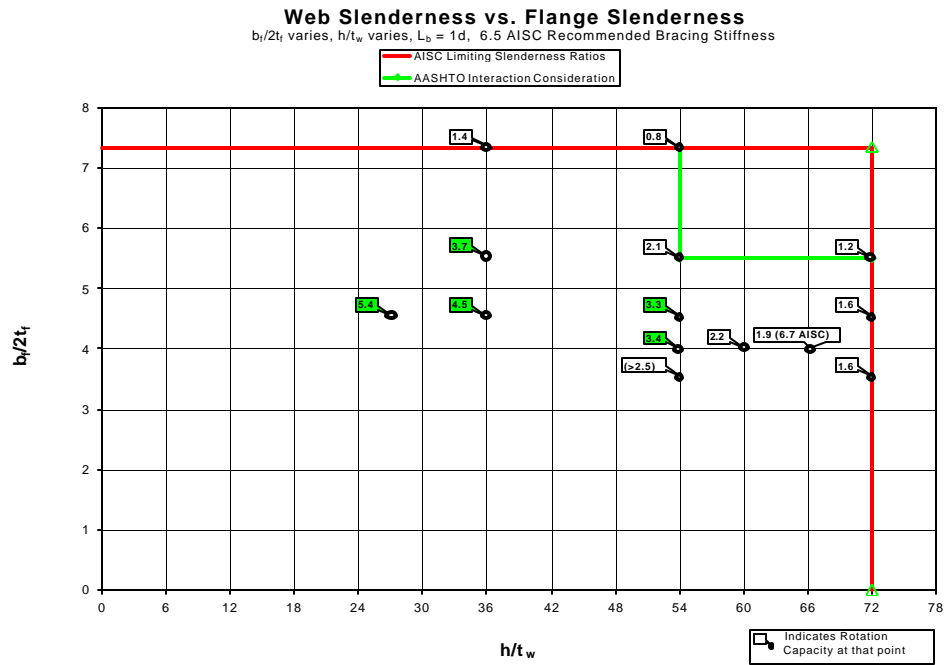
Figure 28 Web Slenderness vs. Flange Slenderness ($b_f/2t_f$ varies, h/t_w varies, $L_b = 1d$, 6.5 AISC Recommended Bracing Stiffness)
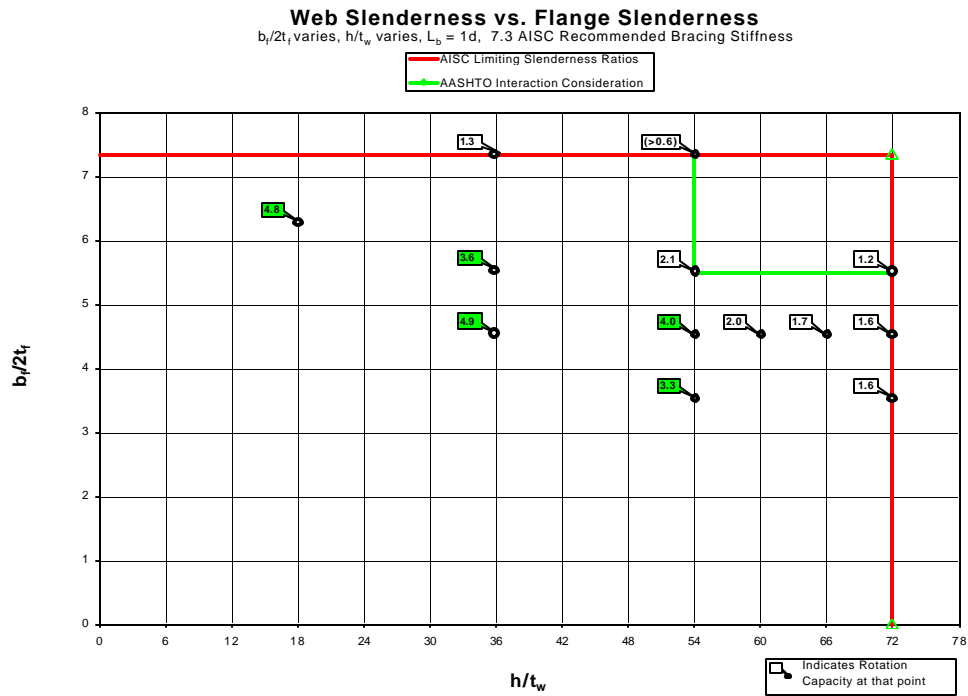
Figure 29 Web Slenderness vs. Flange Slenderness ($b_f/2t_f$ varies, h/t_w varies, $L_b = 1d$, 7.3 AISC Recommended Bracing Stiffness)
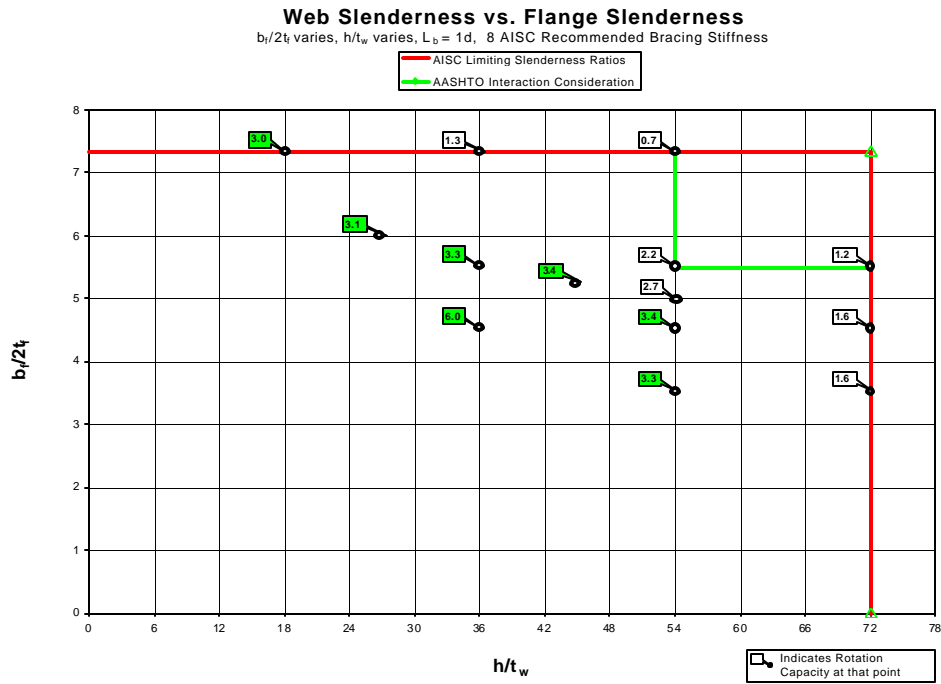
Figure 30 Web Slenderness vs. Flange Slenderness ($b_f/2t_f$ varies, h/t_w varies, $L_b = 1d$, 8 AISC Recommended Bracing Stiffness)
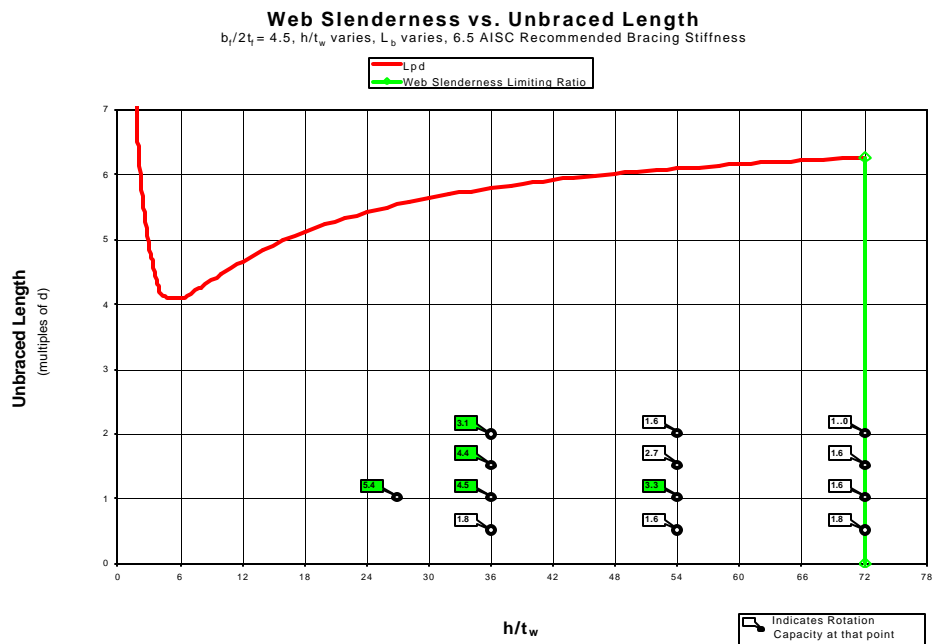
Figure 31 Web Slenderness vs. Unbraced Length ($b_f/2t_f = 4.5$, h/t_w varies, L_b varies, 6.5 AISC Recommended Bracing Stiffness)
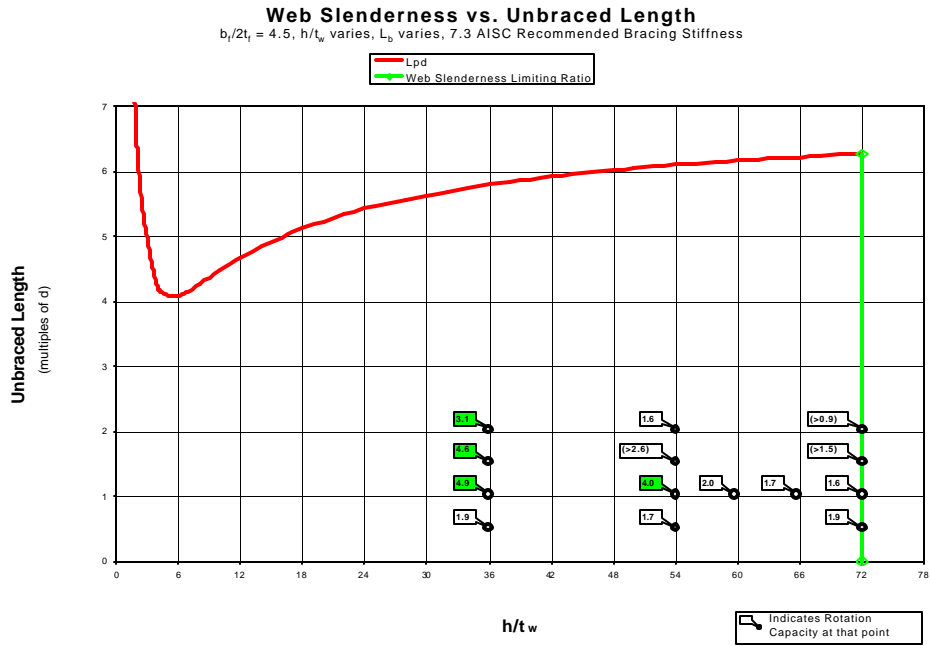
Figure 32 Web Slenderness vs. Unbraced Length ($b_f/2t_f = 4.5$, h/t_w varies, L_b varies, 7.3 AISC Recommended Bracing Stiffness)
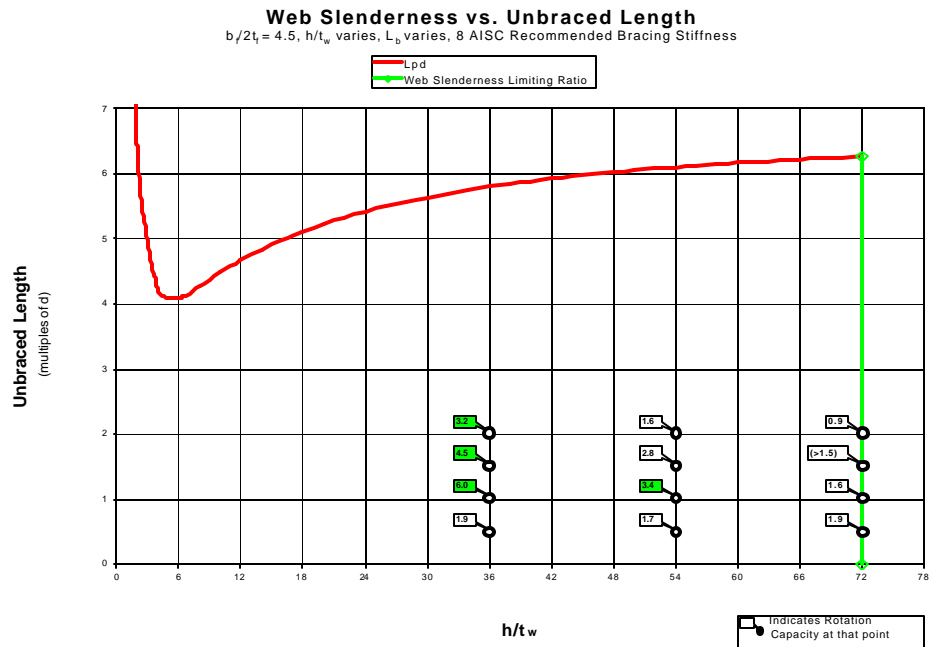
Figure 33 Web Slenderness vs. Unbraced Length ($b_f/2t_f = 4.5$, h/t_w varies, L_b varies, 8 AISC Recommended Bracing Stiffness)

Flange Slenderness vs. Unbraced Length
b$_f$/2t$_f$ varies, h/t$_w$ = 36, L$_b$ varies, 6.5 AISC Recommended Bracing Stiffness
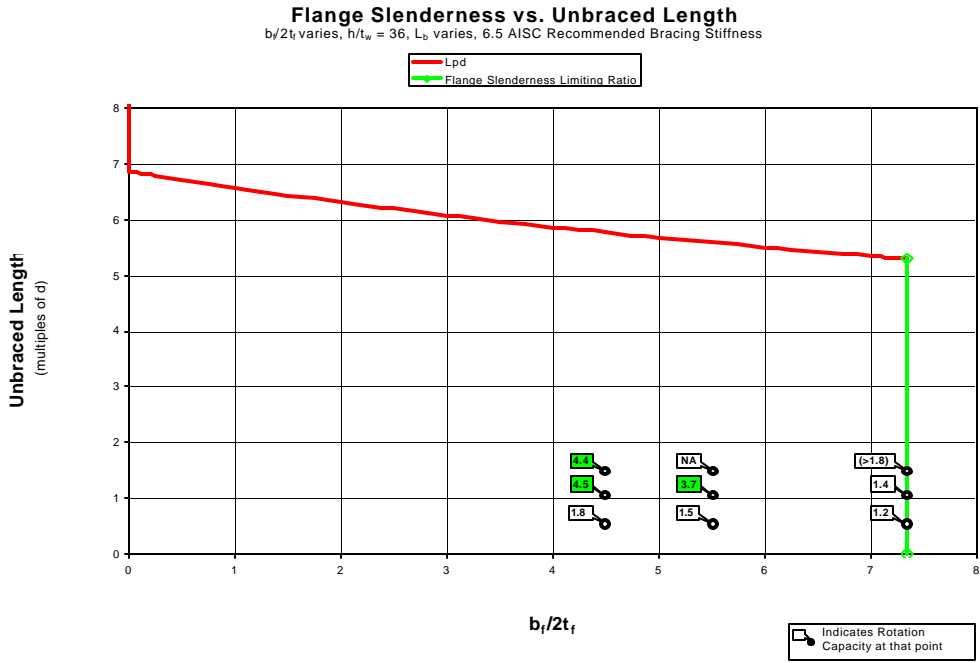
Figure 34 Flange Slenderness vs. Unbraced Length (b$_f$/2t$_f$ varies, h/t$_w$ = 36, L$_b$ varies, 6.5 AISC Recommended Bracing Stiffness)

Flange Slenderness vs. Unbraced Length
b$_f$/2t$_f$ varies, h/t$_w$ = 36, L$_b$ varies, 7.3 AISC Recommended Bracing Stiffness
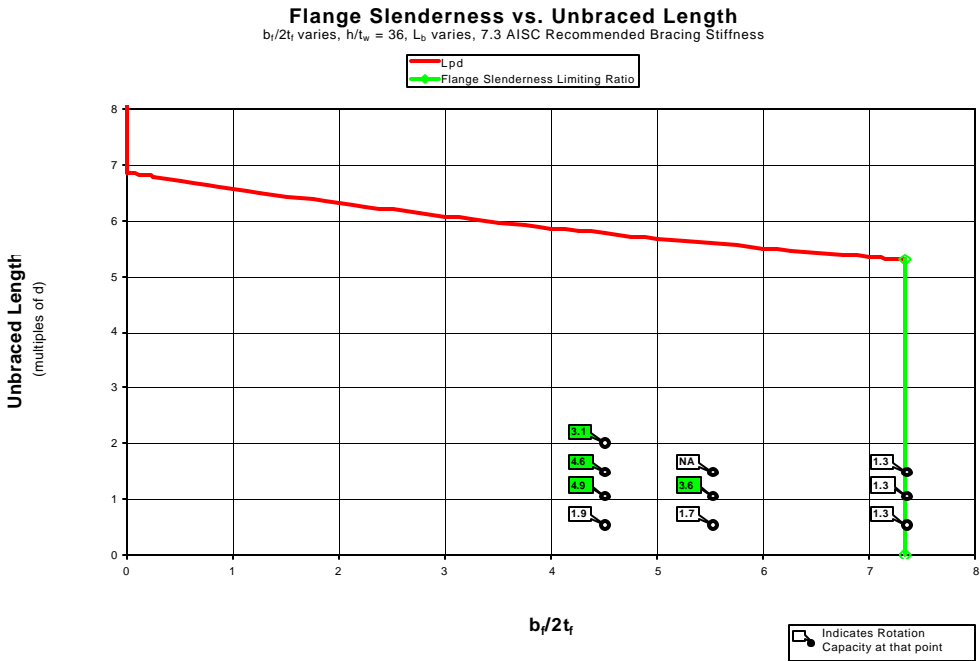
Figure 35 Flange Slenderness vs. Unbraced Length (b$_f$/2t$_f$ varies, h/t$_w$ = 36, L$_b$ varies, 7.3 AISC Recommended Bracing Stiffness)

76

Flange Slenderness vs. Unbraced Length

b$_f$/2t$_f$ varies, h/t$_w$ = 36, L$_b$ varies, 8 AISC Recommended Bracing Stiffness

Figure 36 Flange Slenderness vs. Unbraced Length (b$_f$/2t$_f$ varies, h/t$_w$ = 36, L$_b$ varies, 8 AISC Recommended Bracing Stiffness)

Web Slenderness vs. Bracing Stiffness

b$_f$/2t$_f$ = 4.5, h/t$_w$ varies, L$_b$ = 1d, Bracing Stiffness varies

Figure 37 Web Slenderness vs. Bracing Stiffness (b$_f$/2t$_f$ = 4.5, h/t$_w$ varies, L$_b$ = 1d, Bracing Stiffness varies)

77

Figure 38 Web Slenderness vs. Bracing Stiffness ($b_f/2t_f = 4.5$, h/t_w varies, $L_b = 1.5d$, Bracing Stiffness varies)

Figure 39 Web Slenderness vs. Bracing Stiffness ($b_f/2t_f = 4.5$, h/t_w varies, $L_b = 2d$, Bracing Stiffness varies)

78

Figure 40 Web Slenderness vs. Bracing Stiffness (bf/2tf = 5.5, h/tw varies, Lb = 1d, Bracing Stiffness varies)
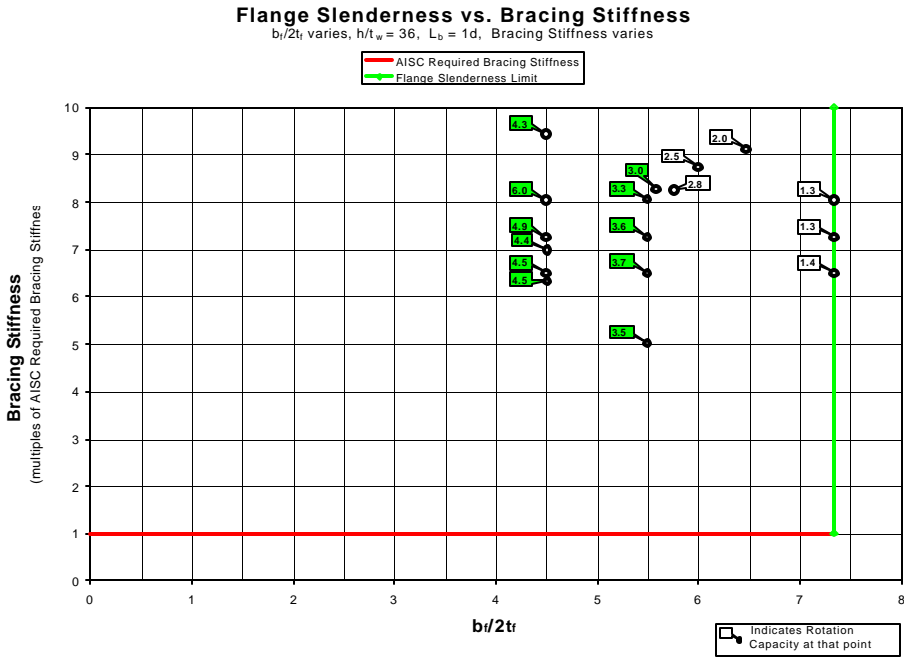
Figure 41 Flange Slenderness vs. Bracing Stiffness (bf/2tf varies, h/tw = 36, Lb = 1d, Bracing Stiffness varies)

79
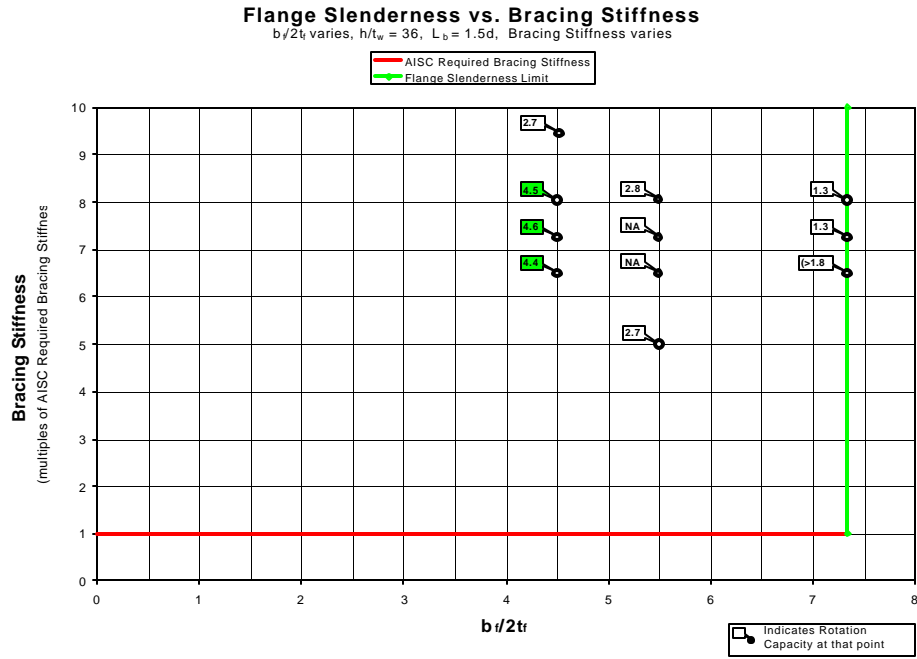
Figure 42 Flange Slenderness vs. Bracing Stiffness ($b_f/2t_f$ varies, $h/t_w = 36$, $L_b = 1.5d$, Bracing Stiffness varies)
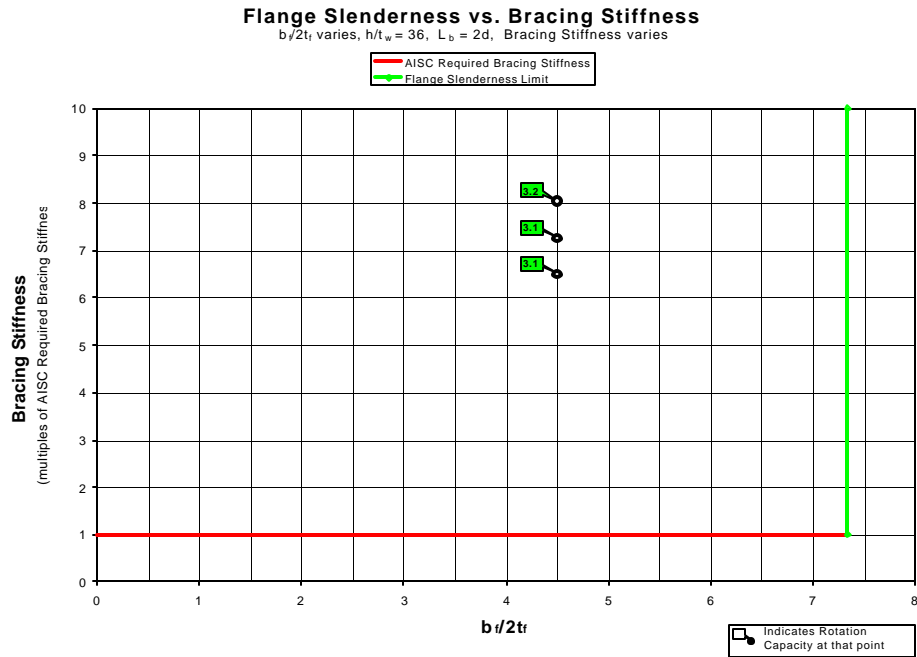
Figure 43 Flange Slenderness vs. Bracing Stiffness ($b_f/2t_f$ varies, $h/t_w = 36$, $L_b = 2d$, Bracing Stiffness varies)

Flange Slenderness vs. Bracing Stiffness

$b_f/2t_f$ varies, $h/t_w = 54$, $L_b = 1d$, Bracing Stiffness varies
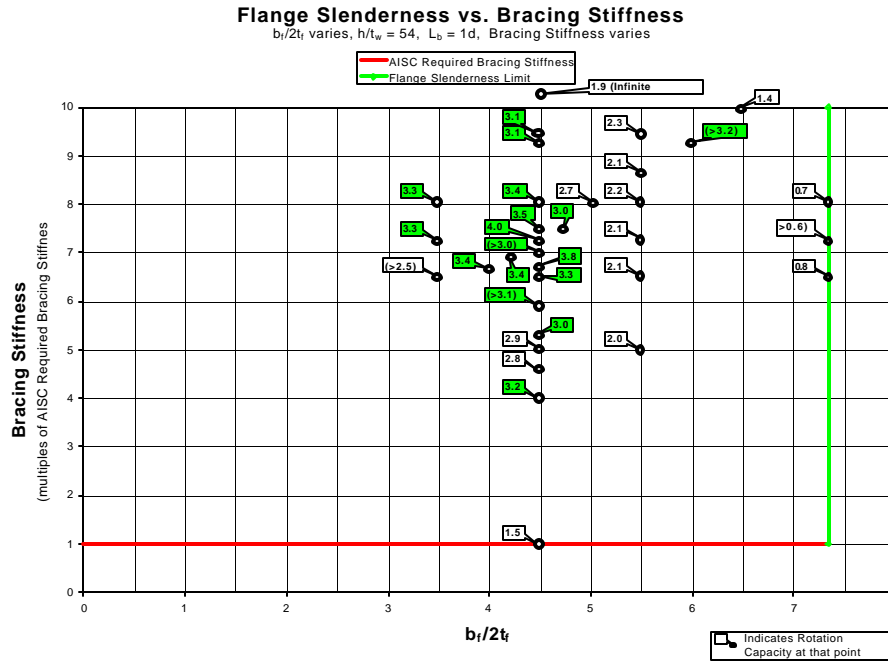
Figure 44 Flange Slenderness vs. Bracing Stiffness ($b_f/2t_f$ varies, $h/t_w = 54$, $L_b = 1d$, Bracing Stiffness varies)

Unbraced Length vs. Bracing Stiffness

$b_f/2t_f = 4.5$, $h/t_w = 36$, L_b varies, Bracing Stiffness varies
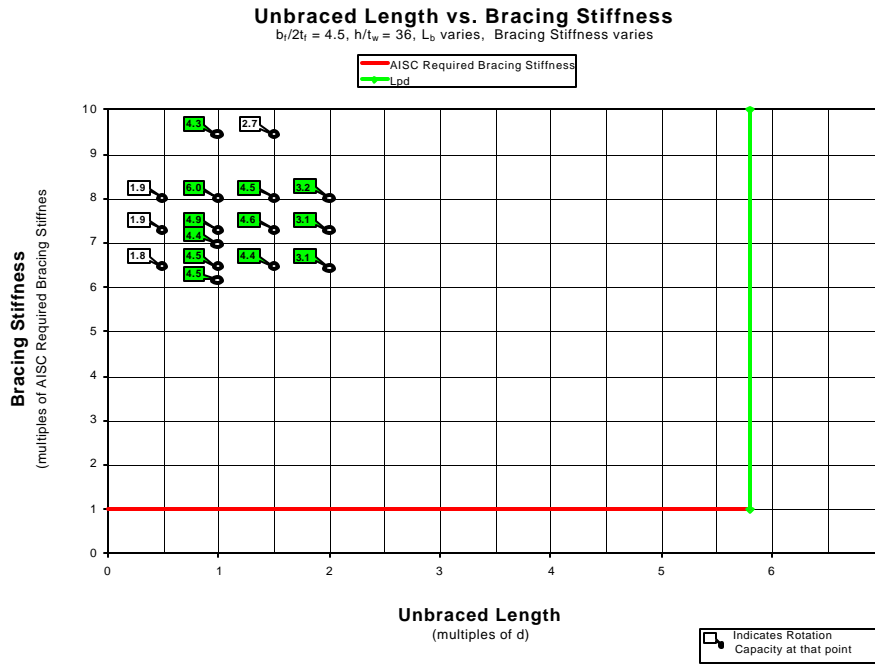
Figure 45 Unbraced Length vs. Bracing Stiffness ($b_f/2t_f = 4.5$, , $h/t_w = 36$, L_b varies, Bracing Stiffness varies)

Unbraced Length vs. Bracing Stiffness

$b_f/2t_f = 4.5$, $h/t_w = 54$, L_b varies, Bracing Stiffness varies

Figure 46 Unbraced Length vs. Bracing Stiffness ($b_f/2t_f = 4.5$, $h/t_w = 54$, L_b varies, Bracing Stiffness varies)

Unbraced Length vs. Bracing Stiffness

$b_f/2t_f = 5.5$, $h/t_w = 36$, L_b varies, Bracing Stiffness varies

Figure 47 Unbraced Length vs. Bracing Stiffness ($b_f/2t_f = 5.5$, $h/t_w = 36$, L_b varies, Bracing Stiffness varies)

5.0 CONCLUSION

Based on the results of the parametric finite element study reported herein, the current provisions for cross-sectional compactness and lateral bracing contained within the AISC LRFD Specification for Structural Steel Buildings (1999) and AASHTO LRFD Bridge Design Specification (1998) as they pertain to plastic analysis and design are not applicable to girders made from A709 HPS483W steel. That is, all criteria relating to flange and web compactness, unbraced length, and bracing stiffness, when considering A709 HPS483W steel, are unconservative and must be re-evaluated. The current approach of de-coupling local and global phenomena from one another when assessing beam ductility is inappropriate and must also be re-evaluated for high performance steel applications.

Despite the current deficiencies in the specifications as they pertain to plastic analysis of high performance steel girders, the results reported herein recommend applicable provisions for ensuring sufficient beam ductility when using A709 HPS483W steel. First, a new lateral bracing scheme is suggested. This new scheme does not require any additional stiffeners or diaphragm members. Rather a repositioning of the two stiffeners and diaphragm members on either side of the bridge pier, so as to be closer together, is all that is required (i.e. moving the existing stiffeners and diaphragm members to a new location d, the depth of the girder, away from the pier on either side).

Secondly, the maximum flange slenderness ratio ($b_f/2t_f$) must not exceed 5.5 and the maximum web slenderness ratio (h/t_w) must not exceed 54. In addition, these

maximum values must not occur at the same time. The results call for a similar flange/web compactness interaction consideration as currently applied by the AASHTO specification. That is, in the case of A709 HPS483W steel, at no time can both slenderness ratios equal their maximum value (as recommended in this report). This is to say that if:

(1) $4.5 \leq b_f/2t_f \leq 5.5$ ($4.5 = 80\%$ of the recommended flange slenderness maximum), then h/t_w must not exceed 36 (67% of its recommended maximum).

(2) $36 \leq h/t_w \leq 54$ ($36 = 67\%$ of the recommended web slenderness maximum), then $b_f/2t_f$ must not exceed 4.5 (80% of its recommended maximum).

These previous provisions apply to an unbraced length of d, only. If the unbraced length must be greater than the d, but not to exceed 2d, then $b_f/2t_f$ must not exceed 4.5 and h/t_w must not exceed 36.

Finally, as long as the previous recommendations are satisfied, then to achieve sufficient beam ductility for moment redistribution using A709 HPS483W steel, the bracing stiffness must be within the range of 5.5 to 9.5 times the current AISC LRFD (1999) recommended bracing stiffness value.

APPENDIX A

APPENDIX A

ROTATION CAPACITY TABLES

All rotation capacities obtained as part of the current research are tabulated in this appendix. The table is presented in eleven different ways so that the results can be compared based on different ordering schemes for the parametric combinations.

Table A-1 Rotation Capacities Ordered by Increasing $b_f/2t_f$, h/t_w, L_b, and β, Respectively

$b_f/2t_f$	h/t_w	L_b	b	R
2	60	1	3.5	1.2
2.5	60	1	4.3	2.1
3	60	1	5.1	2.4
3	72	1	5.2	1.4
3.5	54	0.5	6.5	1.6
3.5	54	0.5	7.3	1.6
3.5	54	0.5	8	1.7
3.5	54	1	6.5	>2.5
3.5	54	1	7.3	3.3
3.5	54	1	8	3.3
3.5	54	1.5	6.5	>2.5
3.5	54	1.5	7.3	2.6
3.5	54	1.5	8	>2.5
3.5	60	1	5.9	2.3
3.5	66	1	5.9	2.1
3.5	72	0.5	6.5	1.5
3.5	72	0.5	7.3	1.5
3.5	72	0.5	8	1.5
3.5	72	1	6	1.6
3.5	72	1	6.5	1.6
3.5	72	1	7.3	1.6
3.5	72	1	8	1.6
3.5	72	1.5	6.5	2
3.5	72	1.5	7.3	1.5
3.5	72	1.5	8	1.6
4	54	1	6.6	3.4
4	60	1	6.6	2.2
4	66	1	6.7	1.9
4.25	54	1	6.9	3.4
4.25	54	1	7	3.5
4.5	18	1	5.3	6
4.5	18	1	5.9	>6
4.5	27	1	6.5	5.4
4.5	36	0.5	6.5	1.8
4.5	36	0.5	7.3	1.9
4.5	36	0.5	8	1.9
4.5	36	1	6.3	4.5
4.5	36	1	6.5	4.5
4.5	36	1	7	4.4
4.5	36	1	7.3	4.9
4.5	36	1	8	6
4.5	36	1	9.5	4.3
4.5	36	1.5	6.5	4.4
4.5	36	1.5	7.3	4.6
4.5	36	1.5	8	4.5
4.5	36	1.5	9.5	2.7
4.5	36	2	6.5	3.1
4.5	36	2	7.3	3.1
4.5	36	2	8	3.2
4.5	45	1	7	4.2
4.5	54	0.5	5	1.6
4.5	54	0.5	6.5	1.6
4.5	54	0.5	7	1.6
4.5	54	0.5	7.3	1.7
4.5	54	0.5	7.5	1.7
4.5	54	0.5	7.7	1.7
4.5	54	0.5	8	1.7
4.5	54	0.5	8.4	1.8
4.5	54	1	1	1.5
4.5	54	1	4	3.2
4.5	54	1	4.6	2.8
4.5	54	1	5	2.9
4.5	54	1	5.3	3
4.5	54	1	5.9	>3.1
4.5	54	1	6.5	3.3
4.5	54	1	6.75	3.8
4.5	54	1	6.8	3.8
4.5	54	1	7	>3
4.5	54	1	7.3	4
4.5	54	1	7.5	3.5
4.5	54	1	8	3.4
4.5	54	1	9.3	3.1
4.5	54	1	9.5	3.1
4.5	54	1	inf	1.9
4.5	54	1.5	5	>2.6
4.5	54	1.5	6.25	>2.6
4.5	54	1.5	6.5	2.7
4.5	54	1.5	6.9	2.8
4.5	54	1.5	7	>2.6
4.5	54	1.5	7.3	>2.6
4.5	54	1.5	7.5	2.8
4.5	54	1.5	8	2.8
4.5	54	1.5	9.5	2.8
4.5	54	2	5.9	1.6
4.5	54	2	6.5	1.6
4.5	54	2	7	1.6
4.5	54	2	7.3	1.6
4.5	54	2	7.5	1.6
4.5	54	2	8	1.6
4.5	60	1	7.3	2
4.5	66	1	7.3	1.7
4.5	72	0.5	5	1.2
4.5	72	0.5	6.5	1.8
4.5	72	0.5	7.3	1.9
4.5	72	0.5	8	1.9
4.5	72	0.5	9.5	1.8
4.5	72	1	5	1.6
4.5	72	1	6.5	1.6
4.5	72	1	6.8	>1.5
4.5	72	1	7.3	1.6
4.5	72	1	7.5	1.6
4.5	72	1	8	1.6
4.5	72	1	9.5	1.6
4.5	72	1.5	5	1.5
4.5	72	1.5	6.5	1.6
4.5	72	1.5	7.3	>1.5
4.5	72	1.5	8	>1.5
4.5	72	1.5	9.5	>1.5
4.5	72	2	6.5	1
4.5	72	2	7.3	>.9
4.5	72	2	8	0.9
4.75	54	1	7.5	3
4.75	54	1	7.6	3
5	54	1	8	2.7
5.25	45	1	8.1	3.4
5.5	36	0.5	6.5	1.5
5.5	36	0.5	7.3	1.7
5.5	36	0.5	8	1.7
5.5	36	1	5	3.5
5.5	36	1	6.5	3.7
5.5	36	1	7.3	3.6
5.5	36	1	8	3.3
5.5	36	1.5	5	2.7
5.5	36	1.5	6.5	NA
5.5	36	1.5	7.3	NA
5.5	36	1.5	8	2.8
5.5	36	1.5	9.5	2.7
5.5	45	1	8.4	2.9
5.5	54	0.5	6.5	1.4
5.5	54	0.5	7.3	1.5
5.5	54	0.5	8	1.6
5.5	54	1	5	2
5.5	54	1	6.5	2.1
5.5	54	1	7.3	2.1
5.5	54	1	8	2.2
5.5	54	1	8.6	2.1
5.5	54	1	9.5	2.3
5.5	54	1.5	6.5	2.2
5.5	54	1.5	7.3	2.3
5.5	54	1.5	8	2.3
5.5	54	1.5	9.5	2.3
5.5	72	0.5	6.5	1.2
5.5	72	0.5	7.3	1.5
5.5	72	0.5	8	1.5
5.5	72	1	6.5	1.2
5.5	72	1	7.3	1.2
5.5	72	1	8	1.2
5.5	72	1	9	1.2
5.5	72	1.5	6.5	1.5
5.5	72	1.5	7.3	1.6
5.5	72	1.5	8	1.5
5.63	36	1	8.3	3
5.67	36	1	8.3	2.9
5.75	36	1	8.3	2.8
6	18	1	7.15	5.2
6	27	1	8.1	3.1
6	36	1	8.7	2.5
6	54	1	9.3	>3.2
6.25	18	1	7.3	4.8
6.25	27	1	8.3	2.8
6.5	18	1	6.8	4.5
6.5	18	1	7.5	3.9
6.5	27	1	8.6	2.6
6.5	36	1	9.2	2
6.5	54	1	10	1.4
6.63	18	1	7.5	3.8
6.63	18	1	7.6	3.8
6.75	18	1	7.7	3.3
6.75	27	1	8.8	2.6
7.34	18	1	8	3
7.34	36	0.5	6.5	1.2
7.34	36	0.5	7.3	1.3
7.34	36	0.5	8	1.4
7.34	36	1	6.5	1.4
7.34	36	1	7.3	1.3
7.34	36	1	8	1.3
7.34	36	1.5	6.5	>1.8
7.34	36	1.5	7.3	1.3
7.34	36	1.5	8	1.3
7.34	54	0.5	6.5	0.9
7.34	54	0.5	7.3	0.9
7.34	54	0.5	8	0.9
7.34	54	1	6.5	0.8
7.34	54	1	7.3	>.6
7.34	54	1	8	0.7
7.34	54	1.5	6.5	0.8
7.34	54	1.5	7.3	0.8
7.34	54	1.5	8	>.5

$b_f/2t_f$	: Flange Slenderness Ratio
h/t_w	: Web Slenderness Ratio
L_b	: Unbraced Length in Multiples of d
b	: # times AISC Recommended Bracing Stiffness
R	: Rotation Capacity Achieved

Table A-2 Rotation Capacities Ordered by Increasing $b_f/2t_f$, L_b, β, and h/t_w, Respectively

$b_f/2t_f$	L_b	b	h/t_w	R
2	1	3.5	60	1.2
2.5	1	4.3	60	2.1
3	1	5.1	60	2.4
3	1	5.2	72	1.4
3.5	0.5	6.5	54	1.6
3.5	0.5	6.5	72	1.5
3.5	0.5	7.3	54	1.6
3.5	0.5	7.3	72	1.5
3.5	0.5	8	54	1.7
3.5	0.5	8	72	1.5
3.5	1	5.9	60	2.3
3.5	1	5.9	66	2.1
3.5	1	6	72	1.6
3.5	1	6.5	54	>2.5
3.5	1	6.5	72	1.6
3.5	1	7.3	54	3.3
3.5	1	7.3	72	1.6
3.5	1	8	54	3.3
3.5	1	8	72	1.6
3.5	1.5	6.5	54	>2.5
3.5	1.5	6.5	72	2
3.5	1.5	7.3	54	2.6
3.5	1.5	7.3	72	1.5
3.5	1.5	8	54	>2.5
3.5	1.5	8	72	1.6
4	1	6.6	54	3.4
4	1	6.6	60	2.2
4	1	6.7	66	1.9
4.25	1	6.9	54	3.4
4.25	1	7	54	3.5
4.5	0.5	5	54	1.6
4.5	0.5	5	72	1.2
4.5	0.5	6.5	36	1.8
4.5	0.5	6.5	54	1.6
4.5	0.5	6.5	72	1.8
4.5	0.5	7	54	1.6
4.5	0.5	7.3	36	1.9
4.5	0.5	7.3	54	1.7
4.5	0.5	7.3	72	1.9
4.5	0.5	7.5	54	1.7
4.5	0.5	7.7	54	1.7
4.5	0.5	8	36	1.9
4.5	0.5	8	54	1.7
4.5	0.5	8	72	1.9
4.5	0.5	8.4	54	1.8
4.5	0.5	9.5	72	1.8
4.5	1	1	54	1.5
4.5	1	4	54	3.2
4.5	1	4.6	54	2.8
4.5	1	5	54	2.9
4.5	1	5	72	1.6
4.5	1	5.3	18	6
4.5	1	5.3	54	3
4.5	1	5.9	18	>6
4.5	1	5.9	54	>3.1
4.5	1	6.3	36	4.5
4.5	1	6.5	27	5.4
4.5	1	6.5	36	4.5
4.5	1	6.5	54	3.3
4.5	1	6.5	72	1.6
4.5	1	6.75	54	3.8
4.5	1	6.8	54	3.8
4.5	1	6.8	72	>1.5
4.5	1	7	36	4.4
4.5	1	7	45	4.2
4.5	1	7	54	>3
4.5	1	7.3	36	4.9
4.5	1	7.3	54	4
4.5	1	7.3	60	2
4.5	1	7.3	66	1.7
4.5	1	7.3	72	1.6
4.5	1	7.5	54	3.5
4.5	1	7.5	72	1.6
4.5	1	8	36	6
4.5	1	8	54	3.4
4.5	1	8	72	1.6
4.5	1	9.3	54	3.1
4.5	1	9.5	36	4.3
4.5	1	9.5	72	1.6
4.5	1	inf	54	1.9
4.5	1.5	5	54	>2.6
4.5	1.5	5	72	1.5
4.5	1.5	6.25	54	>2.6
4.5	1.5	6.5	36	4.4
4.5	1.5	6.5	54	2.7
4.5	1.5	6.5	72	1.6
4.5	1.5	6.9	54	2.8
4.5	1.5	7	54	>2.6
4.5	1.5	7.3	36	4.6
4.5	1.5	7.3	54	>2.6
4.5	1.5	7.3	72	>1.5
4.5	1.5	7.5	54	2.8
4.5	1.5	8	36	4.5
4.5	1.5	8	54	2.8
4.5	1.5	8	72	>1.5
4.5	1.5	9.5	36	2.7
4.5	1.5	9.5	54	2.8
4.5	1.5	9.5	72	>1.5
4.5	2	5.9	54	1.6
4.5	2	6.5	36	3.1
4.5	2	6.5	54	1.6
4.5	2	6.5	72	1
4.5	2	7	54	1.6
4.5	2	7.3	36	3.1
4.5	2	7.3	54	1.6
4.5	2	7.3	72	>.9
4.5	2	7.5	54	1.6
4.5	2	8	36	3.2
4.5	2	8	54	1.6
4.5	2	8	72	0.9
4.75	1	7.5	54	3
4.75	1	7.6	54	3
5	1	8	54	2.7
5.25	1	8.1	45	3.4
5.5	0.5	6.5	36	1.5
5.5	0.5	6.5	54	1.4
5.5	0.5	6.5	72	1.2
5.5	0.5	7.3	36	1.7
5.5	0.5	7.3	54	1.5
5.5	0.5	7.3	72	1.5
5.5	0.5	8	36	1.7
5.5	0.5	8	54	1.6
5.5	0.5	8	72	1.5
5.5	1	5	36	3.5
5.5	1	5	54	2
5.5	1	6.5	36	3.7
5.5	1	6.5	54	2.1
5.5	1	6.5	72	1.2
5.5	1	7.3	36	3.6
5.5	1	7.3	54	2.1
5.5	1	7.3	72	1.2
5.5	1	8	36	3.3
5.5	1	8	54	2.2
5.5	1	8	72	1.2
5.5	1	8.4	45	2.9
5.5	1	8.6	54	2.1
5.5	1	9	72	1.2
5.5	1	9.5	54	2.3
5.5	1.5	5	36	2.7
5.5	1.5	6.5	36	NA
5.5	1.5	6.5	54	2.2
5.5	1.5	6.5	72	1.5
5.5	1.5	7.3	36	NA
5.5	1.5	7.3	54	2.3
5.5	1.5	7.3	72	1.6
5.5	1.5	8	36	2.8
5.5	1.5	8	54	2.3
5.5	1.5	8	72	1.5
5.5	1.5	9.5	36	2.7
5.5	1.5	9.5	54	2.3
5.63	1	8.3	36	3
5.67	1	8.3	36	2.9
5.75	1	8.3	36	2.8
6	1	7.15	18	5.2
6	1	8.1	27	3.1
6	1	8.7	36	2.5
6	1	9.3	54	>3.2
6.25	1	7.3	18	4.8
6.25	1	8.3	27	2.8
6.5	1	6.8	18	4.5
6.5	1	7.5	18	3.9
6.5	1	8.6	27	2.6
6.5	1	9.2	36	2
6.5	1	10	54	1.4
6.63	1	7.5	18	3.8
6.63	1	7.6	18	3.8
6.75	1	7.7	18	3.3
6.75	1	8.8	27	2.6
7.34	0.5	6.5	36	1.2
7.34	0.5	6.5	54	0.9
7.34	0.5	7.3	36	1.3
7.34	0.5	7.3	54	0.9
7.34	0.5	8	36	1.4
7.34	0.5	8	54	0.9
7.34	1	6.5	36	1.4
7.34	1	6.5	54	0.8
7.34	1	7.3	36	1.3
7.34	1	7.3	54	>.6
7.34	1	8	18	3
7.34	1	8	36	1.3
7.34	1	8	54	0.7
7.34	1.5	6.5	36	>1.8
7.34	1.5	6.5	54	0.8
7.34	1.5	7.3	36	1.3
7.34	1.5	7.3	54	0.8
7.34	1.5	8	36	1.3
7.34	1.5	8	54	>.5

$b_f/2t_f$	: Flange Slenderness Ratio
h/t_w	: Web Slenderness Ratio
L_b	: Unbraced Length in Multiples of d
b	: # times AISC Recommended Bracing Stiffness
R	: Rotation Capacity Achieved

Table A-3 Rotation Capacities Ordered by Increasing $b_f/2t_f$, β, h/t_w, and L_b, Respectively

$b_f/2t_f$	b	h/t_w	L_b	R
2	3.5	60	1	1.2
2.5	4.3	60	1	2.1
3	5.1	60	1	2.4
3	5.2	72	1	1.4
3.5	5.9	60	1	2.3
3.5	5.9	66	1	2.1
3.5	6	72	1	1.6
3.5	6.5	54	0.5	1.6
3.5	6.5	54	1	>2.5
3.5	6.5	54	1.5	>2.5
3.5	6.5	72	0.5	1.5
3.5	6.5	72	1	1.6
3.5	6.5	72	1.5	2
3.5	7.3	54	0.5	1.6
3.5	7.3	54	1	3.3
3.5	7.3	54	1.5	2.6
3.5	7.3	72	0.5	1.5
3.5	7.3	72	1	1.6
3.5	7.3	72	1.5	1.5
3.5	8	54	0.5	1.7
3.5	8	54	1	3.3
3.5	8	54	1.5	>2.5
3.5	8	72	0.5	1.5
3.5	8	72	1	1.6
3.5	8	72	1.5	1.6
4	6.6	54	1	3.4
4	6.6	60	1	2.2
4	6.7	66	1	1.9
4.25	6.9	54	1	3.4
4.25	7	54	1	3.5
4.5	1	54	1	1.5
4.5	4	54	1	3.2
4.5	4.6	54	1	2.8
4.5	5	54	0.5	1.6
4.5	5	54	1	2.9
4.5	5	54	1.5	>2.6
4.5	5	72	0.5	1.2
4.5	5	72	1	1.6
4.5	5	72	1.5	1.5
4.5	5.3	18	1	6
4.5	5.3	54	1	3
4.5	5.9	18	1	>6
4.5	5.9	54	1	>3.1
4.5	5.9	54	2	1.6
4.5	6.25	54	1.5	>2.6
4.5	6.3	36	1	4.5
4.5	6.5	27	1	5.4
4.5	6.5	36	0.5	1.8
4.5	6.5	36	1	4.5
4.5	6.5	36	1.5	4.4
4.5	6.5	36	2	3.1
4.5	6.5	54	0.5	1.6
4.5	6.5	54	1	3.3
4.5	6.5	54	1.5	2.7
4.5	6.5	54	2	1.6
4.5	6.5	72	0.5	1.8
4.5	6.5	72	1	1.6
4.5	6.5	72	1.5	1.6
4.5	6.5	72	2	1

$b_f/2t_f$	b	h/t_w	L_b	R
4.5	6.75	54	1	3.8
4.5	6.8	54	1	3.8
4.5	6.8	72	1	>1.5
4.5	6.9	54	1.5	2.8
4.5	7	36	1	4.4
4.5	7	45	1	4.2
4.5	7	54	0.5	1.6
4.5	7	54	1	>3
4.5	7	54	1.5	>2.6
4.5	7	54	2	1.6
4.5	7.3	36	0.5	1.9
4.5	7.3	36	1	4.9
4.5	7.3	36	1.5	4.6
4.5	7.3	36	2	3.1
4.5	7.3	54	0.5	1.7
4.5	7.3	54	1	4
4.5	7.3	54	1.5	>2.6
4.5	7.3	54	2	1.6
4.5	7.3	60	1	2
4.5	7.3	72	0.5	1.9
4.5	7.3	72	1	1.6
4.5	7.3	72	1.5	>1.5
4.5	7.3	72	2	>.9
4.5	7.5	54	0.5	1.7
4.5	7.5	54	1	3.5
4.5	7.5	54	1.5	2.8
4.5	7.5	54	2	1.6
4.5	7.5	72	1	1.6
4.5	7.7	54	0.5	1.7
4.5	8	36	0.5	1.9
4.5	8	36	1	6
4.5	8	36	1.5	4.5
4.5	8	36	2	3.2
4.5	8	54	0.5	1.7
4.5	8	54	1	3.4
4.5	8	54	1.5	2.8
4.5	8	54	2	1.6
4.5	8	72	0.5	1.9
4.5	8	72	1	1.6
4.5	8	72	1.5	>1.5
4.5	8	72	2	0.9
4.5	8.4	54	0.5	1.8
4.5	9.3	54	1	3.1
4.5	9.5	36	1	4.3
4.5	9.5	36	1.5	2.7
4.5	9.5	54	1	3.1
4.5	9.5	54	1.5	2.8
4.5	9.5	72	0.5	1.8
4.5	9.5	72	1	1.6
4.5	9.5	72	1.5	>1.5
4.5	inf	54	1	1.9
4.75	7.5	54	1	3
4.75	7.6	54	1	3
5	8	54	1	2.7
5.25	8.1	45	1	3.4
5.5	5	36	1	3.5
5.5	5	36	1.5	2.7
5.5	5	54	1	2
5.5	6.5	36	0.5	1.5

$b_f/2t_f$	b	h/t_w	L_b	R
5.5	6.5	36	1	3.7
5.5	6.5	36	1.5	NA
5.5	6.5	54	0.5	1.4
5.5	6.5	54	1	2.1
5.5	6.5	54	1.5	2.2
5.5	6.5	72	0.5	1.2
5.5	6.5	72	1	1.2
5.5	6.5	72	1.5	1.5
5.5	7.3	36	0.5	1.7
5.5	7.3	36	1	3.6
5.5	7.3	36	1.5	NA
5.5	7.3	54	0.5	1.5
5.5	7.3	54	1	2.1
5.5	7.3	54	1.5	2.3
5.5	7.3	72	0.5	1.5
5.5	7.3	72	1	1.2
5.5	7.3	72	1.5	1.6
5.5	8	36	0.5	1.7
5.5	8	36	1	3.3
5.5	8	36	1.5	2.8
5.5	8	54	0.5	1.6
5.5	8	54	1	2.2
5.5	8	54	1.5	2.3
5.5	8	72	0.5	1.5
5.5	8	72	1	1.2
5.5	8	72	1.5	1.5
5.5	8.4	45	1	2.9
5.5	8.6	54	1	2.1
5.5	9	72	1	1.2
5.5	9.5	36	1.5	2.7
5.5	9.5	54	1	2.3
5.5	9.5	54	1.5	2.3
5.63	8.3	36	1	3
5.67	8.3	36	1	2.9
5.75	8.3	36	1	2.8
6	7.15	18	1	5.2
6	8.1	27	1	3.1
6	8.7	36	1	2.5
6	9.3	54	1	>3.2
6.25	7.3	18	1	4.8
6.25	8.3	27	1	2.8
6.5	6.8	18	1	4.5
6.5	7.5	18	1	3.9
6.5	8.6	27	1	2.6
6.5	9.2	36	1	2
6.5	10	54	1	1.4
6.63	7.5	18	1	3.8
6.63	7.6	18	1	3.8
6.75	7.7	18	1	3.3
6.75	8.8	27	1	2.6
7.34	6.5	36	0.5	1.2
7.34	6.5	36	1	1.4
7.34	6.5	36	1.5	>1.8
7.34	6.5	54	0.5	0.9
7.34	6.5	54	1	0.8
7.34	6.5	54	1.5	0.8
7.34	7.3	36	0.5	1.3
7.34	7.3	36	1	1.3
7.34	7.3	36	1.5	1.3
7.34	7.3	54	0.5	0.9
7.34	7.3	54	1	>.6
7.34	7.3	54	1.5	0.8
7.34	8	18	1	3
7.34	8	36	0.5	1.4
7.34	8	36	1	1.3
7.34	8	36	1.5	1.3
7.34	8	54	0.5	0.9
7.34	8	54	1	0.7
7.34	8	54	1.5	>.5

$b_f/2t_f$	: Flange Slenderness Ratio
h/t_w	: Web Slenderness Ratio
L_b	: Unbraced Length in Multiples of d
b	: # times AISC Recommended Bracing Stiffness
R	: Rotation Capacity Achieved

Table A-4 Rotation Capacities Ordered by Increasing h/t_w, $b_f/2t_f$, L_b, and β, Respectively

h/t_w	$b_f/2t_f$	L_b	b	R
18	4.5	1	5.3	6
18	4.5	1	5.9	>6
18	6	1	7.15	5.2
18	6.25	1	7.3	4.8
18	6.5	1	6.8	4.5
18	6.5	1	7.5	3.9
18	6.63	1	7.5	3.8
18	6.63	1	7.6	3.8
18	6.75	1	7.7	3.3
18	7.34	1	8	3
27	4.5	1	6.5	5.4
27	6	1	8.1	3.1
27	6.25	1	8.3	2.8
27	6.5	1	8.6	2.6
27	6.75	1	8.8	2.6
36	4.5	0.5	6.5	1.8
36	4.5	0.5	7.3	1.9
36	4.5	0.5	8	1.9
36	4.5	1	6.3	4.5
36	4.5	1	6.5	4.5
36	4.5	1	7	4.4
36	4.5	1	7.3	4.9
36	4.5	1	8	6
36	4.5	1	9.5	4.3
36	4.5	1.5	6.5	4.4
36	4.5	1.5	7.3	4.6
36	4.5	1.5	8	4.5
36	4.5	1.5	9.5	2.7
36	4.5	2	6.5	3.1
36	4.5	2	7.3	3.1
36	4.5	2	8	3.2
36	5.5	0.5	6.5	1.5
36	5.5	0.5	7.3	1.7
36	5.5	0.5	8	1.7
36	5.5	1	5	3.5
36	5.5	1	6.5	3.7
36	5.5	1	7.3	3.6
36	5.5	1	8	3.3
36	5.5	1.5	5	2.7
36	5.5	1.5	6.5	NA
36	5.5	1.5	7.3	NA
36	5.5	1.5	8	2.8
36	5.5	1.5	9.5	2.7
36	5.63	1	8.3	3
36	5.67	1	8.3	2.9
36	5.75	1	8.3	2.8
36	6	1	8.7	2.5
36	6.5	1	9.2	2
36	7.34	0.5	6.5	1.2
36	7.34	0.5	7.3	1.3
36	7.34	0.5	8	1.4
36	7.34	1	6.5	1.4
36	7.34	1	7.3	1.3
36	7.34	1	8	1.3
36	7.34	1.5	6.5	>1.8
36	7.34	1.5	7.3	1.3
36	7.34	1.5	8	1.3
45	4.5	1	7	4.2
45	5.25	1	8.1	3.4

h/t_w	$b_f/2t_f$	L_b	b	R
45	5.5	1	8.4	2.9
54	3.5	0.5	6.5	1.6
54	3.5	0.5	7.3	1.6
54	3.5	0.5	8	1.7
54	3.5	1	6.5	>2.5
54	3.5	1	7.3	3.3
54	3.5	1	8	3.3
54	3.5	1.5	6.5	>2.5
54	3.5	1.5	7.3	2.6
54	3.5	1.5	8	>2.5
54	4	1	6.6	3.4
54	4.25	1	6.9	3.4
54	4.25	1	7	3.5
54	4.5	0.5	5	1.6
54	4.5	0.5	6.5	1.6
54	4.5	0.5	7	1.6
54	4.5	0.5	7.3	1.7
54	4.5	0.5	7.5	1.7
54	4.5	0.5	7.7	1.7
54	4.5	0.5	8	1.7
54	4.5	0.5	8.4	1.8
54	4.5	1	1	1.5
54	4.5	1	4	3.2
54	4.5	1	4.6	2.8
54	4.5	1	5	2.9
54	4.5	1	5.3	3
54	4.5	1	5.9	>3.1
54	4.5	1	6.5	3.3
54	4.5	1	6.75	3.8
54	4.5	1	6.8	3.8
54	4.5	1	7	>3
54	4.5	1	7.3	4
54	4.5	1	7.5	3.5
54	4.5	1	8	3.4
54	4.5	1	9.3	3.1
54	4.5	1	9.5	3.1
54	4.5	1	inf	1.9
54	4.5	1.5	5	>2.6
54	4.5	1.5	6.25	>2.6
54	4.5	1.5	6.5	2.7
54	4.5	1.5	6.9	2.8
54	4.5	1.5	7	>2.6
54	4.5	1.5	7.3	>2.6
54	4.5	1.5	7.5	2.8
54	4.5	1.5	8	2.8
54	4.5	1.5	9.5	2.8
54	4.5	2	5.9	1.6
54	4.5	2	6.5	1.6
54	4.5	2	7	1.6
54	4.5	2	7.3	1.6
54	4.5	2	7.5	1.6
54	4.5	2	8	1.6
54	4.75	1	7.5	3
54	4.75	1	7.6	3
54	5	1	8	2.7
54	5.5	0.5	6.5	1.4
54	5.5	0.5	7.3	1.5
54	5.5	0.5	8	1.6
54	5.5	1	5	2
54	5.5	1	6.5	2.1

h/t_w	$b_f/2t_f$	L_b	b	R
54	5.5	1	8	2.2
54	5.5	1	8.6	2.1
54	5.5	1	9.5	2.3
54	5.5	1.5	6.5	2.2
54	5.5	1.5	7.3	2.3
54	5.5	1.5	8	2.3
54	5.5	1.5	9.5	2.3
54	6	1	9.3	>3.2
54	6.5	1	10	1.4
54	7.34	0.5	6.5	0.9
54	7.34	0.5	7.3	0.9
54	7.34	0.5	8	0.9
54	7.34	1	6.5	0.8
54	7.34	1	7.3	>.6
54	7.34	1	8	0.7
54	7.34	1.5	6.5	0.8
54	7.34	1.5	7.3	0.8
54	7.34	1.5	8	>.5
60	2	1	3.5	1.2
60	2.5	1	4.3	2.1
60	3	1	5.1	2.4
60	3.5	1	5.9	2.3
60	4	1	6.6	2.2
60	4.5	1	7.3	2
66	3.5	1	5.9	2.1
66	4	1	6.7	1.9
66	4.5	1	7.3	1.7
72	3	1	5.2	1.4
72	3.5	0.5	6.5	1.5
72	3.5	0.5	7.3	1.5
72	3.5	0.5	8	1.5
72	3.5	1	6	1.6
72	3.5	1	6.5	1.6
72	3.5	1	7.3	1.6
72	3.5	1	8	1.6
72	3.5	1.5	6.5	2
72	3.5	1.5	7.3	1.5
72	3.5	1.5	8	1.6
72	4.5	0.5	5	1.2
72	4.5	0.5	6.5	1.8
72	4.5	0.5	7.3	1.9
72	4.5	0.5	8	1.9
72	4.5	0.5	9.5	1.8
72	4.5	1	5	1.6
72	4.5	1	6.5	1.6
72	4.5	1	6.8	>1.5
72	4.5	1	7.3	1.6
72	4.5	1	7.5	1.6
72	4.5	1	8	1.6
72	4.5	1	9.5	1.6
72	4.5	1.5	5	1.5
72	4.5	1.5	6.5	1.6
72	4.5	1.5	7.3	>1.5
72	4.5	1.5	8	>1.5
72	4.5	1.5	9.5	>1.5
72	4.5	2	6.5	1
72	4.5	2	7.3	>.9
72	4.5	2	8	0.9
72	5.5	0.5	6.5	1.2
72	5.5	0.5	7.3	1.5
72	5.5	0.5	8	1.5
72	5.5	1	6.5	1.2
72	5.5	1	7.3	1.2
72	5.5	1	8	1.2
72	5.5	1	9	1.2
72	5.5	1.5	6.5	1.5
72	5.5	1.5	7.3	1.6
72	5.5	1.5	8	1.5

$b_f/2t_f$	: Flange Slenderness Ratio
h/t_w	: Web Slenderness Ratio
L_b	: Unbraced Length in Multiples of d
b	: # times AISC Recommended Bracing Stiffness
R	: Rotation Capacity Achieved

Table A-5 Rotation Capacities Ordered by Increasing h/t_w, L_b, β, and $b_f/2t_f$, Respectively

h/t_w	L_b	β	$b_f/2t_f$	R
18	1	5.3	4.5	6
18	1	5.9	4.5	>6
18	1	7.15	6	5.2
18	1	7.3	6.25	4.8
18	1	6.8	6.5	4.5
18	1	7.5	6.5	3.9
18	1	7.5	6.63	3.8
18	1	7.6	6.63	3.8
18	1	7.7	6.75	3.3
18	1	8	7.34	3
27	1	6.5	4.5	5.4
27	1	8.1	6	3.1
27	1	8.3	6.25	2.8
27	1	8.6	6.5	2.6
27	1	8.8	6.75	2.6
36	0.5	6.5	4.5	1.8
36	0.5	7.3	4.5	1.9
36	0.5	8	4.5	1.9
36	1	6.3	4.5	4.5
36	1	6.5	4.5	4.5
36	1	7	4.5	4.4
36	1	7.3	4.5	4.9
36	1	8	4.5	6
36	1	9.5	4.5	4.3
36	1.5	6.5	4.5	4.4
36	1.5	7.3	4.5	4.6
36	1.5	8	4.5	4.5
36	1.5	9.5	4.5	2.7
36	2	6.5	4.5	3.1
36	2	7.3	4.5	3.1
36	2	8	4.5	3.2
36	0.5	6.5	5.5	1.5
36	0.5	7.3	5.5	1.7
36	0.5	8	5.5	1.7
36	1	5	5.5	3.5
36	1	6.5	5.5	3.7
36	1	7.3	5.5	3.6
36	1	8	5.5	3.3
36	1.5	5	5.5	2.7
36	1.5	6.5	5.5	NA
36	1.5	7.3	5.5	NA
36	1.5	8	5.5	2.8
36	1.5	9.5	5.5	2.7
36	1	8.3	5.63	3
36	1	8.3	5.67	2.9
36	1	8.3	5.75	2.8
36	1	8.7	6	2.5
36	1	9.2	6.5	2
36	0.5	6.5	7.34	1.2
36	0.5	7.3	7.34	1.3
36	0.5	8	7.34	1.4
36	1	6.5	7.34	1.4
36	1	7.3	7.34	1.3
36	1	8	7.34	1.3
36	1.5	6.5	7.34	>1.8
36	1.5	7.3	7.34	1.3
36	1.5	8	7.34	1.3
45	1	7	4.5	4.2
45	1	8.1	5.25	3.4

h/t_w	L_b	β	$b_f/2t_f$	R
45	1	8.4	5.5	2.9
54	0.5	6.5	3.5	1.6
54	0.5	7.3	3.5	1.6
54	0.5	8	3.5	1.7
54	1	6.5	3.5	>2.5
54	1	7.3	3.5	3.3
54	1	8	3.5	3.3
54	1.5	6.5	3.5	>2.5
54	1.5	7.3	3.5	2.6
54	1.5	8	3.5	>2.5
54	1	6.6	4	3.4
54	1	6.9	4.25	3.4
54	1	7	4.25	3.5
54	0.5	5	4.5	1.6
54	0.5	6.5	4.5	1.6
54	0.5	7	4.5	1.6
54	0.5	7.3	4.5	1.7
54	0.5	7.5	4.5	1.7
54	0.5	7.7	4.5	1.7
54	0.5	8	4.5	1.7
54	0.5	8.4	4.5	1.8
54	1	1	4.5	1.5
54	1	4	4.5	3.2
54	1	4.6	4.5	2.8
54	1	5	4.5	2.9
54	1	5.3	4.5	3
54	1	5.9	4.5	>3.1
54	1	6.5	4.5	3.3
54	1	6.75	4.5	3.8
54	1	6.8	4.5	3.8
54	1	7	4.5	>3
54	1	7.3	4.5	4
54	1	7.5	4.5	3.5
54	1	8	4.5	3.4
54	1	9.3	4.5	3.1
54	1	9.5	4.5	3.1
54	1	inf	4.5	1.9
54	1.5	5	4.5	>2.6
54	1.5	6.25	4.5	>2.6
54	1.5	6.5	4.5	2.7
54	1.5	6.9	4.5	2.8
54	1.5	7	4.5	>2.6
54	1.5	7.3	4.5	>2.6
54	1.5	7.5	4.5	2.8
54	1.5	8	4.5	2.8
54	1.5	9.5	4.5	2.8
54	2	5.9	4.5	1.6
54	2	6.5	4.5	1.6
54	2	7	4.5	1.6
54	2	7.3	4.5	1.6
54	2	7.5	4.5	1.6
54	2	8	4.5	1.6
54	1	7.5	4.75	3
54	1	7.6	4.75	3
54	1	8	5	2.7
54	0.5	6.5	5.5	1.4
54	0.5	7.3	5.5	1.5
54	0.5	8	5.5	1.6
54	1	5	5.5	2
54	1	6.5	5.5	2.1

h/t_w	L_b	β	$b_f/2t_f$	R
54	1	7.3	5.5	2.1
54	1	8	5.5	2.2
54	1	8.6	5.5	2.1
54	1	9.5	5.5	2.3
54	1.5	6.5	5.5	2.2
54	1.5	7.3	5.5	2.3
54	1.5	8	5.5	2.3
54	1.5	9.5	5.5	2.3
54	1	9.3	6	>3.2
54	1	10	6.5	1.4
54	0.5	6.5	7.34	0.9
54	0.5	7.3	7.34	0.9
54	0.5	8	7.34	0.9
54	1	6.5	7.34	0.8
54	1	7.3	7.34	>.6
54	1	8	7.34	0.7
54	1.5	6.5	7.34	0.8
54	1.5	7.3	7.34	0.8
54	1.5	8	7.34	>.5
60	1	3.5	2	1.2
60	1	4.3	2.5	2.1
60	1	5.1	3	2.4
60	1	5.9	3.5	2.3
60	1	6.6	4	2.2
60	1	7.3	4.5	2
66	1	5.9	3.5	2.1
66	1	6.7	4	1.9
66	1	7.3	4.5	1.7
72	1	5.2	3	1.4
72	0.5	6.5	3.5	1.5
72	0.5	7.3	3.5	1.5
72	0.5	8	3.5	1.5
72	1	6	3.5	1.6
72	1	6.5	3.5	1.6
72	1	7.3	3.5	1.6
72	1	8	3.5	1.6
72	1.5	6.5	3.5	2
72	1.5	7.3	3.5	1.5
72	1.5	8	3.5	1.6
72	0.5	5	4.5	1.2
72	0.5	6.5	4.5	1.8
72	0.5	7.3	4.5	1.9
72	0.5	8	4.5	1.9
72	0.5	9.5	4.5	1.8
72	1	5	4.5	1.6
72	1	6.5	4.5	1.6
72	1	6.8	4.5	>1.5
72	1	7.3	4.5	1.6
72	1	7.5	4.5	1.6
72	1	8	4.5	1.6
72	1	9.5	4.5	1.6
72	1.5	5	4.5	1.5
72	1.5	6.5	4.5	1.6
72	1.5	7.3	4.5	>1.5
72	1.5	8	4.5	>1.5
72	1.5	9.5	4.5	>1.5
72	2	6.5	4.5	1
72	2	7.3	4.5	>.9
72	2	8	4.5	0.9
72	0.5	6.5	5.5	1.2
72	0.5	7.3	5.5	1.5
72	0.5	8	5.5	1.5
72	1	6.5	5.5	1.2
72	1	7.3	5.5	1.2
72	1	8	5.5	1.2
72	1	9	5.5	1.2
72	1.5	6.5	5.5	1.5
72	1.5	7.3	5.5	1.6
72	1.5	8	5.5	1.5

$b_f/2t_f$	: Flange Slenderness Ratio
h/t_w	: Web Slenderness Ratio
L_b	: Unbraced Length in Multiples of d
β	: # times AISC Recommended Bracing Stiffness
R	: Rotation Capacity Achieved

Table A-6 Rotation Capacities Ordered by Increasing h/t$_w$, β, b$_f$/2t$_f$, and L$_b$, Respectively

h/t$_w$	b	b$_f$/2t$_f$	L$_b$	R
18	5.3	4.5	1	6
18	5.9	4.5	1	>6
18	6.8	6.5	1	4.5
18	7.15	6	1	5.2
18	7.3	6.25	1	4.8
18	7.5	6.5	1	3.9
18	7.5	6.63	1	3.8
18	7.6	6.63	1	3.8
18	7.7	6.75	1	3.3
18	8	7.34	1	3
27	6.5	4.5	1	5.4
27	8.1	6	1	3.1
27	8.3	6.25	1	2.8
27	8.6	6.5	1	2.6
27	8.8	6.75	1	2.6
36	5	5.5	1	3.5
36	5	5.5	1.5	2.7
36	6.3	4.5	1	4.5
36	6.5	4.5	0.5	1.8
36	6.5	4.5	1	4.5
36	6.5	4.5	1.5	4.4
36	6.5	4.5	2	3.1
36	6.5	5.5	0.5	1.5
36	6.5	5.5	1	3.7
36	6.5	5.5	1.5	NA
36	6.5	7.34	0.5	1.2
36	6.5	7.34	1	1.4
36	6.5	7.34	1.5	>1.8
36	7	4.5	1	4.4
36	7.3	4.5	0.5	1.9
36	7.3	4.5	1	4.9
36	7.3	4.5	1.5	4.6
36	7.3	4.5	2	3.1
36	7.3	5.5	0.5	1.7
36	7.3	5.5	1	3.6
36	7.3	5.5	1.5	NA
36	7.3	7.34	0.5	1.3
36	7.3	7.34	1	1.3
36	7.3	7.34	1.5	1.3
36	8	4.5	0.5	1.9
36	8	4.5	1	6
36	8	4.5	1.5	4.5
36	8	4.5	2	3.2
36	8	5.5	0.5	1.7
36	8	5.5	1	3.3
36	8	5.5	1.5	2.8
36	8	7.34	0.5	1.4
36	8	7.34	1	1.3
36	8	7.34	1.5	1.3
36	8.3	5.63	1	3
36	8.3	5.67	1	2.9
36	8.3	5.75	1	2.8
36	8.7	6	1	2.5
36	9.2	6.5	1	2
36	9.5	4.5	1	4.3
36	9.5	4.5	1.5	2.7
36	9.5	5.5	1.5	2.7
45	7	4.5	1	4.2
45	8.1	5.25	1	3.4

h/t$_w$	b	b$_f$/2t$_f$	L$_b$	R
45	8.4	5.5	1	2.9
54	1	4.5	1	1.5
54	4	4.5	1	3.2
54	4.6	4.5	1	2.8
54	5	4.5	0.5	1.6
54	5	4.5	1	2.9
54	5	4.5	1.5	>2.6
54	5	5.5	1	2
54	5.3	4.5	1	3
54	5.9	4.5	1	>3.1
54	5.9	4.5	2	1.6
54	6.25	4.5	1.5	>2.6
54	6.5	3.5	0.5	1.6
54	6.5	3.5	1	>2.5
54	6.5	3.5	1.5	>2.5
54	6.5	4.5	0.5	1.6
54	6.5	4.5	1	3.3
54	6.5	4.5	1.5	2.7
54	6.5	4.5	2	1.6
54	6.5	5.5	0.5	1.4
54	6.5	5.5	1	2.1
54	6.5	5.5	1.5	2.2
54	6.5	7.34	0.5	0.9
54	6.5	7.34	1	0.8
54	6.5	7.34	1.5	0.8
54	6.6	4	1	3.4
54	6.75	4.5	1	3.8
54	6.8	4.5	1	3.8
54	6.9	4.25	1	3.4
54	6.9	4.5	1.5	2.8
54	7	4.25	1	3.5
54	7	4.5	0.5	1.6
54	7	4.5	1	>3
54	7	4.5	1.5	>2.6
54	7	4.5	2	1.6
54	7.3	3.5	0.5	1.6
54	7.3	3.5	1	3.3
54	7.3	3.5	1.5	2.6
54	7.3	4.5	0.5	1.7
54	7.3	4.5	1	4
54	7.3	4.5	1.5	>2.6
54	7.3	4.5	2	1.6
54	7.3	5.5	0.5	1.5
54	7.3	5.5	1	2.1
54	7.3	5.5	1.5	2.3
54	7.3	7.34	0.5	0.9
54	7.3	7.34	1	>.6
54	7.3	7.34	1.5	0.8
54	7.5	4.5	0.5	1.7
54	7.5	4.5	1	3.5
54	7.5	4.5	1.5	2.8
54	7.5	4.5	2	1.6
54	7.5	4.75	1	3
54	7.6	4.75	1	3
54	7.7	4.5	0.5	1.7
54	8	3.5	0.5	1.7
54	8	3.5	1	3.3
54	8	3.5	1.5	>2.5
54	8	4.5	0.5	1.7
54	8	4.5	1	3.4

h/t$_w$	b	b$_f$/2t$_f$	L$_b$	R
54	8	4.5	1.5	2.8
54	8	4.5	2	1.6
54	8	5	1	2.7
54	8	5.5	0.5	1.6
54	8	5.5	1	2.2
54	8	5.5	1.5	2.3
54	8	7.34	0.5	0.9
54	8	7.34	1	0.7
54	8	7.34	1.5	>.5
54	8.4	4.5	0.5	1.8
54	8.6	5.5	1	2.1
54	9.3	4.5	1	3.1
54	9.3	6	1	>3.2
54	9.5	4.5	1	3.1
54	9.5	4.5	1.5	2.8
54	9.5	5.5	1	2.3
54	9.5	5.5	1.5	2.3
54	10	6.5	1	1.4
54	inf	4.5	1	1.9
60	3.5	2	1	1.2
60	4.3	2.5	1	2.1
60	5.1	3	1	2.4
60	5.9	3.5	1	2.3
60	6.6	4	1	2.2
60	7.3	4.5	1	2
66	5.9	3.5	1	2.1
66	6.7	4	1	1.9
66	7.3	4.5	1	1.7
72	5	4.5	0.5	1.2
72	5	4.5	1	1.6
72	5	4.5	1.5	1.5
72	5.2	3	1	1.4
72	6	3.5	1	1.6
72	6.5	3.5	0.5	1.5
72	6.5	3.5	1	1.6
72	6.5	3.5	1.5	2
72	6.5	4.5	0.5	1.8
72	6.5	4.5	1	1.6
72	6.5	4.5	1.5	1.6
72	6.5	4.5	2	1
72	6.5	5.5	0.5	1.2
72	6.5	5.5	1	1.2
72	6.5	5.5	1.5	1.5
72	6.8	4.5	1	>1.5
72	7.3	3.5	0.5	1.5
72	7.3	3.5	1	1.6
72	7.3	3.5	1.5	1.5
72	7.3	4.5	0.5	1.9
72	7.3	4.5	1	1.6
72	7.3	4.5	1.5	>1.5
72	7.3	4.5	2	>.9
72	7.3	5.5	0.5	1.5
72	7.3	5.5	1	1.2
72	7.3	5.5	1.5	1.6
72	7.5	4.5	1	1.6
72	8	3.5	0.5	1.5
72	8	3.5	1	1.6
72	8	3.5	1.5	1.6
72	8	4.5	0.5	1.9
72	8	4.5	1	1.6
72	8	4.5	1.5	>1.5
72	8	4.5	2	0.9
72	8	5.5	0.5	1.5
72	8	5.5	1	1.2
72	8	5.5	1.5	1.5
72	9	5.5	1	1.2
72	9.5	4.5	0.5	1.8
72	9.5	4.5	1	1.6
72	9.5	4.5	1.5	>1.5

b$_f$/2t$_f$	:	Flange Slenderness Ratio
h/t$_w$	:	Web Slenderness Ratio
L$_b$	:	Unbraced Length in Multiples of d
b	:	# times AISC Recommended Bracing Stiffness
R	:	Rotation Capacity Achieved

Table A-7 Rotation Capacities Ordered by Increasing L_b, $b_f/2t_f$, h/t_w, and β, Respectively

L_b	$b_f/2t_f$	h/t_w	b	R
0.5	3.5	54	6.5	1.6
0.5	3.5	54	7.3	1.6
0.5	3.5	54	8	1.7
0.5	3.5	72	6.5	1.5
0.5	3.5	72	7.3	1.5
0.5	3.5	72	8	1.5
0.5	4.5	36	6.5	1.8
0.5	4.5	36	7.3	1.9
0.5	4.5	36	8	1.9
0.5	4.5	54	5	1.6
0.5	4.5	54	6.5	1.6
0.5	4.5	54	7	1.6
0.5	4.5	54	7.3	1.7
0.5	4.5	54	7.5	1.7
0.5	4.5	54	7.7	1.7
0.5	4.5	54	8	1.7
0.5	4.5	54	8.4	1.8
0.5	4.5	72	5	1.2
0.5	4.5	72	6.5	1.8
0.5	4.5	72	7.3	1.9
0.5	4.5	72	8	1.9
0.5	4.5	72	9.5	1.8
0.5	5.5	36	6.5	1.5
0.5	5.5	36	7.3	1.7
0.5	5.5	36	8	1.7
0.5	5.5	54	6.5	1.4
0.5	5.5	54	7.3	1.5
0.5	5.5	54	8	1.6
0.5	5.5	72	6.5	1.2
0.5	5.5	72	7.3	1.5
0.5	5.5	72	8	1.5
0.5	7.34	36	6.5	1.2
0.5	7.34	36	7.3	1.3
0.5	7.34	36	8	1.4
0.5	7.34	54	6.5	0.9
0.5	7.34	54	7.3	0.9
0.5	7.34	54	8	0.9
1	2	60	3.5	1.2
1	2.5	60	4.3	2.1
1	3	60	5.1	2.4
1	3	72	5.2	1.4
1	3.5	54	6.5	>2.5
1	3.5	54	7.3	3.3
1	3.5	54	8	3.3
1	3.5	60	5.9	2.3
1	3.5	66	5.9	2.1
1	3.5	72	6	1.6
1	3.5	72	6.5	1.6
1	3.5	72	7.3	1.6
1	3.5	72	8	1.6
1	4	54	6.6	3.4
1	4	60	6.6	2.2
1	4	66	6.7	1.9
1	4.25	54	6.9	3.4
1	4.25	54	7	3.5
1	4.5	18	5.3	6
1	4.5	18	5.9	>6
1	4.5	27	6.5	5.4
1	4.5	36	6.3	4.5
1	4.5	36	6.5	4.5
1	4.5	36	7	4.4
1	4.5	36	7.3	4.9
1	4.5	36	8	6
1	4.5	36	9.5	4.3
1	4.5	45	7	4.2
1	4.5	54	1	1.5
1	4.5	54	4	3.2
1	4.5	54	4.6	2.8
1	4.5	54	5	2.9
1	4.5	54	5.3	3
1	4.5	54	5.9	>3.1
1	4.5	54	6.5	3.3
1	4.5	54	6.75	3.8
1	4.5	54	6.8	3.8
1	4.5	54	7	>3
1	4.5	54	7.3	4
1	4.5	54	7.5	3.5
1	4.5	54	8	3.4
1	4.5	54	9.3	3.1
1	4.5	54	9.5	3.1
1	4.5	54	inf	1.9
1	4.5	60	7.3	2
1	4.5	66	7.3	1.7
1	4.5	72	6.5	1.6
1	4.5	72	6.8	>1.5
1	4.5	72	7.3	1.6
1	4.5	72	7.5	1.6
1	4.5	72	8	1.6
1	4.5	72	9.5	1.6
1	4.75	54	7.5	3
1	4.75	54	7.6	3
1	5	54	8	2.7
1	5.25	45	8.1	3.4
1	5.5	36	5	3.5
1	5.5	36	6.5	3.7
1	5.5	36	7.3	3.6
1	5.5	36	8	3.3
1	5.5	45	8.4	2.9
1	5.5	54	5	2
1	5.5	54	6.5	2.1
1	5.5	54	7.3	2.1
1	5.5	54	8	2.2
1	5.5	54	8.6	2.1
1	5.5	54	9.5	2.3
1	5.5	72	6.5	1.2
1	5.5	72	7.3	1.2
1	5.5	72	8	1.2
1	5.5	72	9	1.2
1	5.63	36	8.3	3
1	5.67	36	8.3	2.9
1	5.75	36	8.3	2.8
1	6	18	7.15	5.2
1	6	27	8.1	3.1
1	6	36	8.7	2.5
1	6	54	9.3	>3.2
1	6.25	18	7.3	4.8
1	6.25	27	8.3	2.8
1	6.5	18	6.8	4.5
1	6.5	18	7.5	3.9
1	6.5	27	8.6	2.6
1	6.5	36	9.2	2
1	6.5	54	10	1.4
1	6.63	18	7.5	3.8
1	6.63	18	7.6	3.8
1	6.75	18	7.7	3.3
1	6.75	27	8.8	2.6
1	7.34	18	8	3
1	7.34	36	6.5	1.4
1	7.34	36	7.3	1.3
1	7.34	36	8	1.3
1	7.34	54	6.5	0.8
1	7.34	54	7.3	>.6
1	7.34	54	8	0.7
1.5	3.5	54	6.5	>2.5
1.5	3.5	54	7.3	2.6
1.5	3.5	54	8	>2.5
1.5	3.5	72	6.5	2
1.5	3.5	72	7.3	1.5
1.5	3.5	72	8	1.6
1.5	4.5	36	6.5	4.4
1.5	4.5	36	7.3	4.6
1.5	4.5	36	8	4.5
1.5	4.5	36	9.5	2.7
1.5	4.5	54	5	>2.6
1.5	4.5	54	6.25	>2.6
1.5	4.5	54	6.5	2.7
1.5	4.5	54	6.9	2.8
1.5	4.5	54	7	>2.6
1.5	4.5	54	7.3	>2.6
1.5	4.5	54	7.5	2.8
1.5	4.5	54	8	2.8
1.5	4.5	54	9.5	2.8
1.5	4.5	72	5	1.5
1.5	4.5	72	6.5	1.6
1.5	4.5	72	7.3	>1.5
1.5	4.5	72	8	>1.5
1.5	4.5	72	9.5	>1.5
1.5	5.5	36	5	2.7
1.5	5.5	36	6.5	NA
1.5	5.5	36	7.3	NA
1.5	5.5	36	8	2.8
1.5	5.5	36	9.5	2.7
1.5	5.5	54	6.5	2.2
1.5	5.5	54	7.3	2.3
1.5	5.5	54	8	2.3
1.5	5.5	54	9.5	2.3
1.5	5.5	72	6.5	1.5
1.5	5.5	72	7.3	1.6
1.5	5.5	72	8	1.5
1.5	7.34	36	6.5	>1.8
1.5	7.34	36	7.3	1.3
1.5	7.34	36	8	1.3
1.5	7.34	54	6.5	0.8
1.5	7.34	54	7.3	0.8
1.5	7.34	54	8	>.5
2	4.5	36	6.5	3.1
2	4.5	36	7.3	3.1
2	4.5	36	8	3.2
2	4.5	54	5.9	1.6
2	4.5	54	6.5	1.6
2	4.5	54	7	1.6
2	4.5	54	7.3	1.6
2	4.5	54	7.5	1.6
2	4.5	54	8	1.6
2	4.5	72	6.5	1
2	4.5	72	7.3	>.9
2	4.5	72	8	0.9

$b_f/2t_f$	: Flange Slenderness Ratio
h/t_w	: Web Slenderness Ratio
L_b	: Unbraced Length in Multiples of d
b	: # times AISC Recommended Bracing Stiffness
R	: Rotation Capacity Achieved

93

Table A-8 Rotation Capacities Ordered by Increasing L_b, h/t_w, $b_f/2t_f$, and β, Respectively

L_b	h/t_w	$b_f/2t_f$	β	R
0.5	36	4.5	6.5	1.8
0.5	36	4.5	7.3	1.9
0.5	36	4.5	8	1.9
0.5	36	5.5	6.5	1.5
0.5	36	5.5	7.3	1.7
0.5	36	5.5	8	1.7
0.5	36	7.34	6.5	1.2
0.5	36	7.34	7.3	1.3
0.5	36	7.34	8	1.4
0.5	54	3.5	6.5	1.6
0.5	54	3.5	7.3	1.6
0.5	54	3.5	8	1.7
0.5	54	4.5	5	1.6
0.5	54	4.5	6.5	1.6
0.5	54	4.5	7	1.6
0.5	54	4.5	7.3	1.7
0.5	54	4.5	7.5	1.7
0.5	54	4.5	7.7	1.7
0.5	54	4.5	8	1.7
0.5	54	4.5	8.4	1.8
0.5	54	5.5	6.5	1.4
0.5	54	5.5	7.3	1.5
0.5	54	5.5	8	1.6
0.5	54	7.34	6.5	0.9
0.5	54	7.34	7.3	0.9
0.5	54	7.34	8	0.9
0.5	72	3.5	6.5	1.5
0.5	72	3.5	7.3	1.5
0.5	72	3.5	8	1.5
0.5	72	4.5	5	1.2
0.5	72	4.5	6.5	1.8
0.5	72	4.5	7.3	1.9
0.5	72	4.5	8	1.9
0.5	72	4.5	9.5	1.8
0.5	72	5.5	6.5	1.2
0.5	72	5.5	7.3	1.5
0.5	72	5.5	8	1.5
1	18	4.5	5.3	6
1	18	4.5	5.9	>6
1	18	6	7.15	5.2
1	18	6.25	7.3	4.8
1	18	6.5	6.8	4.5
1	18	6.5	7.5	3.9
1	18	6.63	7.5	3.8
1	18	6.63	7.6	3.8
1	18	6.75	7.7	3.3
1	18	7.34	8	3
1	27	4.5	6.5	5.4
1	27	6	8.1	3.1
1	27	6.25	8.3	2.8
1	27	6.5	8.6	2.6
1	27	6.75	8.8	2.6
1	36	4.5	6.3	4.5
1	36	4.5	6.5	4.5
1	36	4.5	7	4.4
1	36	4.5	7.3	4.9
1	36	4.5	8	6
1	36	4.5	9.5	4.3
1	36	5.5	5	3.5

L_b	h/t_w	$b_f/2t_f$	β	R
1	36	5.5	6.5	3.7
1	36	5.5	7.3	3.6
1	36	5.5	8	3.3
1	36	5.63	8.3	3
1	36	5.67	8.3	2.9
1	36	5.75	8.3	2.8
1	36	6	8.7	2.5
1	36	6.5	9.2	2
1	36	7.34	6.5	1.4
1	36	7.34	7.3	1.3
1	36	7.34	8	1.3
1	45	4.5	7	4.2
1	45	5.25	8.1	3.4
1	45	5.5	8.4	2.9
1	54	3.5	6.5	>2.5
1	54	3.5	7.3	3.3
1	54	3.5	8	3.3
1	54	4	6.6	3.4
1	54	4.25	6.9	3.4
1	54	4.25	7	3.5
1	54	4.5	1	1.5
1	54	4.5	4	3.2
1	54	4.5	4.6	2.8
1	54	4.5	5	2.9
1	54	4.5	5.3	3
1	54	4.5	5.9	>3.1
1	54	4.5	6.5	3.3
1	54	4.5	6.75	3.8
1	54	4.5	6.8	3.8
1	54	4.5	7	>3
1	54	4.5	7.3	4
1	54	4.5	7.5	3.5
1	54	4.5	8	3.4
1	54	4.5	9.3	3.1
1	54	4.5	9.5	3.1
1	54	4.5	inf	1.9
1	54	4.75	7.5	3
1	54	4.75	7.6	3
1	54	5	8	2.7
1	54	5.5	5	2
1	54	5.5	6.5	2.1
1	54	5.5	7.3	2.1
1	54	5.5	8	2.2
1	54	5.5	8.6	2.1
1	54	5.5	9.5	2.3
1	54	6	9.3	>3.2
1	54	6.5	10	1.4
1	54	7.34	6.5	0.8
1	54	7.34	7.3	>.6
1	54	7.34	8	0.7
1	60	2	3.5	1.2
1	60	2.5	4.3	2.1
1	60	3	5.1	2.4
1	60	3.5	5.9	2.3
1	60	4	6.6	2.2
1	60	4.5	7.3	2
1	66	3.5	5.9	2.1
1	66	4	6.7	1.9
1	66	4.5	7.3	1.7
1	72	3	5.2	1.4

L_b	h/t_w	$b_f/2t_f$	β	R
1	72	3.5	6	1.6
1	72	3.5	6.5	1.6
1	72	3.5	7.3	1.6
1	72	3.5	8	1.6
1	72	4.5	5	1.6
1	72	4.5	6.5	1.6
1	72	4.5	6.8	>1.5
1	72	4.5	7.3	1.6
1	72	4.5	7.5	1.6
1	72	4.5	8	1.6
1	72	4.5	9.5	1.6
1	72	5.5	6.5	1.2
1	72	5.5	7.3	1.2
1	72	5.5	8	1.2
1	72	5.5	9	1.2
1.5	36	4.5	6.5	4.4
1.5	36	4.5	7.3	4.6
1.5	36	4.5	8	4.5
1.5	36	4.5	9.5	2.7
1.5	36	5.5	5	2.7
1.5	36	5.5	6.5	NA
1.5	36	5.5	7.3	NA
1.5	36	5.5	8	2.8
1.5	36	5.5	9.5	2.7
1.5	36	7.34	6.5	>1.8
1.5	36	7.34	7.3	1.3
1.5	36	7.34	8	1.3
1.5	54	3.5	6.5	>2.5
1.5	54	3.5	7.3	2.6
1.5	54	3.5	8	>2.5
1.5	54	4.5	5	>2.6
1.5	54	4.5	6.25	>2.6
1.5	54	4.5	6.5	2.7
1.5	54	4.5	6.9	2.8
1.5	54	4.5	7	>2.6
1.5	54	4.5	7.3	>2.6
1.5	54	4.5	7.5	2.8
1.5	54	4.5	8	2.8
1.5	54	4.5	9.5	2.8
1.5	54	5.5	6.5	2.2
1.5	54	5.5	7.3	2.3
1.5	54	5.5	8	2.3
1.5	54	5.5	9.5	2.3
1.5	54	7.34	6.5	0.8
1.5	54	7.34	7.3	0.8
1.5	54	7.34	8	>.5
1.5	72	3.5	6.5	2
1.5	72	3.5	7.3	1.5
1.5	72	3.5	8	1.6
1.5	72	4.5	5	1.5
1.5	72	4.5	6.5	1.6
1.5	72	4.5	7.3	>1.5
1.5	72	4.5	8	>1.5
1.5	72	4.5	9.5	>1.5
1.5	72	5.5	6.5	1.5
1.5	72	5.5	7.3	1.6
1.5	72	5.5	8	1.5
2	36	4.5	6.5	3.1
2	36	4.5	7.3	3.1
2	36	4.5	8	3.2
2	54	4.5	5.9	1.6
2	54	4.5	6.5	1.6
2	54	4.5	7	1.6
2	54	4.5	7.3	1.6
2	54	4.5	7.5	1.6
2	54	4.5	8	1.6
2	72	4.5	6.5	1
2	72	4.5	7.3	>.9
2	72	4.5	8	0.9

$b_f/2t_f$	: Flange Slenderness Ratio
h/t_w	: Web Slenderness Ratio
L_b	: Unbraced Length in Multiples of d
β	: # times AISC Recommended Bracing Stiffness
R	: Rotation Capacity Achieved

Table A-9 Rotation Capacities Ordered Increasing by L_b, h/t_w, β, and $b_f/2t_f$, Respectively

L_b	h/t_w	β	$b_f/2t_f$	R
0.5	36	6.5	4.5	1.8
0.5	36	6.5	5.5	1.5
0.5	36	6.5	7.34	1.2
0.5	36	7.3	4.5	1.9
0.5	36	7.3	5.5	1.7
0.5	36	7.3	7.34	1.3
0.5	36	8	4.5	1.9
0.5	36	8	5.5	1.7
0.5	36	8	7.34	1.4
0.5	54	5	4.5	1.6
0.5	54	6.5	3.5	1.6
0.5	54	6.5	4.5	1.6
0.5	54	6.5	5.5	1.4
0.5	54	6.5	7.34	0.9
0.5	54	7	4.5	1.6
0.5	54	7.3	3.5	1.6
0.5	54	7.3	4.5	1.7
0.5	54	7.3	5.5	1.5
0.5	54	7.3	7.34	0.9
0.5	54	7.5	4.5	1.7
0.5	54	7.7	4.5	1.7
0.5	54	8	3.5	1.7
0.5	54	8	4.5	1.7
0.5	54	8	5.5	1.6
0.5	54	8	7.34	0.9
0.5	54	8.4	4.5	1.8
0.5	72	5	4.5	1.2
0.5	72	6.5	3.5	1.5
0.5	72	6.5	4.5	1.8
0.5	72	6.5	5.5	1.2
0.5	72	7.3	3.5	1.5
0.5	72	7.3	4.5	1.9
0.5	72	7.3	5.5	1.5
0.5	72	8	3.5	1.5
0.5	72	8	4.5	1.9
0.5	72	8	5.5	1.5
0.5	72	9.5	4.5	1.8
1	18	5.3	4.5	6
1	18	5.9	4.5	>6
1	18	6.8	6.5	4.5
1	18	7.15	6	5.2
1	18	7.3	6.25	4.8
1	18	7.5	6.5	3.9
1	18	7.5	6.63	3.8
1	18	7.6	6.63	3.8
1	18	7.7	6.75	3.3
1	18	8	7.34	3
1	27	6.5	4.5	5.4
1	27	8.1	6	3.1
1	27	8.3	6.25	2.8
1	27	8.6	6.5	2.6
1	27	8.8	6.75	2.6
1	36	5	5.5	3.5
1	36	6.3	4.5	4.5
1	36	6.5	4.5	4.5
1	36	6.5	5.5	3.7
1	36	6.5	7.34	1.4
1	36	7	4.5	4.4
1	36	7.3	4.5	4.9
1	36	7.3	5.5	3.6
1	36	7.3	7.34	1.3
1	36	8	4.5	6
1	36	8	5.5	3.3
1	36	8.3	5.63	3
1	36	8.3	5.67	2.9
1	36	8.3	5.75	2.8
1	36	8.7	6	2.5
1	36	9.2	6.5	2
1	36	9.5	4.5	4.3
1	45	7	4.5	4.2
1	45	8.1	5.25	3.4
1	45	8.4	5.5	2.9
1	54	1	4.5	1.5
1	54	4	4.5	3.2
1	54	4.6	4.5	2.8
1	54	5	4.5	2.9
1	54	5	5.5	2
1	54	5.3	4.5	3
1	54	5.9	4.5	>3.1
1	54	6.5	3.5	>2.5
1	54	6.5	4.5	3.3
1	54	6.5	5.5	2.1
1	54	6.5	7.34	0.8
1	54	6.6	4	3.4
1	54	6.75	4.5	3.8
1	54	6.8	4.5	3.8
1	54	6.9	4.25	3.4
1	54	7	4.25	3.5
1	54	7	4.5	>3
1	54	7.3	3.5	3.3
1	54	7.3	4.5	4
1	54	7.3	5.5	2.1
1	54	7.3	7.34	>.6
1	54	7.5	4.5	3.5
1	54	7.5	4.75	3
1	54	7.6	4.75	3
1	54	8	3.5	3.3
1	54	8	4.5	3.4
1	54	8	5	2.7
1	54	8	5.5	2.2
1	54	8	7.34	0.7
1	54	8.6	5.5	2.1
1	54	9.3	4.5	3.1
1	54	9.3	6	>3.2
1	54	9.5	4.5	3.1
1	54	9.5	5.5	2.3
1	54	10	6.5	1.4
1	54	inf	4.5	1.9
1	60	3.5	2	1.2
1	60	4.3	2.5	2.1
1	60	5.1	3	2.4
1	60	5.9	3.5	2.3
1	60	6.6	4	2.2
1	60	7.3	4.5	2
1	66	5.9	3.5	2.1
1	66	6.7	4	1.9
1	66	7.3	4.5	1.7
1	72	5	4.5	1.6
1	72	5.2	3	1.4
1	72	6	3.5	1.6
1	72	6.5	3.5	1.6
1	72	6.5	4.5	1.6
1	72	6.5	5.5	1.2
1	72	6.8	4.5	>1.5
1	72	7.3	3.5	1.6
1	72	7.3	4.5	1.6
1	72	7.3	5.5	1.2
1	72	7.5	4.5	1.6
1	72	8	3.5	1.6
1	72	8	4.5	1.6
1	72	8	5.5	1.2
1	72	9	5.5	1.2
1	72	9.5	4.5	1.6
1.5	36	5	5.5	2.7
1.5	36	6.5	4.5	4.4
1.5	36	6.5	5.5	NA
1.5	36	6.5	7.34	>1.8
1.5	36	7.3	4.5	4.6
1.5	36	7.3	5.5	NA
1.5	36	7.3	7.34	1.3
1.5	36	8	4.5	4.5
1.5	36	8	5.5	2.8
1.5	36	8	7.34	1.3
1.5	36	9.5	4.5	2.7
1.5	36	9.5	5.5	2.7
1.5	54	5	4.5	>2.6
1.5	54	6.25	4.5	>2.6
1.5	54	6.5	3.5	>2.5
1.5	54	6.5	4.5	2.7
1.5	54	6.5	5.5	2.2
1.5	54	6.5	7.34	0.8
1.5	54	6.9	4.5	2.8
1.5	54	7	4.5	>2.6
1.5	54	7.3	3.5	2.6
1.5	54	7.3	4.5	>2.6
1.5	54	7.3	5.5	2.3
1.5	54	7.3	7.34	0.8
1.5	54	7.5	4.5	2.8
1.5	54	8	3.5	>2.5
1.5	54	8	4.5	2.8
1.5	54	8	5.5	2.3
1.5	54	8	7.34	>.5
1.5	54	9.5	4.5	2.8
1.5	54	9.5	5.5	2.3
1.5	72	5	4.5	1.5
1.5	72	6.5	3.5	2
1.5	72	6.5	4.5	1.6
1.5	72	6.5	5.5	1.5
1.5	72	7.3	3.5	1.5
1.5	72	7.3	4.5	>1.5
1.5	72	7.3	5.5	1.6
1.5	72	8	3.5	1.6
1.5	72	8	4.5	>1.5
1.5	72	8	5.5	1.5
1.5	72	9.5	4.5	>1.5
2	36	6.5	4.5	3.1
2	36	7.3	4.5	3.1
2	36	8	4.5	3.2
2	54	5.9	4.5	1.6
2	54	6.5	4.5	1.6
2	54	7	4.5	1.6
2	54	7.3	4.5	1.6
2	54	7.5	4.5	1.6
2	54	8	4.5	1.6
2	72	6.5	4.5	1
2	72	7.3	4.5	>.9
2	72	8	4.5	0.9

$b_f/2t_f$	: Flange Slenderness Ratio
h/t_w	: Web Slenderness Ratio
L_b	: Unbraced Length in Multiples of d
β	: # times AISC Recommended Bracing Stiffness
R	: Rotation Capacity Achieved

Table A-10 Rotation Capacities Ordered by Increasing β, b_f/2t_f, h/t_w, and L_b, Respectively

b	b_f/2t_f	h/t_w	L_b	R
1	4.5	54	1	1.5
3.5	2	60	1	1.2
4	4.5	54	1	3.2
4.3	2.5	60	1	2.1
4.6	4.5	54	1	2.8
5	4.5	54	0.5	1.6
5	4.5	54	1	2.9
5	4.5	54	1.5	>2.6
5	4.5	72	0.5	1.2
5	4.5	72	1	1.6
5	4.5	72	1.5	1.5
5	5.5	36	1	3.5
5	5.5	36	1.5	2.7
5	5.5	54	1	2
5.1	3	60	1	2.4
5.2	3	72	1	1.4
5.3	4.5	18	1	6
5.3	4.5	54	1	3
5.9	3.5	60	1	2.3
5.9	3.5	66	1	2.1
5.9	4.5	18	1	>6
5.9	4.5	54	1	>3.1
5.9	4.5	54	2	1.6
6	3.5	72	1	1.6
6.25	4.5	54	1.5	>2.6
6.3	4.5	36	1	4.5
6.5	3.5	54	0.5	1.6
6.5	3.5	54	1	>2.5
6.5	3.5	54	1.5	>2.5
6.5	3.5	72	0.5	1.5
6.5	3.5	72	1	1.6
6.5	3.5	72	1.5	2
6.5	4.5	27	1	5.4
6.5	4.5	36	0.5	1.8
6.5	4.5	36	1	4.5
6.5	4.5	36	1.5	4.4
6.5	4.5	36	2	3.1
6.5	4.5	54	0.5	1.6
6.5	4.5	54	1	3.3
6.5	4.5	54	1.5	2.7
6.5	4.5	54	2	1.6
6.5	4.5	72	0.5	1.8
6.5	4.5	72	1	1.6
6.5	4.5	72	1.5	1.6
6.5	4.5	72	2	1
6.5	5.5	36	0.5	1.5
6.5	5.5	36	1	3.7
6.5	5.5	36	1.5	NA
6.5	5.5	54	0.5	1.4
6.5	5.5	54	1	2.1
6.5	5.5	54	1.5	2.2
6.5	5.5	72	0.5	1.2
6.5	5.5	72	1	1.2
6.5	5.5	72	1.5	1.5
6.5	7.34	36	0.5	1.2
6.5	7.34	36	1	1.4
6.5	7.34	36	1.5	>1.8
6.5	7.34	54	0.5	0.9
6.5	7.34	54	1	0.8

b	b_f/2t_f	h/t_w	L_b	R
6.5	7.34	54	1.5	0.8
6.6	4	54	1	3.4
6.6	4	60	1	2.2
6.7	4	66	1	1.9
6.75	4.5	54	1	3.8
6.8	4.5	54	1	3.8
6.8	4.5	72	1	>1.5
6.8	6.5	18	1	4.5
6.9	4.25	54	1	3.4
6.9	4.5	54	1.5	2.8
7	4.25	54	1	3.5
7	4.5	36	1	4.4
7	4.5	45	1	4.2
7	4.5	54	0.5	1.6
7	4.5	54	1	>3
7	4.5	54	1.5	>2.6
7	4.5	54	2	1.6
7.15	6	18	1	5.2
7.3	3.5	54	0.5	1.6
7.3	3.5	54	1	3.3
7.3	3.5	54	1.5	2.6
7.3	3.5	72	0.5	1.5
7.3	3.5	72	1	1.6
7.3	3.5	72	1.5	1.5
7.3	4.5	36	0.5	1.9
7.3	4.5	36	1	4.9
7.3	4.5	36	1.5	4.6
7.3	4.5	36	2	3.1
7.3	4.5	54	0.5	1.7
7.3	4.5	54	1	4
7.3	4.5	54	1.5	>2.6
7.3	4.5	54	2	1.6
7.3	4.5	60	1	2
7.3	4.5	66	1	1.7
7.3	4.5	72	0.5	1.9
7.3	4.5	72	1	1.6
7.3	4.5	72	1.5	>1.5
7.3	4.5	72	2	>.9
7.3	5.5	36	0.5	1.7
7.3	5.5	36	1	3.6
7.3	5.5	36	1.5	NA
7.3	5.5	54	0.5	1.5
7.3	5.5	54	1	2.1
7.3	5.5	54	1.5	2.3
7.3	5.5	72	0.5	1.5
7.3	5.5	72	1	1.2
7.3	5.5	72	1.5	1.6
7.3	6.25	18	1	4.8
7.3	7.34	36	0.5	1.3
7.3	7.34	36	1	1.3
7.3	7.34	36	1.5	1.3
7.3	7.34	54	0.5	0.9
7.3	7.34	54	1	>.6
7.3	7.34	54	1.5	0.8
7.5	4.5	54	0.5	1.7
7.5	4.5	54	1	3.5
7.5	4.5	54	1.5	2.8
7.5	4.5	54	2	1.6
7.5	4.5	72	1	1.6
7.5	4.75	54	1	3

b	b_f/2t_f	h/t_w	L_b	R
7.5	6.5	18	1	3.9
7.5	6.63	18	1	3.8
7.6	4.75	54	1	3
7.6	6.63	18	1	3.8
7.7	4.5	54	0.5	1.7
7.7	6.75	18	1	3.3
8	3.5	54	0.5	1.7
8	3.5	54	1	3.3
8	3.5	54	1.5	>2.5
8	3.5	72	0.5	1.5
8	3.5	72	1	1.6
8	3.5	72	1.5	1.6
8	4.5	36	0.5	1.9
8	4.5	36	1	6
8	4.5	36	1.5	4.5
8	4.5	36	2	3.2
8	4.5	54	0.5	1.7
8	4.5	54	1	3.4
8	4.5	54	1.5	2.8
8	4.5	54	2	1.6
8	4.5	72	0.5	1.9
8	4.5	72	1	1.6
8	4.5	72	1.5	>1.5
8	4.5	72	2	0.9
8	5	54	1	2.7
8	5.5	36	0.5	1.7
8	5.5	36	1	3.3
8	5.5	36	1.5	2.8
8	5.5	54	0.5	1.6
8	5.5	54	1	2.2
8	5.5	54	1.5	2.3
8	5.5	72	0.5	1.5
8	5.5	72	1	1.2
8	5.5	72	1.5	1.5
8	7.34	18	1	3
8	7.34	36	0.5	1.4
8	7.34	36	1	1.3
8	7.34	36	1.5	1.3
8	7.34	54	0.5	0.9
8	7.34	54	1	0.7
8	7.34	54	1.5	>.5
8.1	5.25	45	1	3.4
8.1	6	27	1	3.1
8.3	5.63	36	1	3
8.3	5.67	36	1	2.9
8.3	5.75	36	1	2.8
8.3	6.25	27	1	2.8
8.4	4.5	54	0.5	1.8
8.4	5.5	45	1	2.9
8.6	5.5	54	1	2.1
8.6	6.5	27	1	2.6
8.7	6	36	1	2.5
8.8	6.75	27	1	2.6
9	5.5	72	1	1.2
9.2	6.5	36	1	2
9.3	4.5	54	1	3.1
9.3	6	54	1	>3.2
9.5	4.5	36	1	4.3
9.5	4.5	36	1.5	2.7
9.5	4.5	54	1	3.1
9.5	4.5	54	1.5	2.8
9.5	4.5	72	0.5	1.8
9.5	4.5	72	1	1.6
9.5	4.5	72	1.5	>1.5
9.5	5.5	36	1.5	2.7
9.5	5.5	54	1	2.3
9.5	5.5	54	1.5	2.3
10	6.5	54	1	1.4
inf	4.5	54	1	1.9

b_f/2t_f	: Flange Slenderness Ratio
h/t_w	: Web Slenderness Ratio
L_b	: Unbraced Length in Multiples of d
b	: # times AISC Recommended Bracing Stiffness
R	: Rotation Capacity Achieved

Table A-11 Rotation Capacities Ordered by Increasing β, L_b, $b_f/2t_f$, and h/t_w, Respectively

b	L_b	$b_f/2t_f$	h/t_w	R
1	1	4.5	54	1.5
3.5	1	2	60	1.2
4	1	4.5	54	3.2
4.3	1	2.5	60	2.1
4.6	1	4.5	54	2.8
5	0.5	4.5	54	1.6
5	0.5	4.5	72	1.2
5	1	4.5	54	2.9
5	1	4.5	72	1.6
5	1	5.5	36	3.5
5	1	5.5	54	2
5	1.5	4.5	54	>2.6
5	1.5	4.5	72	1.5
5	1.5	5.5	36	2.7
5.1	1	3	60	2.4
5.2	1	3	72	1.4
5.3	1	4.5	18	6
5.3	1	4.5	54	3
5.9	1	3.5	60	2.3
5.9	1	3.5	66	2.1
5.9	1	4.5	18	>6
5.9	1	4.5	54	>3.1
5.9	2	4.5	54	1.6
6	1	3.5	72	1.6
6.25	1.5	4.5	54	>2.6
6.3	1	4.5	36	4.5
6.5	0.5	3.5	54	1.6
6.5	0.5	3.5	72	1.5
6.5	0.5	4.5	36	1.8
6.5	0.5	4.5	54	1.6
6.5	0.5	4.5	72	1.8
6.5	0.5	5.5	36	1.5
6.5	0.5	5.5	54	1.4
6.5	0.5	5.5	72	1.2
6.5	0.5	7.34	36	1.2
6.5	0.5	7.34	54	0.9
6.5	1	3.5	54	>2.5
6.5	1	3.5	72	1.6
6.5	1	4.5	27	5.4
6.5	1	4.5	36	4.5
6.5	1	4.5	54	3.3
6.5	1	4.5	72	1.6
6.5	1	5.5	36	3.7
6.5	1	5.5	54	2.1
6.5	1	5.5	72	1.2
6.5	1	7.34	36	1.4
6.5	1	7.34	54	0.8
6.5	1.5	3.5	54	>2.5
6.5	1.5	3.5	72	2
6.5	1.5	4.5	36	4.4
6.5	1.5	4.5	54	2.7
6.5	1.5	4.5	72	1.6
6.5	1.5	5.5	36	NA
6.5	1.5	5.5	54	2.2
6.5	1.5	5.5	72	1.5
6.5	1.5	7.34	36	>1.8
6.5	1.5	7.34	54	0.8
6.5	2	4.5	36	3.1
6.5	2	4.5	54	1.6

b	L_b	$b_f/2t_f$	h/t_w	R
6.5	2	4.5	72	1
6.6	1	4	54	3.4
6.6	1	4	60	2.2
6.7	1	4	66	1.9
6.75	1	4.5	54	3.8
6.8	1	4.5	54	3.8
6.8	1	4.5	72	>1.5
6.8	1	6.5	18	4.5
6.9	1	4.25	54	3.4
6.9	1.5	4.5	54	2.8
7	0.5	4.5	54	1.6
7	1	4.25	54	3.5
7	1	4.5	36	4.4
7	1	4.5	45	4.2
7	1	4.5	54	>3
7	1.5	4.5	54	>2.6
7	2	4.5	54	1.6
7.15	1	6	18	5.2
7.3	0.5	3.5	54	1.6
7.3	0.5	3.5	72	1.5
7.3	0.5	4.5	36	1.9
7.3	0.5	4.5	54	1.7
7.3	0.5	4.5	72	1.9
7.3	0.5	5.5	36	1.7
7.3	0.5	5.5	54	1.5
7.3	0.5	5.5	72	1.5
7.3	0.5	7.34	36	1.3
7.3	0.5	7.34	54	0.9
7.3	1	3.5	54	3.3
7.3	1	3.5	72	1.6
7.3	1	4.5	36	4.9
7.3	1	4.5	54	4
7.3	1	4.5	60	2
7.3	1	4.5	66	1.7
7.3	1	4.5	72	1.6
7.3	1	5.5	36	3.6
7.3	1	5.5	54	2.1
7.3	1	5.5	72	1.2
7.3	1	6.25	18	4.8
7.3	1	7.34	36	1.3
7.3	1	7.34	54	>.6
7.3	1.5	3.5	54	2.6
7.3	1.5	3.5	72	1.5
7.3	1.5	4.5	36	4.6
7.3	1.5	4.5	54	>2.6
7.3	1.5	4.5	72	>1.5
7.3	1.5	5.5	36	NA
7.3	1.5	5.5	54	2.3
7.3	1.5	5.5	72	1.6
7.3	1.5	7.34	36	1.3
7.3	1.5	7.34	54	0.8
7.3	2	4.5	36	3.1
7.3	2	4.5	54	1.6
7.3	2	4.5	72	>.9
7.5	0.5	4.5	54	1.7
7.5	1	4.5	54	3.5
7.5	1	4.5	72	1.6
7.5	1	4.75	54	3
7.5	1	6.5	18	3.9
7.5	1	6.63	18	3.8

b	L_b	$b_f/2t_f$	h/t_w	R
7.5	1.5	4.5	54	2.8
7.5	2	4.5	54	1.6
7.6	1	4.75	54	3
7.6	1	6.63	18	3.8
7.7	0.5	4.5	54	1.7
7.7	1	6.75	18	3.3
8	0.5	3.5	54	1.7
8	0.5	3.5	72	1.5
8	0.5	4.5	36	1.9
8	0.5	4.5	54	1.7
8	0.5	4.5	72	1.9
8	0.5	5.5	36	1.7
8	0.5	5.5	54	1.6
8	0.5	5.5	72	1.5
8	0.5	7.34	36	1.4
8	0.5	7.34	54	0.9
8	1	3.5	54	3.3
8	1	3.5	72	1.6
8	1	4.5	36	6
8	1	4.5	54	3.4
8	1	4.5	72	1.6
8	1	5	54	2.7
8	1	5.5	36	3.3
8	1	5.5	54	2.2
8	1	5.5	72	1.2
8	1	7.34	18	3
8	1	7.34	36	1.3
8	1	7.34	54	0.7
8	1.5	3.5	54	>2.5
8	1.5	3.5	72	1.6
8	1.5	4.5	36	4.5
8	1.5	4.5	54	2.8
8	1.5	4.5	72	>1.5
8	1.5	5.5	36	2.8
8	1.5	5.5	54	2.3
8	1.5	5.5	72	1.5
8	1.5	7.34	36	1.3
8	1.5	7.34	54	>.5
8	2	4.5	36	3.2
8	2	4.5	54	1.6
8	2	4.5	72	0.9
8.1	1	5.25	45	3.4
8.1	1	6	27	3.1
8.3	1	5.63	36	3
8.3	1	5.67	36	2.9
8.3	1	5.75	36	2.8
8.3	1	6.25	27	2.8
8.4	0.5	4.5	54	1.8
8.4	1	5.5	45	2.9
8.6	1	5.5	54	2.1
8.6	1	6.5	27	2.6
8.7	1	6	36	2.5
8.8	1	6.75	27	2.6
9	1	5.5	72	1.2
9.2	1	6.5	36	2
9.3	1	4.5	54	3.1
9.3	1	6	54	>3.2
9.5	0.5	4.5	72	1.8
9.5	1	4.5	36	4.3
9.5	1	4.5	54	3.1
9.5	1	4.5	72	1.6
9.5	1	5.5	54	2.3
9.5	1.5	4.5	36	2.7
9.5	1.5	4.5	54	2.8
9.5	1.5	4.5	72	>1.5
9.5	1.5	5.5	36	2.7
9.5	1.5	5.5	54	2.3
10	1	6.5	54	1.4
inf	1	4.5	54	1.9

$b_f/2t_f$	: Flange Slenderness Ratio
h/t_w	: Web Slenderness Ratio
L_b	: Unbraced Length in Multiples of d
b	: # times AISC Recommended Bracing Stiffness
R	: Rotation Capacity Achieved

APPENDIX B

APPENDIX B

MOMENT-ROTATION PLOTS

All moment-rotation plots produced from this research are located in this appendix. They are presented using four different presentation methods to facilitate comparison of the results. Each method is similar except that for each one a different parameter varies (while the other three parameters are held constant). Doing this highlights the influence that a change in the varying parameter has on rotation ductility, as it applies to a given combination of the remaining three parameters.

Appendix B.1

The first presentation method combines the plots such that only the flange slenderness ratio varies. By doing this, it is possible to observe the effect that a change in only flange slenderness has on structural ductility.
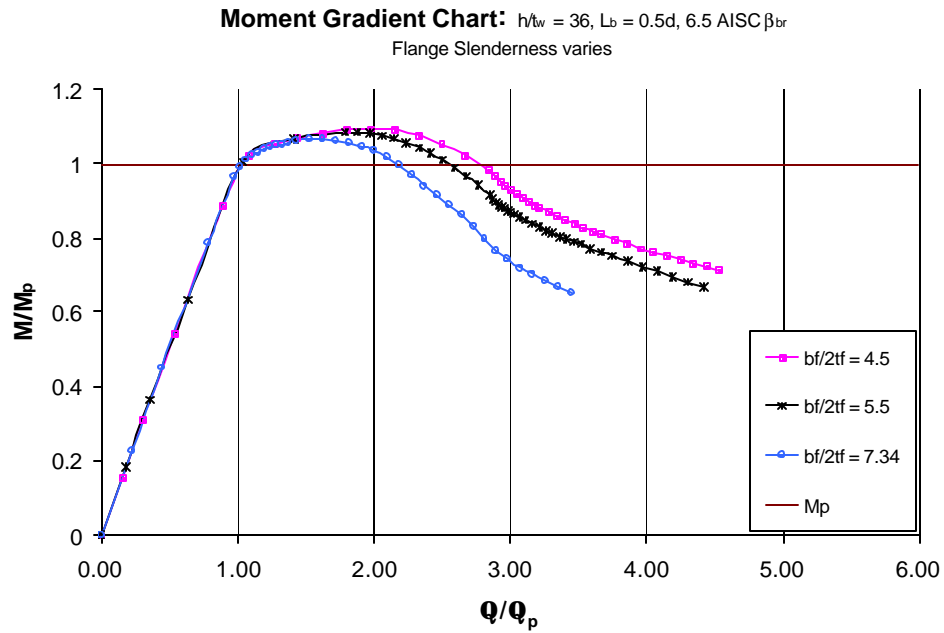
Figure B-1 Moment Rotation Plot ($h/t_w = 36$, $L_b = 0.5d$, 6.5 AISC β_{br} Flange Slenderness Varies)
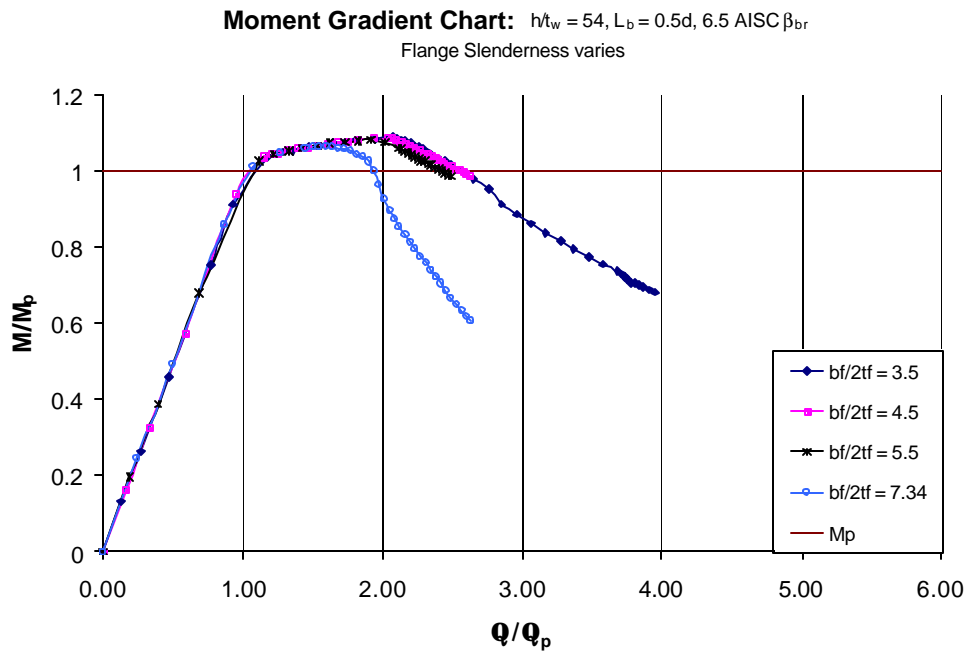
Figure B-2 Moment Rotation Plot ($h/t_w = 54$, $L_b = 0.5d$, 6.5 AISC β_{br} Flange Slenderness Varies)
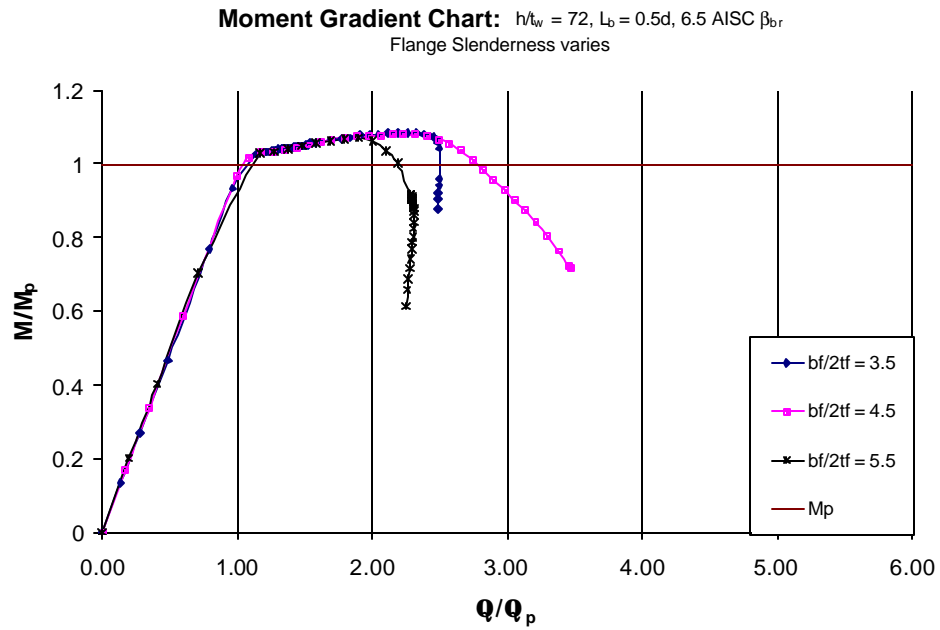
Figure B-3 Moment Rotation Plot (h/t$_w$ = 72, L$_b$ = 0.5d, 6.5 AISC β_{br} Flange Slenderness Varies)
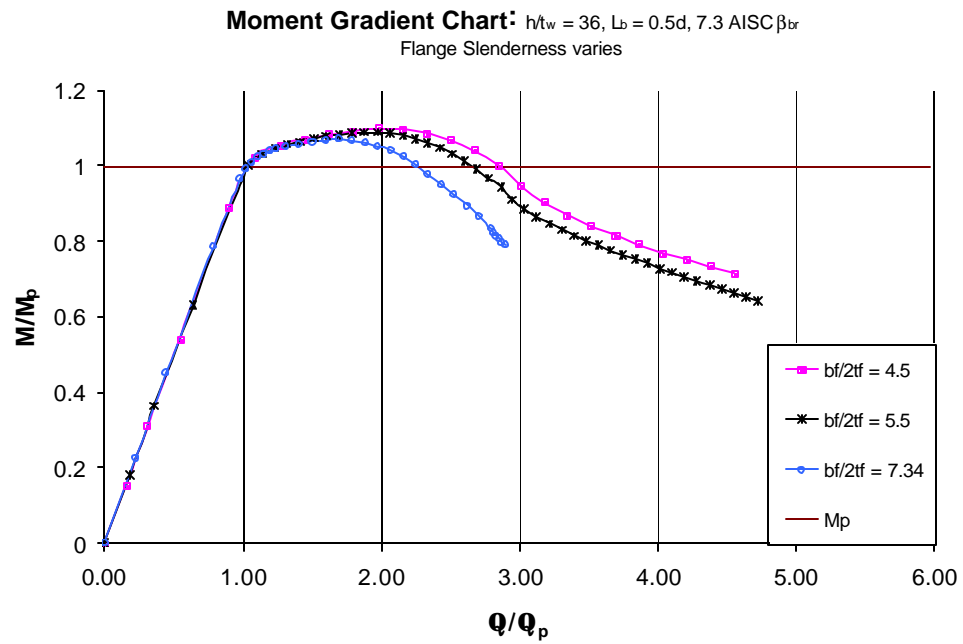
Figure B-4 Moment Rotation Plot (h/t$_w$ = 36, L$_b$ = 0.5d, 7.3 AISC β_{br} Flange Slenderness Varies)
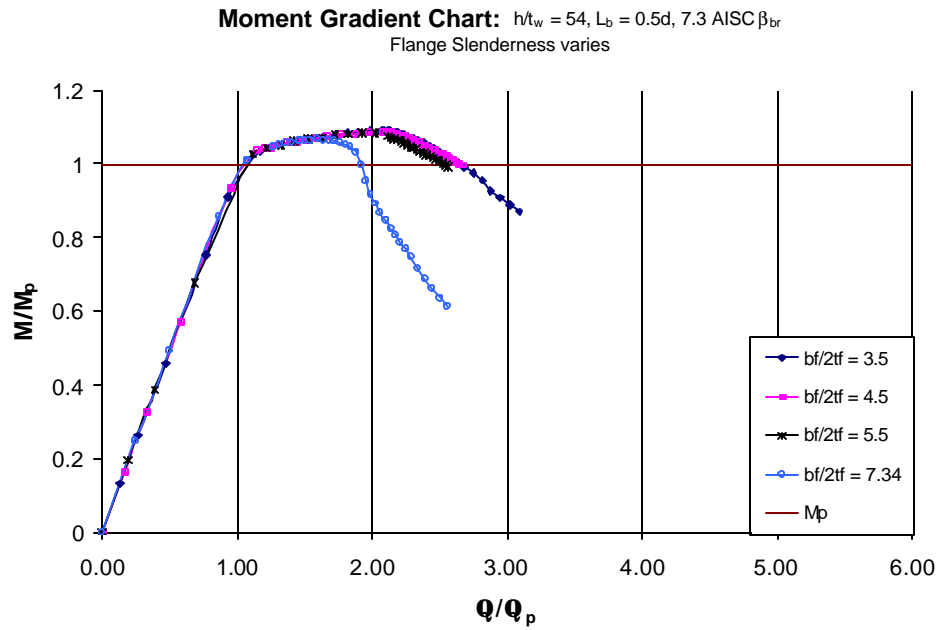
Figure B-5 Moment Rotation Plot (h/t$_w$ = 54, L$_b$ = 0.5d, 7.3 AISC β_{br} Flange Slenderness Varies)
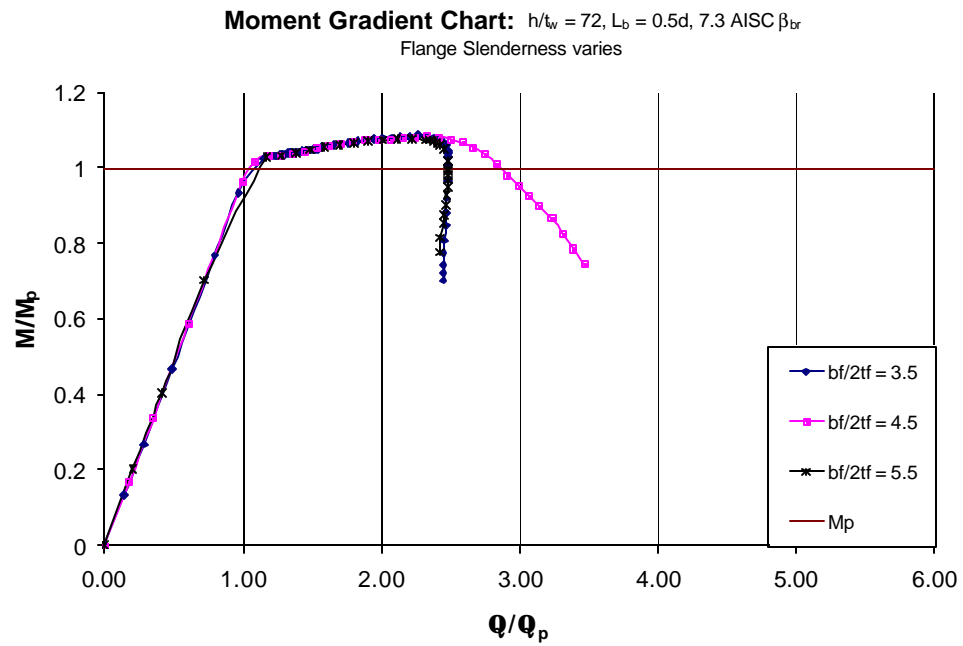
Figure B-6 Moment Rotation Plot (h/t$_w$ = 72, L$_b$ = 0.5d, 7.3 AISC β_{br} Flange Slenderness Varies)
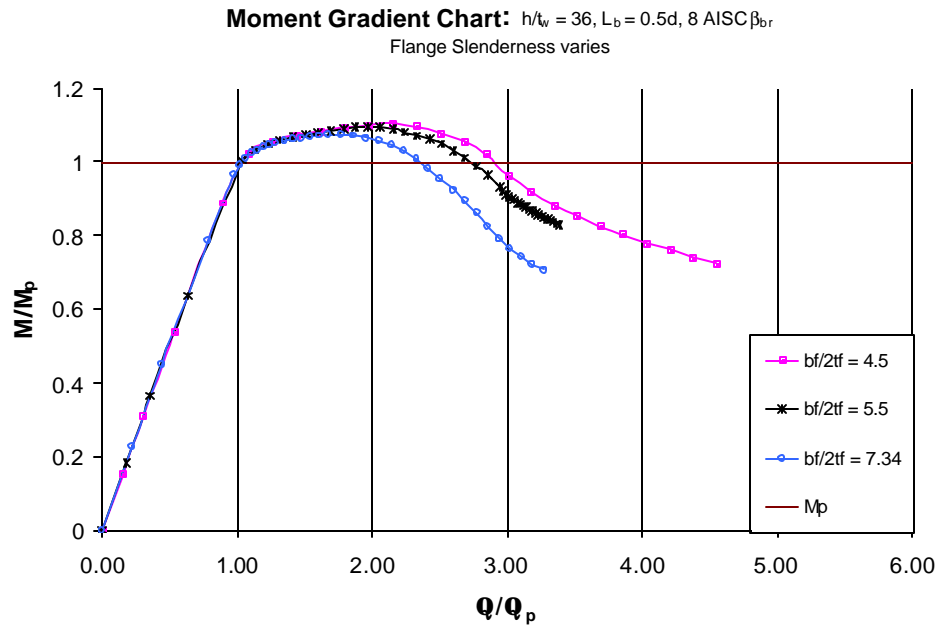
Figure B-7 Moment Rotation Plot ($h/t_w = 36$, $L_b = 0.5d$, 8 AISC β_{br} Flange Slenderness Varies)
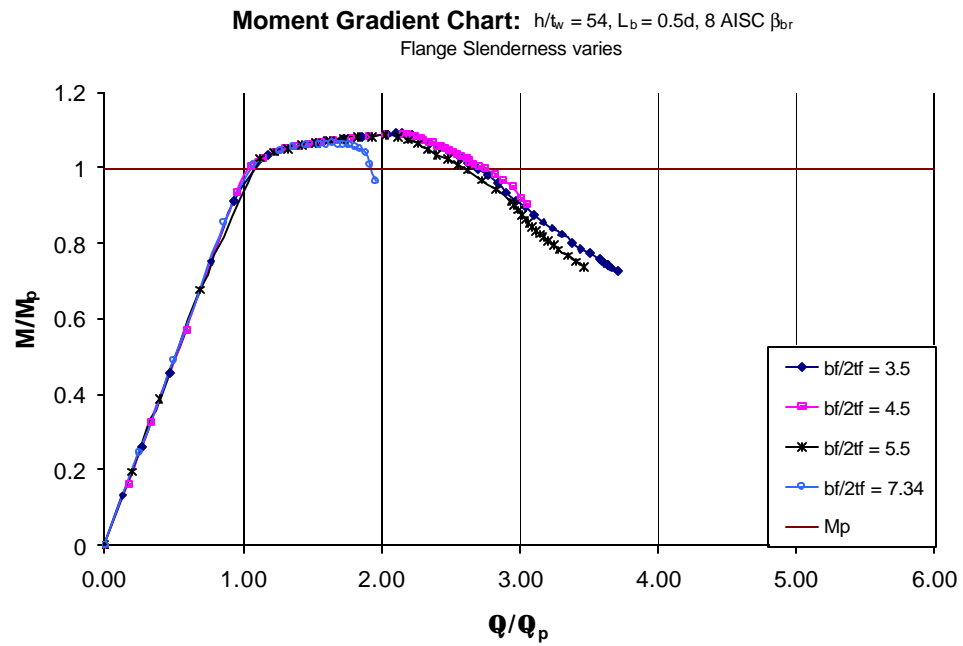
Figure B-8 Moment Rotation Plot ($h/t_w = 54$, $L_b = 0.5d$, 8 AISC β_{br} Flange Slenderness Varies)
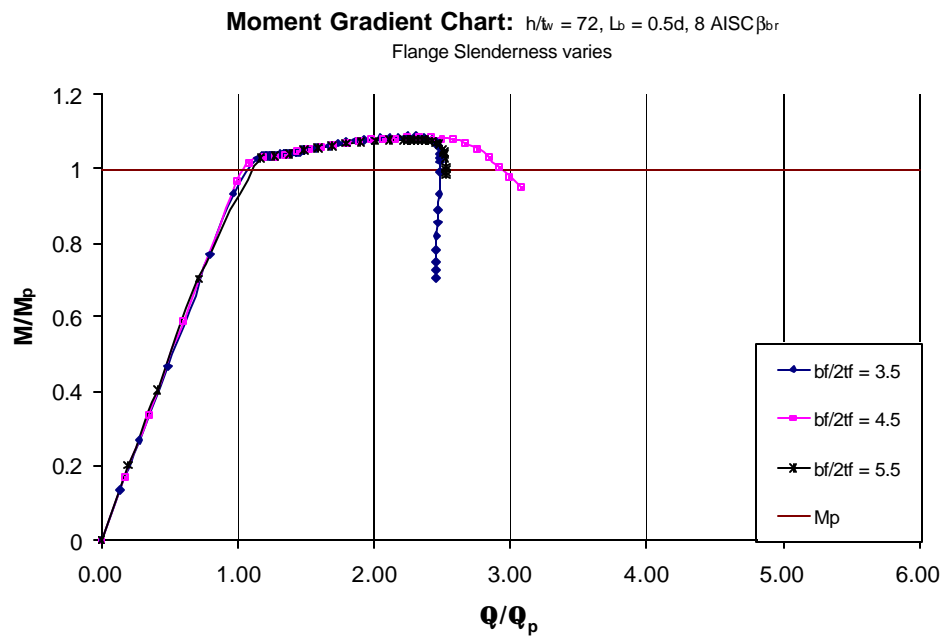
Figure B-9 Moment Rotation Plot ($h/t_w = 72$, $L_b = 0.5d$, 8 AISC β_{br} Flange Slenderness Varies)
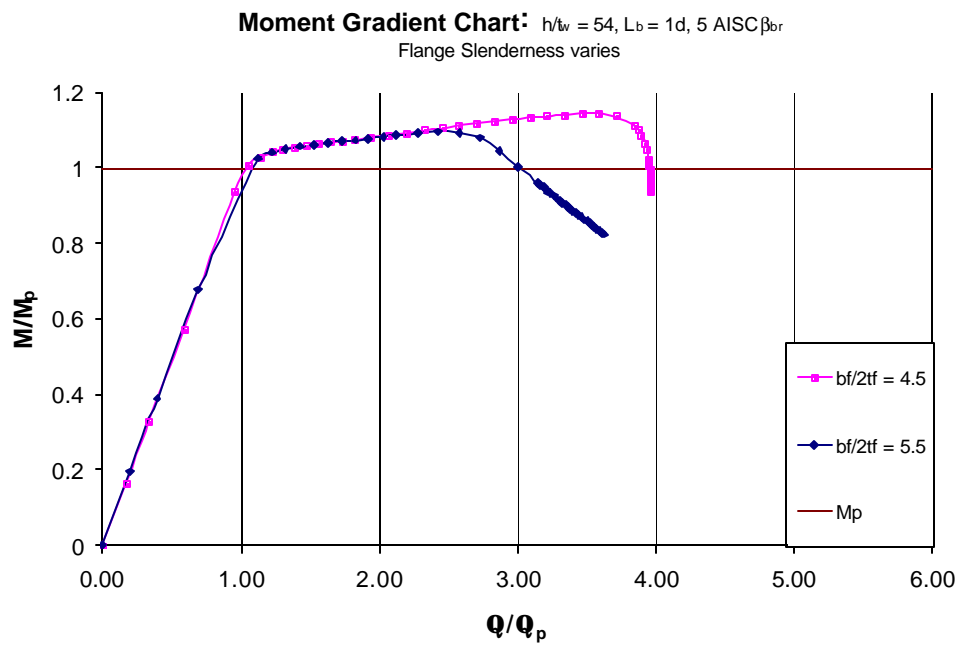
Figure B-10 Moment Rotation Plot ($h/t_w = 54$, $L_b = 1d$, 5 AISC β_{br} Flange Slenderness Varies)
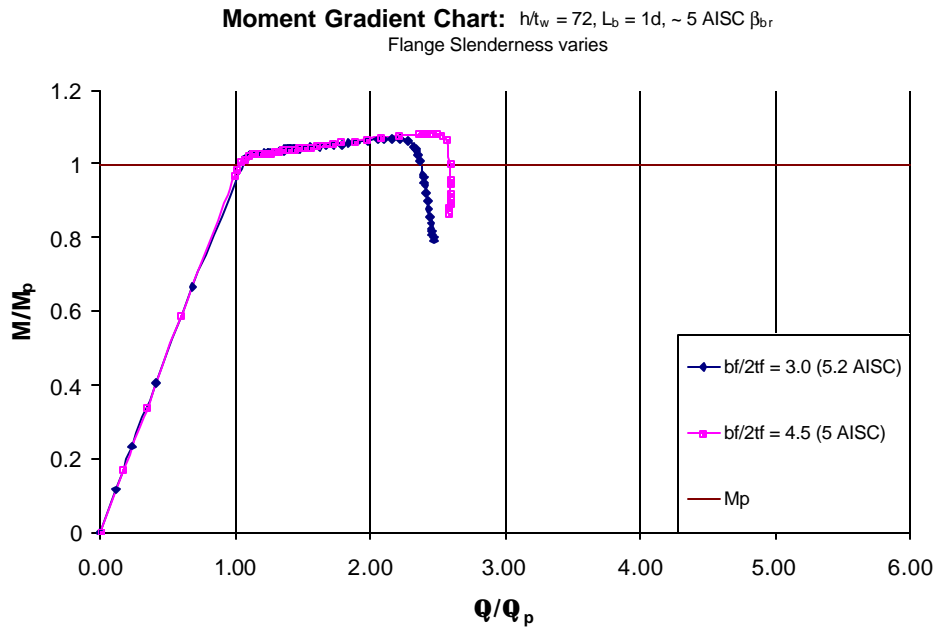
Figure B-11 Moment Rotation Plot (h/t$_w$ = 72, L$_b$ = 1d, ~ 5 AISC β_{br} Flange Slenderness Varies)
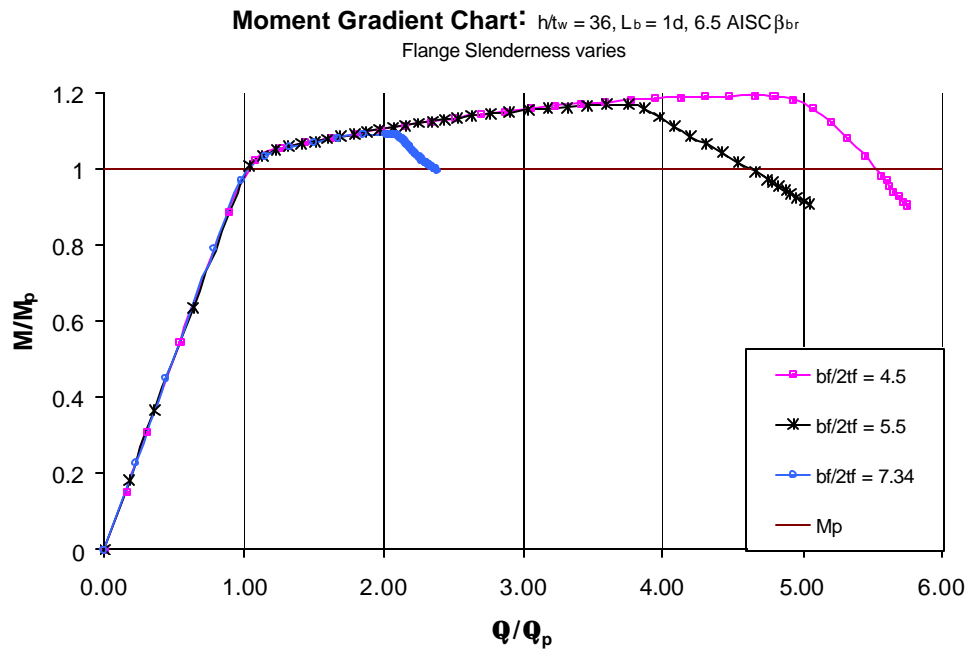
Figure B-12 Moment Rotation Plot (h/t$_w$ = 36, L$_b$ = 1d, 6.5 AISC β_{br} Flange Slenderness Varies)

106

Moment Gradient Chart: h/t$_w$ = 54, L$_b$ = 1d, 6.5 AISC β_{br}
Flange Slenderness varies
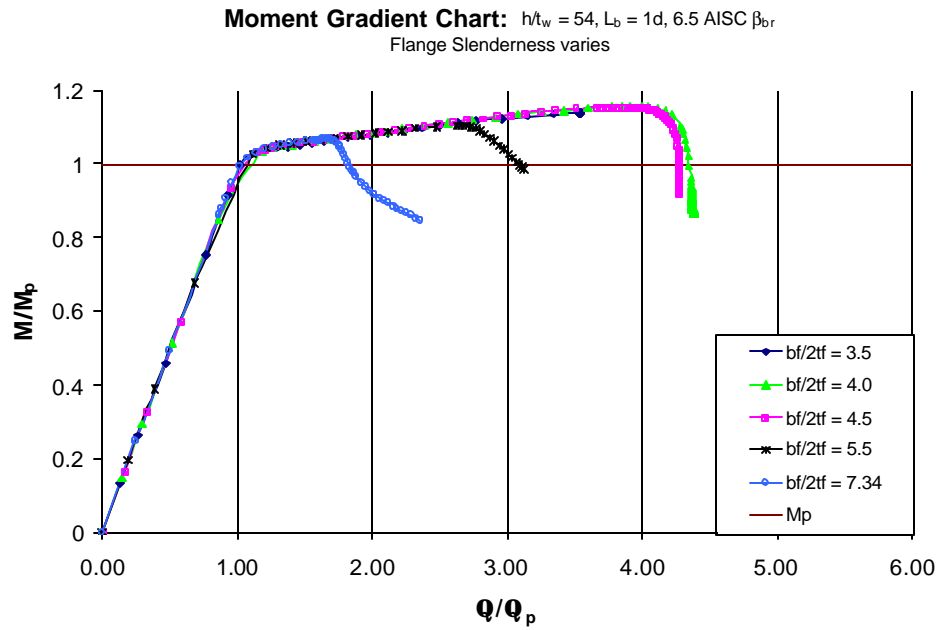
Figure B-13 Moment Rotation Plot (h/t$_w$ = 54, L$_b$ = 1d, 6.5 AISC β_{br} Flange Slenderness Varies)

Moment Gradient Chart: h/t$_w$ = 72, L$_b$ = 1d, 6.5 AISC β_{br}
Flange Slenderness varies
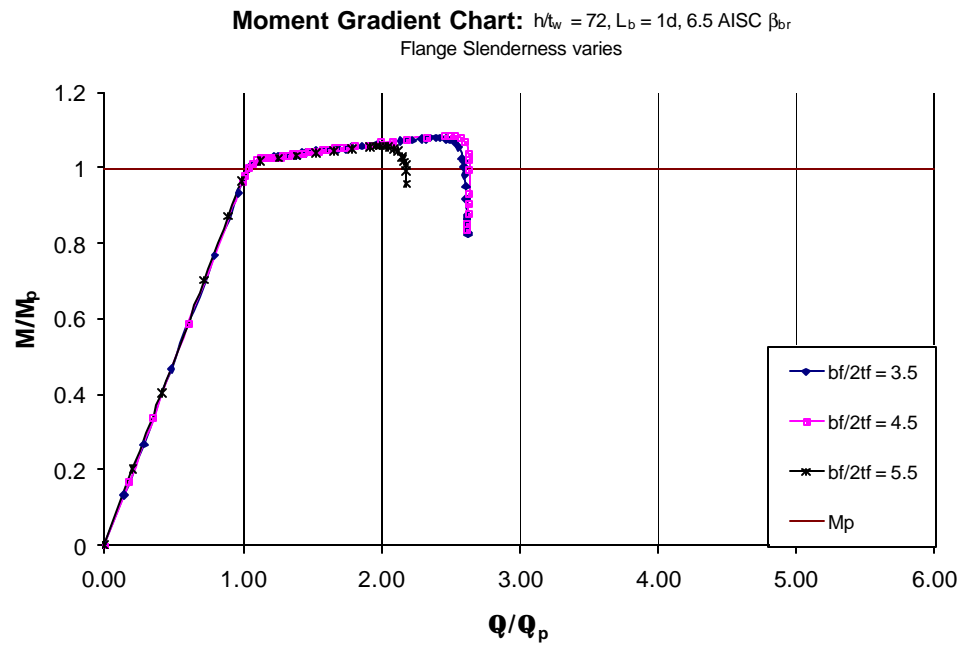
Figure B-14 Moment Rotation Plot (h/t$_w$ = 72, L$_b$ = 1d, 6.5 AISC β_{br} Flange Slenderness Varies)
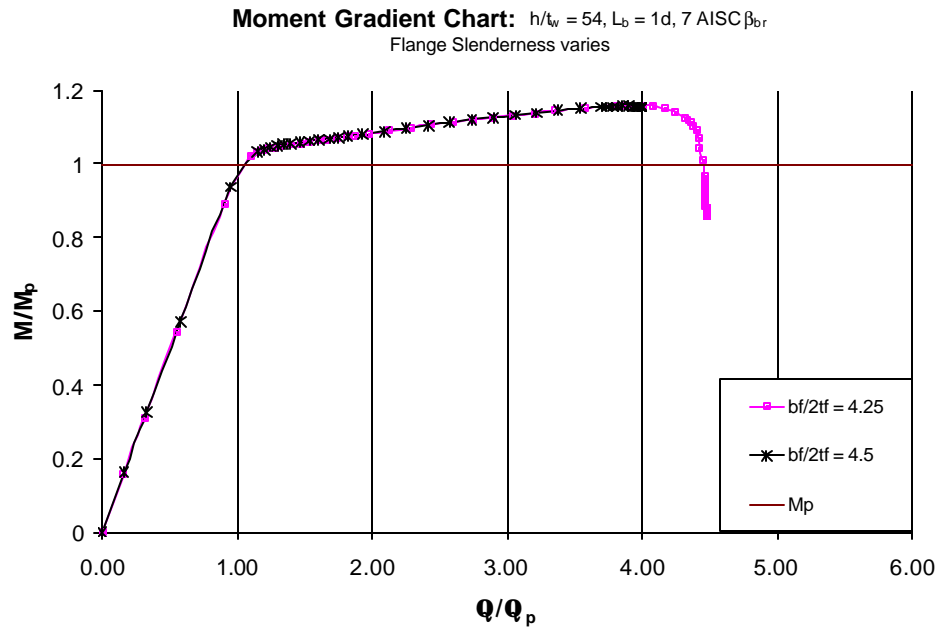
Figure B-15 Moment Rotation Plot ($h/t_w = 54$, $L_b = 1d$, 7 AISC β_{br} Flange Slenderness Varies)
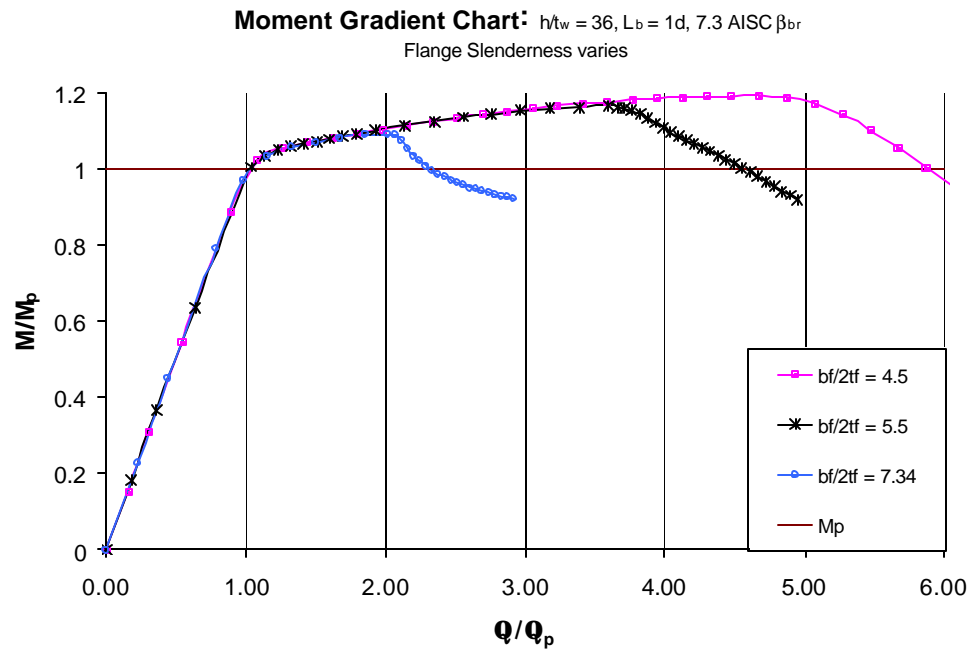
Figure B-16 Moment Rotation Plot ($h/t_w = 36$, $L_b = 1d$, 7.3 AISC β_{br} Flange Slenderness Varies)

Moment Gradient Chart: h/t_w = 54, L_b = 1d, 7.3 AISC β_br
Flange Slenderness varies
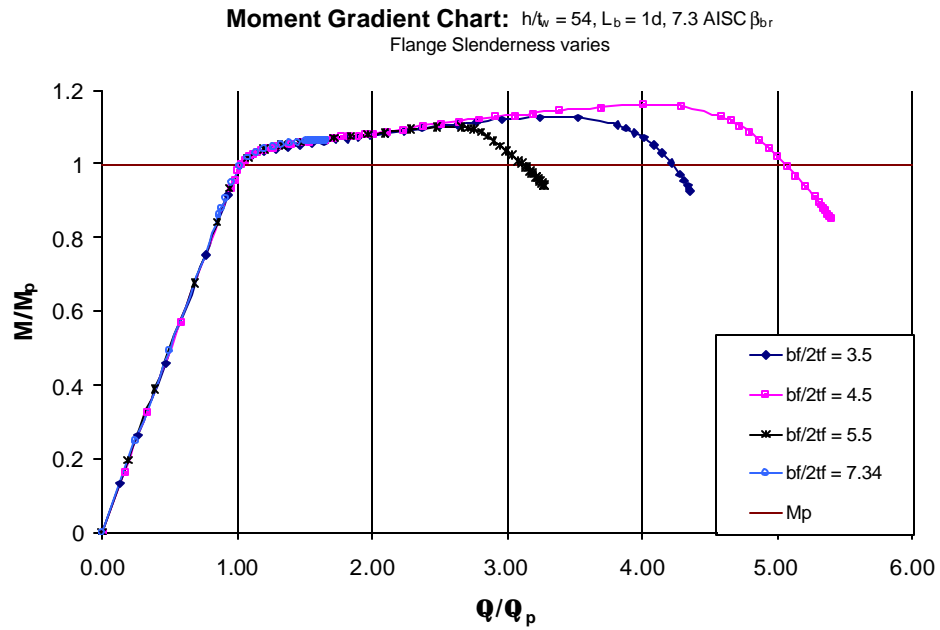
Figure B-17 Moment Rotation Plot ($h/t_w = 54$, $L_b = 1d$, 7.3 AISC β_{br} Flange Slenderness Varies)

Moment Gradient Chart: h/t_w = 72, L_b = 1d, 7.3 AISC β_br
Flange Slenderness varies
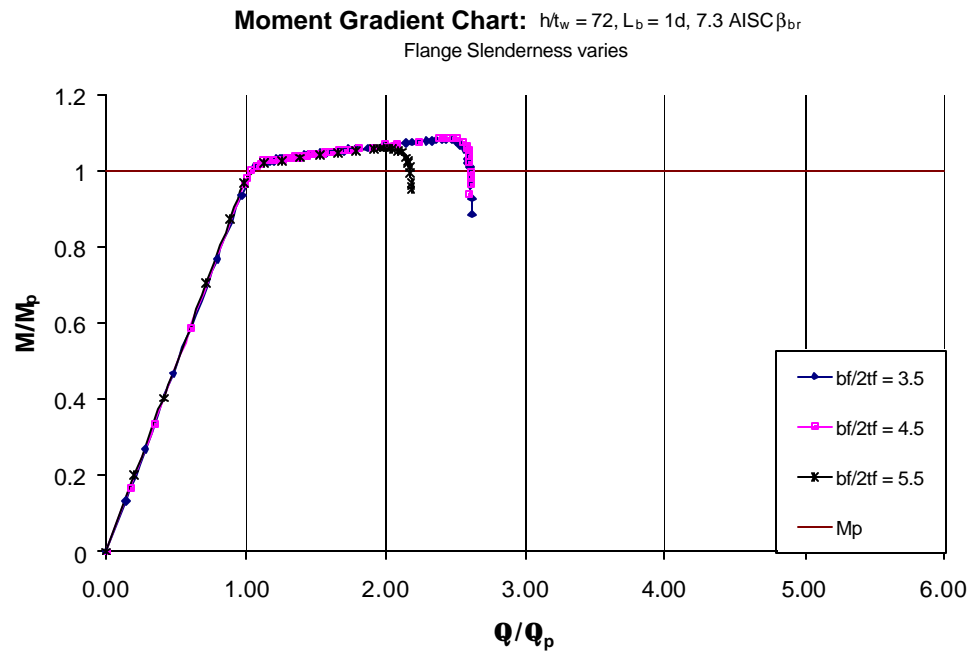
Figure B-18 Moment Rotation Plot ($h/t_w = 72$, $L_b = 1d$, 7.3 AISC β_{br} Flange Slenderness Varies)

Moment Gradient Chart: $h/t_w = 18$, $L_b = 1d$, 7.5 AISC β_{br}
Flange Slenderness varies
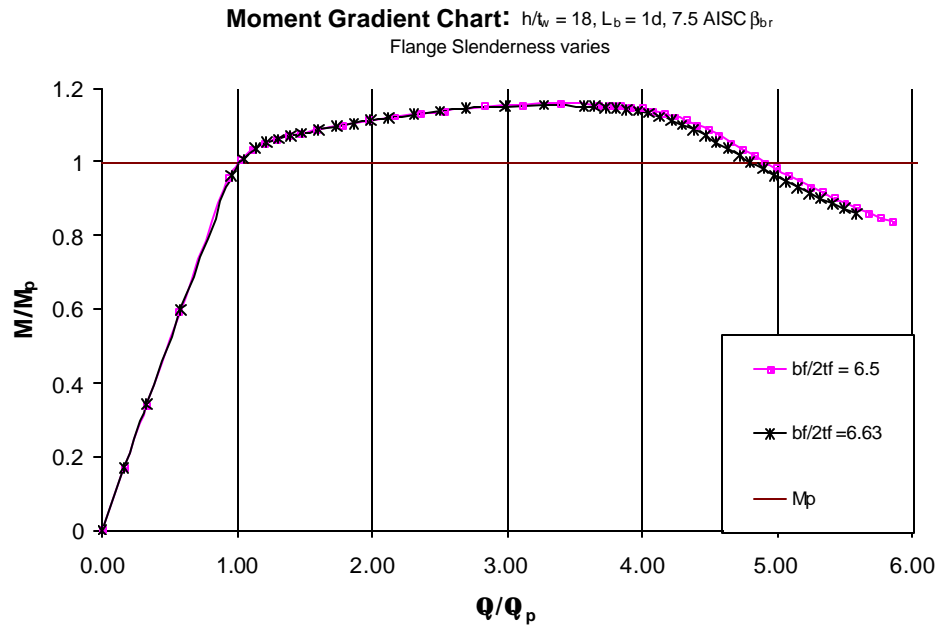
Figure B-19 Moment Rotation Plot ($h/t_w = 18$, $L_b = 1d$, 7.5 AISC β_{br} Flange Slenderness Varies)

Moment Gradient Chart: $h/t_w = 54$, $L_b = 1d$, 7.5 AISC β_{br}
Flange Slenderness varies
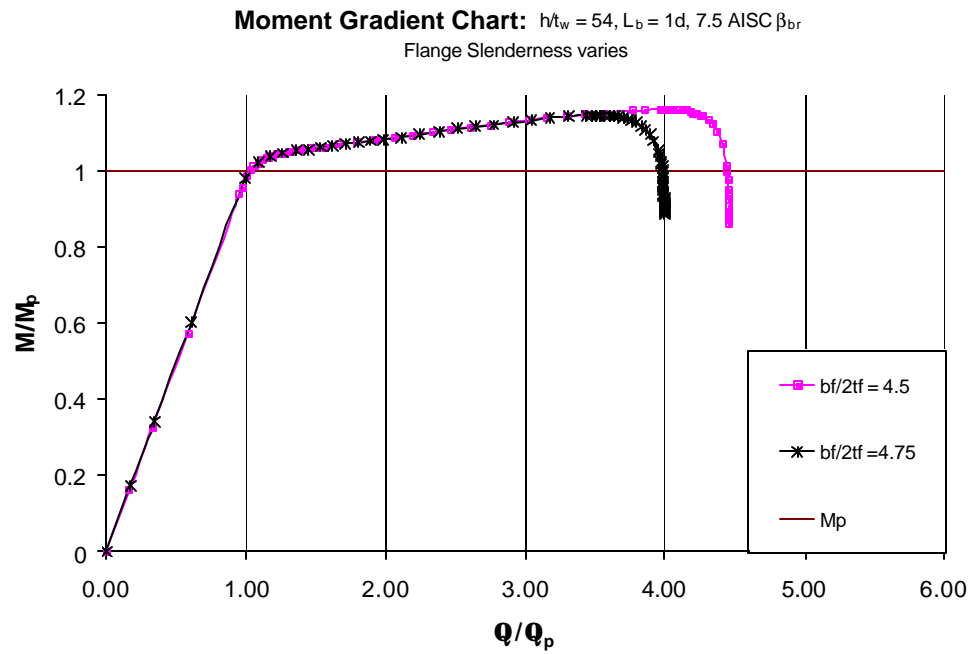
Figure B-20 Moment Rotation Plot ($h/t_w = 54$, $L_b = 1d$, 7.5 AISC β_{br} Flange Slenderness Varies)

Moment Gradient Chart: $h/t_w = 36$, $L_b = 1d$, 8 AISC β_{br}
Flange Slenderness varies
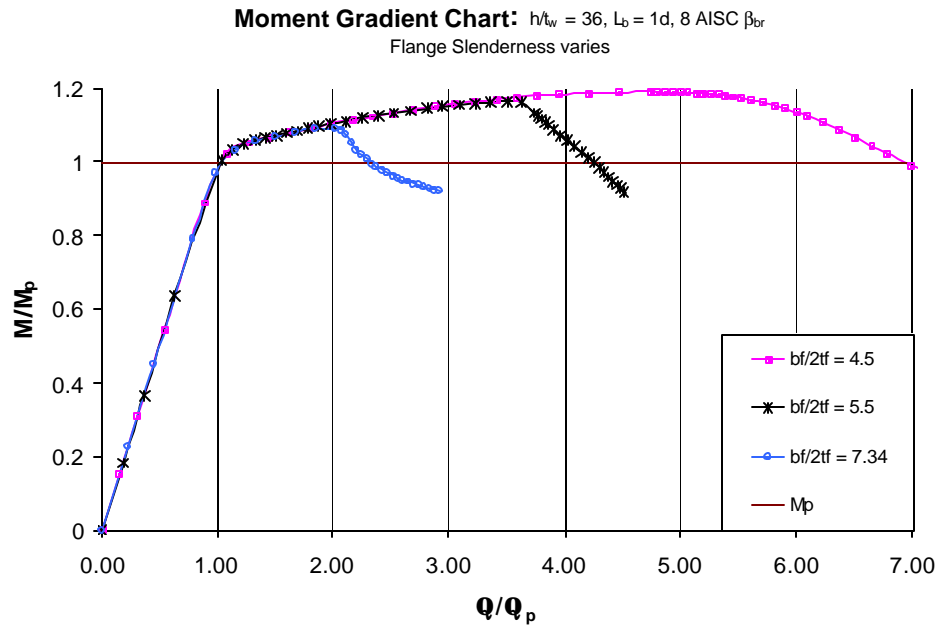
Figure B-21 Moment Rotation Plot ($h/t_w = 36$, $L_b = 1d$, 8 AISC β_{br}
Flange Slenderness Varies)

Moment Gradient Chart: $h/t_w = 54$, $L_b = 1d$, 8 AISC β_{br}
Flange Slenderness varies
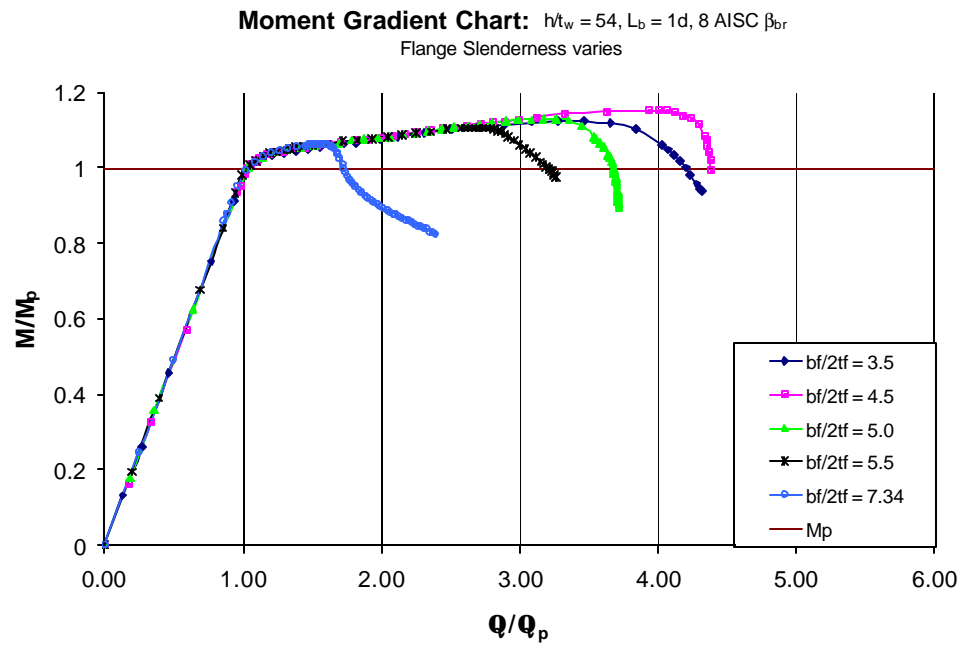
Figure B-22 Moment Rotation Plot ($h/t_w = 54$, $L_b = 1d$, 8 AISC β_{br}
Flange Slenderness Varies)
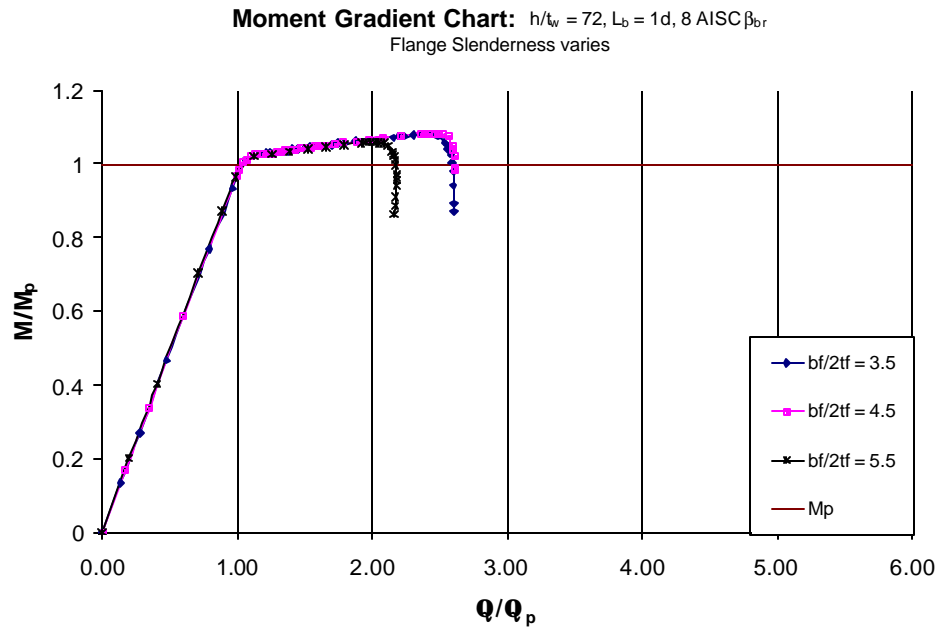
Figure B-23 Moment Rotation Plot ($h/t_w = 72$, $L_b = 1d$, 8 AISC β_{br} Flange Slenderness Varies)
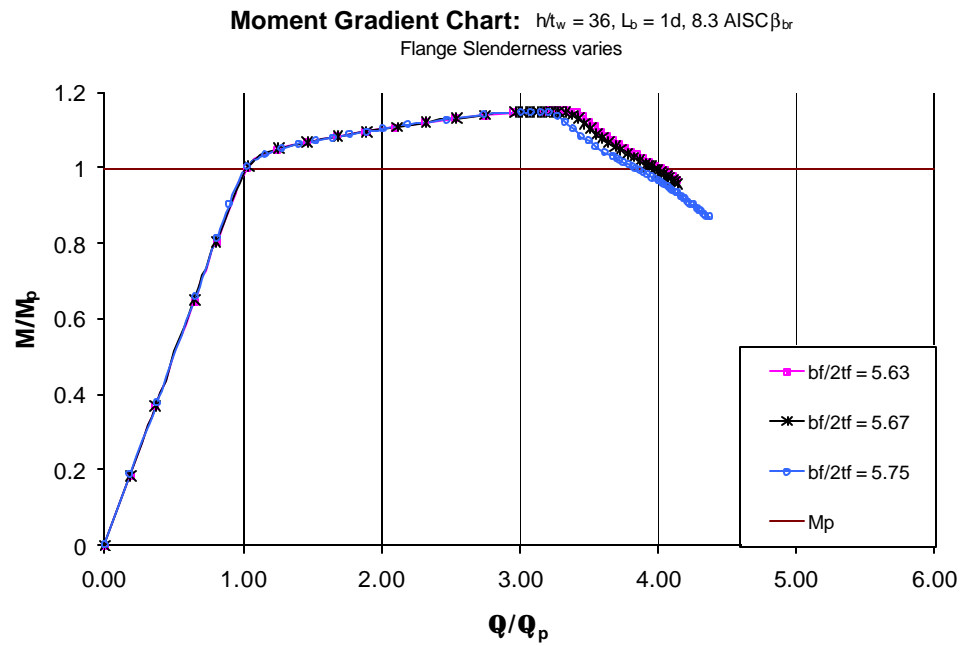
Figure B-24 Moment Rotation Plot ($h/t_w = 36$, $L_b = 1d$, 8.3 AISC β_{br} Flange Slenderness Varies)
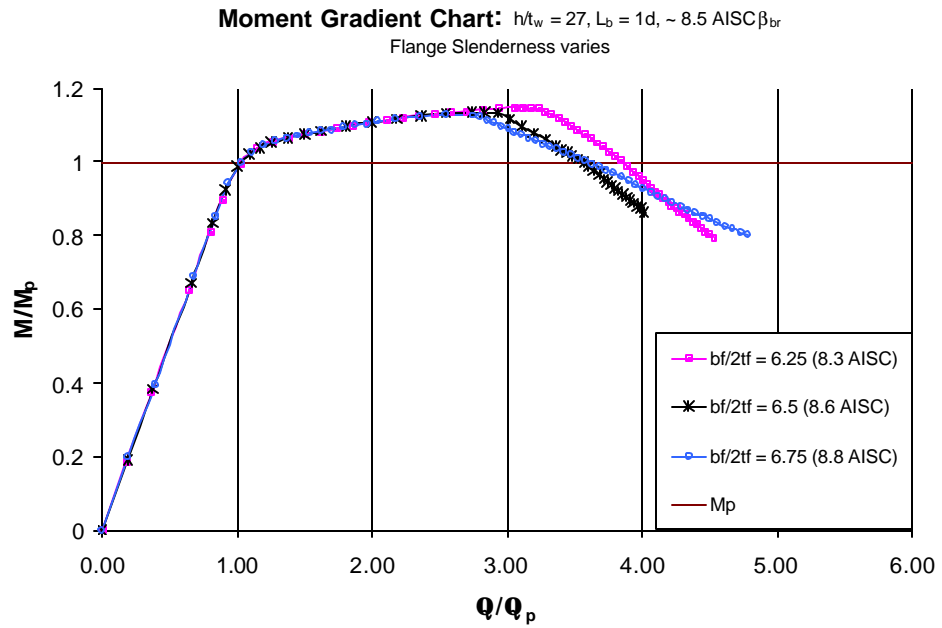
Figure B-25 Moment Rotation Plot ($h/t_w = 27$, $L_b = 1d$, ~ 8.5 AISC β_{br}
Flange Slenderness Varies)
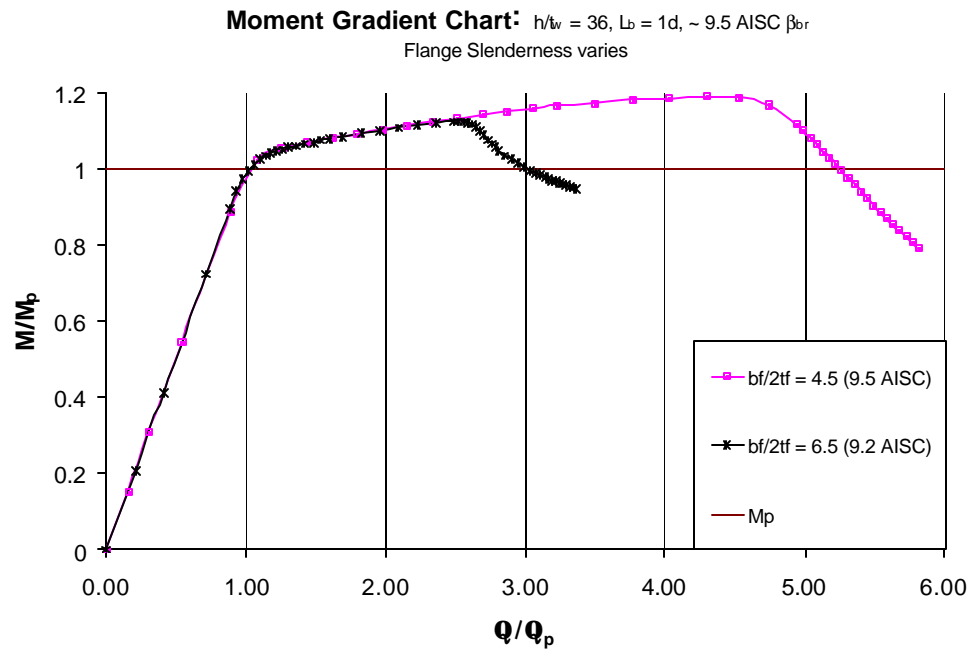
Figure B-26 Moment Rotation Plot ($h/t_w = 36$, $L_b = 1d$, ~ 9.5 AISC β_{br}
Flange Slenderness Varies)

113
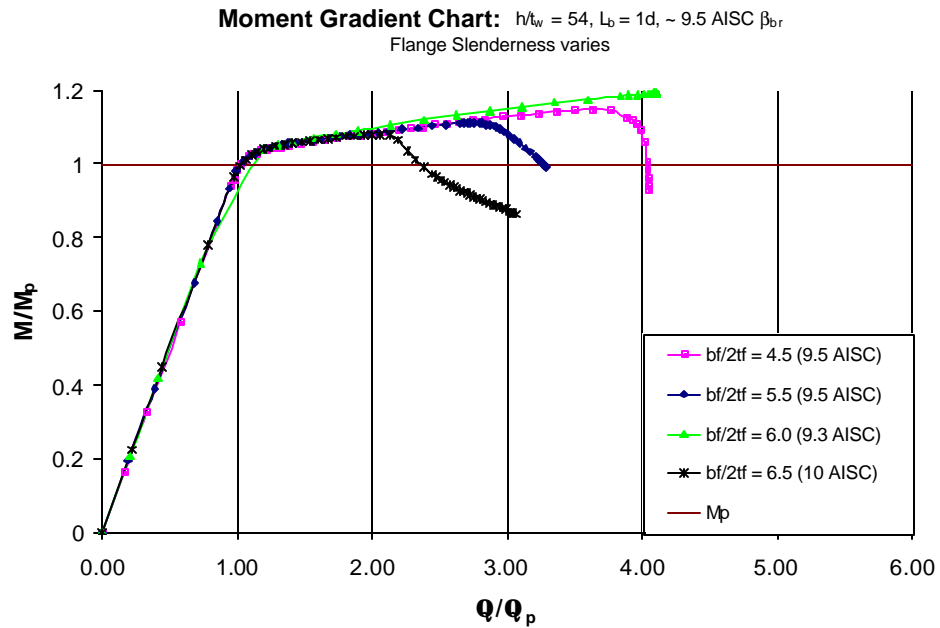
Figure B-27 Moment Rotation Plot ($h/t_w = 54$, $L_b = 1d$, ~ 9.5 AISC β_{br} Flange Slenderness Varies)
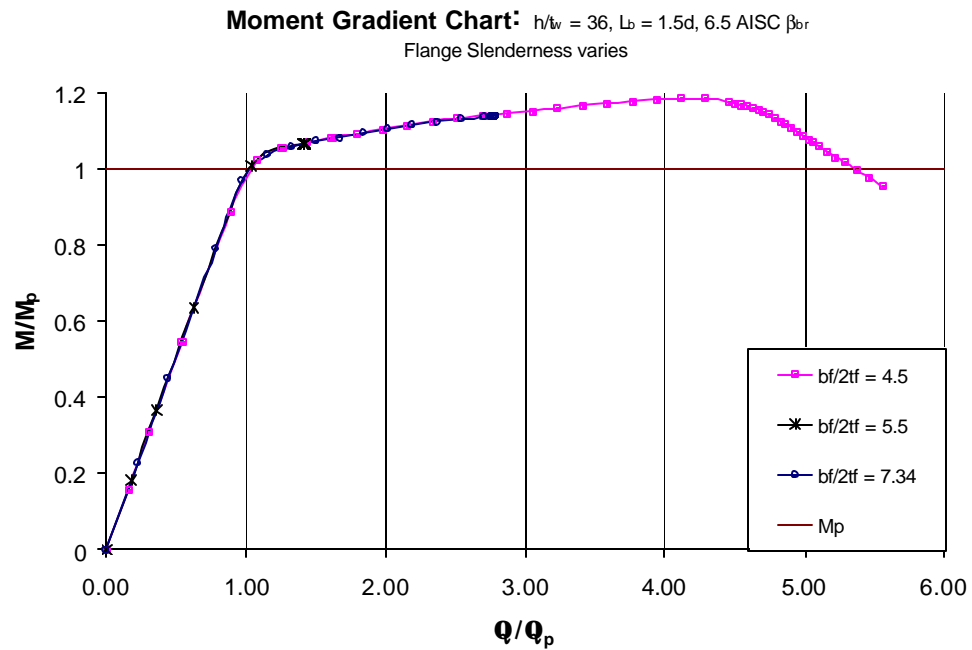
Figure B-28 Moment Rotation Plot ($h/t_w = 36$, $L_b = 1.5d$, 6.5 AISC β_{br} Flange Slenderness Varies)
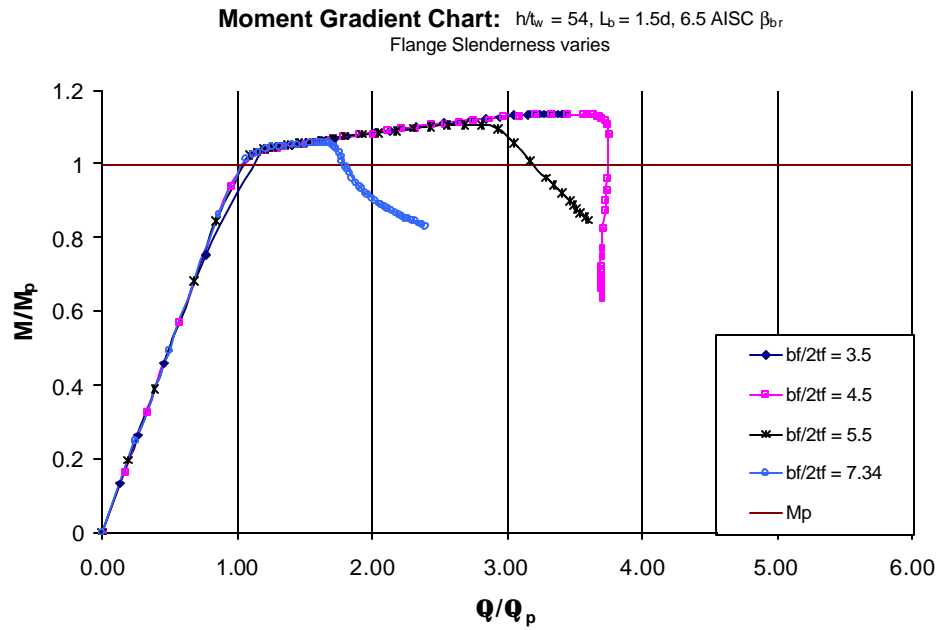
Figure B-29 Moment Rotation Plot (h/t_w = 54, L_b = 1.5d, 6.5 AISC β_{br} Flange Slenderness Varies)
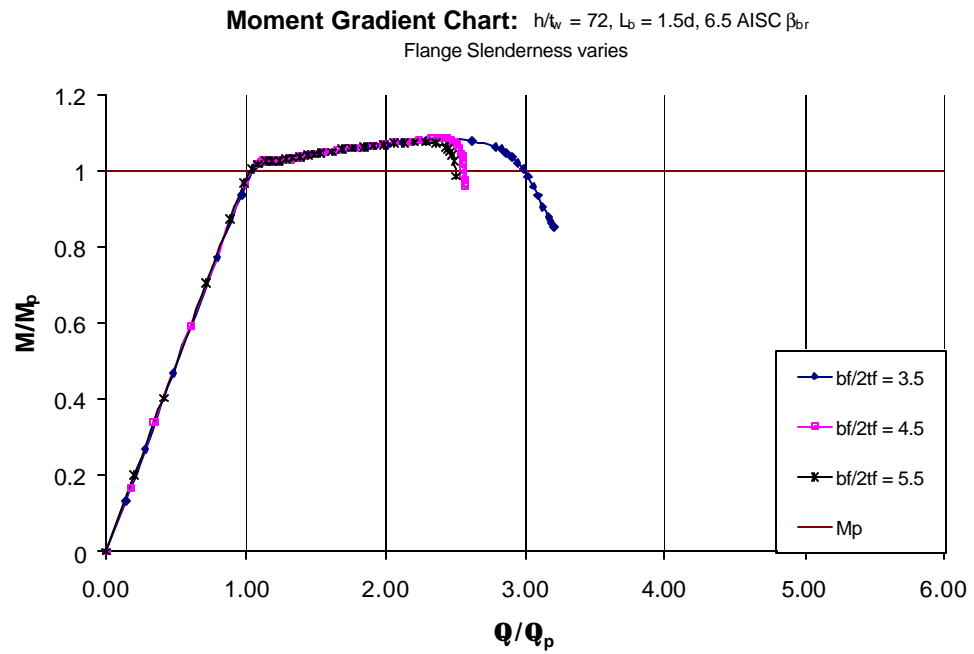
Figure B-30 Moment Rotation Plot (h/t_w = 72, L_b = 1.5d, 6.5 AISC β_{br} Flange Slenderness Varies)

115
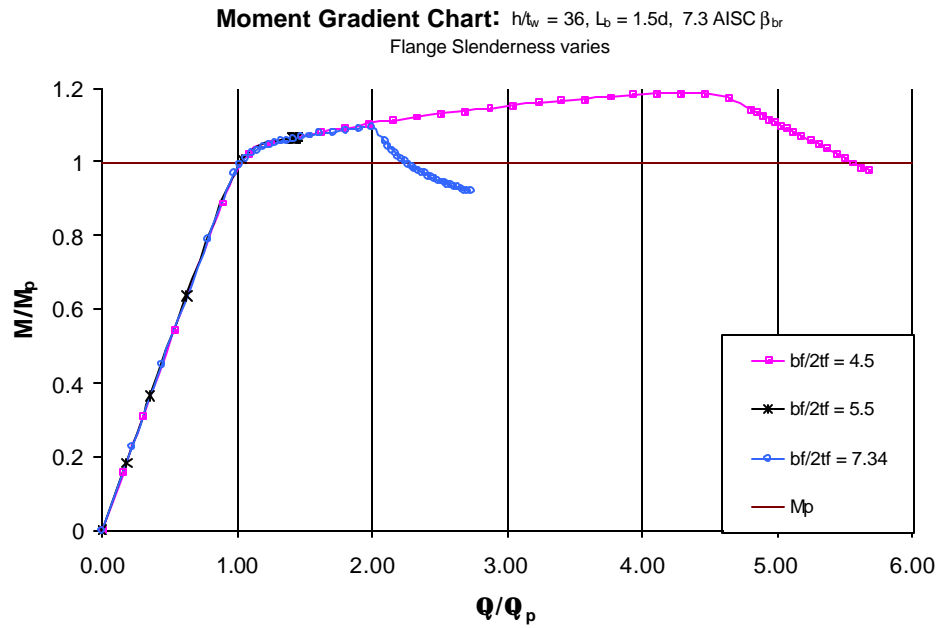
Figure B-31 Moment Rotation Plot ($h/t_w = 36$, $L_b = 1.5d$, 7.3 AISC β_{br} Flange Slenderness Varies)
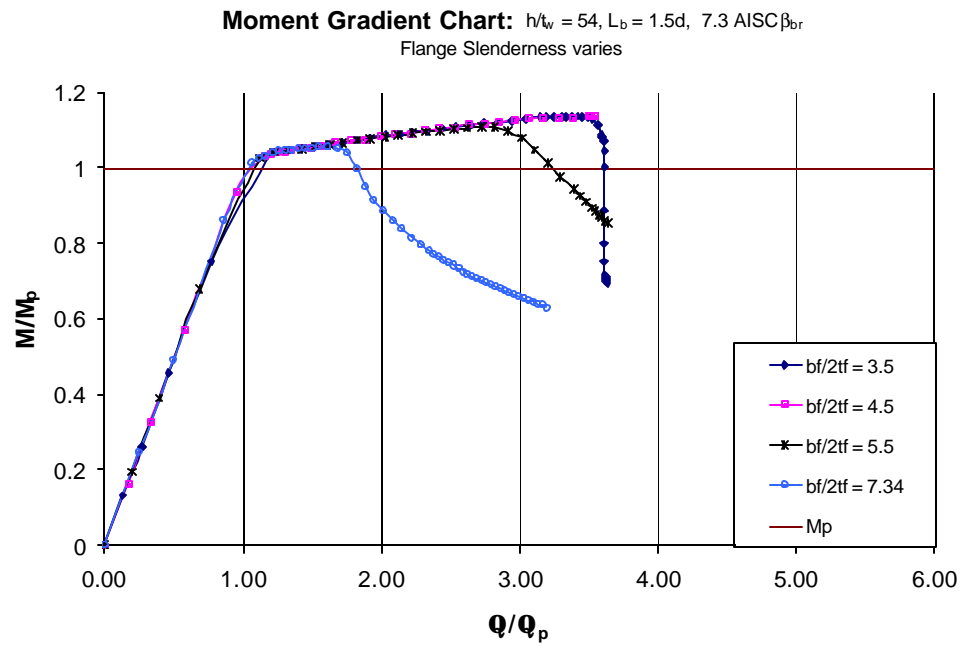
Figure B-32 Moment Rotation Plot ($h/t_w = 54$, $L_b = 1.5d$, 7.3 AISC β_{br} Flange Slenderness Varies)
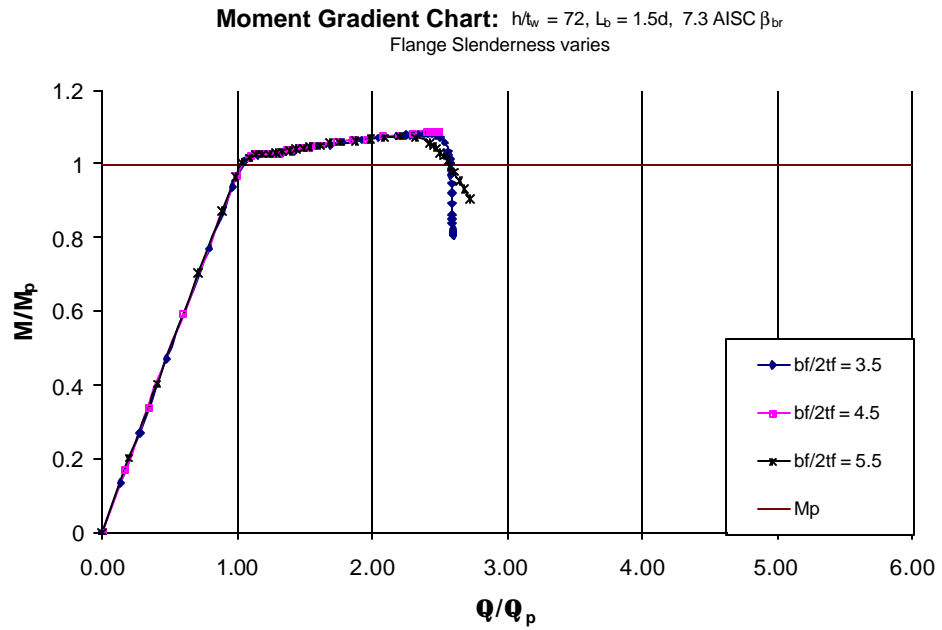
Figure B-33 Moment Rotation Plot (h/t$_w$ = 72, L$_b$ = 1.5d, 7.3 AISC β_{br} Flange Slenderness Varies)
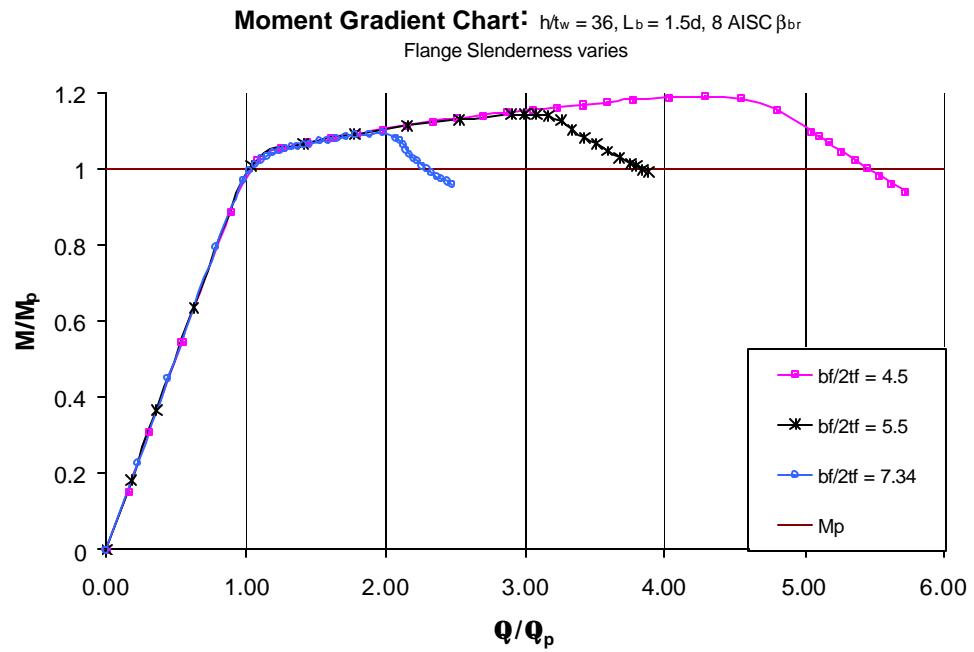
Figure B-34 Moment Rotation Plot (h/t$_w$ = 36, L$_b$ = 1.5d, 8 AISC β_{br} Flange Slenderness Varies)
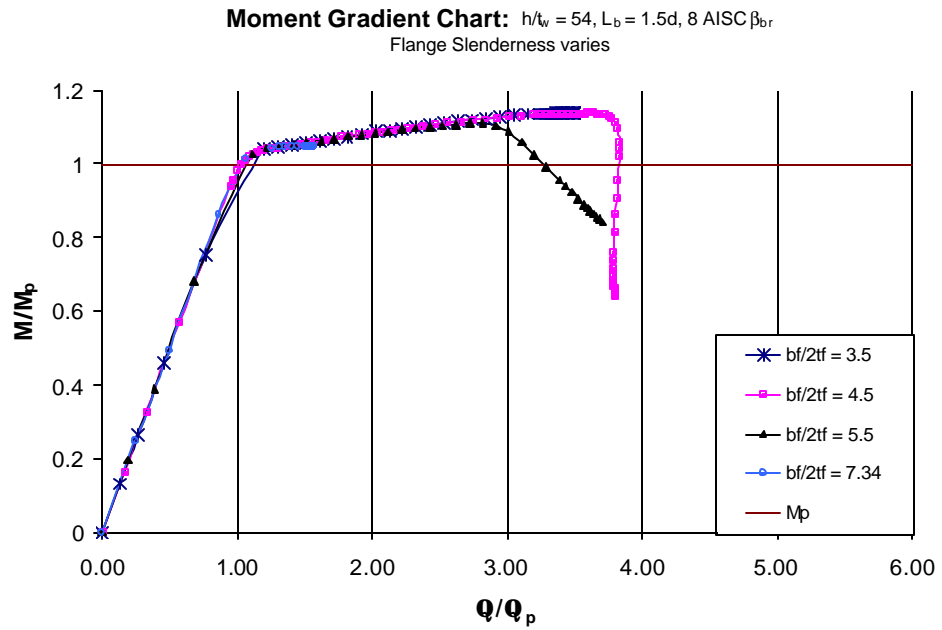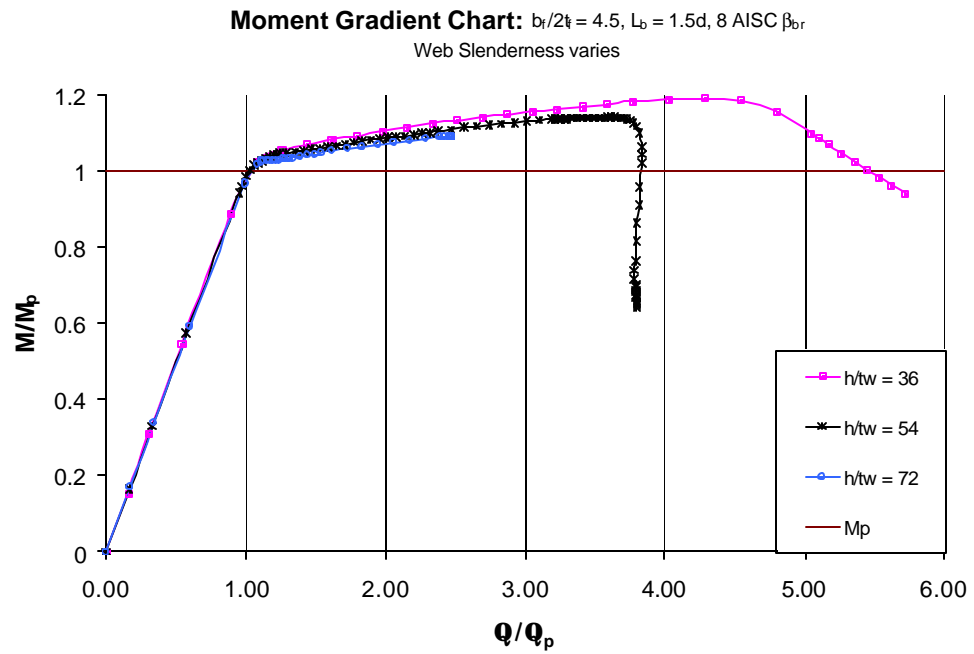
Figure B-35 Moment Rotation Plot ($h/t_w = 54$, $L_b = 1.5d$, 8 AISC β_{br} Flange Slenderness Varies)
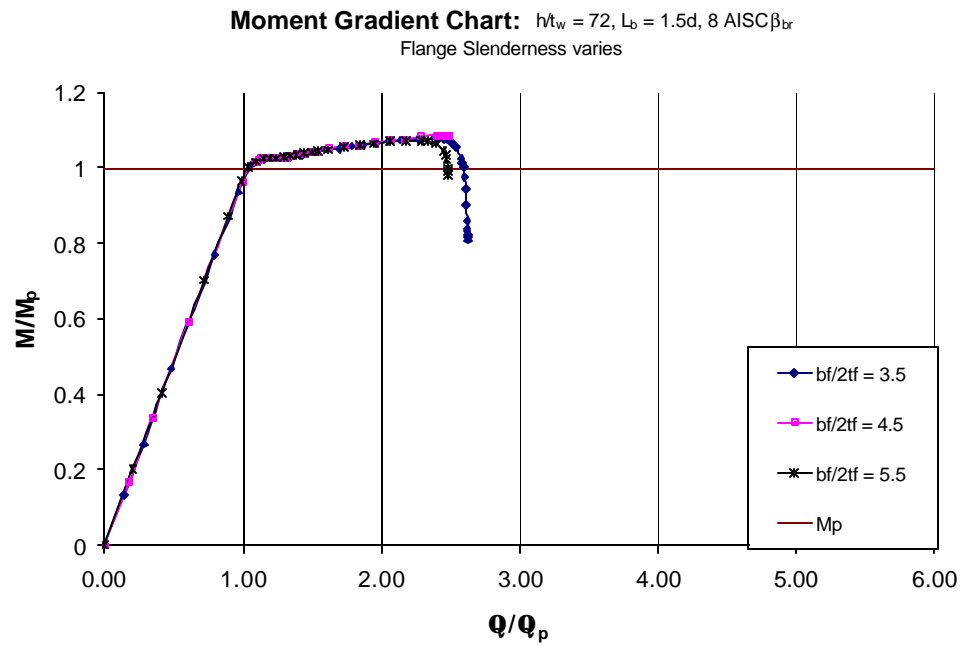
Figure B-36 Moment Rotation Plot ($h/t_w = 72$, $L_b = 1.5d$, 8 AISC β_{br} Flange Slenderness Varies)
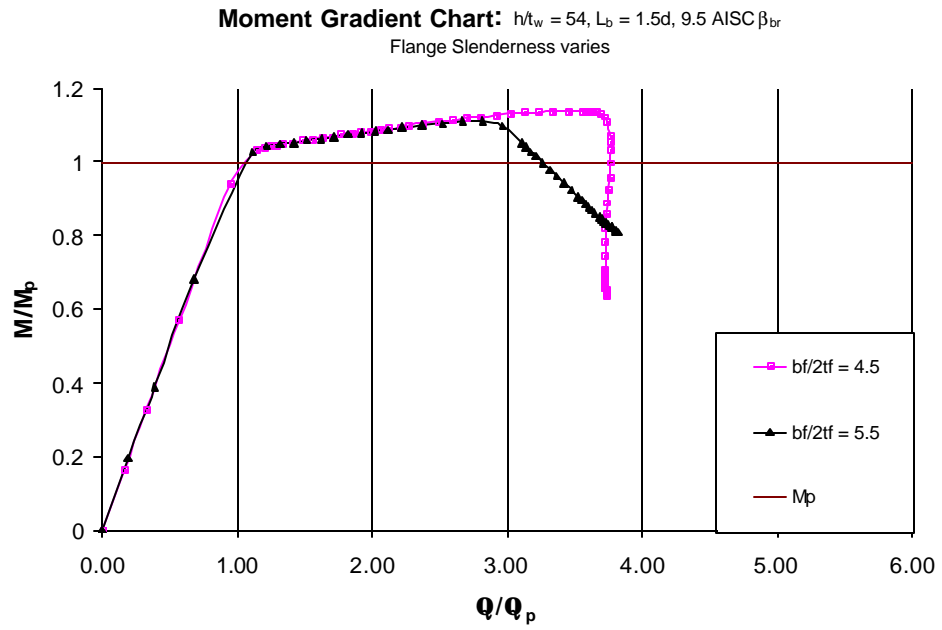
Figure B-37 Moment Rotation Plot (h/t$_w$ = 54, L$_b$ = 1.5d, 9.5 AISC β_{br} Flange Slenderness Varies)

Appendix B.2

The second presentation method combines the plots such that only the web slenderness ratio varies. By doing this, it is possible to observe the effect that a change in only web slenderness has on structural ductility.
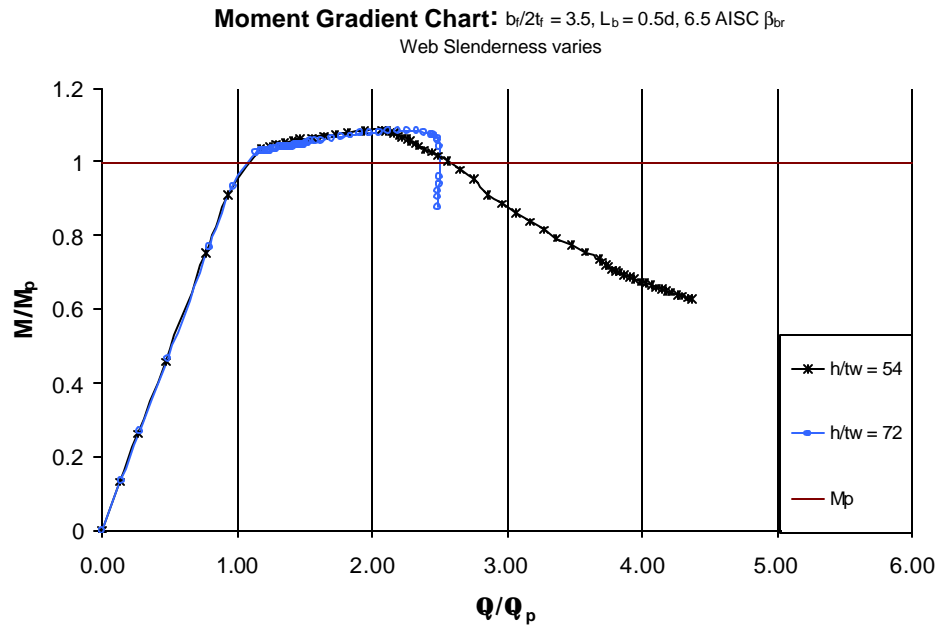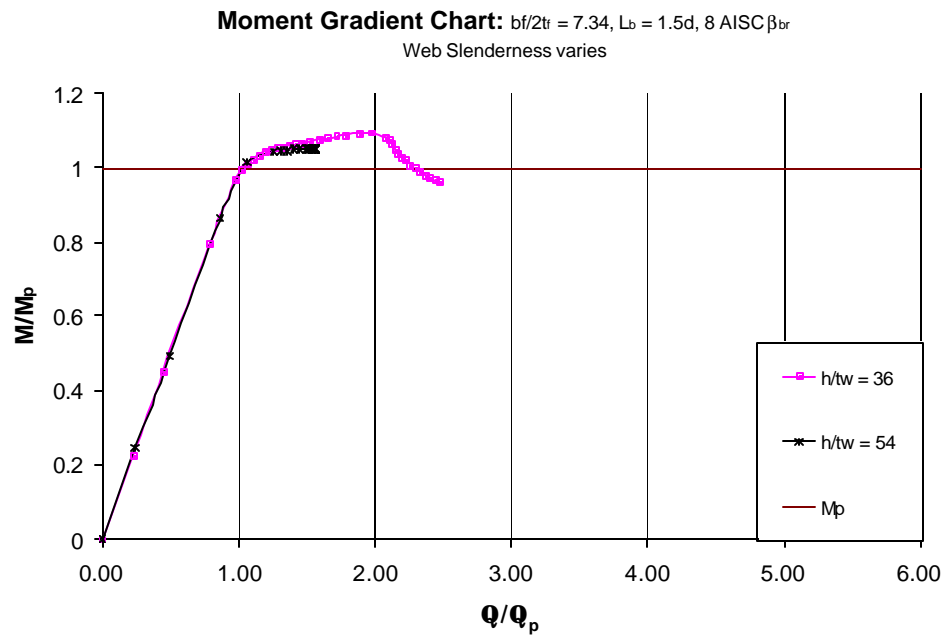
Figure B-38 Moment Rotation Plot ($b_f/2t_f = 3.5$, $L_b = 0.5d$, 6.5 AISC β_{br} Web Slenderness Varies)
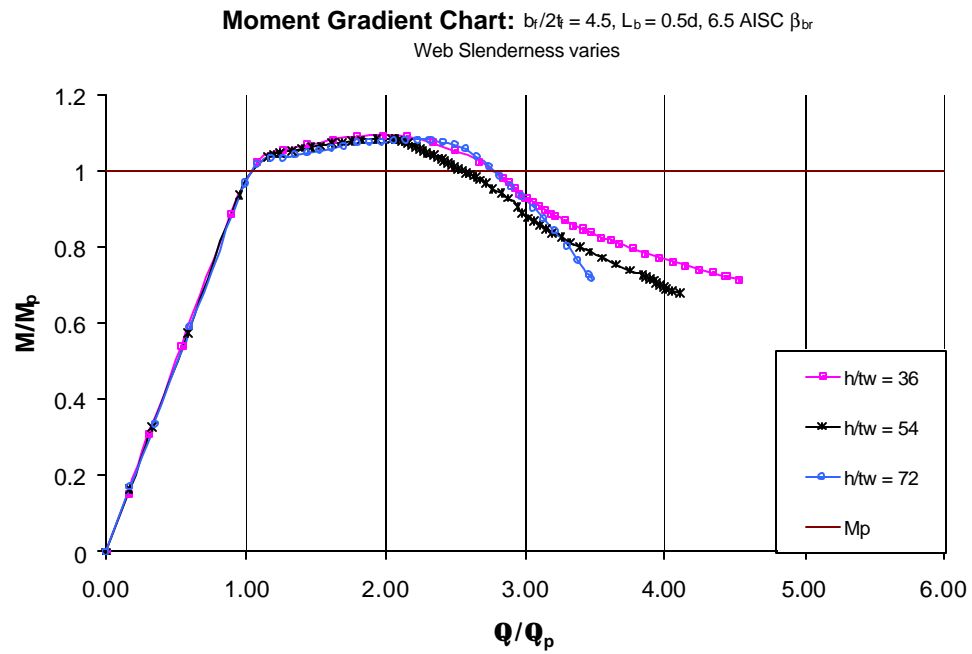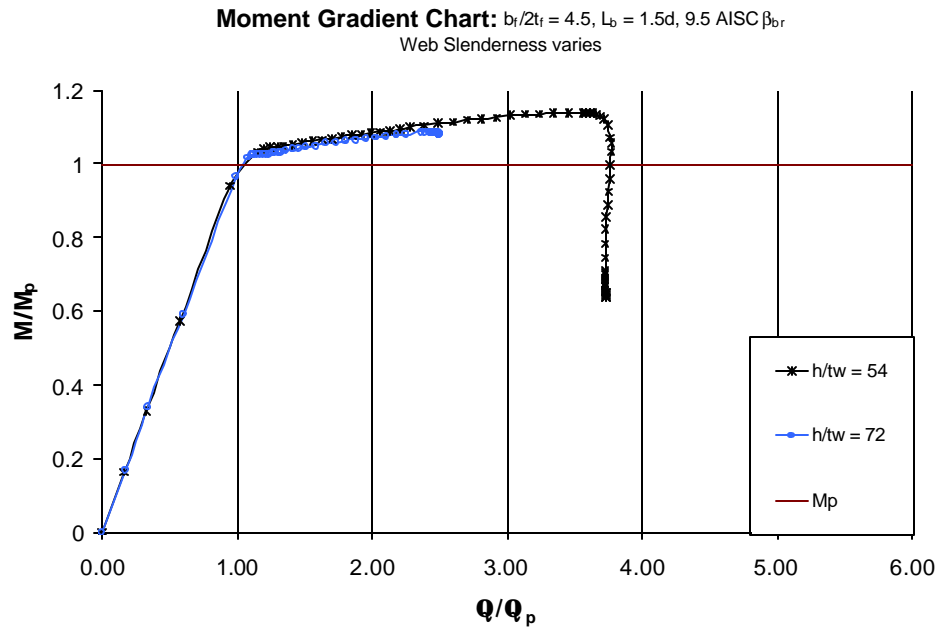

Figure B-39 Moment Rotation Plot ($b_f/2t_f = 4.5$, $L_b = 0.5d$, 6.5 AISC β_{br} Web Slenderness Varies)
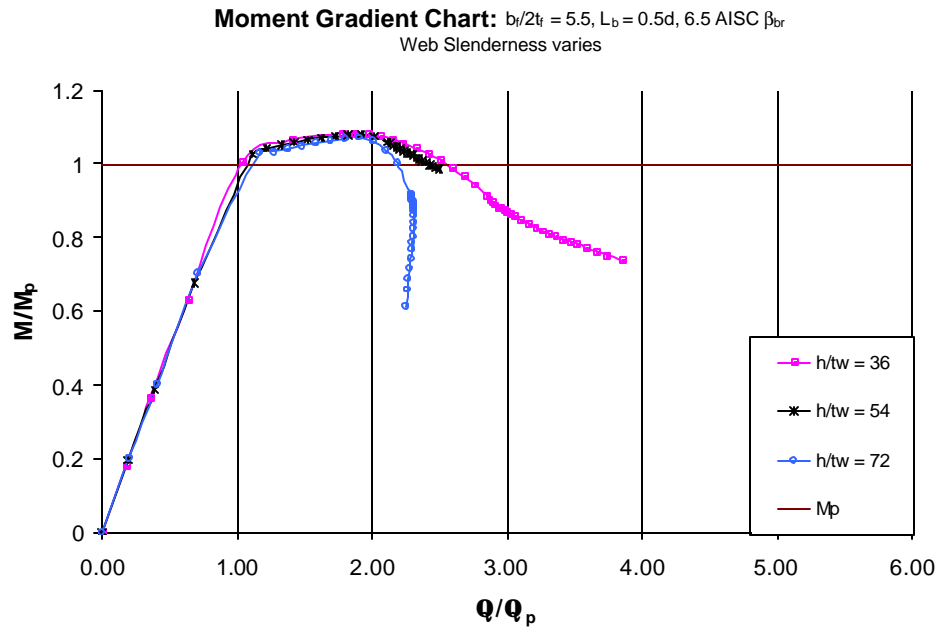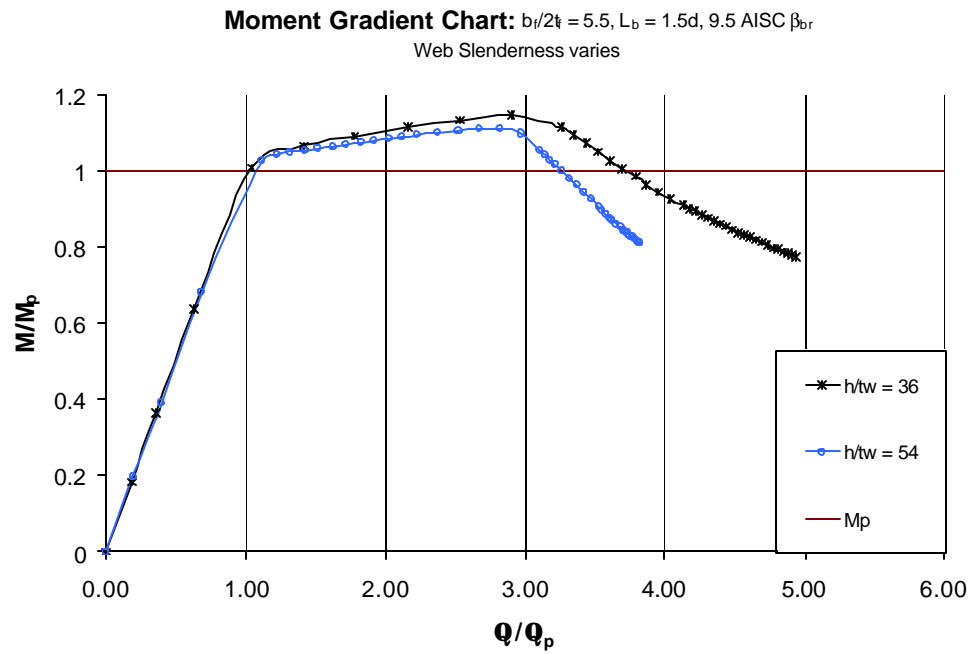
Figure B-40 Moment Rotation Plot ($b_f/2t_f$ = 5.5, L_b = 0.5d, 6.5 AISC β_{br}
Web Slenderness Varies)
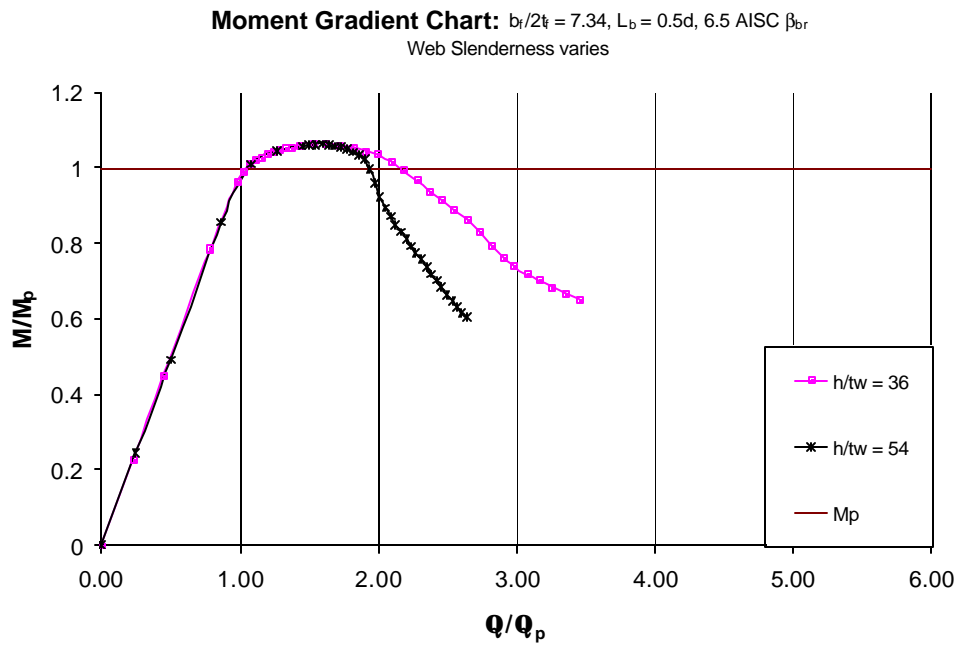
Figure B-41 Moment Rotation Plot ($b_f/2t_f$ = 7.34, L_b = 0.5d, 6.5 AISC β_{br}
Web Slenderness Varies)
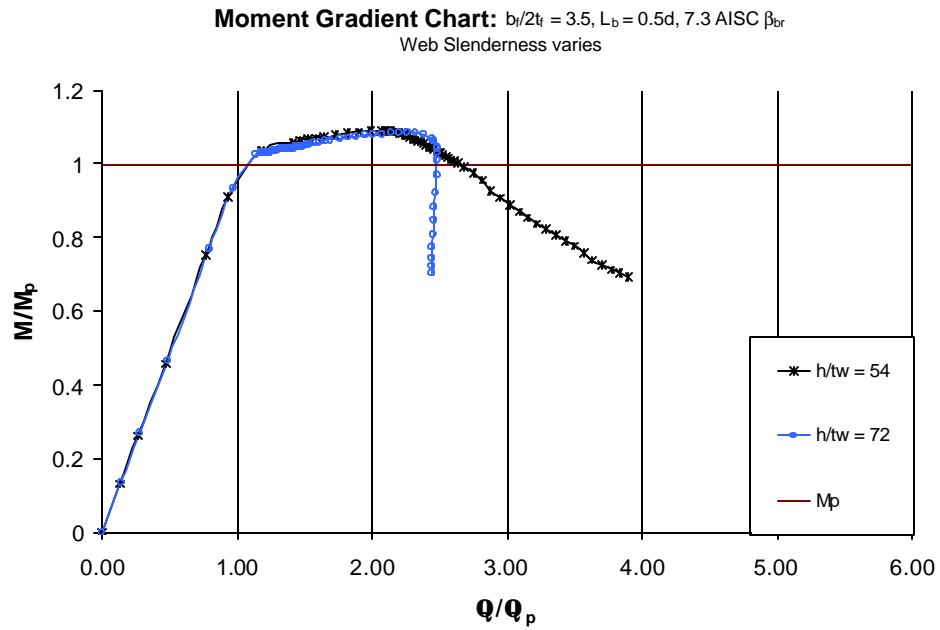
Figure B-42 Moment Rotation Plot ($b_f/2t_f = 3.5$, $L_b = 0.5d$, 7.3 AISC β_{br}
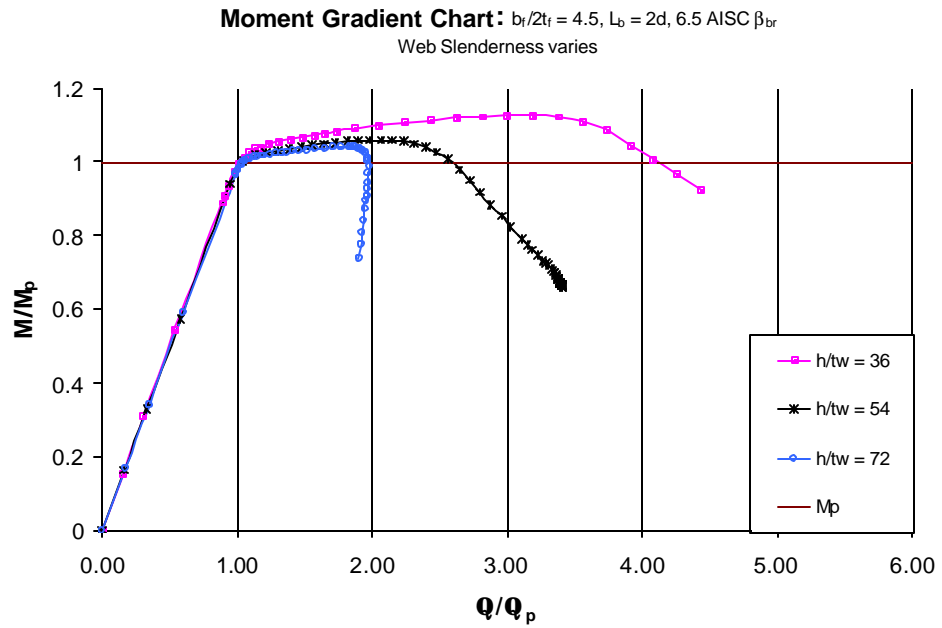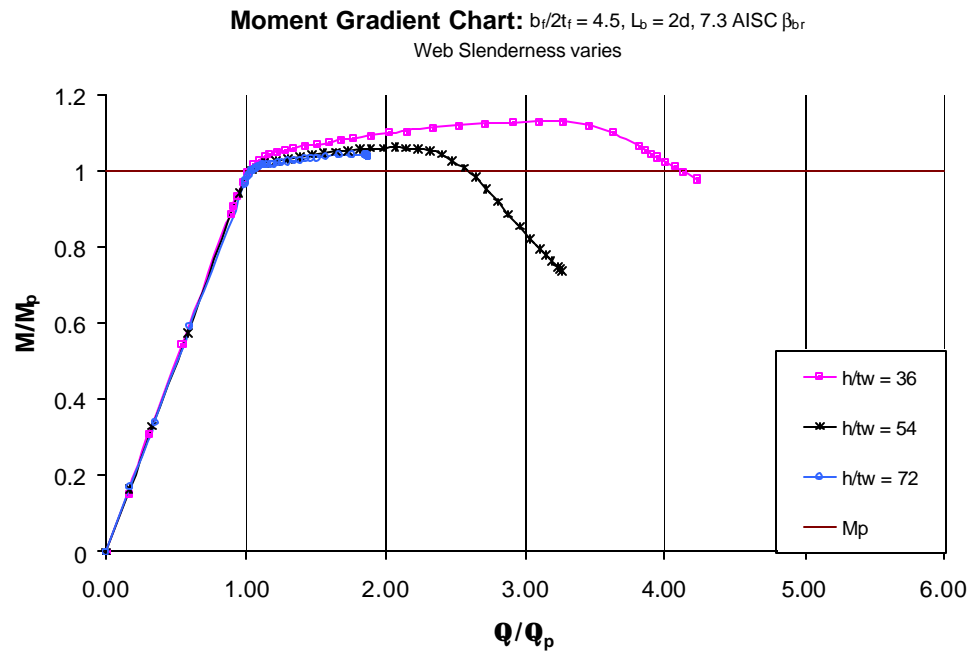Web Slenderness Varies)
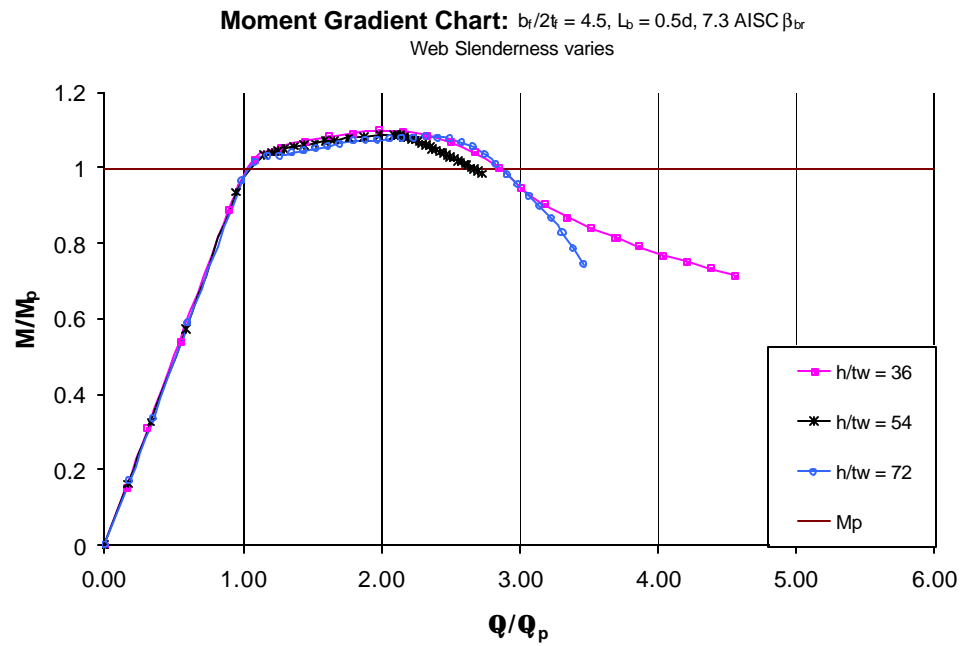
Figure B-43 Moment Rotation Plot ($b_f/2t_f = 4.5$, $L_b = 0.5d$, 7.3 AISC β_{br}
Web Slenderness Varies)
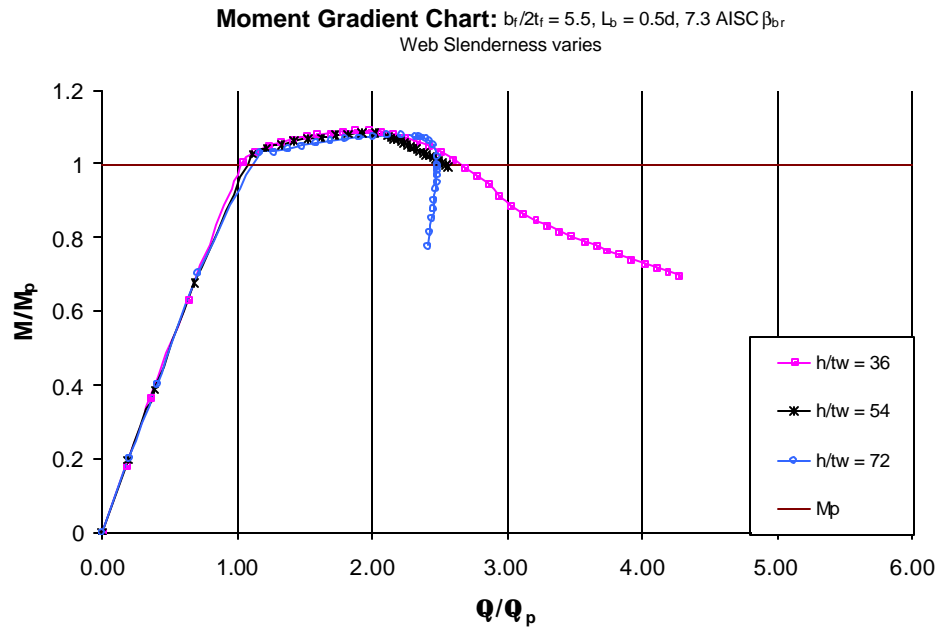
Figure B-44 Moment Rotation Plot ($b_f/2t_f = 5.5$, $L_b = 0.5d$, 7.3 AISC β_{br} Web Slenderness Varies)
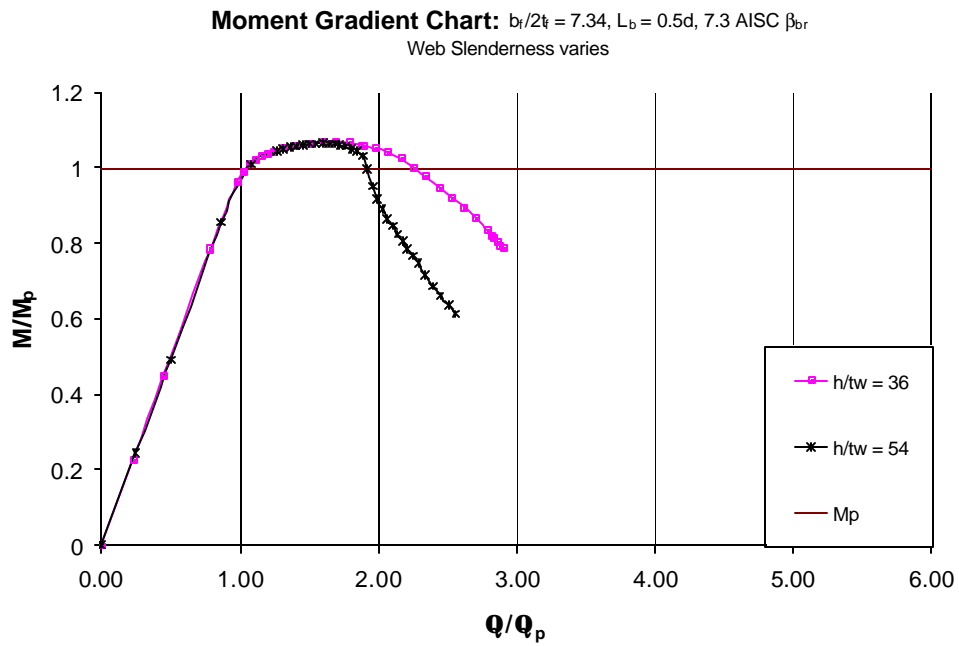
Figure B-45 Moment Rotation Plot ($b_f/2t_f = 7.34$, $L_b = 0.5d$, 7.3 AISC β_{br} Web Slenderness Varies)
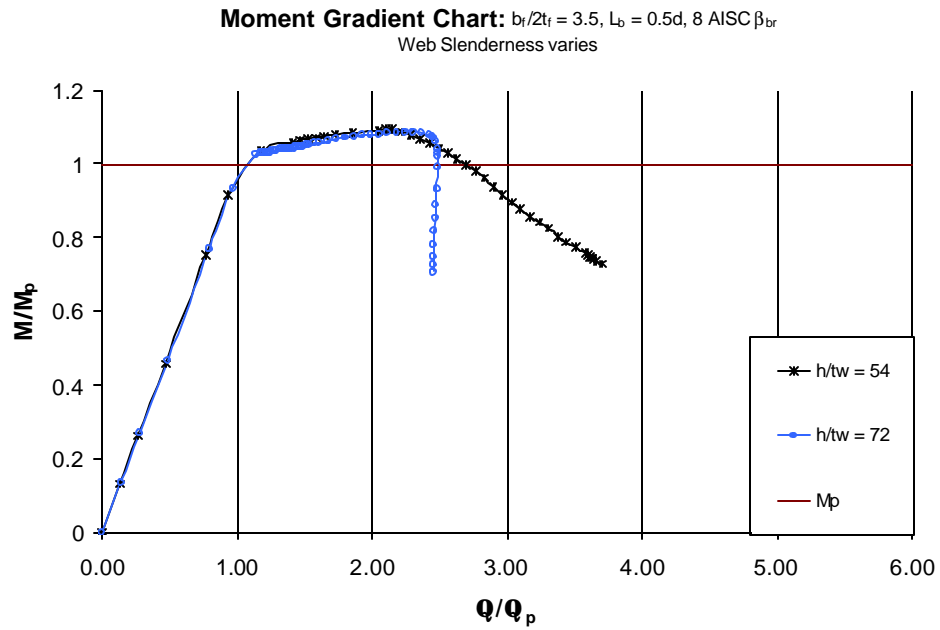
Figure B-46 Moment Rotation Plot ($b_f/2t_f = 3.5$, $L_b = 0.5d$, 8 AISC β_{br} Web Slenderness Varies)
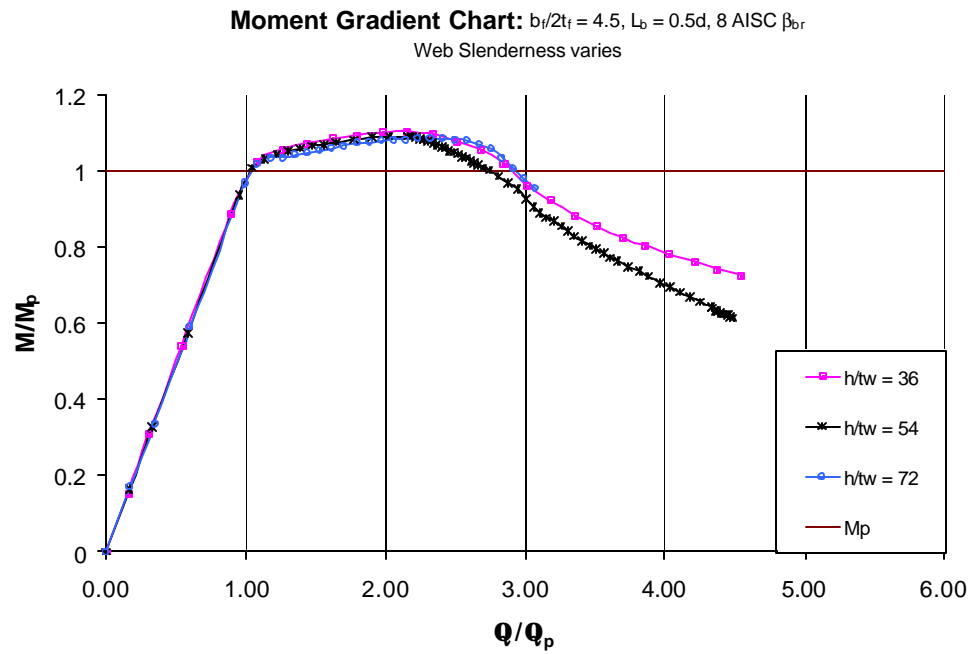
Figure B-47 Moment Rotation Plot ($b_f/2t_f = 4.5$, $L_b = 0.5d$, 8 AISC β_{br} Web Slenderness Varies)

**Moment Gradient Chart:** $b_f/2t_f = 5.5$, $L_b = 0.5d$, 8 AISC β_{br}
Web Slenderness varies
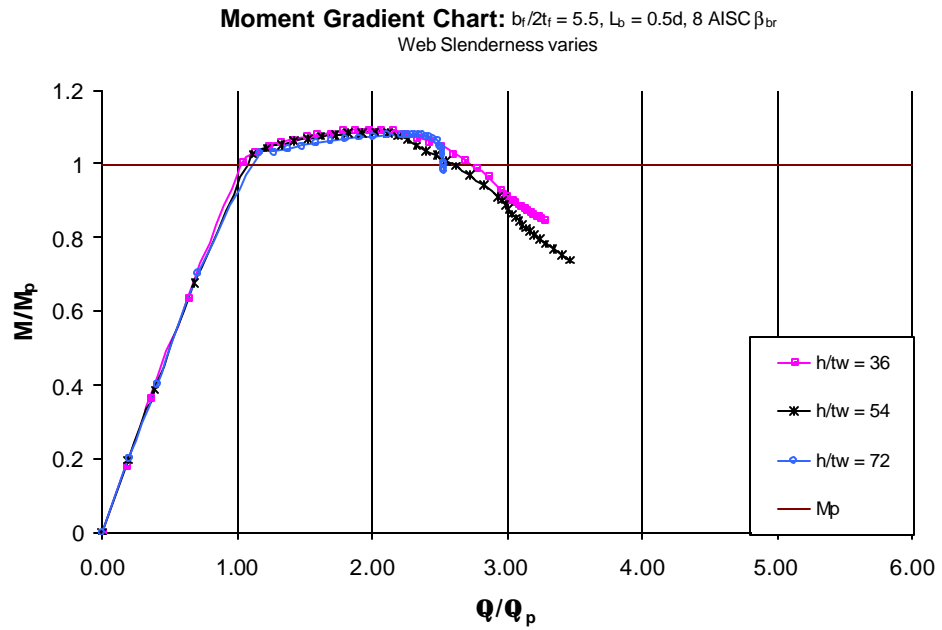
Figure B-48 Moment Rotation Plot ($b_f/2t_f = 5.5$, $L_b = 0.5d$, 8 AISC β_{br} Web Slenderness Varies)

Moment Gradient Chart: $b_f/2t_f = 7.34$, $L_b = 0.5d$, 8 AISC β_{br}
Web Slenderness varies
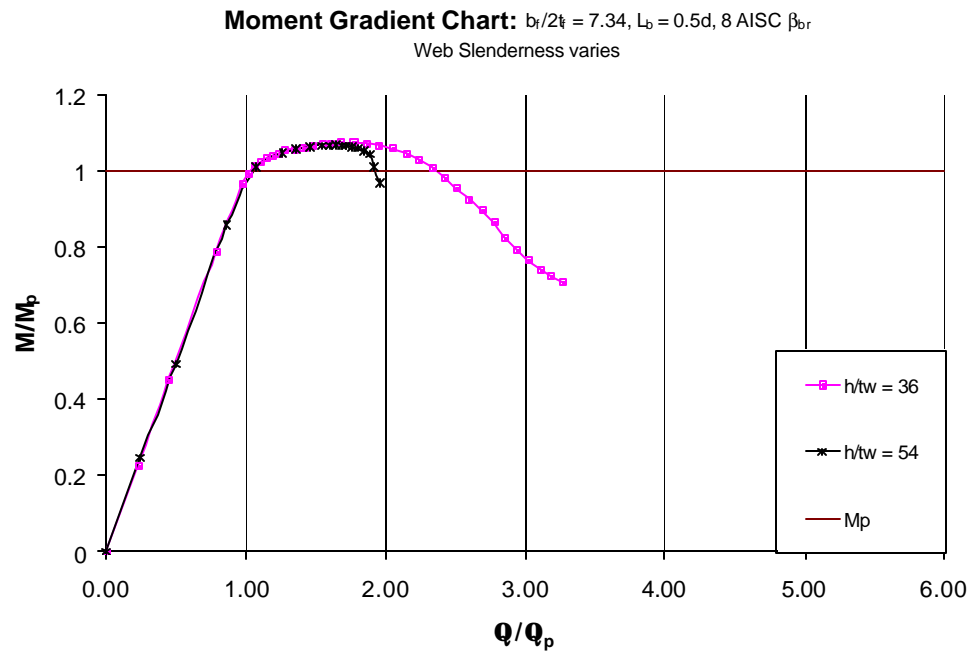
Figure B-49 Moment Rotation Plot ($b_f/2t_f = 7.34$, $L_b = 0.5d$, 8 AISC β_{br} Web Slenderness Varies)

126
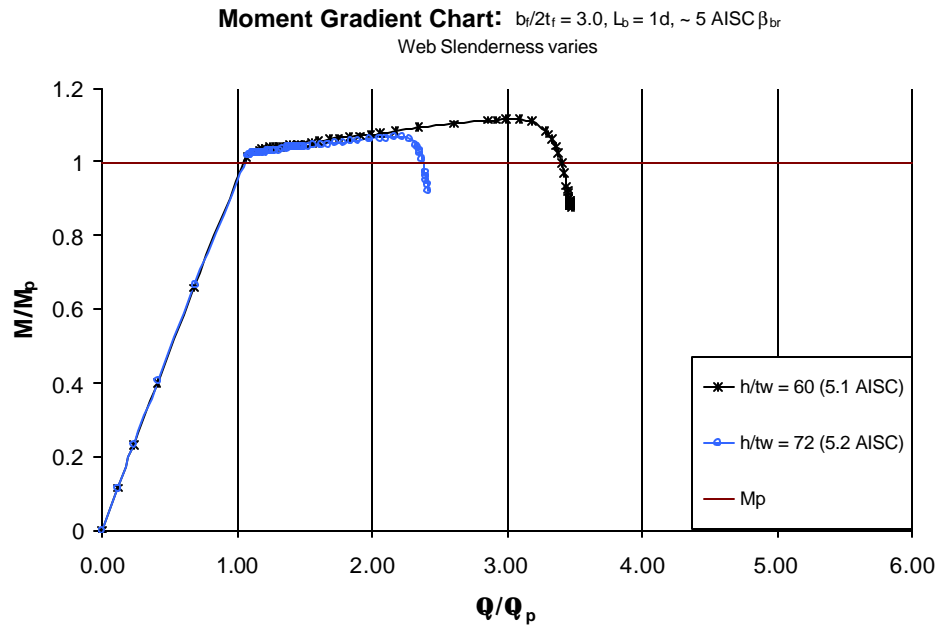
Figure B-50 Moment Rotation Plot ($b_f/2t_f = 3.0$, $L_b = 1d$, ~ 5 AISC β_{br} Web Slenderness Varies)
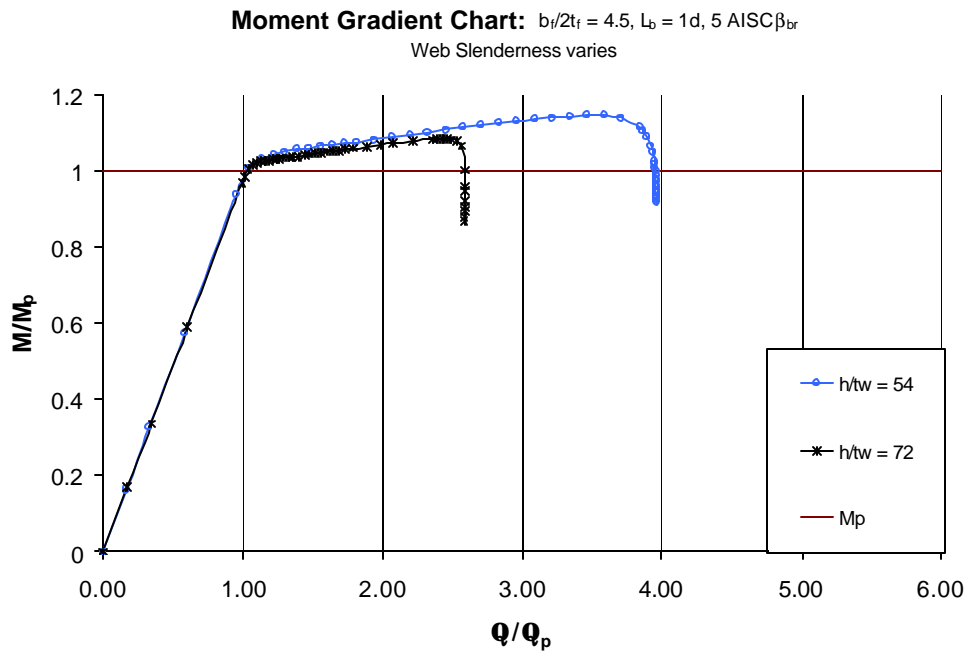
Figure B-51 Moment Rotation Plot ($b_f/2t_f = 4.5$, $L_b = 1d$, 5 AISC β_{br} Web Slenderness Varies)

Moment Gradient Chart: $b_f/2t_f = 5.5$, $L_b = 1d$, 5 AISC β_{br}
Web Slenderness varies
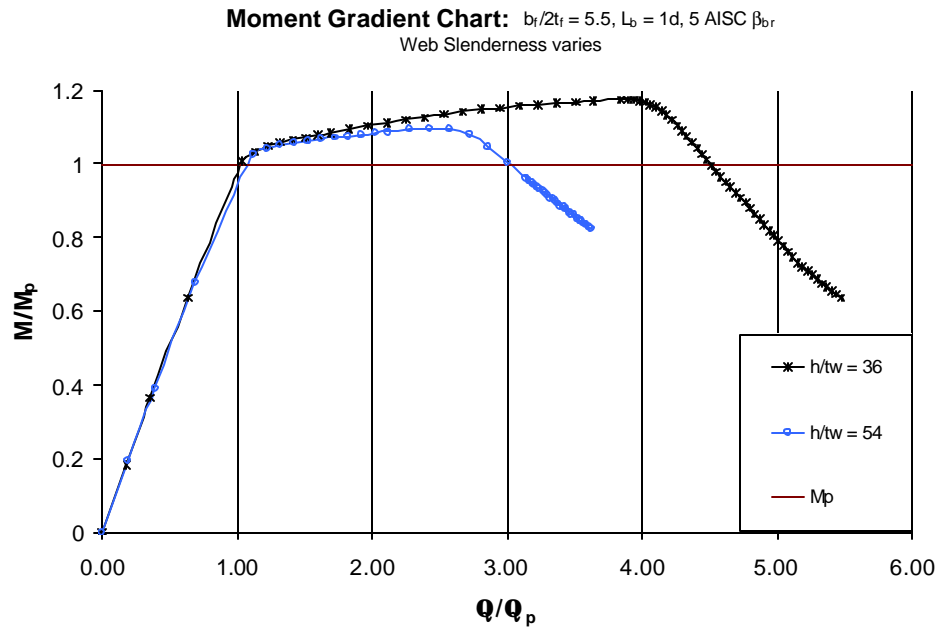
Figure B-52 Moment Rotation Plot ($b_f/2t_f = 5.5$, $L_b = 1d$, 5 AISC β_{br} Web Slenderness Varies)

Moment Gradient Chart: $b_f/2t_f = 4.5$, $L_b = 1d$, 5.3 AISC β_{br}
Web Slenderness varies
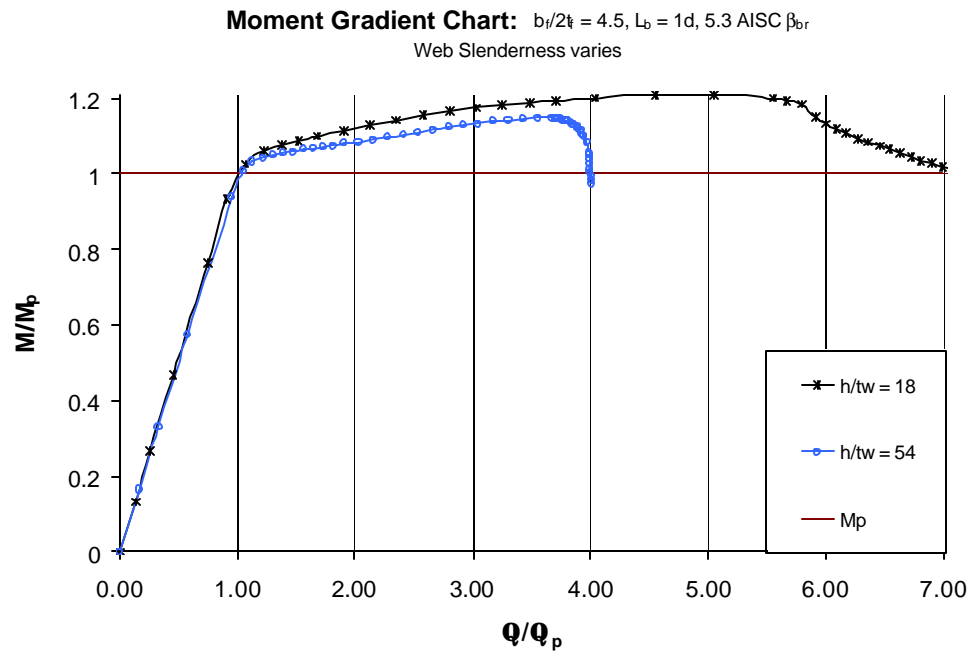
Figure B-53 Moment Rotation Plot ($b_f/2t_f = 4.5$, $L_b = 1d$, 5.3 AISC β_{br} Web Slenderness Varies)

Moment Gradient Chart: $b_f/2t_f = 3.5$, $L_b = 1d$, 5.9 AISC β_{br}
Web Slenderness varies
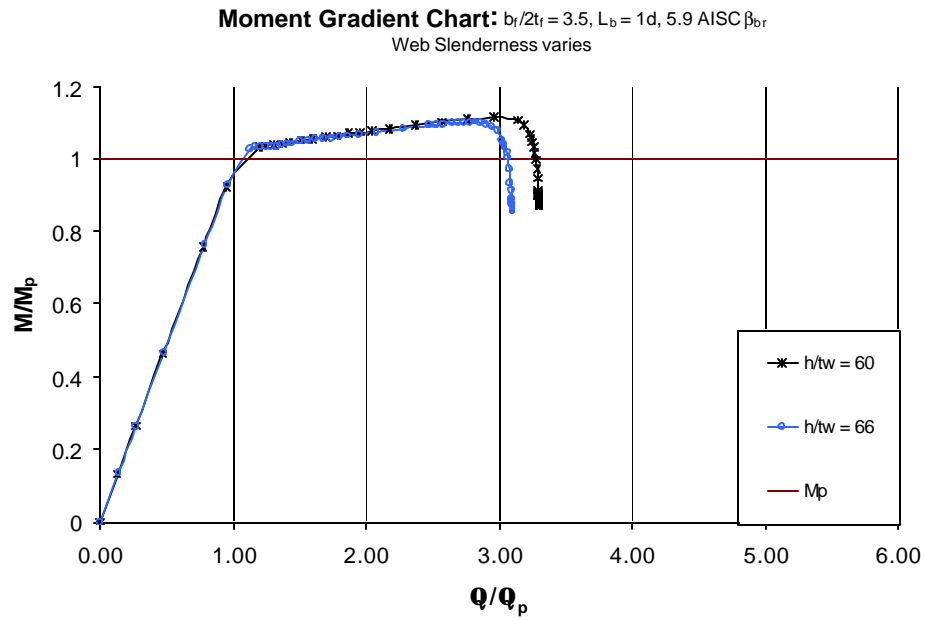
Figure B-54 Moment Rotation Plot ($b_f/2t_f = 3.5$, $L_b = 1d$, 5.9 AISC β_{br} Web Slenderness Varies)

Moment Gradient Chart: $b_f/2t_f = 4.5$, $L_b = 1d$, 5.9 AISC β_{br}
Web Slenderness varies
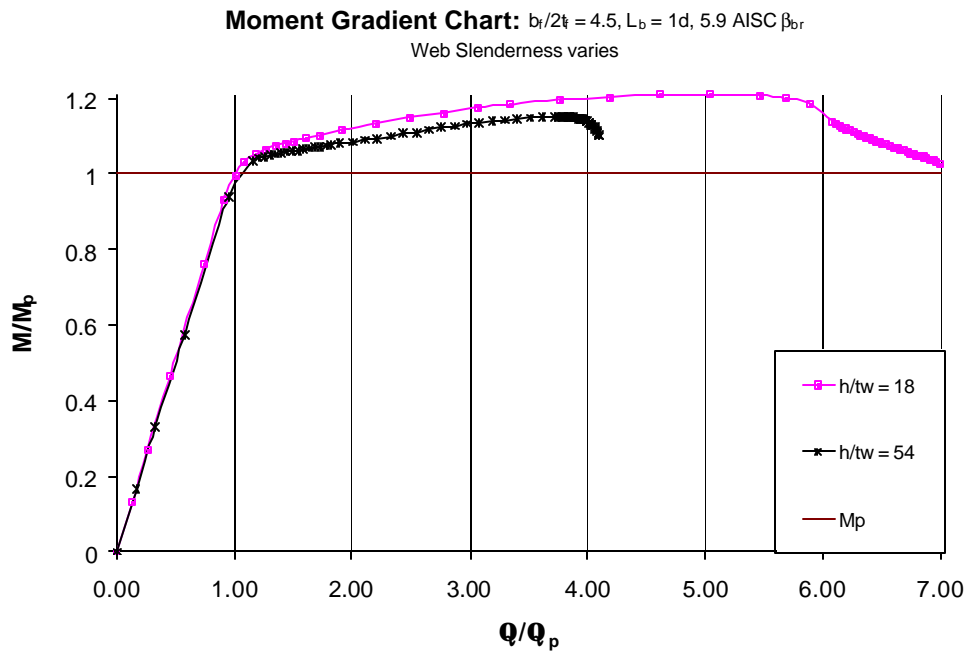
Figure B-55 Moment Rotation Plot ($b_f/2t_f = 4.5$, $L_b = 1d$, 5.9 AISC β_{br} Web Slenderness Varies)
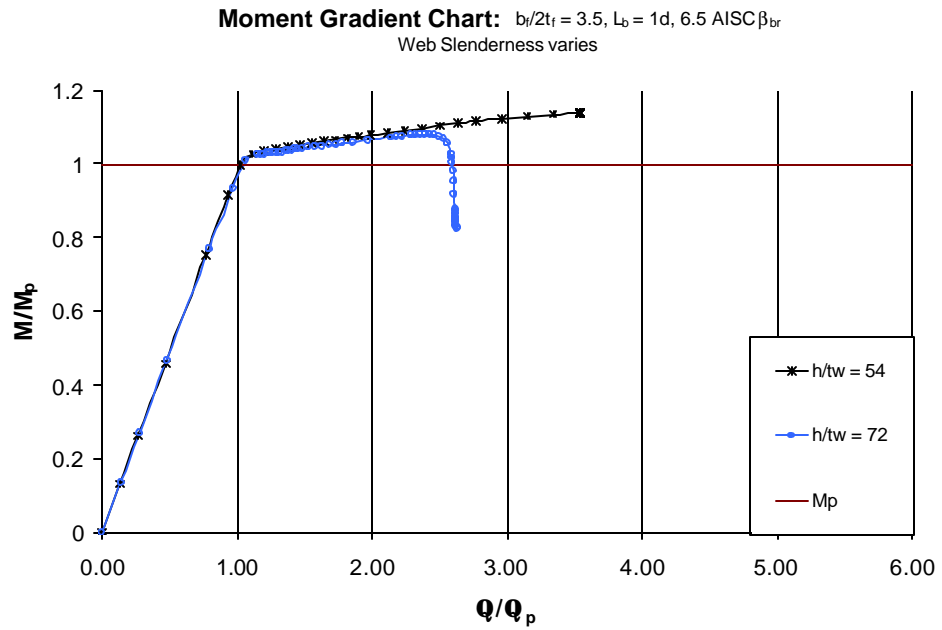
Figure B-56 Moment Rotation Plot ($b_f/2t_f = 3.5$, $L_b = 1d$, 6.5 AISC β_{br} Web Slenderness Varies)
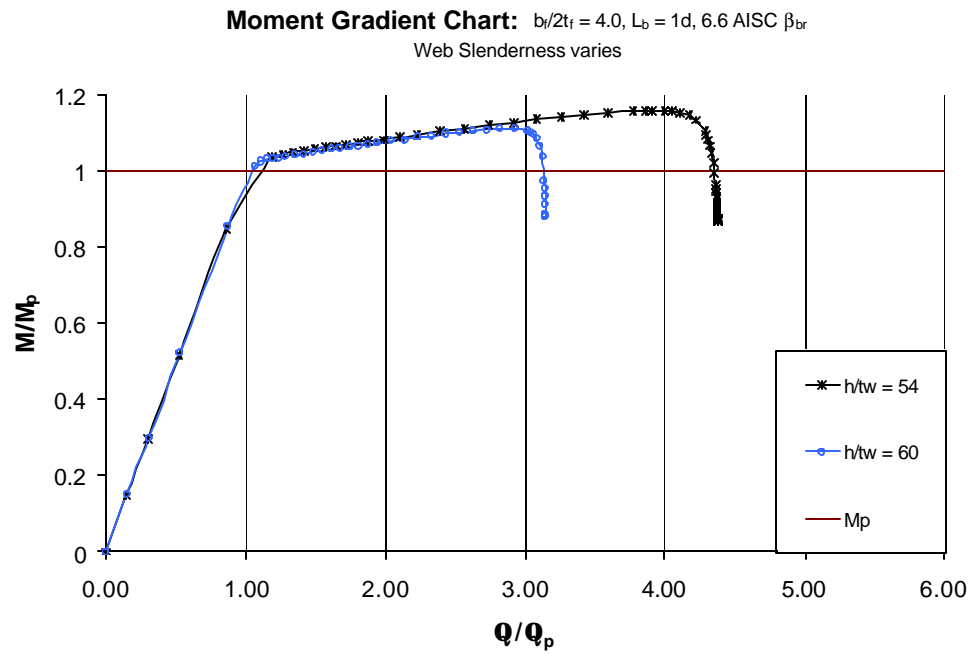
Figure B-57 Moment Rotation Plot ($b_f/2t_f = 4.0$, $L_b = 1d$, 6.6 AISC β_{br} Web Slenderness Varies)
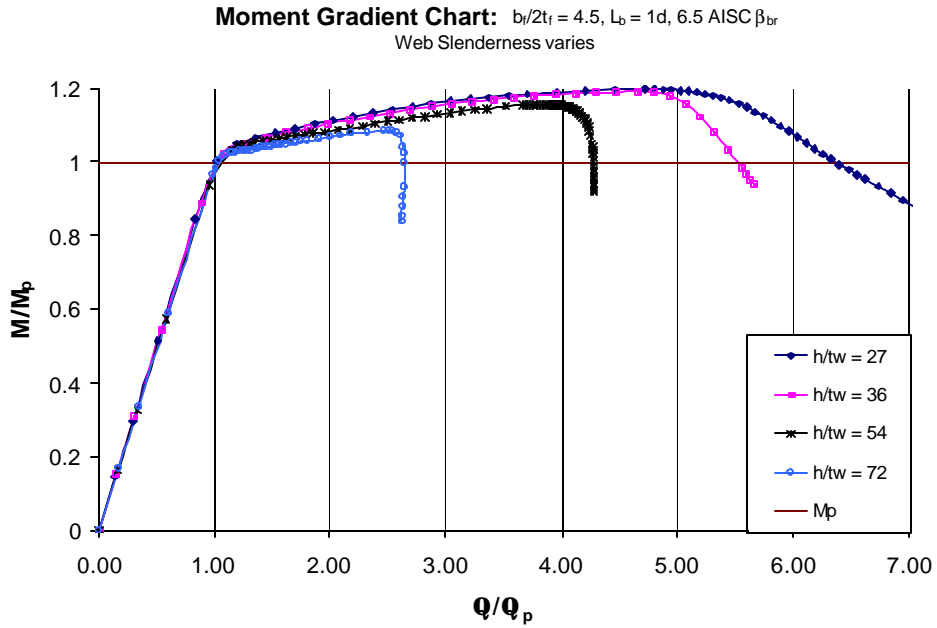
Figure B-58 Moment Rotation Plot ($b_f/2t_f = 4.5$, $L_b = 1d$, 6.5 AISC β_{br} Web Slenderness Varies)
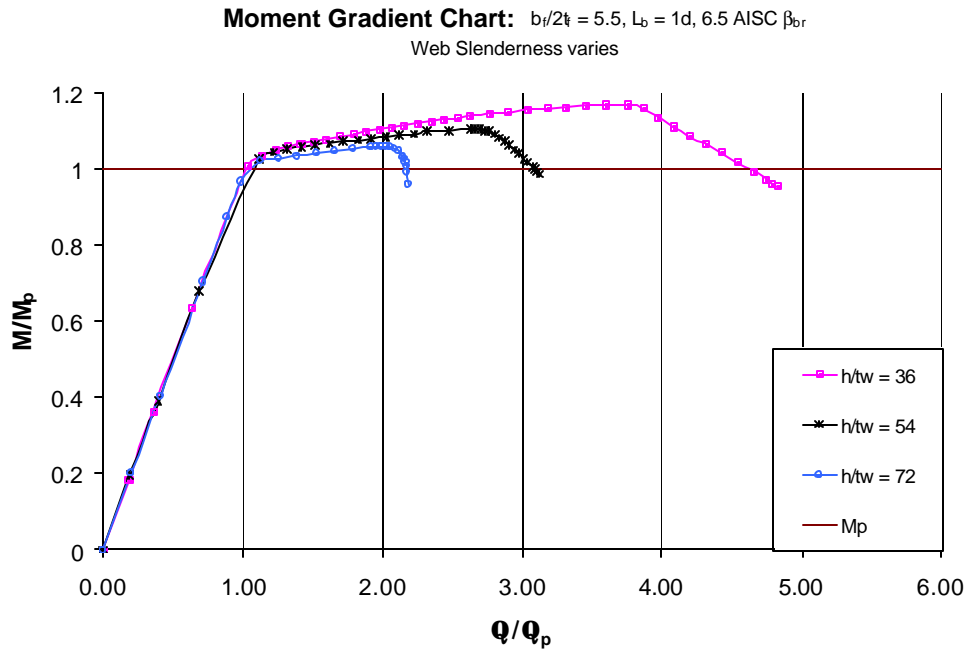
Figure B-59 Moment Rotation Plot ($b_f/2t_f = 5.5$, $L_b = 1d$, 6.5 AISC β_{br} Web Slenderness Varies)

131
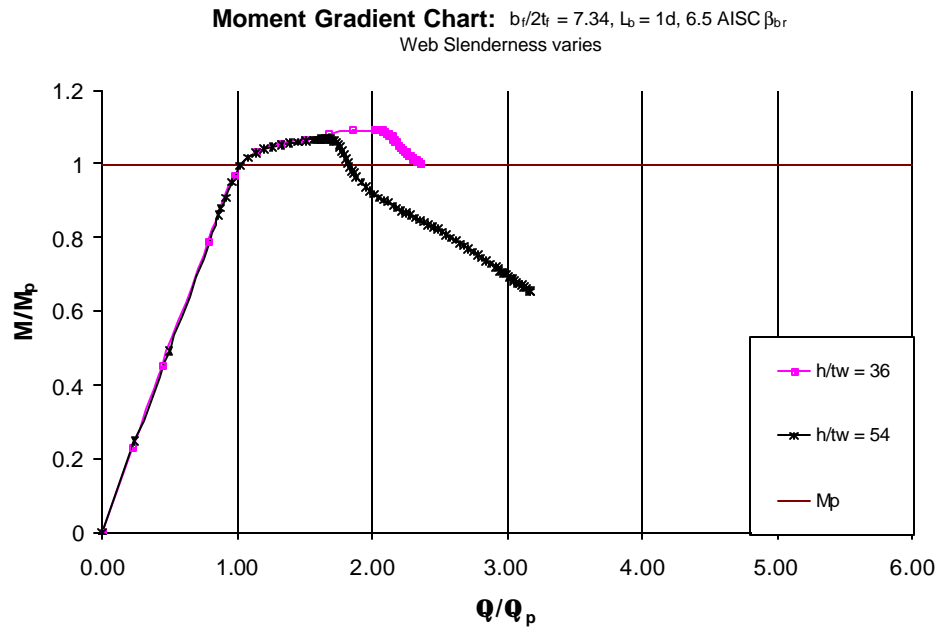
Figure B-60 Moment Rotation Plot ($b_f/2t_f = 7.34$, $L_b = 1d$, 6.5 AISC β_{br} Web Slenderness Varies)
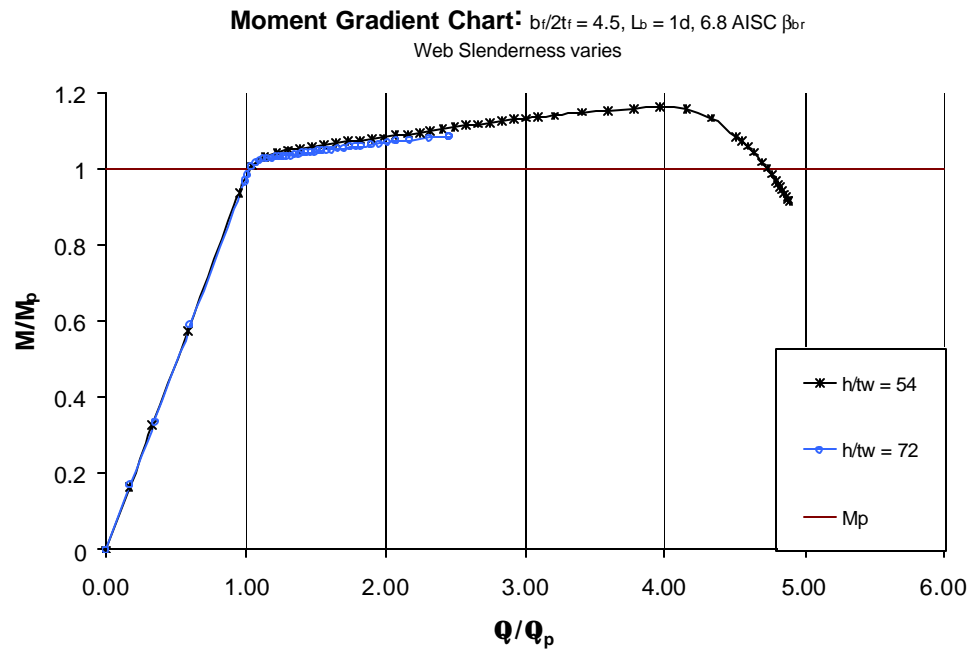
Figure B-61 Moment Rotation Plot ($b_f/2t_f = 4.5$, $L_b = 1d$, 6.8 AISC β_{br} Web Slenderness Varies)
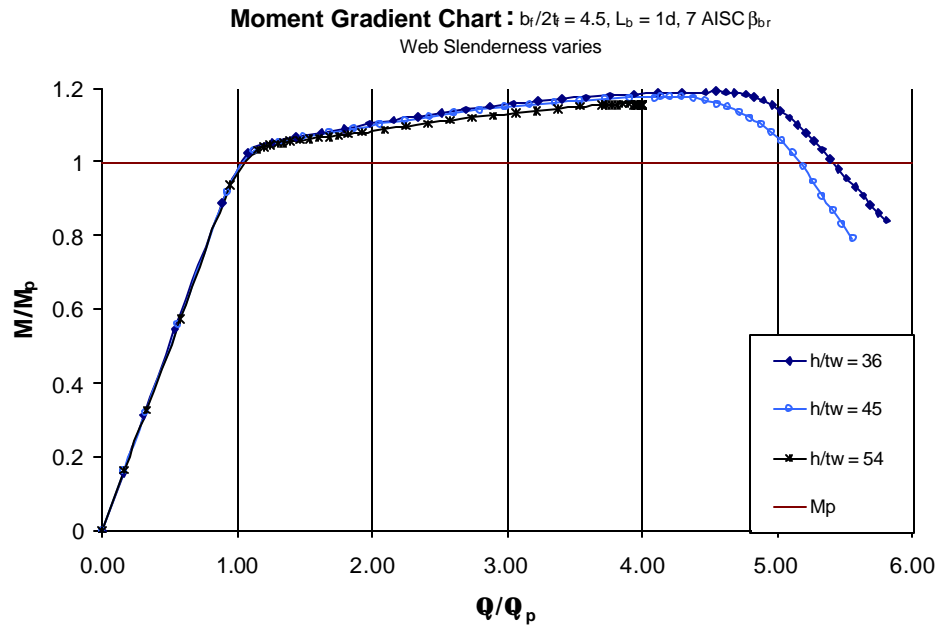
Figure B-62 Moment Rotation Plot ($b_f/2t_f = 4.5$, $L_b = 1d$, 7 AISC β_{br} Web Slenderness Varies)
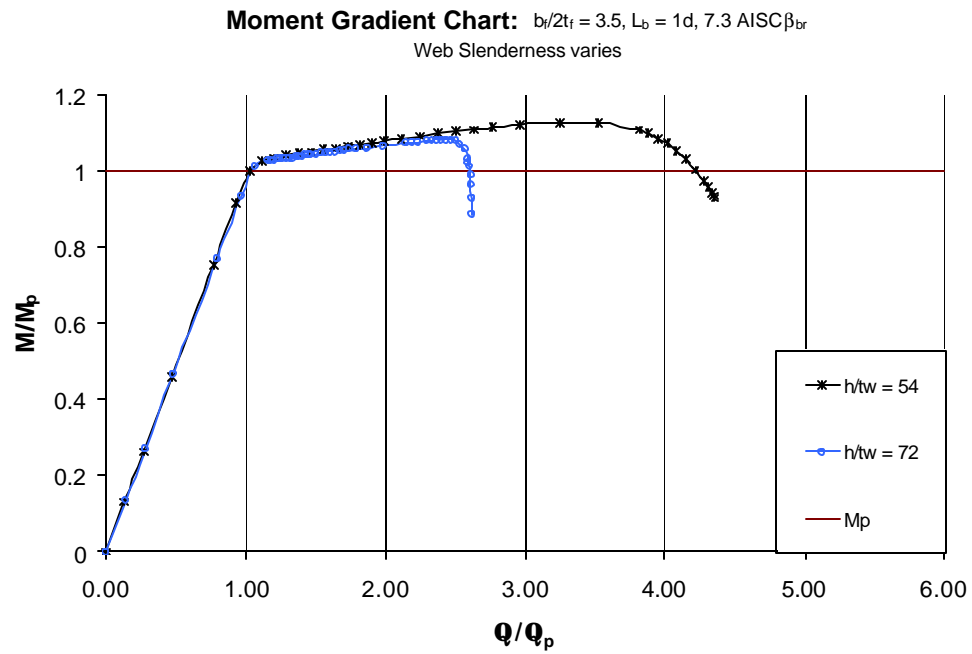
Figure B-63 Moment Rotation Plot ($b_f/2t_f = 3.5$, $L_b = 1d$, 7.3 AISC β_{br} Web Slenderness Varies)
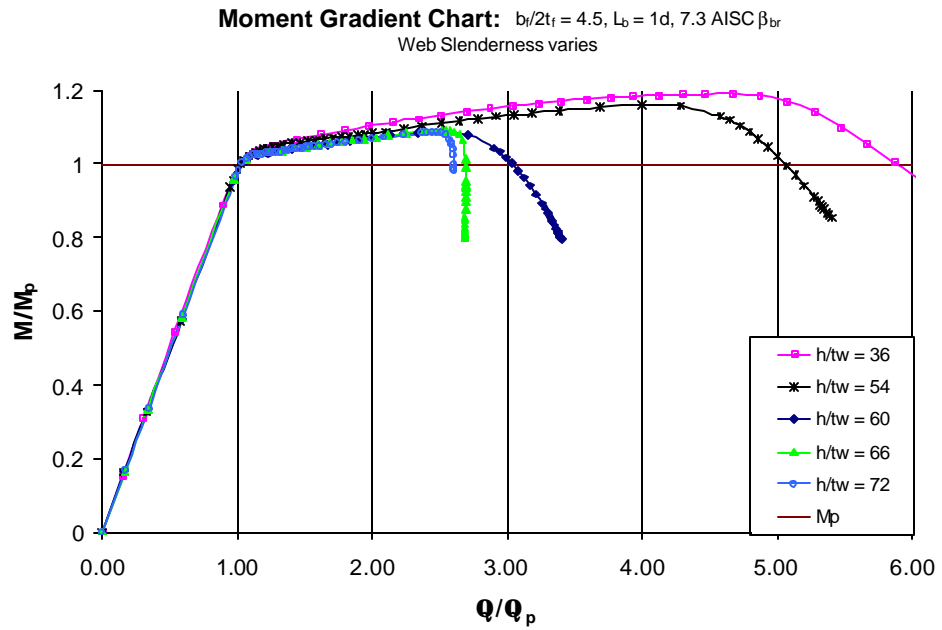
Figure B-64 Moment Rotation Plot ($b_f/2t_f = 4.5$, $L_b = 1d$, 7.3 AISC β_{br} Web Slenderness Varies)
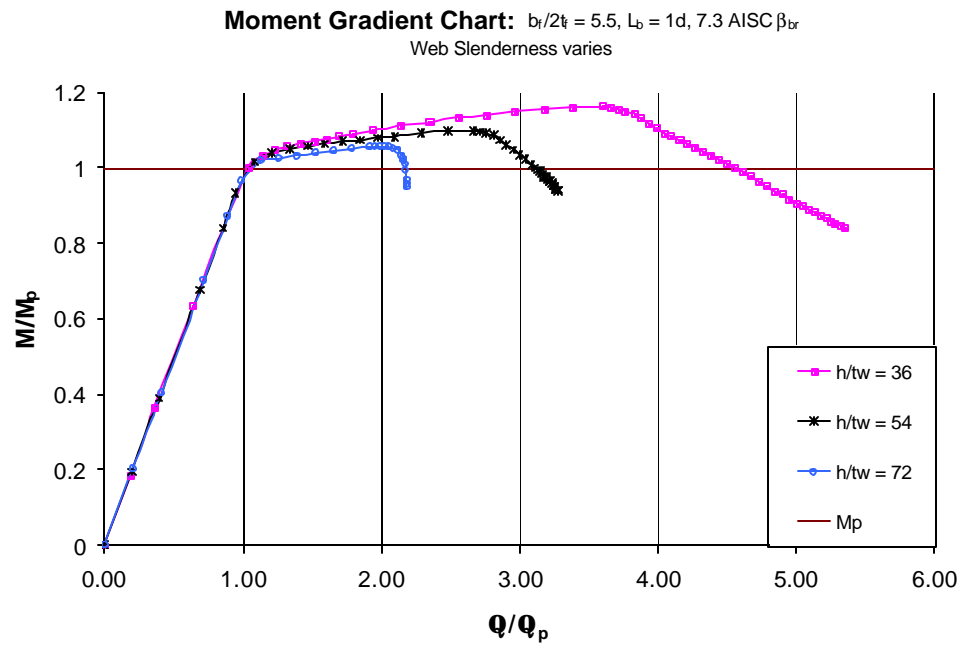
Figure B-65 Moment Rotation Plot ($b_f/2t_f = 5.5$, $L_b = 1d$, 7.3 AISC β_{br} Web Slenderness Varies)
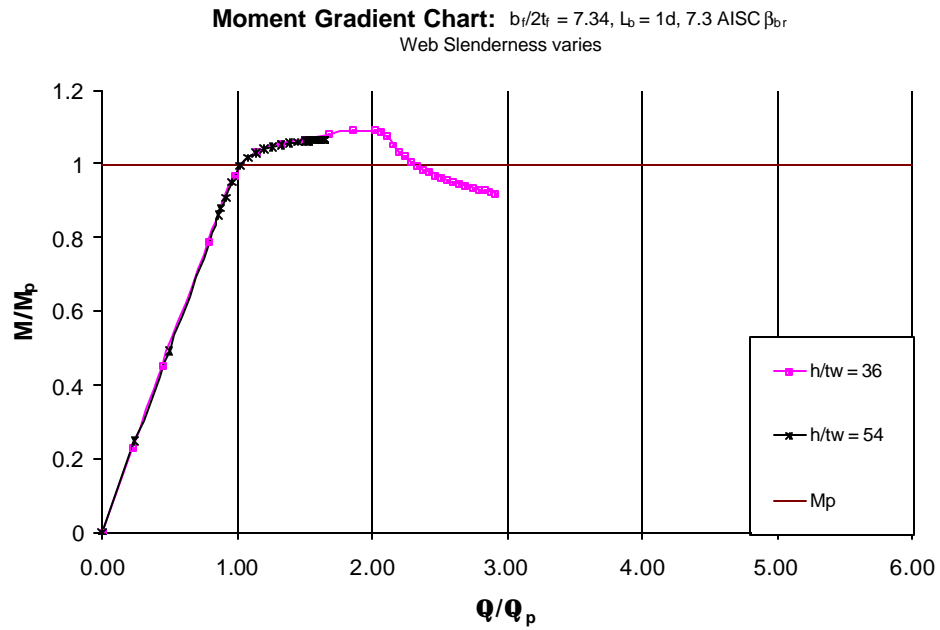
Figure B-66 Moment Rotation Plot ($b_f/2t_f = 7.34$, $L_b = 1d$, 7.3 AISC β_{br}
Web Slenderness Varies)
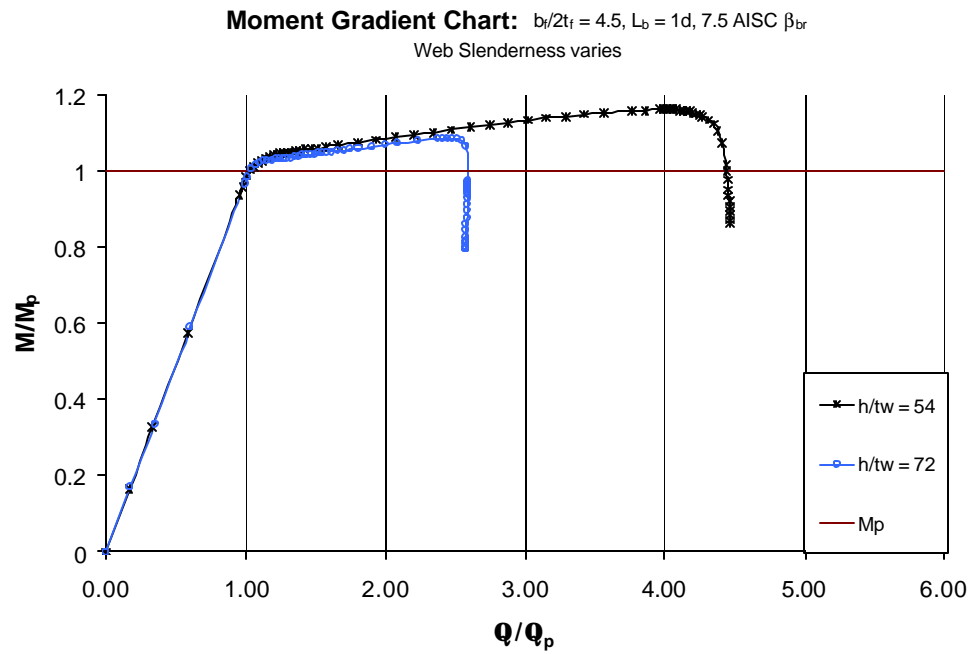
Figure B-67 Moment Rotation Plot ($b_f/2t_f = 4.5$, $L_b = 1d$, 7.5 AISC β_{br}
Web Slenderness Varies)
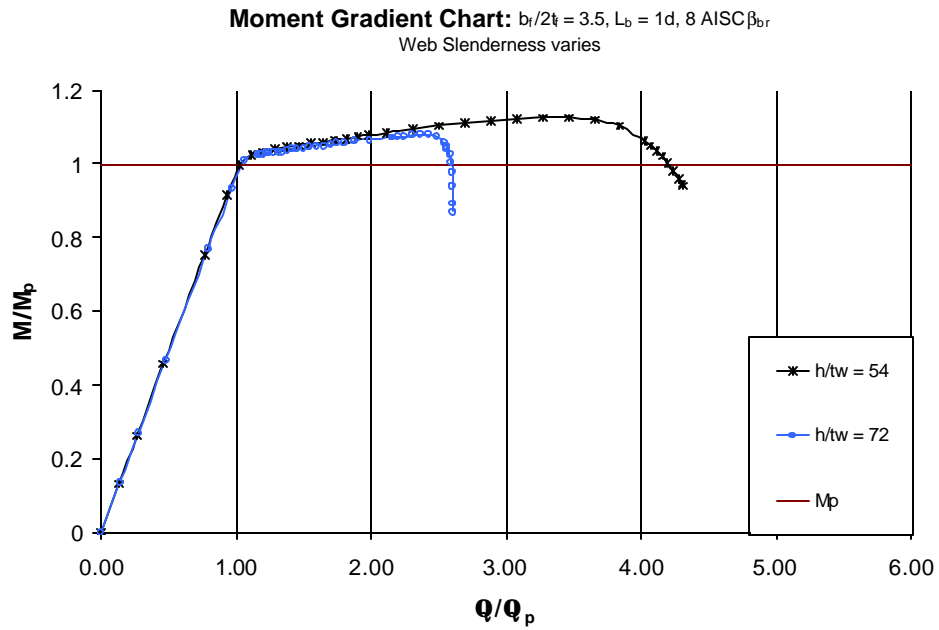
Figure B-68 Moment Rotation Plot ($b_f/2t_f = 3.5$, $L_b = 1d$, 8 AISC β_{br}
Web Slenderness Varies)
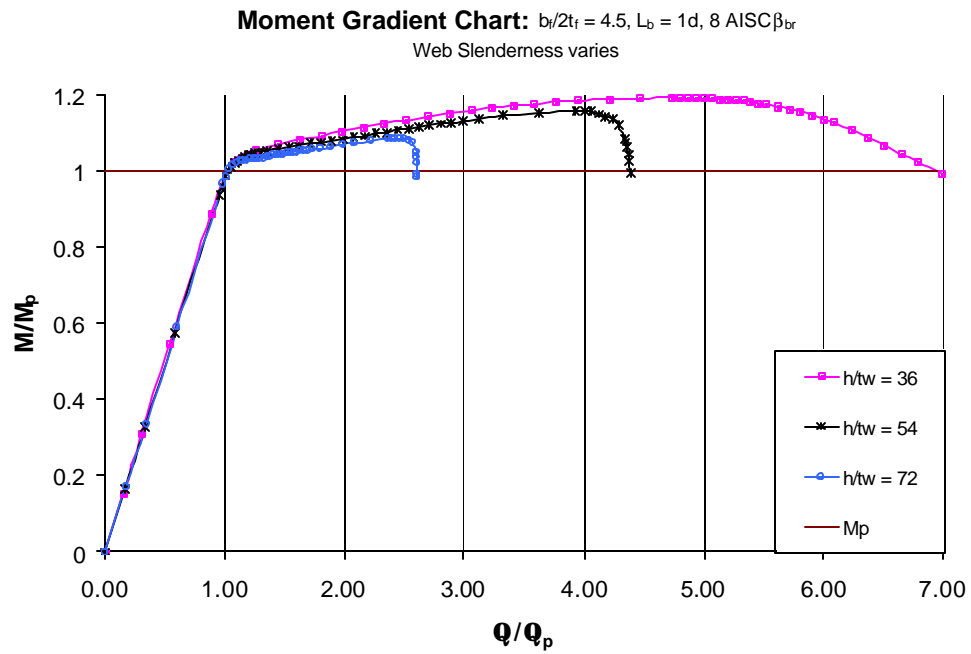
Figure B-69 Moment Rotation Plot ($b_f/2t_f = 4.5$, $L_b = 1d$, 8 AISC β_{br}
Web Slenderness Varies)
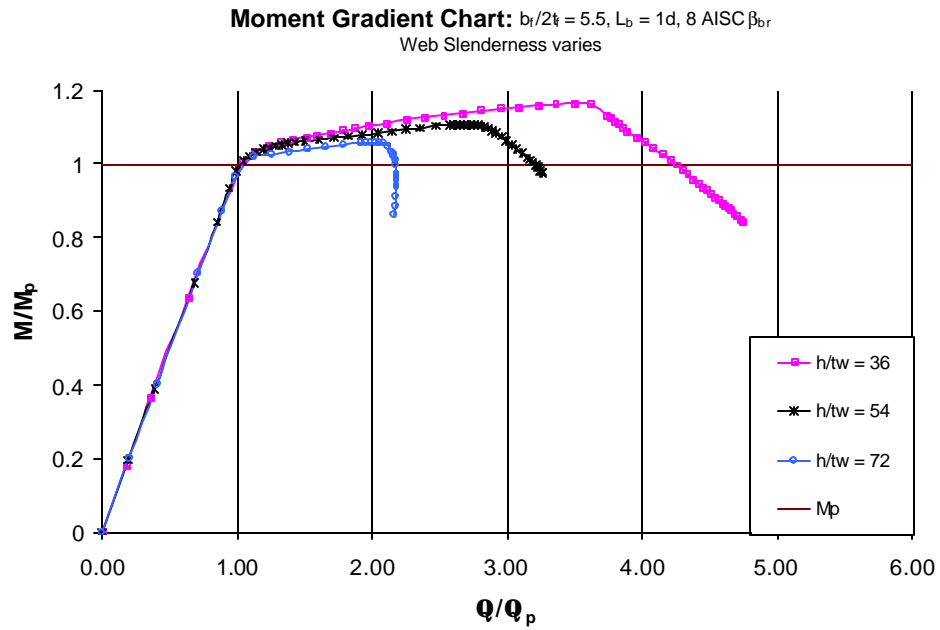
Figure B-70 Moment Rotation Plot ($b_f/2t_f = 5.5$, $L_b = 1d$, 8 AISC β_{br} Web Slenderness Varies)
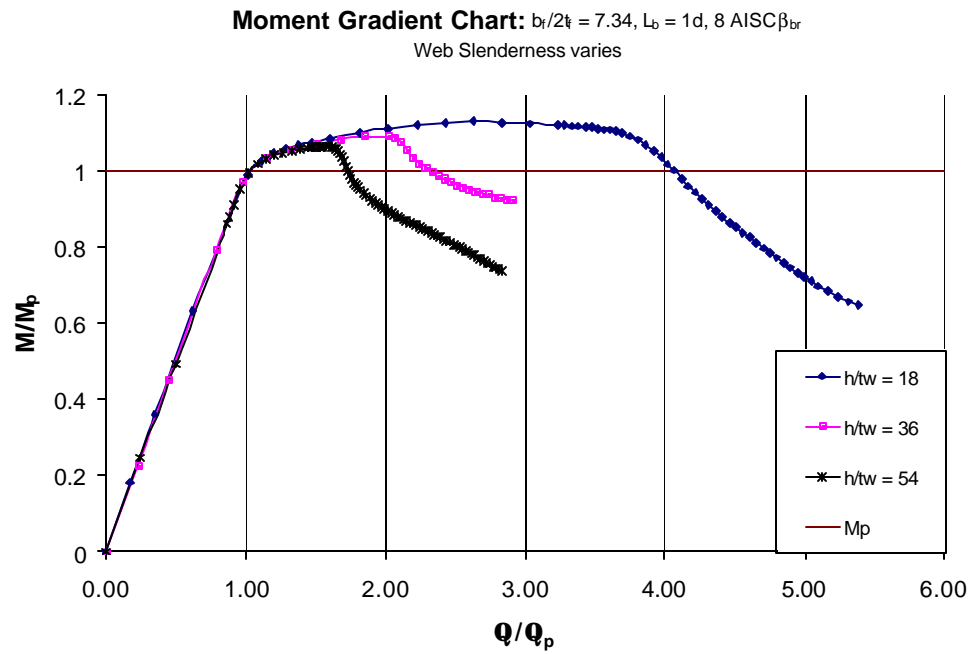
Figure B-71 Moment Rotation Plot ($b_f/2t_f = 7.34$, $L_b = 1d$, 8 AISC β_{br} Web Slenderness Varies)
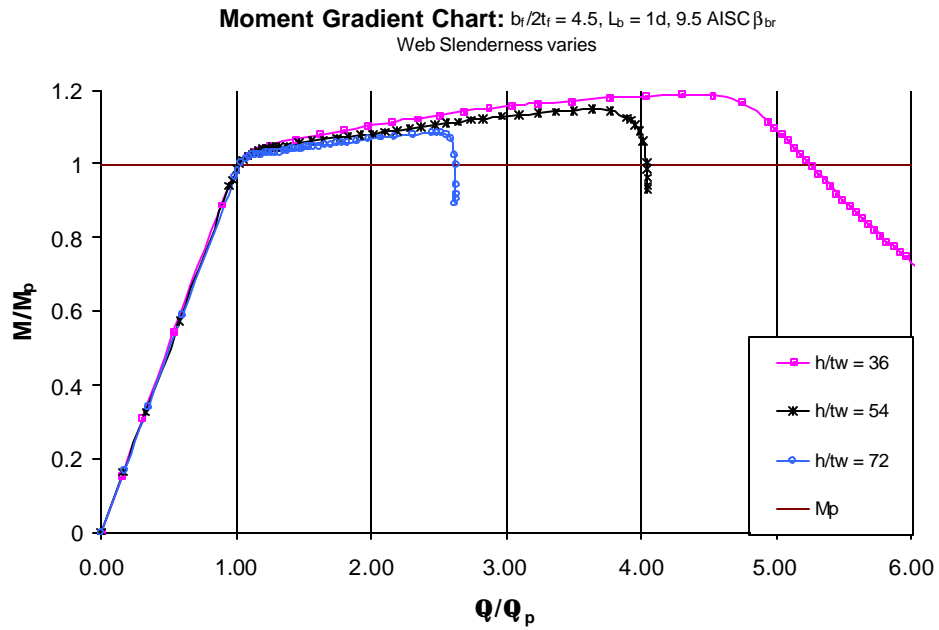
Figure B-72 Moment Rotation Plot ($b_f/2t_f = 4.5$, $L_b = 1d$, 9.5 AISC β_{br} Web Slenderness Varies)
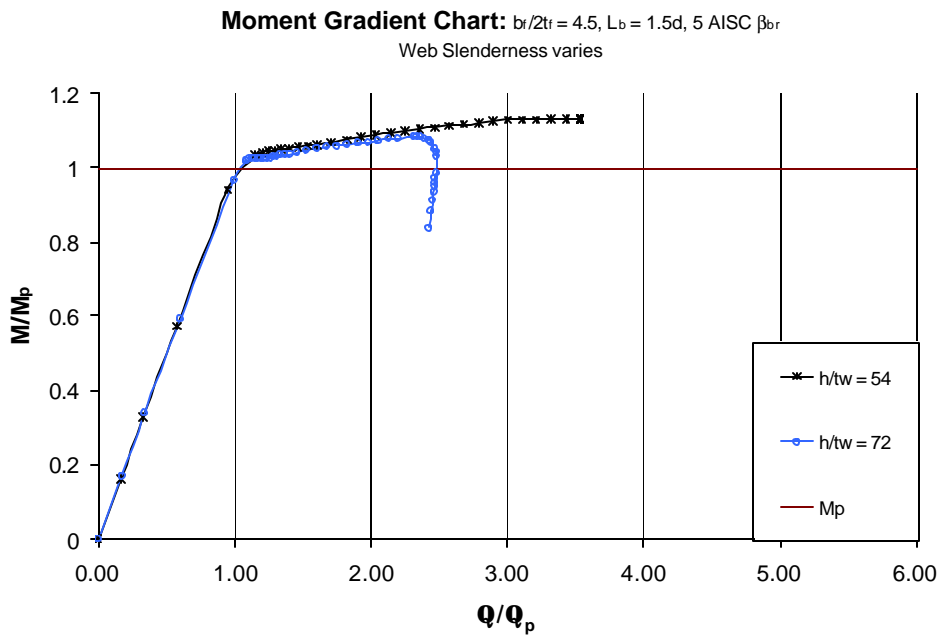
Figure B-73 Moment Rotation Plot ($b_f/2t_f = 4.5$, $L_b = 1.5d$, 5 AISC β_{br} Web Slenderness Varies)
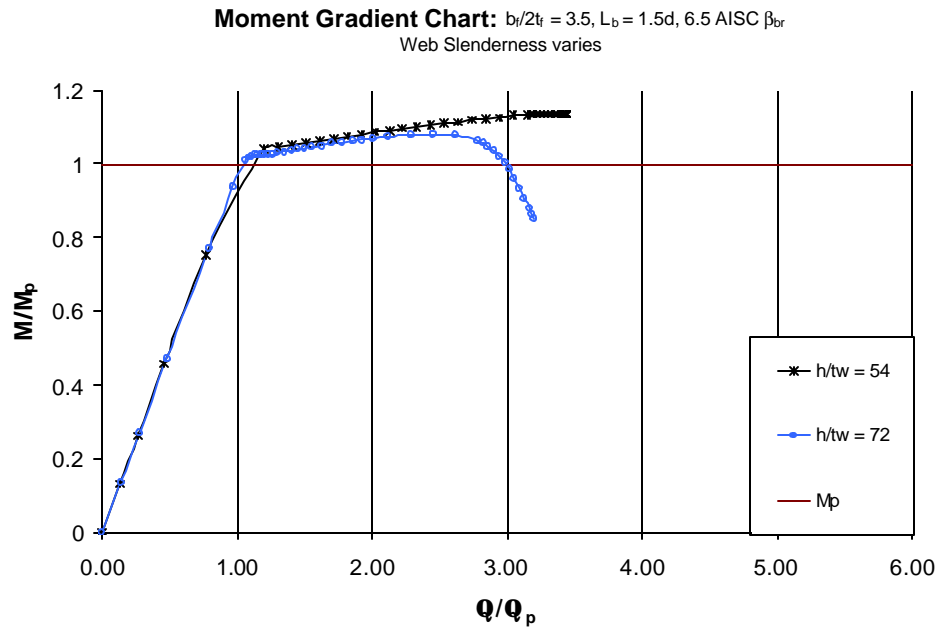
Figure B-74 Moment Rotation Plot ($b_f/2t_f = 3.5$, $L_b = 1.5d$, 6.5 AISC β_{br} Web Slenderness Varies)
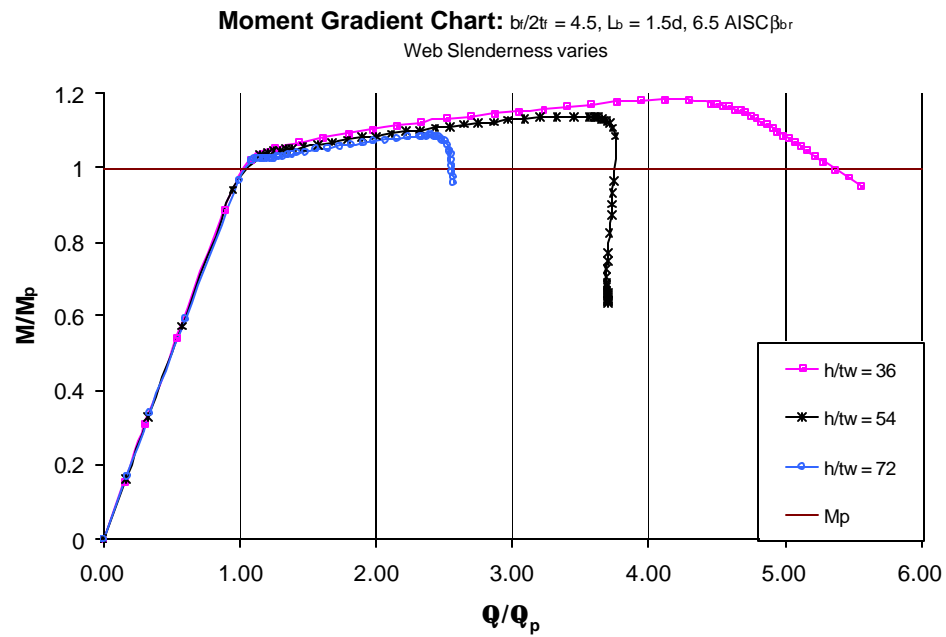
Figure B-75 Moment Rotation Plot ($b_f/2t_f = 4.5$, $L_b = 1.5d$, 6.5 AISC β_{br} Web Slenderness Varies)
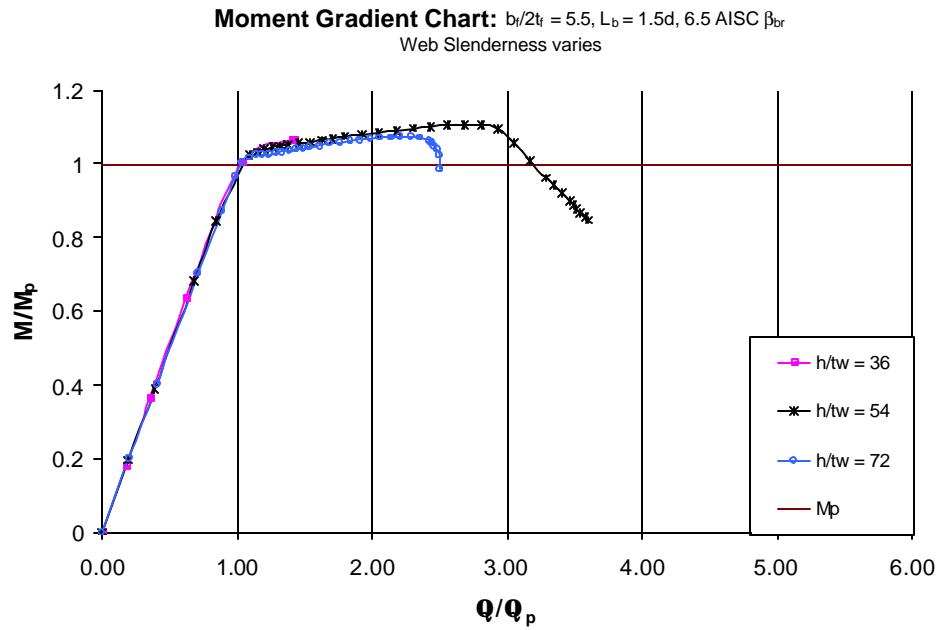
Figure B-76 Moment Rotation Plot ($b_f/2t_f = 5.5$, $L_b = 1.5d$, 6.5 AISC β_{br} Web Slenderness Varies)
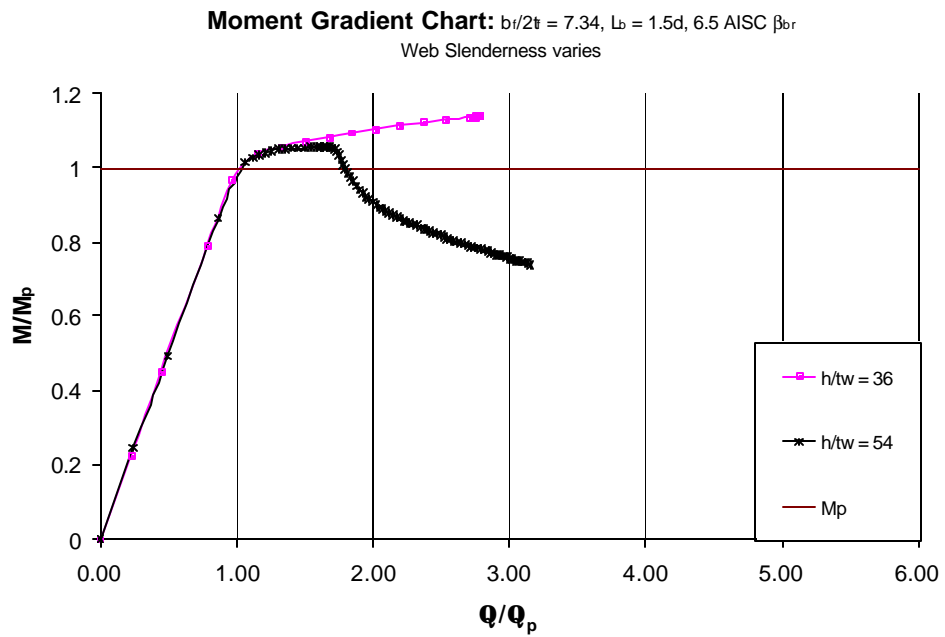
Figure B-77 Moment Rotation Plot ($b_f/2t_f = 7.34$, $L_b = 1.5d$, 6.5 AISC β_{br} Web Slenderness Varies)
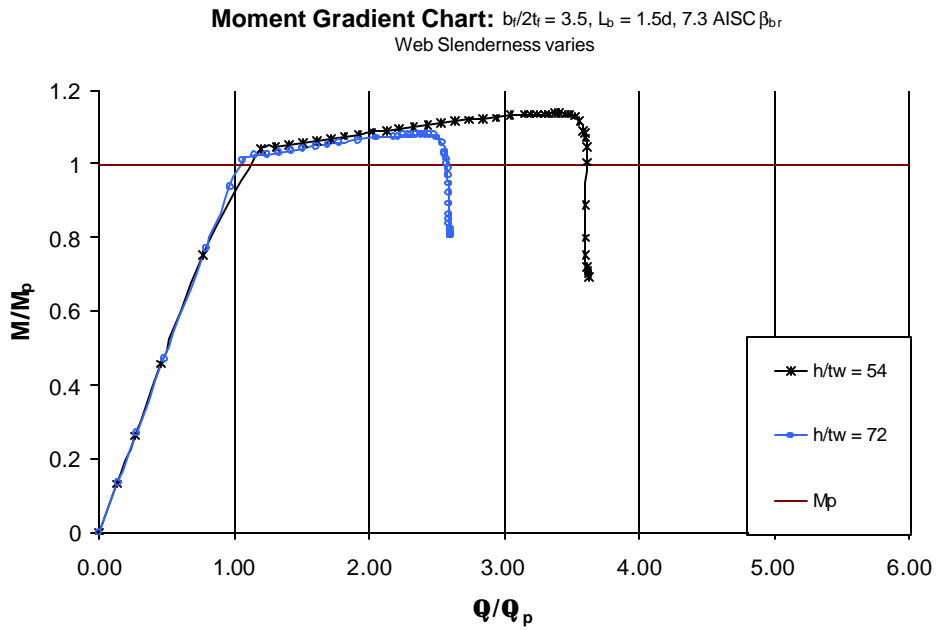
Figure B-78 Moment Rotation Plot ($b_f/2t_f = 3.5$, $L_b = 1.5d$, 7.3 AISC β_{br} Web Slenderness Varies)
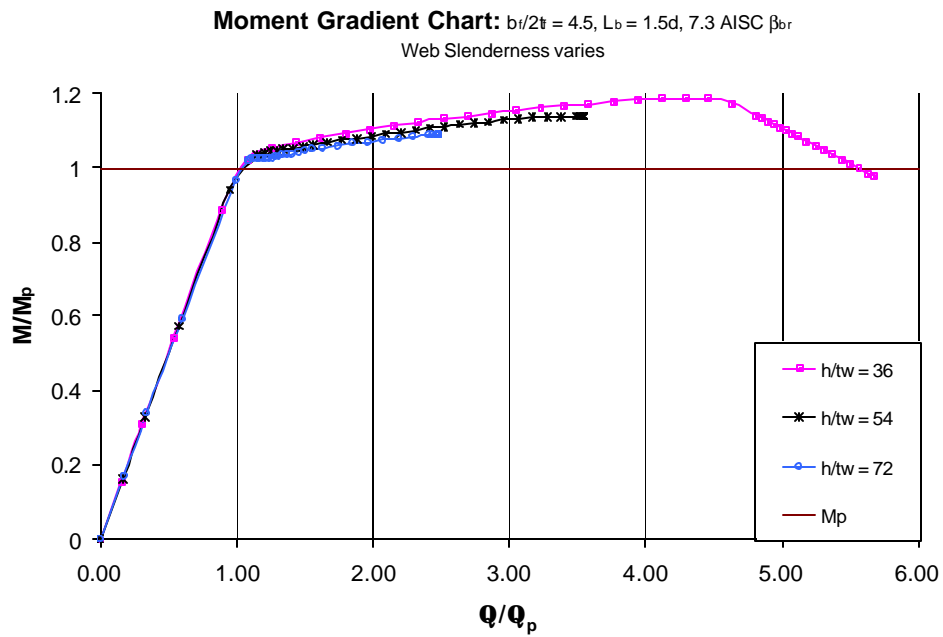
Figure B-79 Moment Rotation Plot ($b_f/2t_f = 4.5$, $L_b = 1.5d$, 7.3 AISC β_{br} Web Slenderness Varies)
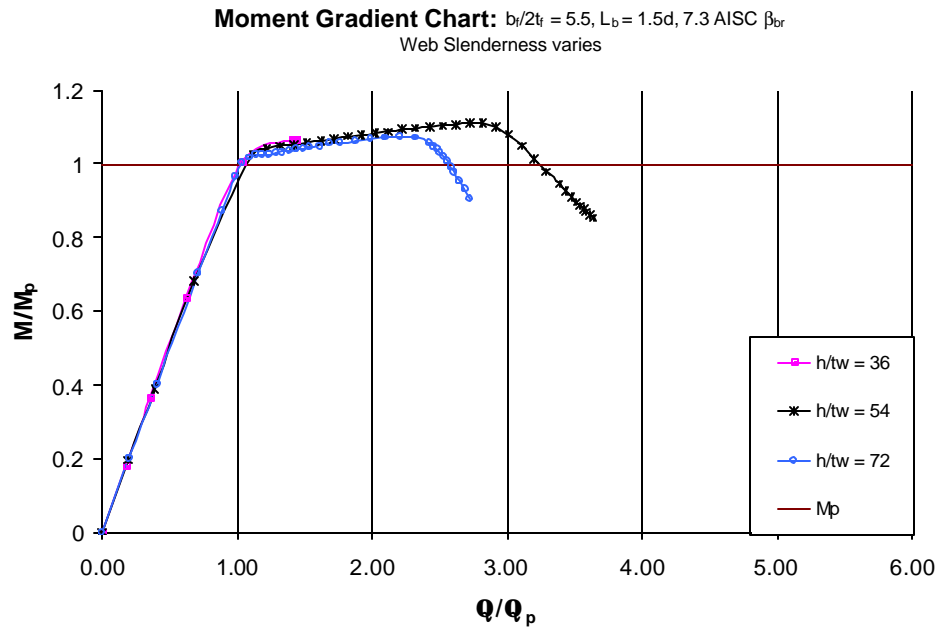
Figure B-80 Moment Rotation Plot ($b_f/2t_f$ = 5.5, L_b = 1.5d, 7.3 AISC β_{br} Web Slenderness Varies)
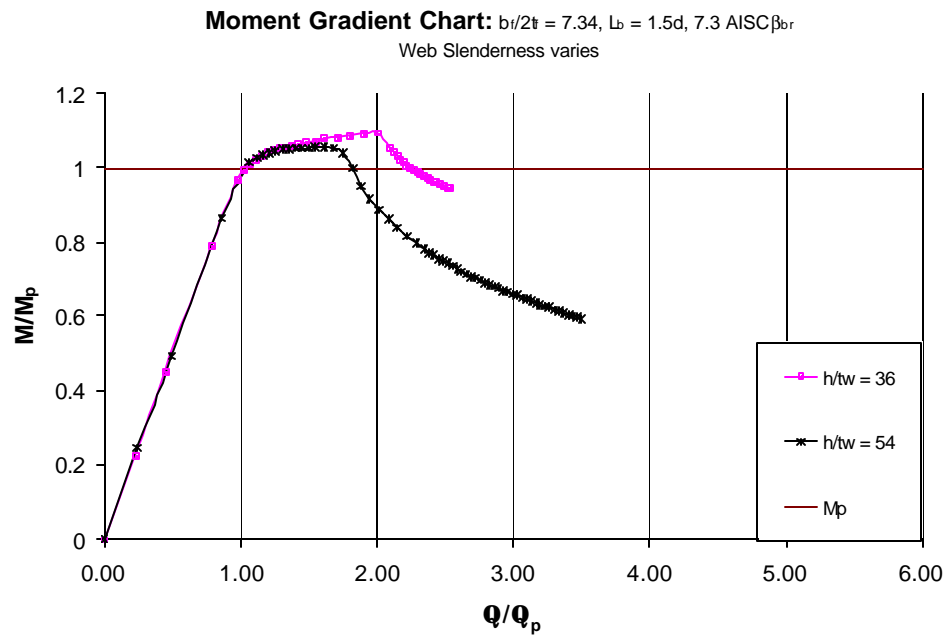
Figure B-81 Moment Rotation Plot ($b_f/2t_f$ = 7.34, L_b = 1.5d, 7.3 AISC β_{br} Web Slenderness Varies)
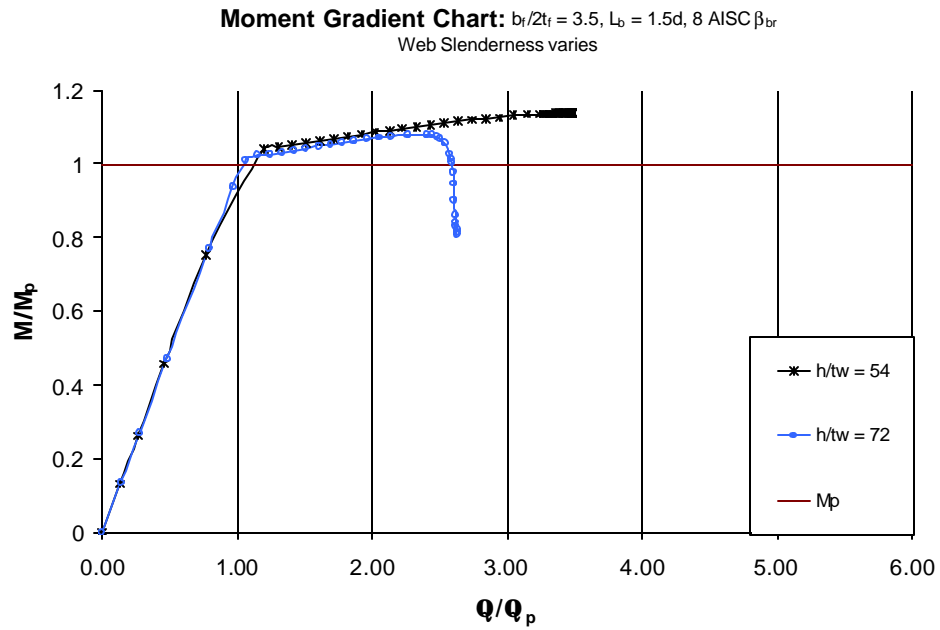
Figure B-82 Moment Rotation Plot ($b_f/2t_f = 3.5$, $L_b = 1.5d$, 8 AISC β_{br} Web Slenderness Varies)

Figure B-83 Moment Rotation Plot ($b_f/2t_f = 4.5$, $L_b = 1.5d$, 8 AISC β_{br} Web Slenderness Varies)

143
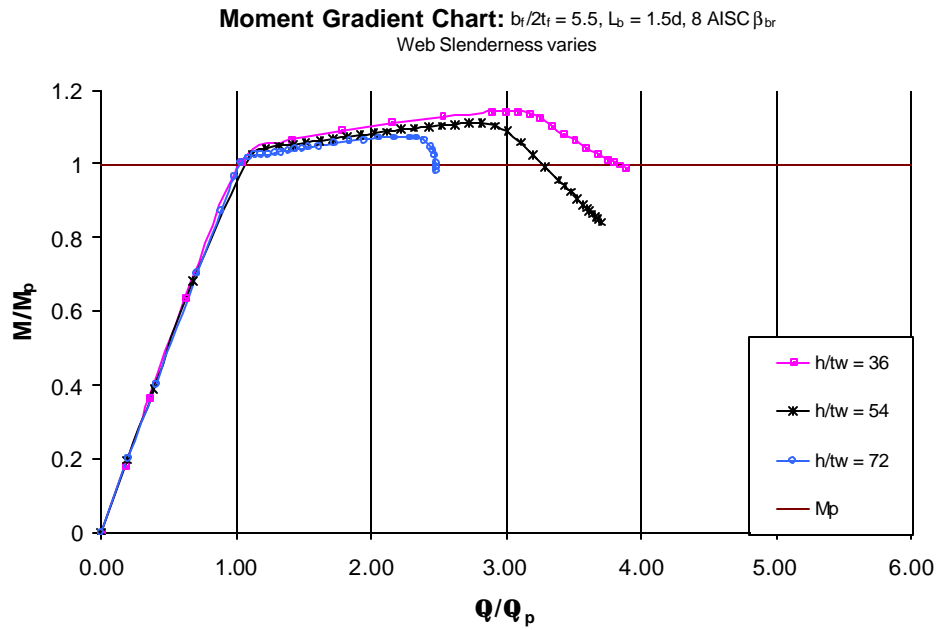
Figure B-84 Moment Rotation Plot ($b_f/2t_f = 5.5$, $L_b = 1.5d$, 8 AISC β_{br} Web Slenderness Varies)

Figure B-85 Moment Rotation Plot ($b_f/2t_f = 7.34$, $L_b = 1.5d$, 8 AISC β_{br} Web Slenderness Varies)

Figure B-86 Moment Rotation Plot ($b_f/2t_f$ = 4.5, L_b = 1.5d, 9.5 AISC β_{br}
Web Slenderness Varies)

Figure B-87 Moment Rotation Plot ($b_f/2t_f$ = 5.5, L_b = 1.5d, 9.5 AISC β_{br}
Web Slenderness Varies)

Figure B-88 Moment Rotation Plot ($b_f/2t_f = 4.5$, $L_b = 2d$, 6.5 AISC β_{br}
Web Slenderness Varies)

Figure B-89 Moment Rotation Plot ($b_f/2t_f = 4.5$, $L_b = 2d$, 7.3 AISC β_{br}
Web Slenderness Varies)
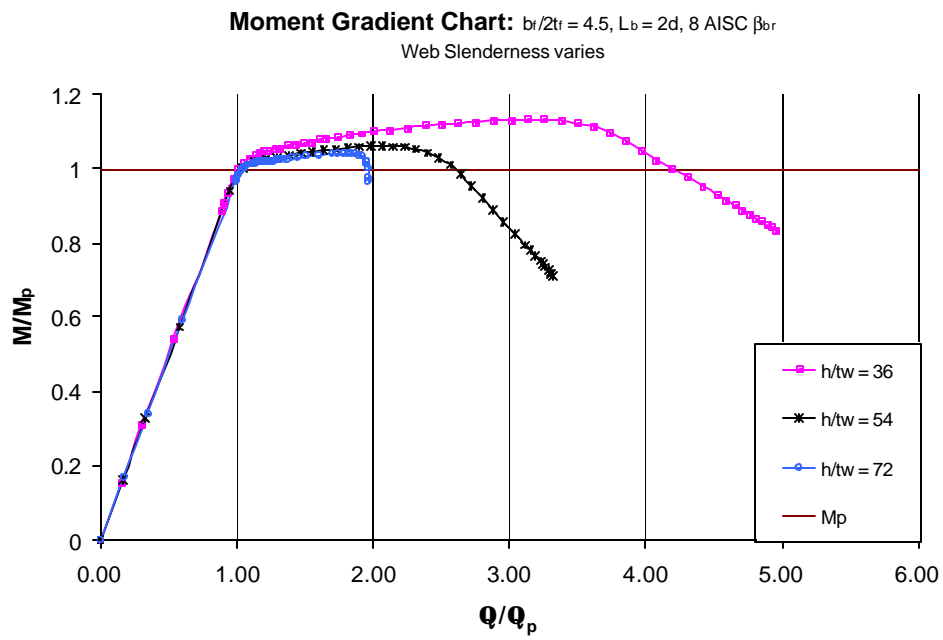
Figure B-90 Moment Rotation Pbt ($b_f/2t_f = 4.5$, $L_b = 2d$, 8 AISC β_{br} Web Slenderness Varies)

Appendix B.3

The third presentation method combines the plots such that only the unbraced length varies. By doing this, it is possible to observe the effect that a change in only unbraced length has on structural ductility.
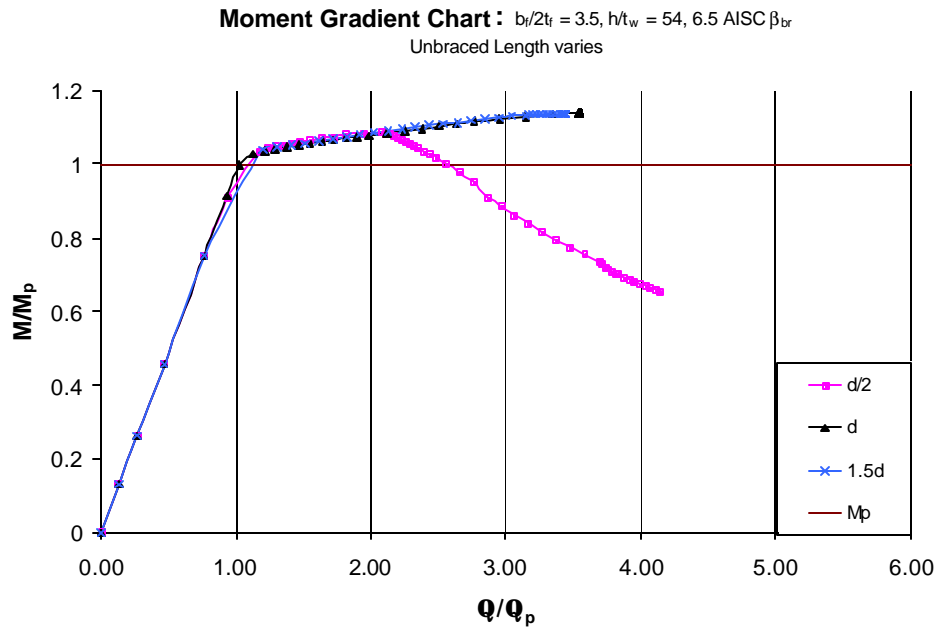
Figure B-91 Moment Rotation Plot ($b_f/2t_f$ = 3.5, h/t_w = 54, 6.5 AISC β_{br} Unbraced Length Varies)
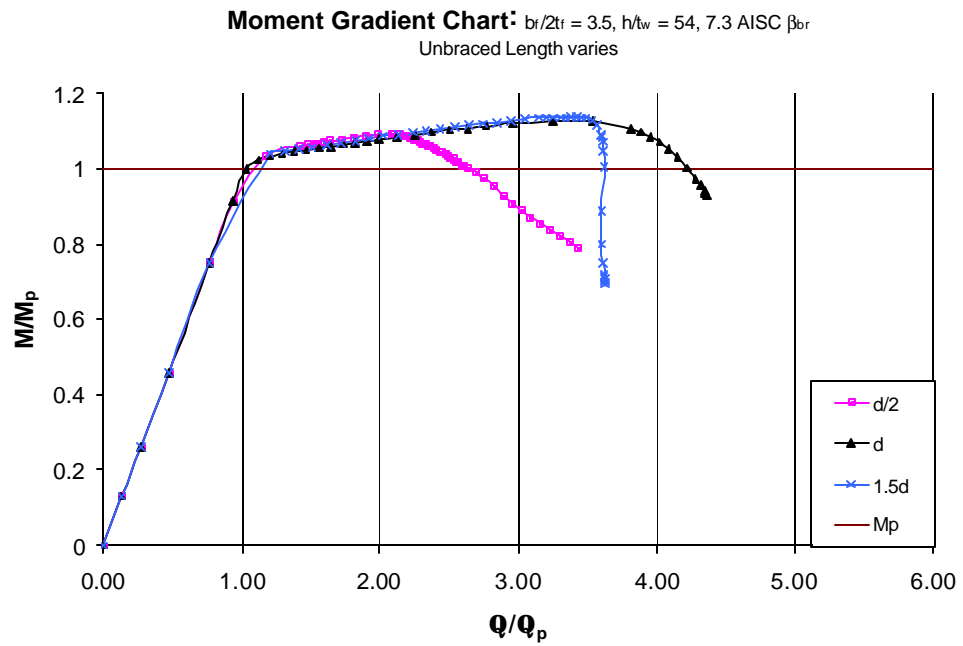
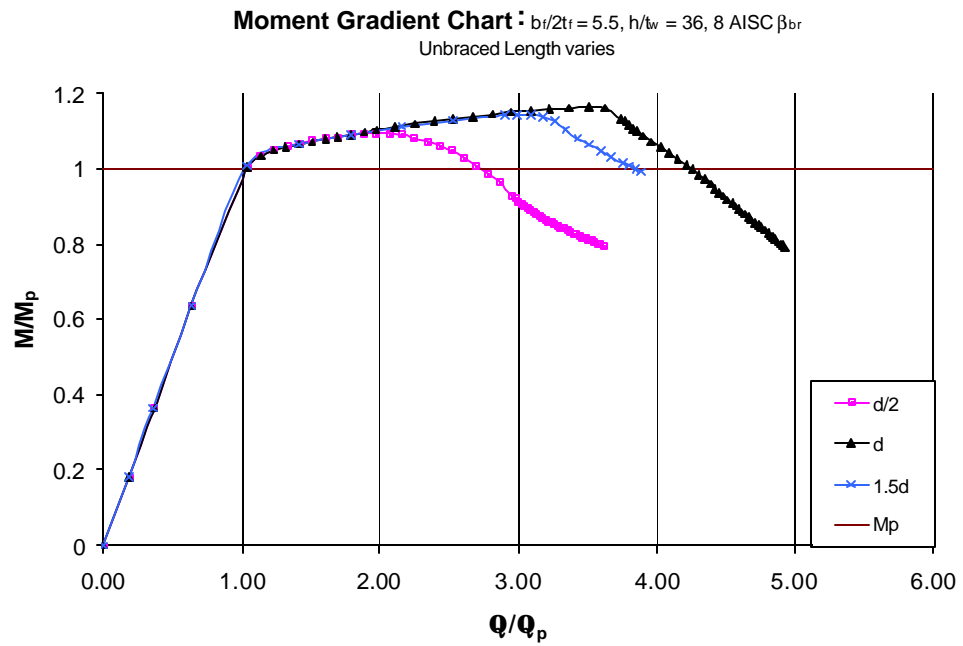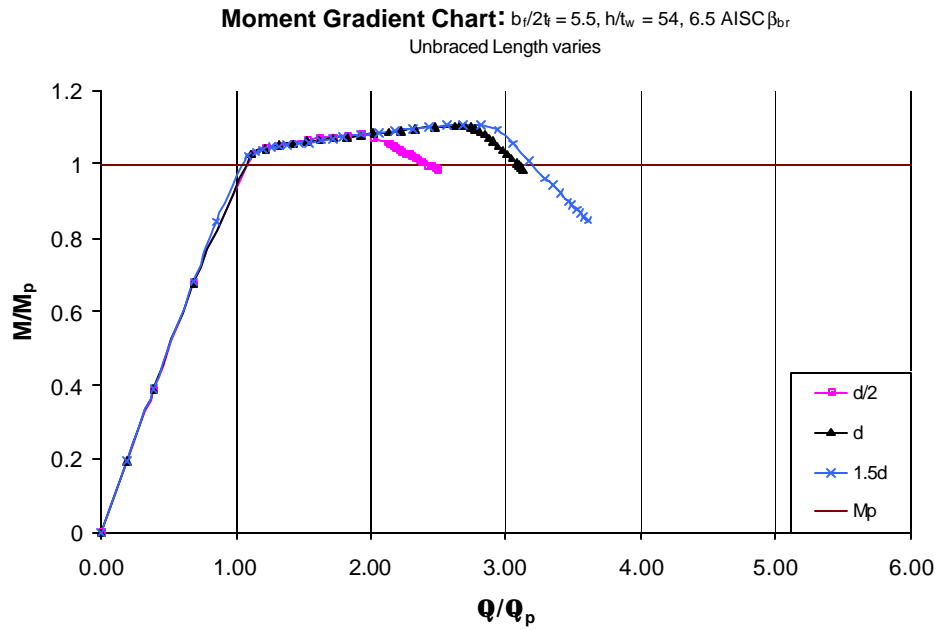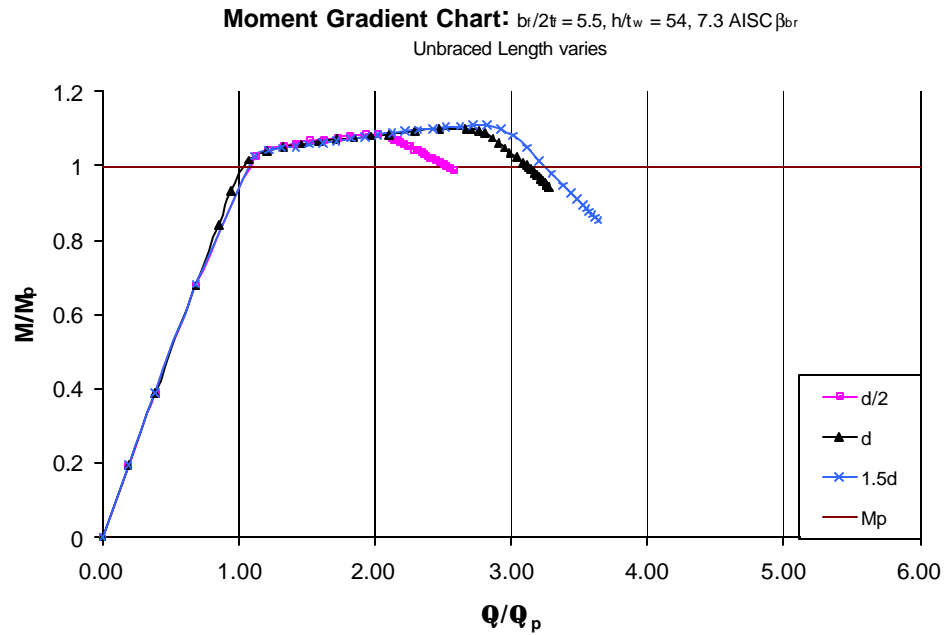**Figure B-92** Moment Rotation Plot ($b_f/2t_f$ = 3.5, h/t_w = 54, 7.3 AISC β_{br} Unbraced Length Varies)
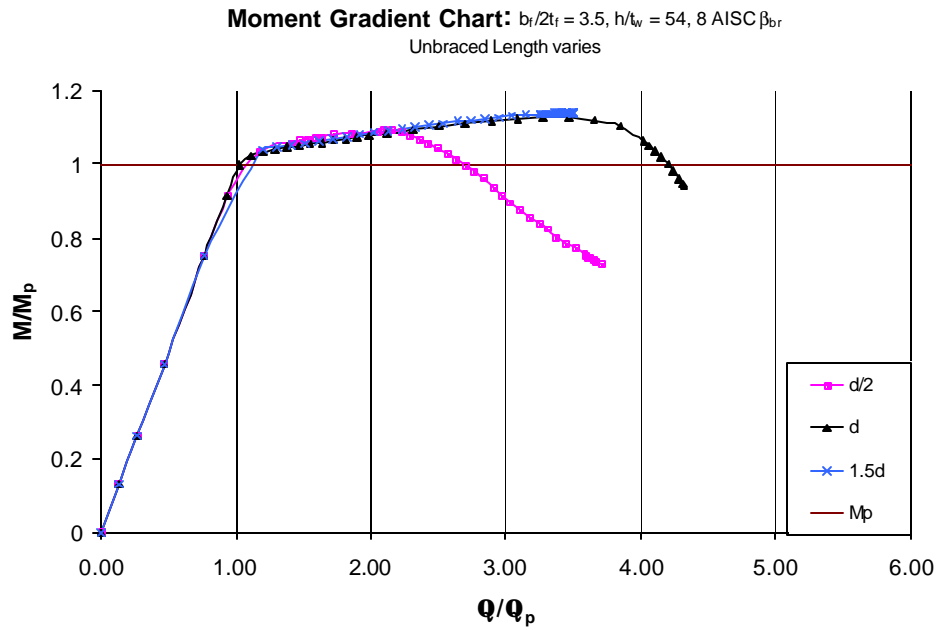
Figure B-93 Moment Rotation Plot ($b_f/2t_f = 3.5$, $h/t_w = 54$, 8 AISC β_{br} Unbraced Length Varies)
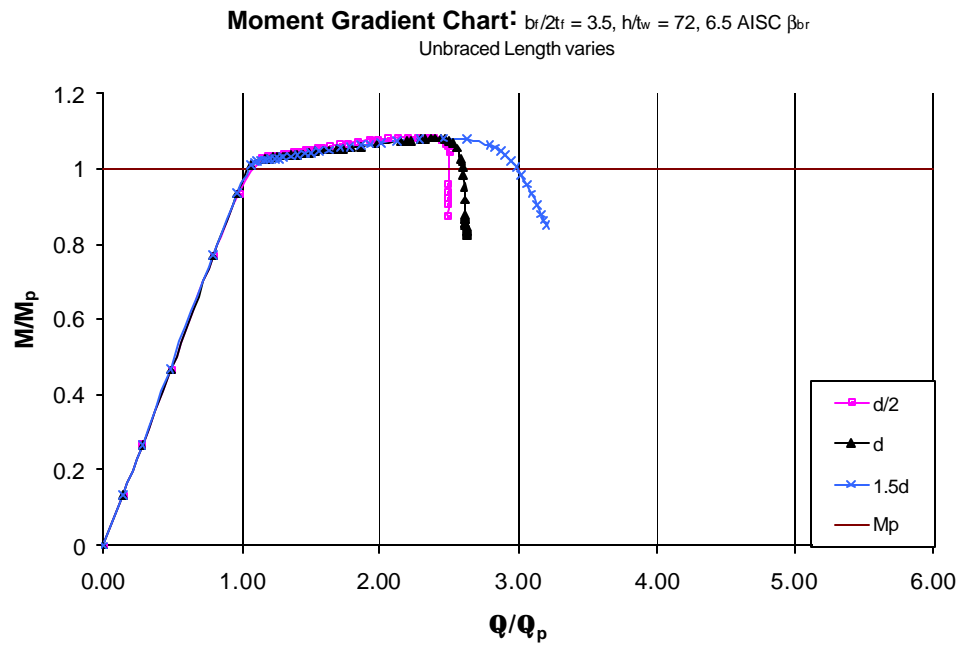
Figure B-94 Moment Rotation Plot ($b_f/2t_f = 3.5$, $h/t_w = 72$, 6.5 AISC β_{br} Unbraced Length Varies)

150
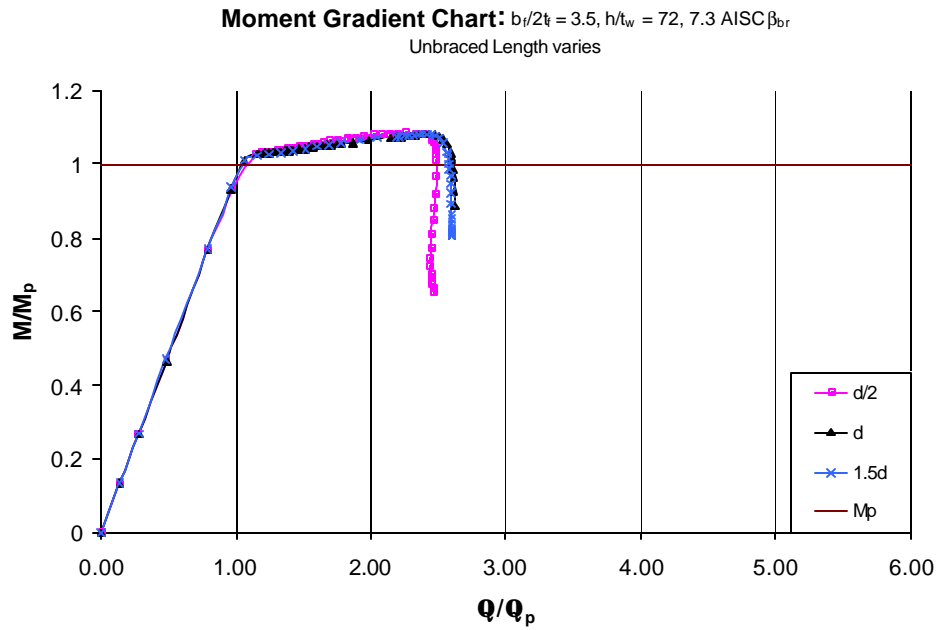
Figure B-95 Moment Rotation Plot ($b_f/2t_f = 3.5$, $h/t_w = 72$, 7.3 AISC β_{br}
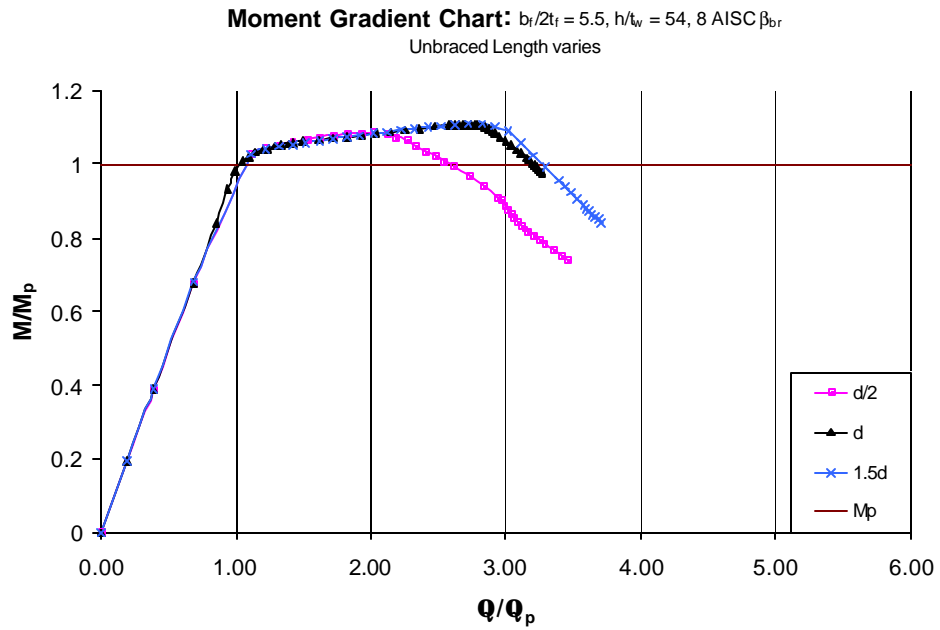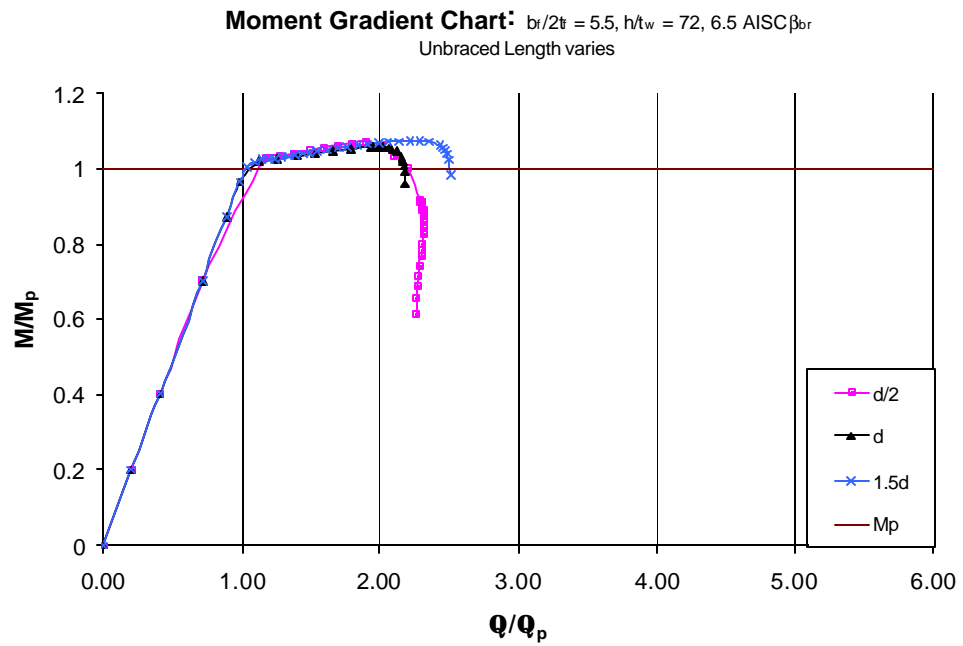Unbraced Length Varies)
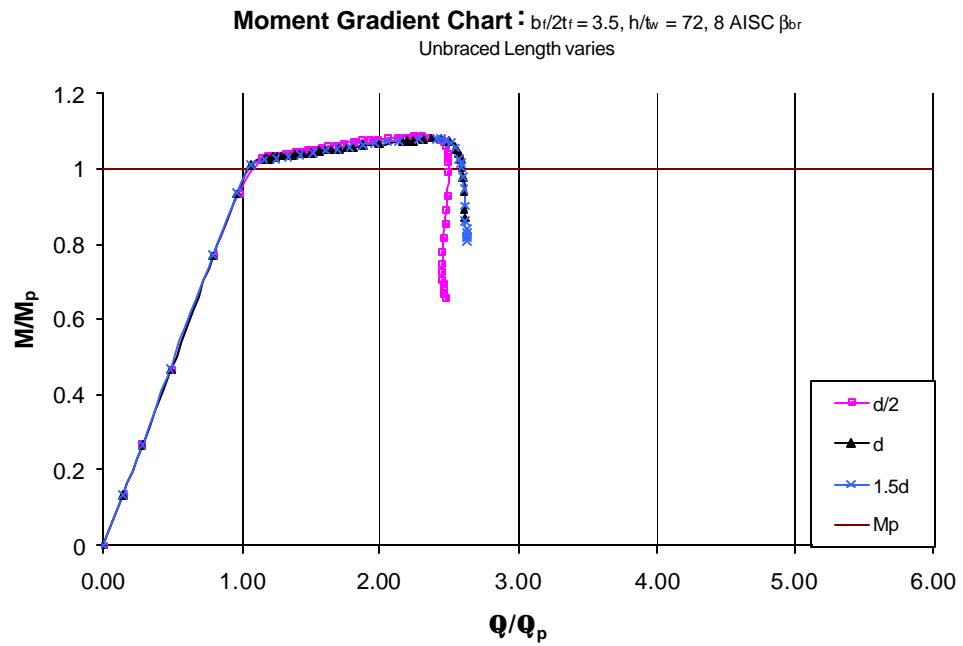
Figure B-96 Moment Rotation Plot ($b_f/2t_f = 3.5$, $h/t_w = 72$, 8 AISC β_{br}
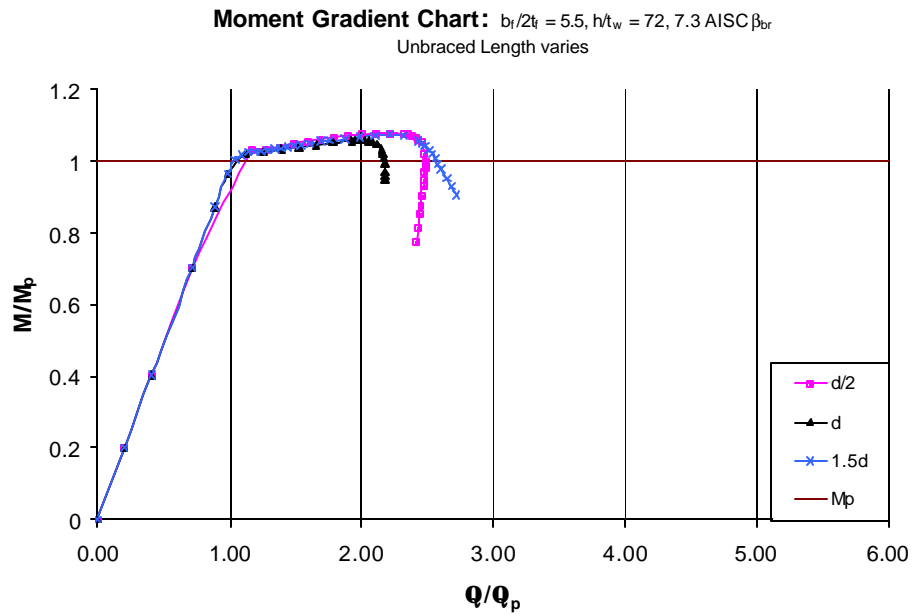Unbraced Length Varies)
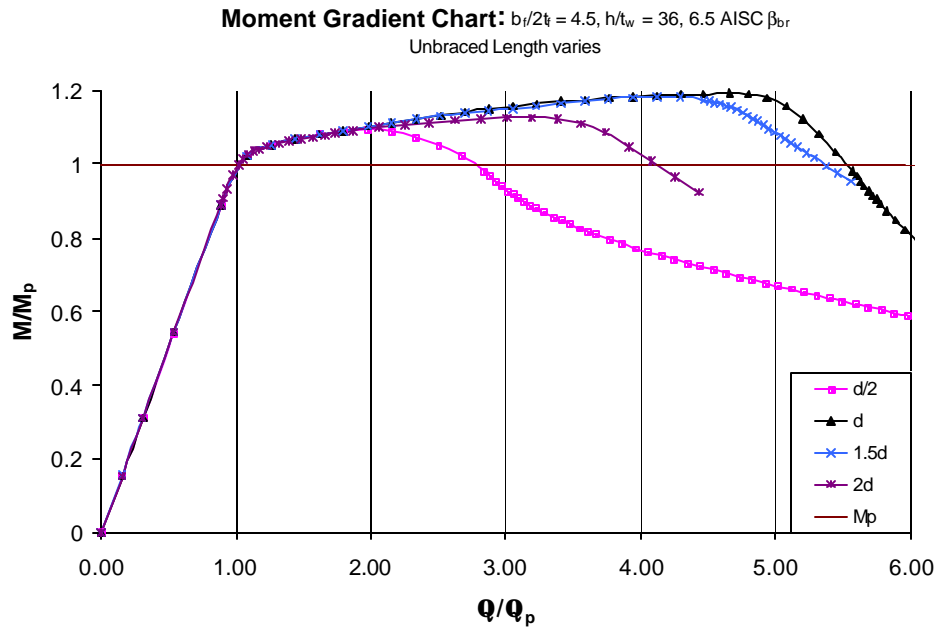
Figure B-97 Moment Rotation Plot ($b_f/2t_f = 4.5$, $h/t_w = 36$, 6.5 AISC β_{br} Unbraced Length Varies)
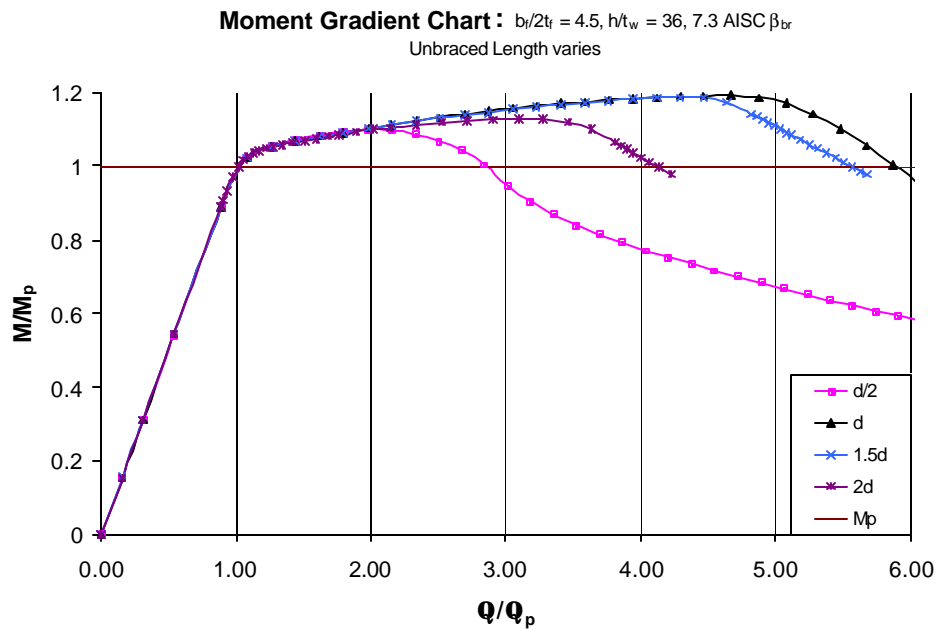
Figure B-98 Moment Rotation Plot ($b_f/2t_f = 4.5$, $h/t_w = 36$, 7.3 AISC β_{br} Unbraced Length Varies)

Moment Gradient Chart: $b_f/2t_f = 4.5$, $h/t_w = 36$, 8 AISC β_{br}
Unbraced Length varies
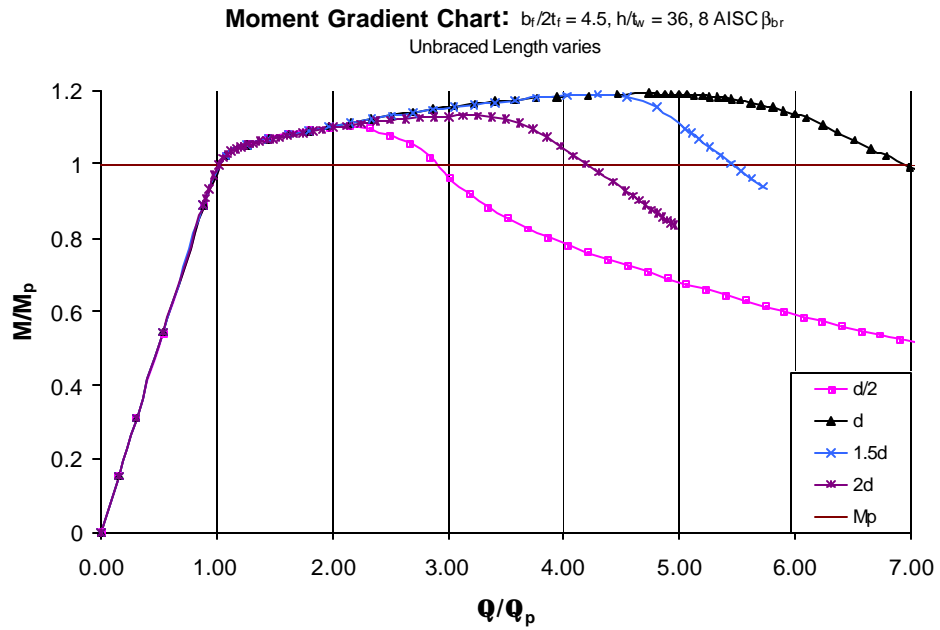
Figure B-99 Moment Rotation Plot ($b_f/2t_f = 4.5$, $h/t_w = 36$, 8 AISC β_{br}
Unbraced Length Varies)

Moment Gradient Chart: $b_f/2t_f = 4.5$, $h/t_w = 54$, 5 AISC β_{br}
Unbraced Length varies
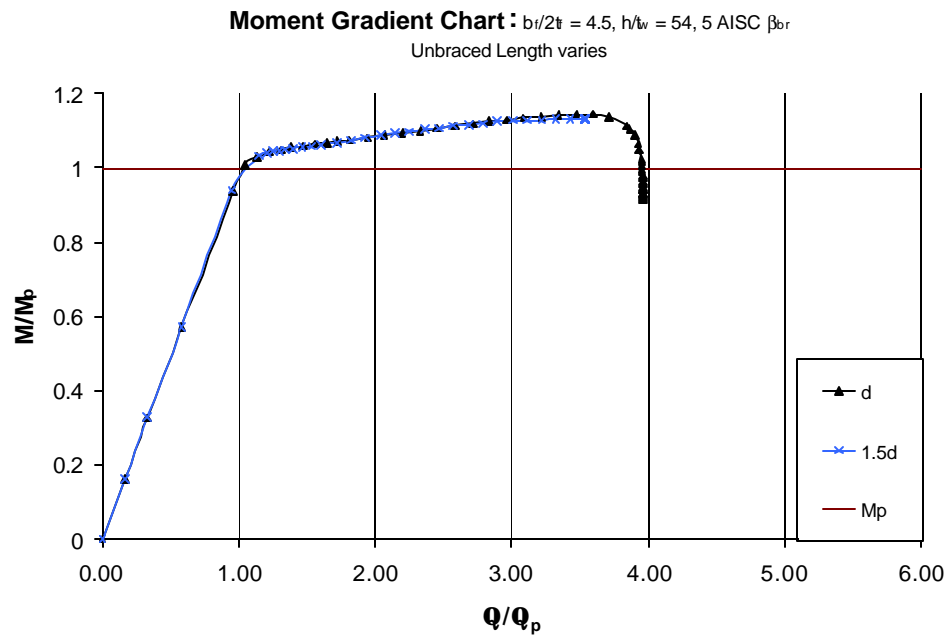
Figure B-100 Moment Rotation Plot ($b_f/2t_f = 4.5$, $h/t_w = 54$, 5 AISC β_{br}
Unbraced Length Varies)

153
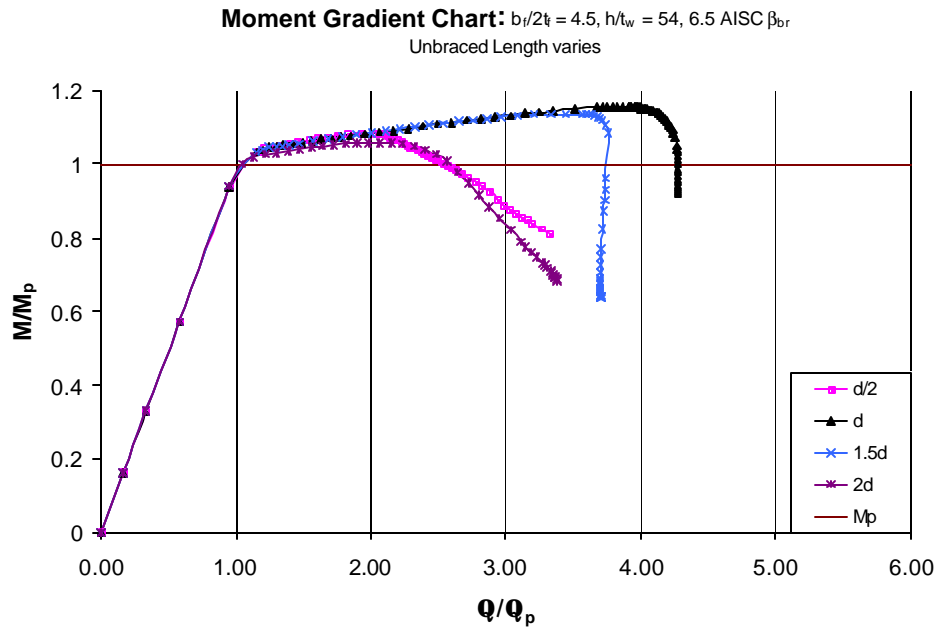
Figure B-101 Moment Rotation Plot ($b_f/2t_f = 4.5$, $h/t_w = 54$, 6.5 AISC β_{br} Unbraced Length Varies)
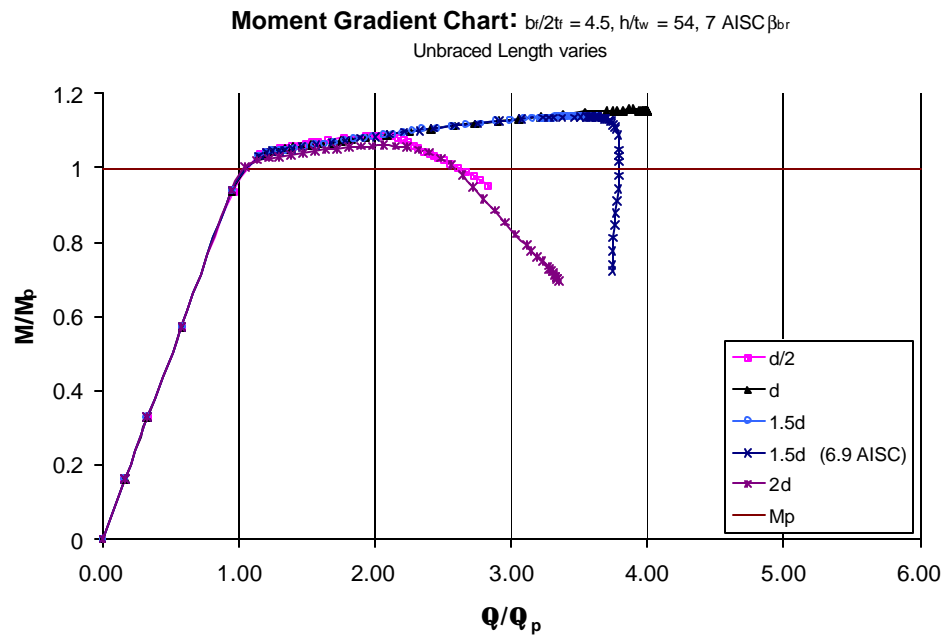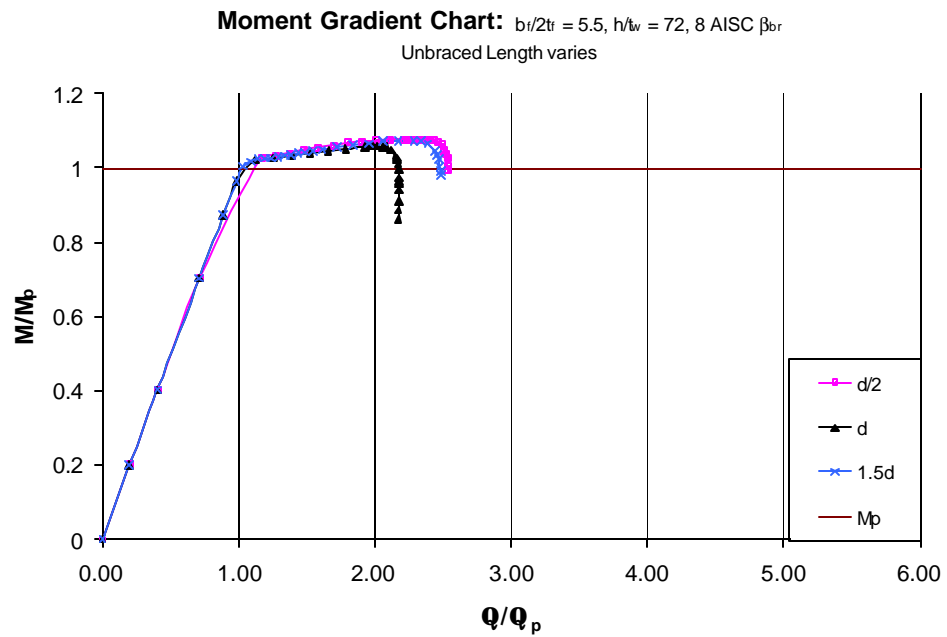

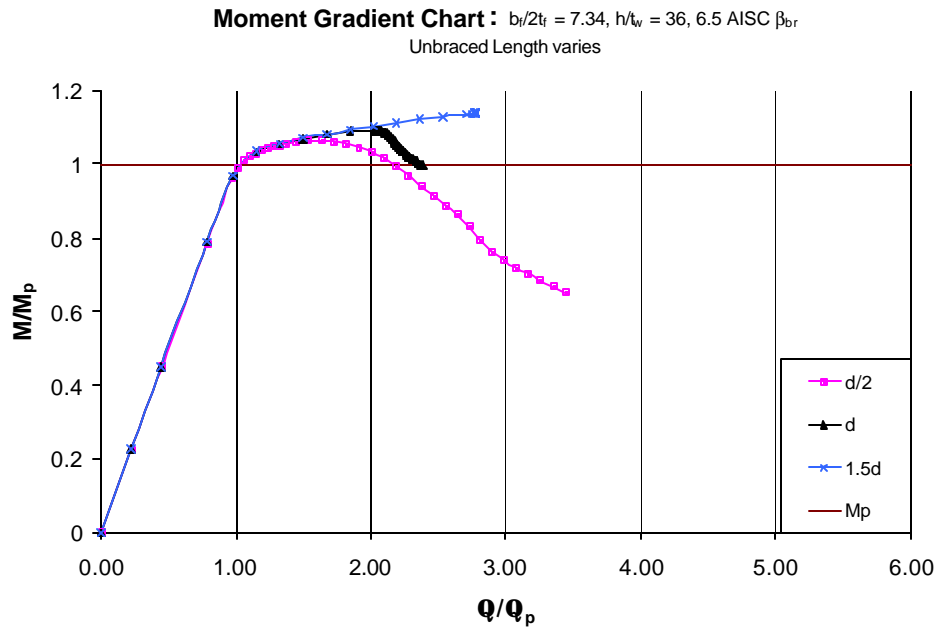**Figure B-102** Moment Rotation Plot ($b_f/2t_f = 4.5$, $h/t_w = 54$, 7 AISC β_{br} Unbraced Length Varies)
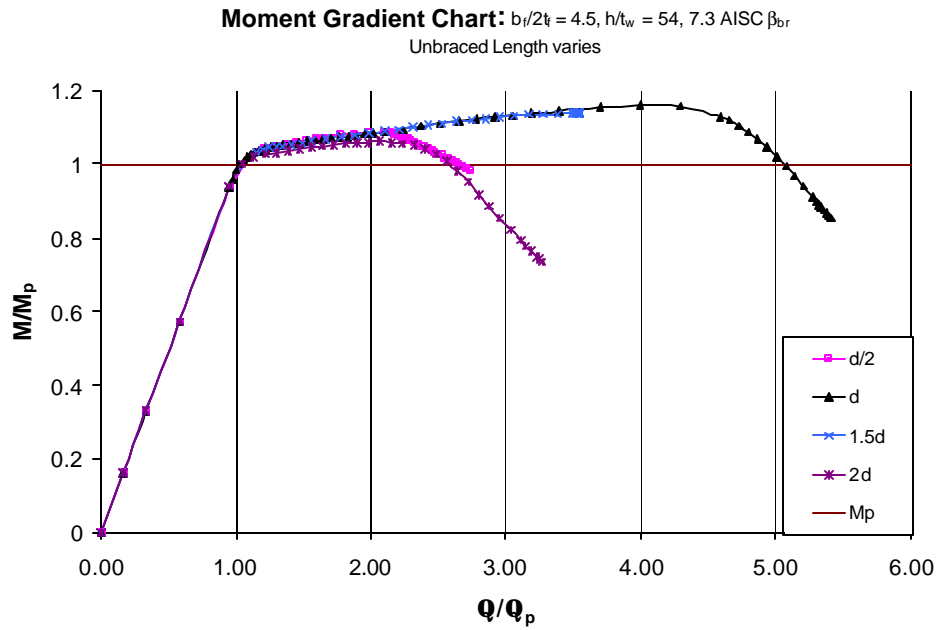
Figure B-103 Moment Rotation Plot ($b_f/2t_f = 4.5$, $h/t_w = 54$, 7.3 AISC β_{br} Unbraced Length Varies)
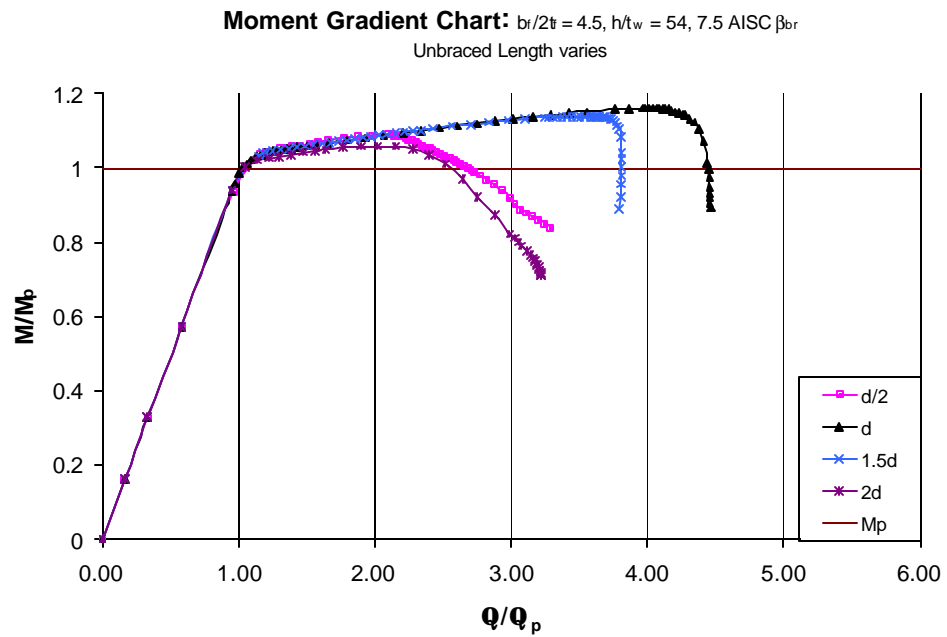
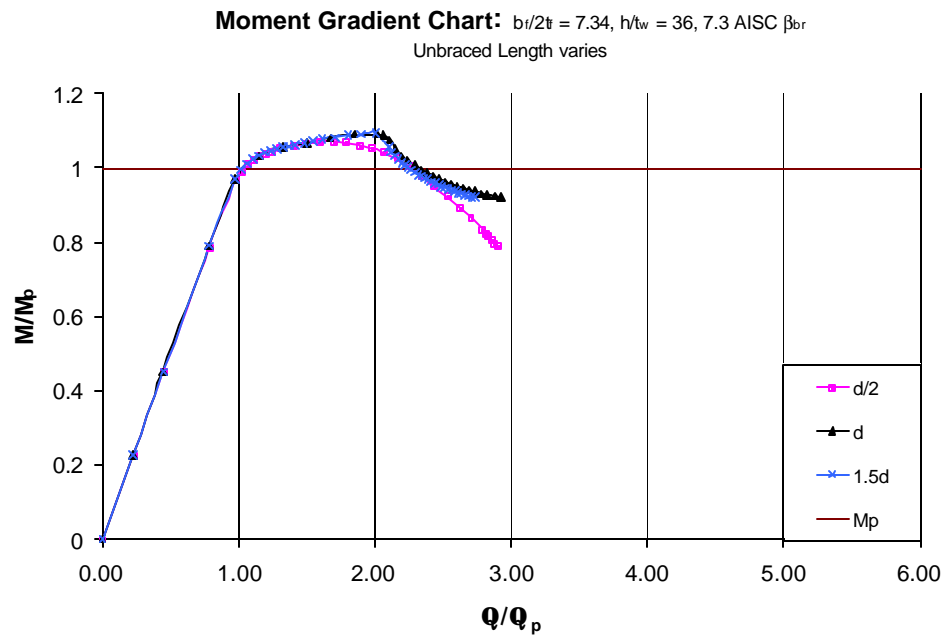**Figure B-104** Moment Rotation Plot ($b_f/2t_f = 4.5$, $h/t_w = 54$, 7.5 AISC β_{br} Unbraced Length Varies)
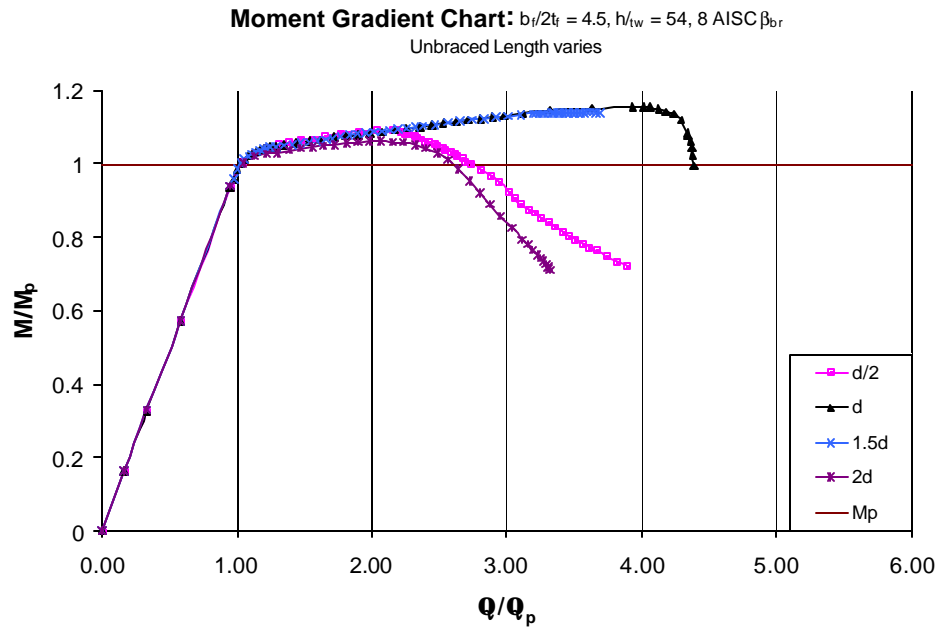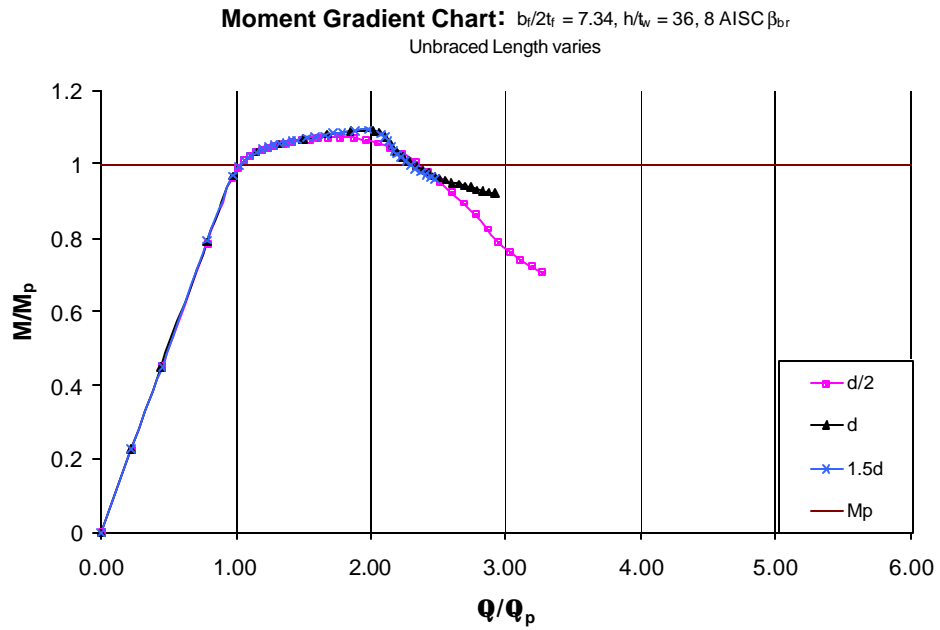
Figure B-105 Moment Rotation Plot ($b_f/2t_f = 4.5$, $h/t_w = 54$, 8 AISC β_{br} Unbraced Length Varies)
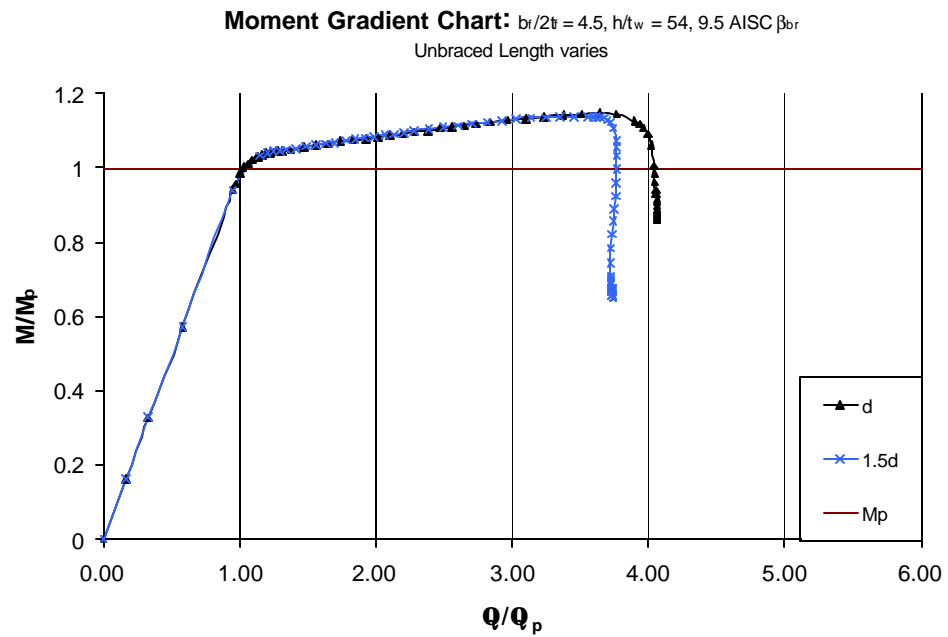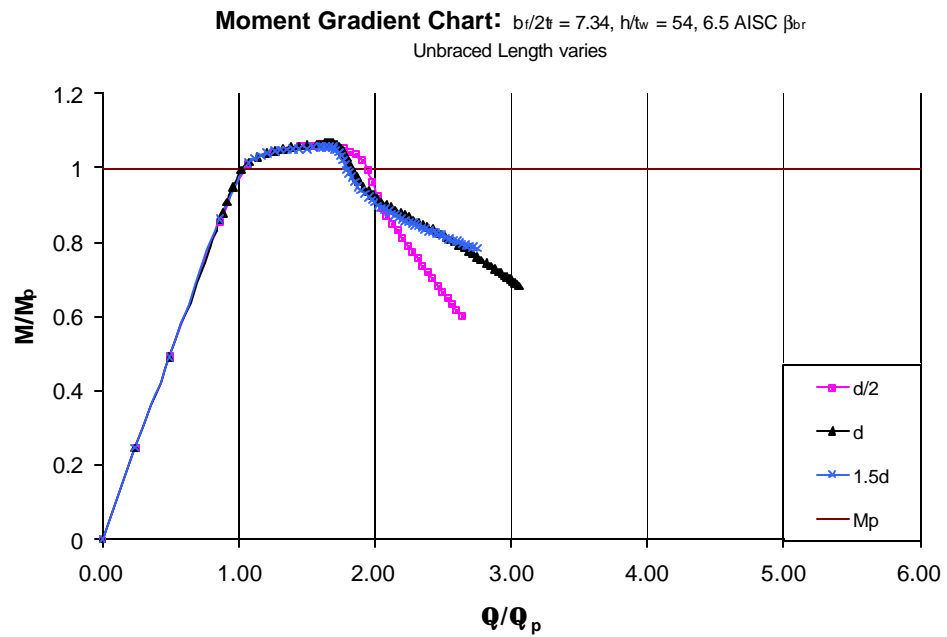

Figure B-106 Moment Rotation Plot ($b_f/2t_f = 4.5$, $h/t_w = 54$, 9.5 AISC β_{br} Unbraced Length Varies)
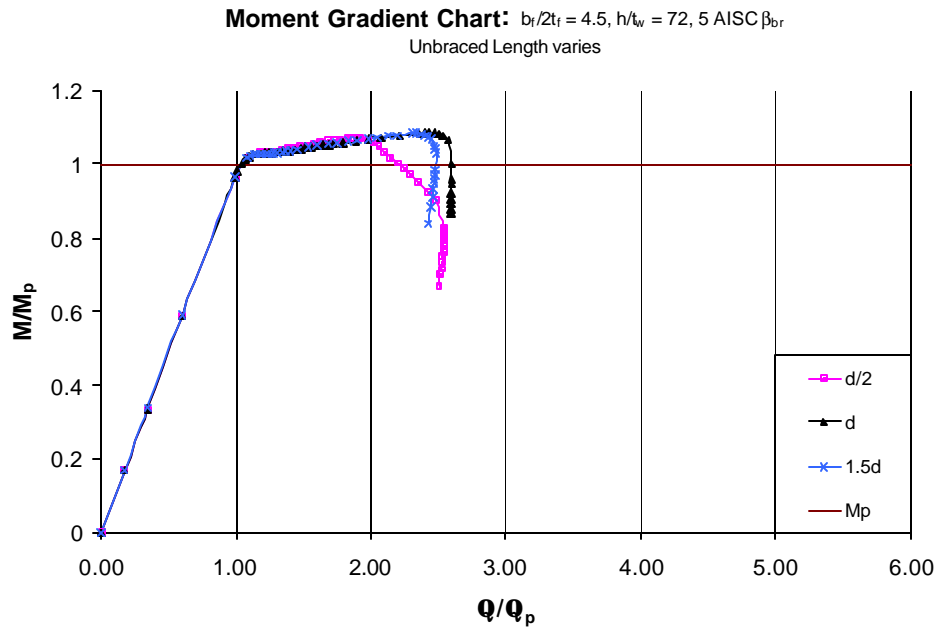
Figure B-107 Moment Rotation Plot ($b_f/2t_f = 4.5$, $h/t_w = 72$, 5 AISC β_{br}
Unbraced Length Varies)
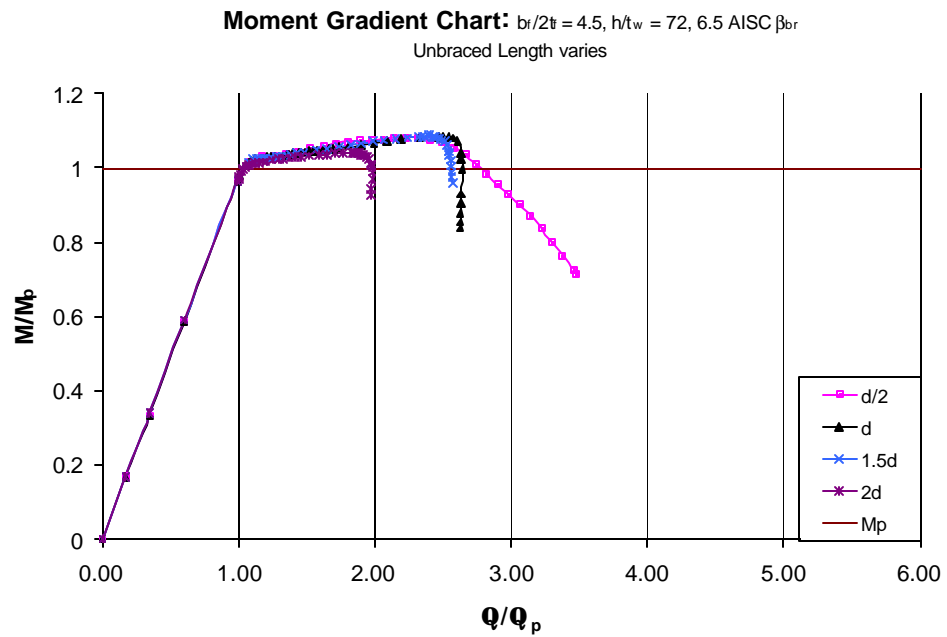
Figure B-108 Moment Rotation Plot ($b_f/2t_f = 4.5$, $h/t_w = 72$, 6.5 AISC β_{br}
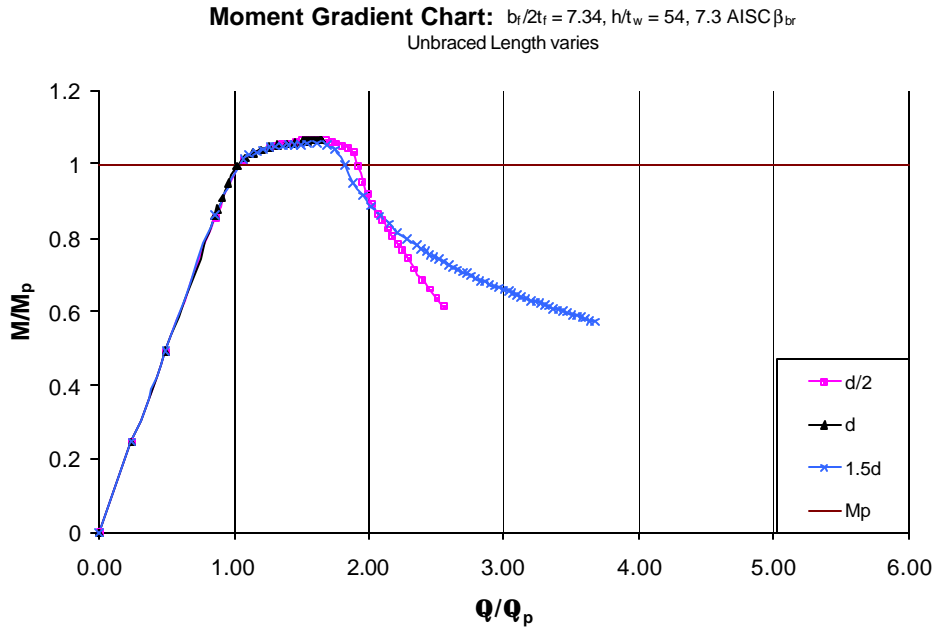Unbraced Length Varies)
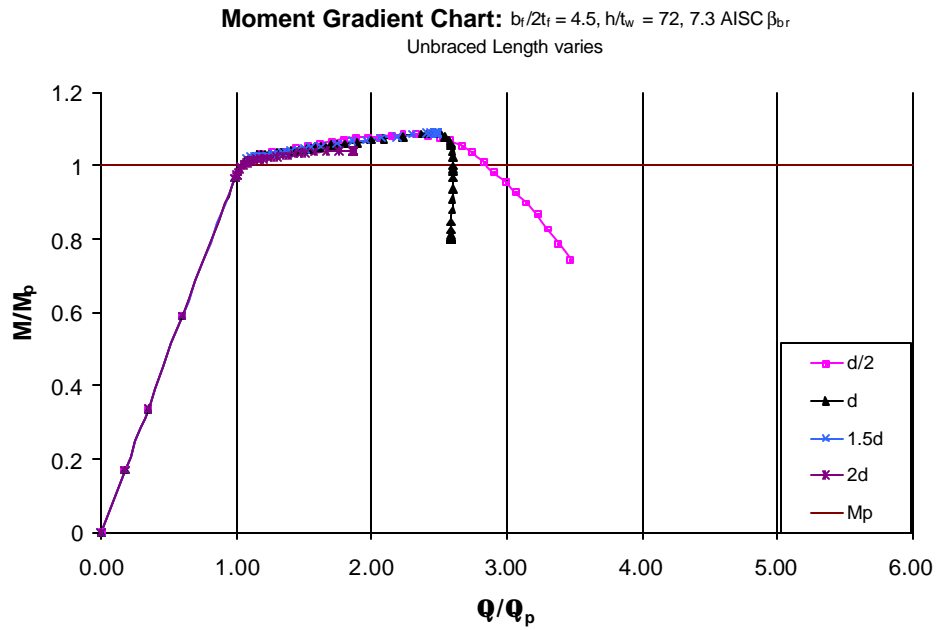
Figure B-109 Moment Rotation Plot ($b_f/2t_f = 4.5$, $h/t_w = 72$, 7.3 AISC β_{br} Unbraced Length Varies)
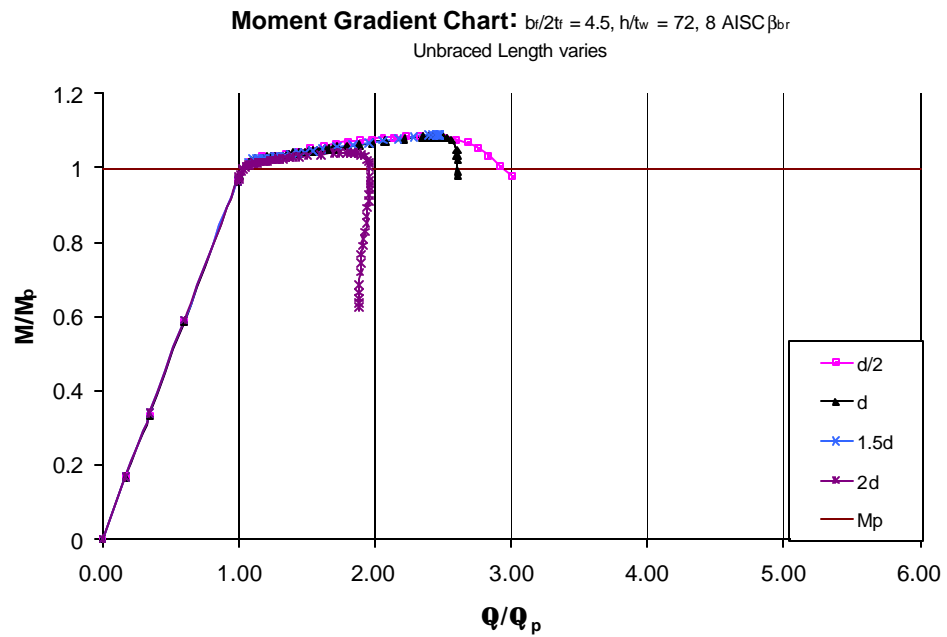
Figure B-110 Moment Rotation Plot ($b_f/2t_f = 4.5$, $h/t_w = 72$, 8 AISC β_{br} Unbraced Length Varies)
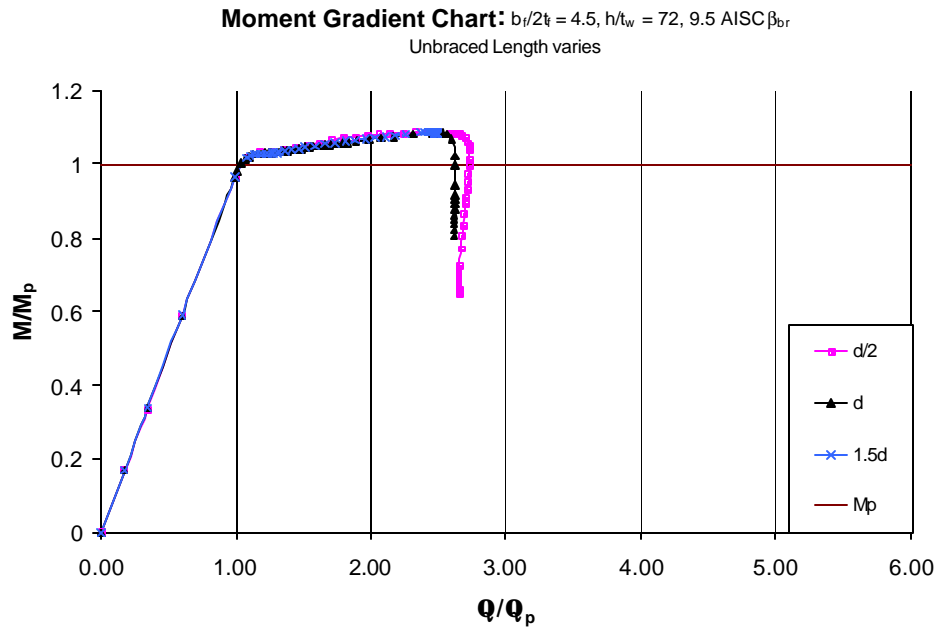
Figure B-111 Moment Rotation Plot ($b_f/2t_f = 4.5$, $h/t_w = 72$, 9.5 AISC β_{br} Unbraced Length Varies)
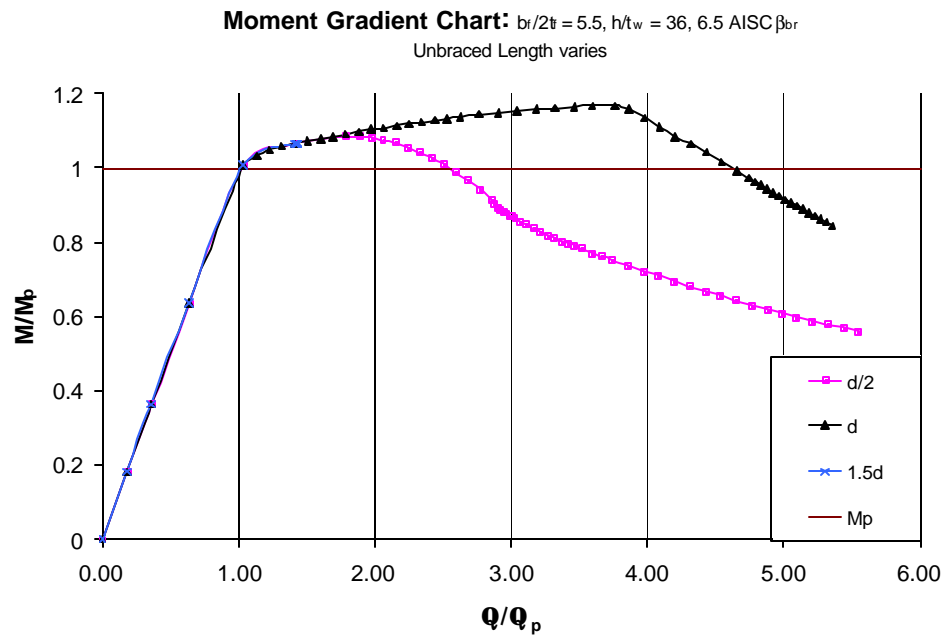
Figure B-112 Moment Rotation Plot ($b_f/2t_f = 5.5$, $h/t_w = 36$, 6.5 AISC β_{br} Unbraced Length Varies)
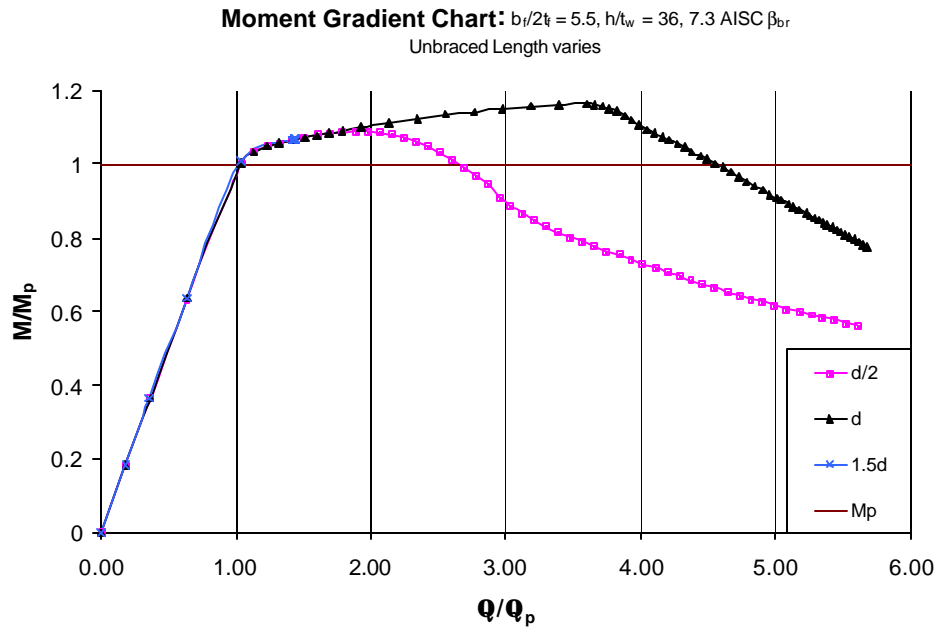
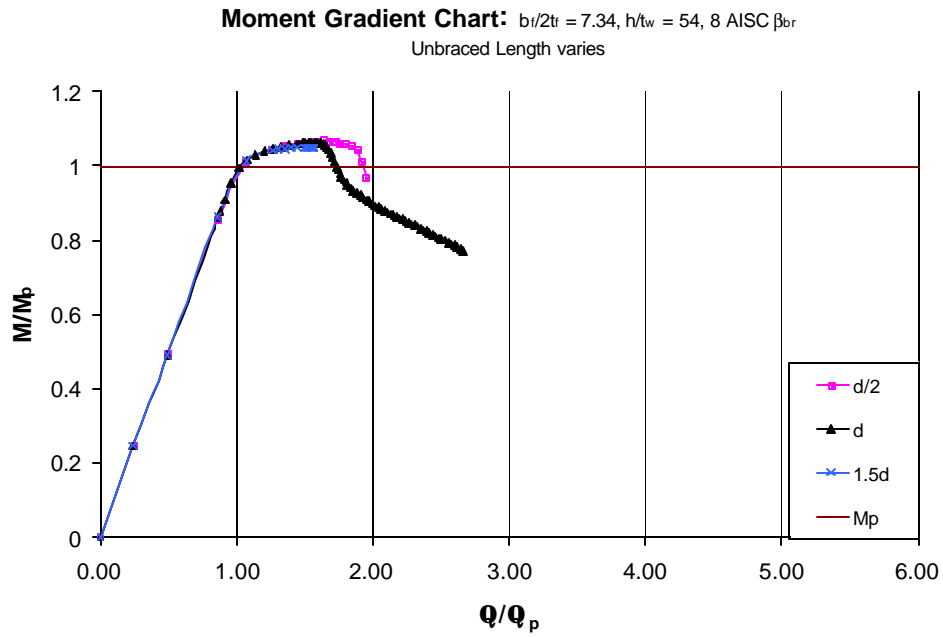**Figure B-113** Moment Rotation Plot ($b_f/2t_f = 5.5$, $h/t_w = 36$, 7.3 AISC β_{br} Unbraced Length Varies)

Figure B-114 Moment Rotation Plot ($b_f/2t_f = 5.5$, $h/t_w = 36$, 8 AISC β_{br} Unbraced Length Varies)

Figure B-115 Moment Rotation Plot ($b_f/2t_f = 5.5$, $h/t_w = 54$, 6.5 AISC β_{br} Unbraced Length Varies)

Figure B-116 Moment Rotation Plot ($b_f/2t_f = 5.5$, $h/t_w = 54$, 7.3 AISC β_{br} Unbraced Length Varies)

Moment Gradient Chart: $b_f/2t_f = 5.5$, $h/t_w = 54$, 8 AISC β_{br}

Unbraced Length varies

Figure B-117 Moment Rotation Plot ($b_f/2t_f = 5.5$, $h/t_w = 54$, 8 AISC β_{br} Unbraced Length Varies)

Moment Gradient Chart: $b_f/2t_f = 5.5$, $h/t_w = 72$, 6.5 AISC β_{br}

Unbraced Length varies

Figure B-118 Moment Rotation Plot ($b_f/2t_f = 5.5$, $h/t_w = 72$, 6.5 AISC β_{br} Unbraced Length Varies)

Figure B-119 Moment Rotation Plot ($b_f/2t_f = 5.5$, $h/t_w = 72$, 7.3 AISC β_{br} Unbraced Length Varies)

Figure B-120 Moment Rotation Plot ($b_f/2t_f = 5.5$, $h/t_w = 72$, 8 AISC β_{br} Unbraced Length Varies)

Figure B-121 Moment Rotation Plot ($b_f/2t_f = 7.34$, $h/t_w = 36$, 6.5 AISC β_{br}
Unbraced Length Varies)

Figure B-122 Moment Rotation Plot ($b_f/2t_f = 7.34$, $h/t_w = 36$, 7.3 AISC β_{br}
Unbraced Length Varies)

Figure B-123 Moment Rotation Pbt ($b_f/2t_f = 7.34$, $h/t_w = 36$, 8 AISC β_{br} Unbraced Length Varies)

Figure B-124 Moment Rotation Plot ($b_f/2t_f = 7.34$, $h/t_w = 54$, 6.5 AISC β_{br} Unbraced Length Varies)

Figure B-125 Moment Rotation Plot ($b_f/2t_f = 7.34$, $h/t_w = 54$, 7.3 AISC β_{br} Unbraced Length Varies)

Figure B-126 Moment Rotation Plot ($b_f/2t_f = 7.34$, $h/t_w = 54$, 8 AISC β_{br} Unbraced Length Varies)

Appendix B.4

The fourth presentation method combines the plots such that only the bracing stiffness varies. By doing this, it is possible to observe the effect that a change in only bracing stiffness has on structural ductility.
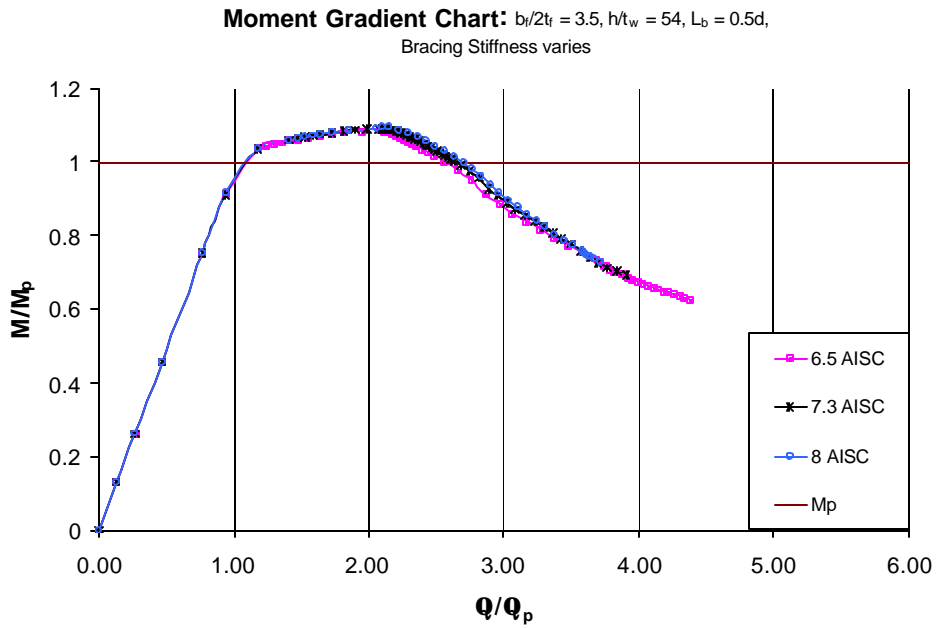
Figure B-127 Moment Rotation Plot ($b_f/2t_f = 3.5$, $h/t_w = 54$, $L_b = 0.5d$ Bracing Stiffness Varies)
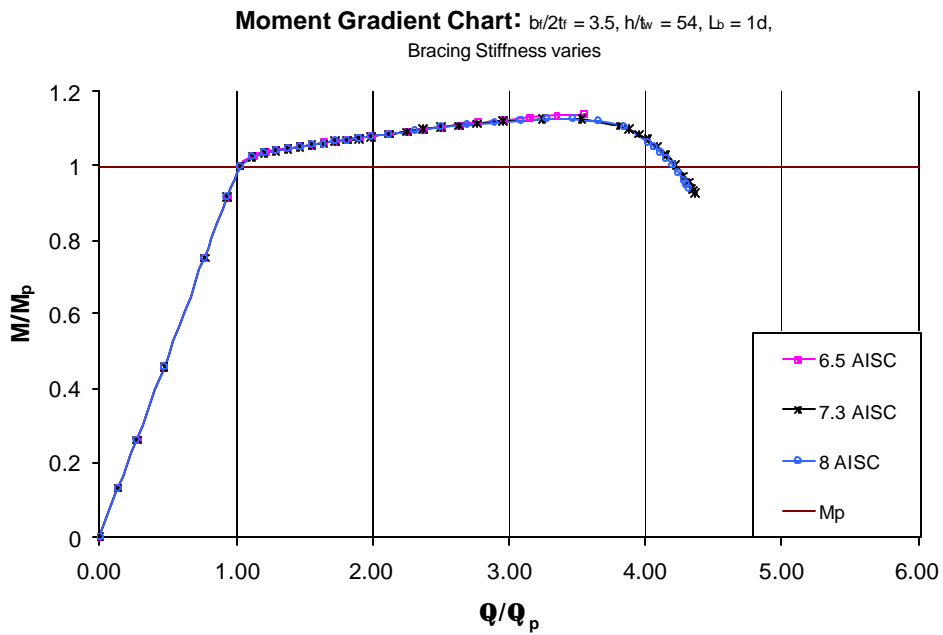
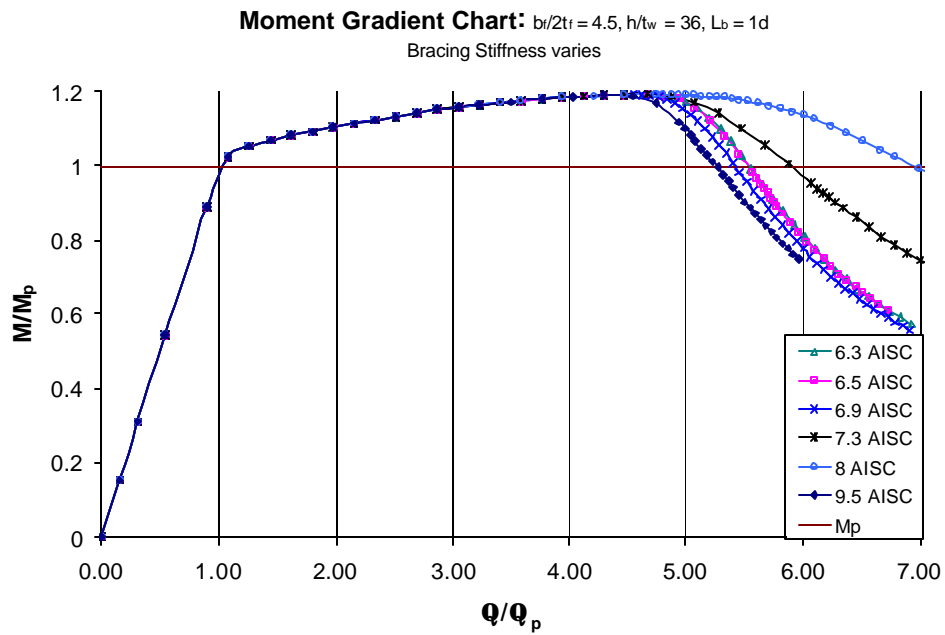**Figure B-128** Moment Rotation Plot ($b_f/2t_f = 3.5$, $h/t_w = 54$, $L_b = 1d$ Bracing Stiffness Varies)
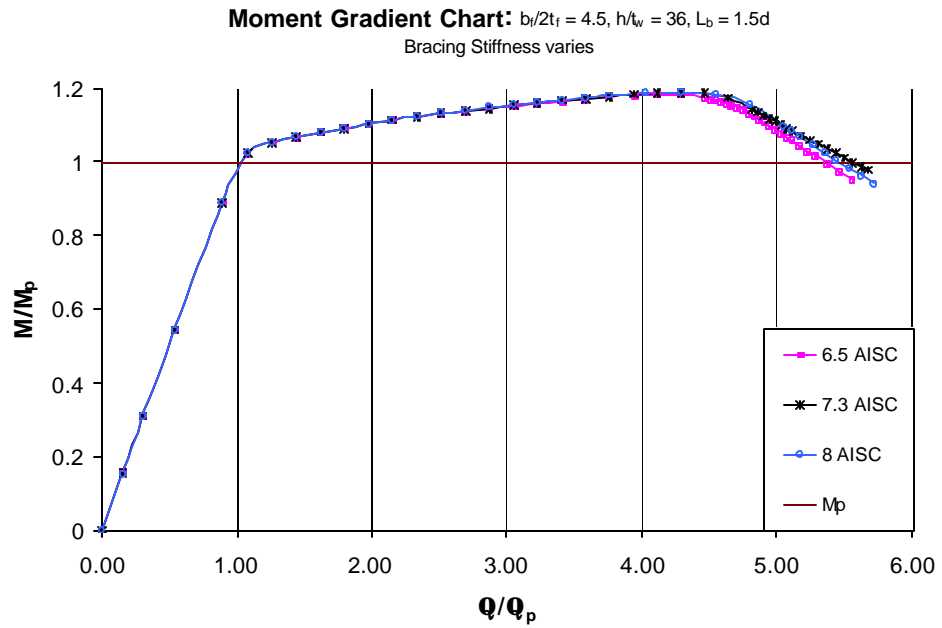
Moment Gradient Chart: $b_f/2t_f = 3.5$, $h/t_w = 54$, $L_b = 1.5d$
Bracing Stiffness varies
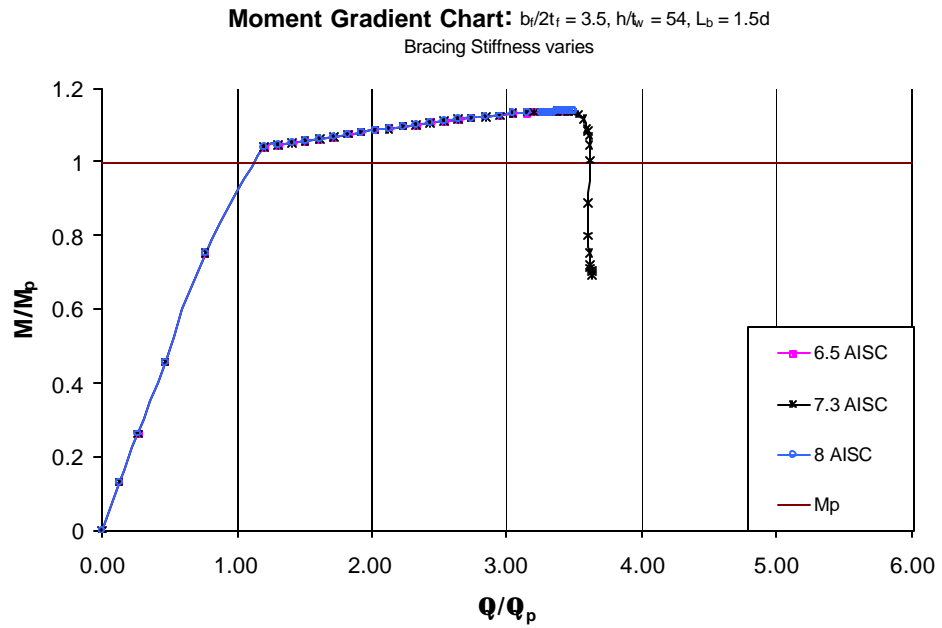
Figure B-129 Moment Rotation Plot ($b_f/2t_f = 3.5$, $h/t_w = 54$, $L_b = 1.5d$ Bracing Stiffness Varies)
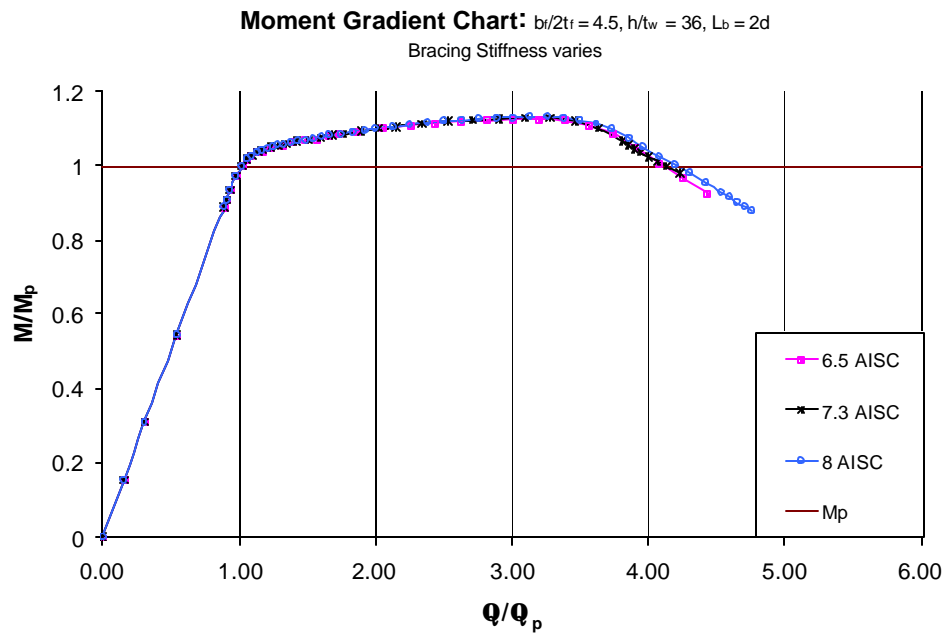
Moment Gradient Chart: $b_f/2t_f = 3.5$, $h/t_w = 72$, $L_b = 0.5d$
Bracing Stiffness varies
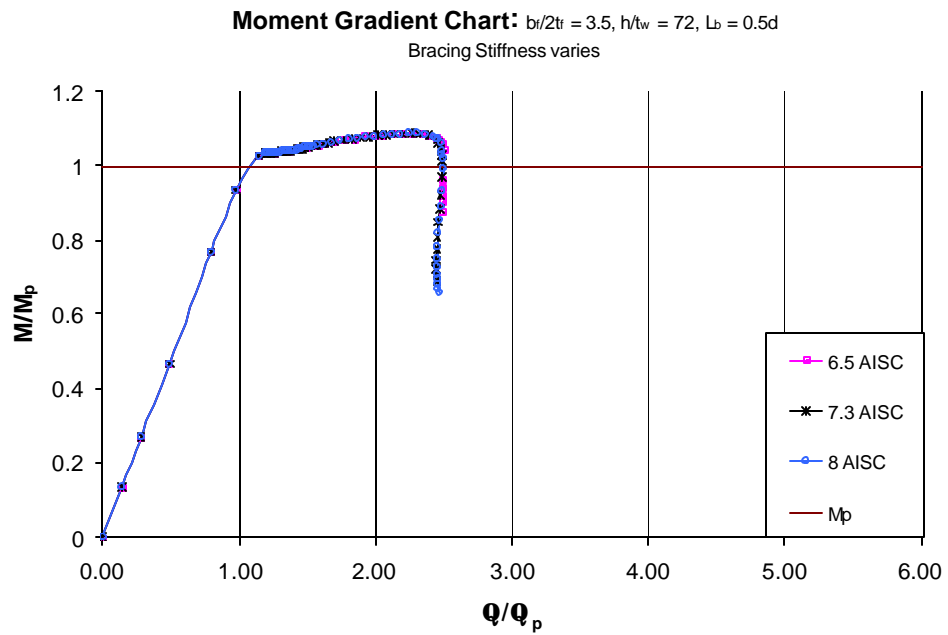
Figure B-130 Moment Rotation Plot ($b_f/2t_f = 3.5$, $h/t_w = 72$, $L_b = 0.5d$ Bracing Stiffness Varies)
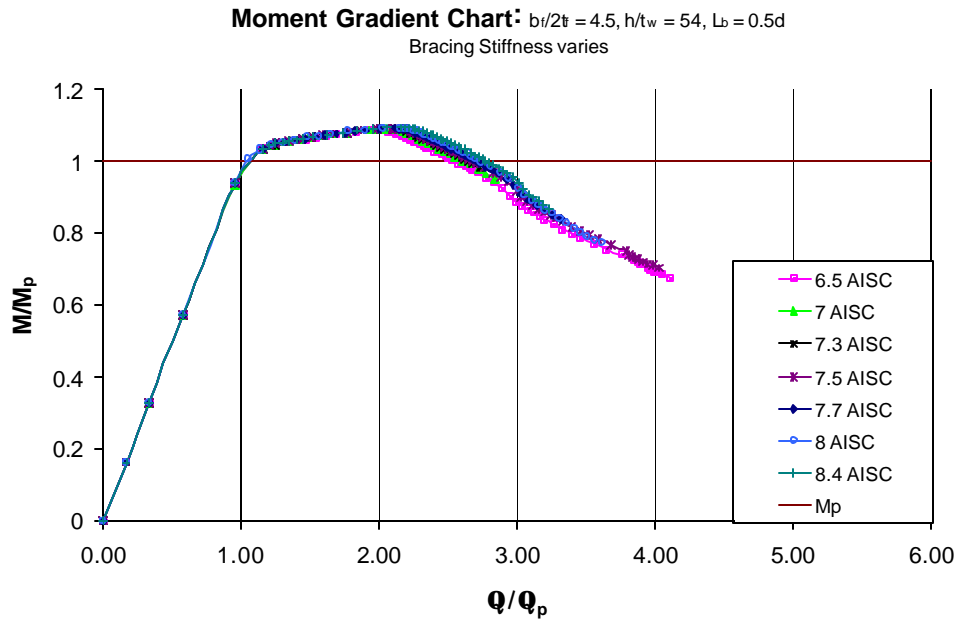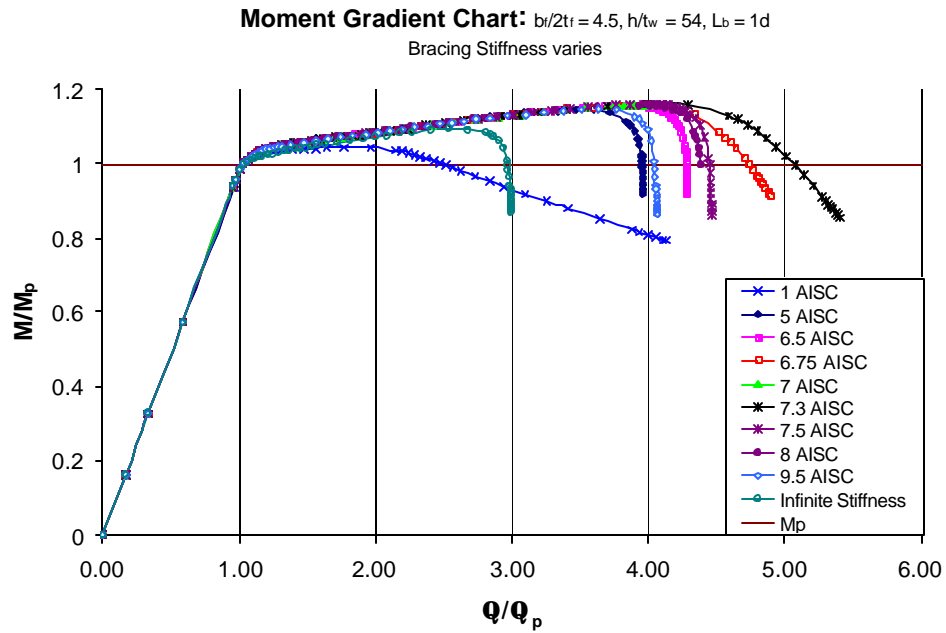
169
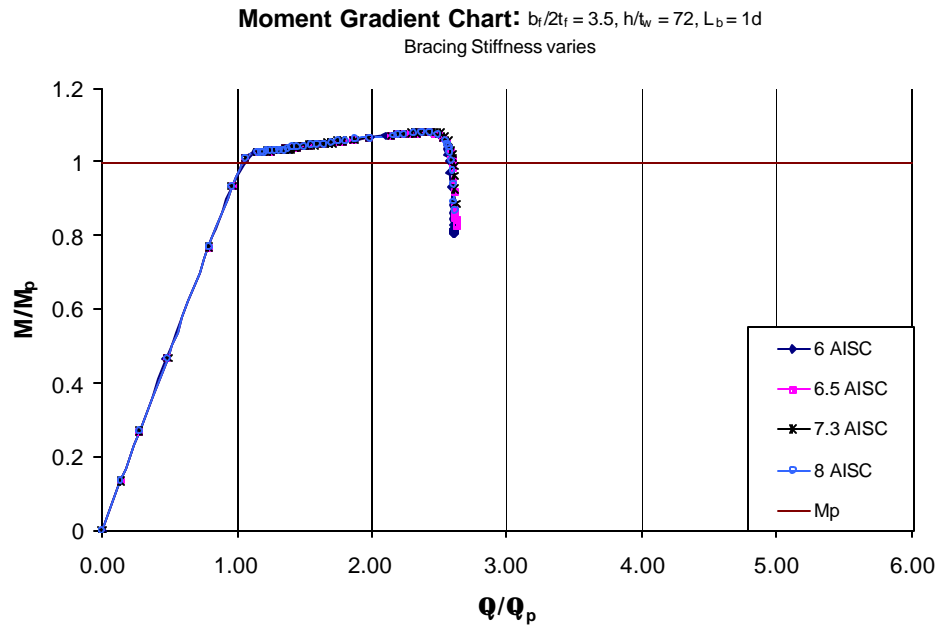
Figure B-131 Moment Rotation Plot ($b_f/2t_f = 3.5$, $h/t_w = 72$, $L_b = 1d$ Bracing Stiffness Varies)
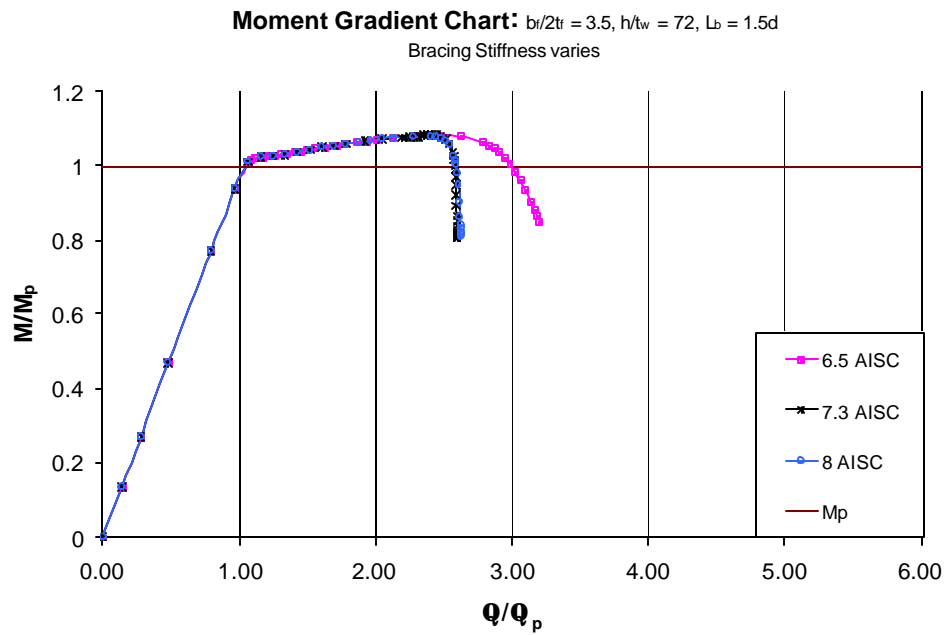
Figure B-132 Moment Rotation Plot ($b_f/2t_f = 3.5$, $h/t_w = 72$, $L_b = 1.5d$ Bracing Stiffness Varies)
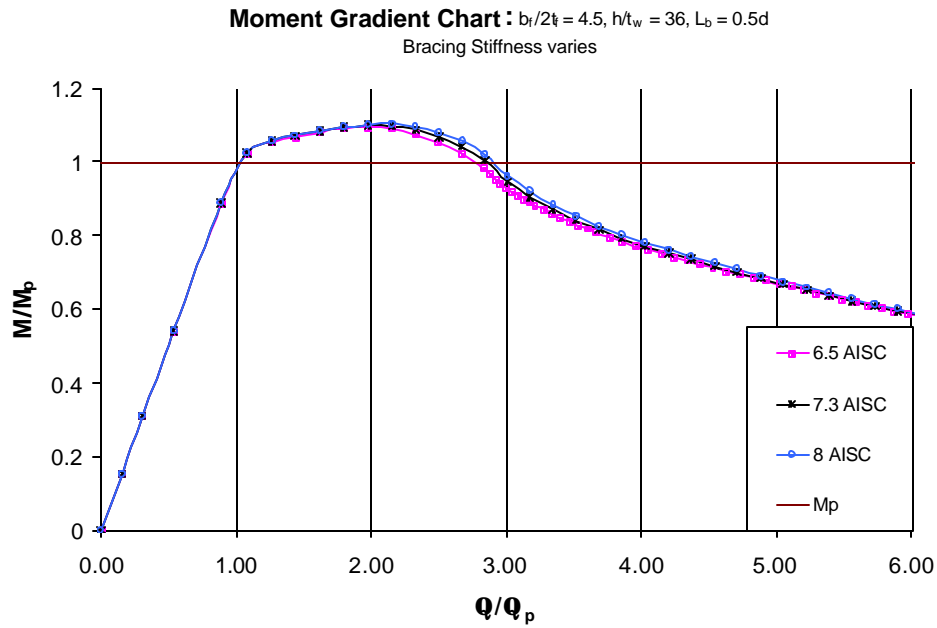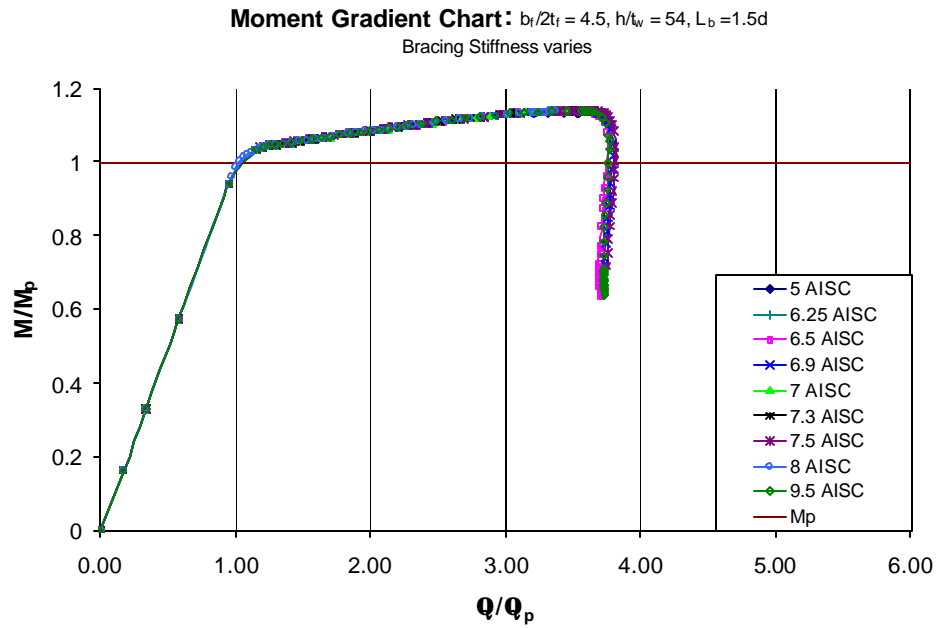
Figure B-133 Moment Rotation Plot ($b_f/2t_f = 4.5$, $h/t_w = 36$, $L_b = 0.5d$ Bracing Stiffness Varies)

Figure B-134 Moment Rotation Plot ($b_f/2t_f = 4.5$, $h/t_w = 36$, $L_b = 1d$ Bracing Stiffness Varies)

Moment Gradient Chart: $b_f/2t_f$ = 4.5, h/t_w = 36, L_b = 1.5d

Bracing Stiffness varies

Figure B-135 Moment Rotation Plot ($b_f/2t_f = 4.5$, $h/t_w = 36$, $L_b = 1.5d$
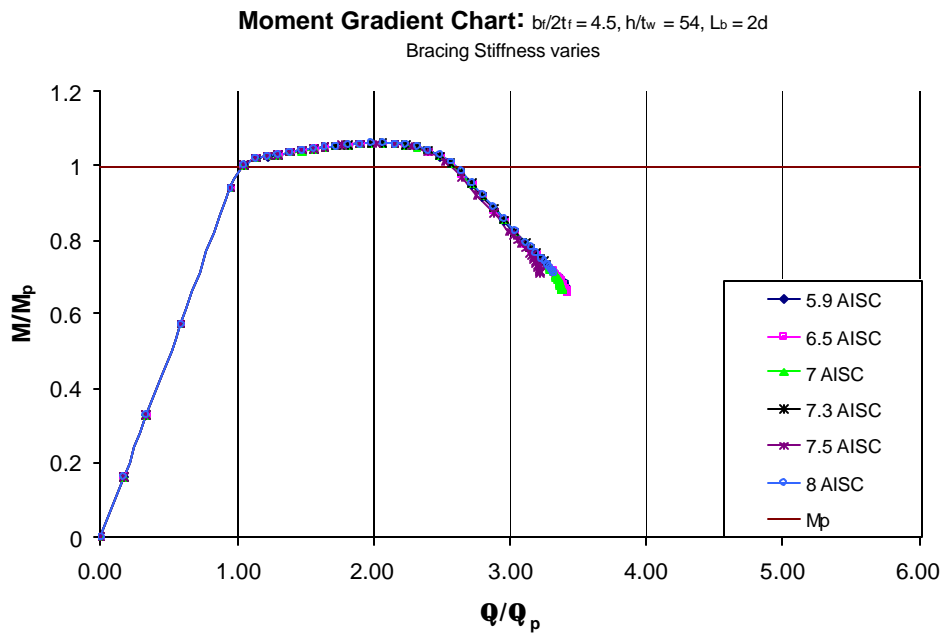Bracing Stiffness Varies)

Moment Gradient Chart: $b_f/2t_f$ = 4.5, h/t_w = 36, L_b = 2d

Bracing Stiffness varies

Figure B-136 Moment Rotation Plot ($b_f/2t_f = 4.5$, $h/t_w = 36$, $L_b = 2d$
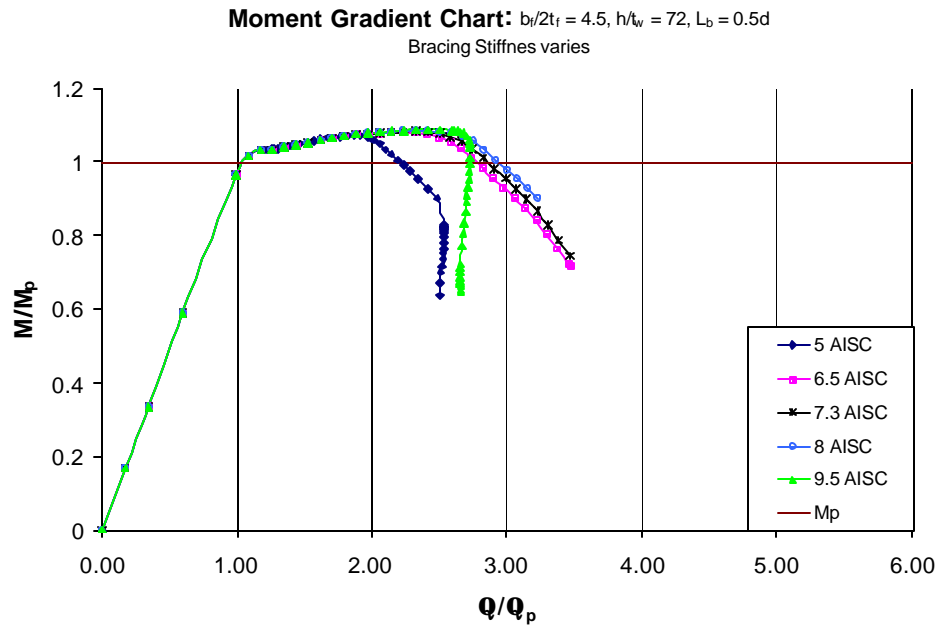Bracing Stiffness Varies)

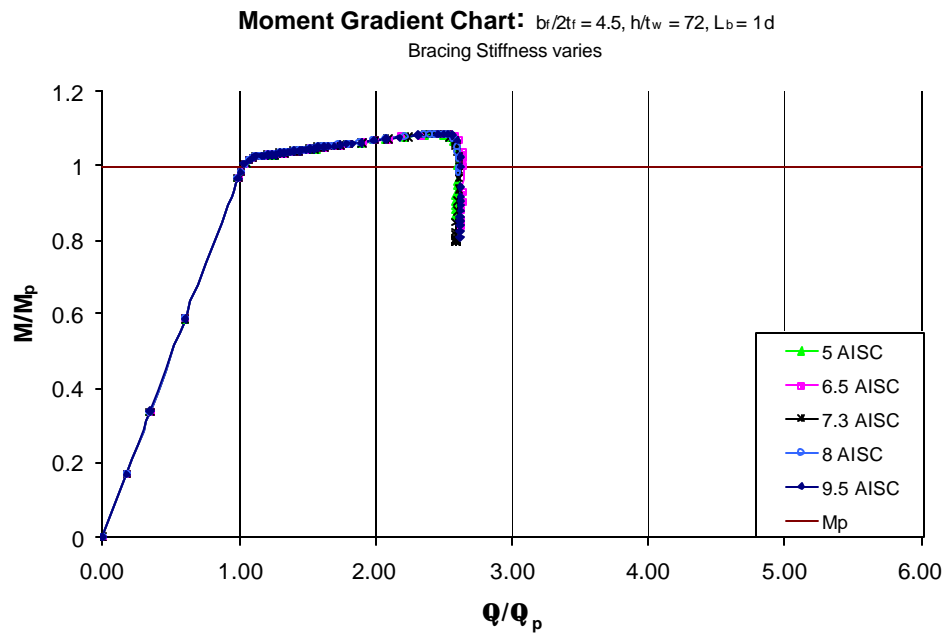**Figure B-137** Moment Rotation Plot ($b_f/2t_f = 4.5$, $h/t_w = 54$, $L_b = 0.5d$ Bracing Stiffness Varies)

Figure B-138 Moment Rotation Plot ($b_f/2t_f = 4.5$, $h/t_w = 54$, $L_b = 1d$ Bracing Stiffness Varies)
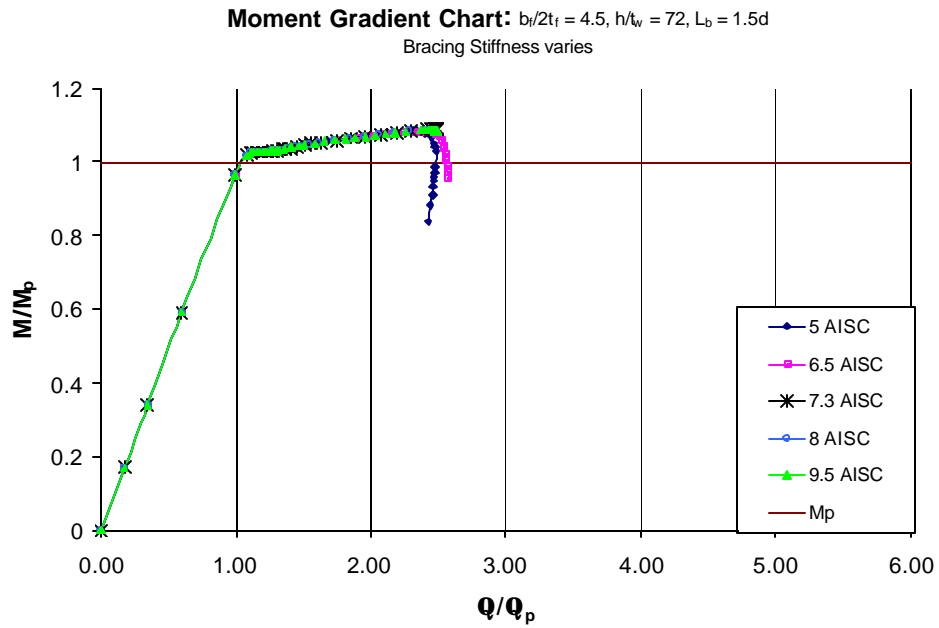
Moment Gradient Chart: $b_f/2t_f = 4.5$, $h/t_w = 54$, $L_b = 1.5d$
Bracing Stiffness varies

Figure B-139 Moment Rotation Plot ($b_f/2t_f = 4.5$, $h/t_w = 54$, $L_b = 1.5d$
Bracing Stiffness Varies)

Moment Gradient Chart: $b_f/2t_f = 4.5$, $h/t_w = 54$, $L_b = 2d$
Bracing Stiffness varies

Figure B-140 Moment Rotation Plot ($b_f/2t_f = 4.5$, $h/t_w = 54$, $L_b = 2d$
Bracing Stiffness Varies)

Figure B-141 Moment Rotation Plot ($b_f/2t_f = 4.5$, $h/t_w = 72$, $L_b = 0.5d$
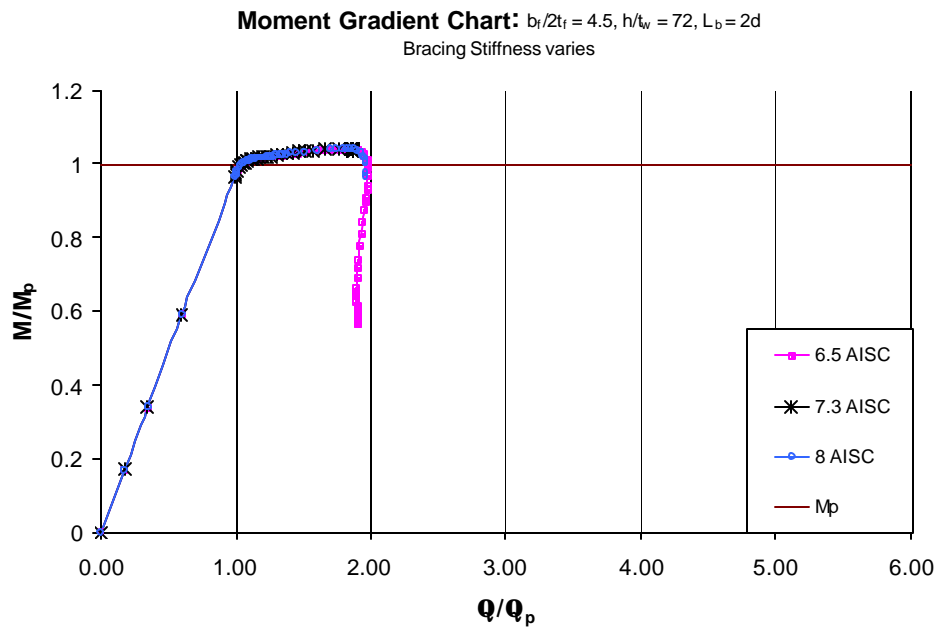Bracing Stiffness Varies)

Figure B-142 Moment Rotation Plot ($b_f/2t_f = 4.5$, $h/t_w = 72$, $L_b = 1d$
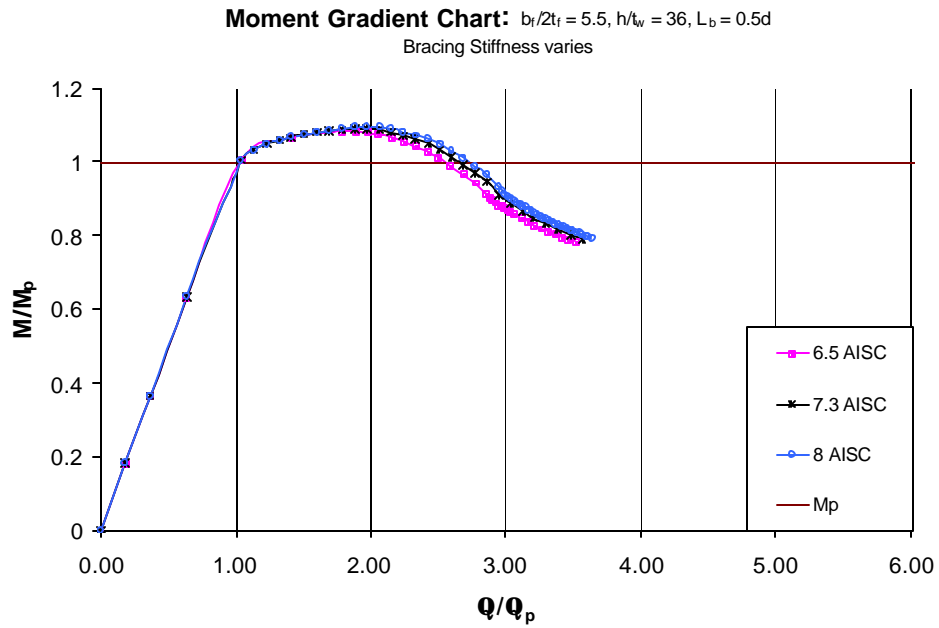Bracing Stiffness Varies)

Moment Gradient Chart: $b_f/2t_f = 4.5$, $h/t_w = 72$, $L_b = 1.5d$
Bracing Stiffness varies

Figure B-143 Moment Rotation Plot ($b_f/2t_f = 4.5$, $h/t_w = 72$, $L_b = 1.5d$
Bracing Stiffness Varies)

Moment Gradient Chart: $b_f/2t_f = 4.5$, $h/t_w = 72$, $L_b = 2d$
Bracing Stiffness varies

Figure B-144 Moment Rotation Plot ($b_f/2t_f = 4.5$, $h/t_w = 72$, $L_b = 2d$
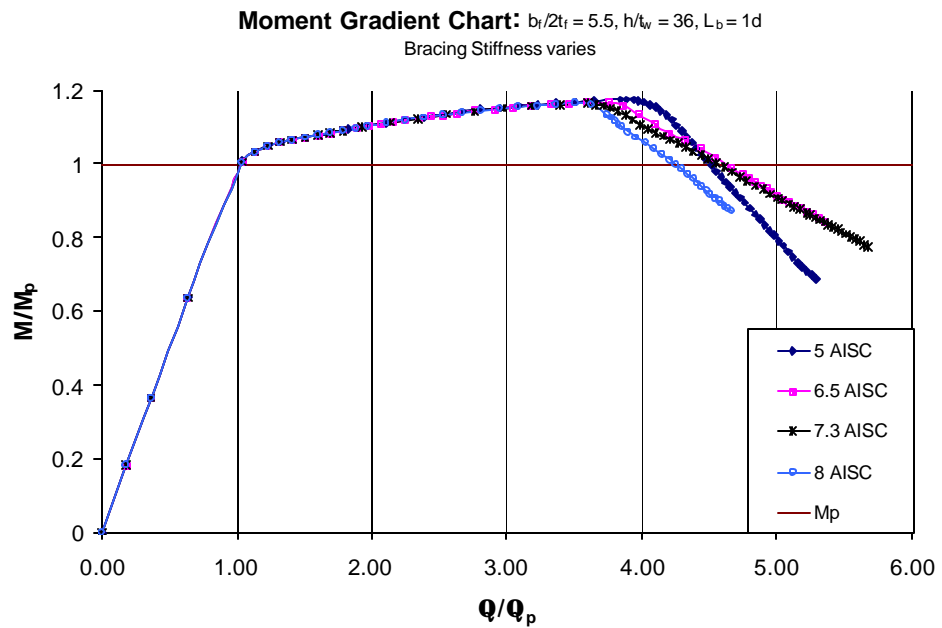Bracing Stiffness Varies)

Moment Gradient Chart: $b_f/2t_f = 5.5$, $h/t_w = 36$, $L_b = 0.5d$

Bracing Stiffness varies

Figure B-145 Moment Rotation Plot ($b_f/2t_f = 5.5$, $h/t_w = 36$, $L_b = 0.5d$ Bracing Stiffness Varies)

Moment Gradient Chart: $b_f/2t_f = 5.5$, $h/t_w = 36$, $L_b = 1d$

Bracing Stiffness varies

Figure B-146 Moment Rotation Plot ($b_f/2t_f = 5.5$, $h/t_w = 36$, $L_b = 1d$ Bracing Stiffness Varies)
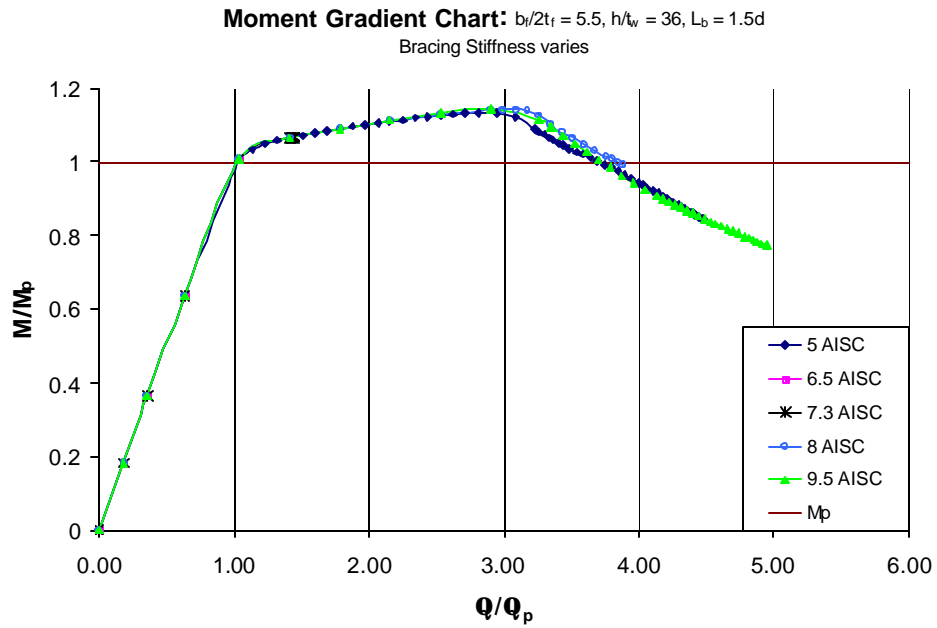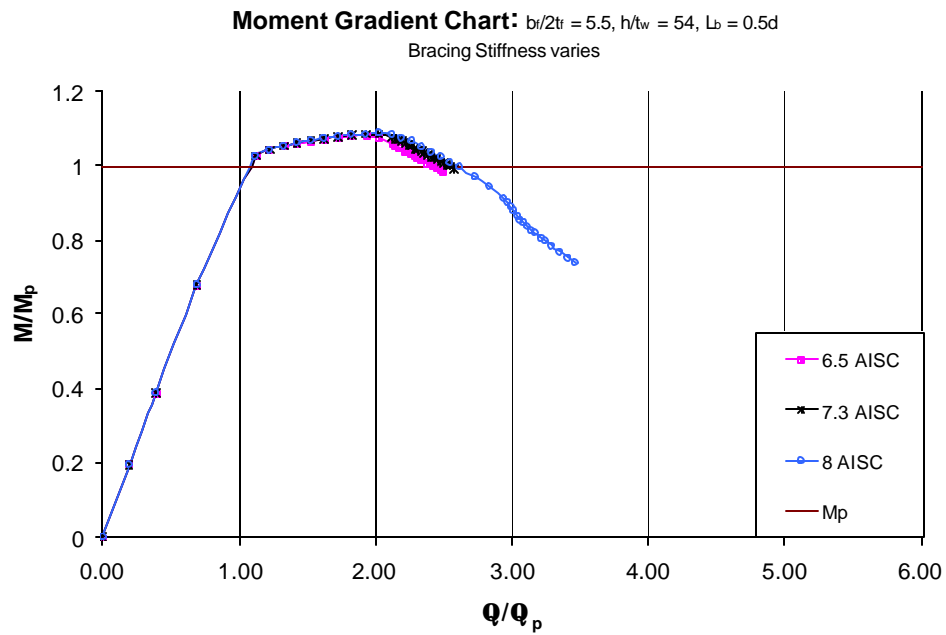
Moment Gradient Chart: $b_f/2t_f = 5.5$, $h/t_w = 36$, $L_b = 1.5d$
Bracing Stiffness varies

Figure B-147 Moment Rotation Plot ($b_f/2t_f = 5.5$, $h/t_w = 36$, $L_b = 1.5d$ Bracing Stiffness Varies)
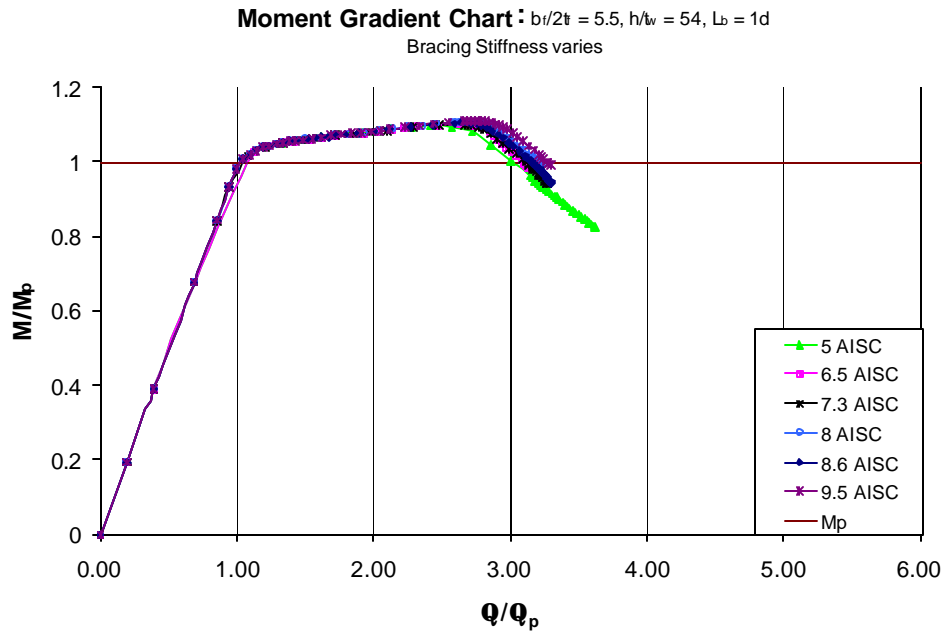
Moment Gradient Chart: $b_f/2t_f = 5.5$, $h/t_w = 54$, $L_b = 0.5d$
Bracing Stiffness varies

Figure B-148 Moment Rotation Plot ($b_f/2t_f = 5.5$, $h/t_w = 54$, $L_b = 0.5d$ Bracing Stiffness Varies)

Figure B-149 Moment Rotation Plot ($b_f/2t_f = 5.5$, $h/t_w = 54$, $L_b = 1d$
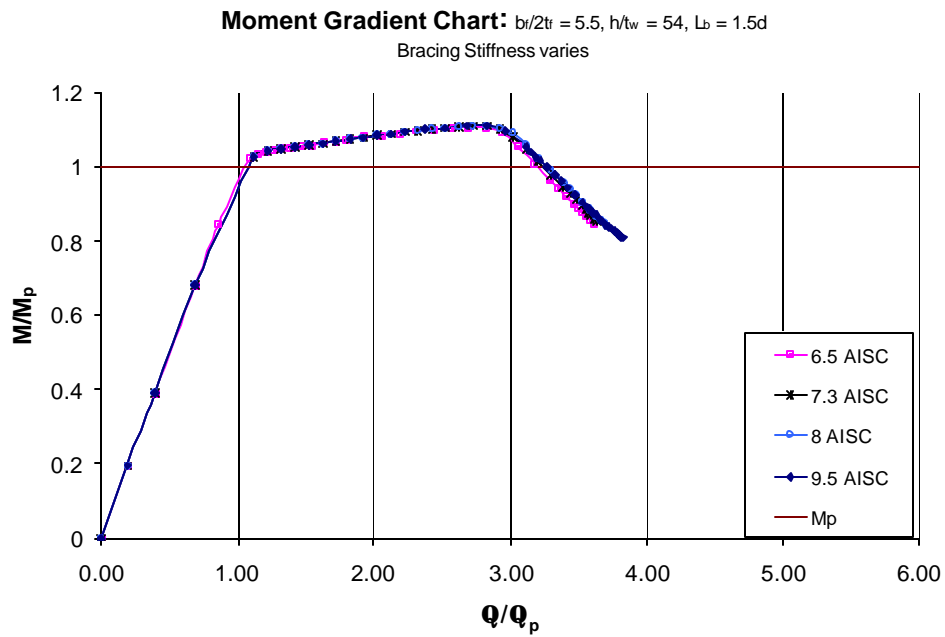Bracing Stiffness Varies)

Figure B-150 Moment Rotation Plot ($b_f/2t_f = 5.5$, $h/t_w = 54$, $L_b = 1.5d$
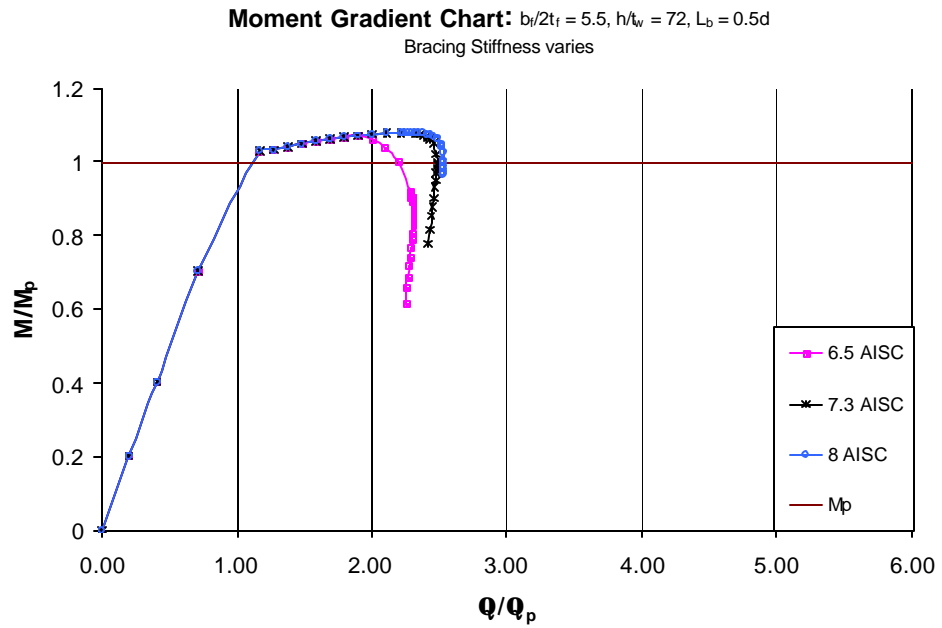Bracing Stiffness Varies)

Moment Gradient Chart: $b_f/2t_f = 5.5$, $h/t_w = 72$, $L_b = 0.5d$
Bracing Stiffness varies

Figure B-151 Moment Rotation Plot ($b_f/2t_f = 5.5$, $h/t_w = 72$, $L_b = 0.5d$
Bracing Stiffness Varies)

Moment Gradient Chart: $b_f/2t_f = 5.5$, $h/t_w = 72$, $L_b = 1d$
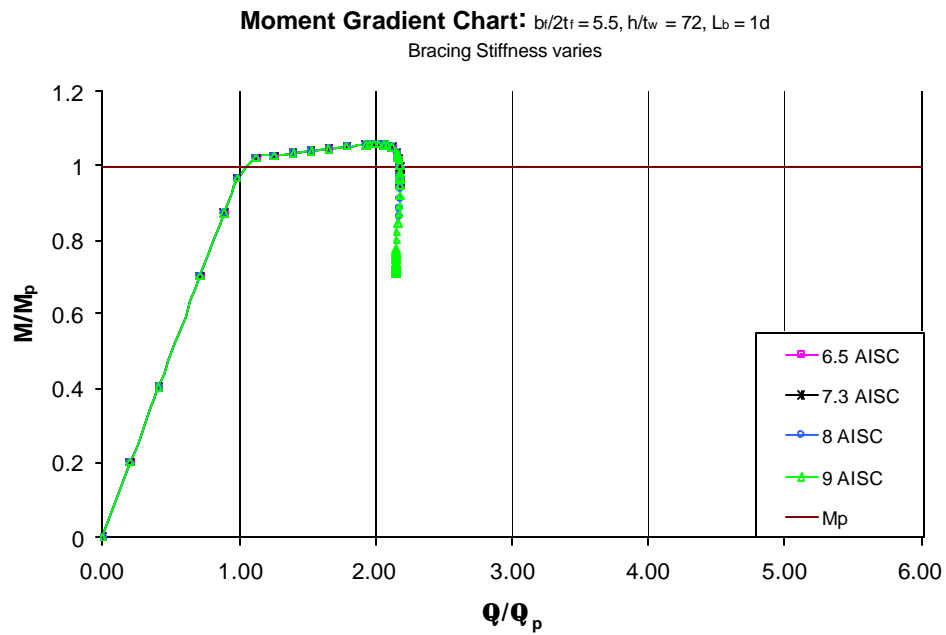Bracing Stiffness varies

Figure B-152 Moment Rotation Plot ($b_f/2t_f = 5.5$, $h/t_w = 72$, $L_b = 1d$
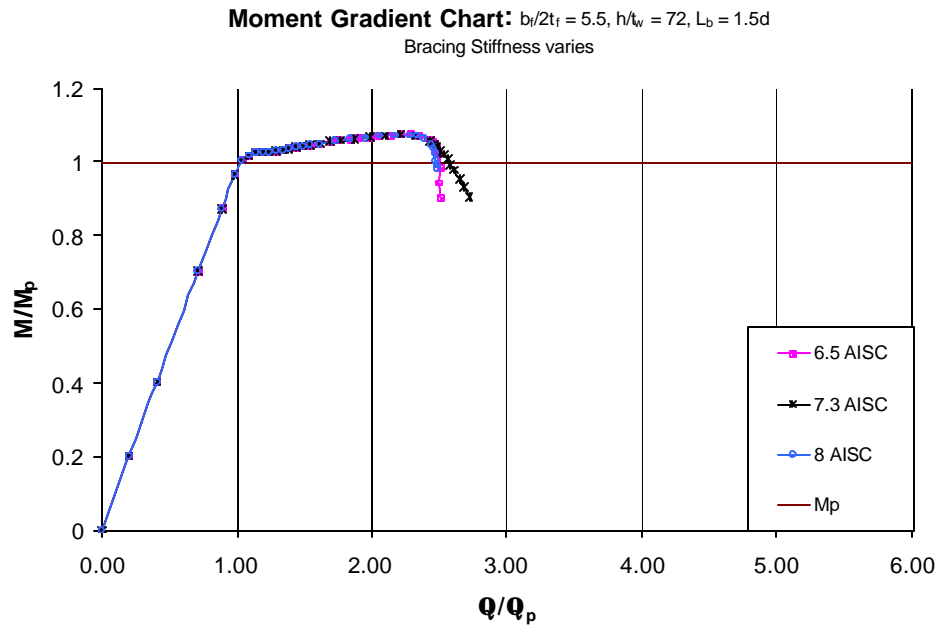Bracing Stiffness Varies)

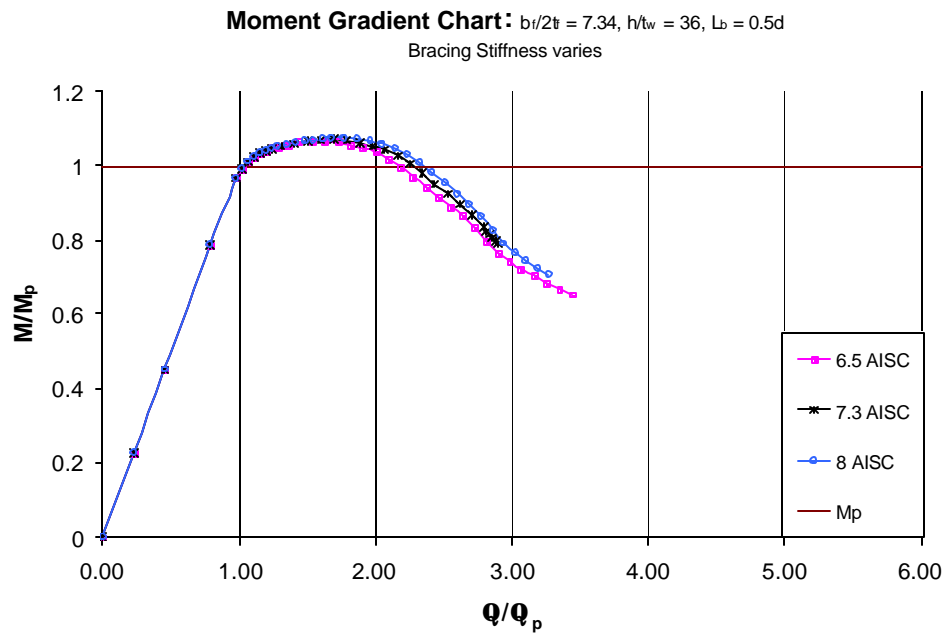**Figure B-153** Moment Rotation Plot ($b_f/2t_f = 5.5$, $h/t_w = 72$, $L_b = 1.5d$ Bracing Stiffness Varies)

Figure B-154 Moment Rotation Plot ($b_f/2t_f = 7.34$, $h/t_w = 36$, $L_b = 0.5d$ Bracing Stiffness Varies)

Moment Gradient Chart: $b_f/2t_f = 7.34$, $h/t_w = 36$, $L_b = 1d$
Bracing Stiffness varies

Figure B155 Moment Rotation Plot ($b_f/2t_f = 7.34$, $h/t_w = 36$, $L_b = 1d$ Bracing Stiffness Varies)

Moment Gradient Chart: $b_f/2t_f = 7.34$, $h/t_w = 36$, $L_b = 1.5d$
Bracing Stiffness varies

Figure B-156 Moment Rotation Plot ($b_f/2t_f = 7.34$, $h/t_w = 36$, $L_b = 1.5d$ Bracing Stiffness Varies)
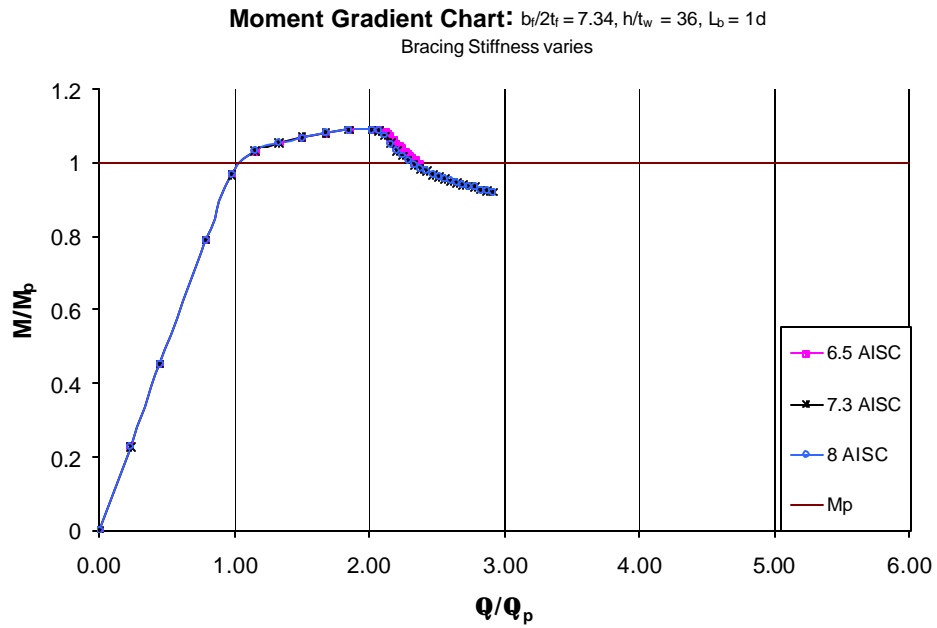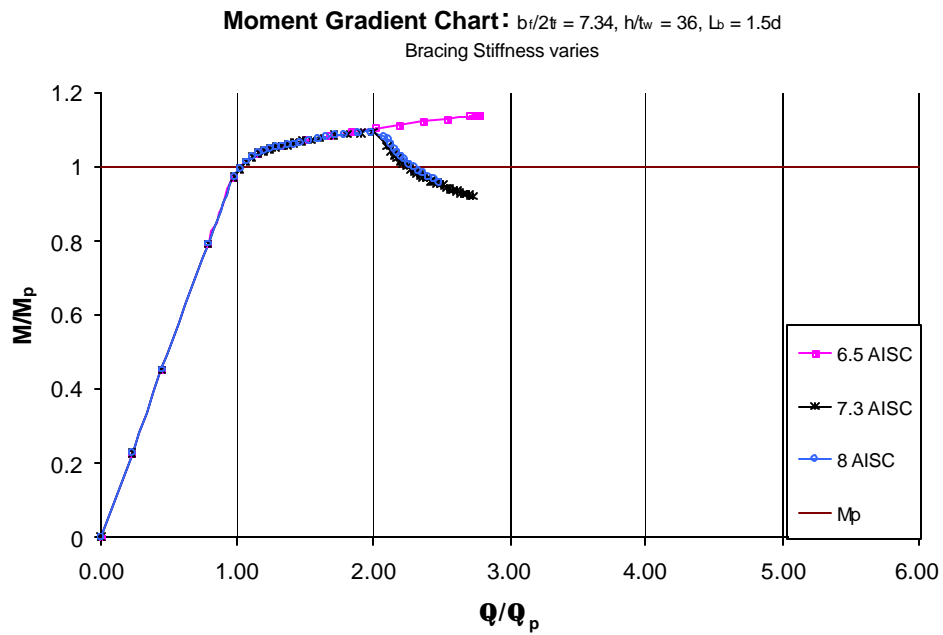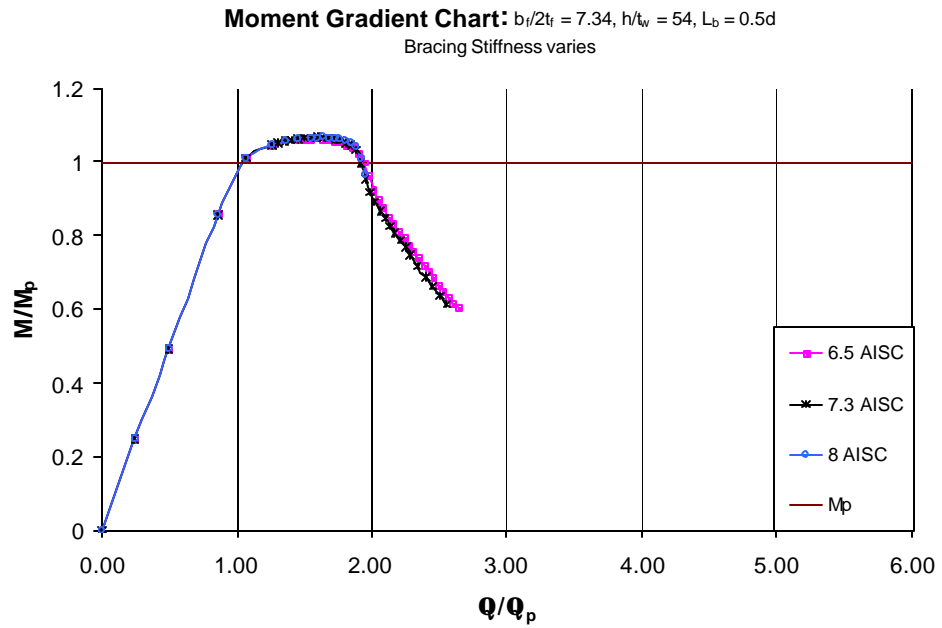
Figure B-157 Moment Rotation Plot ($b_f/2t_f = 7.34$, $h/t_w = 54$, $L_b = 0.5d$
Bracing Stiffness Varies)

Figure B-158 Moment Rotation Plot ($b_f/2t_f = 7.34$, $h/t_w = 54$, $L_b = 1d$
Bracing Stiffness Varies)

Figure B-159 Moment Rotation Plot ($b_f/2t_f = 7.34$, $h/t_w = 54$, $L_b = 1.5d$
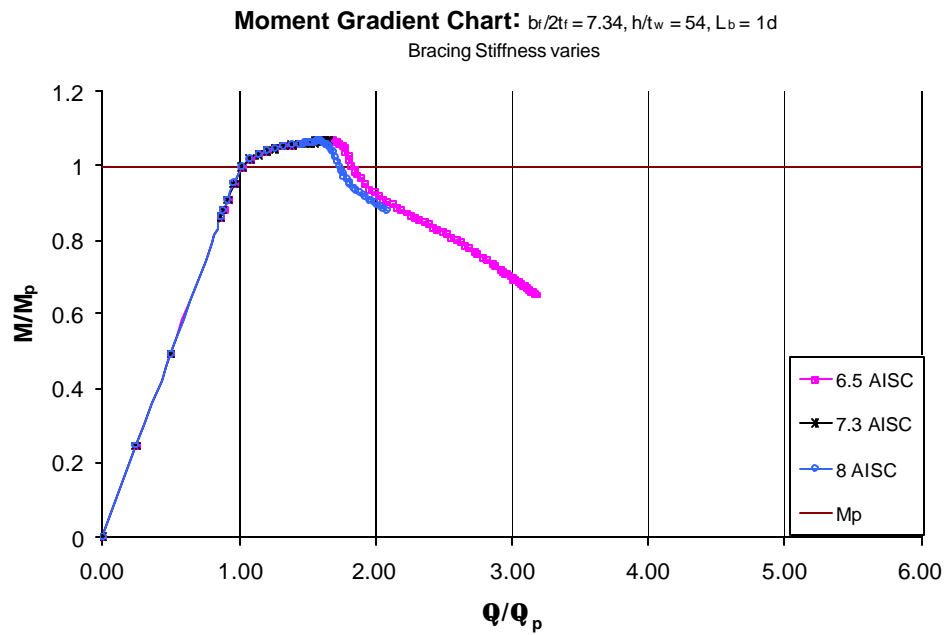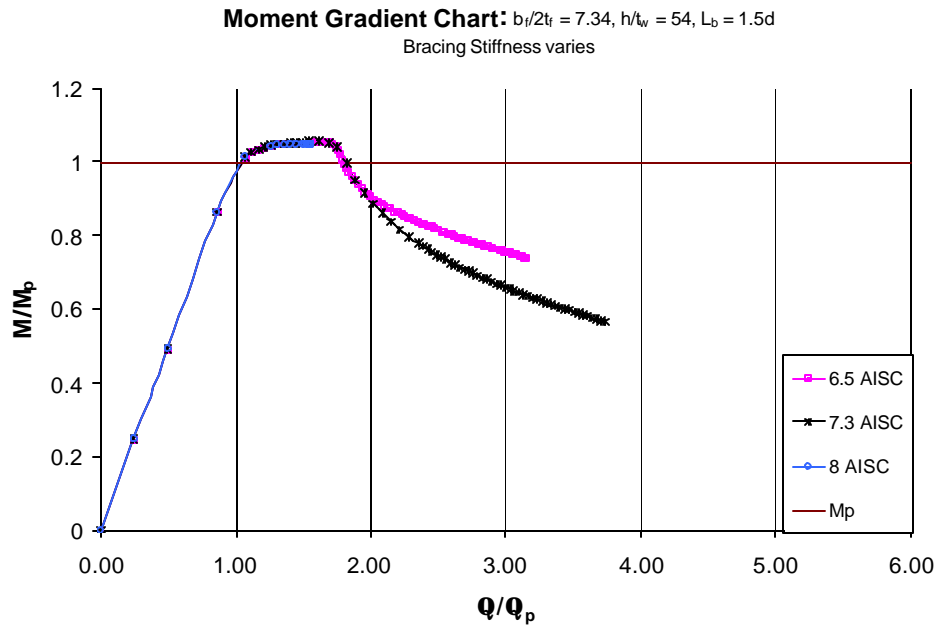Bracing Stiffness Varies)

Appendix B.5

This sub-appendix presents moment-rotation plots for any remaining combinations that were not applicable in any of the previous graphs (i.e. graphs where multiple parameters change simultaneously).
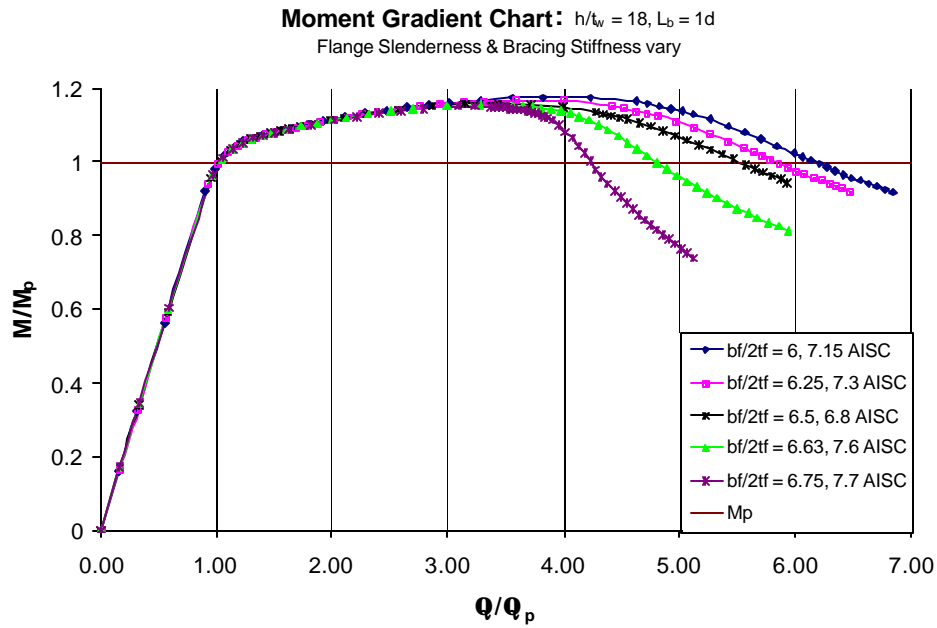
Figure B-160 Moment Rotation Plot ($h/t_w = 18$, $L_b = 1d$
Flange Slenderness & Bracing Stiffness Vary)

Figure B-161 Moment Rotation Plot ($h/t_w = 45$, $L_b = 1d$
Flange Slenderness & Bracing Stiffness Vary)

186

Moment Gradient Chart: h/t_w = 54, L_b = 1d
Flange Slenderness & Bracing Stiffness vary

Figure B-162 Moment Rotation Plot (h/t$_w$ = 54, L$_b$ = 1d Flange Slenderness & Bracing Stiffness Vary)

Moment Gradient Chart: h/t_w = 60, L_b = 1d
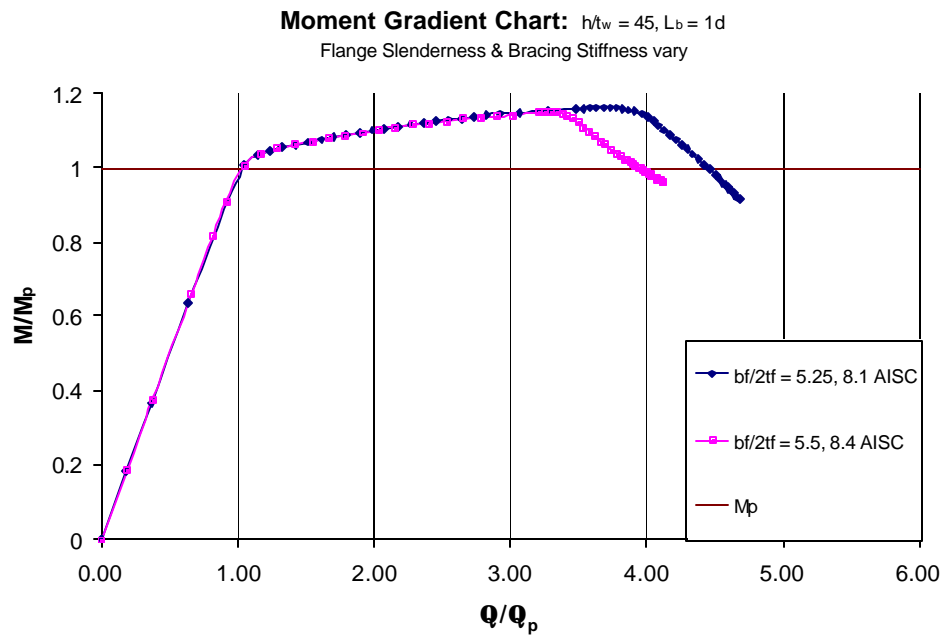Flange Slenderness & Bracing Stiffness vary

Figure B-163 Moment Rotation Plot (h/t$_w$ = 60, L$_b$ = 1d Flange Slenderness & Bracing Stiffness Vary)
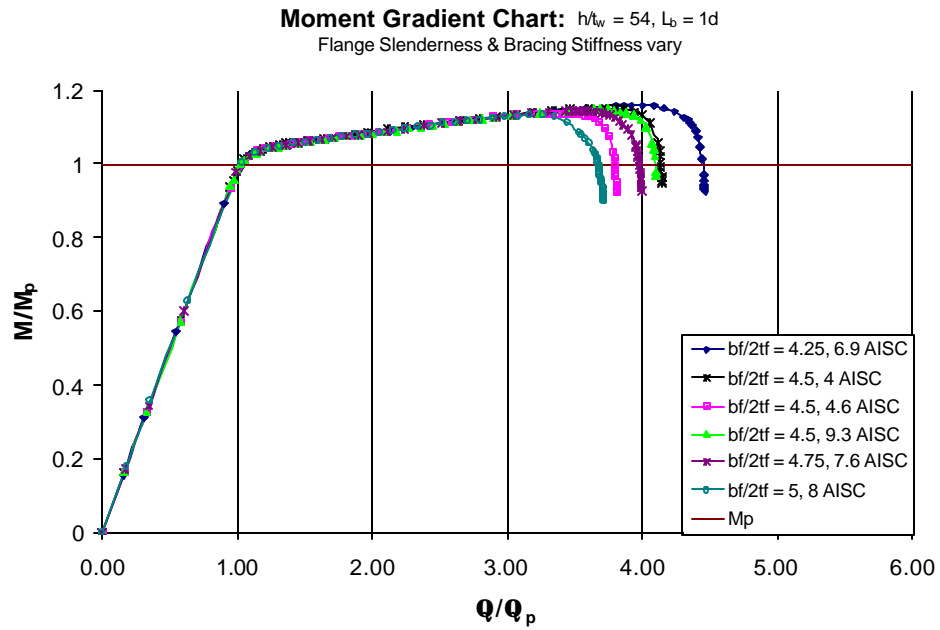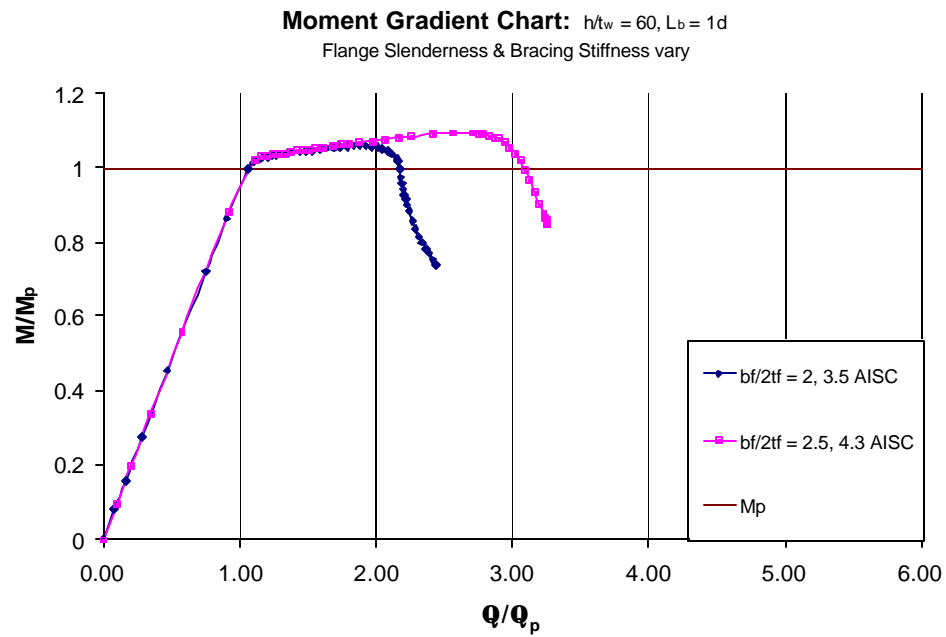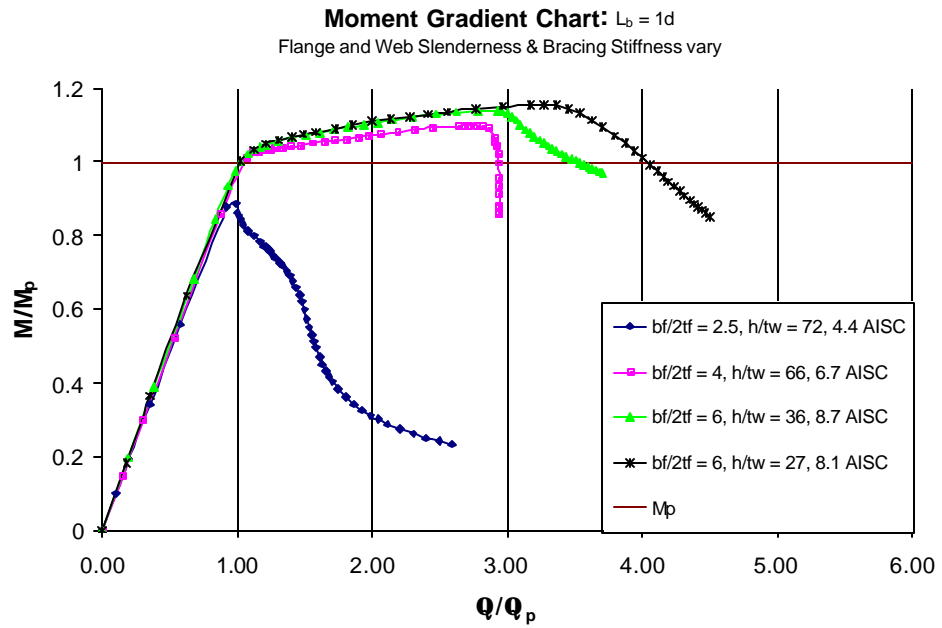
Figure B-164 Moment Rotation Plot (L_b = 1d
Flange and Web Slenderness & Bracing Stiffness Vary)

APPENDIX C

APPENDIX C

INTERACTION PLOTS

All interaction plots produced from the data presented herein are located in this appendix. There exist six different types of interaction plots in which one of the parameters is graphed against another parameter. On each plot, points are marked that indicate combinations of the four parameters that have been tested. Each point is annotated with the rotation capacity that is achieved for that combination of parameters. For ease in reading the graphs, each rotation capacity equal to or greater than 3.0 is highlighted in gray. In addition, the current AISC and/or AASHTO specified criteria are shown on each graph as they apply to A709 HPS483W steel for that combination of parameters to as to indicate where the current "safe zone" is (i.e. where, according to the current specifications, the girder should be capable of achieving a rotation capacity of at least 3.0).

Appendix C.1

The first type of interaction plot located in this sub-appendix graphs web slenderness against flange slenderness. For each combination of unbraced length and bracing stiffness, one of these plots has been produced. For each of these plots there exist numerous combinations of flange and web slenderness ratios for which finite element tests are run. The corresponding rotation capacity for each of these individual tests is shown at its respective point on the graph.

Figure C-1 Interaction Plot: Web Slenderness vs. Flange Slenderness $(b_f/2t_f$ Varies, h/t_w Varies, $L_b = 0.5d$, 6.5 AISC $\beta_{br})$

Figure C-2 Interaction Plot: Web Slenderness vs. Flange Slenderness
($b_f/2t_f$ Varies, h/t_w Varies, $L_b = 0.5d$, 7.3 AISC β_{br})

193

Figure C-3 Interaction Plot: Web Slenderness vs. Flange Slenderness
($b_f/2t_f$ Varies, h/t_w Varies, $L_b = 0.5d$, 8 AISC β_{br})

194

Figure C-4 Interaction Plot: Web Slenderness vs. Flange Slenderness
$(b_f/2t_f$ Varies, h/t_w Varies, $L_b = 1d$, 5 AISC $\beta_{br})$

195

Web Slenderness vs. Flange Slenderness

$b_f/2t_f$ varies, h/t_w varies, $L_b = 1d$, 5.9 AISC Recommended Bracing Stiffness

- AISC Limiting Slenderness Ratios
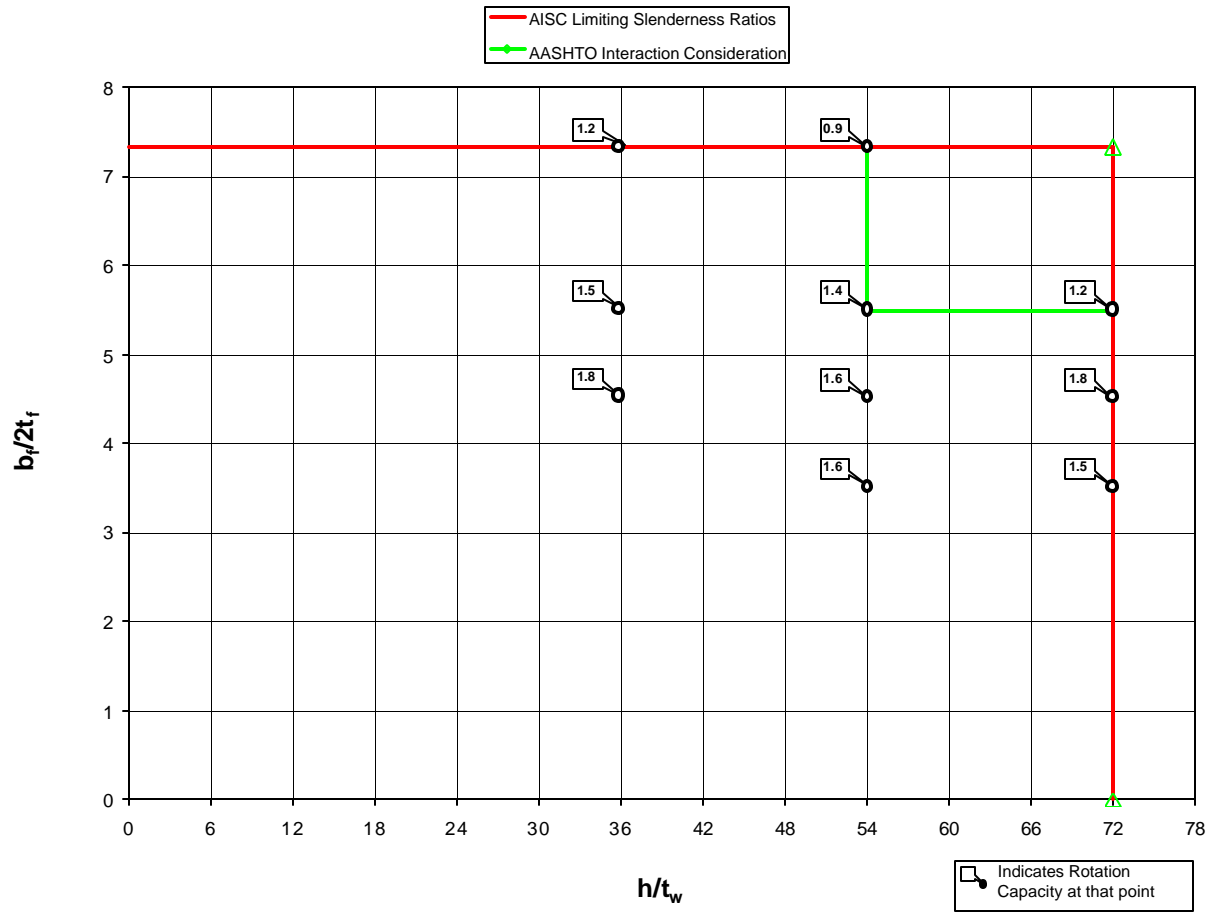- AASHTO Interaction Consideration

Figure C-5 Interaction Plot: Web Slenderness vs. Flange Slenderness
$b_f/2t_f$ Varies, h/t_w Varies, $L_b = 1d$, 5.9AISC β_{br})

Web Slenderness vs. Flange Slenderness

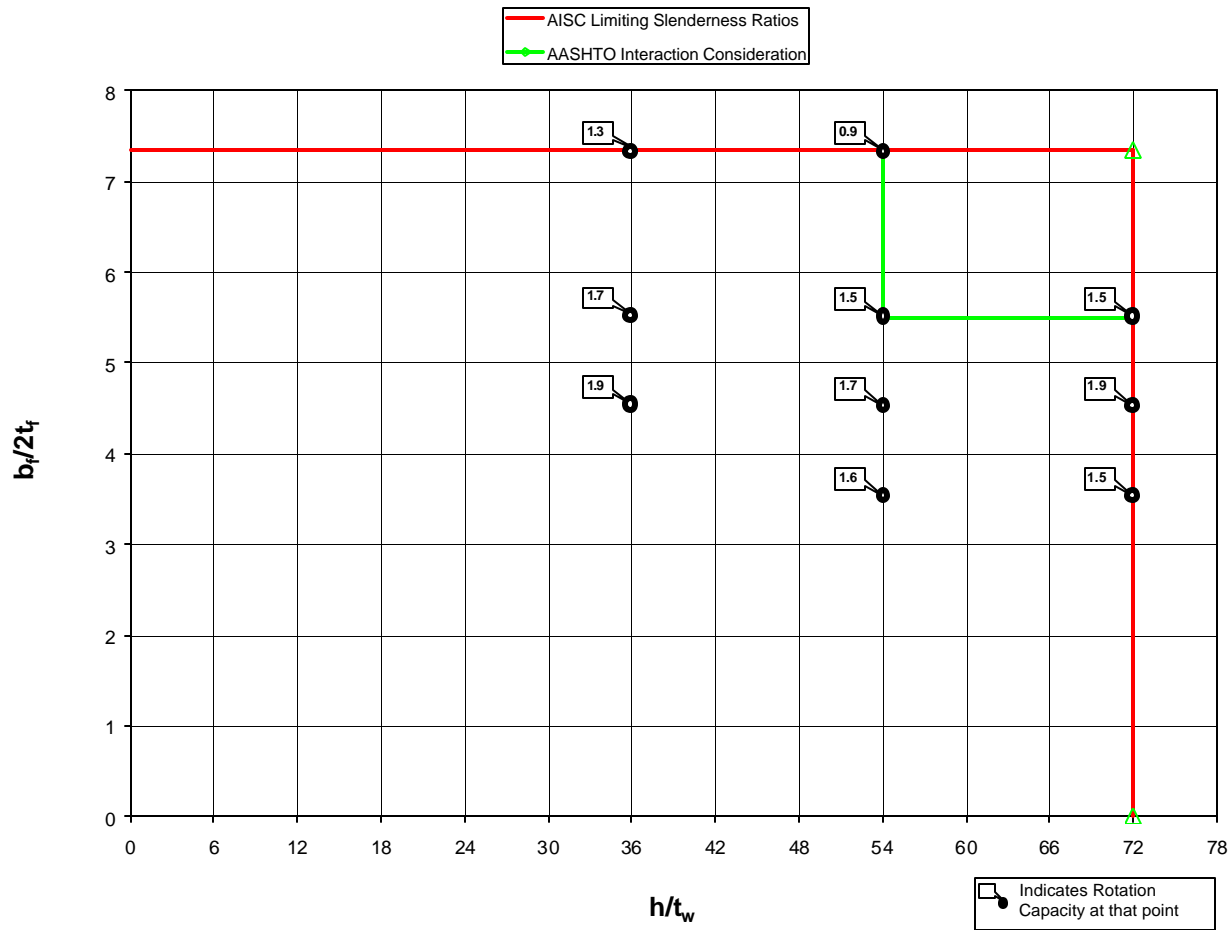$b_f/2t_f$ varies, h/t_w varies, L_b = 1d, 6.5 AISC Recommended Bracing Stiffness

— AISC Limiting Slenderness Ratios

—●— AASHTO Interaction Consideration

Figure C-6 Interaction Plot: Web Slenderness vs. Flange Slenderness
($b_f/2t_f$ Varies, h/t_w Varies, L_b = 1d, 6.5 AISC β_{br})

197

Figure C-7 Interaction Plot: Web Slenderness vs. Flange Slenderness
($b_f/2t_f$ Varies, h/t_w Varies, L_b = 1d, 6.9 AISC β_{br})

198

Figure C-8 Interaction Plot: Web Slenderness vs. Flange Slenderness
($b_f/2t_f$ Varies, h/t_w Varies, L_b = 1d, 7.3 AISC β_{br})

199

Figure C-9 Interaction Plot: Web Slenderness vs. Flange Slenderness
($b_f/2t_f$ Varies, h/t_w Varies, $L_b = 1d$, 7.5 AISC β_{br})
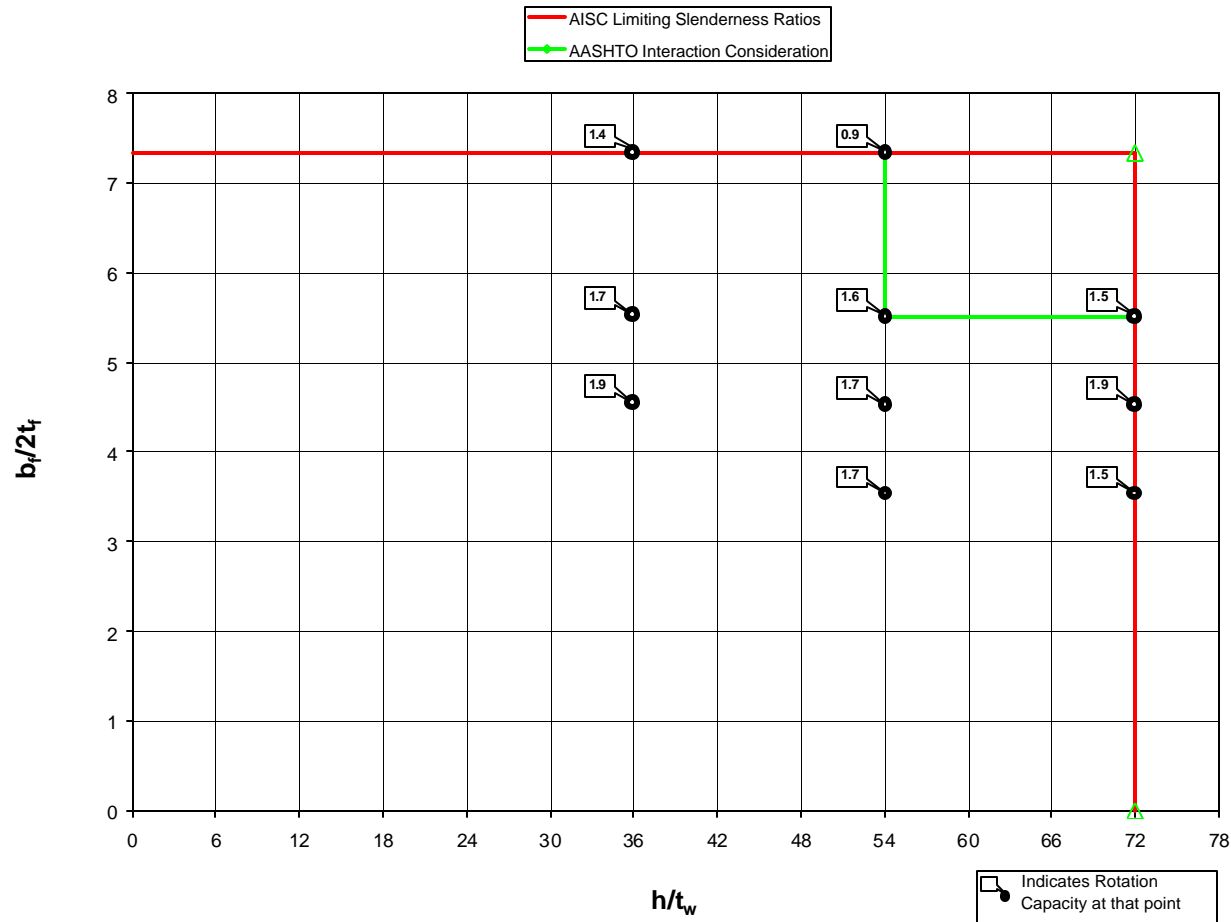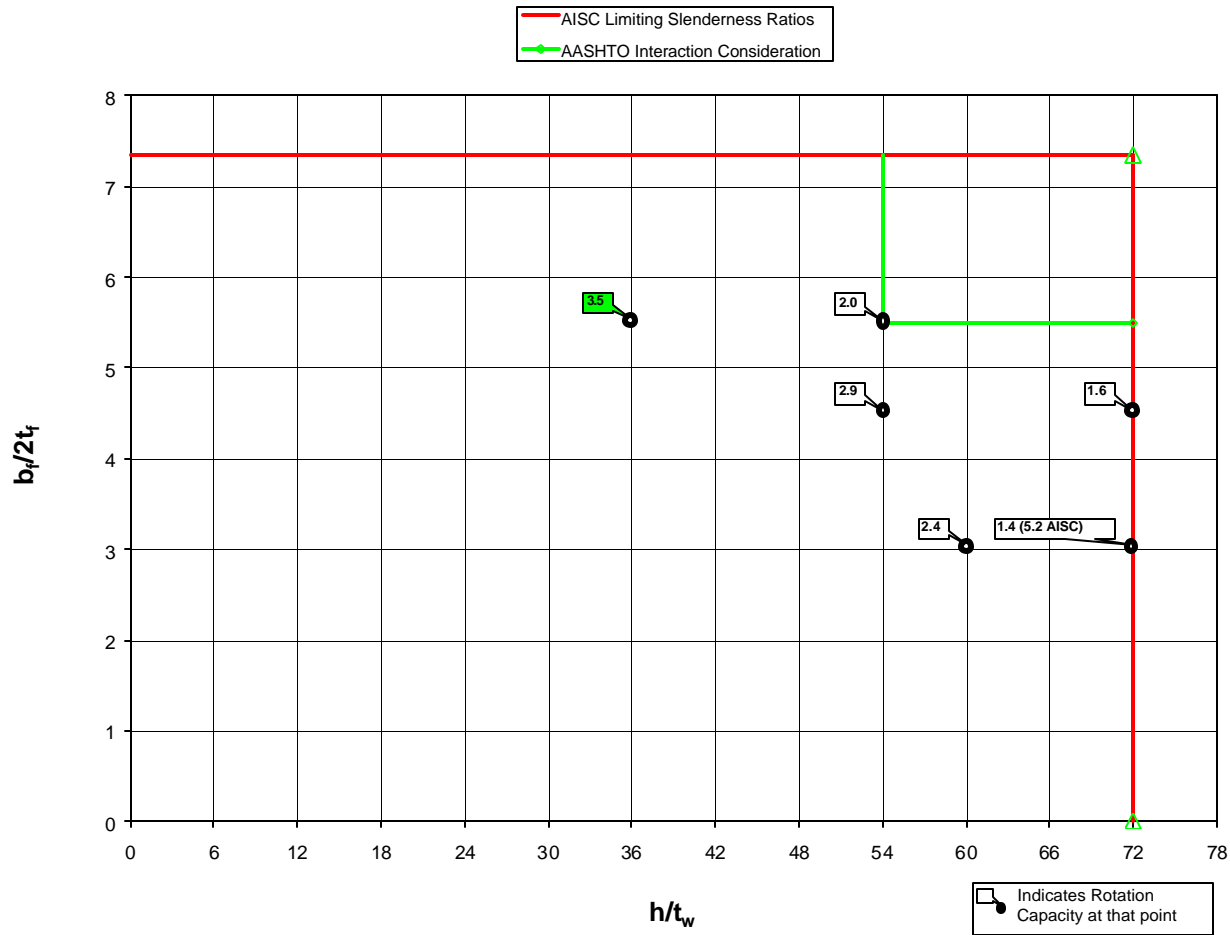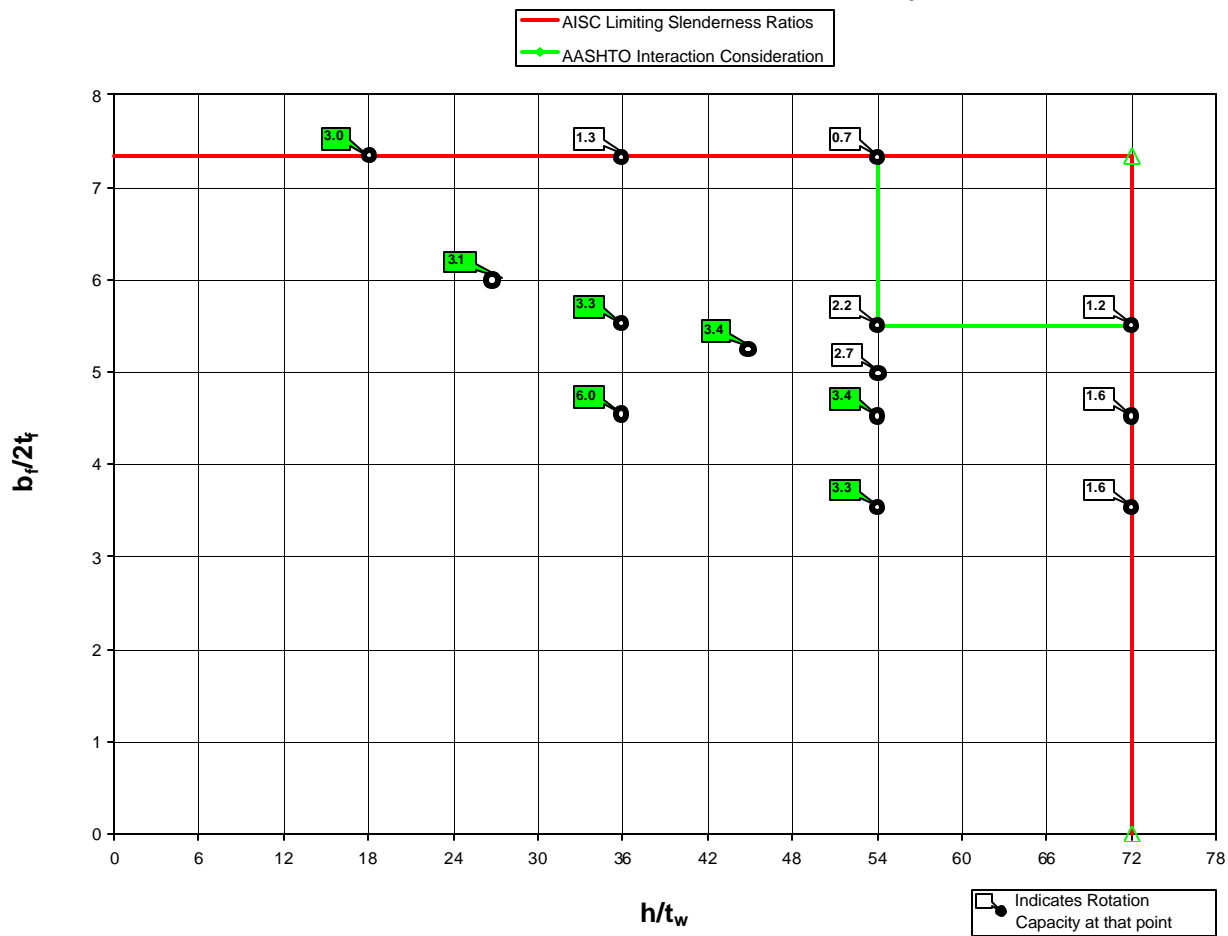
Figure C-10 Interaction Plot: Web Slenderness vs. Flange Slenderness
($b_f/2t_f$ Varies, h/t_w Varies, $L_b = 1d$, 8 AISC β_{br})

201

Web Slenderness vs. Flange Slenderness

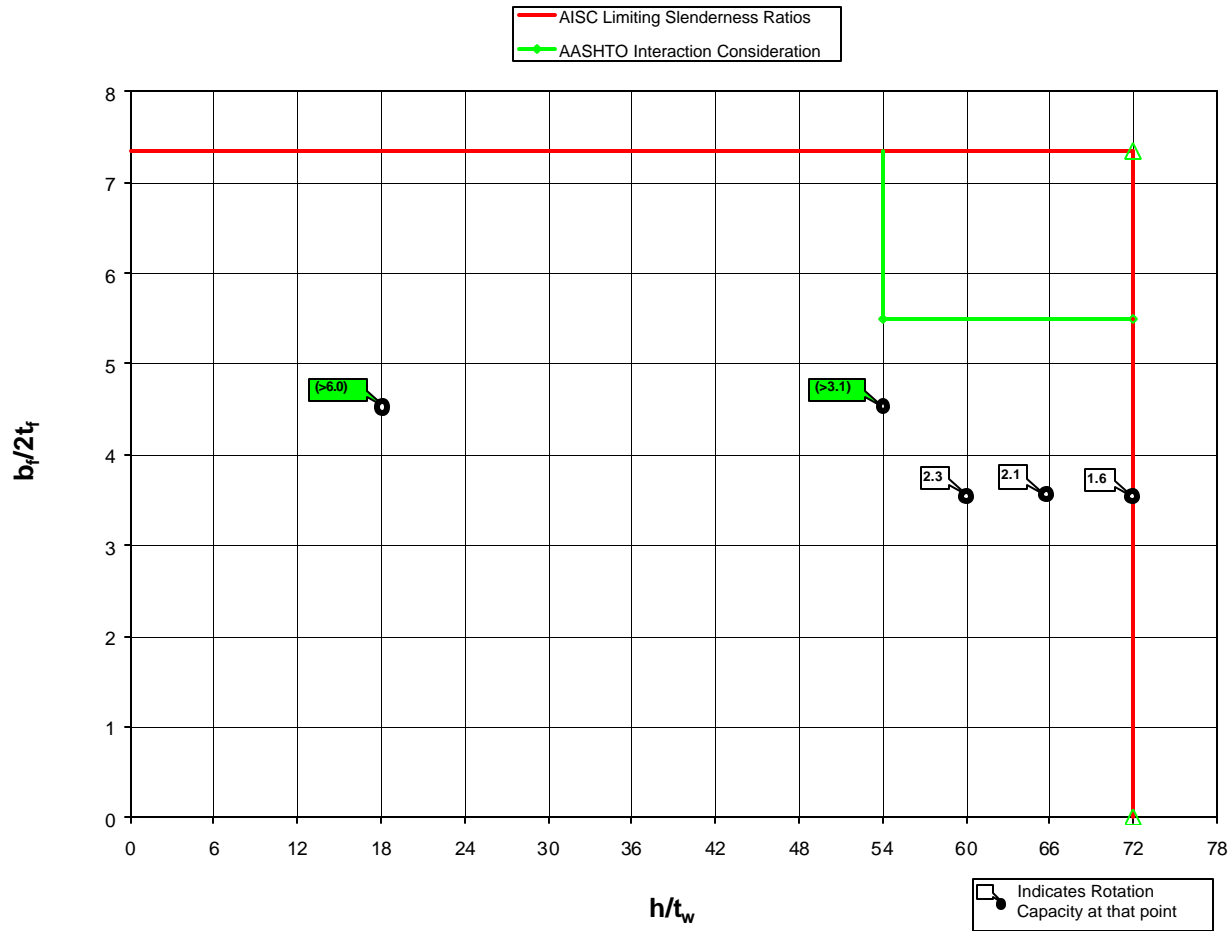$b_f/2t_f$ varies, h/t_w varies, $L_b = 1d$, 8.5 AISC Recommended Bracing Stiffness
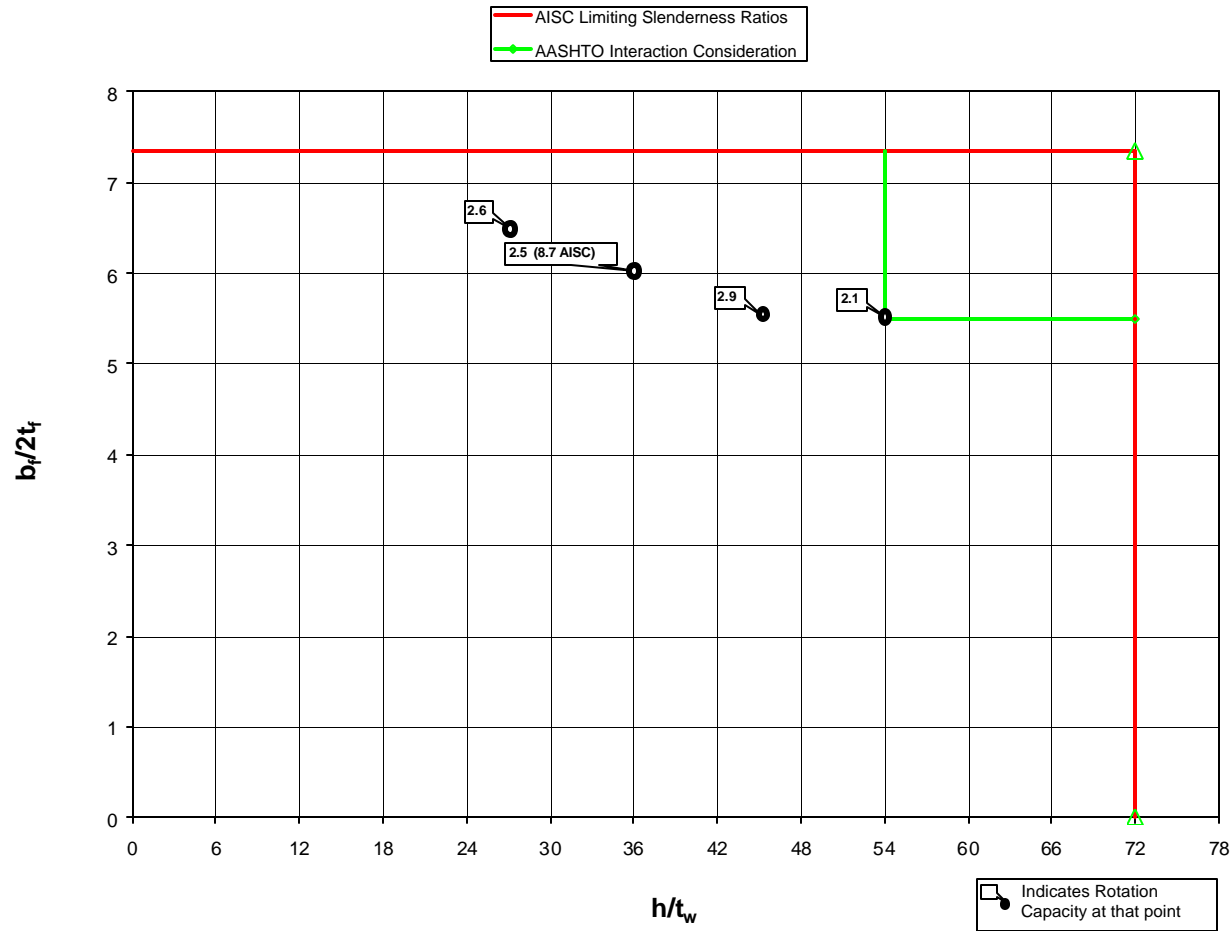
Figure C-11 Interaction Plot: Web Slenderness vs. Flange Slenderness
($b_f/2t_f$ Varies, h/t_w Varies, $L_b = 1d$, 8.5 AISC β_{br})

Figure C-12 Interaction Plot: Web Slenderness vs. Flange Slenderness
($b_f/2t_f$ Varies, h/t_w Varies, $L_b = 1d$, 9.5 AISC β_{br})

203

Figure C-13 Interaction Plot: Web Slenderness vs. Flange Slenderness
($b_f/2t_f$ Varies, h/t_w Varies, $L_b = 1.5d$, 6.5 AISC β_{br})

Figure C-14 Interaction Plot: Web Slenderness vs. Flange Slenderness
($b_f/2t_f$ Varies, h/t_w Varies, $L_b = 1.5d$, 7.3 AISC β_{br})
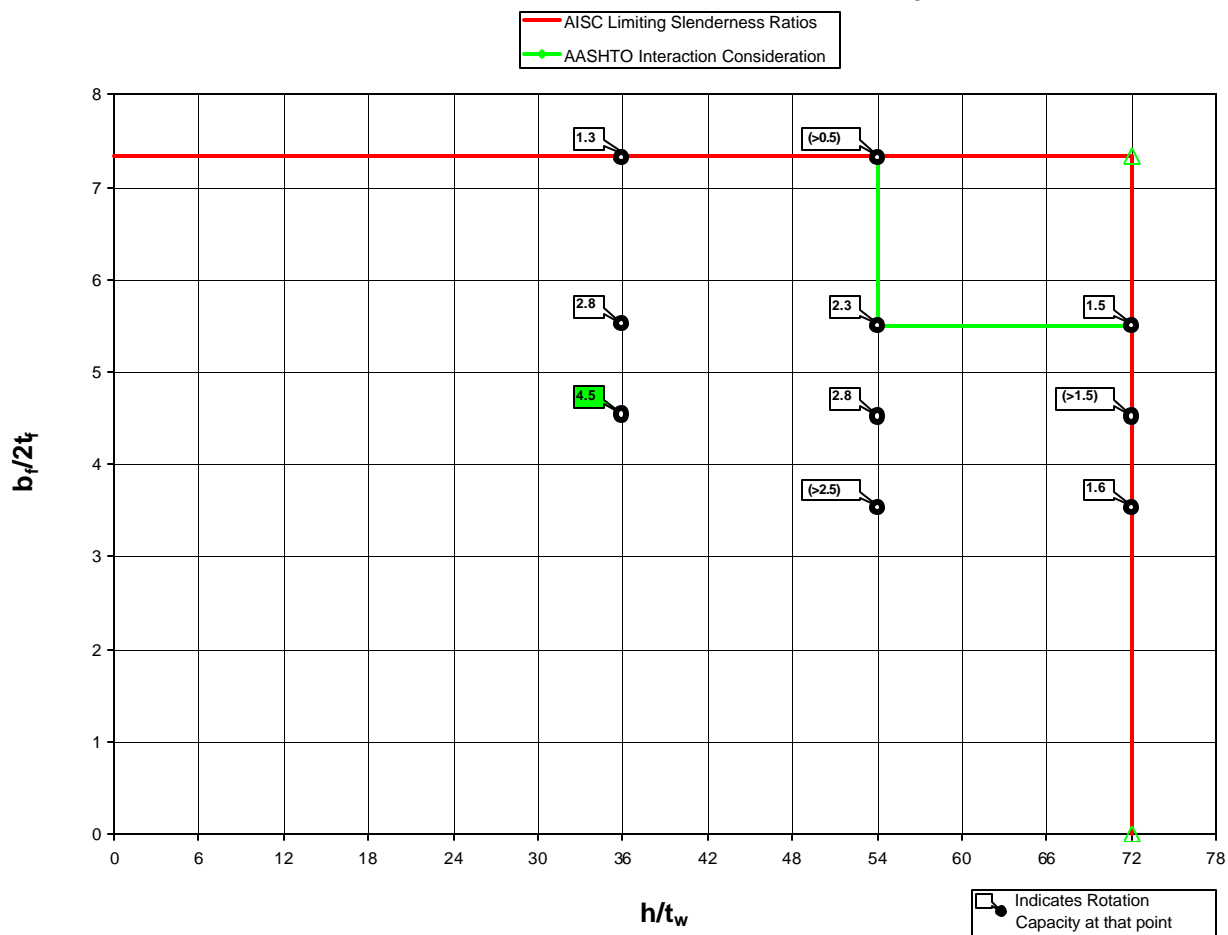
Figure C-15 Interaction Plot: Web Slenderness vs. Flange Slenderness
($b_f/2t_f$ Varies, h/t_w Varies, $L_b = 1.5d$, 8 AISC β_{br})
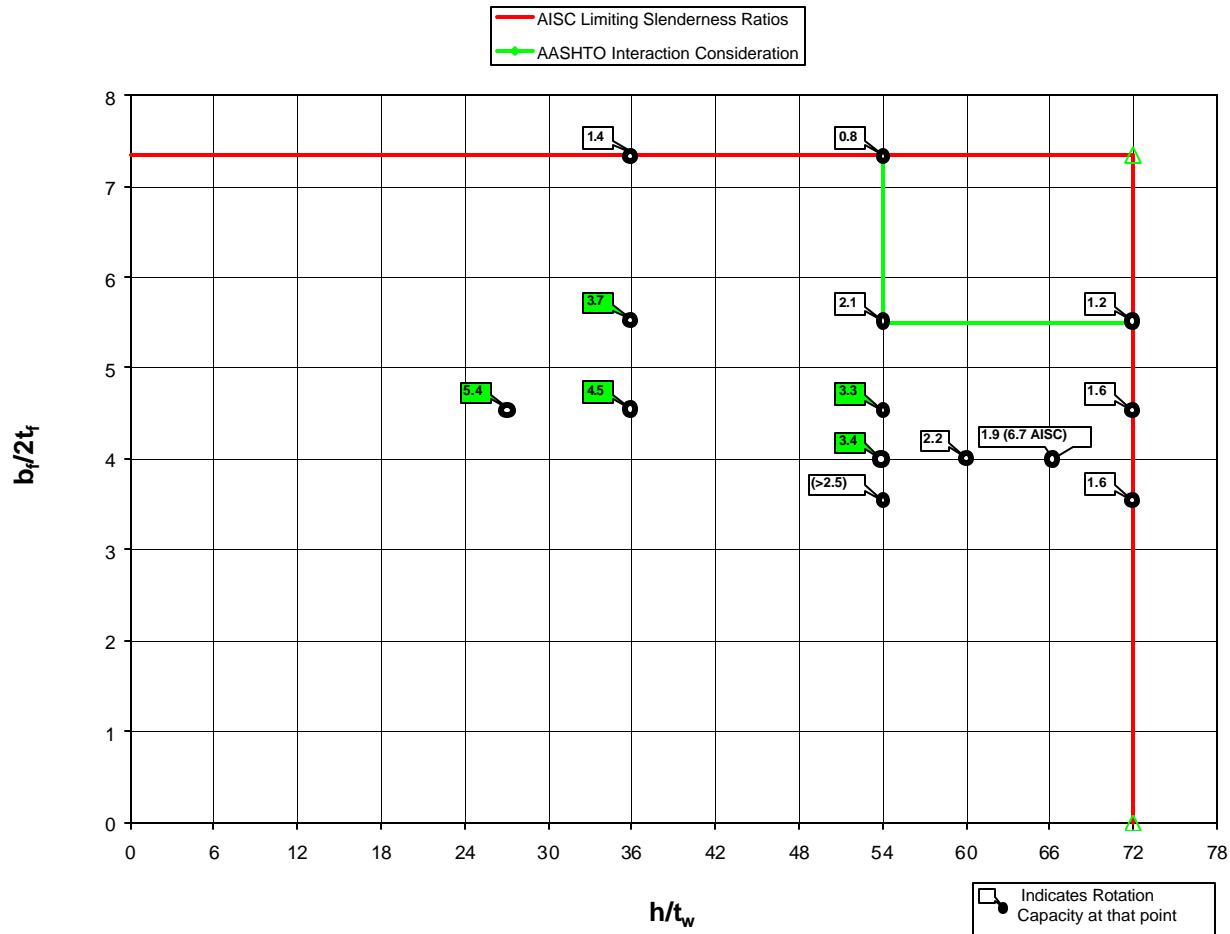
Figure C-16 Interaction Plot: Web Slenderness vs. Flange Slenderness
($b_f/2t_f$ Varies, h/t_w Varies, $L_b = 2$ d, 6.5 AISC β_{br})

Web Slenderness vs. Flange Slenderness

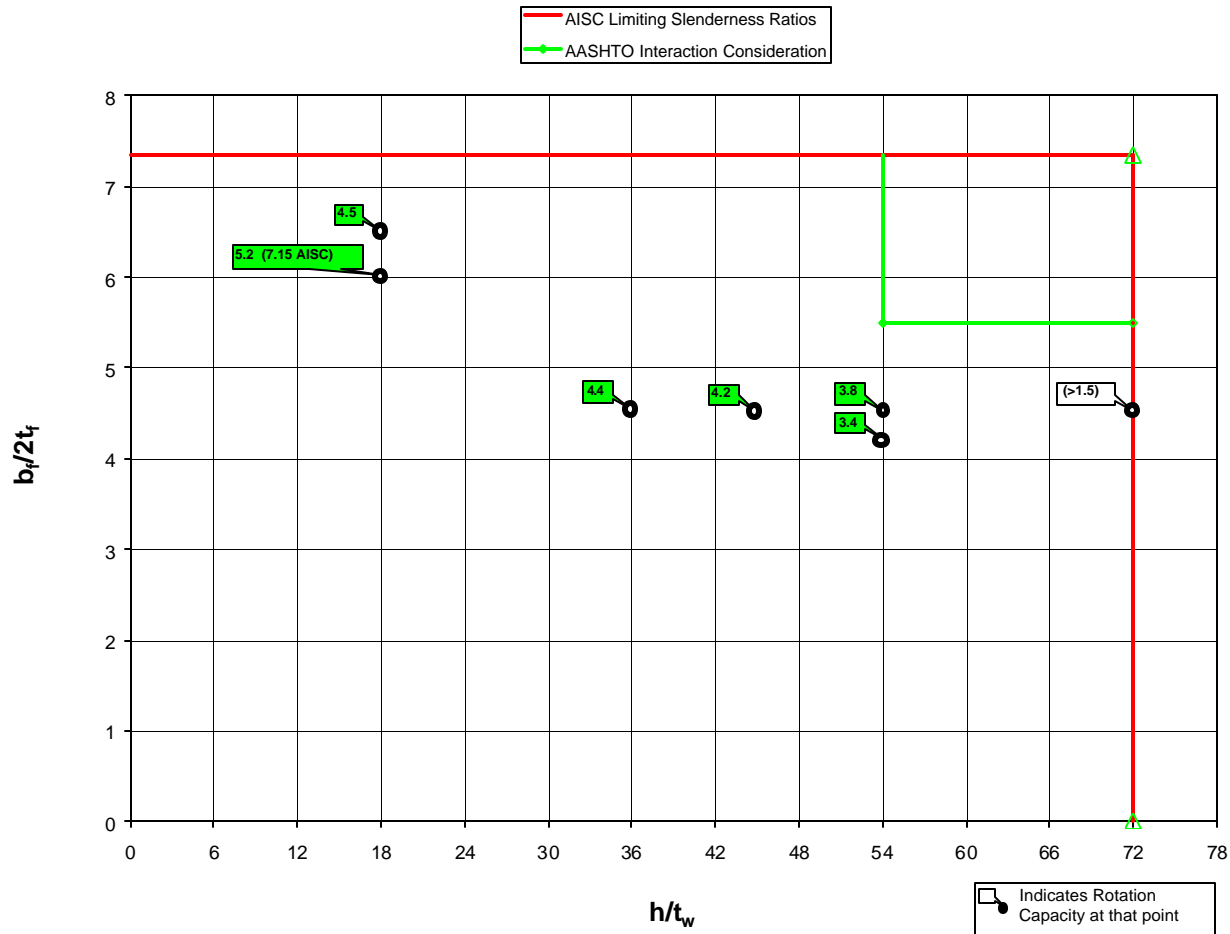$b_f/2t_f$ varies, h/t_w varies, L_b = 2d, 8 AISC Recommended Bracing Stiffness
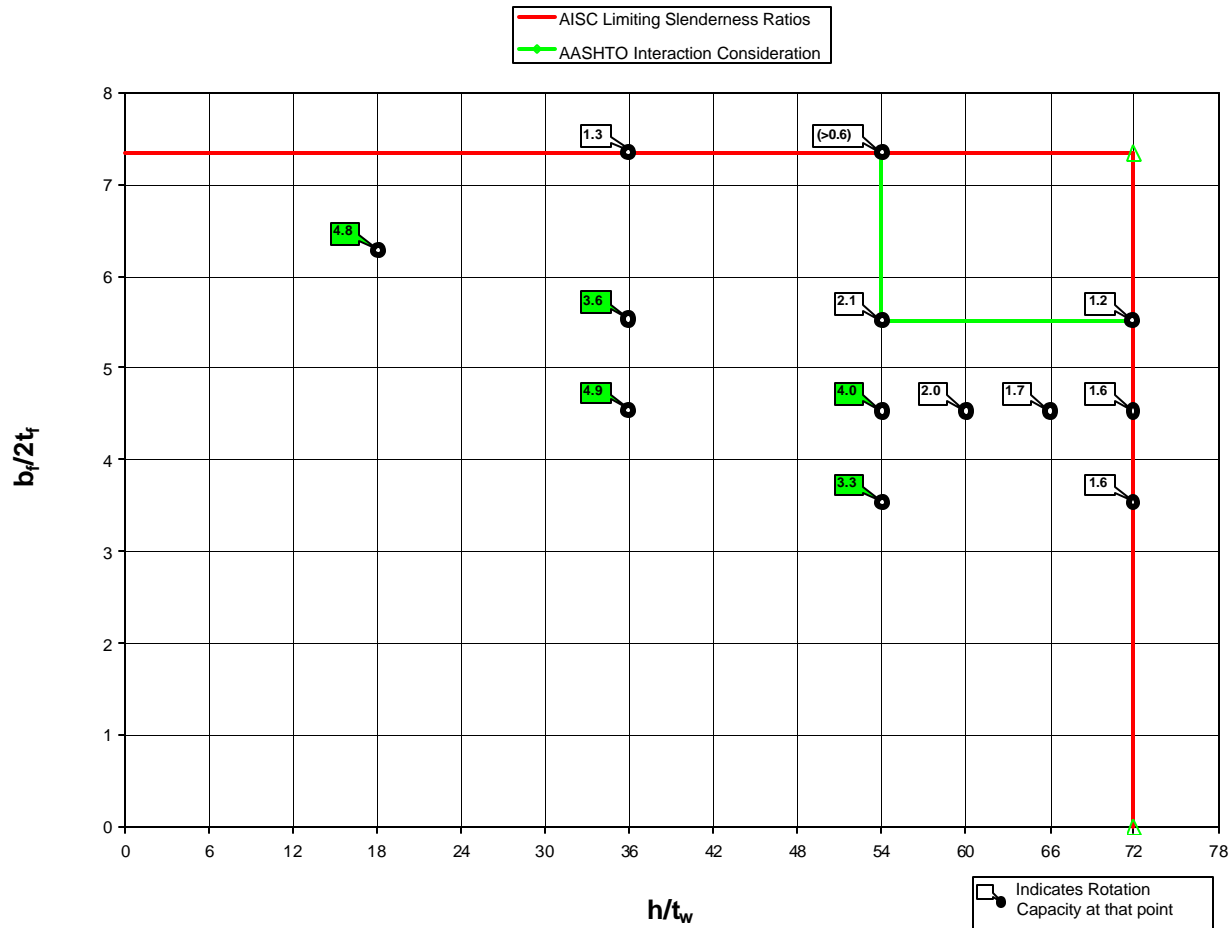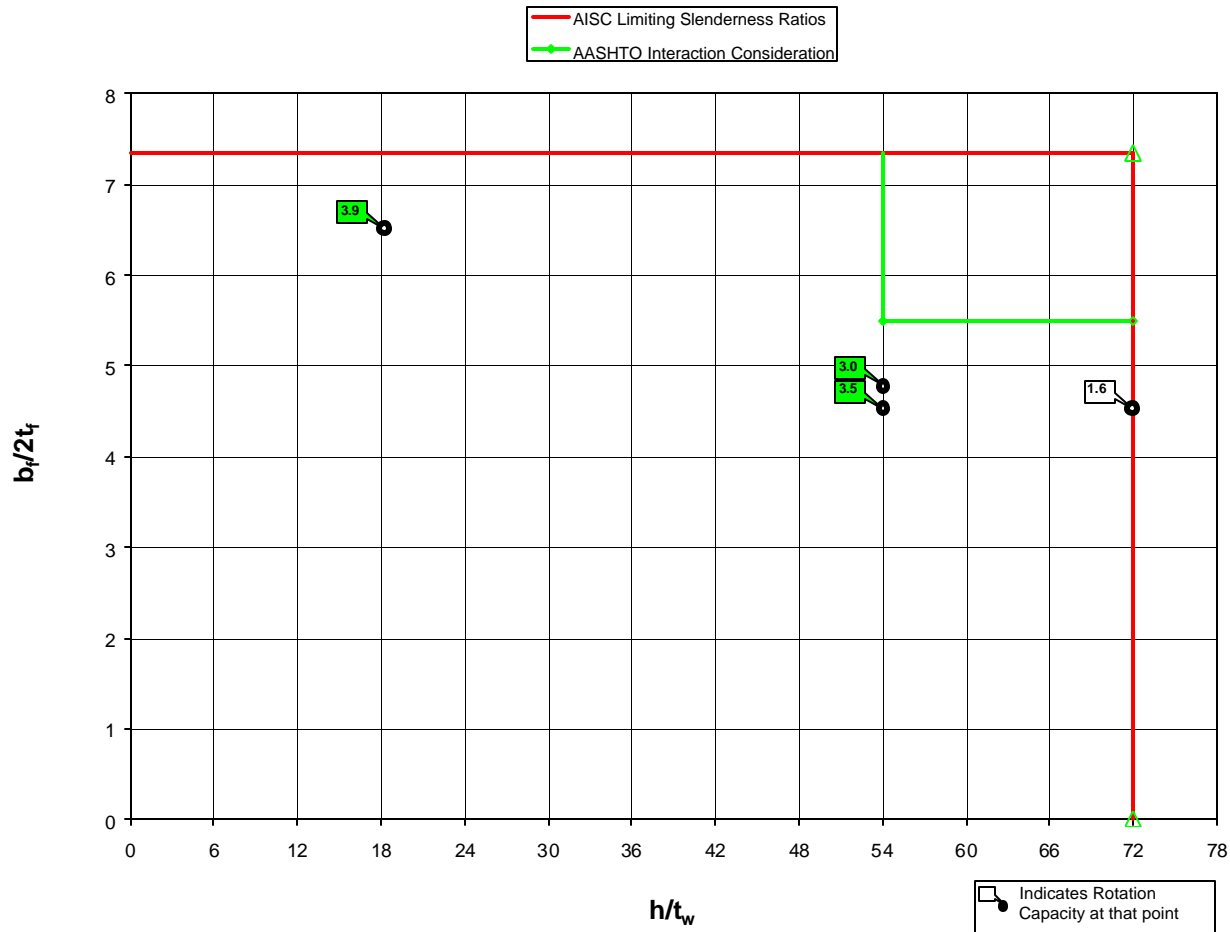
- AISC Limiting Slenderness Ratios
- AASHTO Interaction Consideration
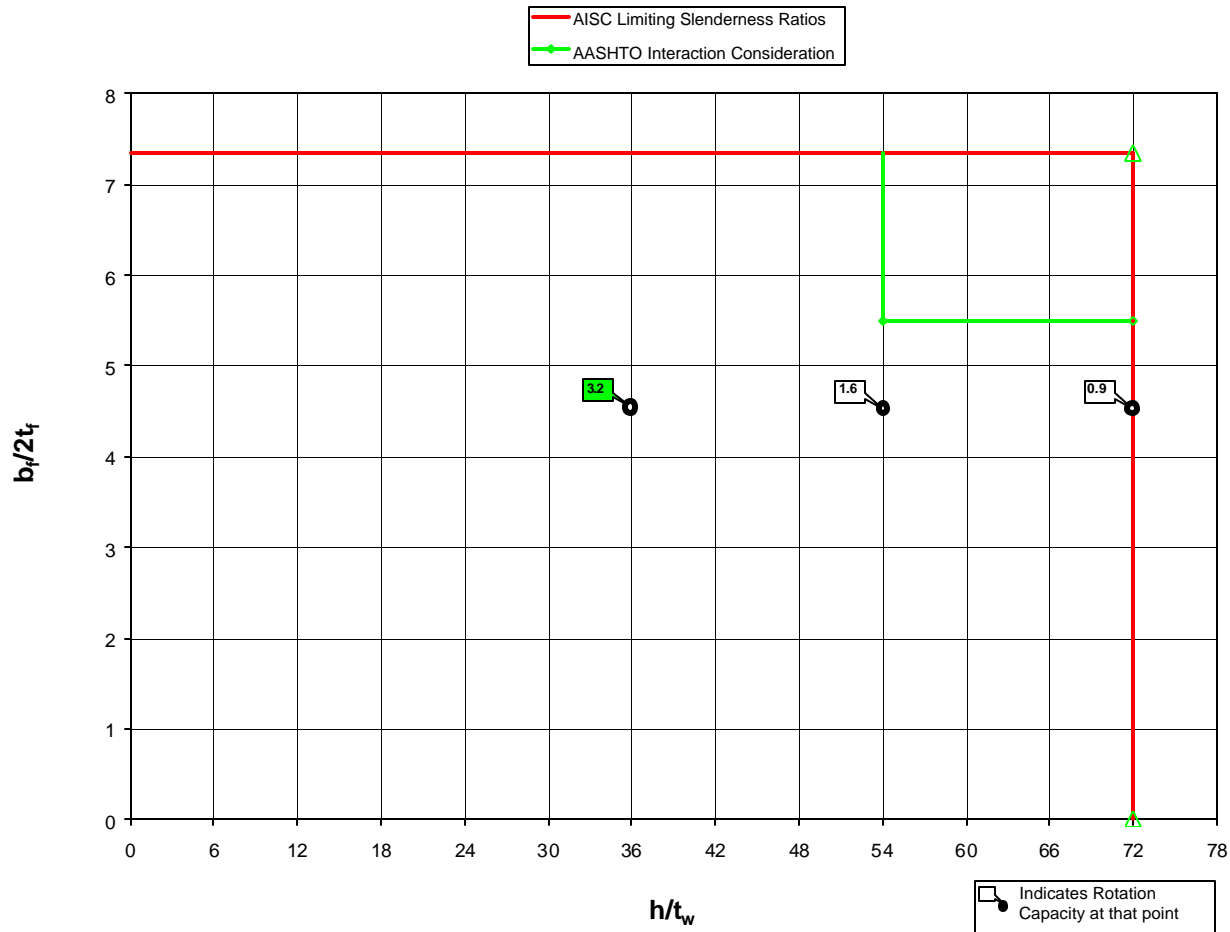
Figure C-17 Interaction Plot: Web Slenderness vs. Flange Slenderness
($b_f/2t_f$ Varies, h/t_w Varies, L_b = 2d, 8 AISC β_{br})

208

Appendix C.2

The second type of interaction plot located in this sub-appendix graphs web slenderness against unbraced length. For each combination of flange slenderness and bracing stiffness, one of these plots has been produced. For each of these plots there exist numerous combinations of web slenderness and unbraced length for which finite element tests are run. The corresponding rotation capacity for each of these individual tests is shown at its respective point on the graph.

Figure C-18 Interaction Plot: Web Slenderness vs. Unbraced Length
$(b_f/2t_f = 3.5, h/t_w$ Varies, L_b Varies, 6 AISC $\beta_{br})$

210

Web Slenderness vs. Unbraced Length

$b_f/2t_f$ = 3.5, h/t_w varies, L_b varies, 6.5 AISC Recommended Bracing Stiffness

Figure C-19 Interaction Plot: Web Slenderness vs. Unbraced Length
($b_f/2t_f$ = 3.5, h/t_w Varies, L_b Varies, 6.5 AISC β_{br})

211

Figure C-20 Interaction Plot: Web Slenderness vs. Unbraced Length
($b_f/2t_f = 3.5$, h/t_w Varies, L_b Varies, 7.3 AISC β_{br})

Web Slenderness vs. Unbraced Length

$b_f/2t_f$ = 3.5, h/t_w varies, L_b varies, 8 AISC Recommended Bracing Stiffness

Legend:
- Lpd
- Web Slenderness Limiting Ratio

Unbraced Length (multiples of d)

h/t_w

Indicates Rotation Capacity at that point

Figure C-21 Interaction Plot: Web Slenderness vs. Unbraced Length
($b_f/2t_f$ = 3.5, h/t_w Varies, L_b Varies, 8 AISC β_{br})

213

Web Slenderness vs. Unbraced Length
$b_f/2t_f = 4.0$, h/t_w varies, L_b varies, 6.6 AISC Recommended Bracing Stiffness

Figure C-22 Interaction Plot: Web Slenderness vs. Unbraced Length
($b_f/2t_f = 4.0$, h/t_w Varies, L_b Varies, 6.6 AISC β_{br})

214
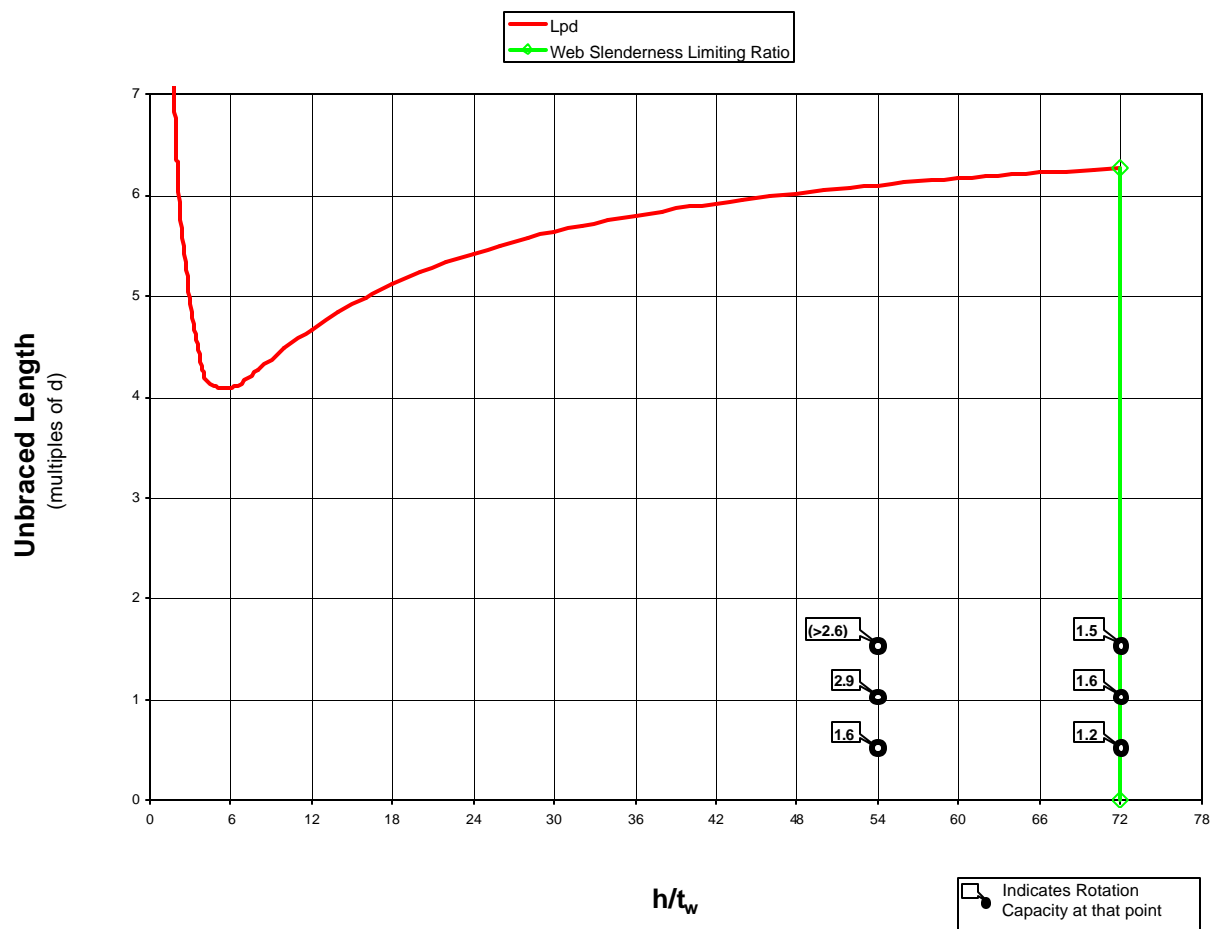
Figure C-23 Interaction Plot: Web Slenderness vs. Unbraced Length
$(b_f/2t_f = 4.5, h/t_w \text{ Varies}, L_b \text{ Varies}, 5 \text{ AISC } \beta_{br})$

Web Slenderness vs. Unbraced Length

$b_f/2t_f = 4.5$, h/t_w varies, L_b varies, 5.9 AISC Recommended Bracing Stiffness
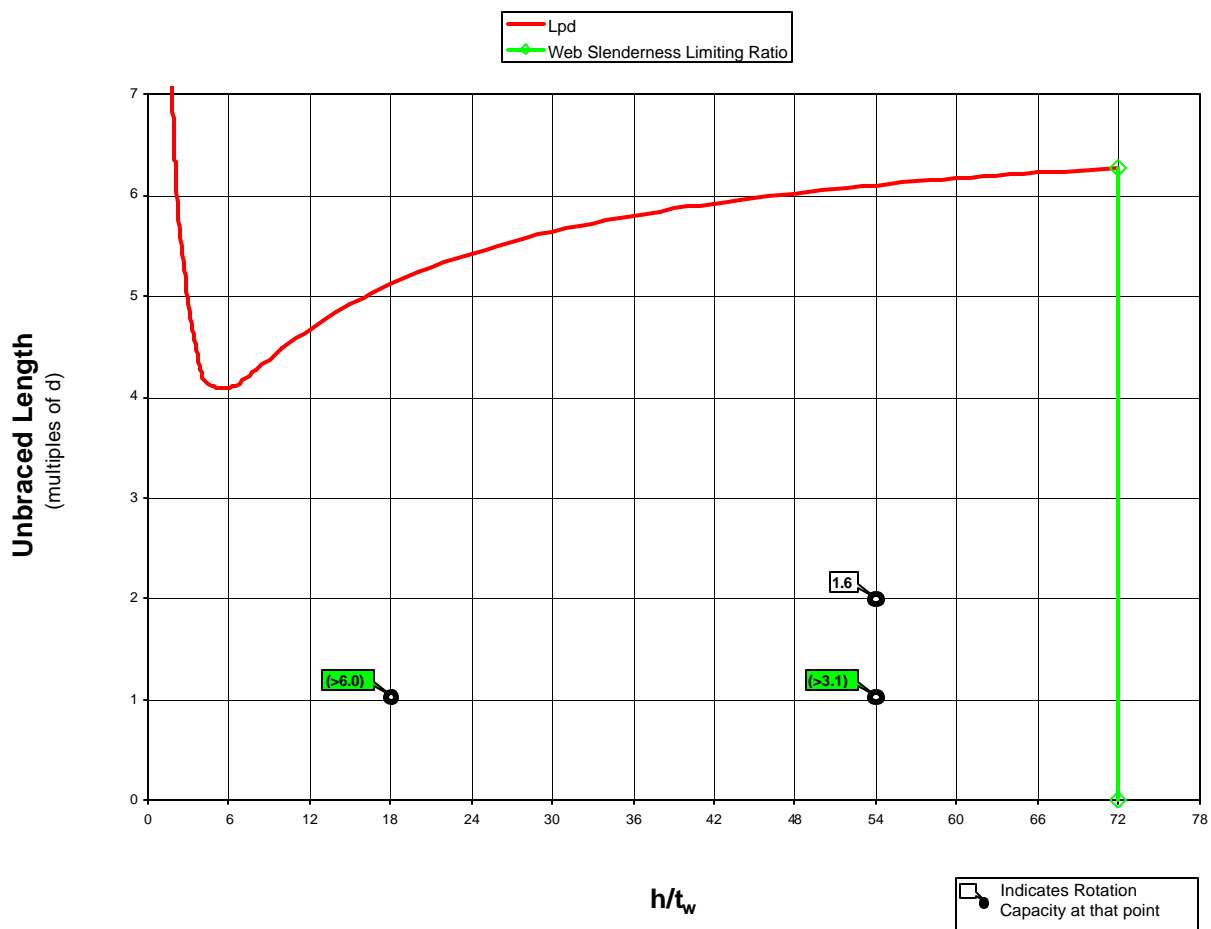
Figure C-24 Interaction Plot: Web Slenderness vs. Unbraced Length
($b_f/2t_f = 4.5$, h/t_w Varies, L_b Varies, 5.9 AISC β_{br})

216
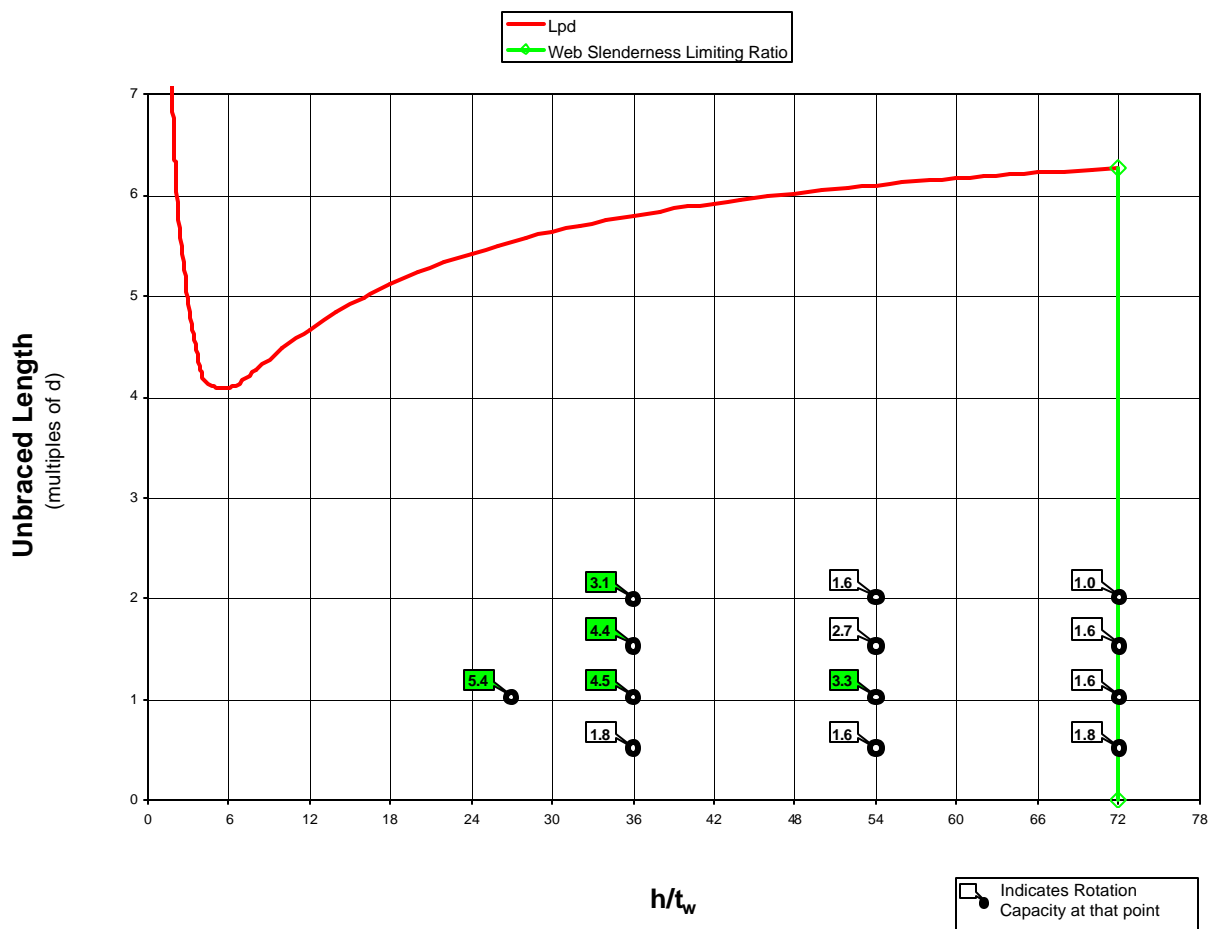
Figure C-25 Interaction Plot: Web Slenderness vs. Unbraced Length
($b_f/2t_f = 4.5$, h/t_w Varies, L_b Varies, 6.5 AISC β_{br})

217
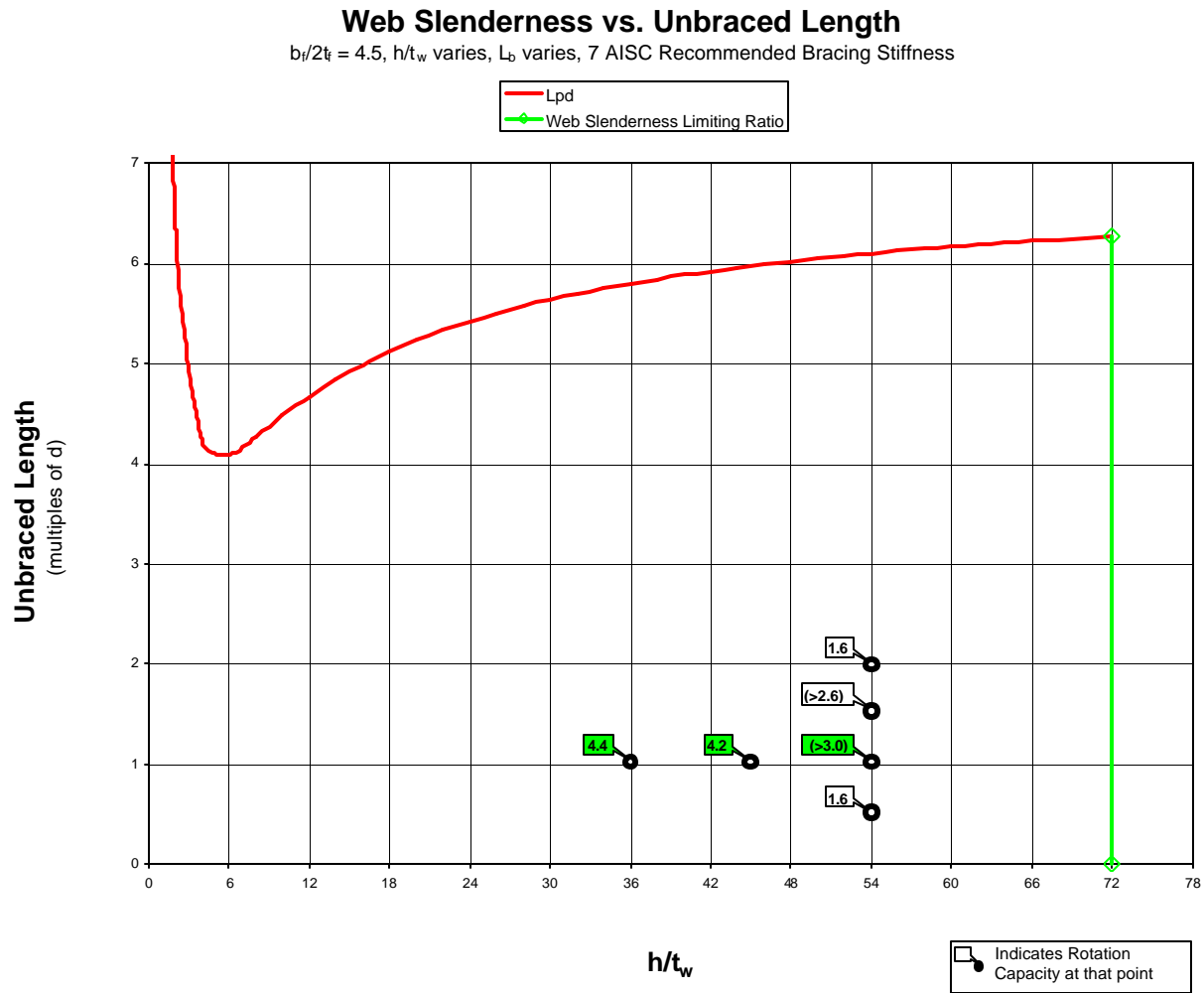
Figure C-26 Interaction Plot: Web Slenderness vs. Unbraced Length
$(b_f/2t_f = 4.5, h/t_w \text{ Varies}, L_b \text{ Varies, 7 AISC } \beta_{br})$

218
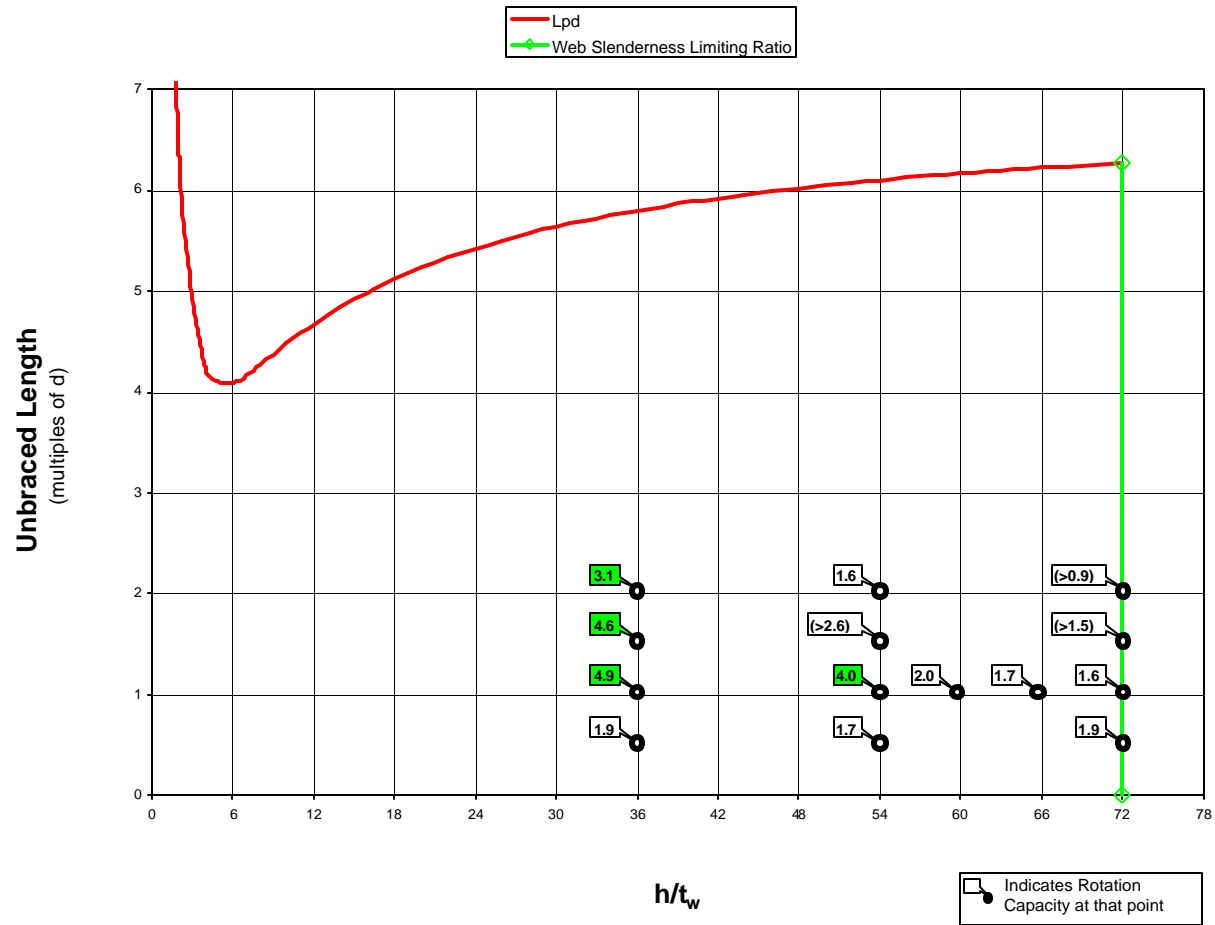
Figure C-27 Interaction Plot: Web Slenderness vs. Unbraced Length
$(b_f/2t_f = 4.5, h/t_w \text{ Varies}, L_b \text{ Varies, 7.3 AISC } \beta_{br})$
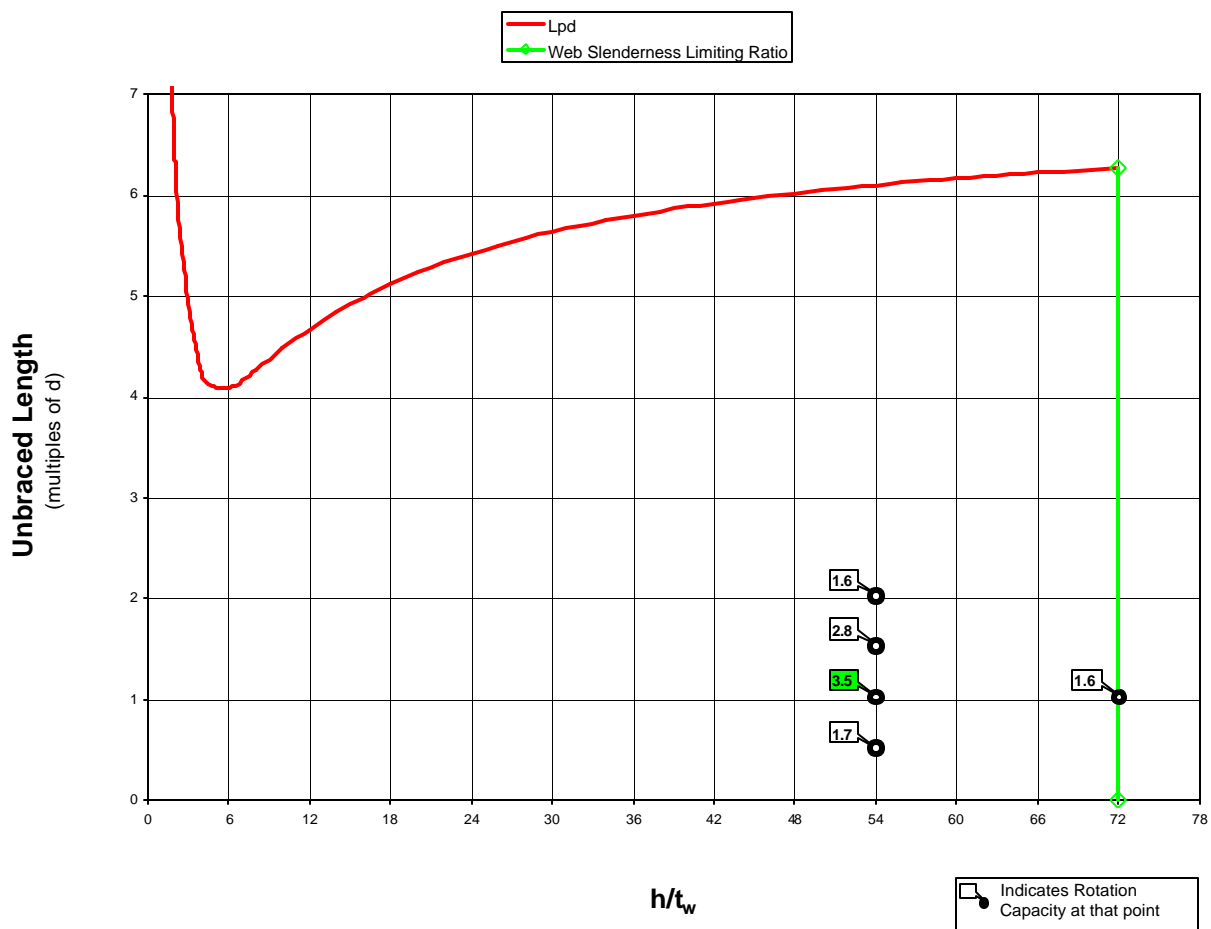
Figure C-28 Interaction Plot: Web Slenderness vs. Unbraced Length
($b_f/2t_f = 4.5$, h/t_w Varies, L_b Varies, 7.5 AISC β_{br})

Web Slenderness vs. Unbraced Length

$b_f/2t_f$ = 4.5, h/t_w varies, L_b varies, 8 AISC Recommended Bracing Stiffness
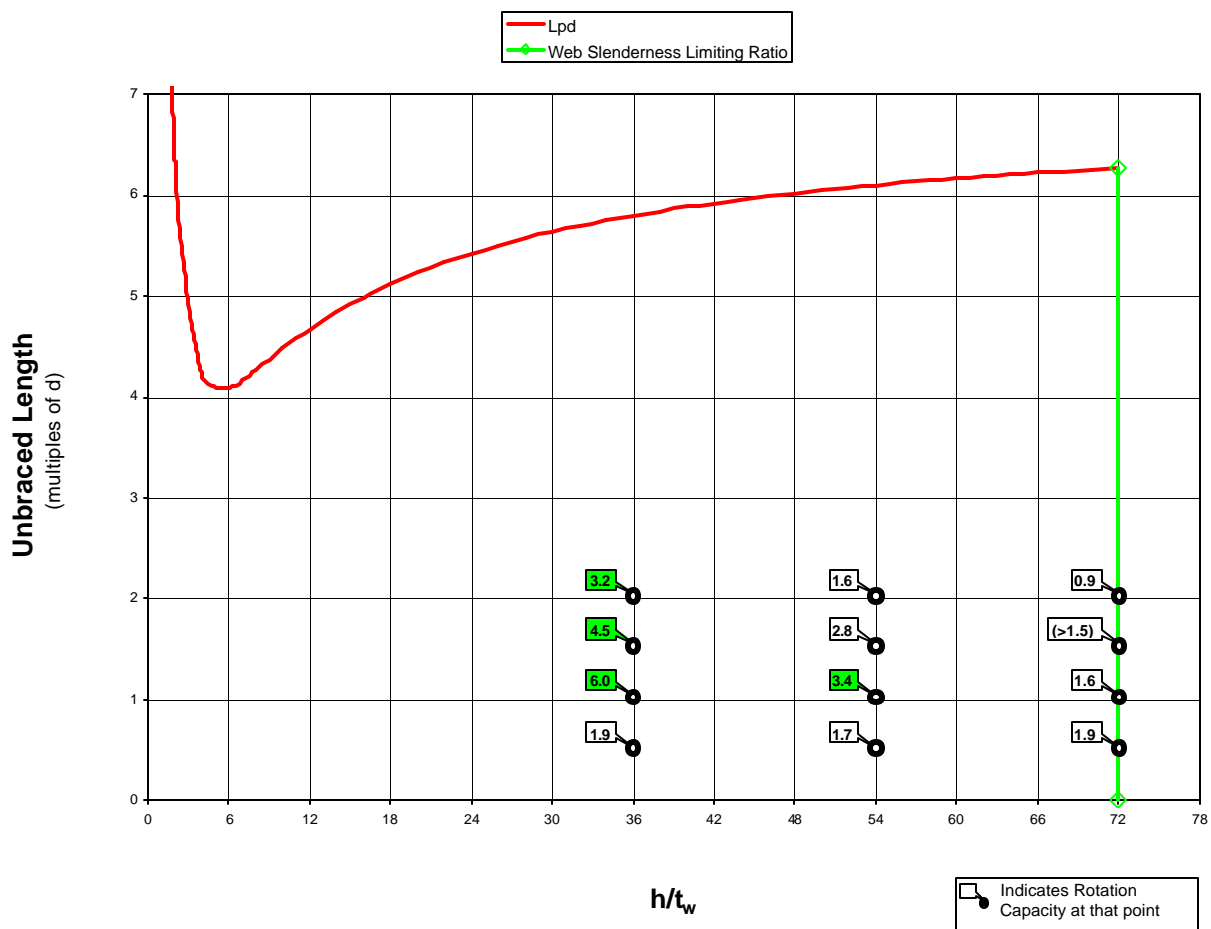
Figure C-29 Interaction Plot: Web Slenderness vs. Unbraced Length
($b_f/2t_f$ = 4.5, h/t_w Varies, L_b Varies, 8 AISC β_{br})

221

Web Slenderness vs. Unbraced Length

$b_f/2t_f$ = 4.5, h/t_w varies, L_b varies, 9.5 AISC Recommended Bracing Stiffness

Legend:
— Lpd
—◆— Web Slenderness Limiting Ratio

(y-axis) **Unbraced Length** (multiples of d)

(x-axis) **h/t_w**

Data labels on plot: 2.7, 2.8, (>1.5), 4.3, 3.1, 1.6, 1.8

Indicates Rotation Capacity at that point
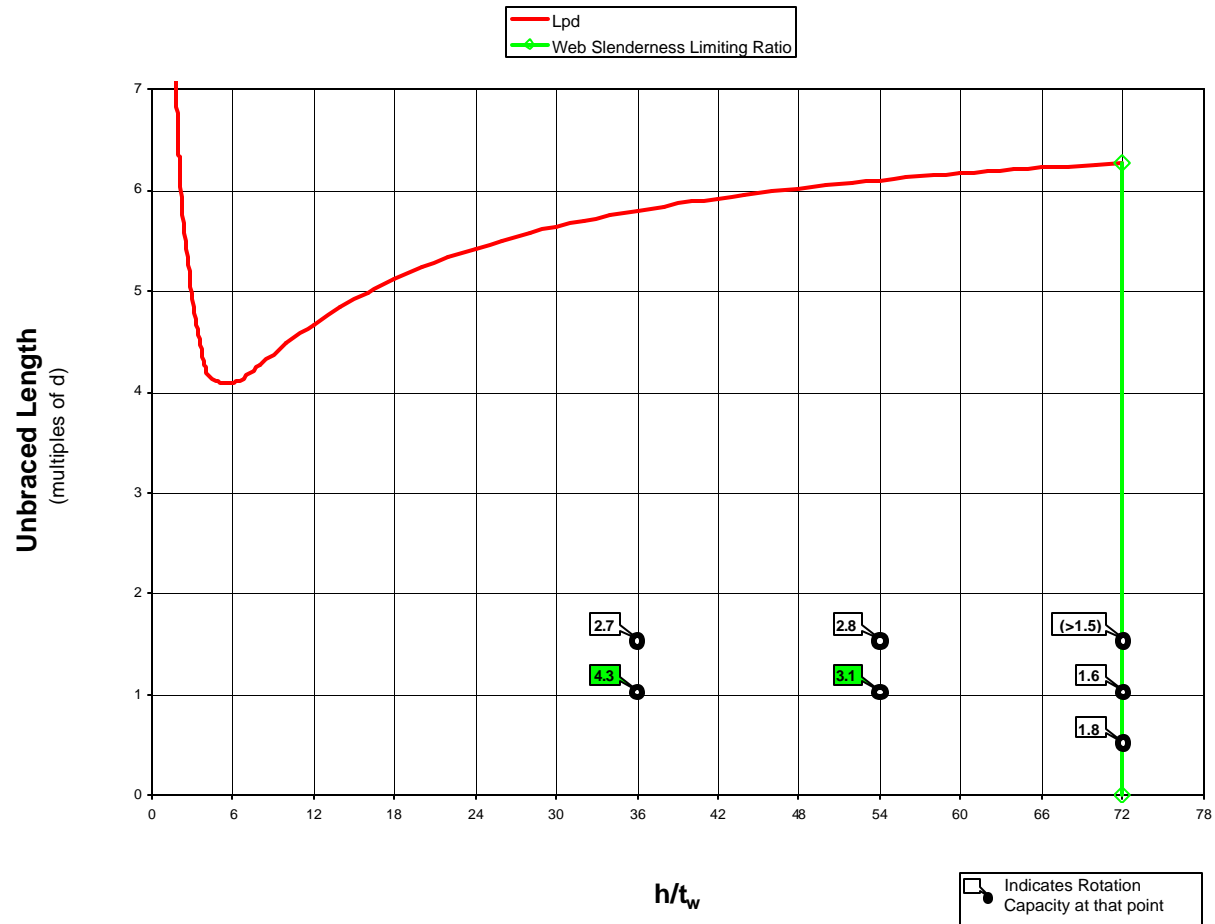
Figure C-30 Interaction Plot: Web Slenderness vs. Unbraced Length
($b_f/2t_f$ = 4.5, h/t_w Varies, L_b Varies, 9.5 AISC β_{br})

Web Slenderness vs. Unbraced Length
$b_f/2t_f = 5.5$, h/t_w varies, L_b varies, 6.5 AISC Recommended Bracing Stiffness
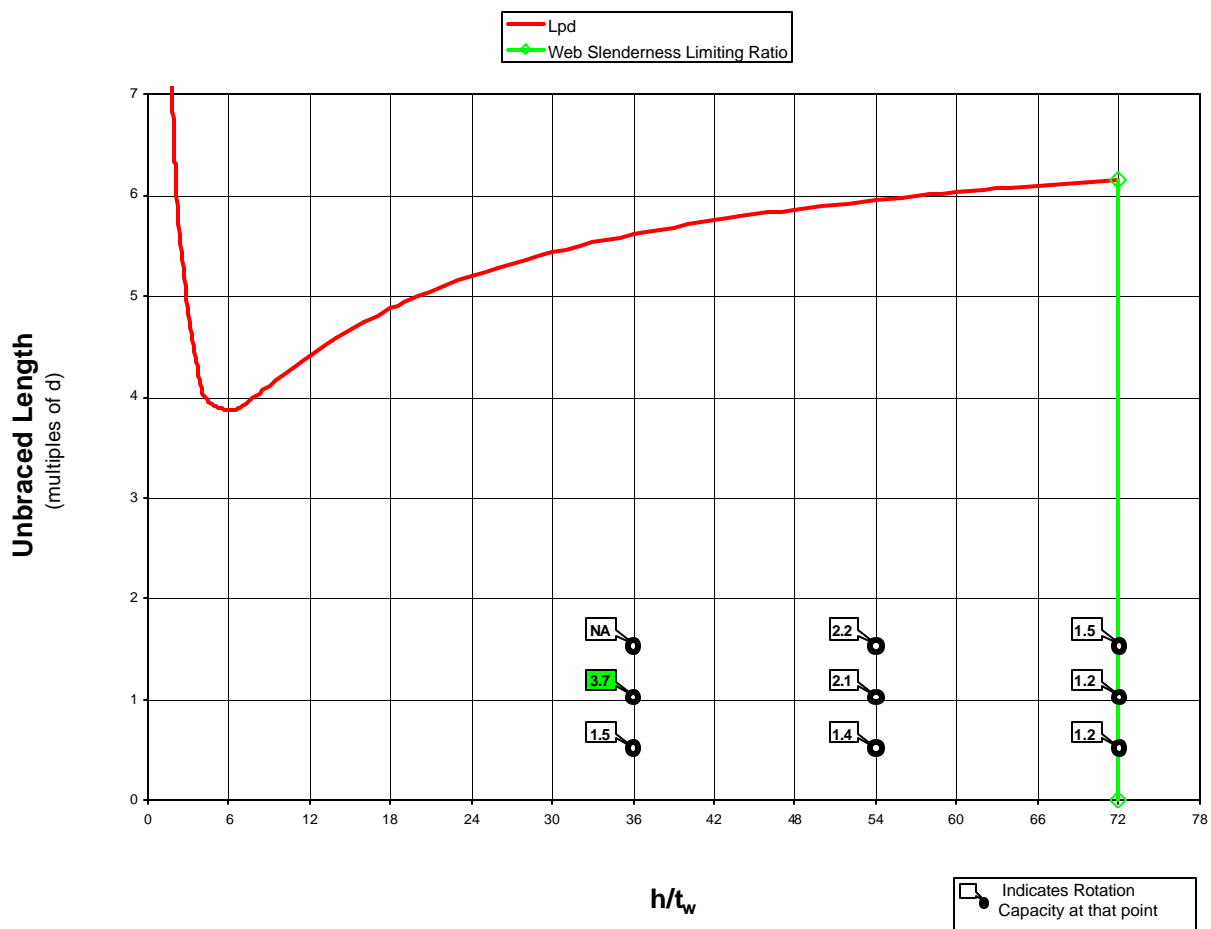
Figure C-31 Interaction Plot: Web Slenderness vs. Unbraced Length
($b_f/2t_f = 5.5$, h/t_w Varies, L_b Varies, 6.5 AISC β_{br})

223
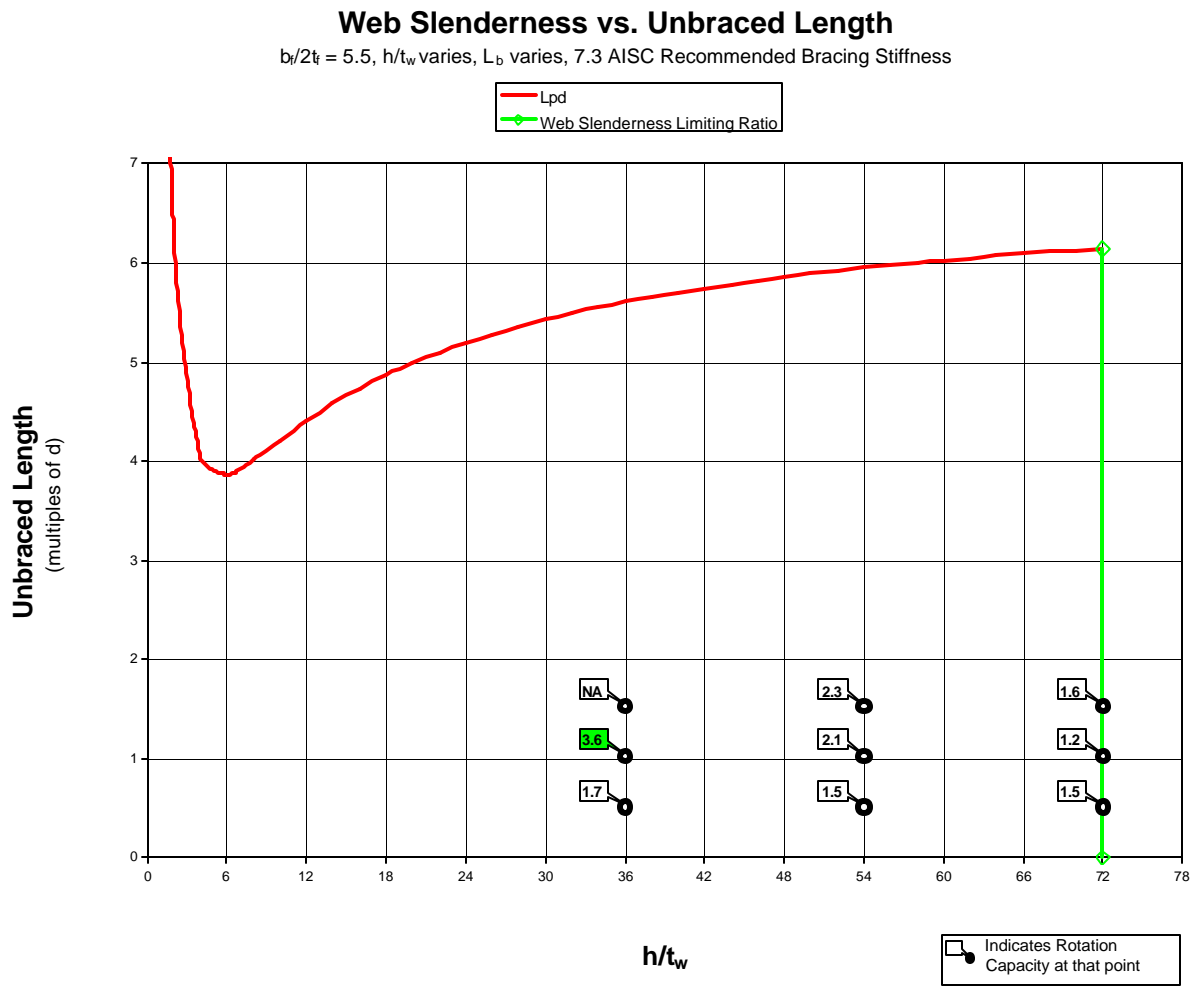
Figure C-32 Interaction Plot: Web Slenderness vs. Unbraced Length
($b_f/2t_f = 5.5$, h/t_w Varies, L_b Varies, 7.3 AISC β_{br})

Web Slenderness vs. Unbraced Length

$b_f/2t_f = 5.5$, h/t_w varies, L_b varies, 8 AISC Recommended Bracing Stiffness
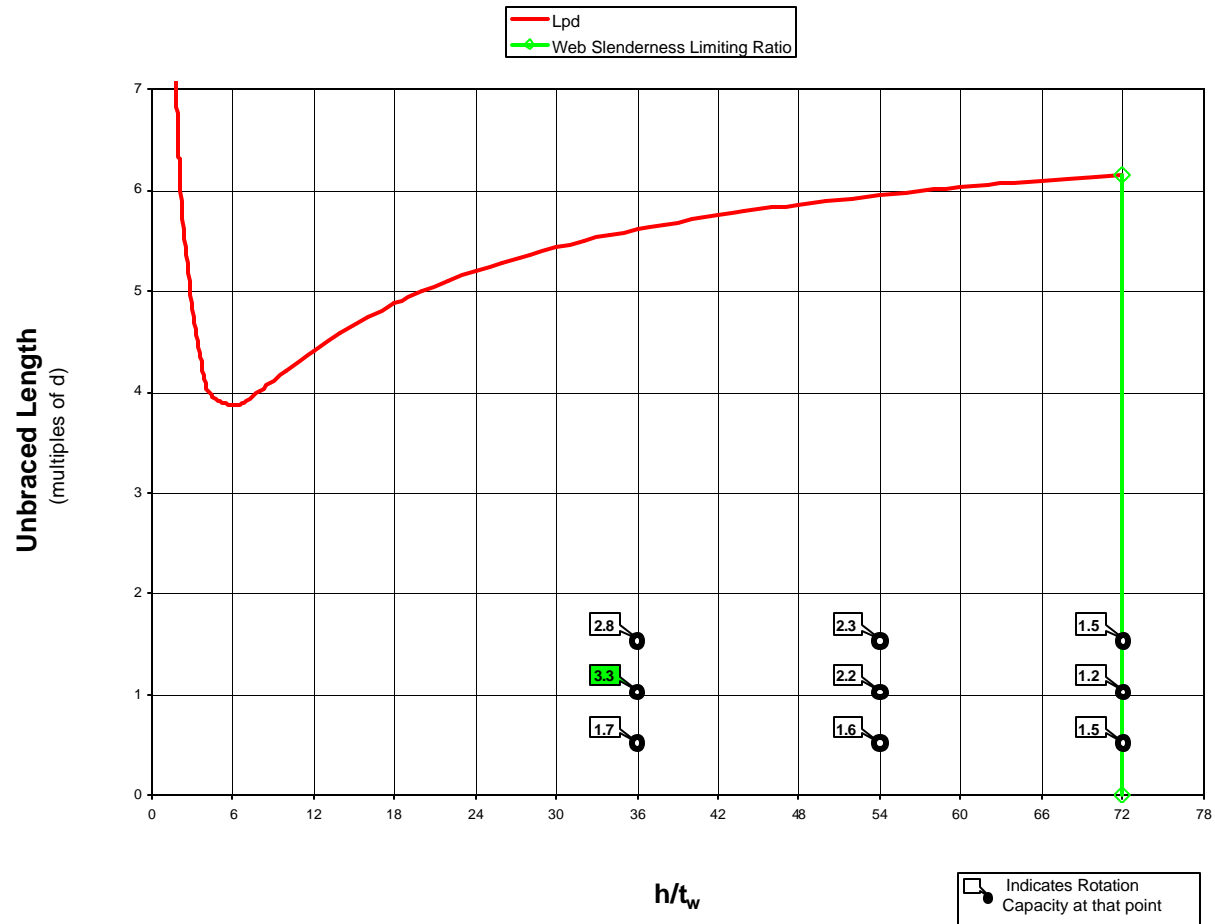
Figure C-33 Interaction Plot: Web Slenderness vs. Unbraced Length
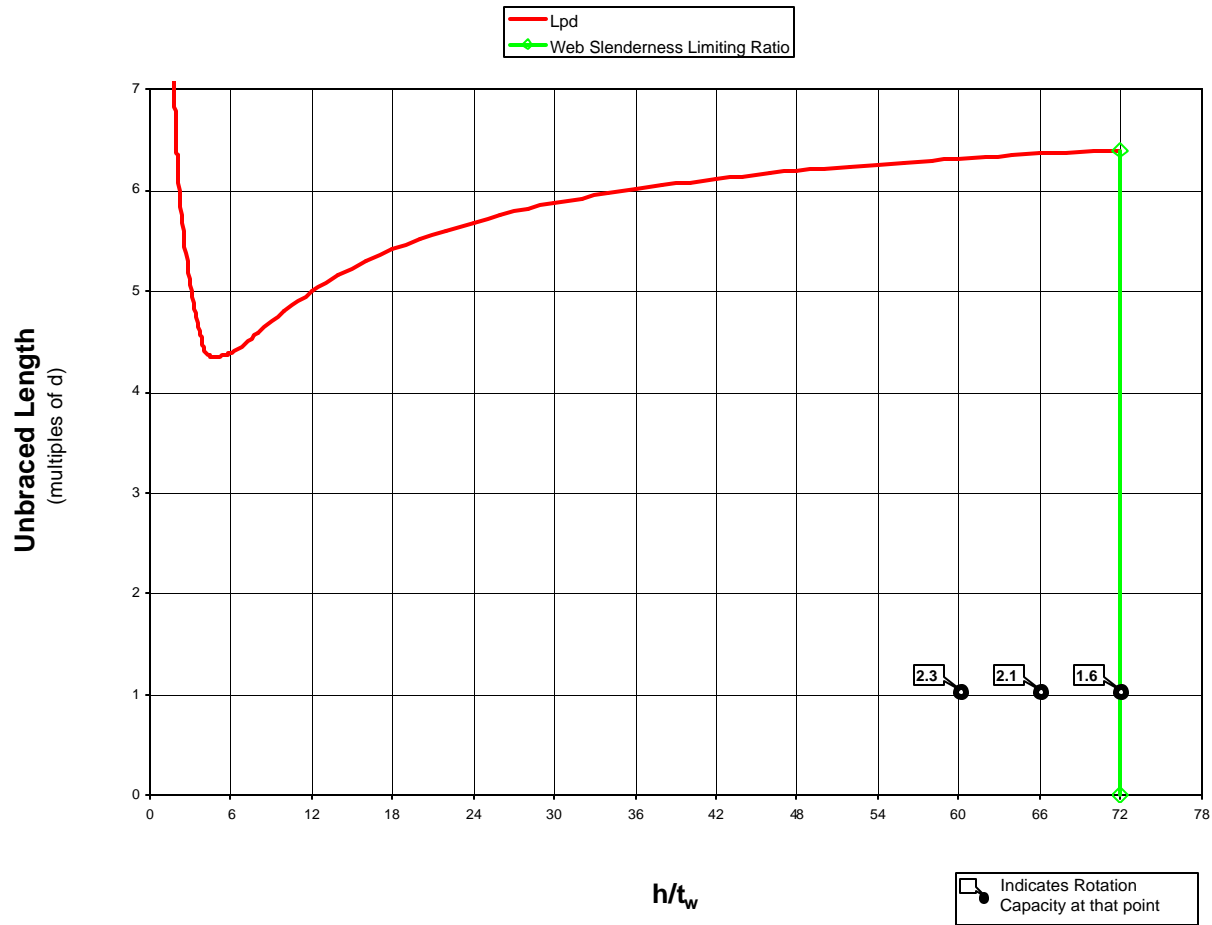($b_f/2t_f = 5.5$, h/t_w Varies, L_b Varies, 8 AISC β_{br})
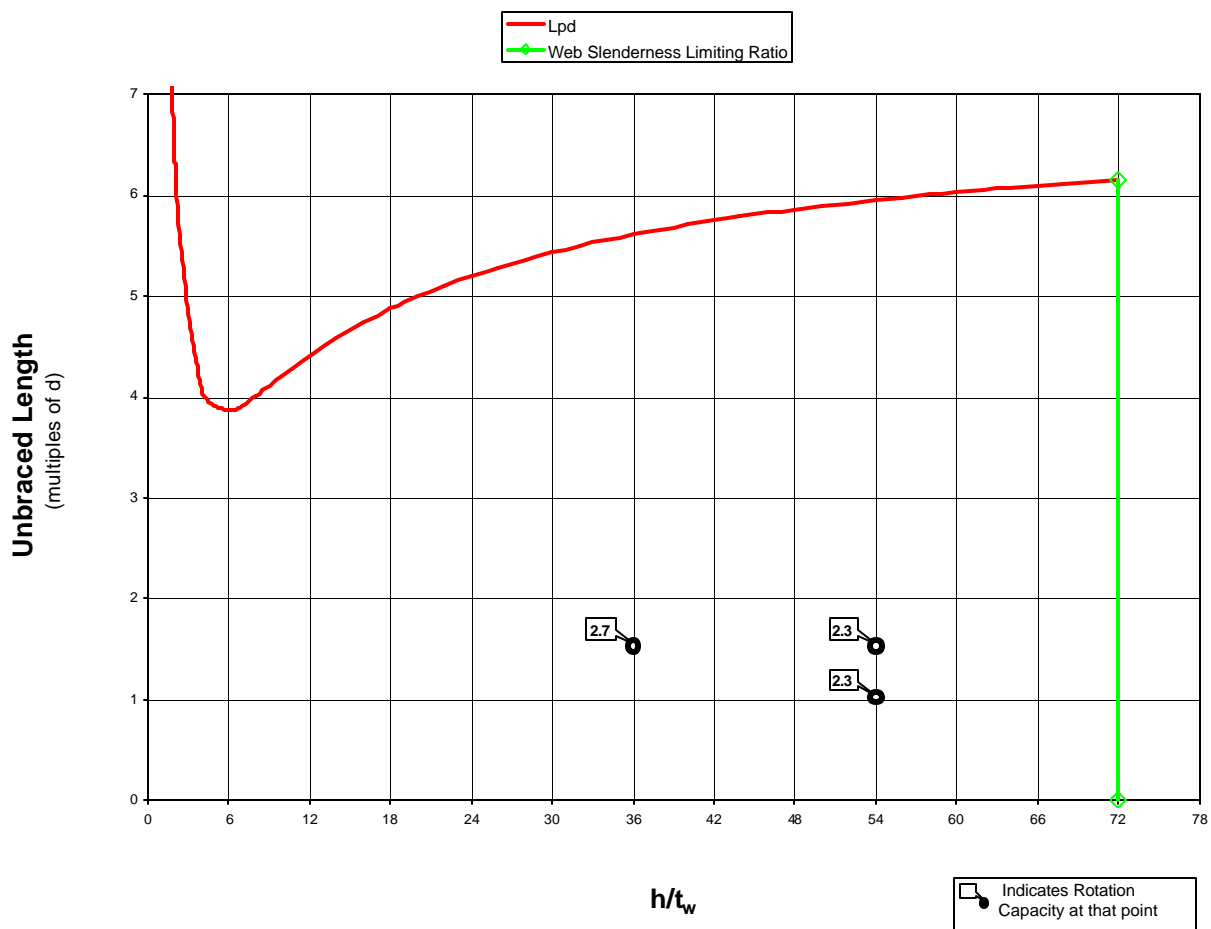
Figure C-34 Interaction Plot: Web Slenderness vs. Unbraced Length
($b_f/2t_f = 5.5$, h/t_w Varies, L_b Varies, 9.5 AISC β_{br})

Web Slenderness vs. Unbraced Length
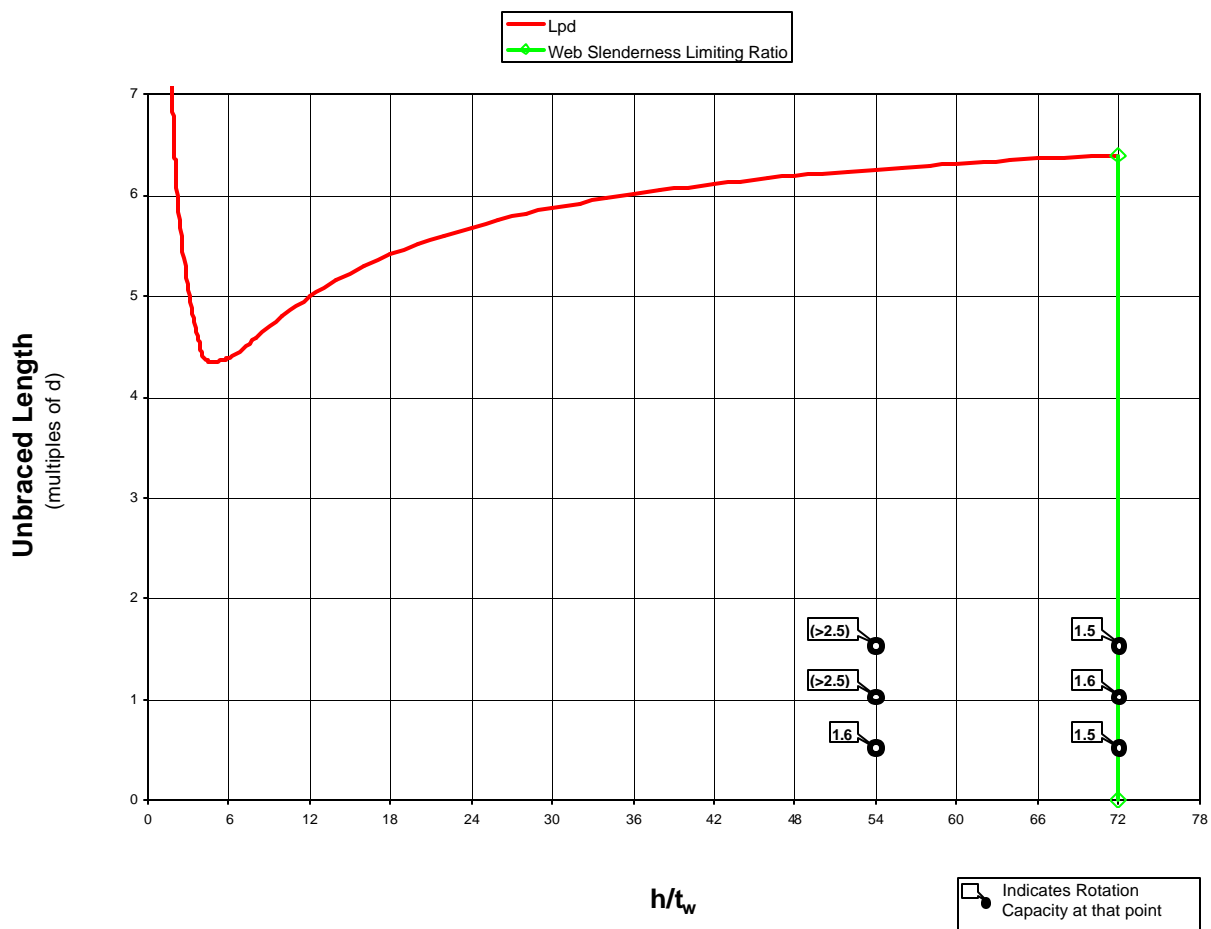$b_f/2t_f = 7.34$, h/t_w varies, L_b varies, 6.5 AISC Recommended Bracing Stiffness
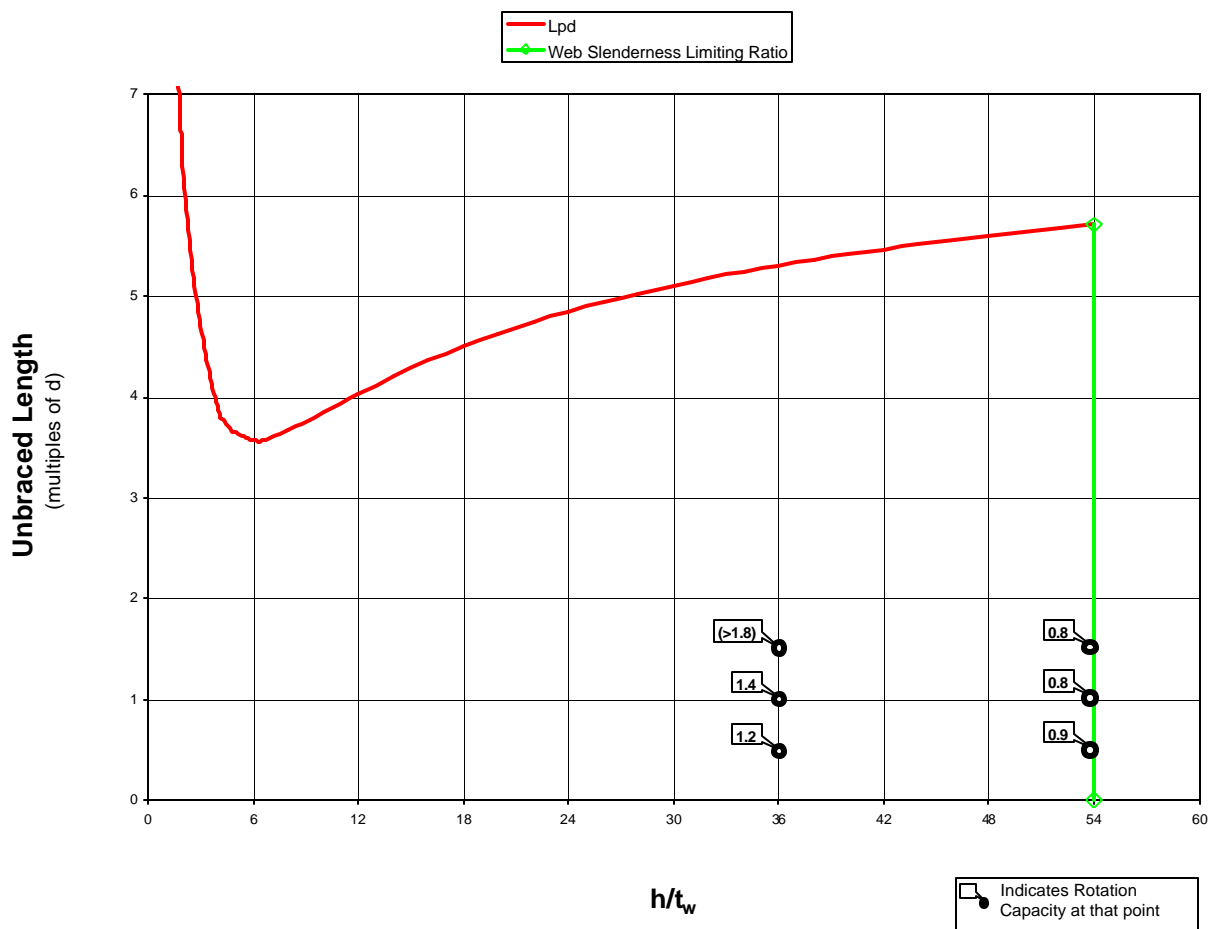
Figure C-35 Interaction Plot: Web Slenderness vs. Unbraced Length
($b_f/2t_f = 7.34$, h/t_w Varies, L_b Varies, 6.5 AISC β_{br})

227

Web Slenderness vs. Unbraced Length

$b_f/2t_f$ = 7.34, h/t_w varies, L_b varies, 7.3 AISC Recommended Bracing Stiffness
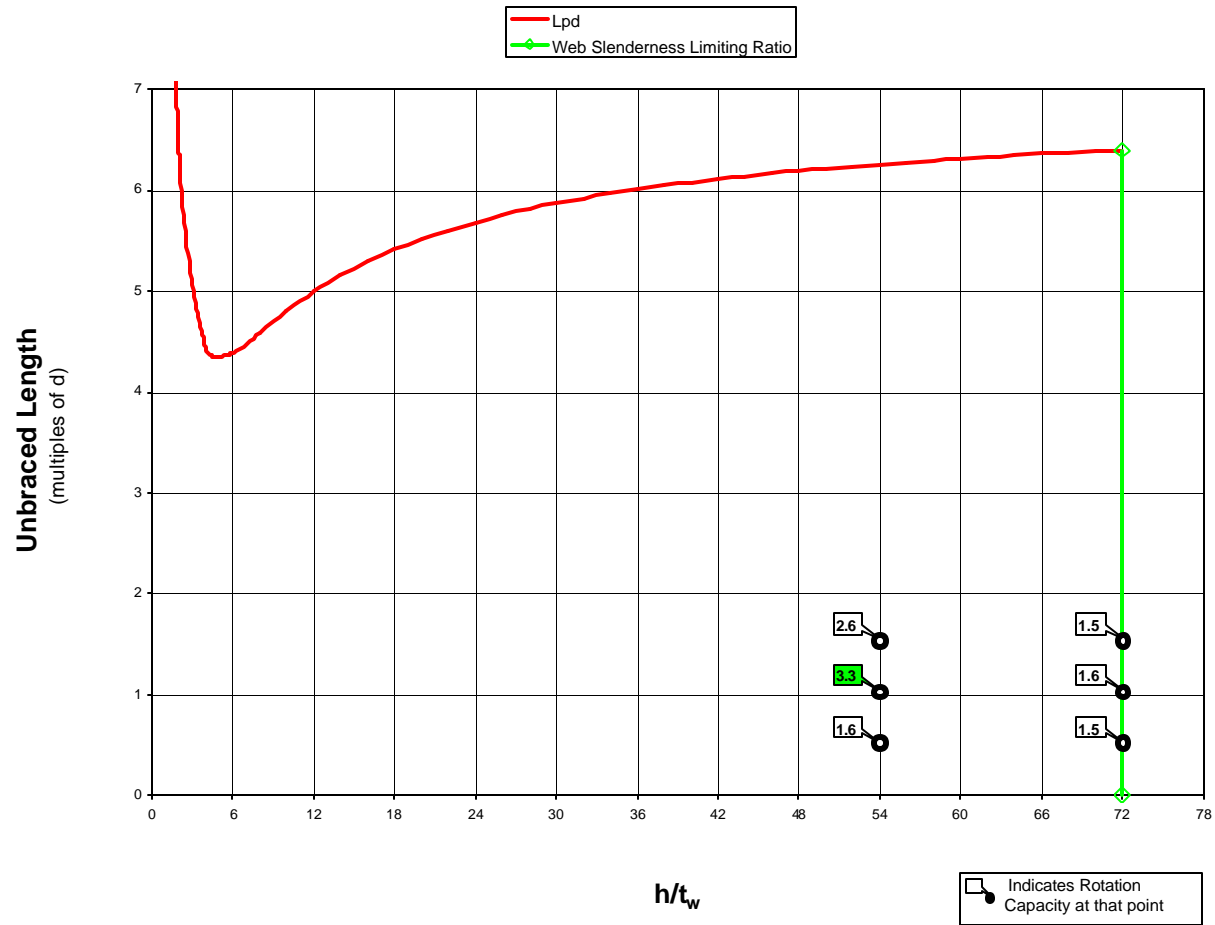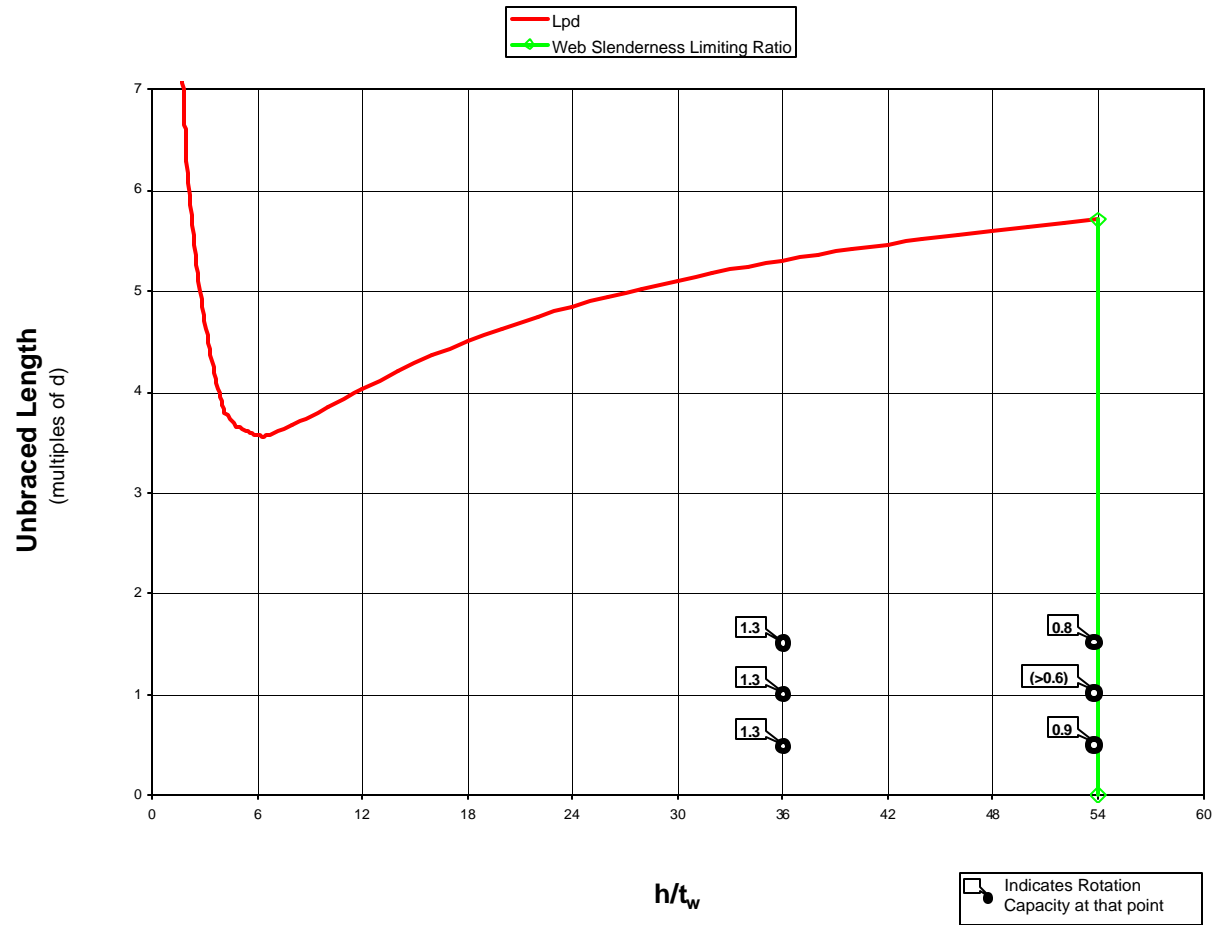
Figure C-36 Interaction Plot: Web Slenderness vs. Unbraced Length
($b_f/2t_f$ = 7.34, h/t_w Varies, L_b Varies, 7.3 AISC β_{br})

228

Web Slenderness vs. Unbraced Length

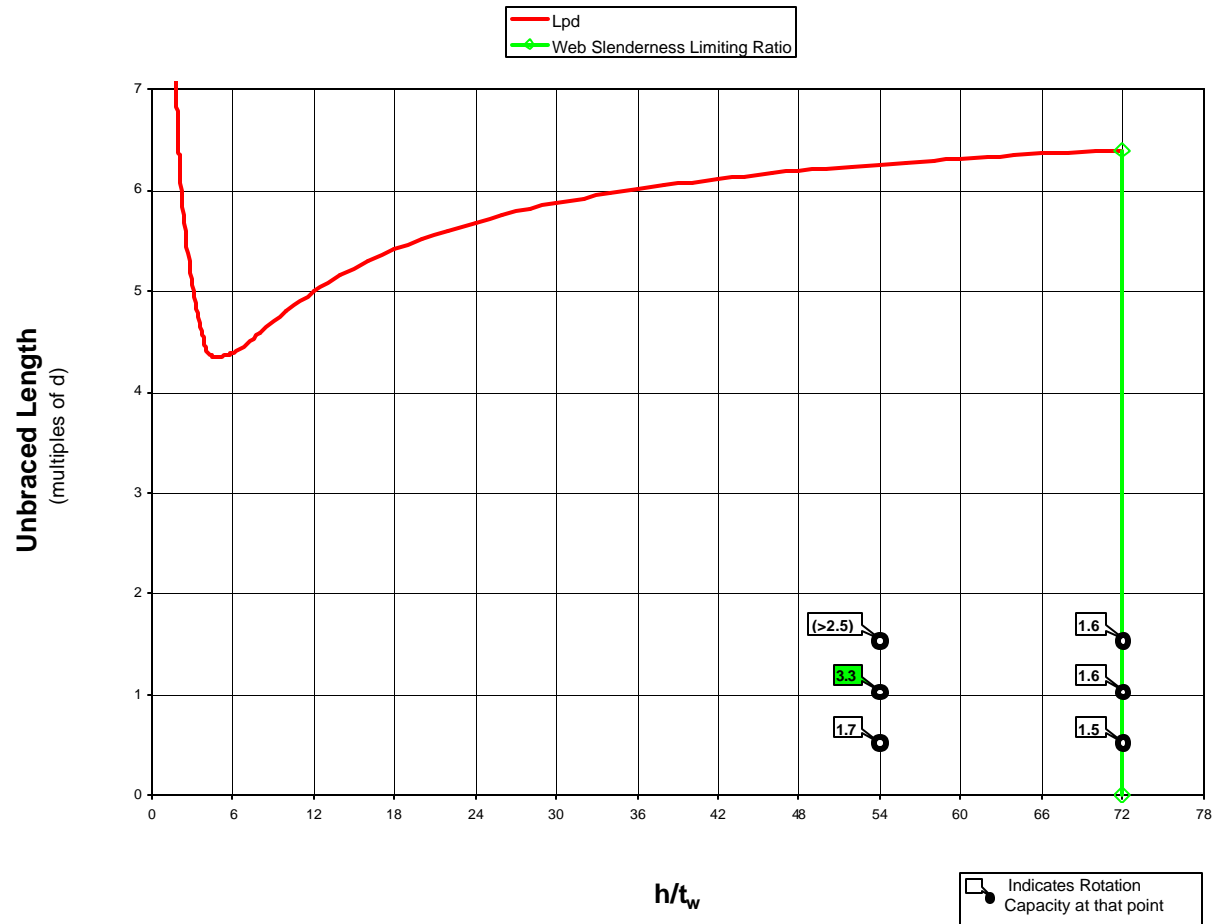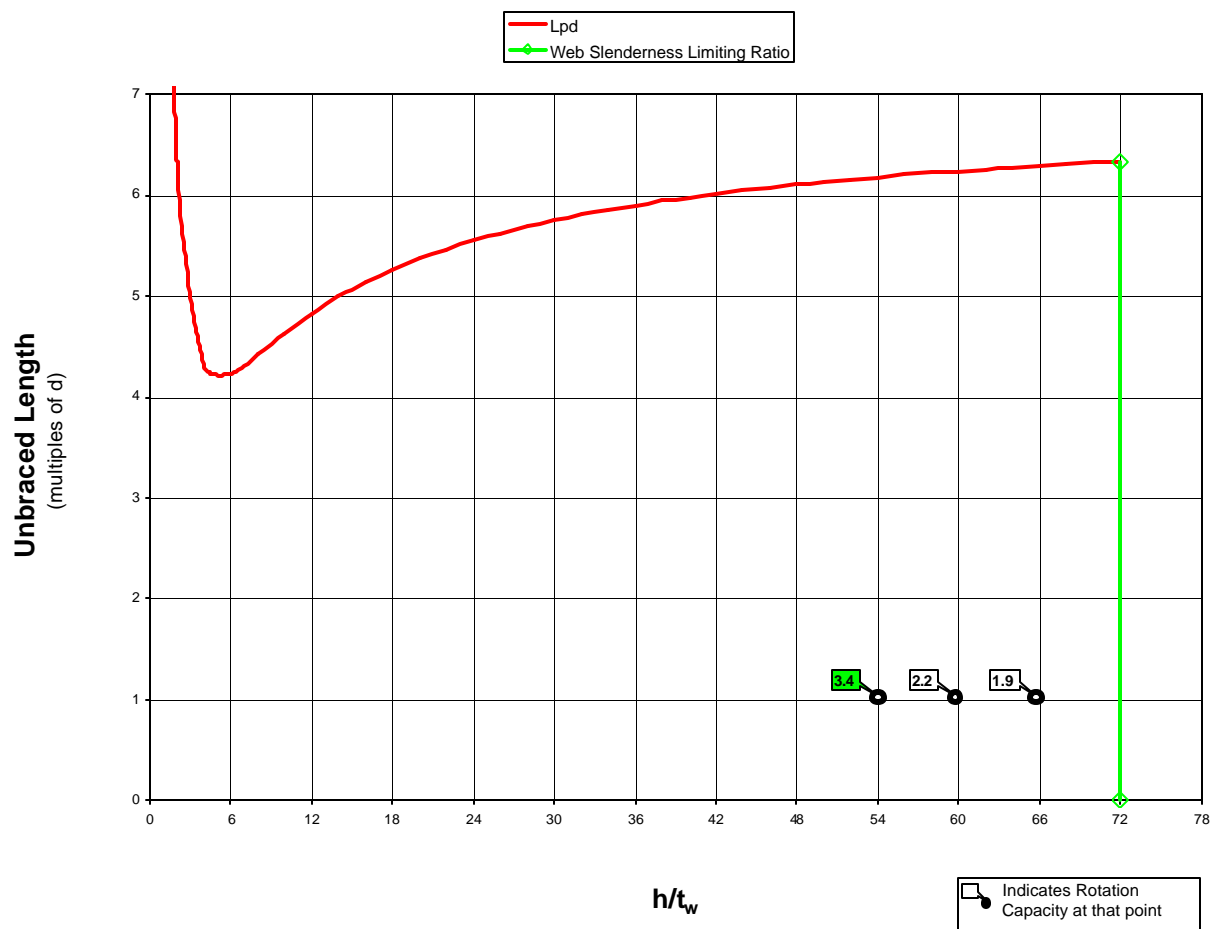$b_f/2t_f = 7.34$, h/t_w varies, L_b varies, 8 AISC Recommended Bracing Stiffness
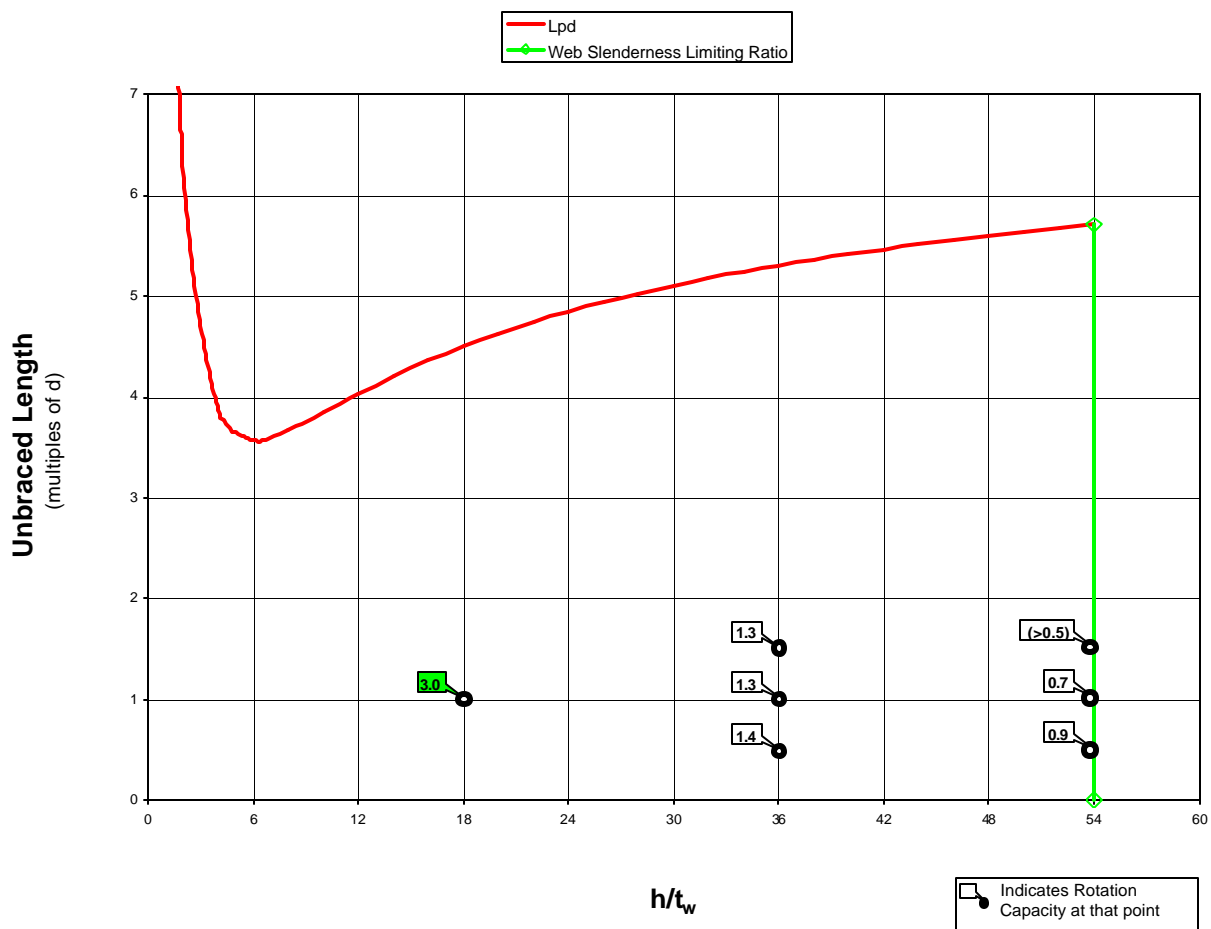
Figure C-37 Interaction Plot: Web Slenderness vs. Unbraced Length
($b_f/2t_f = 7.34$, h/t_w Varies, L_b Varies, 8 AISC β_{br})

Appendix C.3

The third type of interaction plot located in this sub-appendix graphs flange slenderness against unbraced length. For each combination of web slenderness and bracing stiffness, one of these plots has been produced. For each of these plots there exist numerous combinations of flange slenderness and unbraced length for which finite element tests are run. The corresponding rotation capacity for each of these individual tests is shown at its respective point on the graph.

Flange Slenderness vs. Unbraced Length

$b_f/2t_f$ varies, h/t_w = 36, L_b varies, 6.5 AISC Recommended Bracing Stiffness
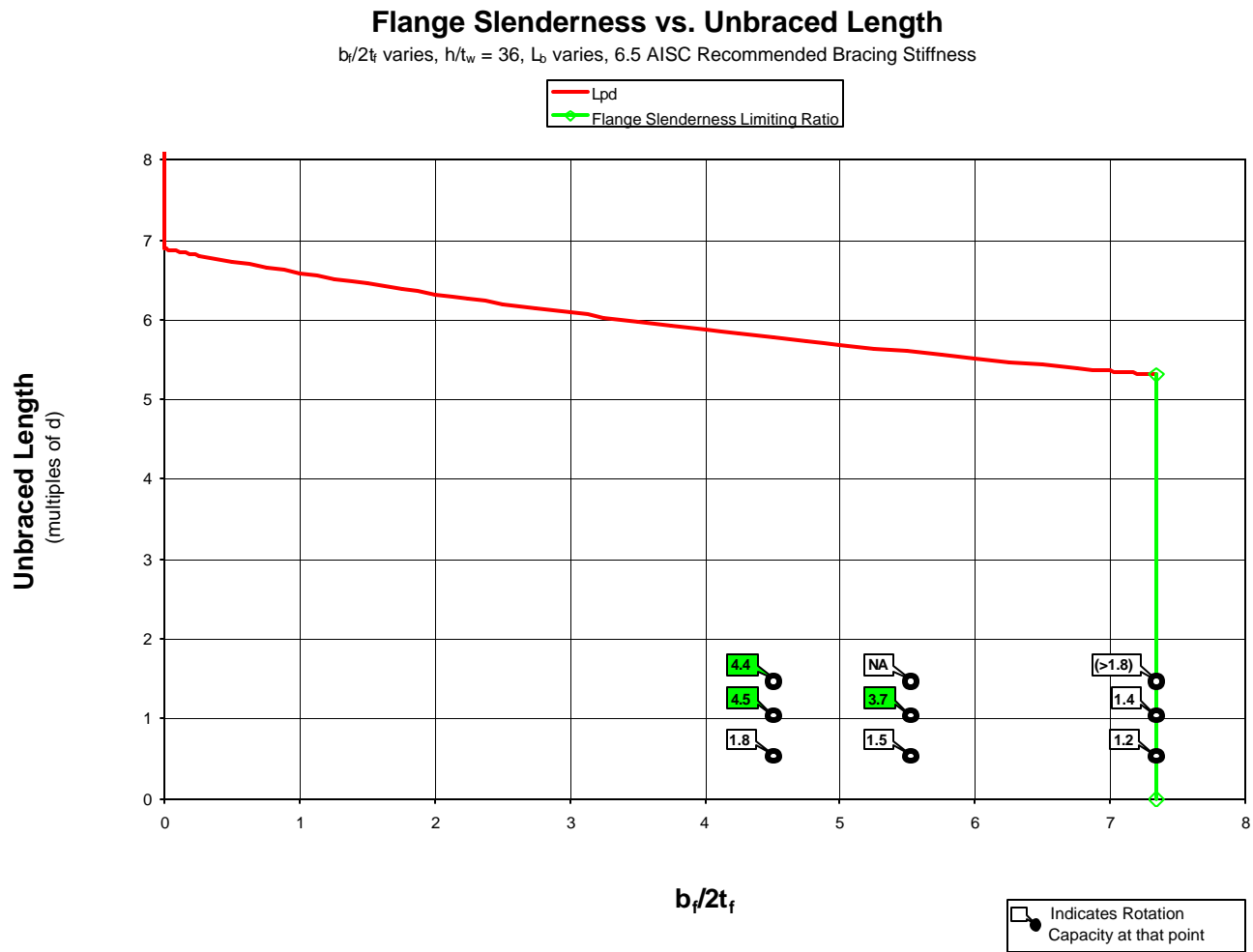
Figure C-38 Interaction Plot: Flange Slenderness vs. Unbraced Length ($b_f/2t_f$ Varies, h/t_w = 36, L_b Varies, 6.5 AISC β_{br})

231

Flange Slenderness vs. Unbraced Length

$b_f/2t_f$ varies, h/t_w = 36, L_b varies, 7.3 AISC Recommended Bracing Stiffness
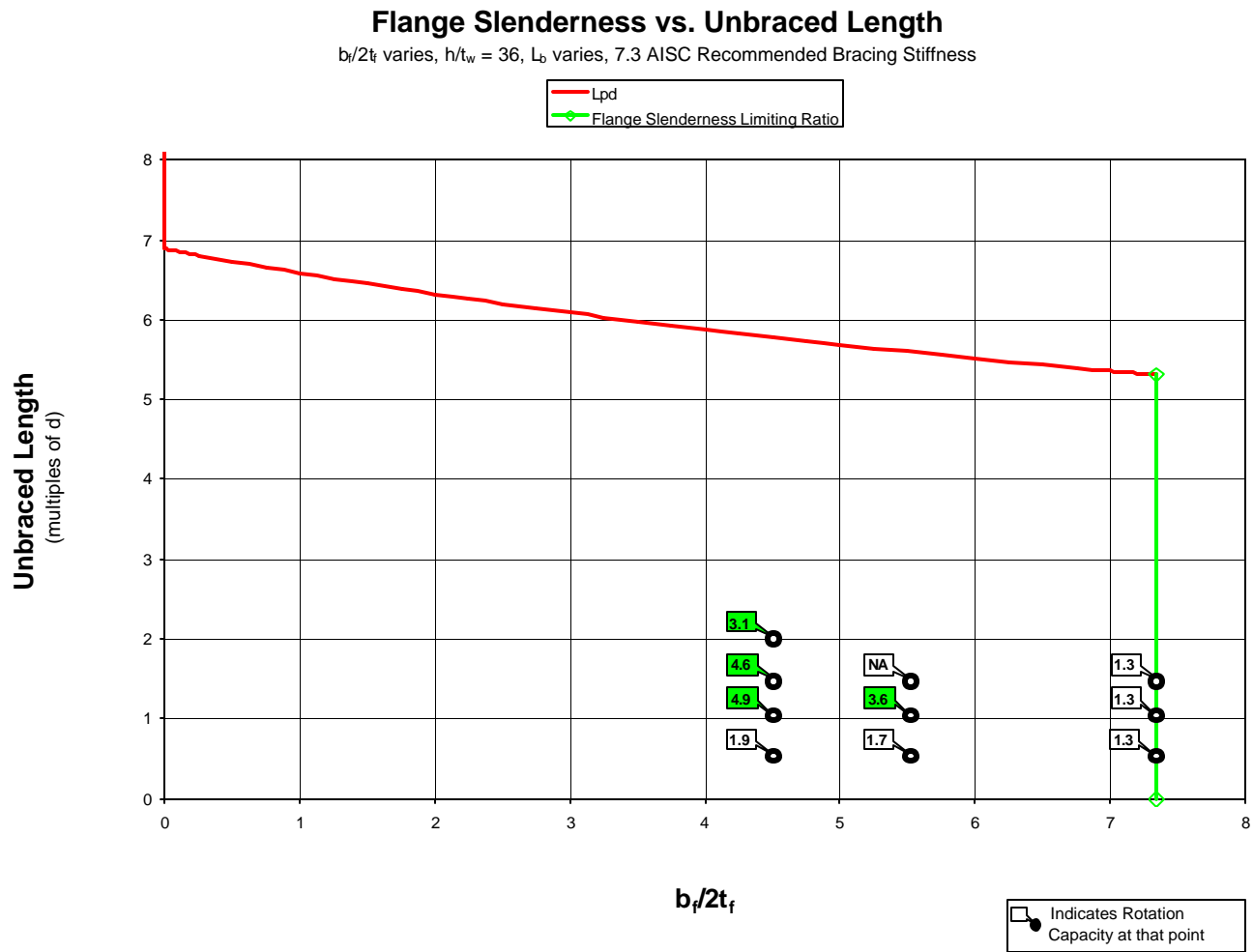
Figure C-39 Interaction Plot: Flange Slenderness vs. Unbraced Length
($b_f/2t_f$ Varies, h/t_w = 36, L_b Varies, 7.3 AISC β_{br})

Flange Slenderness vs. Unbraced Length

$b_f/2t_f$ varies, $h/t_w = 36$, L_b varies, 8 AISC Recommended Bracing Stiffness
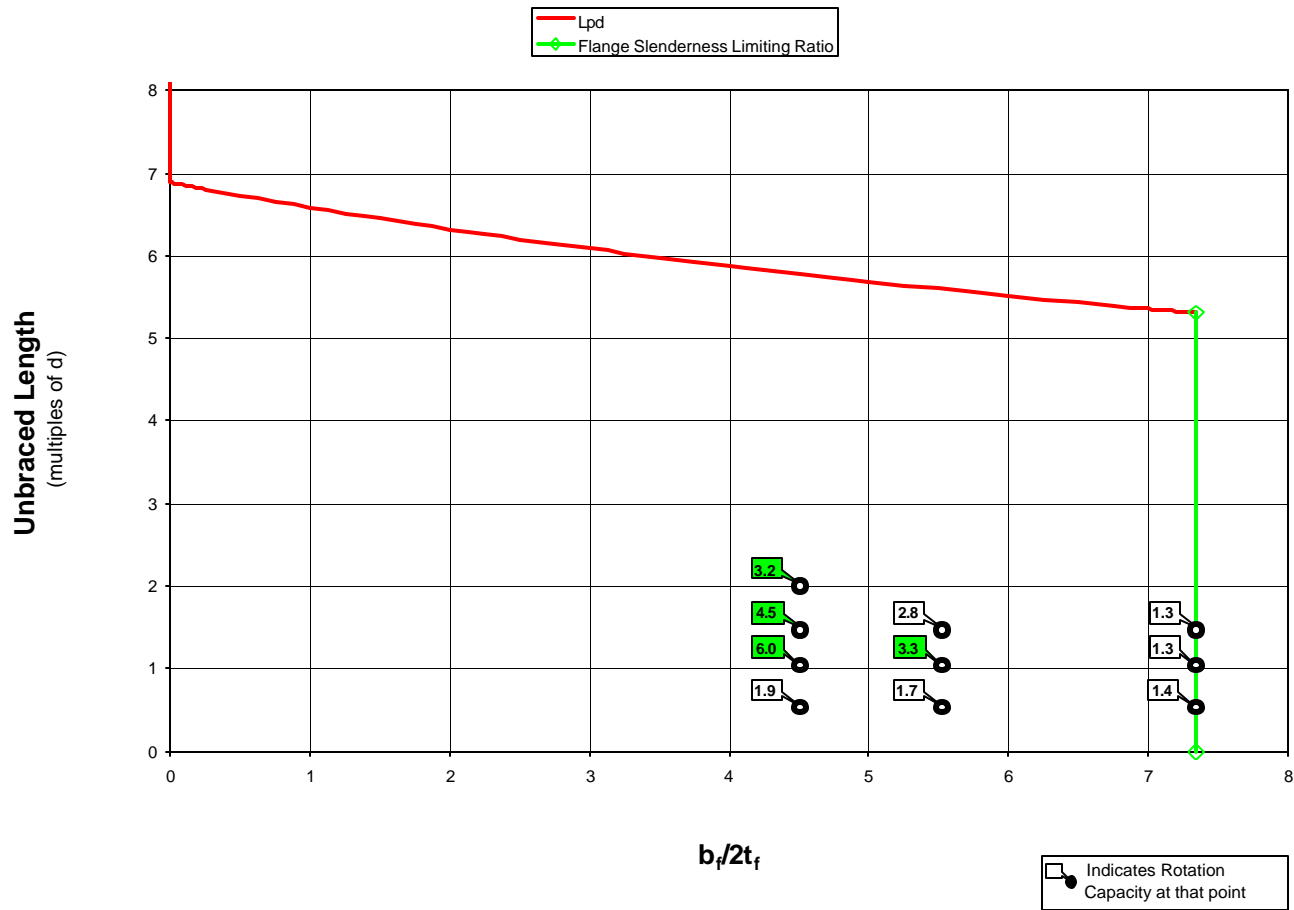
Figure C-40 Interaction Plot: Flange Slenderness vs. Unbraced Length
($b_f/2t_f$ Varies, $h/t_w = 36$, L_b Varies, 8 AISC β_{br})

233
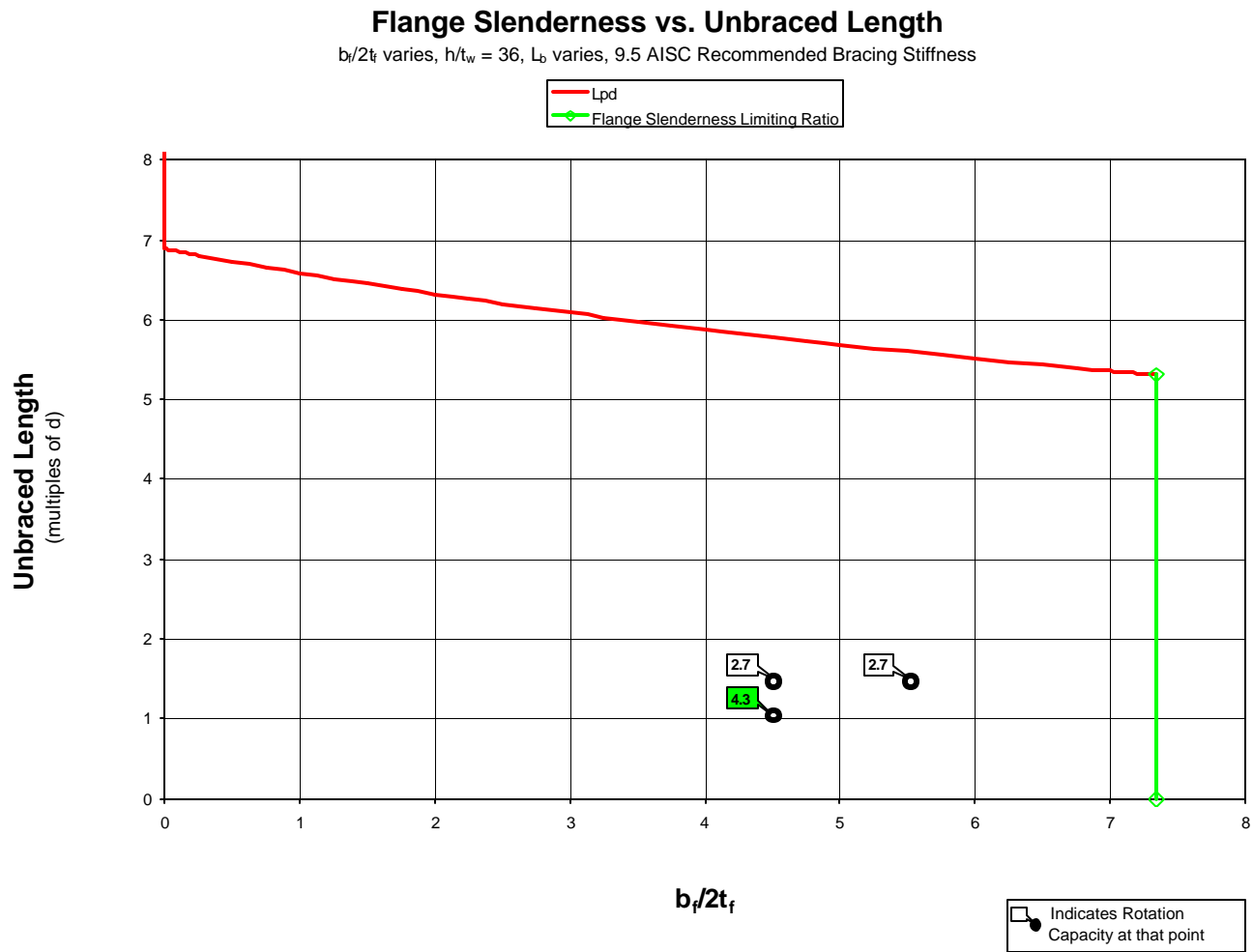
Figure C-41 Interaction Plot: Flange Slenderness vs. Unbraced Length
($b_f/2t_f$ Varies, $h/t_w = 36$, L_b Varies, 9.5 AISC β_{br})

Flange Slenderness vs. Unbraced Length

$b_f/2t_f$ varies, $h/t_w = 54$, L_b varies, 5 AISC Recommended Bracing Stiffness
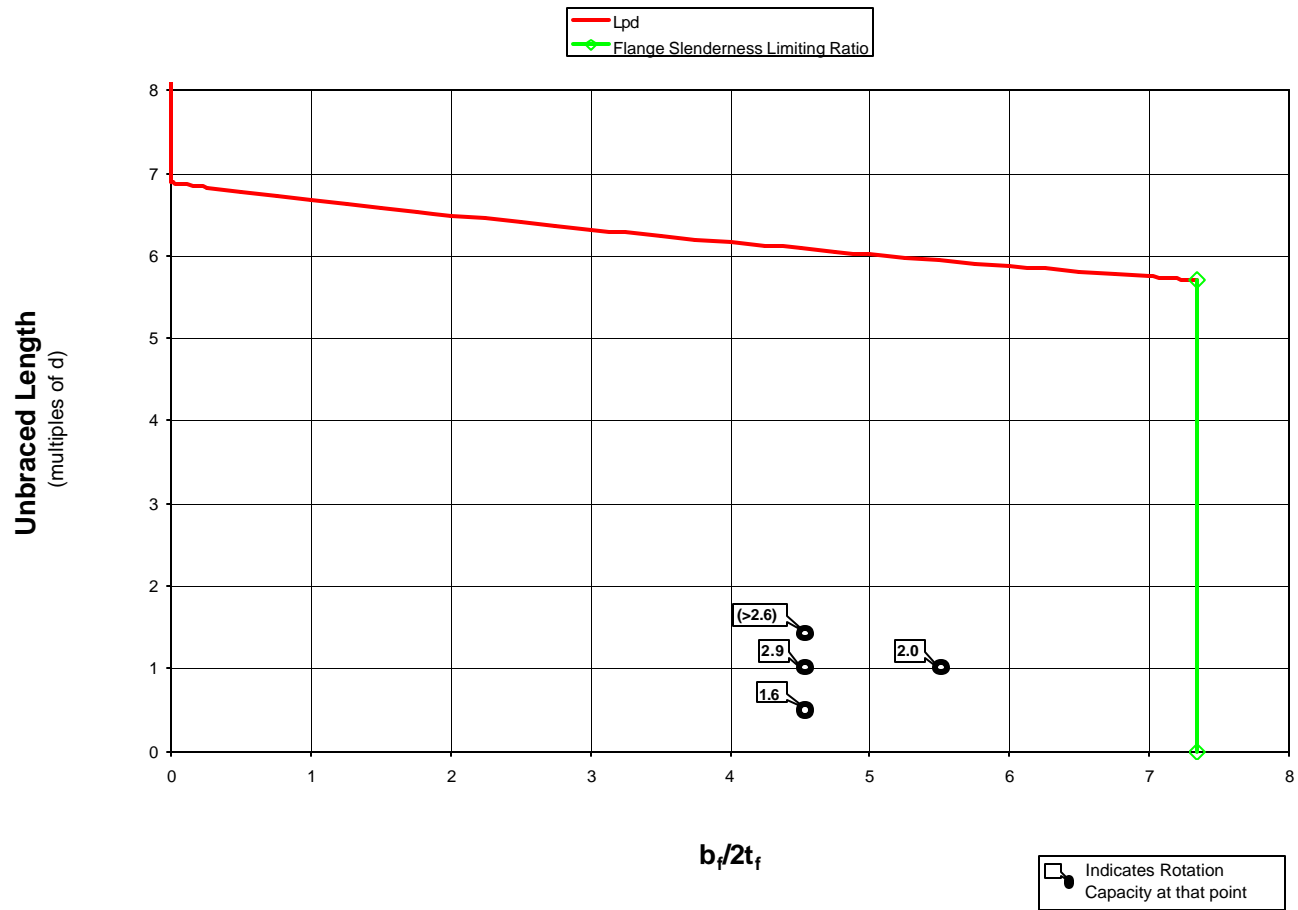
Figure C-42 Interaction Plot: Flange Slenderness vs. Unbraced Length
($b_f/2t_f$ Varies, $h/t_w = 54$, L_b Varies, 5 AISC β_{br})

Figure C-43 Interaction Plot: Flange Slenderness vs. Unbraced Length
($b_f/2t_f$ Varies, h/t_w = 54, L_b Varies, 6.5 AISC β_{br})
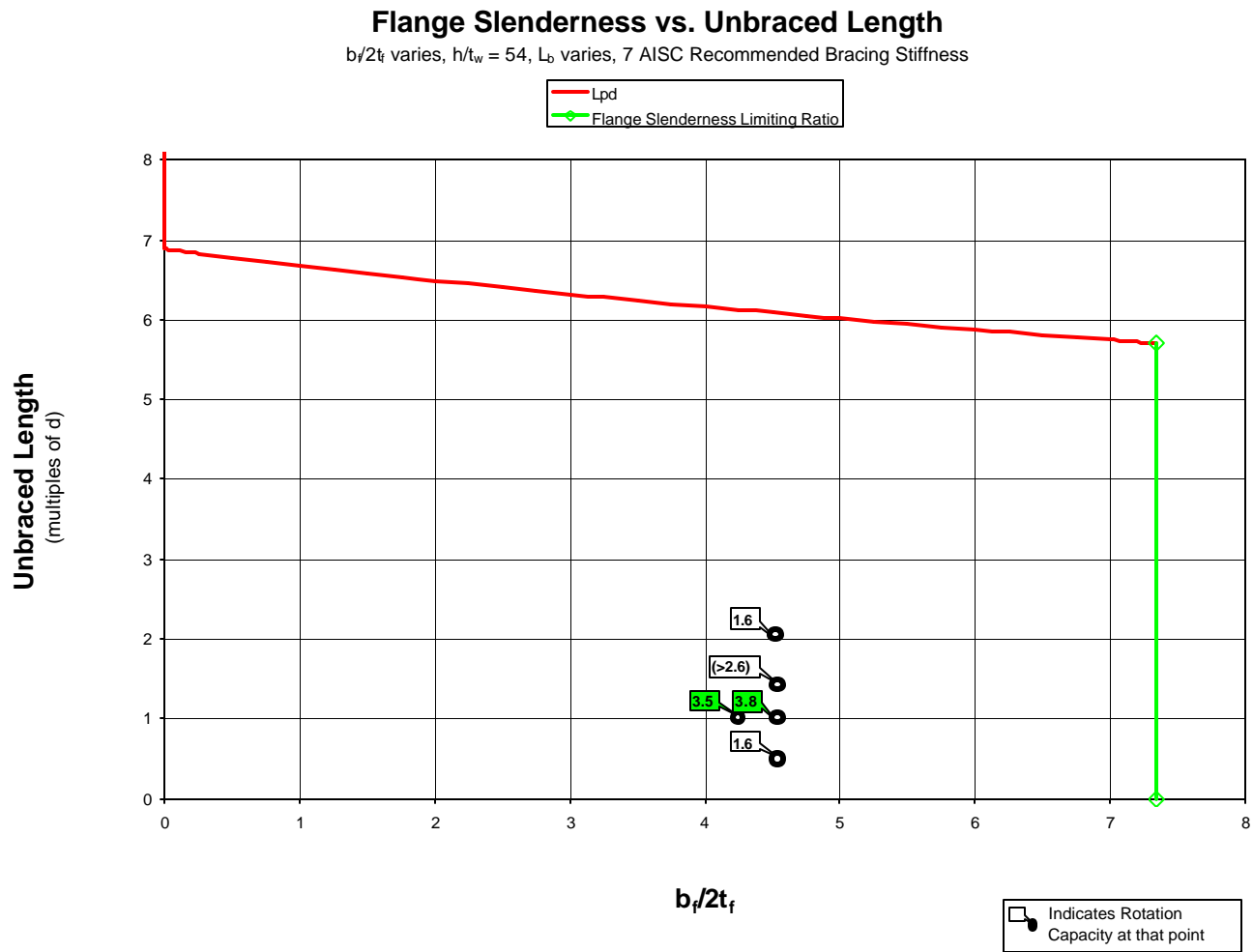
Figure C-44 Interaction Plot: Flange Slenderness vs. Unbraced Length
($b_f/2t_f$ Varies, $h/t_w = 54$, L_b Varies, 7 AISC β_{br})

Flange Slenderness vs. Unbraced Length

$b_f/2t_f$ varies, $h/t_w = 54$, L_b varies, 7.3 AISC Recommended Bracing Stiffness
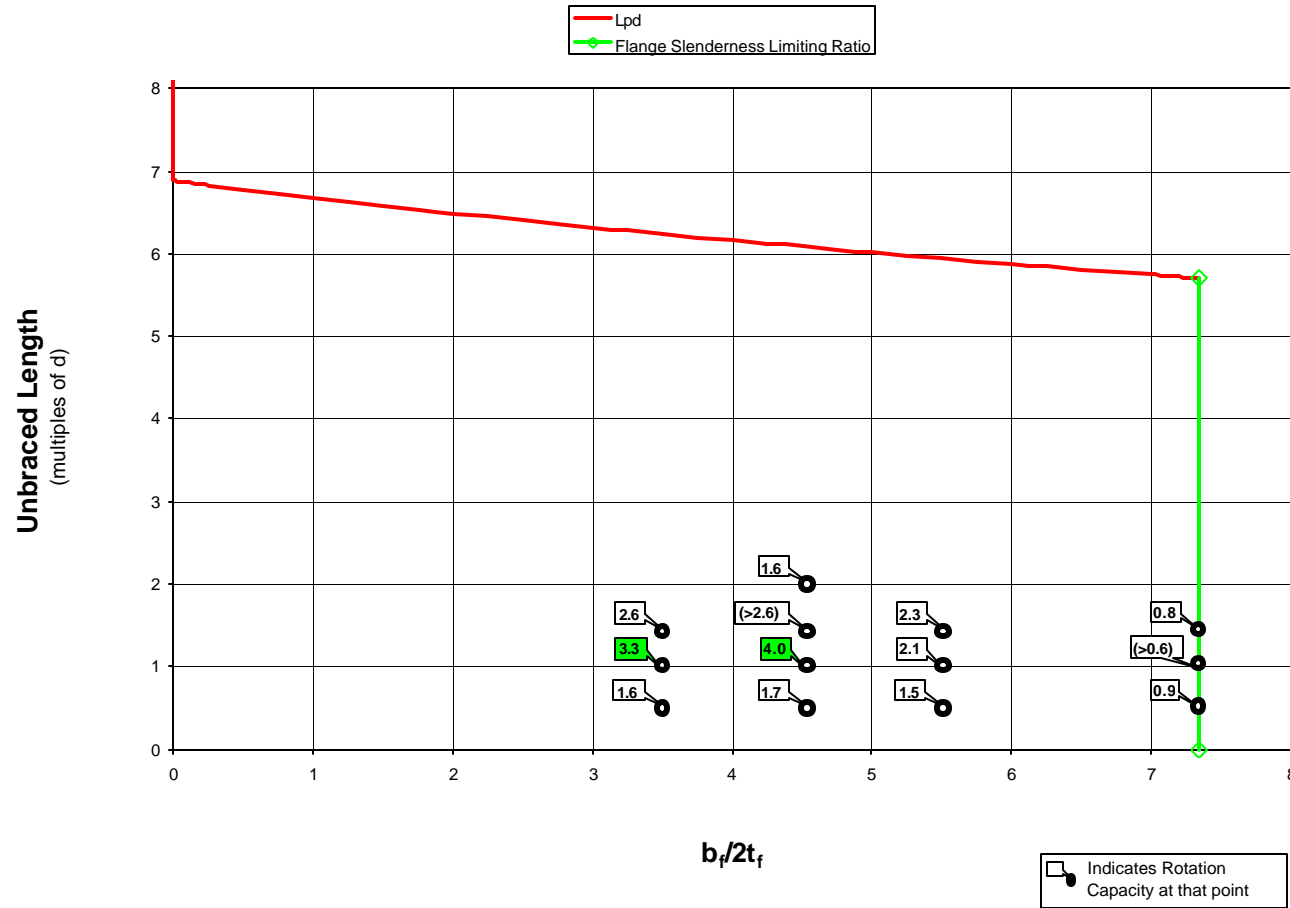
Figure C-45 Interaction Plot: Flange Slenderness vs. Unbraced Length
($b_f/2t_f$ Varies, $h/t_w = 54$, L_b Varies, 7.3 AISC β_{br})

238

Flange Slenderness vs. Unbraced Length

$b_f/2t_f$ varies, $h/t_w = 54$, L_b varies, 7.5 AISC Recommended Bracing Stiffness
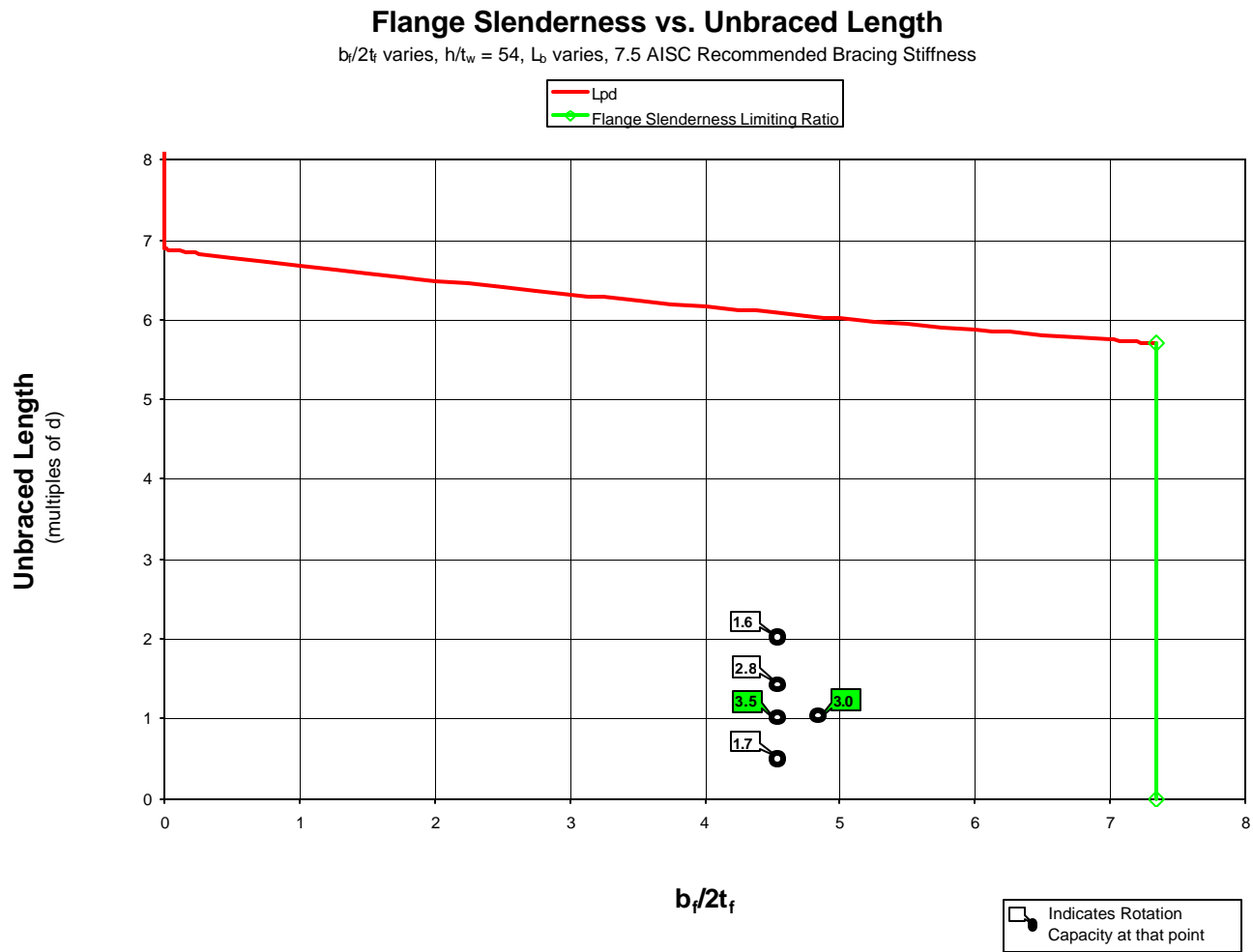
Figure C-46 Interaction Plot: Flange Slenderness vs. Unbraced Length
($b_f/2t_f$ Varies, $h/t_w = 54$, L_b Varies, 7.5 AISC β_{br})

239

Flange Slenderness vs. Unbraced Length

b_f/2t_f varies, h/t_w = 54, L_b varies, 8 AISC Recommended Bracing Stiffness
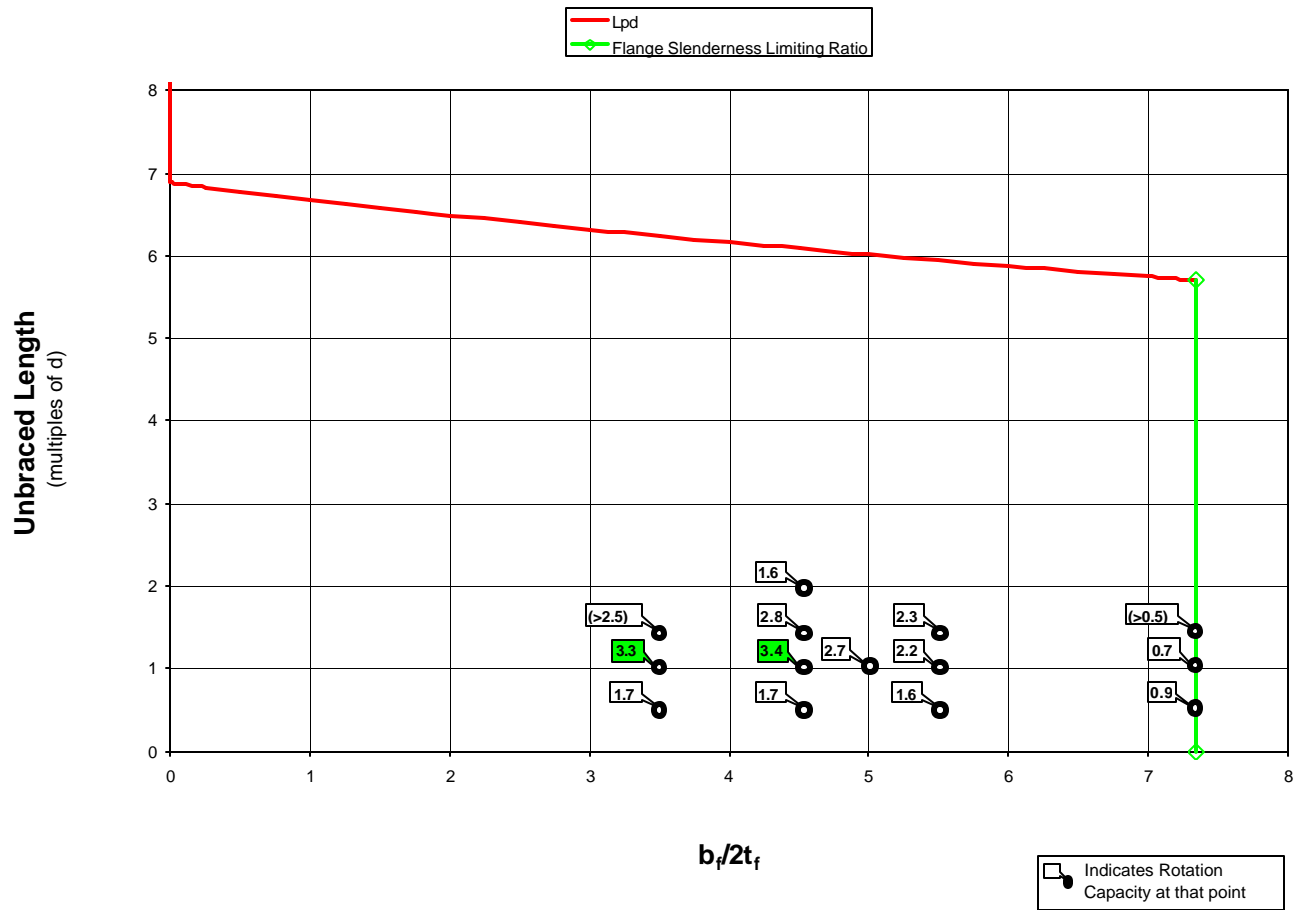
Figure C-47 Interaction Plot: Flange Slenderness vs. Unbraced Length
($b_f/2t_f$ Varies, $h/t_w = 54$, L_b Varies, 8 AISC β_{br})

Flange Slenderness vs. Unbraced Length

$b_f/2t_f$ varies, h/t_w = 54, L_b varies, 9.5 AISC Recommended Bracing Stiffness
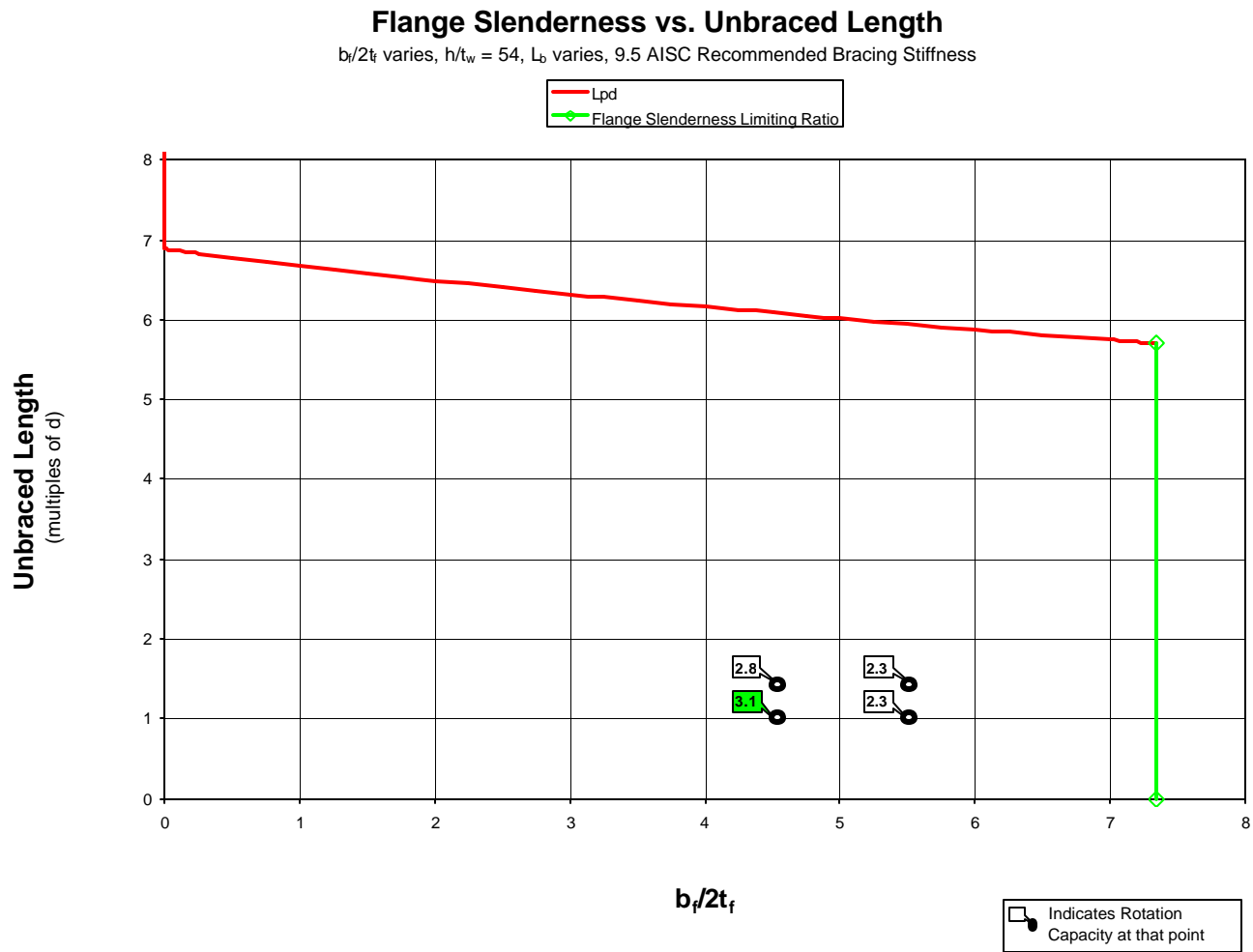
Figure C-48 Interaction Plot: Flange Slenderness vs. Unbraced Length
($b_f/2t_f$ Varies, h/t_w = 54, L_b Varies, 9.5 AISC β_{br})

241

Flange Slenderness vs. Unbraced Length

b$_f$/2t$_f$ varies, h/t$_w$ = 72, L$_b$ varies, 5 AISC Recommended Bracing Stiffness
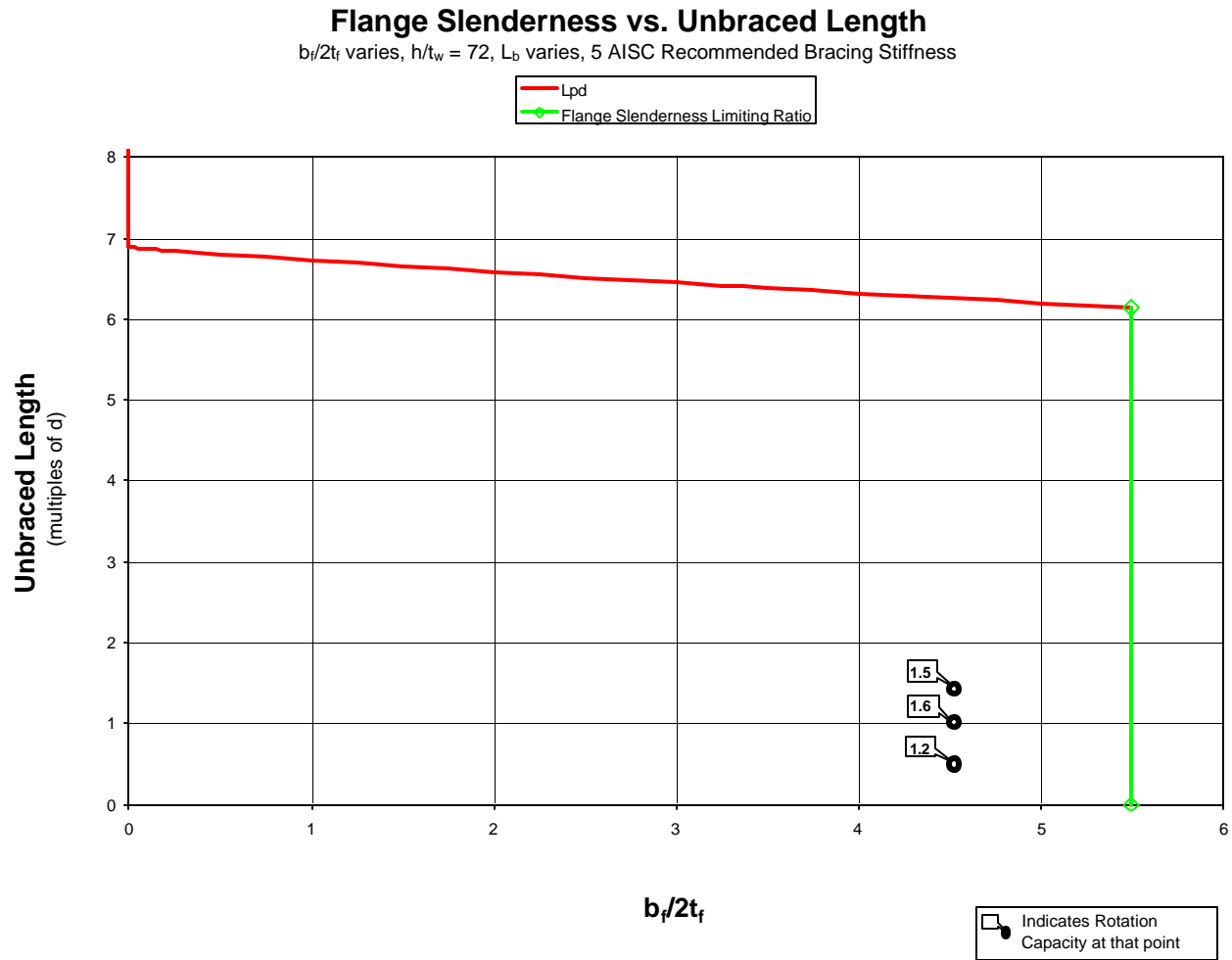
Figure C-49 Interaction Plot: Flange Slenderness vs. Unbraced Length
(b$_f$/2t$_f$ Varies, h/t$_w$ = 72, L$_b$ Varies, 5 AISC β_{br})

242
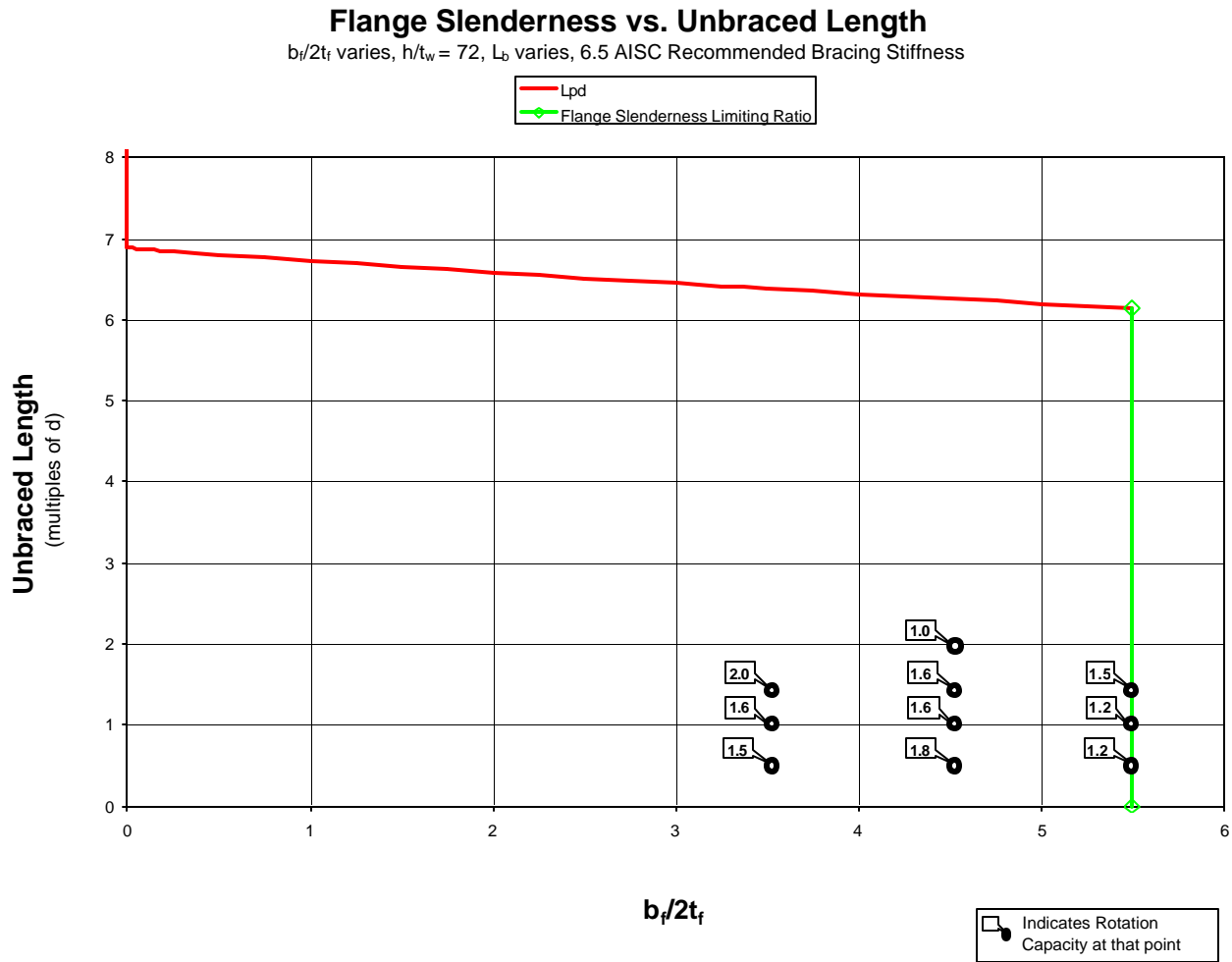
Figure C-50 Interaction Plot: Flange Slenderness vs. Unbraced Length
($b_f/2t_f$ Varies, $h/t_w = 72$, L_b Varies, 6.5 AISC β_{br})

Flange Slenderness vs. Unbraced Length
$b_f/2t_f$ varies, $h/t_w = 72$, L_b varies, 7.3 AISC Recommended Bracing Stiffness
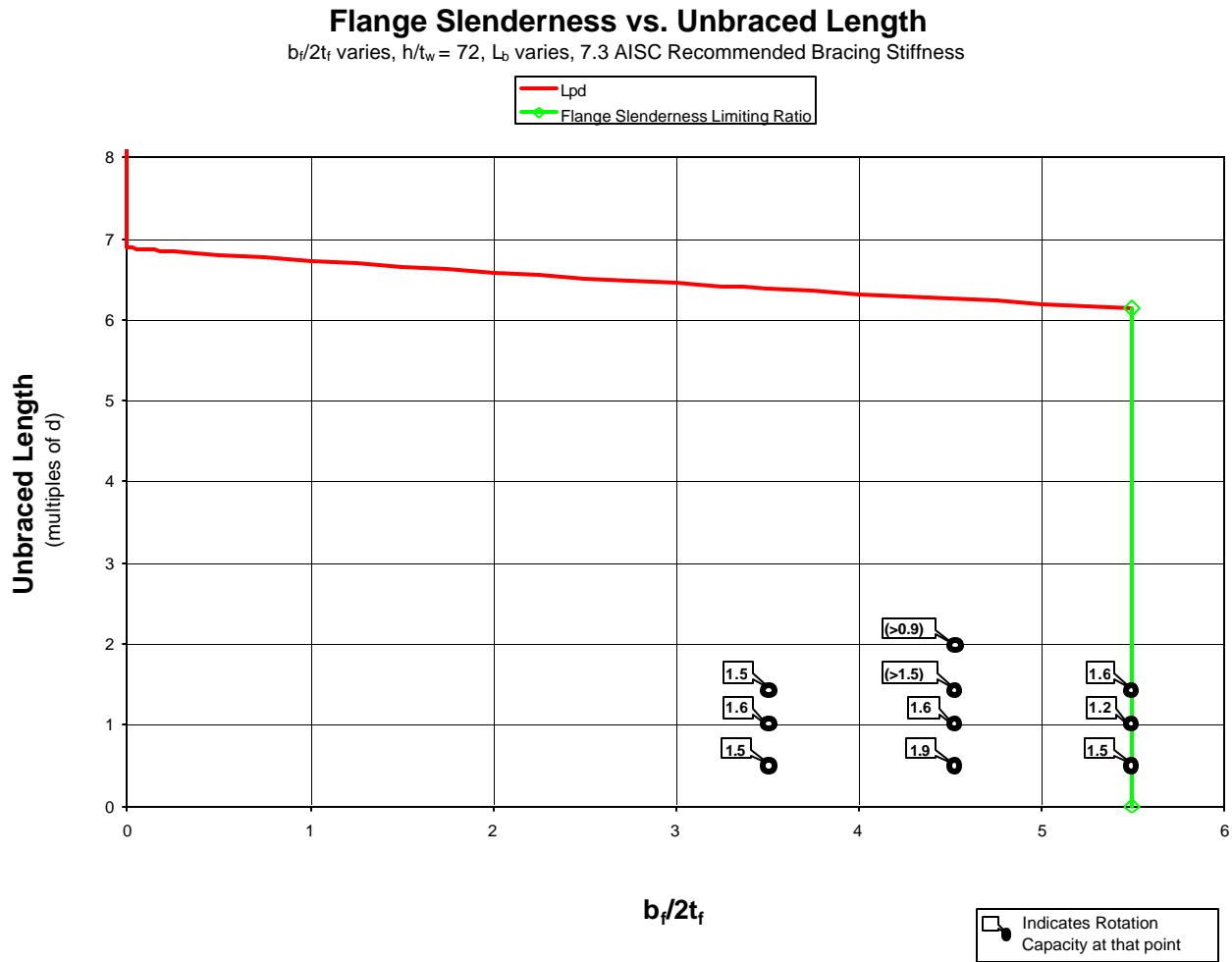
Figure C-51 Interaction Plot: Flange Slenderness vs. Unbraced Length
($b_f/2t_f$ Varies, $h/t_w = 72$, L_b Varies, 7.3 AISC β_{br})

Flange Slenderness vs. Unbraced Length

$b_f/2t_f$ varies, $h/t_w = 72$, L_b varies, 8 AISC Recommended Bracing Stiffness
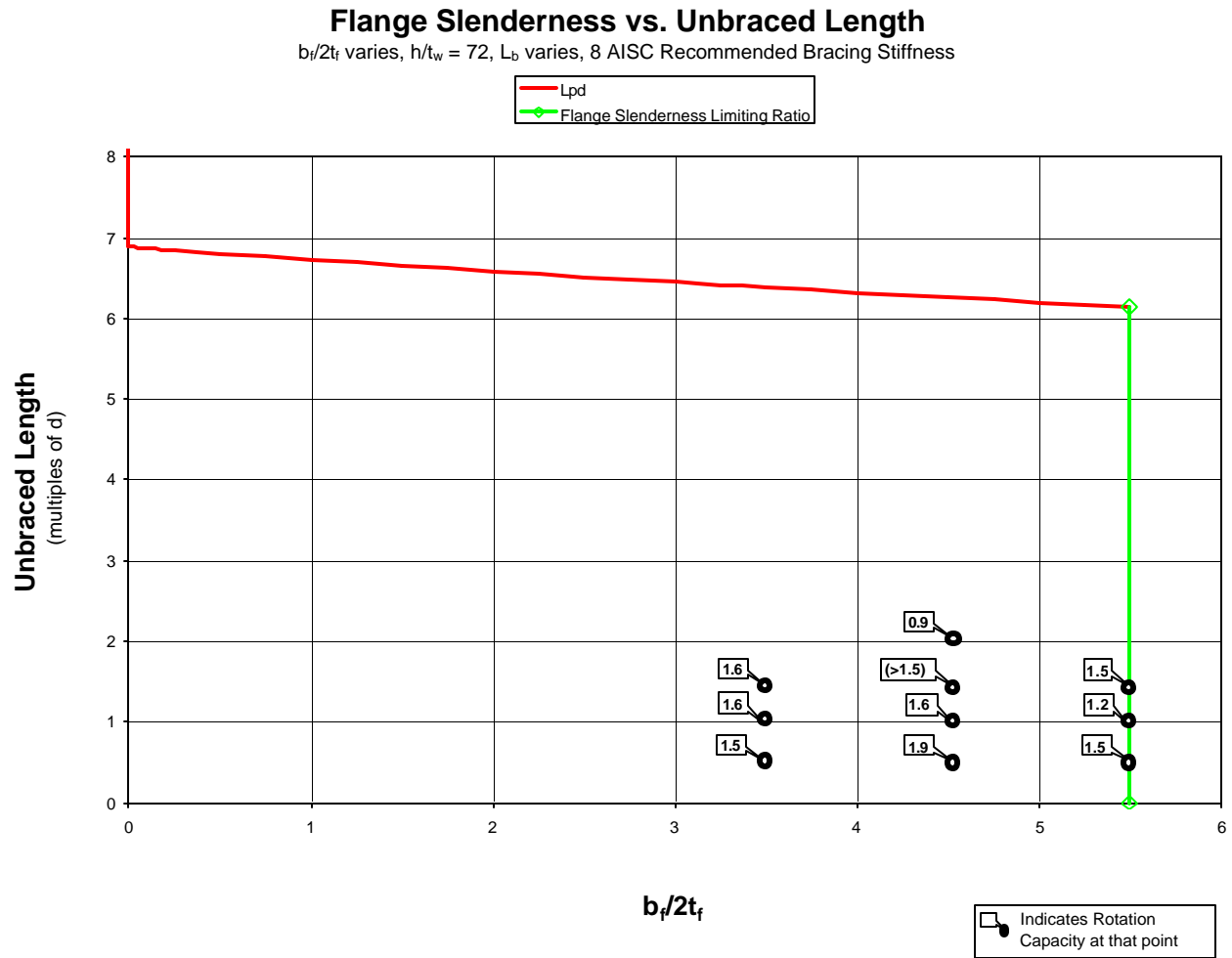
Figure C-52 Interaction Plot: Flange Slenderness vs. Unbraced Length ($b_f/2t_f$ Varies, $h/t_w = 72$, L_b Varies, 8 AISC β_{br})

245

The fourth type of interaction plot located in this sub-appendix graphs web slenderness against bracing stiffness. For each combination of flange slenderness and unbraced length, one of these plots has been produced. For each of these plots there exist numerous combinations of web slenderness and bracing stiffness for which finite element tests are run. The corresponding rotation capacity for each of these individual tests is shown at its respective point on the graph.
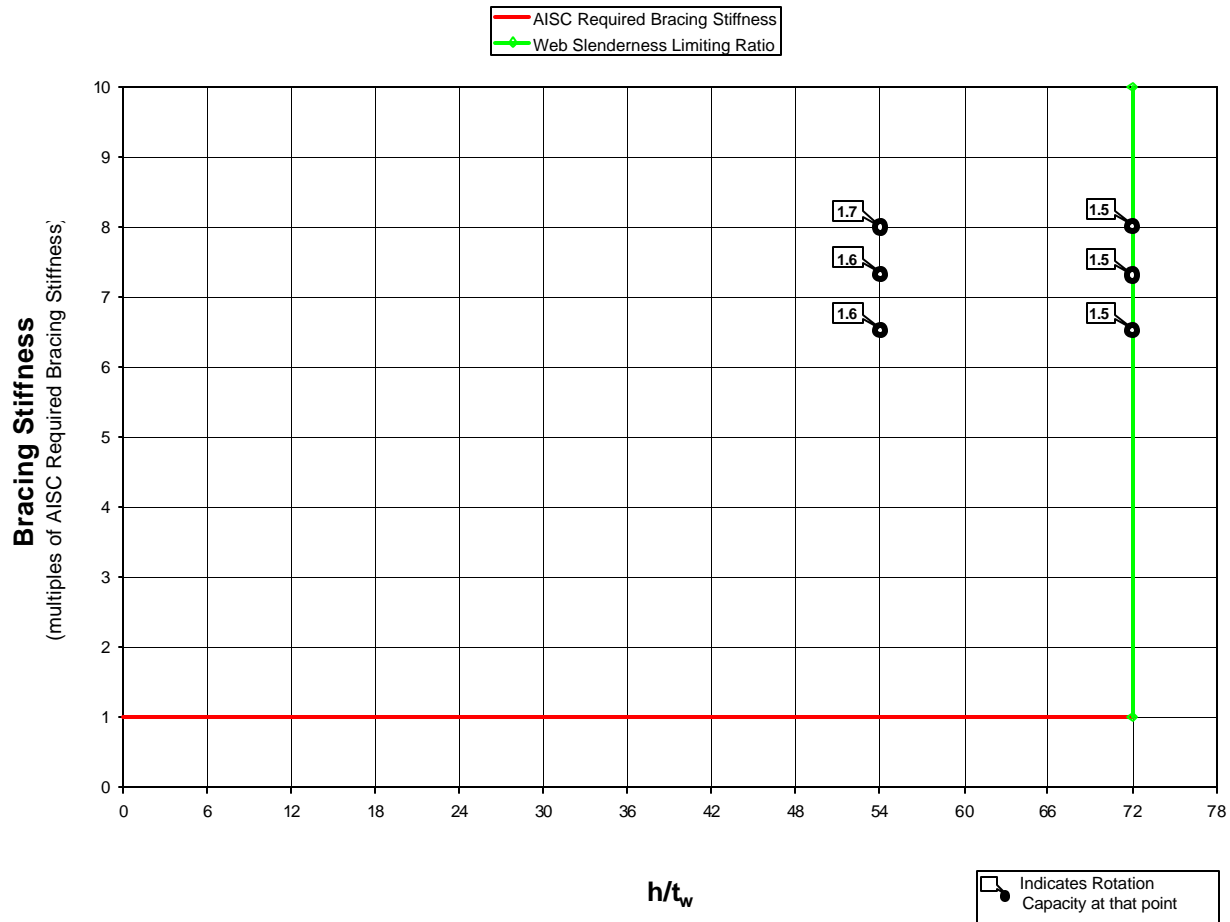
Figure C-53 Interaction Plot: Web Slenderness vs. Bracing Stiffness
($b_f/2t_f$ = 3.5, h/t_w Varies, L_b = 0.5d, Bracing Stiffness Varies)
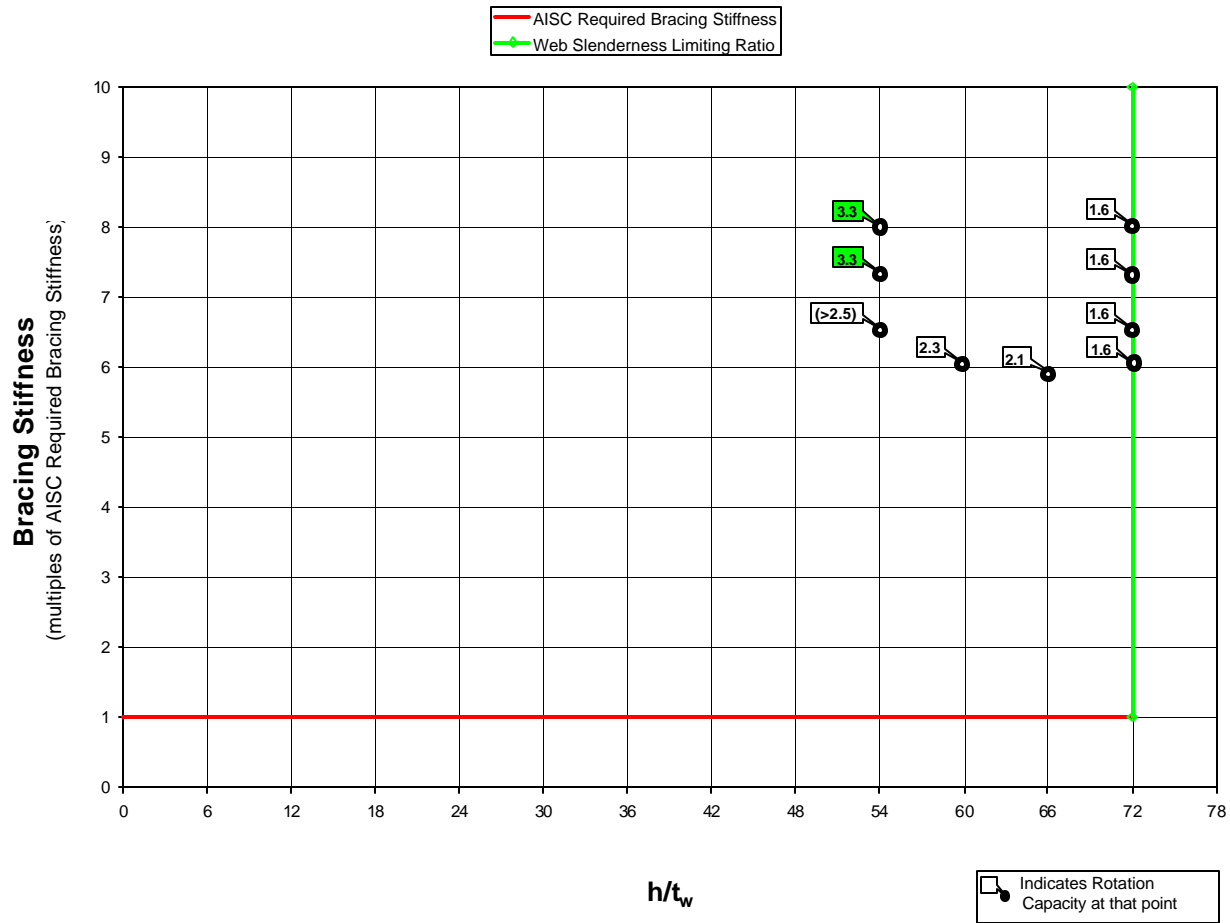
Figure C-54 Interaction Plot: Web Slenderness vs. Bracing Stiffness
($b_f/2t_f = 3.5$, h/t_w Varies, $L_b = 1d$, Bracing Stiffness Varies)
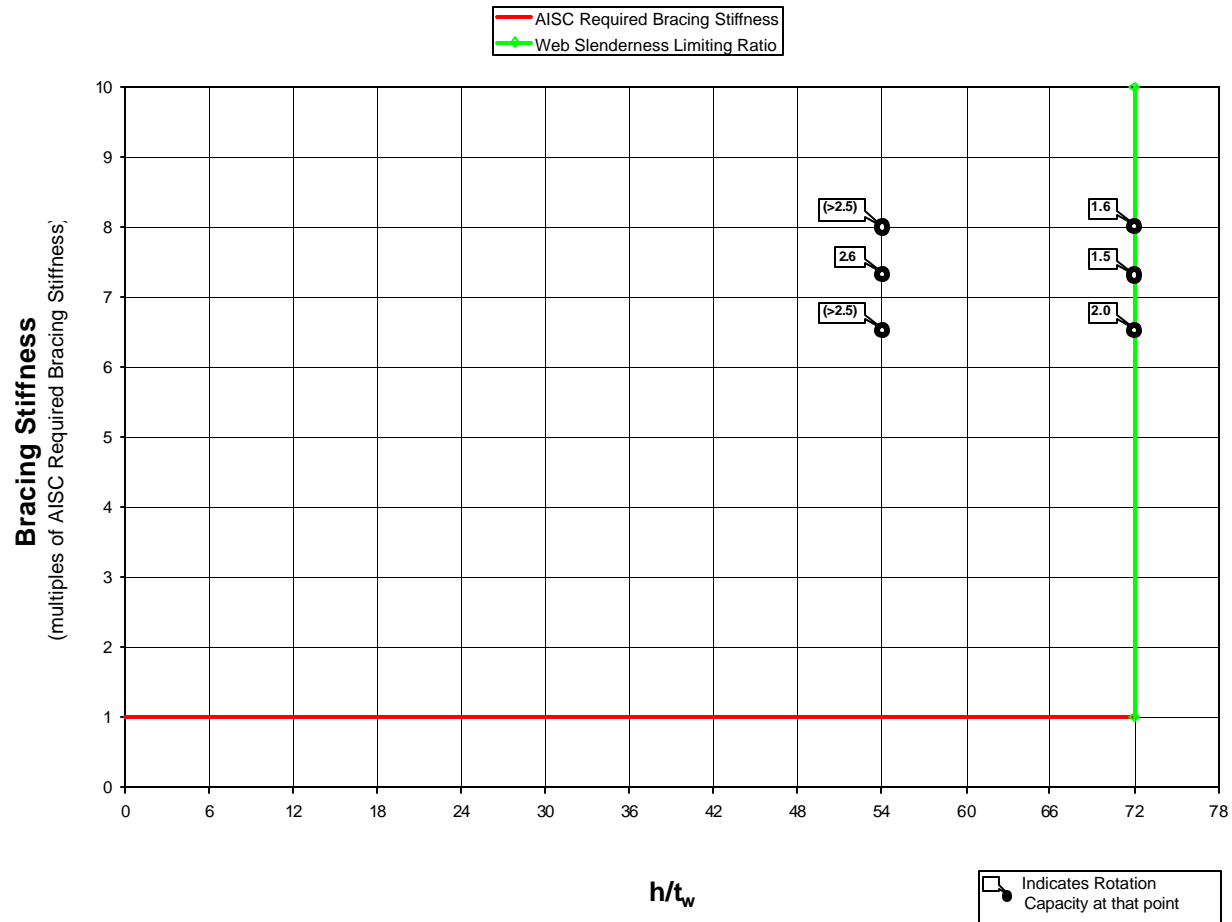
Figure C-55 Interaction Plot: Web Slenderness vs. Bracing Stiffness
($b_f/2t_f$ = 3.5, h/t_w Varies, L_b = 1.5d, Bracing Stiffness Varies)

249

Web Slenderness vs. Bracing Stiffness

$b_f/2t_f = 4$, h/t_w varies, $L_b = 1d$, Bracing Stiffness varies

- AISC Required Bracing Stiffness
- Web Slenderness Limiting Ratio
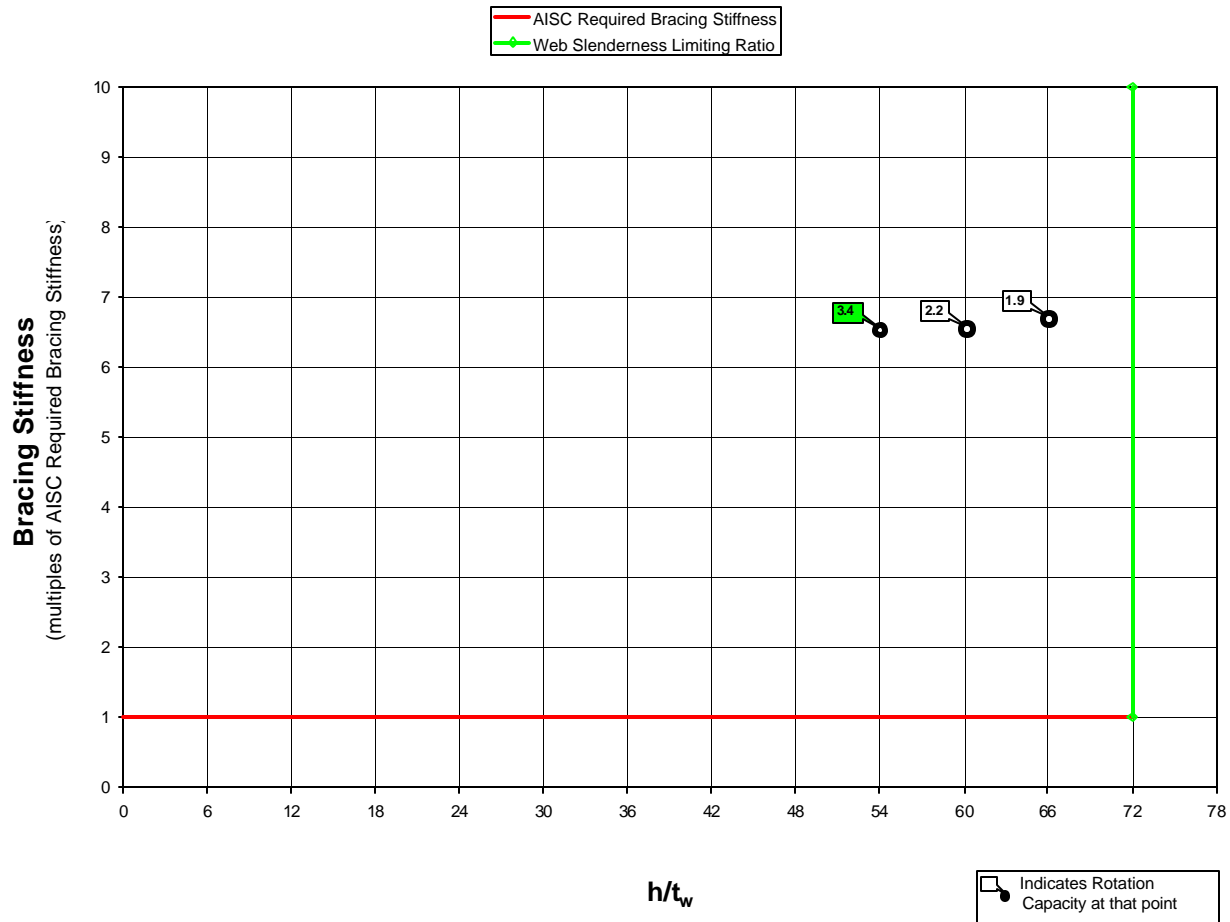
Figure C-56 Interaction Plot: Web Slenderness vs. Bracing Stiffness
($b_f/2t_f = 4.0$, h/t_w Varies, $L_b = 1d$, Bracing Stiffness Varies)

250

Web Slenderness vs. Bracing Stiffness

$b_f/2t_f = 4.5$, h/t_w varies, $L_b = 0.5d$, Bracing Stiffness varies

— AISC Required Bracing Stiffness
◆— Web Slenderness Limiting Ratio

Bracing Stiffness
(multiples of AISC Required Bracing Stiffness)

h/t_w

Indicates Rotation
Capacity at that point
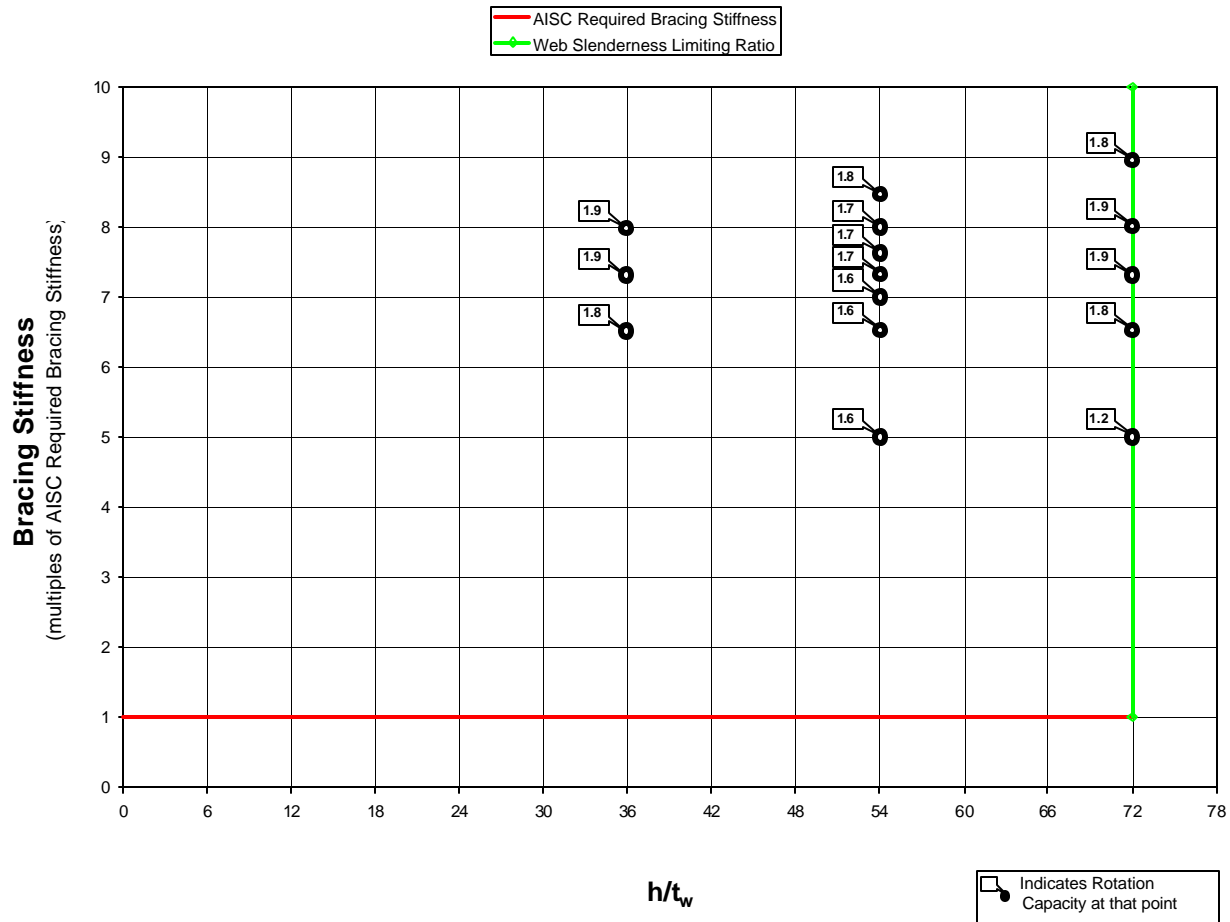
Figure C-57 Interaction Plot: Web Slenderness vs. Bracing Stiffness
($b_f/2t_f = 4.5$, h/t_w Varies, $L_b = 0.5d$, Bracing Stiffness Varies)

251
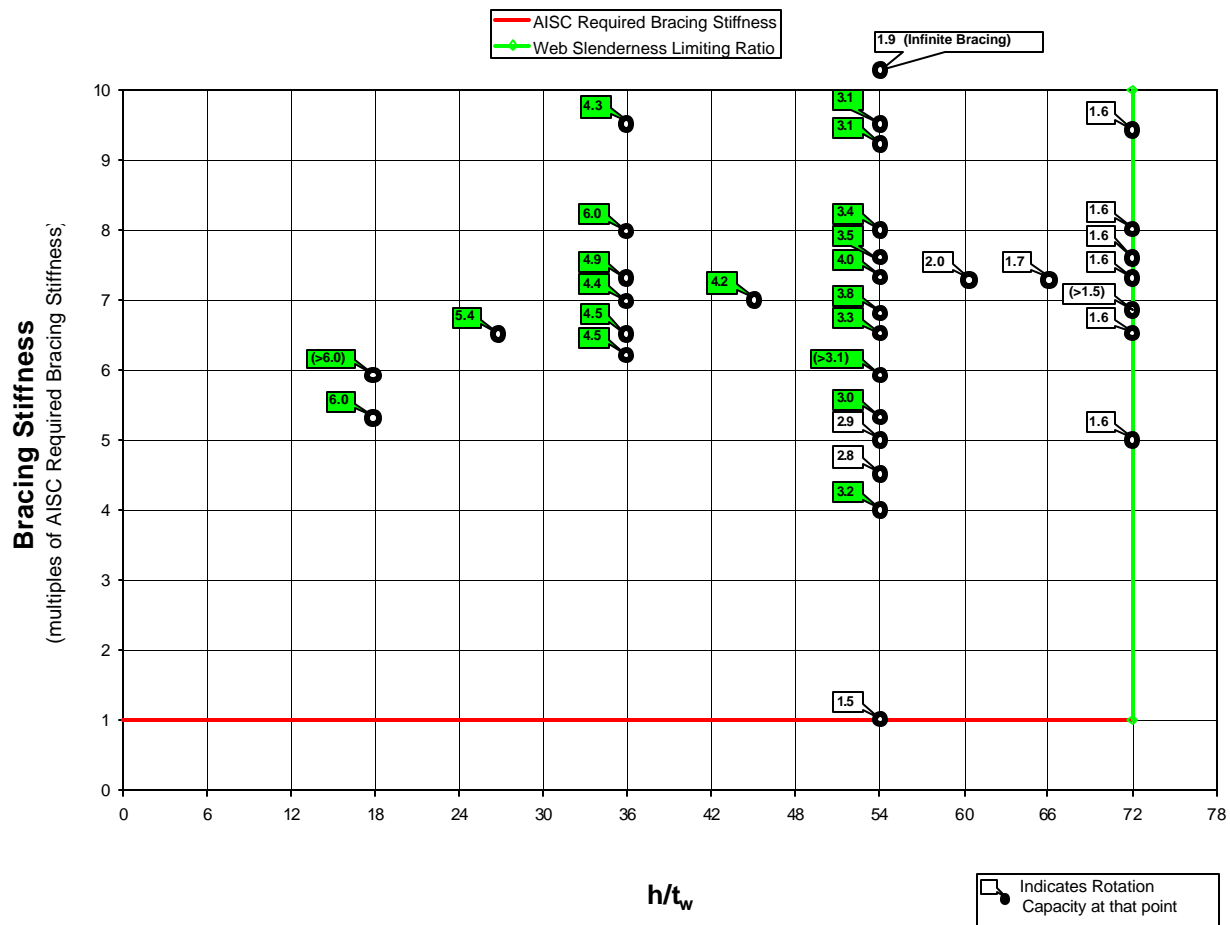
Figure C-58 Interaction Plot: Web Slenderness vs. Bracing Stiffness
($b_f/2t_f$ = 4.5, h/t_w Varies, L_b = 1d, Bracing Stiffness Varies)

252

Web Slenderness vs. Bracing Stiffness

$b_f/2t_f$ = 4.5, h/t_w varies, L_b = 1.5d, Bracing Stiffness varies

AISC Required Bracing Stiffness
Web Slenderness Limiting Ratio

Bracing Stiffness
(multiples of AISC Required Bracing Stiffness)

2.7
4.5
4.6
4.4
2.8
2.8
2.8
(>2.6)
2.8
2.7
(>2.6)
(>2.6)
(>1.5)
(>1.5)
(>1.5)
1.6
1.5

h/t_w

Indicates Rotation
Capacity at that point
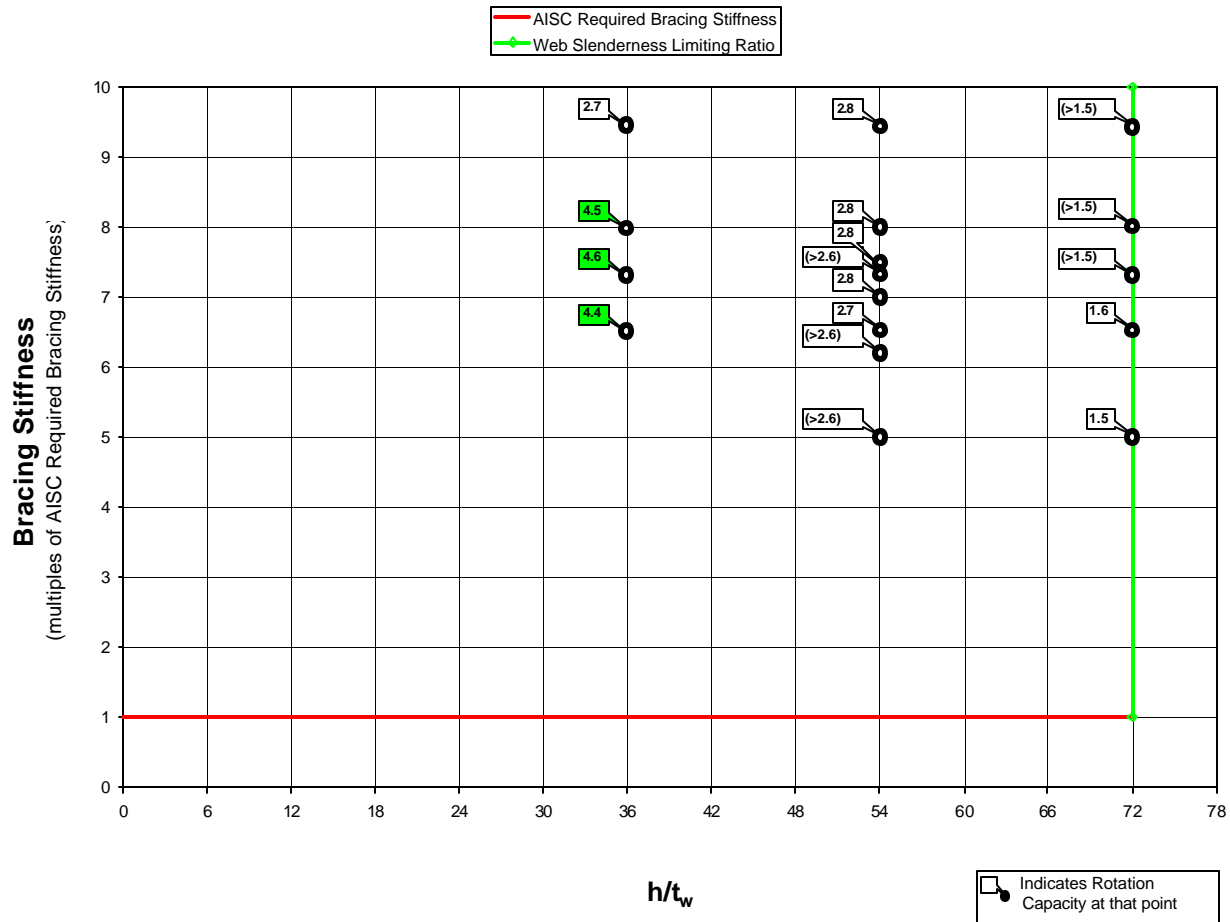
Figure C-59 Interaction Plot: Web Slenderness vs. Bracing Stiffness
($b_f/2t_f$ = 4.5, h/t_w Varies, L_b = 1.5d, Bracing Stiffness Varies)

253
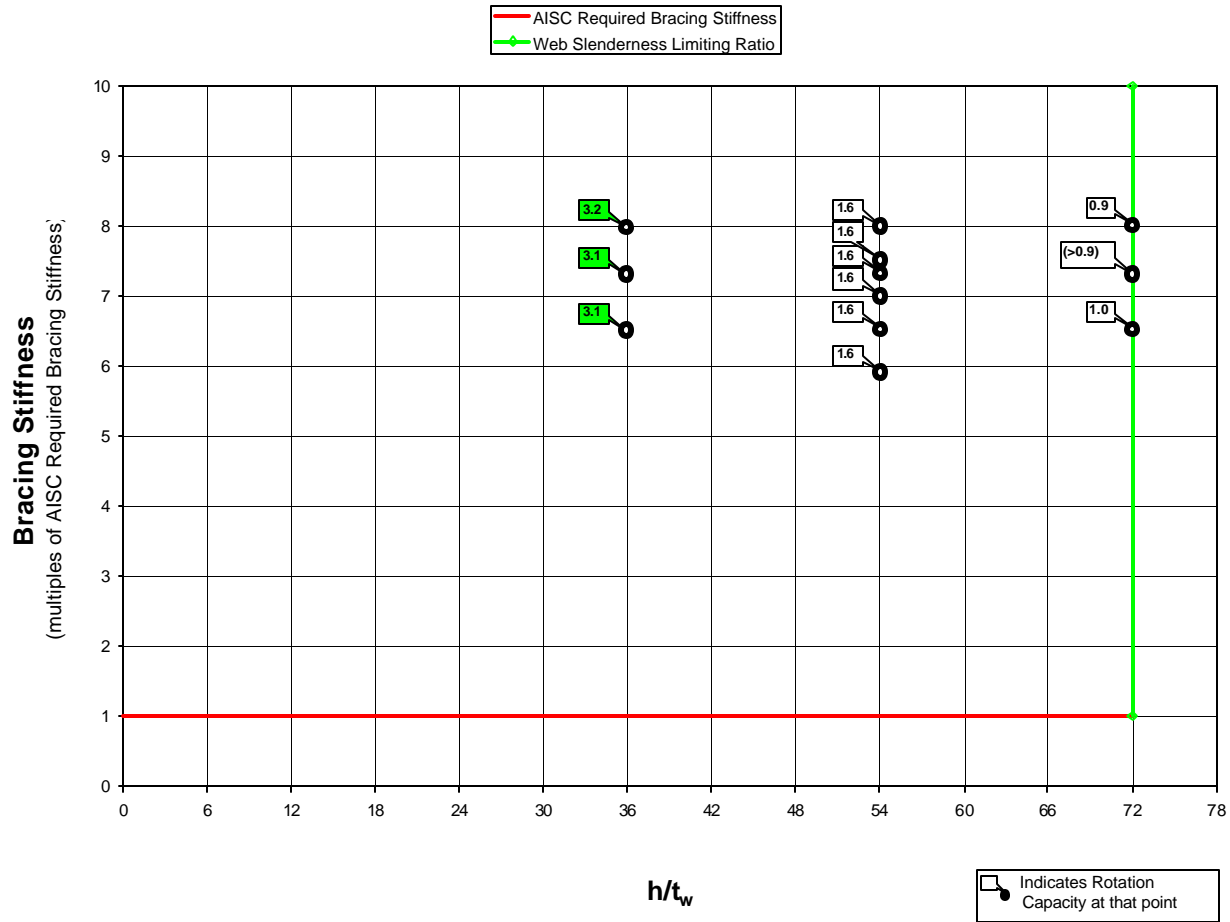
Figure C-60 Interaction Pbt: Web Slenderness vs. Bracing Stiffness
($b_f/2t_f = 4.5$, h/t_w Varies, $L_b = 2d$, Bracing Stiffness Varies)

254
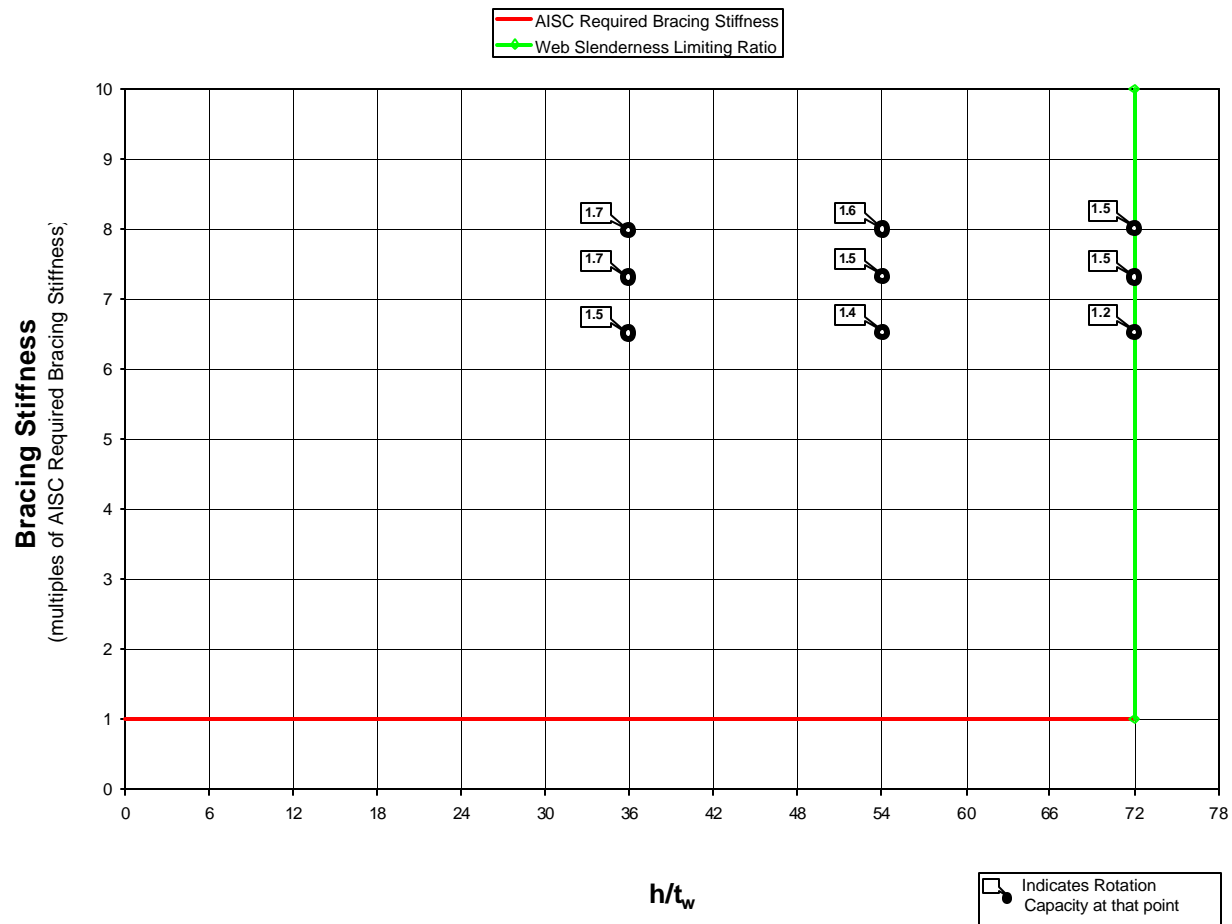
Figure C-61 Interaction Plot: Web Slenderness vs. Bracing Stiffness
($b_f/2t_f = 5.5$, h/t_w Varies, $L_b = 0.5d$, Bracing Stiffness Varies)

255

Web Slenderness vs. Bracing Stiffness

$b_f/2t_f = 5.5$, h/t_w varies, $L_b = 1d$, Bracing Stiffness varies
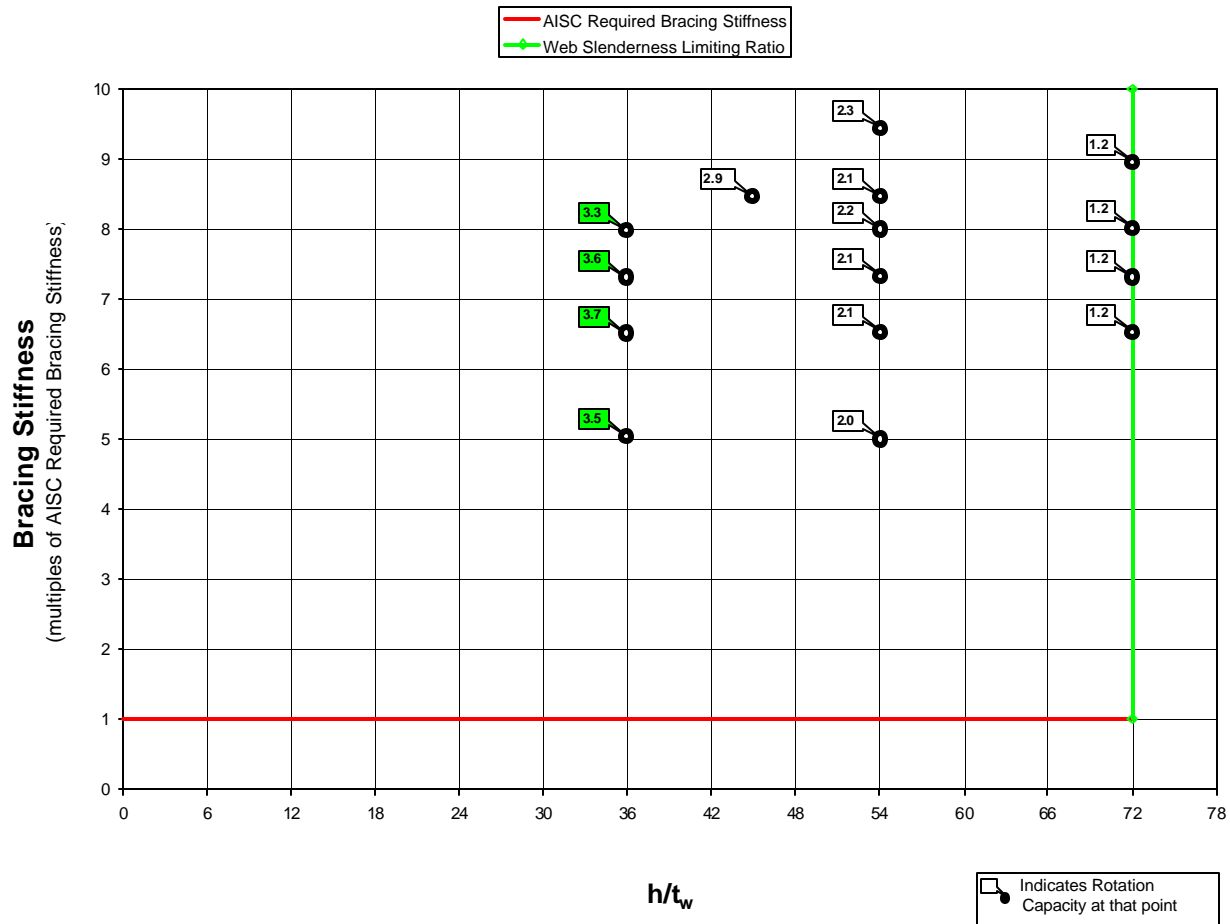
Figure C-62 Interaction Plot: Web Slenderness vs. Bracing Stiffness
($b_f/2t_f = 5.5$, h/t_w Varies, $L_b = 1d$, Bracing Stiffness Varies)

256
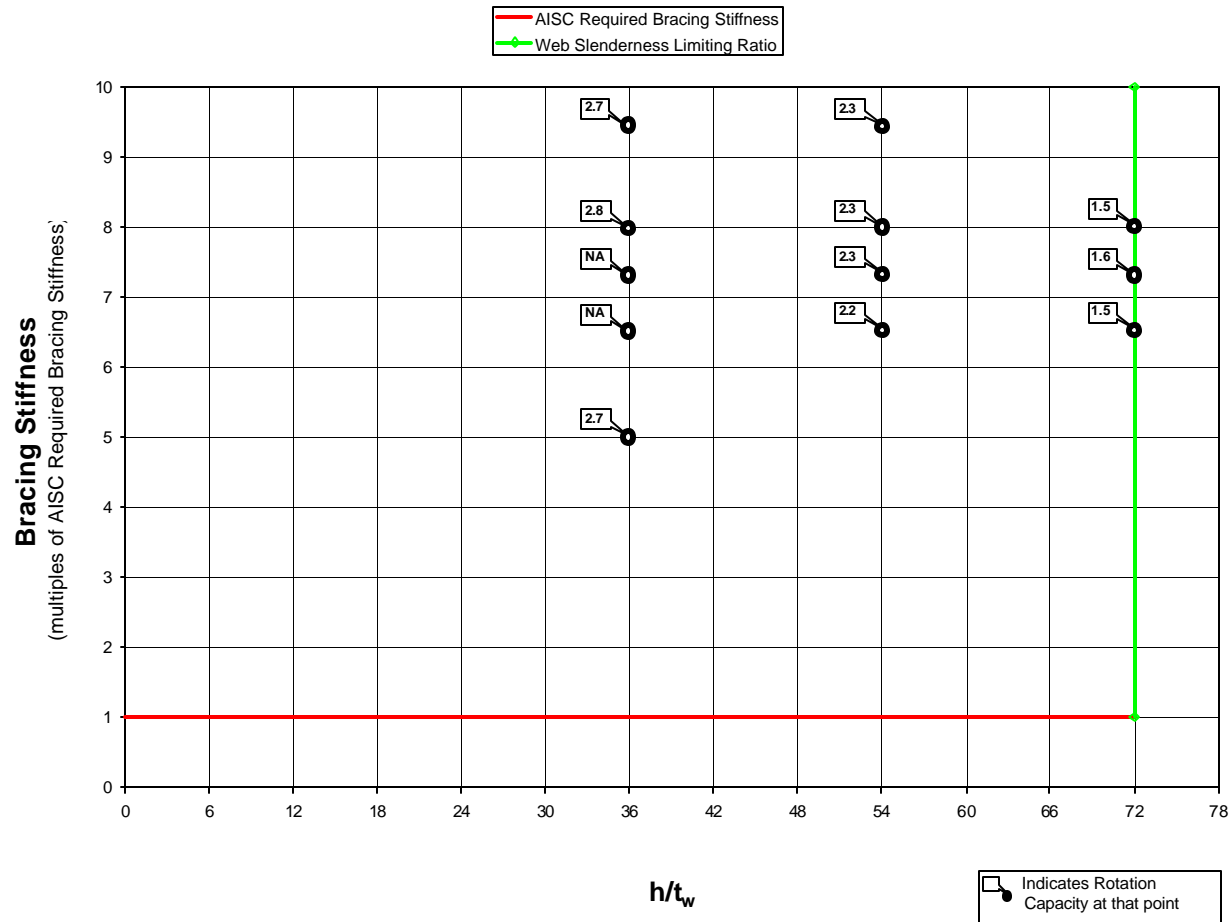
Figure C-63 Interaction Plot: Web Slenderness vs. Bracing Stiffness
($b_f/2t_f$ = 5.5, h/t_w Varies, L_b = 1.5d, Bracing Stiffness Varies)

257
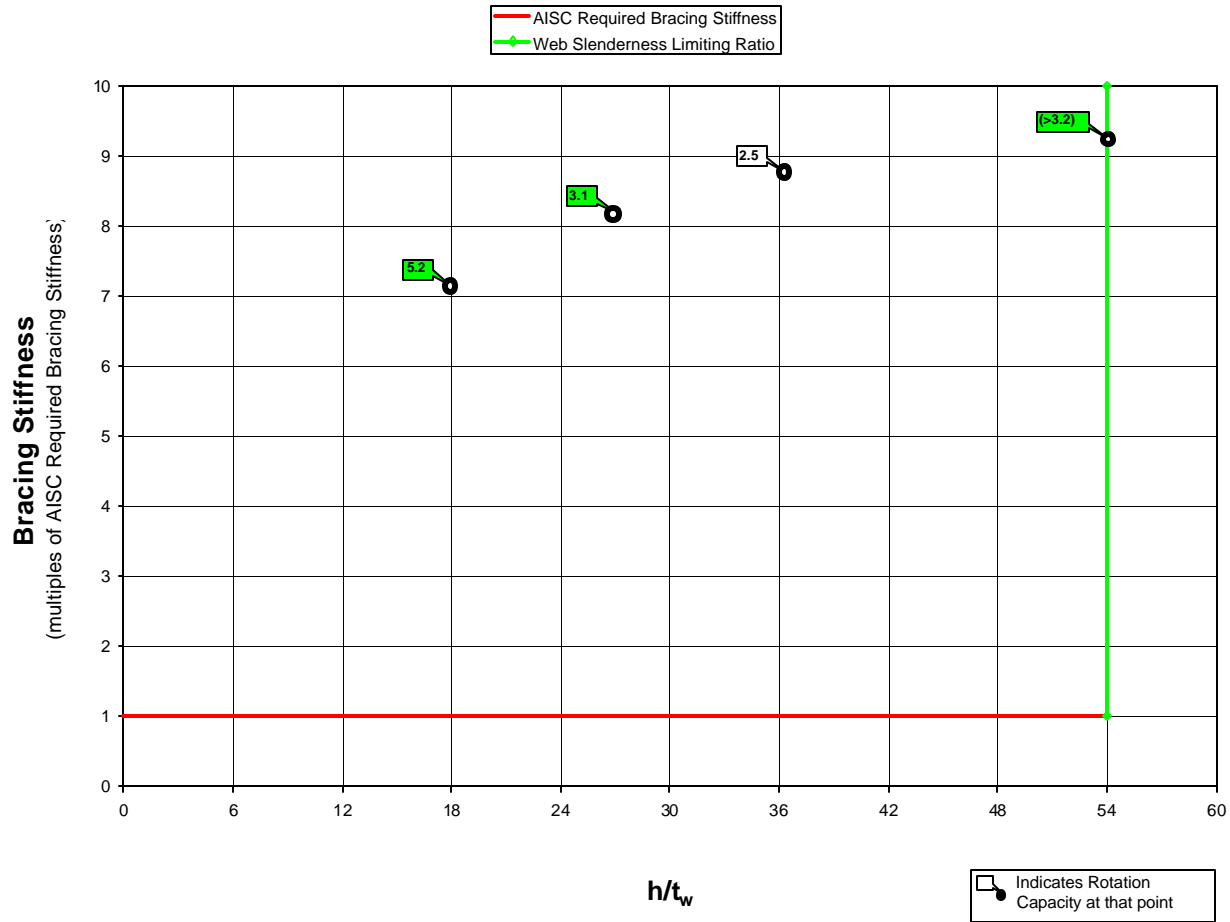
Figure C-64 Interaction Plot: Web Slenderness vs. Bracing Stiffness
($b_f/2t_f$ = 6.0, h/t_w Varies, L_b = 1d, Bracing Stiffness Varies)

258

Web Slenderness vs. Bracing Stiffness

$b_f/2t_f = 6.5$, h/t_w varies, $L_b = 1d$, Bracing Stiffness varies

— AISC Required Bracing Stiffness
— Web Slenderness Limiting Ratio
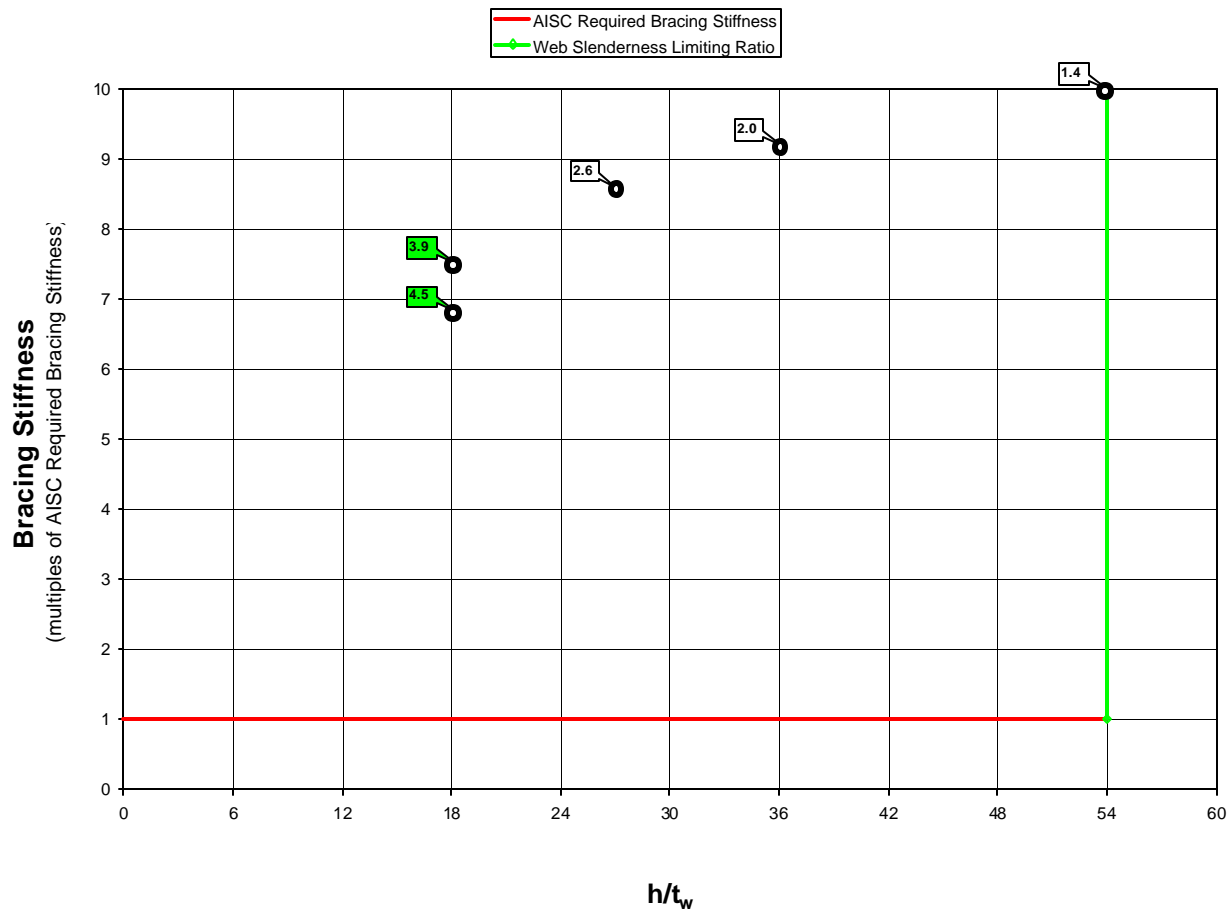
Figure C-65 Interaction Plot: Web Slenderness vs. Bracing Stiffness
($b_f/2t_f = 6.5$, h/t_w Varies, $L_b = 1d$, Bracing Stiffness Varies)

259

Web Slenderness vs. Bracing Stiffness

$b_f/2t_f = 7.34$, h/t_w varies, $L_b = 0.5d$, Bracing Stiffness varies
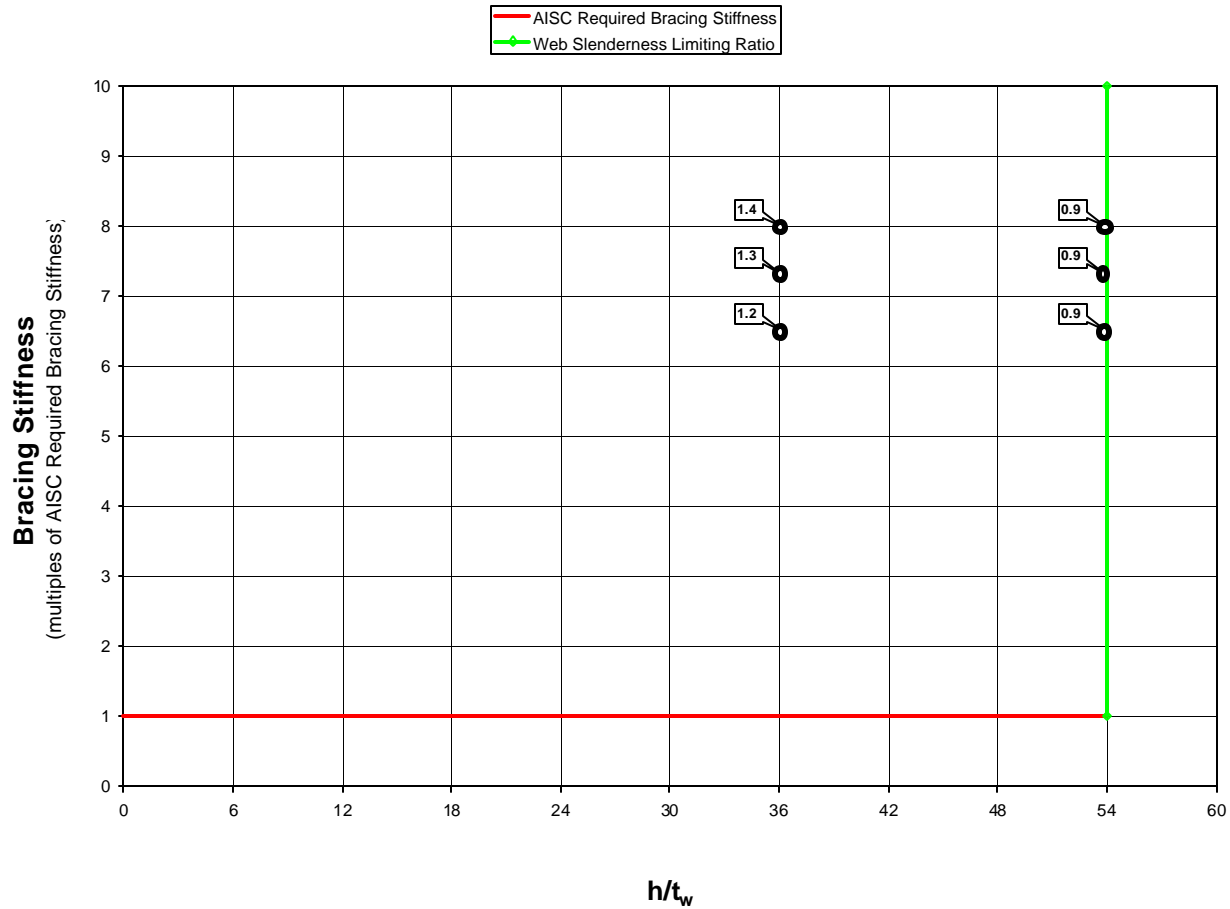
Figure C-66 Interaction Plot: Web Slenderness vs. Bracing Stiffness
($b_f/2t_f = 7.34$, h/t_w Varies, $L_b = 0.5d$, Bracing Stiffness Varies)

260
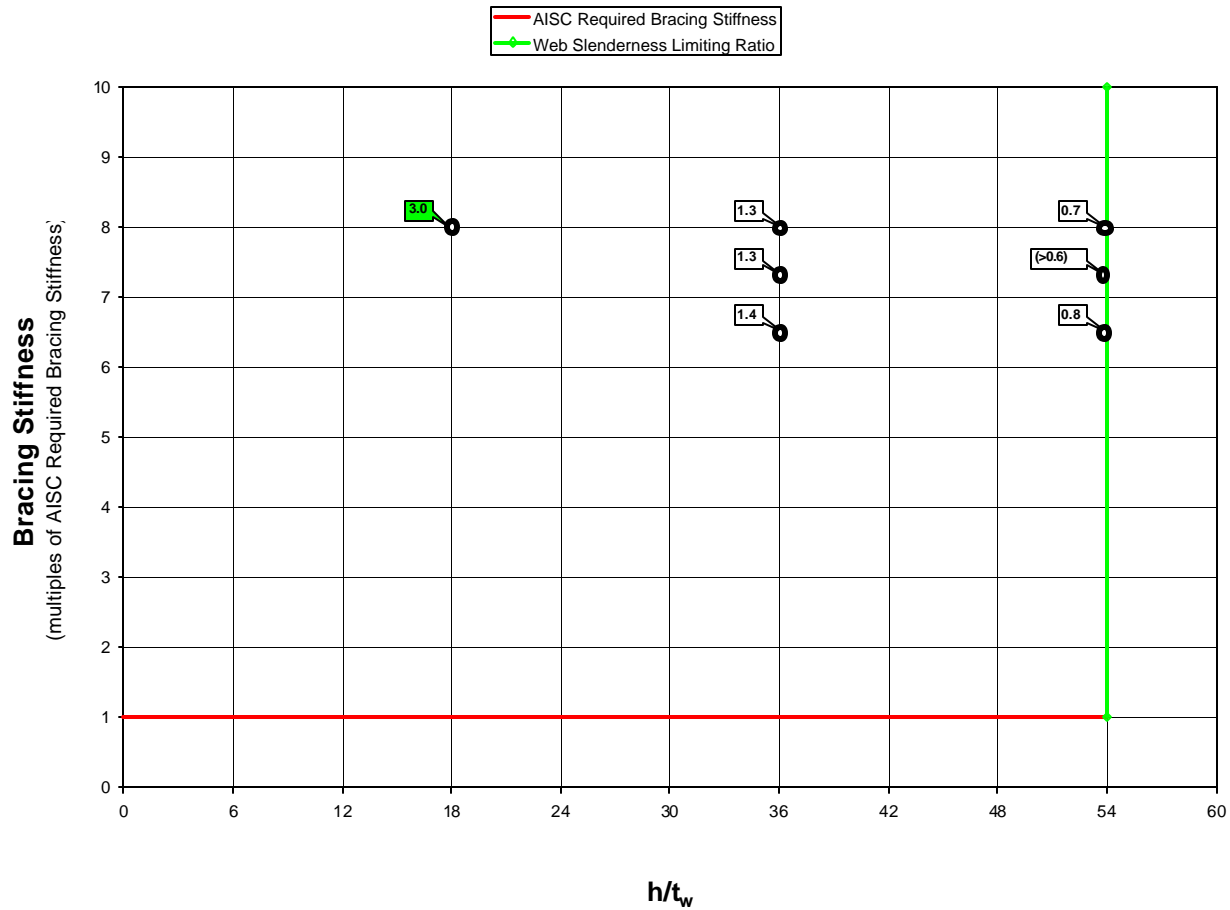
Figure C-67 Interaction Plot: Web Slenderness vs. Bracing Stiffness
($b_f/2t_f$ = 7.34, h/t_w Varies, L_b = 1d, Bracing Stiffness Varies)
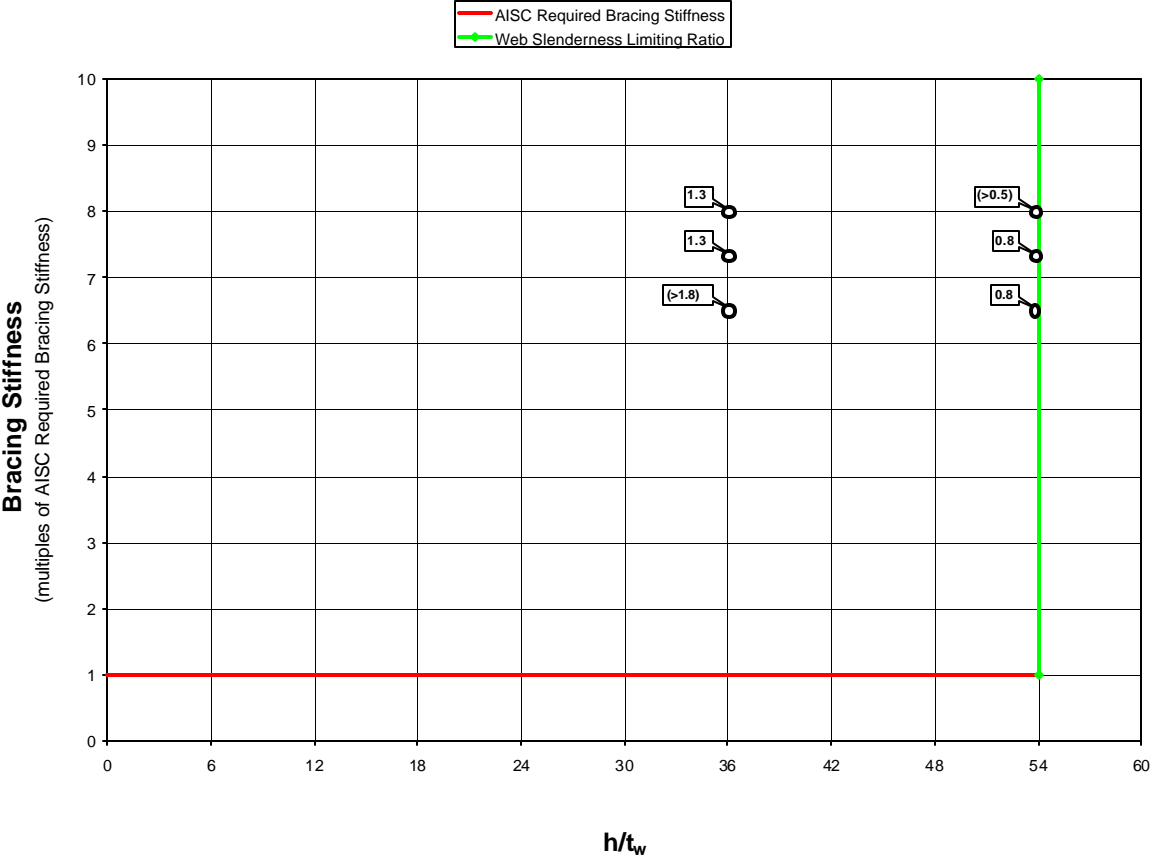
Figure C-68 Interaction Plot: Web Slenderness vs. Bracing Stiffness
($b_f/2t_f = 7.34$, h/t_w Varies, $L_b = 1.5d$, Bracing Stiffness Varies)

Appendix C.5

The fifth type of interaction plot located in this sub-appendix graphs flange slenderness against bracing stiffness. For each combination of web slenderness and unbraced length, one of these plots has been produced. For each of these plots there exist numerous combinations of flange slenderness and bracing stiffness for which finite element tests are run. The corresponding rotation capacity for each of these individual tests is shown at its respective point on the graph.

Figure C-69 Interaction Plot: Flange Slenderness vs. Bracing Stiffness
($b_f/2t_f$ Varies, $h/t_w = 18$, $L_b = 1d$, Bracing Stiffness Varies)

Figure C-70 Interaction Plot: Flange Slenderness vs. Bracing Stiffness
($b_f/2t_f$ Varies, $h/t_w = 27$, $L_b = 1d$, Bracing Stiffness Varies)

Figure C-71 Interaction Plot: Flange Slenderness vs. Bracing Stiffness
($b_f/2t_f$ Varies, $h/t_w = 36$, $L_b = 0.5d$, Bracing Stiffness Varies)
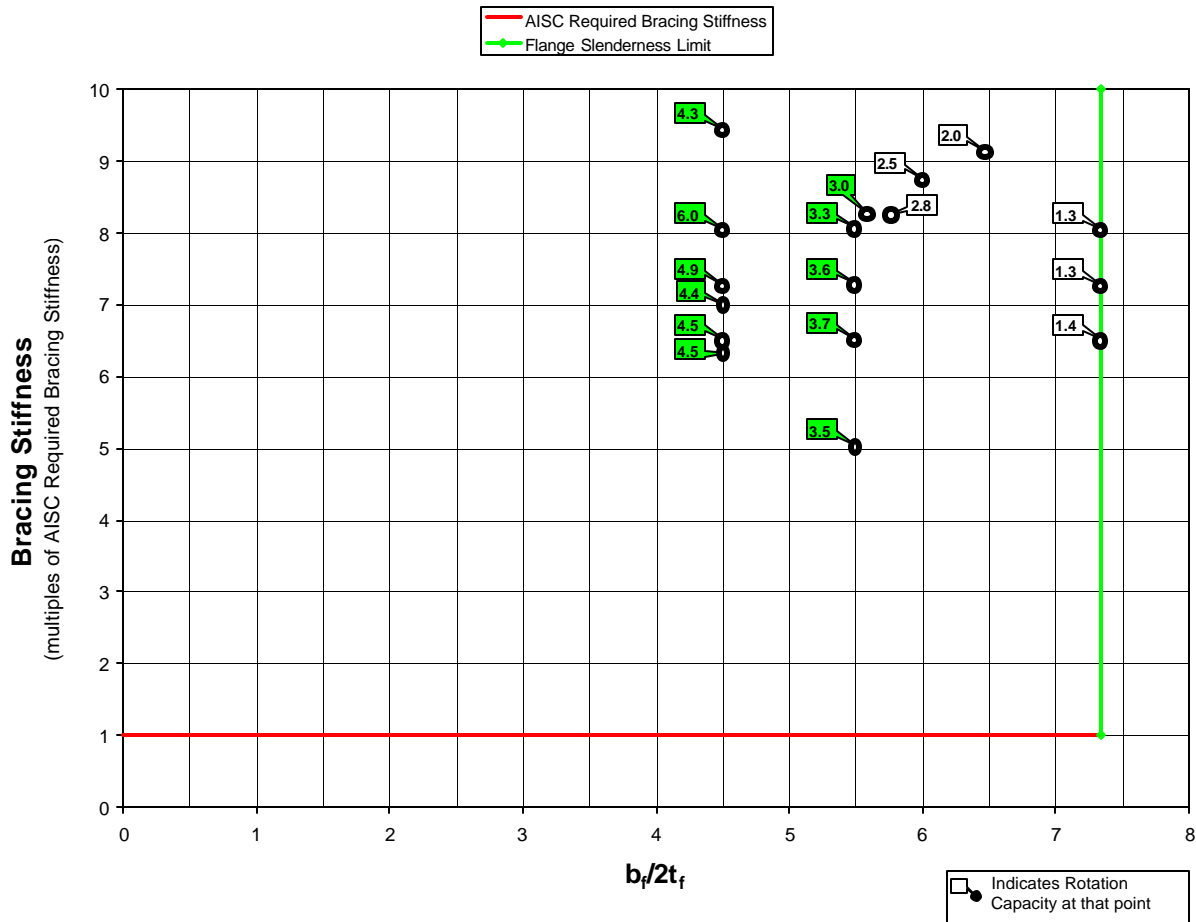
Figure C-72 Interaction Plot: Flange Slenderness vs. Bracing Stiffness
($b_f/2t_f$ Varies, $h/t_w = 36$, $L_b = 1d$, Bracing Stiffness Varies)
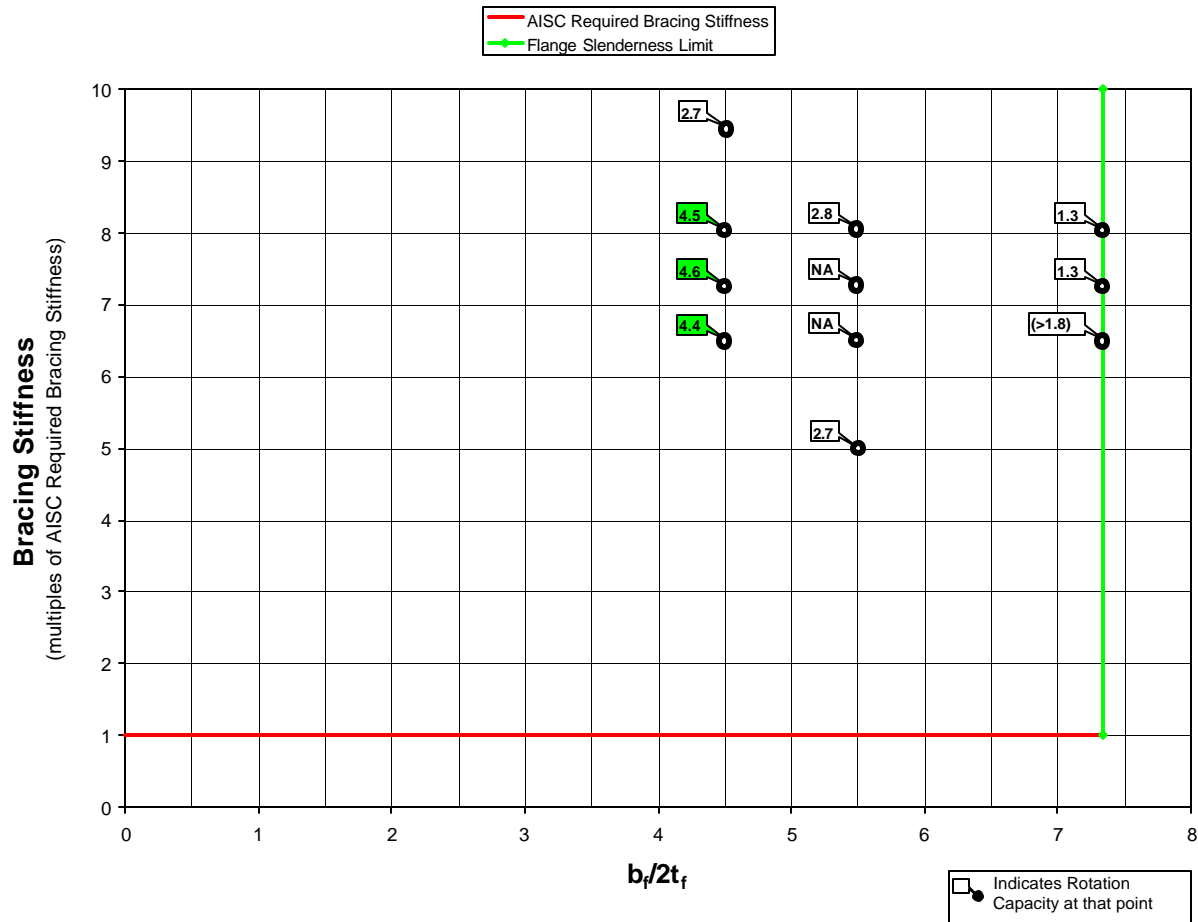
Figure C-73 Interaction Plot: Flange Slenderness vs. Bracing Stiffness
($b_f/2t_f$ Varies, h/t_w = 36, L_b = 1.5d, Bracing Stiffness Varies)
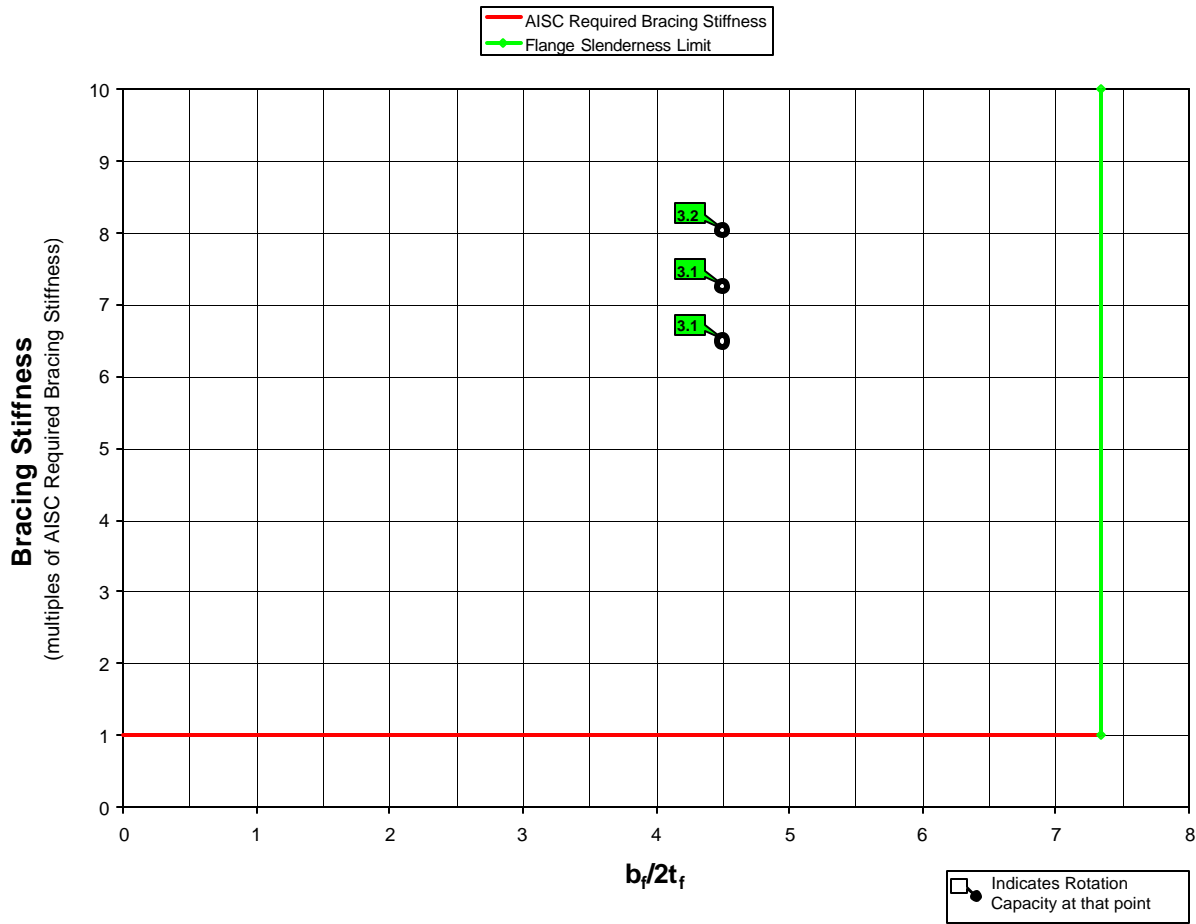
Figure C-74 Interaction Plot: Flange Slenderness vs. Bracing Stiffness
($b_f/2t_f$ Varies, $h/t_w = 36$, $L_b = 2d$, Bracing Stiffness Varies)

Figure C-75 Interaction Plot: Flange Slenderness vs. Bracing Stiffness
($b_f/2t_f$ Varies, $h/t_w = 45$, $L_b = 1d$, Bracing Stiffness Varies)

270

Figure C-76 Interaction Plot: Flange Slenderness vs. Bracing Stiffness
($b_f/2t_f$ Varies, h/t_w = 54, L_b = 0.5d, Bracing Stiffness Varies)

271

Figure C-77 Interaction Plot: Flange Slenderness vs. Bracing Stiffness
($b_f/2t_f$ Varies, $h/t_w = 54$, $L_b = 1d$, Bracing Stiffness Varies)

272

Flange Slenderness vs. Bracing Stiffness

$b_f/2t_f$ varies, $h/t_w = 54$, $L_b = 1.5d$, Bracing Stiffness varies

- AISC Required Bracing Stiffness
- Flange Slenderness Limit

Bracing Stiffness
(multiples of AISC Required Bracing Stiffness)

$b_f/2t_f$

Indicates Rotation
Capacity at that point
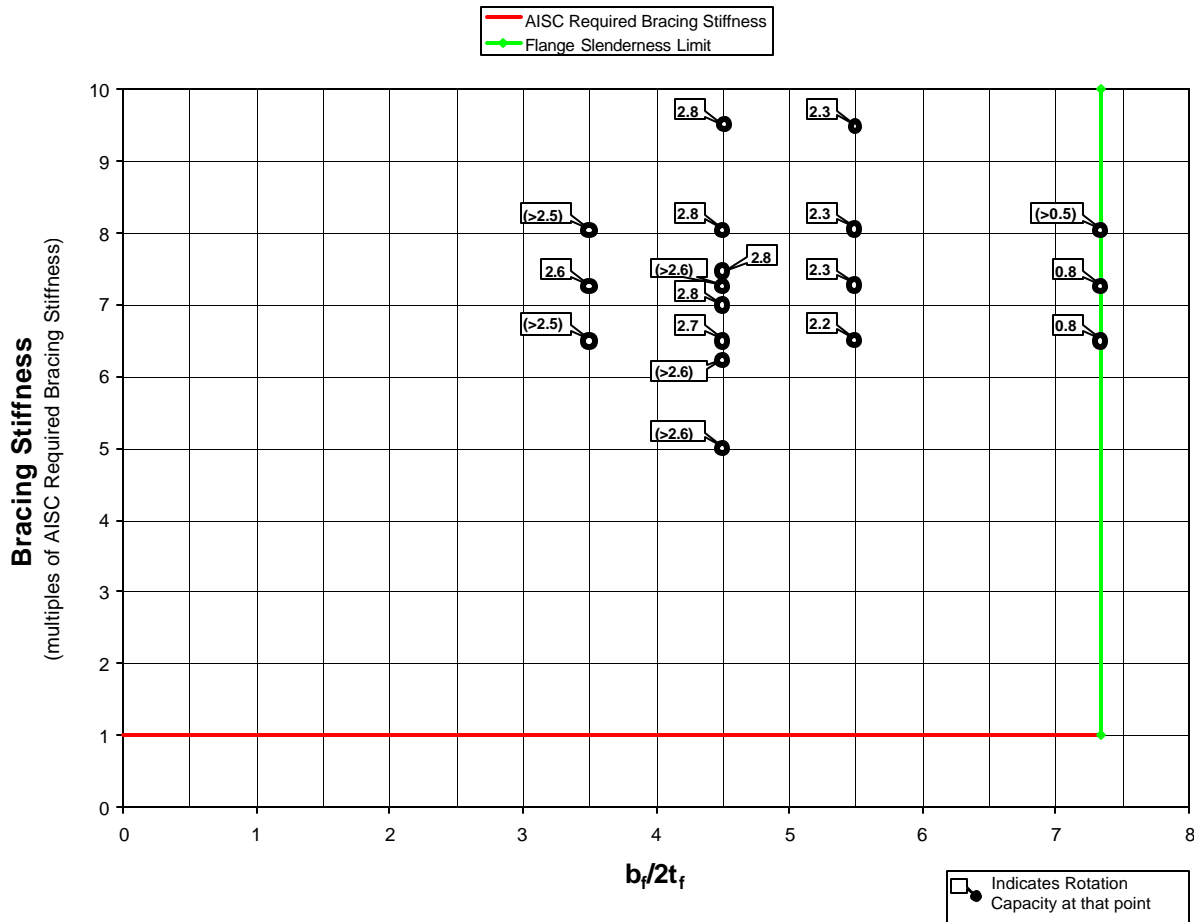
Figure C-78 Interaction Plot: Flange Slenderness vs. Bracing Stiffness
($b_f/2t_f$ Varies, $h/t_w = 54$, $L_b = 1.5d$, Bracing Stiffness Varies)

273

Flange Slenderness vs. Bracing Stiffness

$b_f/2t_f$ varies, $h/t_w = 54$, $L_b = 2d$, Bracing Stiffness varies
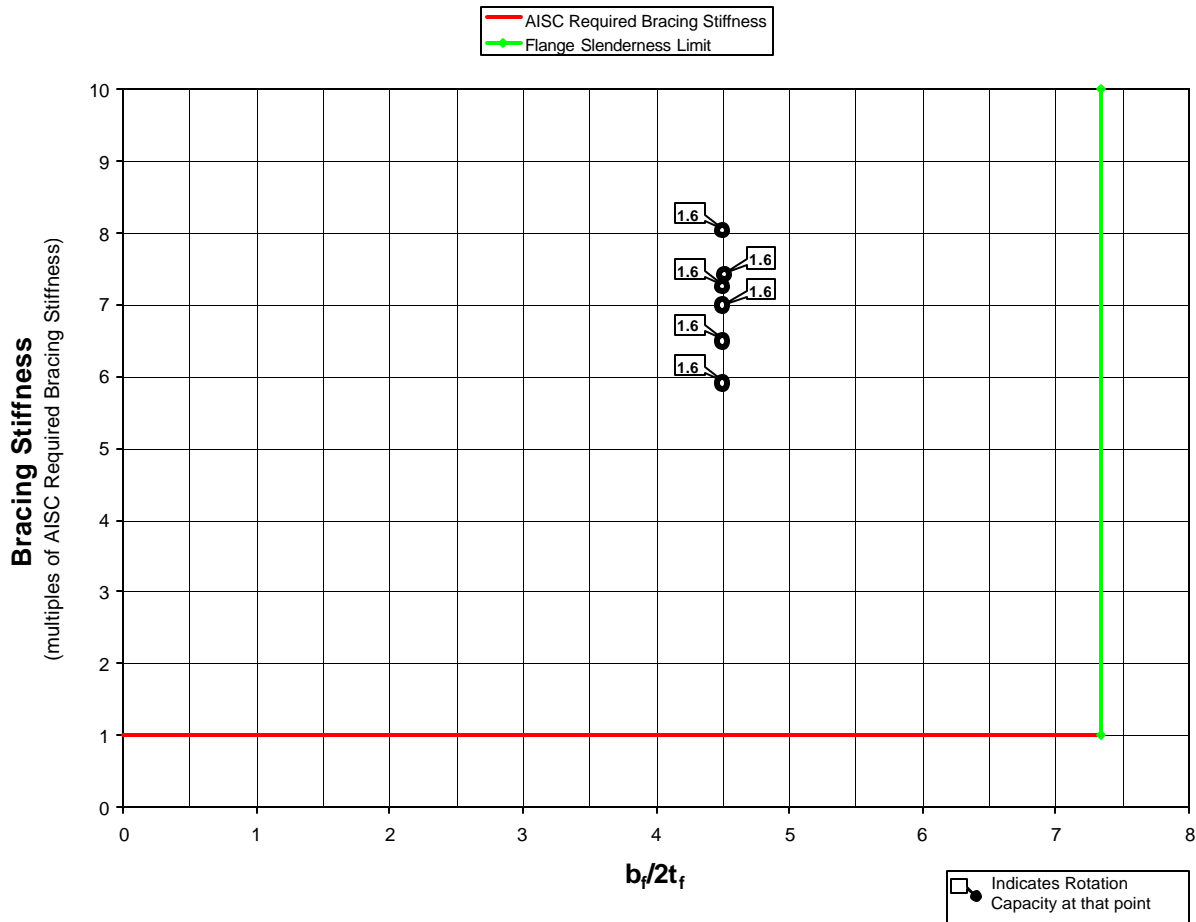
Figure C-79 Interaction Plot: Flange Slenderness vs. Bracing Stiffness
($b_f/2t_f$ Varies, $h/t_w = 54$, $L_b = 2d$, Bracing Stiffness Varies)

Figure C-80 Interaction Plot: Flange Slenderness vs. Bracing Stiffness
($b_f/2t_f$ Varies, $h/t_w = 60$, $L_b = 1d$, Bracing Stiffness Varies)

275

Figure C-81 Interaction Plot: Flange Slenderness vs. Bracing Stiffness
($b_f/2t_f$ Varies, $h/t_w = 66$, $L_b = 1d$, Bracing Stiffness Varies)

276

Figure C-82 Interaction Plot: Flange Slenderness vs. Bracing Stiffness
($b_f/2t_f$ Varies, h/t_w = 72, L_b = 0.5d, Bracing Stiffness Varies)

Figure C-83 Interaction Plot: Flange Slenderness vs. Bracing Stiffness
($b_f/2t_f$ Varies, $h/t_w = 72$, $L_b = 1d$, Bracing Stiffness Varies)

278

Figure C-84 Interaction Plot: Flange Slenderness vs. Bracing Stiffness
($b_f/2t_f$ Varies, $h/t_w = 72$, $L_b = 1.5d$, Bracing Stiffness Varies)

279

Figure C-85 Interaction Plot: Flange Slenderness vs. Bracing Stiffness
($b_f/2t_f$ Varies, $h/t_w = 72$, $L_b = 2d$, Bracing Stiffness Varies)

Appendix C.6

The sixth type of interaction plot located in this sub-appendix graphs unbraced length against bracing stiffness. For each combination of flange slenderness and web slenderness, one of these plots has been produced. For each of these plots there exist numerous combinations of unbraced length and bracing stiffness for which finite element tests are run. The corresponding rotation capacity for each of these individual tests is shown at its respective point on the graph.

Figure C-86 Interaction Plot: Unbraced Length vs. Bracing Stiffness
($b_f/2t_f = 3.5$, $h/t_w = 54$, L_b Varies, Bracing Stiffness Varies)

282

Figure C-87 Interaction Plot: Unbraced Length vs. Bracing Stiffness
($b_f/2t_f = 3.5$, $h/t_w = 72$, L_b Varies, Bracing Stiffness Varies)
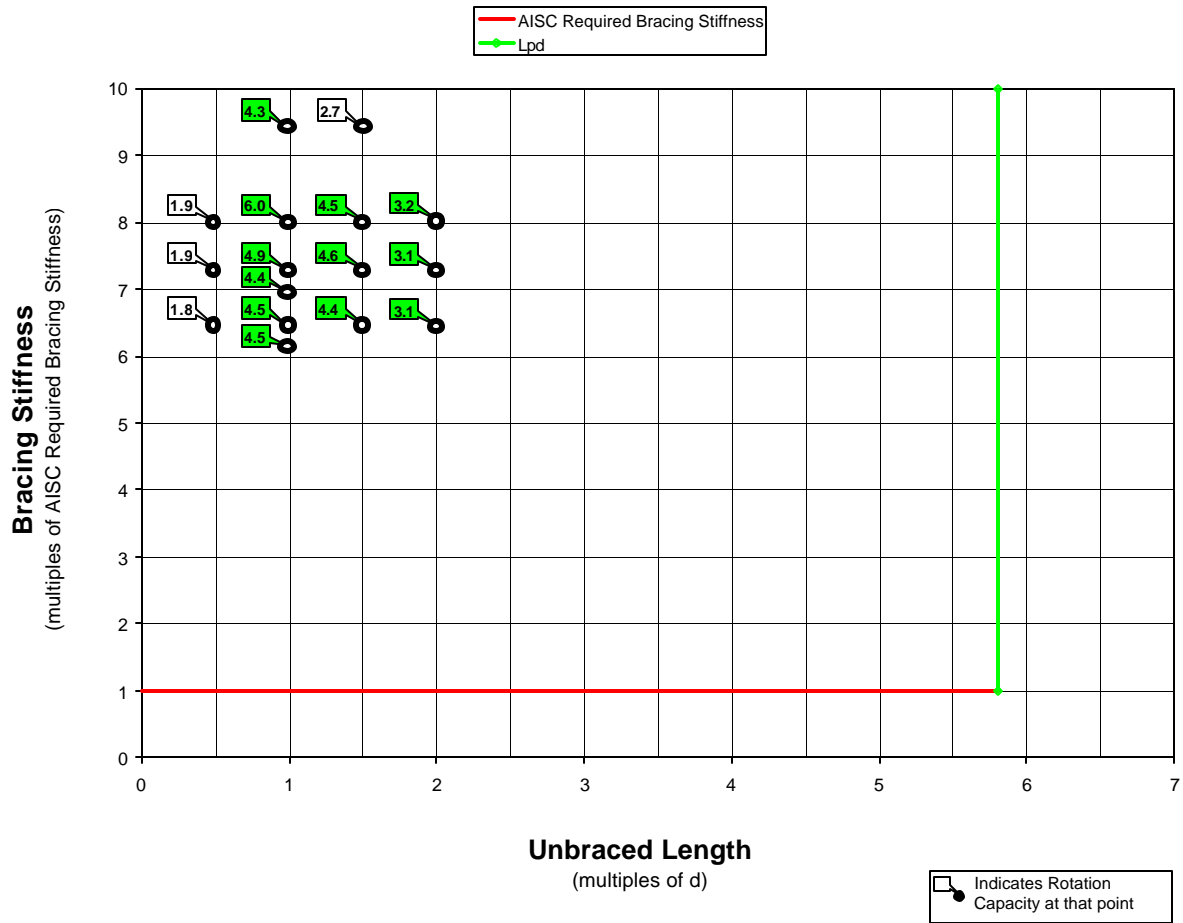
Figure C-88 Interaction Plot: Unbraced Length vs. Bracing Stiffness
($b_f/2t_f$ = 4.5, h/t$_w$ = 36, L$_b$ Varies, Bracing Stiffness Varies)

284
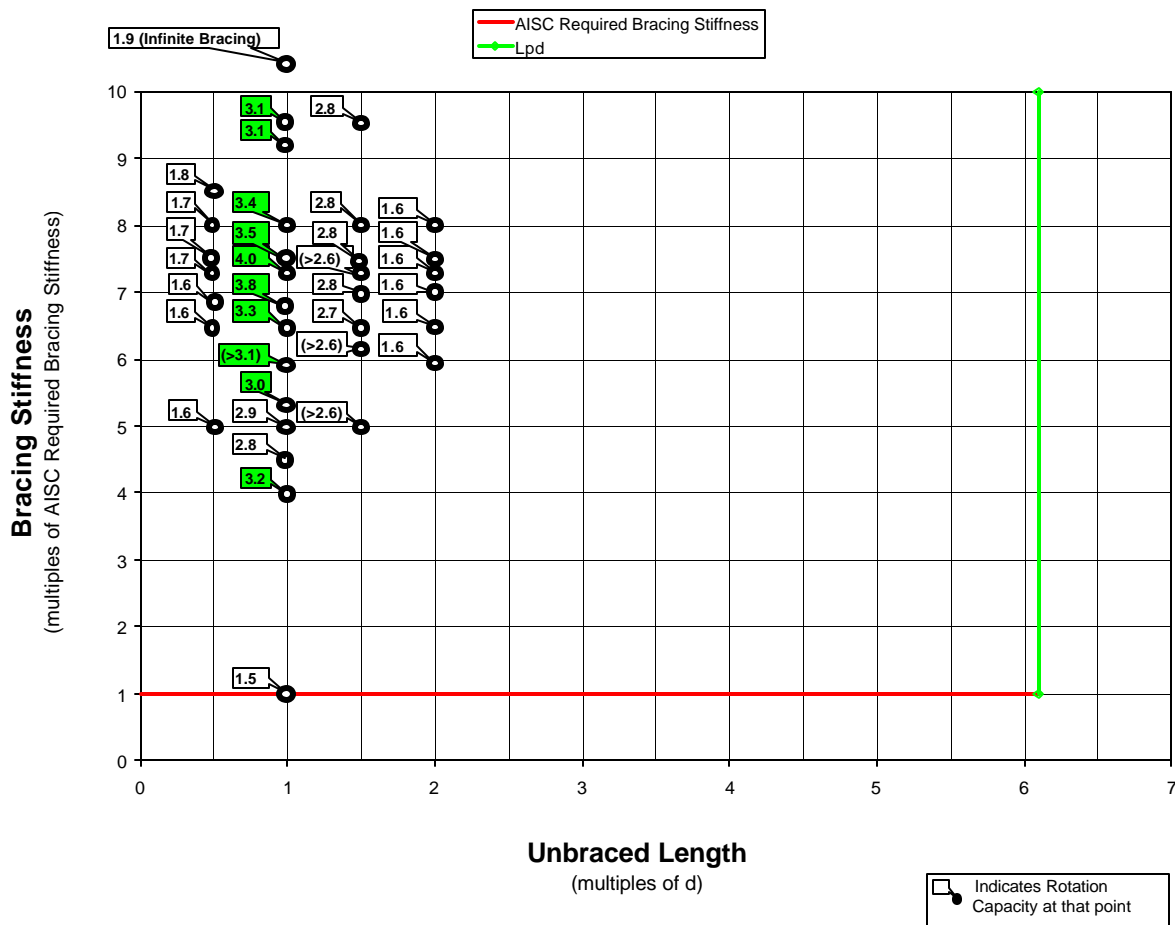
Figure C-89 Interaction Plot: Unbraced Length vs. Bracing Stiffness
($b_f/2t_f$ = 4.5, h/t_w = 54, L_b Varies, Bracing Stiffness Varies)

285

Unbraced Length vs. Bracing Stiffness

$b_f/2t_f = 4.5$, $h/t_w = 72$, L_b varies, Bracing Stiffness varies
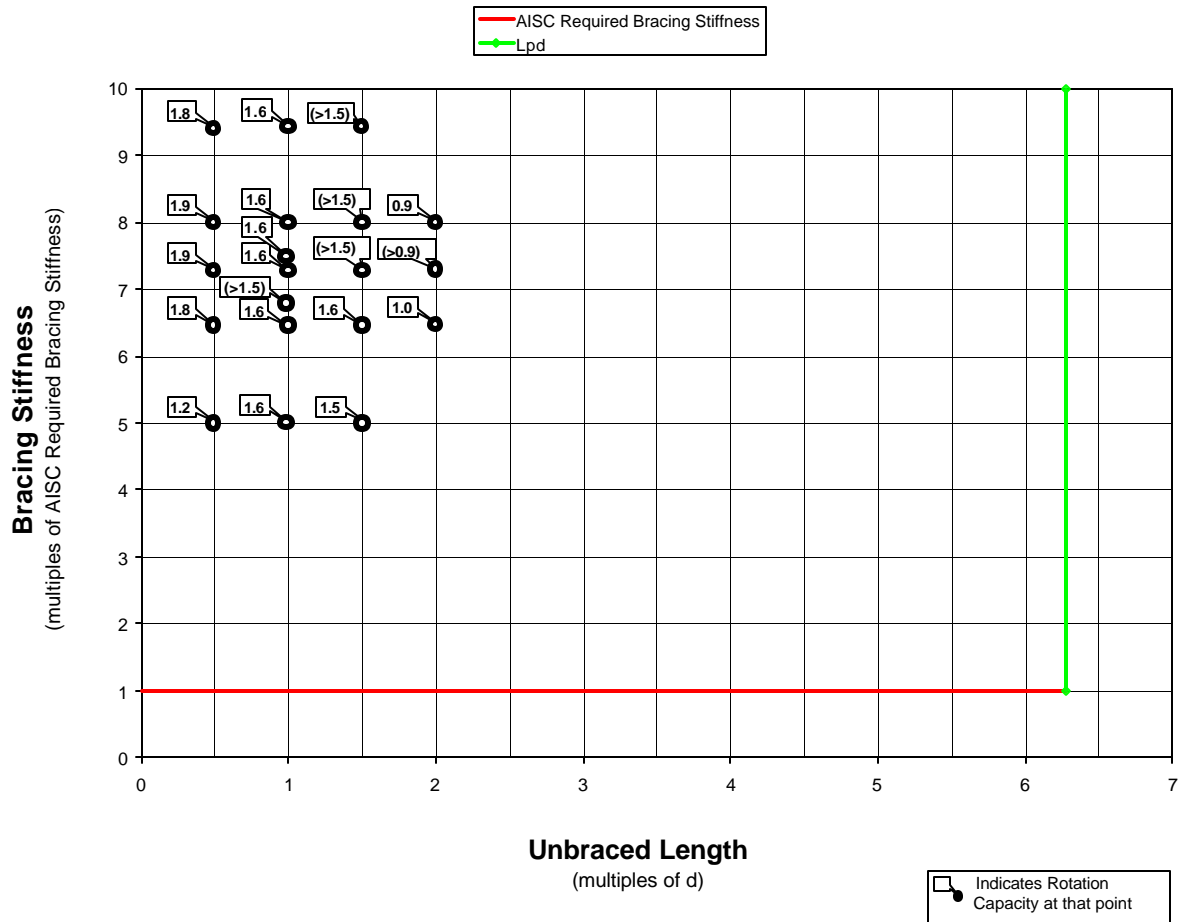
Figure C-90 Interaction Plot: Unbraced Length vs. Bracing Stiffness
($b_f/2t_f = 4.5$, $h/t_w = 72$, L_b Varies, Bracing Stiffness Varies)
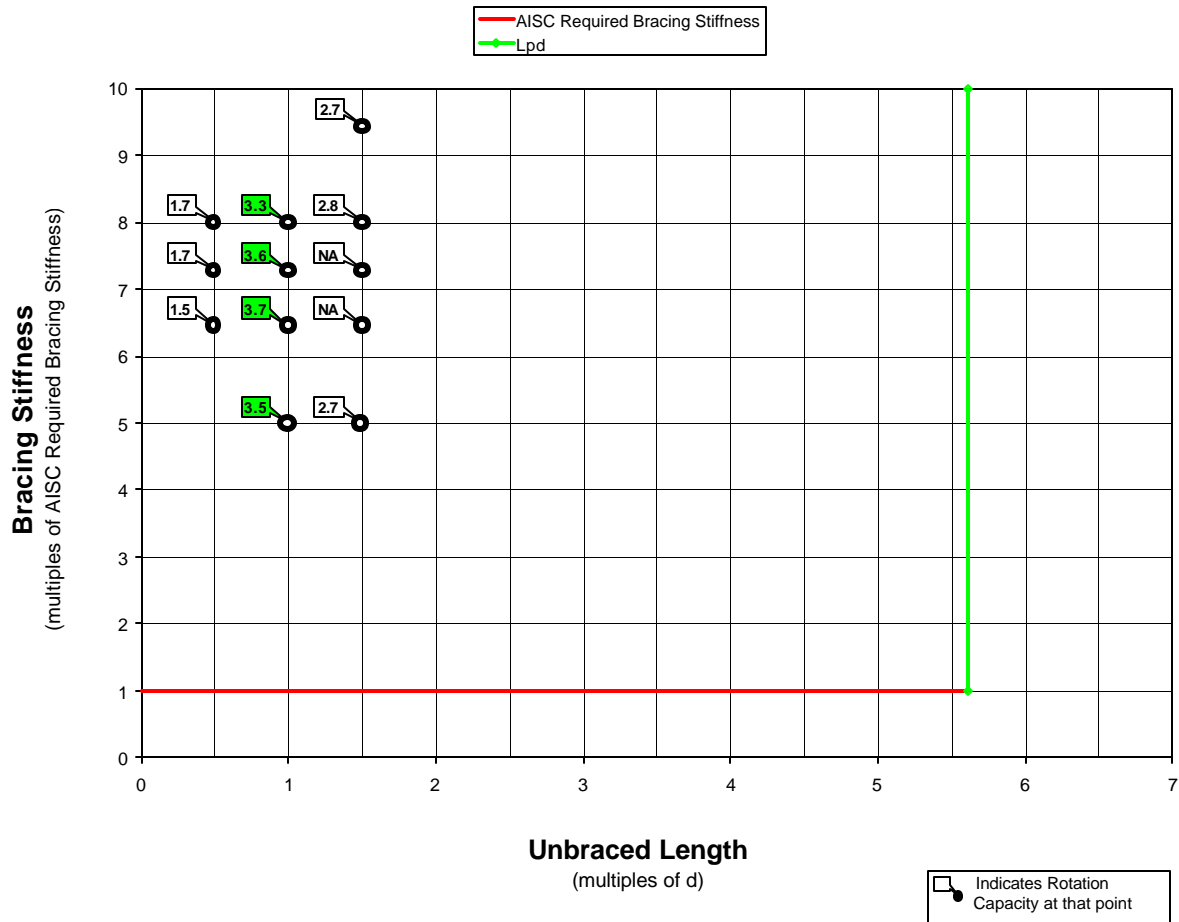
Figure C-91 Interaction Plot: Unbraced Length vs. Bracing Stiffness
($b_f/2t_f = 5.5$, $h/t_w = 36$, L_b Varies, Bracing Stiffness Varies)

287

Unbraced Length vs. Bracing Stiffness

$b_f/2t_f = 5.5$, $h/t_w = 54$, L_b varies, Bracing Stiffness varies
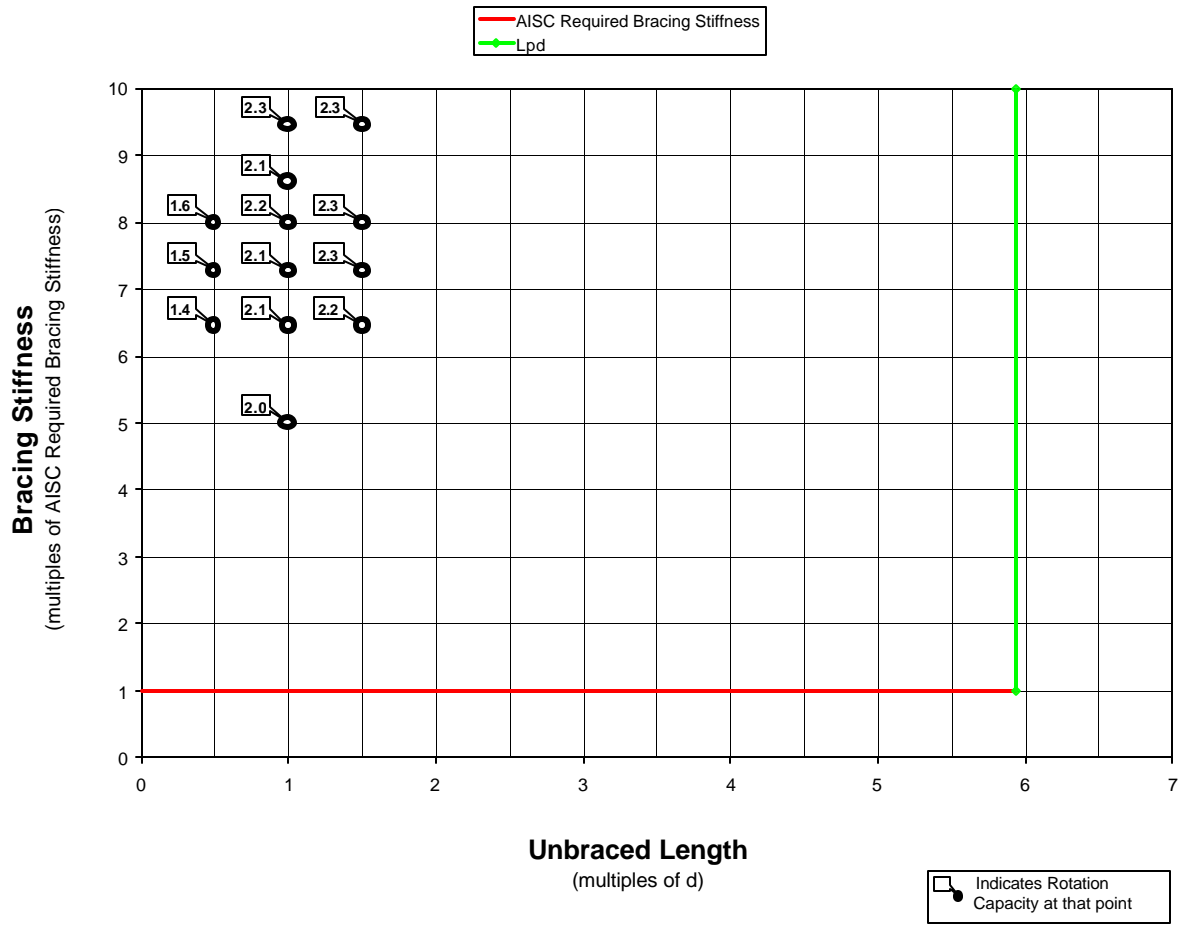
Figure C-92 Interaction Plot: Unbraced Length vs. Bracing Stiffness
($b_f/2t_f = 5.5$, $h/t_w = 54$, L_b Varies, Bracing Stiffness Varies)

288

Unbraced Length vs. Bracing Stiffness

$b_f/2t_f = 5.5$, $h/t_w = 72$, L_b varies, Bracing Stiffness varies
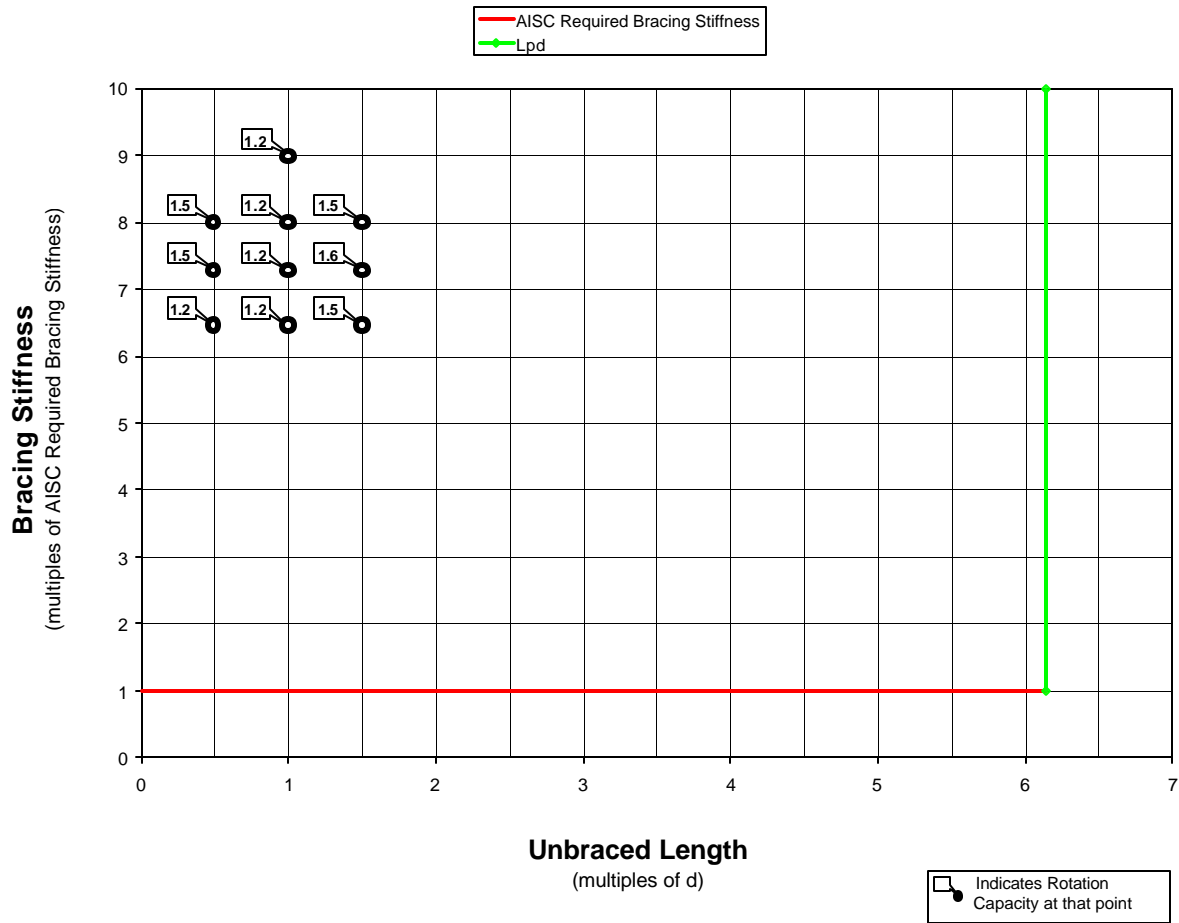
Figure C-93 Interaction Plot: Unbraced Length vs. Bracing Stiffness
($b_f/2t_f = 5.5$, $h/t_w = 72$, L_b Varies, Bracing Stiffness Varies)

289

Figure C-94 Interaction Plot: Unbraced Length vs. Bracing Stiffness
($b_f/2t_f$ = 7.34, h/t_w = 36, L_b Varies, Bracing Stiffness Varies)

Figure C-95 Interaction Plot: Unbraced Length vs. Bracing Stiffness
($b_f/2t_f = 7.34$, $h/t_w = 54$, L_b Varies, Bracing Stiffness Varies)

291

APPENDIX D

APPENDIX D

SAMPLE CALCULATION SHEETS

The following pages provide examples of the excel spreadsheets used for some of the calculations required for this research.

The first page demonstrates how M_p and Θ_p are calculated for $b_f/2t_f = 4.5$ and $h/t_w = 54$. Required as input for this sheet are the beam dimensions and the material properties of the steel (i.e. yield stress and elastic strain modulus). A similar sheet is produced for every combination of flange slenderness and web slenderness.

The remaining pages exemplify the bracing stiffness calculations for the same cross section as above, $b_f/2t_f = 4.5$ and $h/t_w = 54$. Input into these spreadsheets is M_p, Θ_p, r_y (all obtained from the calculation sheet for M_p and Θ_p), and the unbraced length, which varies as part of the parametric study (0.5d, d, 1.5d, or 2d). The spread sheets then calculate the AISC recommended value for the bracing stiffness (β_{br}) as well as the various multiples of this value that were considered in the parametric study. A similar sheet is produced for every combination of flange slenderness, web slenderness, and unbraced length.

Calculation of M_p and Θ_p

$b_f/2t_f$ =	4.5
h/t_w =	54

Enter in the Dimensions of the Beam

Height =	0.781	*
Width =	0.406	
Flange Thickness =	0.0451	
Web Thickness =	0.01363	
L btw Supports =	15.25	
A1 =	0.018311 m^2	
A2 =	0.005015 m^2	
A3 =	0.005015 m^2	
A4 =	0.018311 m^2	

Calculations of the Resultant Forces

R1 =	9899214 N
R2 =	2711333 N
R3 =	2711333 N
R4 =	9899214 N

Enter Stresses in the 4 beam Sections (ksi)			
σ_{y1} =	78.4	=	540627500 Pa **
σ_{y2} =	78.4	=	540627500 Pa **
σ_{y3} =	78.4	=	540627500 Pa **
σ_{y4} =	78.4	=	540627500 Pa **

Cross Sectional Properties	
E =	2E+11 Pa
I_{xx} =	0.006043242 m^4
I_{yy} =	0.000503196 m^4
r_y =	0.103857014 m
S_x =	0.014630776 m^3
P =	2289553.02 N
M_p =	8728920.888 Nm
Θ_p =	0.02753407 rad

* Height is defined from the centroid of the top flange to the centroid of the bottom flange
** Stress in the flange is based on a coupon test from the University of Nebraska.

Figure D-1 Sample Calculation Sheet for M_p and Θ_p

Calculation of Bracing Stiffness

$b_f/2t_f =$	4.5		$M_u =$	8728.9	(KN-m)
$h/t_w =$	54		$r_y =$	0.103857014	(m)
$x (xd) =$	0.05		$x (xd) =$	0.05	

$M_u =$	8728.9	(KN-m)			
$C_d =$	1				
Phi =	1				
$x (xd) =$	0.05		$r_y =$	0.103857014	(m)
$L (x) =$	7.58595	(m)	$L_{pd} =$	4.763921232	(m)
$L_b =$	7.58595				
$H_o =$	0.781	(m)			
β_{br} (AISC)	14733	(KN/m)			
$\beta_{br}/4 =$	3683	(KN/m)			

Factor of β_{br} (AISC)	K ($\beta_{br}/4$) (KN/m)
1	3683
1.5	5525
2	7367
2.5	9208
3	11050
3.5	12892
4	14733
4.5	16575
5	18417
5.5	20258
6	22100
6.5	23942
7	25783
7.3	26888
7.5	27625
8	29466
8.5	31308
9	33150
9.5	34991
10	36833

$K = K_1 = K_2 = K_3 = K_4$
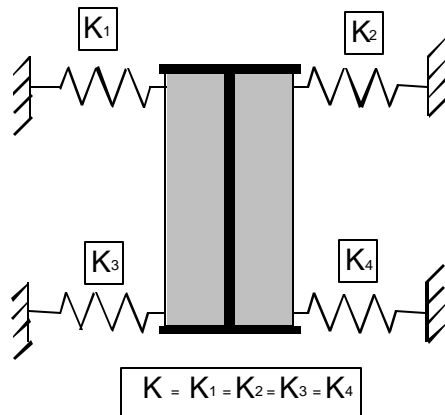
Figure D-2 Sample Calculation Sheet for β_{br} ($L_b = 0.5d$)

Calculation of Bracing Stiffness

$b_f/2t_f =$	4.5	
$h/t_w =$	54	
x (xd) =	1	

$M_u =$	8728.9	(KN-m)
$r_y =$	0.103857014	(m)
x (xd) =	1	

$M_u =$	8728.9	(KN-m)			
$C_d =$	1				
Phi =	1				
x (xd) =	1.00		$r_y =$	0.103857014	(m)
L (x) =	6.844	(m)	$L_{pd} =$	4.763921232	(m)
$L_b =$	6.844				
$H_o =$	0.781	(m)			
β_{br} (AISC)	16330	(KN/m)			
$\beta_{br}/4 =$	4083	(KN/m)			

Factor of β_{br} (AISC)	K ($\beta_{br}/4$) (KN/m)
1	4083
1.5	6124
2	8165
2.5	10207
3	12248
3.5	14289
4	16330
4.5	18372
5	20413
5.5	22454
6	24496
6.5	26537
7	28578
7.3	29803
7.5	30620
8	32661
8.5	34702
9	36744
9.5	38785
10	40826

K_1 K_2

K_3 K_4

$K = K_1 = K_2 = K_3 = K_4$
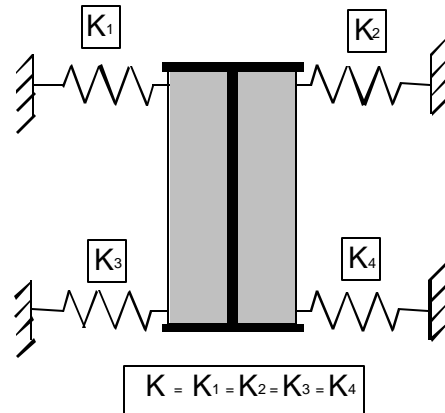
Figure D-3 Sample Calculation Sheet for β_{br} ($L_b = 1d$)

Calculation of Bracing Stiffness

$b_f/2t_f =$	4.5	
$h/t_w =$	54	
x (xd) =	1.5	

$M_u =$	8728.9	(KN-m)
$r_y =$	0.103857014	(m)
x (xd) =	1.5	

$M_u =$	8728.9	(KN-m)			
$C_d =$	1				
Phi =	1				
x (xd) =	1.50		$r_y =$	0.103857014	(m)
L (x) =	6.4535	(m)	$L_{pd} =$	4.763921232	(m)
$L_b =$	6.4535				
$H_o =$	0.781	(m)			
β_{br} (AISC)	17319	(KN/m)			
$\beta_{br}/4 =$	4330	(KN/m)			

Factor of β_{br} (AISC)	K ($\beta_{br}/4$)
	(KN/m)
1	4330
1.5	6494
2	8659
2.5	10824
3	12989
3.5	15154
4	17319
4.5	19483
5	21648
5.5	23813
6	25978
6.5	28143
7	30308
7.3	31606
7.5	32472
8	34637
8.5	36802
9	38967
9.5	41132
10	43297

$$K = K_1 = K_2 = K_3 = K_4$$
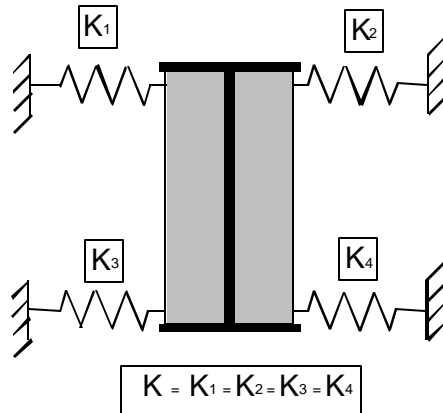
Figure D-4 Sample Calculation Sheet for β_{br} (L_b = 1.5d)

Calculation of Bracing Stiffness

$b_f/2t_f$ =	4.5	
h/t_w =	54	
x (xd) =	2	

M_u =	8728.9	(KN-m)
r_y =	0.103857014	(m)
x (xd) =	2	

M_u =	8728.9	(KN-m)			
C_d =	1				
Phi =	1				
x (xd) =	2.00		r_y =	0.103857014	(m)
L (x) =	6.063	(m)	L_{pd} =	4.763921232	(m)
L_b =	6.063				
H_o =	0.781	(m)			
β_{br} (AISC)	18434	(KN/m)			
$\beta_{br}/4$ =	4609	(KN/m)			

Factor of β_{br} (AISC)	K ($\beta_{br}/4$) (KN/m)
1	4609
1.5	6913
2	9217
2.5	11521
3	13826
3.5	16130
4	18434
4.5	20738
5	23043
5.5	25347
6	27651
6.5	29955
7	32260
7.3	33642
7.5	34564
8	36868
8.5	39172
9	41477
9.5	43781
10	46085

$$K = K_1 = K_2 = K_3 = K_4$$
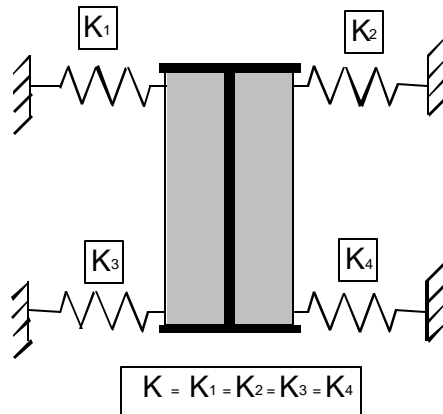
Figure D-5 Sample Calculation Sheet for β_{br} (L_b = 2d)

APPENDIX E

APPENDIX E

COMMON VALUES

The tables included within this appendix provide some of the more commonly used values for M_p, Θ_p, and β_{br}.

Table E-1 Commonly Used Values for M_p

Commonly Used Values for M_p
(KN-m)

Flange Slenderness Ratio	Web Slenderness Ratio							
	18	27	36	45	54	60	66	72
2.5						14732		14596
3						112449		12308
3.5					10906	10810	10730	10665
4					9682	9584	9503	
4.5	10708	9710	9211	8912	8712	8612	8530	8462
5			8474		7970			
5.5			7855	7550	7346			7090
6	8879	7851	7336		6823			
6.5	8455	7420	6901		6384			
7.34	7884		6316		5794			

Table E-2 Commonly Used Values for Θ_p

Commonly Used Values for Θ_p
(rad)

Flange Slenderness Ratio	Web Slenderness Ratio							
	18	27	36	45	54	60	66	72
2.5						0.02690		0.02680
3						0.02704		0.02693
3.5					0.02727	0.02718	0.02711	0.02705
4					0.02740	0.02731	0.02722	
4.5	0.02943	0.02855	0.02806	0.02775	0.02754	0.02743	0.02734	0.02726
5			0.02823		0.02766			
5.5			0.02839	0.02803	0.02778			0.02745
6	0.03018	0.02914	0.02855		0.02790			
6.5	0.03040	0.02933	0.02870		0.02801			
7.34	0.03075		0.02895		0.02820			

Table E-3 Commonly Used Values for β_{br} ($L_b = 0.5d$)

Commonly Used Values for $\mathbf{b}_{br}$ (AISC Recommended Bracing Stiffness)
(KN/m)
(For $L_b = 0.5d$)

		Web Slenderness Ratio		
		36	54	72
Flange Slenderness Ratio	3.5		19301	18875
	4.5	16301	15419	14977
	5.5	13902	13001	12549
	7.34	11178	10254	

Table E-4 Commonly Used Values for β_{br} ($L_b = 1d$)

Commonly Used Values for $\mathbf{b}_{br}$ (AISC Recommended Bracing Stiffness)
(KN/m)
(For $L_b = 1d$)

		Web Slenderness Ratio							
		18	27	36	45	54	60	66	72
Flange Slenderness Ratio	2.5						27560		27308
	3						23292		23028
	3.5					20402	20224	20076	19952
	4					18112	17932	17780	
	4.5	20032	18164	17231	16672	16299	16112	15960	15832
	5			15852		14908			
	5.5			14696	14124	13742			13265
	6	16612	14688	13724		12764			
	6.5	15820	13880	12912		11944			
	7.34	14752		11816		10839			

Table E-5 Commonly Used Values for β_{br} ($L_b = 1.5d$)

Commonly Used Values for b_{br} (AISC Recommended Bracing Stiffness)
(KN/m)
(For $L_b = 1.5d$)

		Web Slenderness Ratio		
		36	54	72
Flange Slenderness Ratio	3.5		21637	21159
	4.5	18274	17285	16790
	5.5	15585	14574	14068
	7.34	12531	11495	

APPENDIX F

APPENDIX F

ABAQUS INPUT FILES

This appendix includes an example of the ABAQUS input file and imperfection file written for this parametric study. Both files are for the case of $b_f/2t_f = 4.5$, $h/t_w = 54$, $L_b = 1d$, and 7.3 times the AISC recommended bracing stiffness.

*HEADING
```
********************************************************************************
**                        PARAMETRIC STUDY                                    *
**                    HIGH STRENGTH STEEL PROJECT                              *
**                                                                            *
** S. S. BEAM   (Using Non linear geometry and Riks Wempner method)           *
** OBTAINING PERTURBATION FOR THE BEAM USING FIRST BUCKLING MODE              *
**                                                                            *
**                 -------X----------------------X--------                     *
**                   7.625          15.25 m        7.625                       *
**                                                                            *
** bf/2tf= 4.5,  h/tw= 54;  1d spacing;   7.3 AISC bracing                     *
**                                                                            *
**   1-horiz;   2- vert;   UNITS: KN-METER                                     *
**                                                                            *
**   ELEMENT TYPE: S4R                                                         *
**   IMPERFECTION --> L/1000                                                   *
**                                                 BUCKLE FILE                 *
********************************************************************************
**
```
*NODE
1, 0, 0, 0
1053, 30.5, 0, 0
7372, 0, 0, -0.203
8424, 30.5, 0, -0.203
14743, 0, 0, -0.406
15795, 30.5, 0, -0.406
16001, 0, 0.781, 0
17053, 30.5, 0.781, 0
23372, 0, 0.781, -0.203
24424, 30.5, 0.781, -0.203
30743, 0, 0.781, -0.406
31795, 30.5, 0.781, -0.406
32001, 0, 0.03, -0.203
33053, 30.5, 0.03, -0.203
57273, 0, 0.75096, -0.203
58325, 30.5, 0.75096, -0.203
**
**STIFFENERS
**
60001, 0, 0, -0.058
60027, 0, 0.781, -0.058
60136, 0, 0, -0.203
60162, 0, 0.781, -0.203
60301, 0, 0, -0.203
60327, 0, 0.781, -0.203
60436, 0, 0, -0.348
60462, 0, 0.781, -0.348
**
60601, 7.625, 0, -0.058
60627, 7.625, 0.781, -0.058
60736, 7.625, 0, -0.203
60762, 7.625, 0.781, -0.203

60901, 7.625, 0, -0.203
60927, 7.625, 0.781, -0.203
61036, 7.625, 0, -0.348
61062, 7.625, 0.781, -0.348
**
61201, 15.25, 0, 0
61227, 15.25, 0.781, 0
61390, 15.25, 0, -0.203
61416, 15.25, 0.781, -0.203
61501, 15.25, 0, -0.203
61527, 15.25, 0.781, -0.203
61690, 15.25, 0, -0.406
61716, 15.25, 0.781, -0.406
**
61801, 22.875, 0, -0.058
61827, 22.875, 0.781, -0.058
61936, 22.875, 0, -0.203
61962, 22.875, 0.781, -0.203
62101, 22.875, 0, -0.203
62127, 22.875, 0.781, -0.203
62236, 22.875, 0, -0.348
62262, 22.875, 0.781, -0.348
**
62401, 30.5, 0, -0.058
62427, 30.5, 0.781, -0.058
62536, 30.5, 0, -0.203
62562, 30.5, 0.781, -0.203
62701, 30.5, 0, -0.203
62727, 30.5, 0.781, -0.203
62836, 30.5, 0, -0.348
62862, 30.5, 0.781, -0.348
**
**INTERMEDIATE STIFFENERS (VARIABLE)
**
63101, 14.46720532, 0, -0.058
63127, 14.46720532, 0.781, -0.058
63236, 14.46720532, 0, -0.203
63262, 14.46720532, 0.781, -0.203
63301, 14.46720532, 0, -0.203
63327, 14.46720532, 0.781, -0.203
63436, 14.46720532, 0, -0.348
63462, 14.46720532, 0.781, -0.348
**
63501, 16.03279468, 0, -0.058
63527, 16.03279468, 0.781, -0.058
63636, 16.03279468, 0, -0.203
63662, 16.03279468, 0.781, -0.203
63701, 16.03279468, 0, -0.203
63727, 16.03279468, 0.781, -0.203
63836, 16.03279468, 0, -0.348
63862, 16.03279468, 0.781, -0.348
****
****

```
*NGEN, NSET=BLFLTIP
1, 1053, 1
*NGEN, NSET=BINT
7372, 8424, 1
*NGEN, NSET=BRFLTIP
14743, 15795, 1
*NGEN, NSET=TLFLTIP
16001, 17053, 1
*NGEN, NSET=TINT
23372, 24424, 1
*NGEN, NSET=TRFLTIP
30743, 31795, 1
*NGEN, NSET=BWEB
32001, 33053, 1
*NGEN, NSET=TWEB
57273, 58325, 1
*********
*********
**
**STIFFENERS
**
*NGEN, NSET=LBS1E
60001, 60027, 1
*NGEN, NSET=LBS1I
60136, 60162, 1
*NGEN, NSET=RBS1I
60301, 60327, 1
*NGEN, NSET=RBS1E
60436, 60462, 1
*NGEN, NSET=LBS2E
60601, 60627, 1
*NGEN, NSET=LBS2I
60736, 60762, 1
*NGEN, NSET=RBS2I
60901, 60927, 1
*NGEN, NSET=RBS2E
61036, 61062, 1
*NGEN, NSET=LBS3E
61201, 61227, 1
*NGEN, NSET=LBS3I
61390, 61416, 1
*NGEN, NSET=RBS3I
61501, 61527, 1
*NGEN, NSET=RBS3E
61690, 61716, 1
*NGEN, NSET=LBS4E
61801, 61827, 1
*NGEN, NSET=LBS4I
61936, 61962, 1
*NGEN, NSET=RBS4I
62101, 62127, 1
*NGEN, NSET=RBS4E
62236, 62262, 1
```

```
*NGEN, NSET=LBS5E
62401, 62427, 1
*NGEN, NSET=LBS5I
62536, 62562, 1
*NGEN, NSET=RBS5I
62701, 62727, 1
*NGEN, NSET=RBS5E
62836, 62862, 1
**
**INTERMEDIATE STIFFENERS
**
*NGEN, NSET=LBS6E
63101, 63127, 1
*NGEN, NSET=LBS6I
63236, 63262, 1
*NGEN, NSET=RBS6I
63301, 63327, 1
*NGEN, NSET=RBS6E
63436, 63462, 1
**
*NGEN, NSET=LBS7E
63501, 63527, 1
*NGEN, NSET=LBS7I
63636, 63662, 1
*NGEN, NSET=RBS7I
63701, 63727, 1
*NGEN, NSET=RBS7E
63836, 63862, 1
********
********
*NFILL, NSET=BLFLANGE
BLFLTIP, BINT, 7, 1053
*NFILL, NSET=BRFLANGE
BINT, BRFLTIP, 7, 1053
*NFILL, NSET=TLFLANGE
TLFLTIP, TINT, 7, 1053
*NFILL, NSET=TRFLANGE
TINT, TRFLTIP, 7, 1053
*NFILL, NSET=WEB
BWEB, TWEB, 24, 1053
********
********
**
**STIFFENERS
**
*NFILL, NSET=LBS1
LBS1E, LBS1I, 5, 27
*NFILL, NSET=RBS1
RBS1I, RBS1E, 5, 27
*NFILL, NSET=LBS2
LBS2E, LBS2I, 5, 27
*NFILL, NSET=RBS2
RBS2I, RBS2E, 5, 27
```

```
*NFILL, NSET=LBS3
LBS3E, LBS3I, 7, 27
*NFILL, NSET=RBS3
RBS3I, RBS3E, 7, 27
*NFILL, NSET=LBS4
LBS4E, LBS4I, 5, 27
*NFILL, NSET=RBS4
RBS4I, RBS4E, 5, 27
*NFILL, NSET=LBS5
LBS5E, LBS5I, 5, 27
*NFILL, NSET=RBS5
RBS5I, RBS5E, 5, 27
**
**INTERMEDIATE STIFFENERS
**
*NFILL, NSET=LBS6
LBS6E, LBS6I, 5, 27
*NFILL, NSET=RBS6
RBS6I, RBS6E, 5, 27
*NFILL, NSET=LBS7
LBS7E, LBS7I, 5, 27
*NFILL, NSET=RBS7
RBS7I, RBS7E, 5, 27
*********
*********
*NSET, NSET=PINNED, GENERATE
264, 15006, 1053
*NSET, NSET=ROLLER, GENERATE
790, 15532, 1053
*NSET, NSET=MIDTOP, GENERATE
16527, 31269, 1053
*NSET, NSET=TFLANGE
TLFLANGE, TRFLANGE
**
*NSET, NSET=LBS1EX, GENERATE
60002, 60026, 1
*NSET, NSET=RBS1EX, GENERATE
60437, 60461, 1
*NSET, NSET=LBS2EX, GENERATE
60602, 60626, 1
*NSET, NSET=RBS2EX, GENERATE
61037, 61061, 1
*NSET, NSET=LBS3EX, GENERATE
61202, 61226, 1
*NSET, NSET=RBS3EX, GENERATE
61691, 61715, 1
*NSET, NSET=LBS4EX, GENERATE
61802, 61826, 1
*NSET, NSET=RBS4EX, GENERATE
62237, 62261, 1
*NSET, NSET=LBS5EX, GENERATE
62402, 62426, 1
```

```
*NSET, NSET=RBS5EX, GENERATE
62837, 62861, 1
*NSET, NSET=LBS6EX, GENERATE
63102, 63126, 1
*NSET, NSET=RBS6EX, GENERATE
63437, 63461, 1
*NSET, NSET=LBS7EX, GENERATE
63502, 63526, 1
*NSET, NSET=RBS7EX, GENERATE
63837, 63861, 1
*NSET, NSET=LBS1BF, GENERATE
60001, 60136, 27
*NSET, NSET=RBS1BF, GENERATE
60301, 60436, 27
*NSET, NSET=LBS2BF, GENERATE
60601, 60736, 27
*NSET, NSET=RBS2BF, GENERATE
60901, 61036, 27
*NSET, NSET=LBS3BF, GENERATE
61201, 61390, 27
*NSET, NSET=RBS3BF, GENERATE
61501, 61690, 27
*NSET, NSET=LBS4BF, GENERATE
61801, 61936, 27
*NSET, NSET=RBS4BF, GENERATE
62101, 62236, 27
*NSET, NSET=LBS5BF, GENERATE
62401, 62536, 27
*NSET, NSET=RBS5BF, GENERATE
62701, 62836, 27
*NSET, NSET=LBS6BF, GENERATE
63101, 63236, 27
*NSET, NSET=RBS6BF, GENERATE
63301, 63436, 27
*NSET, NSET=LBS7BF, GENERATE
63501, 63636, 27
*NSET, NSET=RBS7BF, GENERATE
63701, 63836, 27
*NSET, NSET=LBS1TF, GENERATE
60027, 60162, 27
*NSET, NSET=RBS1TF, GENERATE
60327, 60462, 27
*NSET, NSET=LBS2TF, GENERATE
60627, 60762, 27
*NSET, NSET=RBS2TF, GENERATE
60927, 61062, 27
*NSET, NSET=LBS3TF, GENERATE
61227, 61416, 27
*NSET, NSET=RBS3TF, GENERATE
61527, 61716, 27
*NSET, NSET=LBS4TF, GENERATE
61827, 61962, 27
```

*NSET, NSET=RBS4TF, GENERATE
62127, 62262, 27
*NSET, NSET=LBS5TF, GENERATE
62427, 62562, 27
*NSET, NSET=RBS5TF, GENERATE
62727, 62862, 27
*NSET, NSET=LBS6TF, GENERATE
63127, 63262, 27
*NSET, NSET=RBS6TF, GENERATE
63327, 63462, 27
*NSET, NSET=LBS7TF, GENERATE
63527, 63662, 27
*NSET, NSET=RBS7TF, GENERATE
63727, 63862, 27
*NSET, NSET=LBS1WEB, GENERATE
60137, 60161, 1
*NSET, NSET=RBS1WEB, GENERATE
60302, 60326, 1
*NSET, NSET=LBS2WEB, GENERATE
60737, 60761, 1
*NSET, NSET=RBS2WEB, GENERATE
60902, 60926, 1
*NSET, NSET=LBS3WEB, GENERATE
61391, 61415, 1
*NSET, NSET=RBS3WEB, GENERATE
61502, 61526, 1
*NSET, NSET=LBS4WEB, GENERATE
61937, 61961, 1
*NSET, NSET=RBS4WEB, GENERATE
62102, 62126, 1
*NSET, NSET=LBS5WEB, GENERATE
62537, 62561, 1
*NSET, NSET=RBS5WEB, GENERATE
62702, 62726, 1
*NSET, NSET=LBS6WEB, GENERATE
63237, 63261, 1
*NSET, NSET=RBS6WEB, GENERATE
63302, 63326, 1
*NSET, NSET=LBS7WEB, GENERATE
63637, 63661, 1
*NSET, NSET=RBS7WEB, GENERATE
63702, 63726, 1
**
*NSET, NSET=BF1LBS, GENERATE
2107, 7372, 1053
*NSET, NSET=BF1RBS, GENERATE
7372, 12637, 1053
*NSET, NSET=BF2LBS, GENERATE
2370, 7635, 1053
*NSET, NSET=BF2RBS, GENERATE
7635, 12900, 1053
*NSET, NSET=BF3LBS, GENERATE
527, 7898, 1053

```
*NSET, NSET=BF3RBS, GENERATE
7898, 15269, 1053
*NSET, NSET=BF4LBS, GENERATE
2896, 8161, 1053
*NSET, NSET=BF4RBS, GENERATE
8161, 13426, 1053
*NSET, NSET=BF5LBS, GENERATE
3159, 8424, 1053
*NSET, NSET=BF5RBS, GENERATE
8424, 13689, 1053
*NSET, NSET=BF6LBS, GENERATE
2606, 7871, 1053
*NSET, NSET=BF6RBS, GENERATE
7871, 13136, 1053
*NSET, NSET=BF7LBS, GENERATE
2660, 7925, 1053
*NSET, NSET=BF7RBS, GENERATE
7925, 13190, 1053
*NSET, NSET=TF1LBS, GENERATE
18107, 23372, 1053
*NSET, NSET=TF1RBS, GENERATE
23372, 28637, 1053
*NSET, NSET=TF2LBS, GENERATE
18370, 23635, 1053
*NSET, NSET=TF2RBS, GENERATE
23635, 28900, 1053
*NSET, NSET=TF3LBS, GENERATE
16527, 23898, 1053
*NSET, NSET=TF3RBS, GENERATE
23898, 31269, 1053
*NSET, NSET=TF4LBS, GENERATE
18896, 24161, 1053
*NSET, NSET=TF4RBS, GENERATE
24161, 29426, 1053
*NSET, NSET=TF5LBS, GENERATE
19159, 24424, 1053
*NSET, NSET=TF5RBS, GENERATE
24424, 29689, 1053
*NSET, NSET=TF6LBS, GENERATE
18606, 23871, 1053
*NSET, NSET=TF6RBS, GENERATE
23871, 29136, 1053
*NSET, NSET=TF7LBS, GENERATE
18660, 23925, 1053
*NSET, NSET=TF7RBS, GENERATE
23925, 29190, 1053
*NSET, NSET=WEB1BS, GENERATE
32001, 57273, 1053
*NSET, NSET=WEB2BS, GENERATE
32264, 57536, 1053
*NSET, NSET=WEB3BS, GENERATE
32527, 57799, 1053
```

*NSET, NSET=WEB4BS, GENERATE
32790, 58062, 1053
*NSET, NSET=WEB5BS, GENERATE
33053, 58325, 1053
*NSET, NSET=WEB6BS, GENERATE
32500, 57772, 1053
*NSET, NSET=WEB7BS, GENERATE
32554, 57826, 1053
****
****
*ELEMENT, TYPE=S4R
1, 1, 1054, 1055, 2
*ELGEN, ELSET=BFLANGE
1, 1052, 1, 1, 14, 1053, 1052
**
*ELEMENT, TYPE=S4R
16001, 16001, 17054, 17055, 16002
*ELGEN, ELSET=TFLANGEL
16001, 263, 1, 1, 14, 1053, 263
**
*ELEMENT, TYPE=S4R
19683, 16264, 17317, 17318, 16265
*ELGEN, ELSET=TFLANGEM
19683, 526, 1, 1, 14, 1053, 526
**
*ELEMENT, TYPE=S4R
27047, 16790, 17843, 17844, 16791
*ELGEN, ELSET=TFLANGER
27047, 263, 1, 1, 14, 1053, 263
**
*ELEMENT, TYPE=S4R
32001, 7372, 32001, 32002, 7373
*ELGEN, ELSET=BWEB
32001, 1052, 1, 1
**
*ELEMENT, TYPE=S4R
33053, 32001, 33054, 33055, 32002
*ELGEN, ELSET=WEB
33053, 1052, 1, 1, 24, 1053, 1052
**
*ELEMENT, TYPE=S4R
58301, 57273, 23372, 23373, 57274
*ELGEN, ELSET=TWEB
58301, 1052, 1, 1
**
**STIFFENERS
**
*ELEMENT, TYPE=S4R
60001, 60001, 60028, 60029, 60002
*ELGEN, ELSET=LBS1
60001, 26, 1, 1, 5, 27, 26
*ELEMENT, TYPE=S4R
60301, 60301, 60328, 60329, 60302

```
*ELGEN, ELSET=RBS1
60301, 26, 1, 1, 5, 27, 26
*ELEMENT, TYPE=S4R
60601, 60601, 60628, 60629, 60602
*ELGEN, ELSET=LBS2
60601, 26, 1, 1, 5, 27, 26
*ELEMENT, TYPE=S4R
60901, 60901, 60928, 60929, 60902
*ELGEN, ELSET=RBS2
60901, 26, 1, 1, 5, 27, 26
**
*ELEMENT, TYPE=S4R
61201, 61201, 61228, 61229, 61202
*ELGEN, ELSET=LBS3
61201, 26, 1, 1, 7, 27, 26
*ELEMENT, TYPE=S4R
61501, 61501, 61528, 61529, 61502
*ELGEN, ELSET=RBS3
61501, 26, 1, 1, 7, 27, 26
**
*ELEMENT, TYPE=S4R
61801, 61801, 61828, 61829, 61802
*ELGEN, ELSET=LBS4
61801, 26, 1, 1, 5, 27, 26
*ELEMENT, TYPE=S4R
62101, 62101, 62128, 62129, 62102
*ELGEN, ELSET=RBS4
62101, 26, 1, 1, 5, 27, 26
**
*ELEMENT, TYPE=S4R
62401, 62401, 62428, 62429, 62402
*ELGEN, ELSET=LBS5
62401, 26, 1, 1, 5, 27, 26
*ELEMENT, TYPE=S4R
62701, 62701, 62728, 62729, 62702
*ELGEN, ELSET=RBS5
62701, 26, 1, 1, 5, 27, 26
**
**INTERMEDIATE STIFFENERS
**
*ELEMENT, TYPE=S4R
63101, 63101, 63128, 63129, 63102
*ELGEN, ELSET=LBS6
63101, 26, 1, 1, 5, 27, 26
*ELEMENT, TYPE=S4R
63301, 63301, 63328, 63329, 63302
*ELGEN, ELSET=RBS6
63301, 26, 1, 1, 5, 27, 26
**
*ELEMENT, TYPE=S4R
63501, 63501, 63528, 63529, 63502
*ELGEN, ELSET=LBS7
63501, 26, 1, 1, 5, 27, 26
```

```
*ELEMENT, TYPE=S4R
63701, 63701, 63728, 63729, 63702
*ELGEN, ELSET=RBS7
63701, 26, 1, 1, 5, 27, 26
********
********
**
**FLANGE THICKNESS
**
*SHELL SECTION, MATERIAL=STEEL, ELSET=BFLANGE
0.045
*SHELL SECTION, MATERIAL=STEEL, ELSET=TFLANGEL
0.045
*SHELL SECTION, MATERIAL=STEEL, ELSET=TFLANGER
0.045
*SHELL SECTION, MATERIAL=STEEL, ELSET=TFLANGEM
0.045
**
**WEB THICKNESS
**
*SHELL SECTION, MATERIAL=STEEL, ELSET=BWEB
0.01363
*SHELL SECTION, MATERIAL=STEEL, ELSET=TWEB
0.01363
*SHELL SECTION, MATERIAL=STEEL, ELSET=WEB
0.01363
**
**STIFFENER THICKNESS
**
*SHELL SECTION, MATERIAL=STEEL, ELSET=LBS1
0.012
*SHELL SECTION, MATERIAL=STEEL, ELSET=RBS1
0.012
*SHELL SECTION, MATERIAL=STEEL, ELSET=LBS2
0.012
*SHELL SECTION, MATERIAL=STEEL, ELSET=RBS2
0.012
*SHELL SECTION, MATERIAL=STEEL, ELSET=LBS3
0.025
*SHELL SECTION, MATERIAL=STEEL, ELSET=RBS3
0.025
*SHELL SECTION, MATERIAL=STEEL, ELSET=LBS4
0.012
*SHELL SECTION, MATERIAL=STEEL, ELSET=RBS4
0.012
*SHELL SECTION, MATERIAL=STEEL, ELSET=LBS5
0.012
*SHELL SECTION, MATERIAL=STEEL, ELSET=RBS5
0.012
*SHELL SECTION, MATERIAL=STEEL, ELSET=LBS6
0.012
*SHELL SECTION, MATERIAL=STEEL, ELSET=RBS6
0.012
```

```
*SHELL SECTION, MATERIAL=STEEL, ELSET=LBS7
0.012
*SHELL SECTION, MATERIAL=STEEL, ELSET=RBS7
0.012
********
********
**MATERAL PROPERTIES
**
*MATERIAL, NAME=STEEL
*ELASTIC
2.E8, 0.3
*PLASTIC
540627.5106,0.
550799.7165,0.009667822
653885.595, 0.049084972
704579.612, 0.091786387
720592.785, 0.114179156
720213.571, 0.157666165
*********
*********
**
**BOUNDARY CONDITIONS
**
*BOUNDARY
PINNED, 1,3
ROLLER, 2
ROLLER, 3
60002, 3
60026, 3
60437, 3
60461, 3
60602, 3
60626, 3
61037, 3
61061, 3
61202, 3
61226, 3
61691, 3
61715, 3
61802, 3
61826, 3
62237, 3
62261, 3
62402, 3
62426, 3
62837, 3
62861, 3
**
**FLEXIBLE LATERAL BRACING
**
*ELEMENT, TYPE=SPRING1, ELSET=BRACE
80000, 63102
80001, 63126
```

80002, 63437
80003, 63461
**
80004, 63502
80005, 63526
80006, 63837
80007, 63861
**
**FLEXIBLE BRACING STIFFNESS
**
*SPRING, ELSET=BRACE
3
29803
****
****
*MPC
TIE, LBS1BF, BF1LBS
TIE, RBS1BF, BF1RBS
TIE, LBS2BF, BF2LBS
TIE, RBS2BF, BF2RBS
TIE, LBS3BF, BF3LBS
TIE, RBS3BF, BF3RBS
TIE, LBS4BF, BF4LBS
TIE, RBS4BF, BF4RBS
TIE, LBS5BF, BF5LBS
TIE, RBS5BF, BF5RBS
TIE, LBS6BF, BF6LBS
TIE, RBS6BF, BF6RBS
TIE, LBS7BF, BF7LBS
TIE, RBS7BF, BF7RBS
TIE, LBS1TF, TF1LBS
TIE, RBS1TF, TF1RBS
TIE, LBS2TF, TF2LBS
TIE, RBS2TF, TF2RBS
TIE, LBS3TF, TF3LBS
TIE, RBS3TF, TF3RBS
TIE, LBS4TF, TF4LBS
TIE, RBS4TF, TF4RBS
TIE, LBS5TF, TF5LBS
TIE, RBS5TF, TF5RBS
TIE, LBS6TF, TF6LBS
TIE, RBS6TF, TF6RBS
TIE, LBS7TF, TF7LBS
TIE, RBS7TF, TF7RBS
TIE, LBS1WEB, WEB1BS
TIE, RBS1WEB, WEB1BS
TIE, LBS2WEB, WEB2BS
TIE, RBS2WEB, WEB2BS
TIE, LBS3WEB, WEB3BS
TIE, RBS3WEB, WEB3BS
TIE, LBS4WEB, WEB4BS
TIE, RBS4WEB, WEB4BS
TIE, LBS5WEB, WEB5BS

```
TIE, RBS5WEB, WEB5BS
TIE, LBS6WEB, WEB6BS
TIE, RBS6WEB, WEB6BS
TIE, LBS7WEB, WEB7BS
TIE, RBS7WEB, WEB7BS
**
*STEP
*BUCKLE
3,,20,80
**
*CLOAD
MIDTOP, 2, -250
**
*RESTART, WRITE, FREQUENCY=1
*NODE FILE,LAST MODE=1,GLOBAL=YES
U
*END STEP
```

*HEADING
****
**   PARAMETRIC STUDY   *
**   HIGH STRENGTH STEEL PROJECT   *
**   *
** S. S. BEAM   (Using Non linear geometry and Riks Wempner method)   *
** APPLYING PERTURBATION TO THE BEAM FOR FULL NONLINEAR ANALYSIS   *
**   *
**   -------X----------------------X--------   *
**   7.625   15.25 m   7.625   *
**   *
** bf/2tf= 4.5, h/tw= 54; 1d spacing;   7.3 AISC bracing   *
**   *
** 1-horiz;   2- vert;   UNITS: KN-METER   *
**   *
**   ELEMENT TYPE: S4R   *
**   IMPERFECTION --> L/1000   *
**   *
****
**
*NODE
1, 0, 0, 0
1053, 30.5, 0, 0
7372, 0, 0, -0.203
8424, 30.5, 0, -0.203
14743, 0, 0, -0.406
15795, 30.5, 0, -0.406
16001, 0, 0.781, 0
17053, 30.5, 0.781, 0
23372, 0, 0.781, -0.203
24424, 30.5, 0.781, -0.203
30743, 0, 0.781, -0.406
31795, 30.5, 0.781, -0.406
32001, 0, 0.03, -0.203
33053, 30.5, 0.03, -0.203
57273, 0, 0.75096, -0.203
58325, 30.5, 0.75096, -0.203
**
**STIFFENERS
**
60001, 0, 0, -0.058
60027, 0, 0.781, -0.058
60136, 0, 0, -0.203
60162, 0, 0.781, -0.203
60301, 0, 0, -0.203
60327, 0, 0.781, -0.203
60436, 0, 0, -0.348
60462, 0, 0.781, -0.348
**
60601, 7.625, 0, -0.058
60627, 7.625, 0.781, -0.058
60736, 7.625, 0, -0.203
60762, 7.625, 0.781, -0.203

60901, 7.625, 0, -0.203
60927, 7.625, 0.781, -0.203
61036, 7.625, 0, -0.348
61062, 7.625, 0.781, -0.348
**
61201, 15.25, 0, 0
61227, 15.25, 0.781, 0
61390, 15.25, 0, -0.203
61416, 15.25, 0.781, -0.203
61501, 15.25, 0, -0.203
61527, 15.25, 0.781, -0.203
61690, 15.25, 0, -0.406
61716, 15.25, 0.781, -0.406
**
61801, 22.875, 0, -0.058
61827, 22.875, 0.781, -0.058
61936, 22.875, 0, -0.203
61962, 22.875, 0.781, -0.203
62101, 22.875, 0, -0.203
62127, 22.875, 0.781, -0.203
62236, 22.875, 0, -0.348
62262, 22.875, 0.781, -0.348
**
62401, 30.5, 0, -0.058
62427, 30.5, 0.781, -0.058
62536, 30.5, 0, -0.203
62562, 30.5, 0.781, -0.203
62701, 30.5, 0, -0.203
62727, 30.5, 0.781, -0.203
62836, 30.5, 0, -0.348
62862, 30.5, 0.781, -0.348
**
**INTERMEDIATE STIFFENERS (VARIABLE)
**
63101, 14.46720532, 0, -0.058
63127, 14.46720532, 0.781, -0.058
63236, 14.46720532, 0, -0.203
63262, 14.46720532, 0.781, -0.203
63301, 14.46720532, 0, -0.203
63327, 14.46720532, 0.781, -0.203
63436, 14.46720532, 0, -0.348
63462, 14.46720532, 0.781, -0.348
**
63501, 16.03279468, 0, -0.058
63527, 16.03279468, 0.781, -0.058
63636, 16.03279468, 0, -0.203
63662, 16.03279468, 0.781, -0.203
63701, 16.03279468, 0, -0.203
63727, 16.03279468, 0.781, -0.203
63836, 16.03279468, 0, -0.348
63862, 16.03279468, 0.781, -0.348

```
*********
*********
*NGEN, NSET=BLFLTIP
1, 1053, 1
*NGEN, NSET=BINT
7372, 8424, 1
*NGEN, NSET=BRFLTIP
14743, 15795, 1
*NGEN, NSET=TLFLTIP
16001, 17053, 1
*NGEN, NSET=TINT
23372, 24424, 1
*NGEN, NSET=TRFLTIP
30743, 31795, 1
*NGEN, NSET=BWEB
32001, 33053, 1
*NGEN, NSET=TWEB
57273, 58325, 1
*********
*********
**
**STIFFENERS
**
*NGEN, NSET=LBS1E
60001, 60027, 1
*NGEN, NSET=LBS1I
60136, 60162, 1
*NGEN, NSET=RBS1I
60301, 60327, 1
*NGEN, NSET=RBS1E
60436, 60462, 1
*NGEN, NSET=LBS2E
60601, 60627, 1
*NGEN, NSET=LBS2I
60736, 60762, 1
*NGEN, NSET=RBS2I
60901, 60927, 1
*NGEN, NSET=RBS2E
61036, 61062, 1
*NGEN, NSET=LBS3E
61201, 61227, 1
*NGEN, NSET=LBS3I
61390, 61416, 1
*NGEN, NSET=RBS3I
61501, 61527, 1
*NGEN, NSET=RBS3E
61690, 61716, 1
*NGEN, NSET=LBS4E
61801, 61827, 1
*NGEN, NSET=LBS4I
61936, 61962, 1
*NGEN, NSET=RBS4I
62101, 62127, 1
```

*NGEN, NSET=RBS4E
62236, 62262, 1
*NGEN, NSET=LBS5E
62401, 62427, 1
*NGEN, NSET=LBS5I
62536, 62562, 1
*NGEN, NSET=RBS5I
62701, 62727, 1
*NGEN, NSET=RBS5E
62836, 62862, 1
**
**INTERMEDIATE STIFFENERS
**
*NGEN, NSET=LBS6E
63101, 63127, 1
*NGEN, NSET=LBS6I
63236, 63262, 1
*NGEN, NSET=RBS6I
63301, 63327, 1
*NGEN, NSET=RBS6E
63436, 63462, 1
**
*NGEN, NSET=LBS7E
63501, 63527, 1
*NGEN, NSET=LBS7I
63636, 63662, 1
*NGEN, NSET=RBS7I
63701, 63727, 1
*NGEN, NSET=RBS7E
63836, 63862, 1
****
****
*NFILL, NSET=BLFLANGE
BLFLTIP, BINT, 7, 1053
*NFILL, NSET=BRFLANGE
BINT, BRFLTIP, 7, 1053
*NFILL, NSET=TLFLANGE
TLFLTIP, TINT, 7, 1053
*NFILL, NSET=TRFLANGE
TINT, TRFLTIP, 7, 1053
*NFILL, NSET=WEB
BWEB, TWEB, 24, 1053
****
****
**
**STIFFENERS
**
*NFILL, NSET=LBS1
LBS1E, LBS1I, 5, 27
*NFILL, NSET=RBS1
RBS1I, RBS1E, 5, 27
*NFILL, NSET=LBS2

LBS2E, LBS2I, 5, 27
*NFILL, NSET=RBS2
RBS2I, RBS2E, 5, 27
*NFILL, NSET=LBS3
LBS3E, LBS3I, 7, 27
*NFILL, NSET=RBS3
RBS3I, RBS3E, 7, 27
*NFILL, NSET=LBS4
LBS4E, LBS4I, 5, 27
*NFILL, NSET=RBS4
RBS4I, RBS4E, 5, 27
*NFILL, NSET=LBS5
LBS5E, LBS5I, 5, 27
*NFILL, NSET=RBS5
RBS5I, RBS5E, 5, 27
**
**INTERMEDIATE STIFFENERS
**
*NFILL, NSET=LBS6
LBS6E, LBS6I, 5, 27
*NFILL, NSET=RBS6
RBS6I, RBS6E, 5, 27
*NFILL, NSET=LBS7
LBS7E, LBS7I, 5, 27
*NFILL, NSET=RBS7
RBS7I, RBS7E, 5, 27
****
****
*NSET, NSET=PINNED, GENERATE
264, 15006, 1053
*NSET, NSET=ROLLER, GENERATE
790, 15532, 1053
*NSET, NSET=MIDTOP, GENERATE
16527, 31269, 1053
*NSET, NSET=TFLANGE
TLFLANGE, TRFLANGE
**
*NSET, NSET=LBS1EX, GENERATE
60002, 60026, 1
*NSET, NSET=RBS1EX, GENERATE
60437, 60461, 1
*NSET, NSET =LBS2EX, GENERATE
60602, 60626, 1
*NSET, NSET=RBS2EX, GENERATE
61037, 61061, 1
*NSET, NSET=LBS3EX, GENERATE
61202, 61226, 1
*NSET, NSET=RBS3EX, GENERATE
61691, 61715, 1
*NSET, NSET=LBS4EX, GENERATE
61802, 61826, 1
*NSET, NSET=RBS4EX, GENERATE
62237, 62261, 1

*NSET, NSET=LBS5EX, GENERATE
62402, 62426, 1
*NSET, NSET=RBS5EX, GENERATE
62837, 62861, 1
*NSET, NSET=LBS6EX, GENERATE
63102, 63126, 1
*NSET, NSET=RBS6EX, GENERATE
63437, 63461, 1
*NSET, NSET=LBS7EX, GENERATE
63502, 63526, 1
*NSET, NSET=RBS7EX, GENERATE
63837, 63861, 1
*NSET, NSET=LBS1BF, GENERATE
60001, 60136, 27
*NSET, NSET=RBS1BF, GENERATE
60301, 60436, 27
*NSET, NSET=LBS2BF, GENERATE
60601, 60736, 27
*NSET, NSET=RBS2BF, GENERATE
60901, 61036, 27
*NSET, NSET=LBS3BF, GENERATE
61201, 61390, 27
*NSET, NSET=RBS3BF, GENERATE
61501, 61690, 27
*NSET, NSET=LBS4BF, GENERATE
61801, 61936, 27
*NSET, NSET=RBS4BF, GENERATE
62101, 62236, 27
*NSET, NSET=LBS5BF, GENERATE
62401, 62536, 27
*NSET, NSET=RBS5BF, GENERATE
62701, 62836, 27
*NSET, NSET=LBS6BF, GENERATE
63101, 63236, 27
*NSET, NSET=RBS6BF, GENERATE
63301, 63436, 27
*NSET, NSET=LBS7BF, GENERATE
63501, 63636, 27
*NSET, NSET=RBS7BF, GENERATE
63701, 63836, 27
*NSET, NSET=LBS1TF, GENERATE
60027, 60162, 27
*NSET, NSET=RBS1TF, GENERATE
60327, 60462, 27
*NSET, NSET=LBS2TF, GENERATE
60627, 60762, 27
*NSET, NSET=RBS2TF, GENERATE
60927, 61062, 27
*NSET, NSET=LBS3TF, GENERATE
61227, 61416, 27
*NSET, NSET=RBS3TF, GENERATE
61527, 61716, 27

*NSET, NSET=LBS4TF, GENERATE
61827, 61962, 27
*NSET, NSET=RBS4TF, GENERATE
62127, 62262, 27
*NSET, NSET=LBS5TF, GENERATE
62427, 62562, 27
*NSET, NSET=RBS5TF, GENERATE
62727, 62862, 27
*NSET, NSET=LBS6TF, GENERATE
63127, 63262, 27
*NSET, NSET=RBS6TF, GENERATE
63327, 63462, 27
*NSET, NSET=LBS7TF, GENERATE
63527, 63662, 27
*NSET, NSET=RBS7TF, GENERATE
63727, 63862, 27
*NSET, NSET=LBS1WEB, GENERATE
60137, 60161, 1
*NSET, NSET=RBS1WEB, GENERATE
60302, 60326, 1
*NSET, NSET=LBS2WEB, GENERATE
60737, 60761, 1
*NSET, NSET=RBS2WEB, GENERATE
60902, 60926, 1
*NSET, NSET=LBS3WEB, GENERATE
61391, 61415, 1
*NSET, NSET=RBS3WEB, GENERATE
61502, 61526, 1
*NSET, NSET=LBS4WEB, GENERATE
61937, 61961, 1
*NSET, NSET=RBS4WEB, GENERATE
62102, 62126, 1
*NSET, NSET=LBS5WEB, GENERATE
62537, 62561, 1
*NSET, NSET=RBS5WEB, GENERATE
62702, 62726, 1
*NSET, NSET=LBS6WEB, GENERATE
63237, 63261, 1
*NSET, NSET=RBS6WEB, GENERATE
63302, 63326, 1
*NSET, NSET=LBS7WEB, GENERATE
63637, 63661, 1
*NSET, NSET=RBS7WEB, GENERATE
63702, 63726, 1
**
*NSET, NSET=BF1LBS, GENERATE
2107, 7372, 1053
*NSET, NSET=BF1RBS, GENERATE
7372, 12637, 1053
*NSET, NSET=BF2LBS, GENERATE
2370, 7635, 1053
*NSET, NSET=BF2RBS, GENERATE
7635, 12900, 1053

326

*NSET, NSET=BF3LBS, GENERATE
527, 7898, 1053
*NSET, NSET=BF3RBS, GENERATE
7898, 15269, 1053
*NSET, NSET=BF4LBS, GENERATE
2896, 8161, 1053
*NSET, NSET=BF4RBS, GENERATE
8161, 13426, 1053
*NSET, NSET=BF5LBS, GENERATE
3159, 8424, 1053
*NSET, NSET=BF5RBS, GENERATE
8424, 13689, 1053
*NSET, NSET=BF6LBS, GENERATE
2606, 7871, 1053
*NSET, NSET=BF6RBS, GENERATE
7871, 13136, 1053
*NSET, NSET=BF7LBS, GENERATE
2660, 7925, 1053
*NSET, NSET=BF7RBS, GENERATE
7925, 13190, 1053
*NSET, NSET=TF1LBS, GENERATE
18107, 23372, 1053
*NSET, NSET=TF1RBS, GENERATE
23372, 28637, 1053
*NSET, NSET=TF2LBS, GENERATE
18370, 23635, 1053
*NSET, NSET=TF2RBS, GENERATE
23635, 28900, 1053
*NSET, NSET=TF3LBS, GENERATE
16527, 23898, 1053
*NSET, NSET=TF3RBS, GENERATE
23898, 31269, 1053
*NSET, NSET=TF4LBS, GENERATE
18896, 24161, 1053
*NSET, NSET=TF4RBS, GENERATE
24161, 29426, 1053
*NSET, NSET=TF5LBS, GENERATE
19159, 24424, 1053
*NSET, NSET=TF5RBS, GENERATE
24424, 29689, 1053
*NSET, NSET=TF6LBS, GENERATE
18606, 23871, 1053
*NSET, NSET=TF6RBS, GENERATE
23871, 29136, 1053
*NSET, NSET=TF7LBS, GENERATE
18660, 23925, 1053
*NSET, NSET=TF7RBS, GENERATE
23925, 29190, 1053
*NSET, NSET=WEB1BS, GENERATE
32001, 57273, 1053
*NSET, NSET=WEB2BS, GENERATE
32264, 57536, 1053

```
*NSET, NSET=WEB3BS, GENERATE
32527, 57799, 1053
*NSET, NSET=WEB4BS, GENERATE
32790, 58062, 1053
*NSET, NSET=WEB5BS, GENERATE
33053, 58325, 1053
*NSET, NSET=WEB6BS, GENERATE
32500, 57772, 1053
*NSET, NSET=WEB7BS, GENERATE
32554, 57826, 1053
*********
*********
*ELEMENT, TYPE=S4R
1, 1, 1054, 1055, 2
*ELGEN, ELSET=BFLANGE
1, 1052, 1, 1, 14, 1053, 1052
**
*ELEMENT, TYPE=S4R
16001, 16001, 17054, 17055, 16002
*ELGEN, ELSET=TFLANGEL
16001, 263, 1, 1, 14, 1053, 263
**
*ELEMENT, TYPE=S4R
19683, 16264, 17317, 17318, 16265
*ELGEN, ELSET=TFLANGEM
19683, 526, 1, 1, 14, 1053, 526
**
*ELEMENT, TYPE=S4R
27047, 16790, 17843, 17844, 16791
*ELGEN, ELSET=TFLANGER
27047, 263, 1, 1, 14, 1053, 263
**
*ELEMENT, TYPE=S4R
32001, 7372, 32001, 32002, 7373
*ELGEN, ELSET=BWEB
32001, 1052, 1, 1
**
*ELEMENT, TYPE=S4R
33053, 32001, 33054, 33055, 32002
*ELGEN, ELSET=WEB
33053, 1052, 1, 1, 24, 1053, 1052
**
*ELEMENT, TYPE=S4R
58301, 57273, 23372, 23373, 57274
*ELGEN, ELSET=TWEB
58301, 1052, 1, 1
**
**STIFFENERS
**
*ELEMENT, TYPE=S4R
60001, 60001, 60028, 60029, 60002
*ELGEN, ELSET=LBS1
60001, 26, 1, 1, 5, 27, 26
```

```
*ELEMENT, TYPE=S4R
60301, 60301, 60328, 60329, 60302
*ELGEN, ELSET=RBS1
60301, 26, 1, 1, 5, 27, 26
*ELEMENT, TYPE=S4R
60601, 60601, 60628, 60629, 60602
*ELGEN, ELSET=LBS2
60601, 26, 1, 1, 5, 27, 26
*ELEMENT, TYPE=S4R
60901, 60901, 60928, 60929, 60902
*ELGEN, ELSET=RBS2
60901, 26, 1, 1, 5, 27, 26
**
*ELEMENT, TYPE=S4R
61201, 61201, 61228, 61229, 61202
*ELGEN, ELSET=LBS3
61201, 26, 1, 1, 7, 27, 26
*ELEMENT, TYPE=S4R
61501, 61501, 61528, 61529, 61502
*ELGEN, ELSET=RBS3
61501, 26, 1, 1, 7, 27, 26
**
*ELEMENT, TYPE=S4R
61801, 61801, 61828, 61829, 61802
*ELGEN, ELSET=LBS4
61801, 26, 1, 1, 5, 27, 26
*ELEMENT, TYPE=S4R
62101, 62101, 62128, 62129, 62102
*ELGEN, ELSET=RBS4
62101, 26, 1, 1, 5, 27, 26
**
*ELEMENT, TYPE=S4R
62401, 62401, 62428, 62429, 62402
*ELGEN, ELSET=LBS5
62401, 26, 1, 1, 5, 27, 26
*ELEMENT, TYPE=S4R
62701, 62701, 62728, 62729, 62702
*ELGEN, ELSET=RBS5
62701, 26, 1, 1, 5, 27, 26
**
**INTERMEDIATE STIFFENERS
**
*ELEMENT, TYPE=S4R
63101, 63101, 63128, 63129, 63102
*ELGEN, ELSET=LBS6
63101, 26, 1, 1, 5, 27, 26
*ELEMENT, TYPE=S4R
63301, 63301, 63328, 63329, 63302
*ELGEN, ELSET=RBS6
63301, 26, 1, 1, 5, 27, 26
**
*ELEMENT, TYPE=S4R
63501, 63501, 63528, 63529, 63502
```

*ELGEN, ELSET=LBS7
63501, 26, 1, 1, 5, 27, 26
*ELEMENT, TYPE=S4R
63701, 63701, 63728, 63729, 63702
*ELGEN, ELSET=RBS7
63701, 26, 1, 1, 5, 27, 26
****
****
**
**FLANGE THICKNESS
**
*SHELL SECTION, MATERIAL=STEEL, ELSET=BFLANGE
0.045
*SHELL SECTION, MATERIAL=STEEL, ELSET=TFLANGEL
0.045
*SHELL SECTION, MATERIAL=STEEL, ELSET=TFLANGER
0.045
*SHELL SECTION, MATERIAL=STEEL, ELSET=TFLANGEM
0.045
**
**WEB THICKNESS
**
*SHELL SECTION, MATERIAL=STEEL, ELSET=BWEB
0.01363
*SHELL SECTION, MATERIAL=STEEL, ELSET=TWEB
0.01363
*SHELL SECTION, MATERIAL=STEEL, ELSET=WEB
0.01363
**
**STIFFENER THICKNESS
**
*SHELL SECTION, MATERIAL=STEEL, ELSET=LBS1
0.012
*SHELL SECTION, MATERIAL=STEEL, ELSET=RBS1
0.012
*SHELL SECTION, MATERIAL=STEEL, ELSET=LBS2
0.012
*SHELL SECTION, MATERIAL=STEEL, ELSET=RBS2
0.012
*SHELL SECTION, MATERIAL=STEEL, ELSET=LBS3
0.025
*SHELL SECTION, MATERIAL=STEEL, ELSET=RBS3
0.025
*SHELL SECTION, MATERIAL=STEEL, ELSET=LBS4
0.012
*SHELL SECTION, MATERIAL=STEEL, ELSET=RBS4
0.012
*SHELL SECTION, MATERIAL=STEEL, ELSET=LBS5
0.012
*SHELL SECTION, MATERIAL=STEEL, ELSET=RBS5
0.012
*SHELL SECTION, MATERIAL=STEEL, ELSET=LBS6
0.012

```
*SHELL SECTION, MATERIAL=STEEL, ELSET=RBS6
0.012
*SHELL SECTION, MATERIAL=STEEL, ELSET=LBS7
0.012
*SHELL SECTION, MATERIAL=STEEL, ELSET=RBS7
0.012
********
********
**
**IMPERFECTION CONIDERATION
**
*IMPERFECTION, FILE=fs45ws54-1d73AISC_buckle, STEP=1
1, 0.01525
********
********
**MATERAL PROPERTIES
**
*MATERIAL, NAME=STEEL
*ELASTIC
2.E8, 0.3
*PLASTIC
540627.5106,0.
550799.7165,0.009667822
653885.595, 0.049084972
704579.612, 0.091786387
720592.785, 0.114179156
720213.571, 0.157666165
*********
*********
**
**BOUNDARY CONDITIONS
**
*BOUNDARY
PINNED, 1,3
ROLLER, 2
ROLLER, 3
60002, 3
60026, 3
60437, 3
60461, 3
60602, 3
60626, 3
61037, 3
61061, 3
61202, 3
61226, 3
61691, 3
61715, 3
61802, 3
61826, 3
62237, 3
62261, 3
62402, 3
```

62426, 3
62837, 3
62861, 3
**
**FLEXIBLE LATERAL BRACING
**
*ELEMENT, TYPE=SPRING1, ELSET=BRACE
80000, 63102
80001, 63126
80002, 63437
80003, 63461
**
80004, 63502
80005, 63526
80006, 63837
80007, 63861
**
**FLEXIBLE BRACING STIFFNESS
**
*SPRING, ELSET=BRACE
3
29803
****
****
*MPC
TIE, LBS1BF, BF1LBS
TIE, RBS1BF, BF1RBS
TIE, LBS2BF, BF2LBS
TIE, RBS2BF, BF2RBS
TIE, LBS3BF, BF3LBS
TIE, RBS3BF, BF3RBS
TIE, LBS4BF, BF4LBS
TIE, RBS4BF, BF4RBS
TIE, LBS5BF, BF5LBS
TIE, RBS5BF, BF5RBS
TIE, LBS6BF, BF6LBS
TIE, RBS6BF, BF6RBS
TIE, LBS7BF, BF7LBS
TIE, RBS7BF, BF7RBS
TIE, LBS1TF, TF1LBS
TIE, RBS1TF, TF1RBS
TIE, LBS2TF, TF2LBS
TIE, RBS2TF, TF2RBS
TIE, LBS3TF, TF3LBS
TIE, RBS3TF, TF3RBS
TIE, LBS4TF, TF4LBS
TIE, RBS4TF, TF4RBS
TIE, LBS5TF, TF5LBS
TIE, RBS5TF, TF5RBS
TIE, LBS6TF, TF6LBS
TIE, RBS6TF, TF6RBS
TIE, LBS7TF, TF7LBS
TIE, RBS7TF, TF7RBS

```
TIE, LBS1WEB, WEB1BS
TIE, RBS1WEB, WEB1BS
TIE, LBS2WEB, WEB2BS
TIE, RBS2WEB, WEB2BS
TIE, LBS3WEB, WEB3BS
TIE, RBS3WEB, WEB3BS
TIE, LBS4WEB, WEB4BS
TIE, RBS4WEB, WEB4BS
TIE, LBS5WEB, WEB5BS
TIE, RBS5WEB, WEB5BS
TIE, LBS6WEB, WEB6BS
TIE, RBS6WEB, WEB6BS
TIE, LBS7WEB, WEB7BS
TIE, RBS7WEB, WEB7BS
**
*STEP, NLGEOM, INC=75
*STATIC, RIKS
0.1, 1., 1.e-12
**
*CONTROLS, ANALYSIS=DISCONTINUOUS
*CLOAD
MIDTOP, 2, -250
**
*RESTART, WRITE, FREQUENCY=1
*EL PRINT, FREQUENCY=10
S, MISES
*NODE PRINT, FREQUENCY=10
U
RF
*END STEP
```

BIBLIOGRAPHY

BIBLIOGRAPHY

1. American Association of State Highway and Transportation Officials (AASHTO), (1998), LRFD Bridge Design Specifications, Cusotmary U.S. Units, Second Addition, Washington, D.C.

2. American Association of State Highway and Transportation Officials (AASHTO), (1998), LRFD Bridge Design Specifications, S.I. Units, Second Addition, Washington, D.C.

3. ABAQUS, (1998), ABAQUS Standard User's Manual, Version 5.8, Volumes 1 to 3, Hibbit, Karlsson & Sorensen, Inc., Pawtucket, Rhode Island, USA.

4. ABAQUS, (1998), ABAQUS Theory Manual, Hibbitt, Karlsson & Sorensen, Inc., Pawtucket, Rhode Island, USA.

5. American Institute of Steel Construction (AISC), (1999), Load and Resistance Factor Design (LRFD) Specification for Structural Steel Buildings, Chicago, Illinois.

6. American Society of Civil Engineers (ASCE), (1971), Plastic Design in Steel, A Guide and Commentary, American Society of Civil Engineers, New York, p. 80.

7. Axhag F., Johnsson B., (1998), "Tension Flange Instability of I Beams," Journal of Constructional Steel Research, Elsevier Science Ltd., Great Britain, Vol. 49, No. 1, pp. 69-81.

8. Azizinamini, A., Mans, P., and Yakel, A.J., (1998), Flexural Capacity of HPS-70W Bridge Girders, National Bridge Research Organization (NaBRO), Lincoln, Nebraska

9. Barth Karl E., White Donald W. and Bobb Betsy M., (2000), "Negative bending resistance of HPS70W girders," Journal of Constructional Steel Research, Vol. 53, January, pp. 1-31.

10. Clough, Ray W., (1965), "The Finite Element Method in Structural Mechanics," Stress Analysis: Recent Development in Numerical and Experimental Methods, John Wiley & Sons Ltd, 1956.

11. Earls C.J., (1999) "On the Inelastic Failure of High Strength Steel I-Shaped Beams," Journal of Constructional Steel Research, Elsevier Science Ltd., Great Britain, Vol. 49, No. 1, pp. 1-24.

12. Earls C. J., (2000a) "On Geometric Factors Influencing the Structural Ductility of Compact I-Shaped Beams," Journal of Structural Engineering, American Society of Civil Engineers, Reston, Virginia, Vol. 126, No. 7, pp. 780-789.

13. Earls C. J., (2000b) "The Influence of Material Effects on the Structural Ductility of Compact I-Shaped Beams," Journal of Structural Engineering, American Society of Civil Engineers, Reston, Virginia, Vol. 126, No. 11, pp. 1268-1278.

14. Earls, C.J. and Shah, B.J., (2001), "High Performance Steel Bridge Girder Compactness," Journal of Constructional Steel Research, In Press, Uncorrected Proof, pp. 1-22.

15. Greco, N. and Earls, C.J., (2002), "Structural Ductility in Hybrid High Performance Steel Beams," Report No. CE/ST 23, Department of Civil and Environmental Engineering, University of Pittsburgh, Pittsburgh, Pennsylvania.

16. Green, P.S., Sauce, R., and Ricles, J.M., (2002), "Strength and Ductility of HPS Flexural Members," Journal of Constructional Steel Research, In Press, Uncorrected Proof, pp. 2-35.

17. Green P. S., Sooi T. K., Ricles J. M., Sauce R., Kelly T., (1994), "Inelastic behavior of Structural members Fabricated from High Performance Steel," Proceedings, Structural Stability Research Council, Lehigh University, Bethlehem, Pennsylvania, USA, pp. 435-455.

18. Huang P. C., (1994), "Finite Element Analysis of Inelastic Behavior of Structural Beams and Bridge Girders," Ph. D. Dissertation, School of Civil & Environmental Engineering, Cornell University, Ithaca, New York.

19. Moen L. A., Matteis G., De Hopperstad O. S., Langseth M., Landolfo R. and Mazzolani F. M., (August, 1999), "Rotational capacity of Aluminium beams under Moment Gradient," Journal of structural Engineering, Vol. 125, No. 8, pp. 921-928.

20. Morcos S. S., (1988), "Moment –Rotation Tests of Steel Bridge Girders for Autostress Design," MS Thesis, University of Pittsburgh, Pittsburgh, Pennsylvania.

21. Ricles J. M., Sauce R., Green P. S., (1998), "High Strength Steel: Implications of material and geometric characteristics on inelastic Flexural behavior," Engineering Structures, Elsevier Science Ltd., Great Britain, Vol. 20, pp. 323-335.

22. Salmon, C. G., Johnson, J. E., (1996), Steel Structures, Design and Behavior, Fourth Edition, HarperCollins Publishers Inc., New York, New York.

23. Teh L.H., Clarke M.J., (1999) "Tracing Secondary Equilibrium Paths of Elastic Framed Structures," Journal of Engineering Mechanics, Vol. 125, No. 12, American Society of Civil Engineers, Reston, Virginia, pp. 1358-1364.

24. White, D. W., (1987), "Analysis of the Inelastic Moment-Rotation Behavior of Non-compact Steel Bridge Girders," Report CE-STR-94-1, School of Civil Engineering, Purdue University, West Lafayette, Indiana.

25. White D. W., Ramirez J. A., Barth K. E., (1997), "Moment-Rotation Relationships for Unified Autostress Designs of Continuous-span bridge beams and Girders," Report FHWA/IN/JTRP-97/8, Federal Highway Administration, Washington D. C.

26. White D. W., Barth K. E., (1998), "Strength and Ductility of Compact-Flange I-Girders in Negative Bending," Journal of Constructional Steel Research, Elsevier Science Ltd.,
Great Britain, Vol. 45, No. 3, pp. 241-280.

27. Yura, J.A., Galambos, T.V., and Ravindra, M.K., (1978), "The Bending Resistance of Steel Beams," Journal of the Structural Division, ASCE, Vol. 104, No. ST9, September, pp. 1355-1369.

28. Yura, J.A., Helwig, T.A. (2001) "Bracing for Stability," Notes from a Short Course Sponsored by the Structural Stability Research Council and the American Institute of Steel Construction.

REFERENCES NOT CITED

1. Barker, R. M. and Puckett, J. A., (1997), *Design of Highway Bridges, Based on AASHTO LRFD, Bridge Design Specifications,* John Wiley and Sons, Inc., New York, New York.

2. Beer, F. P. and Johnston, Jr., E.R., (1992), *Mechanics of Material*, Mc-Graw Hill, Inc. New York, New York.

3. Boresi A. P., Schmidt R. J., and Sidebottom O. M., (1993), *Advanced Mechanics of Materials*, Fifth Ed. John Wiley & Sons, Inc.

4. Earls C.J., (1995), "On the Use of Nonlinear Finite Element Analysis Techniques to Model Structural Steel Angle Response," Ph. D. Dissertation, University of Minnesota, Minneapolis, USA.

5. Earls, C.J., (2001), "Constant Moment Behavior of High Performance Steel I-Shaped Beams," *Journal of Constructional Steel Research,* Volume 57, No. 7, July, pp. 711-728.

6. Galambos, T.V., (1977), "History of Steel Beam Design," Engineering Journal, AISC, Vol. 14, Fourth Quarter, pp. 141-147.

7. Logan, D.L., (1993), *A First Course In the Finite Element Method*, PWS Publishing Company, Boston, MA.